PRELIMINARY EXPLORATION (G-3) FOR REE AND ASSOCIATED MINERALS IN BORANA BLOCK, BHILWARA DISTRICT, RAJASTHAN

Name of the Block: **Borana Block**

Explored block area**: 1.14 Sq. Km**

Toposheet No. 45 K/03

Submitted to

खान मंत्रालय
MINISTRY OF
MINES
सत्यमेव जयते

National Mineral Exploration and Development Trust (NMEDT)

Ministry of Mines, Government of India

Submitted by:

GeoExpOre Pvt.Ltd

GeoExpOre Private Limited

Bangalore, Karnataka, 560040

www.geoexpore.com

e-mail: info@geoexpore.com

July 2026

CONTENTS

1. CHAPTER 1 - EXECUTIVE SUMMARY 24

1.1 EXECUTIVE SUMMARY (ENGLISH) 24

1.2 कार्यकारी सारांश 27

2. CHAPTER 2 - DETAILS OF THE QUALIFIED PERSON(S) / EXPLORATION AGENCY 30

2.1 DETAILS OF THE EXPLORATION AGENCY 30

2.2 DETAILS OF QUALIFICATION AND EXPERIENCE OF PERSONS ASSOCIATED WITH VARIOUS ASPECTS OF EXPLORATION ASSESSMENT OF RESOURCES AND RESERVES 30

3. CHAPTER 3 – TITLE AND OWNERSHIP 33

3.1 NAME OF THE EXPLORER/ MINING OR PROSPECTING RIGHTS HOLDER 33

3.2 DETAILS OF PERIOD OF PROSPECTING/MINERAL RIGHT IF ANY: 33

4. CHAPTER 4 - DETAILS OF THE AREA UNDER STUDY 34

4.1 VILLAGE, DISTRICT, STATE 34

4.2 SURVEY OF INDIA TOPOSHEET NO. & DIFFERENTIAL GLOBAL POSITIONING SYSTEM (DGPS) COORDINATES OF ALL CORNER POINTS OF THE AREA AND BOREHOLE POINTS IN LATITUDE AND LONGITUDE (DEGREE MINUTES SECOND) FORMAT WGS-84 DATUM 34

4.3 CADASTRAL DETAILS OF THE AREA WITH LAND USE, AREA UNDER FOREST WITH TYPE OF FOREST. IN CASE THE CADASTRAL DETAILS ARE NOT AVAILABLE AN INDICATIVE DATA OF BREAKUP OF GOVERNMENT, PRIVATE AND FOREST LAND 35

4.4 MINERAL(S) UNDER INVESTIGATION OR GRANTED UNDER LICENCE OR LEASE 36

5. CHAPTER 5 – PHYSIOGRAPHY AND ENVIRONMENT 37

5.1 RELIEF OF THE AREA WITH MINIMUM AND MAXIMUM ELEVATION, DRAINAGE PATTERN, NATURAL WATER COURSES, RESERVOIRS, ETC. 37

5.2 ROADS, RAILWAY TRACK, ELECTRIC TRANSMISSION LINE, TELEPHONE LINE, ETC., PASSING THROUGH THE AREA OR NEARBY **39**

5.3 HOST POPULATION (LOCAL TRIBES), HUMAN SETTLEMENTS WITHIN AND NEARBY THE AREA **39**

5.4 SOCIO DEMOGRAPHIC PROFILE OF THE AREA AND NEARBY **39**

5.5 HISTORICAL SITES AND ARCHAEOLOGICAL MONUMENTS, PLACES OF WORSHIP, PUBLIC UTILITIES ETC. WITHIN OR NEAR BY **40**

5.6 FORESTS, SANCTUARIES, NATIONAL PARK AND WILD LIFE SANCTUARIES; GRAZING LAND AND GOCHAR LAND WITHIN OR NEAR BY THE AREA WITH DISTANCE FROM PERIPHERY OF THE AREA EXPLORED. **40**

5.7 FLORA AND FAUNA WITHIN AND NEARBY **40**

5.8 WATER BODIES SUCH AS RIVER, NALA, STREAM, RESERVOIR, ETC., WITHIN OR NEARBY **41**

5.9 CLIMATIC CONDITIONS: **41**

5.10 ANY OTHER PHYSIOGRAPHIC, SOCIAL AND ENVIRONMENTAL FACTOR HAVING POTENTIAL TO AFFECT THE VIABILITY OF THE PROJECT AND ASSESSMENT OF RESOURCES AND RESERVES. **41**

6. CHAPTER 6 – INFRASTRUCTURE **42**

6.1 LOCAL INFRASTRUCTURE DETAILS **42**

7. CHAPTER 7 – GEOLOGY **43**

7.1 BRIEF REGIONAL GEOLOGY OF THE AREA OUTLINING THE BROAD GEOLOGICAL, STRATIGRAPHICAL AND STRUCTURAL FRAMEWORK. **43**

7.2 LOCAL GEOLOGICAL SETTING DETAILING THE COMMON ROCK TYPES, CONTROLS OF MINERALIZATION, DETAILS OF OLD WORKINGS IF ANY, SURFACE EXPOSURES, ETC., OF THE AREA UNDER STUDY ALSO OF ADJOINING NEARBY AREAS, IF THE INFORMATION IS LIKELY TO HAVE AN IMPACT ON THE AREA UNDER STUDY. **46**

7.2.1 OUTCROP MAPPING *46*

7.2.2 GEOLOGICAL MAPPING *47*

7.2.3 DESCRIPTION OF ROCK TYPES *48*

7.2.3.1 Migmatite Gneiss 48

7.2.3.2 Syenite/alkali syenite 49

7.2.3.3 Amphibolite 50

7.2.3.4 Pegmatite 51

7.2.4 PETROGRAPHY *52*
7.2.4.1 Migmatite gneiss 53
7.2.4.2 Syenite 61
7.2.4.3 Amphibolite 71
7.2.4.4 Pegmatite 75
7.2.5 ORE MICROSCOPY *76*
7.2.5.1 Migmatite Gneiss 76
7.2.5.2 Syenite 77
7.2.5.3 Amphibolite 79
7.3 STRUCTURAL DETAILS OF THE AREA SUCH AS DIP, STRIKE, FOLDS, FAULTS, ETC. 79
7.3.1 DETAILED STRUCTURAL DISPOSITION *80*
7.3.1.1 Planar Structure: 80
7.3.1.1.1 Gneissic Banding 80
7.3.1.2 Linear structures 81
7.3.1.2.1 Mineral lineation 81
7.3.1.2.2 Joints 81
7.3.1.2.3 Folds 81
7.3.1.2.4 Faults 81
7.3.1.2.5 Epidote veins 81
7.3.2 DETAILED STRUCTURAL DISPOSITION AND ITS RELATIONSHIP WITH MINERALIZATION *83*
7.4 A DISCUSSION ON THE TYPE OF THE DEPOSIT BASED ON THE STYLE OF MINERALISATION AND MINERALS UNDER INVESTIGATION. SUGGESTED EXPLORATION PLAN WITH SPACING OF THE SAMPLING POINTS AND DEPTH OF EXPLORATION COMMENSURATE WITH THE STAGE OF EXPLORATION. 83
7.5 THE EXTENT AND VARIABILITY OF THE MINERALISATION EXPRESSED AS LENGTH (IN METER) (ALONG STRIKE OR OTHERWISE), PLAN WIDTH, AND DEPTH BELOW SURFACE TO THE UPPER AND LOWER LIMITS OF THE MINERAL RESOURCE. 84

8. CHAPTER 8 - PREVIOUS EXPLORATION 85

8.1 NAME AND ADDRESS OF PROSPECTING AGENCY OR PERMIT HOLDER OR LICENSEE INVOLVED IN THE EXPLORATION OF THE AREA WITH YEAR AND PERIOD OF EXPLORATION (IF MORE THAN ONE AGENCY IS INVOLVED DETAILS TO BE GIVEN SEPARATELY FOR EACH AGENCY) 85

8.2 BRIEF DETAILS OF THE EXPLORATION CARRIED OUT (TO BE GIVEN SEPARATELY FOR EACH AGENCY) 86

8.3 RESERVES OR RESOURCES ESTIMATED, IF ANY, DURING THE PREVIOUS EXPLORATION CAMPAIGN WITH QUANTITY AND GRADE UNDER VARIOUS CATEGORIES 88

9. CHAPTER 9 - AERIAL OR GROUND GEOPHYSICAL OR GEOCHEMICAL DATA 89

9.1 PREVIOUS GEOPHYSICAL STUDIES 89

9.2 PREVIOUS GEOCHEMICAL INVESTIGATIONS 89

10. CHAPTER 10 - EXPLORATION UNDERTAKEN DURING CURRENT INVESTIGATION 91

10.1 OBJECTIVES OF INVESTIGATION 91

10.2 BASIS FOR TAKING UP INVESTIGATION 91

10.3 DETAILS OF NATURE AND QUANTUM OF WORK APPROVED VS ACHIEVEMENT 92

10.3.1 NATURE OF WORK 92

10.4 MODE OF OPERATION OF DIFFERENT WORK COMPONENTS AND ASSOCIATED AGENCY 96

10.5 DETAILS OF PITTING, TRENCHING, DRILLING, ETC., WITH SPACING AND DISTRIBUTION OF THE SAMPLE POINTS ALONG WITH GEOGRAPHICAL CO-ORDINATES. 96

10.5.1 TRENCHING 96

10.5.1.1 Trenching Methodology 96

10.5.1.2 Trench description 97

10.5.1.2.1 Trench 1-RJBO/T1/2024-25 97

10.5.1.2.2 Trench 2-RJBO/T2/2024-25 100

10.5.1.2.3 Trench-3 RJBO/T3/2024-25 103

10.5.1.2.4 Trench-4 RJBO/T4/2024-25 106

10.5.1.2.5 Trench-5 RJBO/T5/2024-25 108

10.5.2 DRILLING 111

10.6 DATA SPACING FOR REPORTING OF EXPLORATION RESULTS: 112

11. CHAPTER 11 - LOCATION OF DATA POINT 113

11.1 ACCURACY AND QUALITY OF SURVEYS USED TO LOCATE DRILL HOLES (COLLAR AND DOWN-HOLE SURVEYS, AZIMUTH, INCLINATION, COORDINATES OF BORE HOLES ETC), TRENCHES, MINE WORKINGS AND OTHER LOCATIONS USED

IN MINERAL RESOURCE ESTIMATION. 113

11.2 QUALITY AND ADEQUACY OF TOPOGRAPHIC CONTROL. 113

12. CHAPTER 12 - SAMPLING TECHNIQUE 114

12.1 NATURE AND QUALITY OF SAMPLING (EG. CUT CHANNELS, RANDOM CHIPS, ETC.) AND MEASURES TAKEN TO ENSURE SAMPLE REPRESENTATION. 114

12.1.1 BED ROCK SAMPLING 114

12.1.2 TRENCH SAMPLING 115

12.1.3 CORE SAMPLING 116

12.1.4 EXTERNAL CHECK SAMPLING 116

13. CHAPTER 13 - DRILLING TECHNIQUE AND DRILL SAMPLING EMPLOYED 117

13.1 DRILL TYPE (EG. CORE, REVERSE CIRCULATION, OPEN-HOLE HAMMER, ROTARY AIR BLAST, AUGER, BANGKA, SONIC, ETC.) AND DETAILS (EG. CORE DIAMETER, TRIPLE OR STANDARD TUBE). 117

13.2 WHETHER CORE AND CHIP SAMPLE RECOVERIES HAVE BEEN PROPERLY RECORDED AND RESULTS ASSESSED. 117

13.3 MEASURES TAKEN TO MAXIMIZE SAMPLE RECOVERY AND ENSURE REPRESENTATIVE NATURE OF THE SAMPLES. 117

13.4 WHETHER A RELATIONSHIP EXISTS BETWEEN SAMPLE RECOVERY AND GRADE AND WHETHER SAMPLE BIAS COULD HAVE OCCURRED DUE TO PREFERENTIAL LOSS OR GAIN OF FINE OR COARSE MATERIAL. 118

13.5 LOGGING: -WHETHER CORE AND CHIP SAMPLES HAVE BEEN LOGGED TO A LEVEL OF DETAIL TO SUPPORT APPROPRIATE MINERAL RESOURCE ESTIMATION, MINING STUDIES AND METALLURGICAL STUDIES. 118

13.6 EXPLORATION SYSTEMATIC DRILLING 119

13.6.1 DRILL CORE LOGGING 120

13.6.2 DRILL CORE SAMPLING 123

13.7 DRILL CORE PRESERVATION 123

13.8 DISCUSSION ON THE ANALYSIS RESULTS OF HANDHELD X-RAY FLUORESCENCE (XRF), IF USED IN THE INVESTIGATION. 124

14. CHAPTER 14 - SUB-SAMPLING TECHNIQUES AND SAMPLE PREPARATION 125

14.1 IF CORE, WHETHER CUT OR SAWN AND WHETHER QUARTER, HALF OR ALL CORE TAKEN. 125

14.2 IF NON-CORE, WHETHER RIFFLED, TUBE SAMPLED, ROTARY SPLIT, ETC., AND WHETHER SAMPLED WET OR DRY. 125

14.2.1 FOR ALL SAMPLE TYPES, THE NATURE, QUALITY AND APPROPRIATENESS OF THE SAMPLE PREPARATION TECHNIQUE. 125

14.3 QUALITY CONTROL PROCEDURES ADOPTED FOR ALL SUB-SAMPLING STAGES TO MAXIMIZE REPRESENTATION OF SAMPLES. 126

14.4 MEASURES TAKEN TO ENSURE THAT THE SAMPLING IS REPRESENTATIVE OF THE IN-SITU MATERIAL COLLECTED. 126

14.5 WHETHER SAMPLE SIZES ARE APPROPRIATE TO THE GRAIN SIZE OF THE MATERIAL BEING SAMPLED. 126

15. CHAPTER 15 - QUALITY OF ASSAY DATA AND LABORATORY TESTS 127

15.1 EPMA ANALYSIS 127

15.2 XRD ANALYSIS 131

15.3 WHOLE ROCK ELEMENTAL ANALYSIS 133

15.4 TRACE ELEMENTAL ANALYSIS 134

15.5 RARE EARTH ELEMENTAL ANALYSIS 135

15.5.1 RARE EARTH ELEMENTAL ANALYSIS IN MIGMATITE GNEISS 135

15.5.2 RARE EARTH ELEMENTAL ANALYSIS IN SYENITE 136

15.5.3 RARE EARTH ELEMENTAL ANALYSIS IN AMPHIBOLITE 136

15.5.4 RARE EARTH ELEMENTAL ANALYSIS IN PEGMATITE 136

15.6 BIVARIATE GEOCHEMICAL RELATIONSHIPS OF TOTAL RARE EARTH ELEMENTS (TREE) AND SELECTED MAJOR AND TRACE ELEMENTS 136

15.7 DISCUSSION 141

15.7.1 DETAILED INTERPRETATION OF CHEMICAL ANALYTICAL DATA 141

15.7.2 REE SCENARIO FROM REFERENCE ANALYTICAL DATA 153

15.8 CHECK ANALYSIS OF AT LEAST 10% OF SAMPLES SHOULD BE ANALYZED FROM THIRD PARTY NATIONAL ACCREDITATION BOARD FOR TESTING AND CALIBRATION LABORATORIES (NABL) ACCREDITED OR DEPARTMENT OF SCIENCE AND TECHNOLOGY (DST) OR BUREAU OF INDIAN STANDARDS (BIS) RECOGNIZED LABORATORIES OR GOVERNMENT LABORATORIES FOR ASSESSING THE ACCEPTABLE LEVELS OF ACCURACY. 154

15.9 INTEGRATION OF GEOLOGY, GEOPHYSICS AND GEOCHEMICAL EXPLORATION AND THE INTERPRETATION 157

15.10 MINERAL PROSPECT 160

15.10.1 MINERALIZATION 160

15.10.2 SURFACE INDICATION OF MINERALIZATION 160

15.10.3 MODE OF OCCURRENCE 161

15.10.4 STRIKE LENGTH AND WIDTH OF ANOMALIES IDENTIFIED BASED ON GEOLOGY AND GEOCHEMICAL EXPLORATION 161

15.10.5 GENESIS OF MINERALIZATION 162

16. CHAPTER 16 - MOISTURE 163

17. CHAPTER 17 – BULK DENSITY 164

18. CHAPTER 18 – BENEFICIATION STUDIES AS MAY BE REQUIRED 165

19. CHAPTER 19 – RESOURCE ESTIMATION TECHNIQUES 166

19.1 DISCUSSION ON SUFFICIENT DATA DENSITY TO ASSURE CONTINUITY OF MINERALISATION AND SYNTHESIS ADEQUATE DATA BASE FOR ESTIMATION PROCEDURE USED. 166

19.2 WHETHER PREVIOUS EXPLORATION DATA HAS BEEN USED AND INTEGRATED WITH THE CURRENT EXPLORATION DATA FOR ASSESSMENT OF THE UPDATED RESOURCES. 166

19.3 THE NATURE AND APPROPRIATENESS OF THE ESTIMATION TECHNIQUE(S) APPLIED AND KEY ASSUMPTIONS,VINCLUDING TREATMENT OF EXTREME GRADE VALUES, DOMAINING, INTERPOLATION PARAMETERS, MAXIMUM DISTANCE OF EXTRAPOLATION FROM DATA POINTS 167

19.4 THE BASIS FOR THE CLASSIFICATION OF THE MINERAL RESOURCES INTO VARYING CONFIDENCE CLASSES. 167

19.5 THE ASSUMPTIONS MADE REGARDING RECOVERY OF BY-PRODUCTS. 167

19.6 DETAILED DESCRIPTION OF THE METHOD USED AND THE ASSUMPTIONS MADE TO ESTIMATE TONNAGES AND GRADES (SECTION, POLYGON, INVERSE DISTANCE, GEOSTATISTICAL, OR OTHER METHOD). 168

19.7 DESCRIPTION OF HOW THE GEOLOGICAL INTERPRETATION WAS USED TO CONTROL THE RESOURCE ESTIMATES.169

19.8 DISCUSSION OF BASIS FOR USING OR NOT USING GRADE CUTTING OR CAPPING. IF ANY COMPUTER SOFTWARE WAS USED FOR ESTIMATION OF RESOURCES THEN NAME OF THE SOFTWARE WITH THE VERSION AND METHOD CHOSEN, DESCRIPTION OF PROGRAMMES AND PARAMETERS USED. 169

19.9 GEOSTATISTICAL METHODS ARE EXTREMELY VARIED AND SHOULD BE DESCRIBED IN DETAIL. THE METHOD CHOSEN SHOULD BE JUSTIFIED. THE GEOSTATISTICAL PARAMETERS, INCLUDING THE VARIOGRAM, AND THEIR COMPATIBILITY WITH THE GEOLOGICAL INTERPRETATION SHOULD BE DISCUSSED. EXPERIENCE GAINED IN APPLYING GEO-STATISTICS TO SIMILAR

DEPOSITS SHOULD BE TAKEN INTO ACCOUNT. 169

19.10 DATA VERIFICATION OR VALIDATION PROCEDURES USED, INCLUDING PEER REVIEW REPORT. 170

20. CHAPTER 20 – REPORTING OF RESOURCES 171

20.1 REE RESOURCE ESTIMATION (1000 PPM CUT-OFF GRADE) 173

20.1.1 OVERALL REE RESOURCE 175

20.2 REE RESOURCE ESTIMATION (1200 PPM CUTOFF GRADE) 177

20.2.1 OVERALL REE RESOURCE 178

21. CHAPTER 21 - SUMMARY AND RECOMMENDATIONS 180

21.1 SUMMARY 180

21.2 RECOMMENDATIONS 183

22. CHAPTER 22 – PLATES AND MAPS 186

23. CHAPTER 23 – ANNEXURES OR ENCLOSURES TO THE REPORT 198

23.1 ANNEXURE I – SAMPLE DESCRIPTION 198

23.2 ANNEXURE II- PETROGRAPHY REPORT 203

23.2.1 BRS PETROGRAPHY REPORT 203

23.2.2 CORE PETROGRAPHY REPORT 222

23.3 ANNEXURE III- XRD 235

23.4 ANNEXURE IV- BULK DENSITY 236

23.5 ANNEXURE V- EPMA 237

23.6 ANNEXURE VI- WHOLE ROCK ANALYSES 239

23.7 ANNEXURE VII- DETAILS OF 34 TRACE ELEMENTAL ANALYSES IN BORANA BLOCK, BHILWARA DISTRICT, RAJASTHAN 240

23.8 ANNEXURE VIII- REE ANALYSIS 243

23.8.1 DETAILS OF REE ELEMENTAL ANALYSES OF BRS SAMPLES IN BORANA BLOCK, BHILWARA DISTRICT, RAJASTHAN 243

23.8.2 DETAILS OF REE ELEMENTAL ANALYSES OF TRENCH NO 1 SAMPLES IN BORANA BLOCK, BHILWARA DISTRICT,

RAJASTHAN *250*

23.8.3 DETAILS OF REE ELEMENTAL ANALYSES OF TRENCH NO 2 SAMPLES IN BORANA BLOCK, BHILWARA DISTRICT, RAJASTHAN *251*

23.8.4 DETAILS OF REE ELEMENTAL ANALYSES OF TRENCH NO 3 SAMPLES IN BORANA BLOCK, BHILWARA DISTRICT, RAJASTHAN *252*

23.8.5 DETAILS OF REE ELEMENTAL ANALYSES OF TRENCH NO 4 SAMPLES IN BORANA BLOCK, BHILWARA DISTRICT, RAJASTHAN *253*

23.8.6 DETAILS OF REE ELEMENTAL ANALYSES OF TRENCH NO 5 SAMPLES IN BORANA BLOCK, BHILWARA DISTRICT, RAJASTHAN *254*

23.8.7 REE ELEMENTAL ANALYSES OF CORE SAMPLES, BH-1 IN BORANA BLOCK, BHILWARA DISTRICT, RAJASTHAN *255*

23.8.8 REE ELEMENTAL ANALYSES OF CORE SAMPLES, BH-2 IN BORANA BLOCK, BHILWARA DISTRICT, RAJASTHAN *257*

23.8.9 REE ELEMENTAL ANALYSES OF CORE SAMPLES, BH-3 IN BORANA BLOCK, BHILWARA DISTRICT, RAJASTHAN *260*

23.8.10 REE ELEMENTAL ANALYSES OF CORE SAMPLES, BH-4 IN BORANA BLOCK, BHILWARA DISTRICT, RAJASTHAN *263*

23.9 ANNEXURE IX- EXTERNAL CHECK SAMPLES (IISC LAB) **266**

23.10 ANNEXURE X- LOGSHEETS **268**

23.11 ANNEXURE XI- SANCTION ORDER **329**

23.12 ANNEXURE XII- OFFICIALS INVOLVED IN THE EXPLORATION PROJECT **335**

23.13 ANNEXURE XIII- PROJECT REVIEWED AT VARIOUS STAGES **336**

23.14 ANNEXURE XIV- FIELD INSPECTION PHOTOGRAPHS **337**

24. CHAPTER 24 - ANY OTHER INFORMATION **338**

24.1 REFERENCES **338**

24.2 LOCALITY INDEX **340**

24.3 REVIEWER'S COMMENTS **341**

25. CHAPTER 25 - CERTIFICATE FROM THE QUALIFIED PERSON WITH NAME, DATE AND SIGNATURE 345

LIST OF FIGURES

Fig 4.1 Location map of Borana block 36

Fig 5.1 2D contour map and corresponding 3D elevation model of the Borana Block showing topographic variation and cardinal points with contour interval: 1m (source: Google earth pro).37

Fig 5.2 Geomorphological map of the Borana block (source: NGDR website) 38

Fig 7.1 Regional geology map of the Mangalwar Complex 45

Fig 7.2 Field photographs of Migmatite Gneiss 49

Fig 7.3 Field photographs of Syenite 50

Fig 7.4 Field photographs of Amphibolite 51

Fig 7.5 Field photograph of Pegmatites 52

Fig 7.6a Photomicrograph showing dark and light colour bands of biotite, hornblende and K-feldspars, quartz, plagioclase respectively under CPL (Sample no. RJBO/BRS24/24-25). 55

Fig 7.6b Photomicrograph showing Allanite (Aln) with radial cracks under CPL (Sample no. RJBO/BRS-24/24-25). 55

Fig 7.7a Photomicrograph showing biotite foliation defined by biotite (Bt) under PPL (sample no. RJBO/BRS93/2024-25). 56

Fig 7.7b Photomicrograph showing irregular shaped allanite (Aln) with radial cracks developed the surrounding quartz grains under PPL (sample no. RJBO/BRS93/2024-25) 56

Fig 7.7c Photomicrograph showing Zircon (Zrn) and Apatite (Ap) under PPL (sample no. RJBO/BRS93/2024-25). 56

Fig 7.7d Photomicrograph showing xenomorphic garnet (Grt) under PPL (RJBO/BRS93/2024-25). 56

Fig 7.8a Photomicrograph showing mineral assemblages and intergrowth of plagioclase and quartz exhibits myrmekite texture under CPL (sample no. RJBO/BRS36/2024-25). 57

Fig 7.8b Photomicrograph showing schistosity defined by biotite and magnetite (opaques) are seen under PPL (sample no. RJBO/BRS36/202425). 57

Fig 7.9 Photomicrograph of an elongated monazite grain associated with hornblende and plagioclase and close to epidote seen in cross polarized light (sample no. RJBO/BRS25/2024-25). 57

Fig 7.10a Hand sample of drill core sample of migmatite gneiss (RJBO-02/CS-77) 58

Fig 7.10b Photomicrograph displays alternations of mafic and felsic bands/layers, mafic band composed of Biotite-hornblende and felsic band composed of quartz-plagioclase under plane polar view (RJBO-02/CS-77) 58
Fig 7.10c Photomicrograph showing alteration of biotite by chlorite under cross polar view (RJBO-02/CS-77) 58
Fig 7.10d Photomicrograph of plagioclase (Pl) showing sub grain formation due to metamorphic activity under cross polar view (RJBO-02/CS-77) 58
Fig 7.10e Photomicrograph cluster of zircon (Zrn) grains under plane polar view (RJBO-02/CS-77) 59
Fig. 7.11a Drill core sample of migmatite gneiss (RJBO-03/CS-37) 59
Fig 7.11b Photomicrograph displays epidote (Ep) veins along with major minerals like biotite (Bt), plagioclase (Pl) and microcline (Mc) under cross polarized light (RJBO-03/CS-37) 59
Fig 7.11c Photomicrograph showing cluster of titanite along the boundary of plagioclase and biotite under plane polarized light (RJBO-03/CS-37) 60
Fig 7.11d Photomicrograph showing a long prismatic allanite (Aln) with radial cracks under plane polar view (RJBO-03/CS-37) 60
Fig 7.11e Photomicrograph showing Allanite grain in Migmatite Gneiss from Borehole 3 at 95 m depth 60
Fig 7.11f Photomicrograph showing Allanite grain in Migmatite Gneiss from Borehole 3 at 95 m depth 61
Fig 7.12a A Photomicrograph of syenite showing different mineral assemblages like microcline, quartz, orthoclase and zoisite under XPL (Sample no RJBO/BRS-107/2024-25). 64
Fig 7.12b Photomicrograph showing epidote vein cross cutting under XPL (Sample no. RJBO/BRS-107/2024-25). 64
Fig 7.12c Photomicrograph showing of xenomorphic garnet in syenite (Sample no. RJBO/BRS-107/2024-25). 64
Fig 7.12d Photomicrograph along prismatic allanite with radial cracks in syenite under PPL (Sample no. RJBO/BRS-107/2024-25). 64
Fig 7.13a Photomicrograph showing epidote (ep)- zoisite (zo) veins intruded into the syenite under the cross-polar view (Sample no. RJBO/BRS-108/24-25). 65
Fig 7.13b Photomicrograph showing a large allanite (aln) crystal altered marginally by epidote

(ep) under the cross-polar view (Sample no. RJBO/BRS-108/24-25). 65
Fig 7.14a Photomicrograph showing Monazite (Mnz) associated with K-feldspars (Kfs) under cross-polar view (Sample no. RJBO/BRS-29/24-25). 65
Fig 7.14b Photomicrograph showing an elongated allanite (aln) with distinct radial cracks associated with K-feldspars (k-spar) and magnetite (mag), under plane polar view (Sample no. RJBO/BRS-29/24-25). 65
Fig 7.15c Photomicrograph showing granular monazite grains associated with K-feldspars and quartz in syenite under cross polar view (Sample no. RJBO/BRS26/24-25). 66
Fig 7.16a Drill core sample of alkali feldspar syenite (RJBO-02/CS-36) 67
Fig 7.16b Photomicrograph of syenite showing assemblage of plagioclase (Pl), and microcline (Mc) displaying Sub-hypidiomorphic texture under cross polar view (RJBO-02/CS-36) 67
Fig 7.16c Photomicrograph showing clusters of zircon (zrn) grains under plane polar view (RJBO-02/CS-36) 67
Fig 7.17a Hand sample of drill core sample of Alkali feldspar syenite (RJBO-04/CS-25) 68
Fig 7.17b. Photomicrograph showing myrmekite texture along with plagioclase and microcline; subgrain formation of Plagioclase (Pl) in the alkali feldspar syenite under cross polar view (RJBO-04/CS-25) 68
Fig 7.17c Photomicrograph showing granular Monazite (Mz) grains associated with plagioclase under Cross polar view (RJBO-04/CS-25) 68
Fig 7.17d Photomicrograph showing Allanite grain in Syenite from Borehole 4 at 50 m depth 69
Fig 7.18a Photomicrograph showing ribbon quartz (Qz) with epidote (Ep) veins under Cross Polar view (Sample no. RJBO/BRS-24/24-25) 69
Fig 7.18b Photomicrograph showing primary allanite (Aln) under plane polar view (Sample no. RJB-4 (50mts). 69
Fig 7.19a Drill core sample of alkali feldspar syenite (RJBO-04/CS-23) 70
Fig 7.19b Photomicrograph alkali-feldspar syenite showing mineral assemblages such as plagioclase (Pl) and epidote (Ep) vein which intruded the syenite at earlier stage under CPL (RJBO-04/CS-23) 70
Fig 7.19c Photomicrograph showing a late-stage epidote and carbonate veins are cross-cutting the alkali feldspar syenite under CPL (RJBO-04/CS-23) 70
Fig 7.19d Photomicrograph showing primary allanite (Aln) rimmed by epidote (Ep) and

plagioclase (Pl) under plane polarized light (RJBO-04/CS-23) 70
Fig 7.19e Photomicrograph showing cluster of Monazite (Mnz) and plagioclase (Pl) under cross polarized light (RJBO-04/CS-23) 71
Fig 7.20a Photomicrograph of amphibolite showing assemblage of plagioclase (Pl), hornblende (Hbl) and epidote (Ep) exhibiting granulose texture under plane polar view (Sample no. RJBO/BRS-7/24-25) 73
Fig 7.20b Photomicrograph showing minor plagioclase inclusion in hornblende and secondary plagioclase under plane polar view (Sample no. RJBO/BRS-7/24-25) 73
Fig 7.21a Drill core sample of alkali amphibolite (RJB0-01/CS-25) (75mts) 73
Fig 7.21b Photomicrograph of Alkali amphibolite showing mineral assemblages (K-Amp) under cross polar view (RJB0-01/CS-25) (75mts) 73
Fig 7.21c Photomicrograph showing yellow to bluish grey alkali amphiboles under cross polar view (RJB0-01/CS-25) (75mts) 74
Fig 7.21d Photomicrograph showing Clinopyroxene (cpx) along with alkali amphiboles and titanite under cross polar view (RJB0-01/CS-25) (75mts) 74
Fig 7.21e Photomicrograph showing cluster of titanite (Ttn) along the boundary of alkali amphiboles under cross polar view (RJB0-01/CS-25) (75mts) 74
Fig 7.22a Photomicrograph of Pegmatite showing mineral assemblages under CPL (Sample no. RJBO/BRS-11/24-25). 75
Fig 7.22b Photomicrograph of Polygonal mosaic texture in Pegmatite under CPL (Sample no. RJBO/BRS-11/24-25). 75
Fig 7.22c Photomicrograph showing epidotes in Pegmatite under CPL (Sample no. RJBO/BRS-11/24-25). 75
Fig 7.23 Photomicrograph showing magnetite (Mag) veinlet and discrete magnetite associated with biotite under reflected light (Sample no. RJBO/BRS-24/24-25) 76
Fig 7.24 Photomicrograph showing discrete/ disseminated magnetite grains in the biotite gneiss, under reflected light (sample no. RJBO/BRS36/2024-25) 76
Fig 7.25 Photomicrograph showing a euhedral magnetite replaced by hematite and subsequently by goethite at the margin under reflected light (sample no. RJBO/BRS25/2024-25). 77
Fig 7.26a Photomicrograph showing disseminated chalcopyrite (Ccp), and pyrite (Py) under reflected light (RJBO-02/CS-77) (154mts) 77

Fig 7.26b Photomicrograph showing magnetite (Mag) under reflected light (RJBO-02/CS-77) (154mts) 77
Fig 7.27a Photomicrograph showing Pinkish to grey tinge of irregularly shaped magnetite (Mag) replaced marginally by hematite (Hem) under reflected light (Sample no. RJBO/BRS29/24-25). 78
Fig 7.27b Photomicrograph showing magnetite replaced by hematite (Hem) and goethite (Gth) exhibits colloform structure under reflected light (Sample no. RJBO/BRS-29/24-25) 78
Fig 7.28 Photomicrograph showing pyrite. Chalcopyrite and magnetite in association with silicates under reflected light (RJBO-02/CS-36) (71mts) 78
Fig 7.29 Photomicrograph showing euhedral pyrite (Py) under reflected light (RJBO-04/CS-25) (50mts) 78
Fig 7.30a Photomicrograph showing subhedral hematite (Hem), associated with silicates under reflected light (RJB0-01/CS-25(75mts) 79
Fig 7.30b Photomicrograph showing irregular form of pyrite (Py), chalcopyrite (Ccp) and magnetite (Mag) associated with alkali amphiboles under reflected light (Sample no. RJB-1 (75mts). RJB0-01/CS-25(75mts) 79
Fig 7.31 Gneissic bandings 82
Fig 7.34 Chevron fold 82
Fig 7.37 Epidote veins cross-cutting 82
Fig 10.1a Trench no RJBO/T1/2024-25(i) represent demarcated trench photographs before excavating (ii) represents trench dug with the collection of composite samples and (iii) represents after excavation trench properly closed and backfilled 98
Fig 10.1b Cross section of Trench-1 (RJBO/T1/2024-25) 99
Fig 10.1c Cross section of Trench-1 with TREE vs distance along Trench (RJBO/T1/2024-25)99
Fig 10.1d LREE and HREE proportion with its **ratio (LREE: HREE= 20.70: 1)** in Trench-1(RJBO/T1/2024-25) 100
Fig 10.2a Trench no RJBO/T2/2024-25 (i) represent demarcated trench photographs before excavating (ii) represents trench dug with the collection of composite samples and 101
(iii) represents after excavation trench properly closed and backfilled 101
Fig 10.2b Cross section of Trench-2 (RJBO/T2/2024-25) 101
Fig 10.2c Cross section of Trench-2 with REE (TREE) vs trench width plot (RJBO/T2/2024-25)

102
Fig 10.2d LREE and HREE proportion with **ratio (LREE: HREE= 5.87: 1**) in Trench-2 (RJBO/T25/2024-25) 103
Fig 10.3a Trench no RJBO/T3/2024-25 (i) represent demarcated trench photographs before excavating (ii) represents trench dug with the collection of composite samples and (iii) represents after excavation trench properly closed and backfilled 104
Fig 10.3b Cross section of Trench-3 (RJBO/T3/2024-25) 105
Fig 10.3c Cross section of Trench-3 with REE (TREE) vs trench width plot (RJBO/T3/2024-25) 105
Fig 10.3d LREE and HREE proportion with **ratio (LREE: HREE= 15.68:1)** in Trench-3(RJBO/T3/2024-25) 106
Fig 10.4a Trench no RJBO/T4/2024-25 (i) represent demarcated trench photographs before excavating (ii) represents trench dug with the collection of composite samples and (iii) represents after excavation trench properly closing and backfilling 107
Fig 10.4b Cross section of Trench-4 (RJBO/T4/2024-25) 107
Fig 10.4c Cross section of Trench-4 with REE (TREE) vs trench width plot (RJBO/T4/2024-25) 108
Fig 10.4d LREE and HREE proportion with **ratio (LREE: HREE= 11.70: 1)** in Trench-4 (RJBO/T4/2024-25) 108
Fig 10.5a Trench no RJBO/T5/2024-25 (i) represent demarcated trench photographs before excavating (ii) represents trench dug with the collection of composite samples and (iii) represents after excavation trench properly closing and backfilling 109
Fig 10.5b Cross section of Trench-5 (RJBO/T4/2024-25) 110
Fig 10.5c Cross section of Trench-5 with REE (TREE) vs trench width plot (RJBO/T5/2024-25) 110
111
Fig 10.5d LREE and HREE proportion with **ratio (LREE: HREE= 13.41: 1)** in Trench-5 (RJBO/T5/2024-25) 111
Fig 13.1 Drilling 120
Fig 13.2 Drill core recovery with REE mineralization 121
Fig 13.3 Drill core showing Albitization and Epidotization 122

Fig 13.4 Drill core showing Sulfides mineralization 122
Fig 13.5 Boreholes Lithology Section 123
Fig 13.6: Photograph showing drill core boxes with appropriate labelling. 124
Fig 15.1a BSE image of monazite within migmatite gneiss in sample no RJBO/BRS-93 128
Fig 15.1b BSE image of zircon within migmatite gneiss in sample no RJBO/BRS-93 128
Fig 15.2 BSE image of zircon within migmatite gneiss in sample no RJB-03(95mts) 128
Fig 15.3a & Fig 15.3b BSE image of zircon within syenite in sample no RJBO/BRS-26 129
Fig 15.4 BSE image of zircon within syenite in sample no RJB-04(50mts) 129
Fig 15.5a & Fig 15.5b BSE image of chalcopyrite and pyrite within amphibolite 130
in sample no BRS-03(75 mts) 130
Fig 15.6a BSE image of chalcopyrite within amphibolite in sample no BRS-03(75 mts) 130
Fig 15.6b BSE image of pyrite within amphibolite in sample no BRS-03(75 mts) 130
Fig 15.7a BSE image of pyrite within amphibolite in sample no BRS-03(75 mts) 131
Fig 15.7b BSE image of magnetite within amphibolite in sample no BRS-03(75 mts) 131
Fig 15.8 BSE image of magnetite within amphibolite in sample no BRS-03(75 mts) 131
Fig 15.9 Bivariate geochemical relationships between Total Rare Earth Elements (TREE) and selected major oxides elements 137
Fig 15.10 Bivariate geochemical relationships between Total Rare Earth Elements (TREE) and selected Trace elements. 139
Fig 15.11 TAS diagram for Borana block 141
Fig 15.12 AFM diagram for Borana block 142
Fig 15.13 Harker bivariant diagrams SiO2 vs different elements for different rock types of Borana block 143
Fig 15.14 Harker bivariant diagrams SiO2 vs different elements for different rock types of Borana block 144
Fig 15.15 A/NK-A/CNK diagram for different rock types of Borana block (After Shand, 1943) 146
Fig 15.16 Fe(t) + Ti - Al - Mg ternary plot for different rock types of Borana block (Jensen, 1976) 147
Fig 15.17 FeOT-MgO-Al2O3 ternary plot for different rock types of Borana block. (after Pearce et al., 1977) 148

Fig 15.18 Chondrite normalized pattern for different BRS of Borana block (Nakamura, 1974) 150
Fig 15.19 Chondrite normalized pattern for different trench samples of Borana block (Nakamura, 1974) 151
Fig 15.20 Comparison of BRS, Trench and Check Sample Total REE values between Shiva Analytical Labs and Indian Institute of Science (IISc) Bengaluru 156
Fig 19.1 The Longitudinal section on inclined plane (45°) 168
Fig 20.1 ΣREE values depth wise for Borana Boreholes 172
Fig 20.2 Histogram showing distribution of total REE 173
Fig 20.3 Longitudinal section on inclined plane (45°) for 1000ppm showing mineralized and non-mineralized bodies 173
Fig 20.4 Longitudinal section on inclined plane (45°) for 1000ppm showing mineralized and non-mineralized bodies of entire area 174
Fig 20.5 Longitudinal section on inclined plane (45°) for 1200ppm showing mineralized and non-mineralized bodies 177
Fig 20.6 Longitudinal section on inclined plane (45°) for 1200ppm showing mineralized and non-mineralized bodies of entire area 177

LIST OF TABLES

Table 2.1: Personnel involved 30
Table 4.1: Boundary Co-ordinates of the Borana block 35
Table 4.2: Borehole location details with total depth 35
Table 7.1: Regional Lithotectonic stratigraphic succession of the area 44
Table 7.2: Lithostratigraphy of the proposed block (After GSI FSP:2018-19) 46
Table 7.3: Details of sample subjected for petrographic study 52
Table 8.1 Brief Details of Exploration Carried Out 86
Table 10.1: Nature of Work 92
Table 10.2: Quantum of Approved Work vs Achievements 94
Table 10.3: Represents the location and bearing of the Trenches 97
Table 10.4: The average, maximum and minimum REE values obtained from Trench-1 (RJBO/T1/2024-25) 100
Table 10.5: The average, maximum and minimum REE values obtained from Trench-2(RJBO/T2/2024-25) 102
Table 10.6: The average, maximum and minimum REE values obtained fromTrench-3(RJBO/T3/2024-25) 105
Table 10.7: The average, maximum and minimum REE values obtained fromTrench-4(RJBO/T4/2024-25) 108
Table 10.8: The average, maximum and minimum REE values obtained fromTrench-5(RJBO/T5/2024-25) 111
Table 11.1 Co-ordinates of the base station for DGPS Survey 113
Table 13.1 Borehole Details 119
Table 15.1: Details of Samples collected for EPMA study in Borana block 127
Table 15.2: Details of Samples analyzed for XRD in Borana block 132
Table 15.3: Check Samples Borana 154
Table 17.1: Bulk Density Analysis 164
Table 20.1: Ore resource estimation for 1000 ppm cut-off 174
Table 20.2: Resource Estimation 175
Table 20.3: Different elements metal resource of all four boreholes: 176

Table 20.4: Ore resource estimation for 1200 ppm cut-off 178
Table 20.5: Different elements metal resource of all four boreholes: 179

LIST OF PLATES

Sr. No.	Plates	Page No.
1	Outcrop Map of Borana Block, Bhilwara District, Rajasthan	186
2	Geological Map of Borana Block, Bhilwara District, Rajasthan	187
3	Sample Location Map on Geological Map of Borana Block, Bhilwara District, Rajasthan	188
4	Geochemical Dispersion Map of Borana Block, Bhilwara District, Rajasthan	189
5	Borehole selection on Geochemical Dispersion Map of Borana Block, Bhilwara District, Rajasthan	190
6	Transverse cross section for BH - 01	191
7	Transverse cross section for BH - 02	192
8	Transverse cross section for BH - 03	193
9	Transverse cross section for BH - 04	194
10	Longitudinal lithological section on inclined plane (45°)	195
11	Longitudinal section on inclined plane (45°) for 1000ppm showing mineralized body and non-mineralized body	196
12	Longitudinal section on inclined plane (45°) for 1000ppm showing mineralized body and non-mineralized body of entire area	196
13	Longitudinal section on inclined plane (45°) for 1200ppm showing mineralized body and non-mineralized body	197
14	Longitudinal section on inclined plane (45°) for 1200ppm showing mineralized body and non-mineralized body of entire area	197

LIST OF ANNEXURES

Sr. No.	Annexures	Page No.
1	Sample Description	198
2	Petrography Report – BRS & Core Samples	203
3	XRD	235
4	Bulk Density	236
5	EPMA	237
6	Whole Rock Analysis	239
7	Trace Elements Analysis	240
8	REE Analysis: BRS, Trench & Core Samples	243
9	External Check Samples	266
10	Log Sheets	268
11	Sanction Order	329
12	Officials involved in the Exploration Project	335
13	Project Reviewed at various stages	336
14	Field Inspection Photographs	337

LIST OF ABBREVATIONS

Abbreviation	Description
GSI	Geological Survey of India
SOI	Survey of India
NMET	National Mineral Exploration Trust
NMEDT	National Mineral Exploration and Development Trust
NMEP	National Mineral Exploration Policy
MoM	Ministry or Mines
TCC	Technical cum Cost Committee
EC	Executive committee
DMG	Department of Mines and Geology
NQT	Nature, Quantum and Target
REE	Rare Earth Element
DGPS	Differential Global Positioning System
PPM	Parts per Million
Km^2	Square Kilometer
ENE	East - North – East
WSW	West - South – West
NE	North-East
SW	South-west
NW	North-West
SE	South-East
ICP-MS	Inductively coupled plasma mass spectrometry
ICP-OES	Inductively coupled plasma optical emission spectroscopy
EPMA	Electron probe Microanalysis
BGC	Basement Gneissic Complex
BH	Borehole
XRD	X-ray Diffraction
BRS	Bed Rock Sampling
mts	Meters
PPL	Plane polarized light
XPL	Cross polarized light

TREE	Total Rare Earth Elements (La to Lu)
LREE	Light Rare Earth Elements (La to Eu)
HREE	Heavy Rare Earth Elements (Gd to Lu)
LSM	Large Scale Mapping
Cu. m	Cubic meter
MSL	Mean Sea Level

CHAPTER 1 - EXECUTIVE SUMMARY

1.1 Executive Summary (English)

A G3-stage investigation into Rare Earth Element (REE) mineralization titled "Preliminary Survey(G3-Stage) for REE and associated minerals in Borana Block, Bhilwara District, Rajasthan" was carried out under the sanctioned letter F.No.23/464/2024 – NMEDT131, dated 10th June 2024 and revised office memorandum – F.No.23/4642024 – NMEDT/881, dated 21st February 2025. Borana area is situated in western part of Bhilwara District, Rajasthan. The main objective of this exploration was to evaluate 'REE' mineralization in and around Borana area, Bhilwara District, Rajasthan. The work was stated to have been undertaken as follow-up to REE anomalies reported during earlier G4 reconnaissance exploration during GSI FS 2018-19.

The Borana project area was reported within Survey of India toposheet 45K/03 and was stated to cover approximately 1.14 km², between latitudes 25°26'08" N to 25°25'33" N and longitudes 74°07'44" E to 74°06'47" E. The coordinate reference system used was WGS-1984 with UTM, where applicable. The work mainly involved Detailed geological mapping at 1:2,000 scales of 1.14 sq. km was done during which bedrock samples were collected. A total of 108 numbers of bed rock samples, 100 numbers of trench samples, 222 numbers of core samples have been collected and sent for chemical analysis to evaluate the REE potentiality of the area.

Geologically the area belongs to the Mangalwar Complex of the Bhilwara Supergroup. The terrain comprises a Mesoarchean basement dominated by granitic gneisses containing enclaves of amphibolite, metasediments, and granitoid intrusions collectively referred to as the Banded Gneissic Complex (BGC). The main lithological units mapped in Borana block include syenite, migmatite gneiss, amphibolite and pegmatite.

Among the 108 BRS samples collected, the TREE values range from 5.04 ppm to 2971.05 ppm with average of 1416.68 ppm. A total of five trenches, each measuring 20 m in length, 1 m in width, and 1 m in depth, were excavated, amounting to 100 cubic meters of trenching. The trenching was undertaken to assess the subsurface strike extension and depth persistence of potential mineralized

units and to enable representative sampling. Among the 100 Trench samples collected, the TREE values range from 130.82 ppm to 2645.85 ppm with average of 1163.98 ppm.

The drilling comprised four inclined boreholes at 45° inclination (BH-01 to BH-04), aggregating 474.64 m of drilling, were completed at 200 m spacing between boreholes. The TREE values in the study area lie between 30.58 ppm and 3081.88 ppm across different boreholes, with average of 1267.29 ppm.

Geochemical classification and discrimination plots were referenced in support of lithological differentiation; amphibolite samples were reported as plotting in mafic fields indicating a mafic affinity characterized by low silica content, while felsic lithologies (pegmatite, syenite, migmatite gneiss) were reported as plotting in granite–granodiorite fields reflecting their felsic composition with comparatively high silica content.

The Borana Block hosts appreciable rare earth element (REE) mineralization, predominantly associated with syenite/alkali syenite and migmatite gneiss of the Mangalwar Complex. Among these lithologies, syenite/alkali syenite exhibits comparatively higher REE enrichment.

In syenite/alkali syenite, bedrock samples record TREE values ranging from 778.08 ppm to 2742.54 ppm, with an average of 1522.94 ppm (n = 45). Trench samples range from 904.23 to 2645.85 ppm, with an average of 1775.28 ppm (n = 26), while core samples range from 333.63 ppm to 3397.12 ppm, averaging 1423.71 ppm (n = 112).

In migmatite gneiss, bedrock samples show total REE concentrations ranging from 194.10 to 2853.19 ppm, with an average of 1376.46 ppm (n = 59). Trench samples range from 130.82 to 1748.22 ppm, averaging 956.45 ppm (n = 74), whereas core samples range from 411.51 to 3081.88 ppm, with an average of 1235.06 ppm (n = 98).

The amphibolite core samples contain sulfide mineralization, represented by Pyrite and Chalcopyrite, along with evident Albitization, suggesting hydrothermal alteration and potential mineralizing fluid activity.

Based on drill core analytical data, the REE resource was estimated. At a cut-off grade of 1000 ppm, the total Rare Earth Element (REE) resource estimated from all four boreholes is 39,340 tonnes,

whereas at a cut-off grade of 1200 ppm, the estimated REE resource is 37,098 tonnes. The identified anomaly zones are described below.

In Syenite

i) Zone I: The anomaly extends for approximately 200 m with an average width of 100 m in the northwestern part.
ii) Zone II: The anomaly measures about 170 m × 50 m and is located in the eastern-central part.
iii) Zone III: The anomaly extends for approximately 160 m with an average width of 100 m in the north-central part.

In Migmatite Gneiss

i) Zone I: The main anomaly extends for approximately 1 km with an average width of 300 m in the central part, trending towards the northeastern side.
ii) Zone II: The anomaly extends for about 200 m with an average width of 150 m in the central-eastern part.
iii) Zone III: The anomaly measures approximately 100 m × 80 m and is located in the western part.
iv) Zone IV: The anomaly measures about 100 m × 200 m and occurs in the northern part.
v) Zone V: The anomaly extends for approximately 140 m with an average width of 50 m in the northwestern part.
vi) Zone VI: The anomaly measures approximately 70 m × 70 m and is located in the northwestern part.

The investigation successfully achieved all assigned targets, integrating surface and sub-surface exploration techniques. Syenite and migmatite gneiss serve as the principal hosts for mineralization. Hence, it is recommended that the detailed mapping in higher level of investigation G2 stage of exploration may be taken up. Considering the wide borehole spacing and limited number of drill holes, the estimated resource is categorized as Inferred Resource. Based on these encouraging results, it is recommended to upgrade the project to a G-2 level of exploration.

1.2 कार्यकारी सारांश

दुर्लभ मृदा तत्वों (Rare Earth Elements - REE) के खनिजीकरण पर G3-स्तरीय अन्वेषण, जिसका शीर्षक "राजस्थान के भीलवाड़ा जिले के बोराना ब्लॉक में REE एवं संबद्ध खनिजों हेतु प्रारंभिक अन्वेषण (G3-Stage)" है, स्वीकृति पत्र F.No.23/464/2024–NMEDT/131 दिनांक 10 जून 2024 तथा संशोधित कार्यालय ज्ञापन F.No.23/464/2024–NMEDT/881 दिनांक 21 फरवरी 2025 के अंतर्गत संपादित किया गया। यह कार्य GSI द्वारा वर्ष 2018-19 के G4 स्तर के पुनर्संधान (Reconnaissance Exploration) के दौरान प्रतिवेदित REE विसंगतियों (Anomalies) के अनुवर्ती अन्वेषण के रूप में किया गया।

बोराना परियोजना क्षेत्र Survey of India के टोपोशीट 45K/03 में स्थित है तथा इसका क्षेत्रफल लगभग 1.14 वर्ग किलोमीटर है। यह क्षेत्र 25°26'08" N से 25°25'33" N अक्षांश तथा 74°07'44" E से 74°06'47" E देशांतर के मध्य स्थित है। जहाँ आवश्यक था, वहाँ WGS-1984 निर्देशांक संदर्भ प्रणाली के साथ UTM प्रक्षेपण का उपयोग किया गया।

भूवैज्ञानिक दृष्टि से यह क्षेत्र भीलवाड़ा सुपरग्रुप के मंगलवार कॉम्प्लेक्स का भाग है। यह भूभाग मुख्यतः मेसोआर्कियन (Mesoarchean) आधारशिला से निर्मित है, जिसमें ग्रेनाइटिक ग्नाइस प्रमुख है तथा इसके भीतर एम्फिबोलाइट, मेटासेडिमेंट तथा ग्रेनिटोइड अंतःक्षेप पाए जाते हैं, जिन्हें सामूहिक रूप से बैंडेड ग्नाइसिक कॉम्प्लेक्स (BGC) कहा जाता है । बोराना ब्लॉक में मानचित्रित प्रमुख शैल इकाइयों में साइनाइट, मिग्माटाइट ग्नाइस, एम्फिबोलाइट तथा पेग्माटाइट सम्मिलित हैं।

परियोजना क्षेत्र के 1.14 वर्ग किलोमीटर में 1:2,000 पैमाने पर विस्तृत भूवैज्ञानिक मानचित्रण किया गया, जिसके दौरान आधारशिला (Bedrock) के नमूने एकत्रित किए गए। संकलित 108 Bedrock Samples (BRS) में कुल REE (TREE) का मान 5.04 ppm से 2971.05 ppm के मध्य पाया गया, जिसका औसत 1416.68 ppm है।

कुल 5 ट्रेंच, प्रत्येक 20 मीटर लंबी, 1 मीटर चौड़ी एवं 1 मीटर गहरी, खोदी गईं, जिससे कुल 100 घन मीटर ट्रेंचिंग कार्य संपन्न हुआ। ट्रेंचिंग का उद्देश्य संभावित खनिजीकृत इकाइयों के उपसतही स्ट्राइक विस्तार एवं गहराई में निरंतरता का आकलन करना तथा प्रतिनिधिक नमूनों का संग्रह करना था। संकलित 100 ट्रेंच नमूनों में TREE का मान 130.82 ppm से 2645.85 ppm के मध्य पाया गया, जिसका औसत 1163.98 ppm है।

ड्रिलिंग कार्य के अंतर्गत 45° झुकाव पर चार तिर्यक बोरहोल (BH-01 से BH-04) किए गए, जिनकी कुल ड्रिलिंग लंबाई 474.64 मीटर रही। बोरहोलों के मध्य दूरी 200 मीटर रखी गई। अध्ययन क्षेत्र के विभिन्न बोरहोलों में TREE का मान 30.58 ppm से 3081.88 ppm के मध्य पाया गया, जिसका औसत 1267.29 ppm है।

भू-रासायनिक वर्गीकरण एवं विभेदन आरेखों का उपयोग विभिन्न शैल प्रकारों के विभेदन के समर्थन में किया गया। एम्फिबोलाइट नमूनों को मैफिक क्षेत्र (Mafic Field) में स्थित पाया गया, जो कम सिलिका युक्त मैफिक प्रकृति को दर्शाता है, जबकि फेल्सिक शैलें (पेग्माटाइट, साइनाइट एवं मिग्माटाइट ग्नाइस) ग्रेनाइट–ग्रैनोडियोराइट क्षेत्र में स्थित पाई गईं, जो उनकी उच्च सिलिका युक्त फेल्सिक प्रकृति को प्रतिबिंबित करती हैं।

बोराना ब्लॉक में दुर्लभ मृदा तत्वों (REE) का उल्लेखनीय खनिजीकरण पाया गया है, जो मुख्यतः साइनाइट/क्षारीय साइनाइट (Alkali Syenite) तथा मिग्माटाइट ग्नाइस में विकसित है। इन शैलों में साइनाइट/क्षारीय साइनाइट में तुलनात्मक रूप से अधिक REE संवर्धन पाया गया।

साइनाइट/क्षारीय साइनाइट में आधारशिला नमूनों में TREE का मान 778.08 ppm से 2742.54 ppm तक पाया गया, जिसका औसत 1522.94 ppm (n = 45) है। ट्रेंच नमूनों में TREE का मान 904.23 ppm से 2645.85 ppm तक पाया गया, जिसका औसत 1775.28 ppm (n = 26) है, जबकि ड्रिल कोर नमूनों में TREE का मान 333.63 ppm से 3397.12 ppm तक पाया गया, जिसका औसत 1423.71 ppm (n = 112) है।

मिग्माटाइट ग्नाइस में आधारशिला नमूनों में कुल REE का मान 194.10 ppm से 2853.19 ppm तक पाया गया, जिसका औसत 1376.46 ppm (n = 59) है। ट्रेंच नमूनों में TREE का मान 130.82 ppm से 1748.22 ppm तक पाया गया, जिसका औसत 956.45 ppm (n = 74) है, जबकि ड्रिल कोर नमूनों में TREE का मान 411.51 ppm से 3081.88 ppm तक पाया गया, जिसका औसत 1235.06 ppm (n = 98) है।

एम्फिबोलाइट के ड्रिल कोर नमूनों में पाइराइट (Pyrite) एवं चैल्कोपाइराइट (Chalcopyrite) के रूप में सल्फाइड खनिजीकरण पाया गया है। साथ ही स्पष्ट अल्बिटीकरण (Albitization) भी देखा गया, जो हाइड्रोथर्मल परिवर्तन (Hydrothermal Alteration) तथा संभावित खनिजीकृत द्रवों (Mineralizing Fluids) की सक्रियता का संकेत देता है।

ड्रिल कोर के रासायनिक विश्लेषण के आधार पर REE संसाधन का आकलन किया गया। 1000 ppm कट-ऑफ ग्रेड पर चारों बोरहोलों से अनुमानित कुल REE संसाधन 39,340 टन है, जबकि 1200 ppm कट-ऑफ ग्रेड पर अनुमानित REE संसाधन 37,098 टन है। पहचाने गए विसंगति (Anomaly) क्षेत्र निम्नानुसार हैं।

साइनाइट में

i) ज़ोन-I: विसंगति उत्तर-पश्चिमी भाग में लगभग 200 मीटर तक फैली हुई है तथा इसकी औसत चौड़ाई 100 मीटर है।

ii) ज़ोन-II: विसंगति का विस्तार लगभग 170 मीटर × 50 मीटर है तथा यह पूर्वी-मध्य भाग में स्थित है।

iii) ज़ोन-III: विसंगति उत्तर-मध्य भाग में लगभग 160 मीटर तक फैली हुई है तथा इसकी औसत चौड़ाई 100 मीटर है।

मिग्माटाइट ग्नाइस में

i) ज़ोन-I: मुख्य विसंगति केंद्रीय भाग से उत्तर-पूर्व दिशा की ओर लगभग 1 किलोमीटर तक फैली हुई है तथा इसकी औसत चौड़ाई 300 मीटर है।
ii) ज़ोन-II: विसंगति केंद्रीय-पूर्वी भाग में लगभग 200 मीटर तक फैली हुई है तथा इसकी औसत चौड़ाई 150 मीटर है।
iii) ज़ोन-III: विसंगति का विस्तार लगभग 100 मीटर × 80 मीटर है तथा यह पश्चिमी भाग में स्थित है।
iv) ज़ोन-IV: विसंगति लगभग 100 मीटर × 200 मीटर क्षेत्र में उत्तरी भाग में स्थित है।
v) ज़ोन-V: विसंगति उत्तर-पश्चिमी भाग में लगभग 140 मीटर तक फैली हुई है तथा इसकी औसत चौड़ाई 50 मीटर है।
vi) ज़ोन-VI: विसंगति का विस्तार लगभग 70 मीटर × 70 मीटर है तथा यह उत्तर-पश्चिमी भाग में स्थित है।

इस अन्वेषण में सतही एवं उपसतही दोनों प्रकार की अन्वेषण तकनीकों का समन्वित उपयोग करते हुए निर्धारित सभी उद्देश्यों की सफलतापूर्वक प्राप्ति की गई। साइनाइट एवं मिग्माटाइट ग्नाइस इस क्षेत्र में खनिजीकरण की प्रमुख आश्रयी शैलें (Host Rocks) हैं। बोरहोलों के मध्य अपेक्षाकृत अधिक दूरी तथा सीमित संख्या में ड्रिल होलों को ध्यान में रखते हुए अनुमानित संसाधन को अनुमानित संसाधन (Inferred Resource) श्रेणी में वर्गीकृत किया गया है।

इन उत्साहवर्धक परिणामों के आधार पर परियोजना को G-2 स्तर के अन्वेषण में उन्नत किए जाने की अनुशंसा की जाती है।

CHAPTER 2 - DETAILS OF THE QUALIFIED PERSON(S) / EXPLORATION AGENCY

2.1 Details of the Exploration Agency

(a) Name: GeoExpOre Pvt. Ltd.

(b) Address: #45(S), 2nd A Main Road, 2nd Cross, Chandra Layout, Bengaluru, 560040

(c) Contact Mobile No: 9591167745

(d) E-Mail id: info@geoexpore.com

(e) Qualification: NA

(f) Experience: NA

(g) Affiliation to any organization/ company, if yes, specify the name of the organization or company: NA

2.2 Details of qualification and experience of persons associated with various aspects of exploration assessment of resources and reserves

As per the requirement based on the quantum of work assigned by NMEDT, GeoExpOre Pvt. Ltd. had assigned a Project Coordinator, Senior Geologist, Geologist, Laborers (for sampling), etc., to complete the project.

Table 2.1: Personnel involved

Sr. No.	Name	Qualification and Experience	Designation	Main Contributions
1	Ms. Mansi Kesarwani* (mansi@geoexpore.com)	M.Sc., MTech with 1 year of experience	Assistant Manager-Geoscience Strategy	Interpretation of data, map preparation and report writing
2	Dr. Abrar Ahmed*	M.Sc., PhD with 8	Senior	Core drilling, selection of

	(abrar@geoexpore.com)	years of experience	Geologist	samples for chemical analysis, and interpretation of data, map preparation, and report writing
3	Mr. Mohammad Muslemeen (mohammad@geoexpore.com)	M.Sc with 15 years of experience	Senior Geologist	Geological mapping, topographic survey, core drilling, selection of samples for chemical analysis, core drilling, interpretation of data, map preparation, and report writing
4	Mr. Manoj Kumar (manoj@geoexpore.com)	M.Sc , M.Tech with 8 years of experience	Senior Geologist	Geological mapping, topographic survey, core drilling, selection of samples for chemical analysis, and interpretation of data, map preparation,
5	Dr. R. Chandrasekaran (chandru@geoexpore.com)	M.Sc , Ph.D with 8 years of experience	Project Coordinator	Geological mapping, topographic survey, core drilling, selection of samples for chemical analysis.
6	Mr. Sandeep Hamilton (sandeep@geoexpore.com)	M.Sc (35 years of experience). Formerly Additional Director , Atomic Mineral Directorate (AMD)	Project Coordinator	Guidance throughout the field season, sample processing, analysis and report writing
				*yet to be assessed by NABET
7	Mr. Channamallikarjun B. Patil	M.Tech with 25 years of experience	Project Director	Supervision and guidance in geological mapping,

	(cm@geoexpore.com)			topographic survey, core drilling, selection of samples for chemical analysis, and interpretation of data, map preparation and report writing.
8	Dr. Yerriswamy Pateel (ypateel@geoexpore.com)	M.Tech, Ph. D with 28years of experience	Project Director	Supervision and guidance in geological mapping, topographic survey, core drilling, selection of samples for chemical analysis, and interpretation of data, map preparation, and report writing.

CHAPTER 3 – TITLE AND OWNERSHIP

Title of the Report

Preliminary Exploration (G3) for REE and associated minerals around Borana Block, Bhilwara District, Rajasthan

3.1 Name of the explorer/ Mining or prospecting rights holder

GeoExpOre Private Limited, Bangalore is a notified private exploration agency accredited by QCI-NABET (Govt. of India) based in Bengaluru, Karnataka.

Address: #45(S), 2nd A Main Road, 2nd Cross, Chandra Layout, Bengaluru, 560040

Telephone No: 9591167745

E-Mail i.d.: info@geoexpore.com

3.2 Details of period of prospecting/mineral right if any:

Nil (Exploration carried out under NMEDT sanction; no prospecting/mineral right granted). Chemical analysis of the collected samples was outsourced to Shiva Analyticals (India) Pvt. Ltd., an NABL-accredited laboratory, for analysis as per the approved Scope of Work.

In case of a licence or lease: NA.

CHAPTER 4 - DETAILS OF THE AREA UNDER STUDY

4.1 Village, District, State

The Borana village is situated in Raipur Tehsil, Bhilwara District, of Rajasthan State, India. It lies within the Ajmer Division. The main villages included in the study area are Borana, Borana Ka Khera and Gujjaron Ka Khera along with parts of Raipur village.

4.2 Survey of India Toposheet No. & Differential Global Positioning System (DGPS) coordinates of all corner points of the area and borehole points in latitude and longitude (Degree Minutes Second) format WGS-84 Datum

The area under investigation forms a part of Survey of India Toposheet No. 45 K/03. The area is mostly occupied by Government and by Private land (Agricultural).

Differential Global Positioning System (DGPS) survey was carried out in Borana Block to establish accurate ground control for the proposed drilling programme. A total of five DGPS points were surveyed and fixed, including one base point and four borehole fixation points. The base point was first established and observed for a sufficient duration to obtain highly accurate corrected coordinates, which served as the primary reference for the entire survey. Using this base station, four additional points corresponding to the planned borehole locations were surveyed.

The Differential Global Positioning System (DGPS) coordinates of all corner points of the area and borehole points in latitude and longitude (Degree Minutes Second) format WGS-84 Datum are as follows:

Table 4.1: Boundary Co-ordinates of the Borana block

Points	Latitude	Longitude
A	25°26'00"N	74°06'47"E
B	25°26'08"N	74°07'05"E
C	25°26'00"N	74°07'16"E
D	25°25'54"N	74°07'08"E
E	25°25'51"N	74°07'11"E
F	25°25'57"N	74°07'22"E
G	25°25'57"N	74°07'44"E
H	25°25'33"N	74°07'44"E
I	25°25'33"N	74°06'56"E
J	25°25'51"N	74°06'56"E

Table 4.2: Borehole location details with total depth

Point name	code	Original Latitude	Original Longitude	Original Altitude	Antenna Height (m)	Northing (mts)	Easting (mts)	Elevation (m)
1	BH-01	25°25'53.9427"	74°07'32.6900"	507.092	1.8	2813033.252	412087.949	554.233
2	BH-02	25°25'51.0366"	74°07'26.2560"	513.358	1.8	2812945.034	411907.664	560.497
3	BH-03	25°25'44.5360"	74°07'22.7573"	507.692	1.8	2812745.706	411808.588	554.831
4	BH-04	25°25'40.5262"	74°07'18.0708"	504.521	1.8	2812623.215	411676.861	551.66
5	TBM-1	25°25'54.1206"	74°07'33.4274"	508.389	1.8	2813038.591	412108.584	555.53

4.3 Cadastral details of the area with land use, area under forest with type of forest. In case the cadastral details are not available an indicative data of breakup of government, private and forest land

The location map of Borana block has been prepared and presented in Fig 4.1. The block covers an area of 1.14 sq.km. No forest area is present. Details of breakup of government, private and forest land are not available.

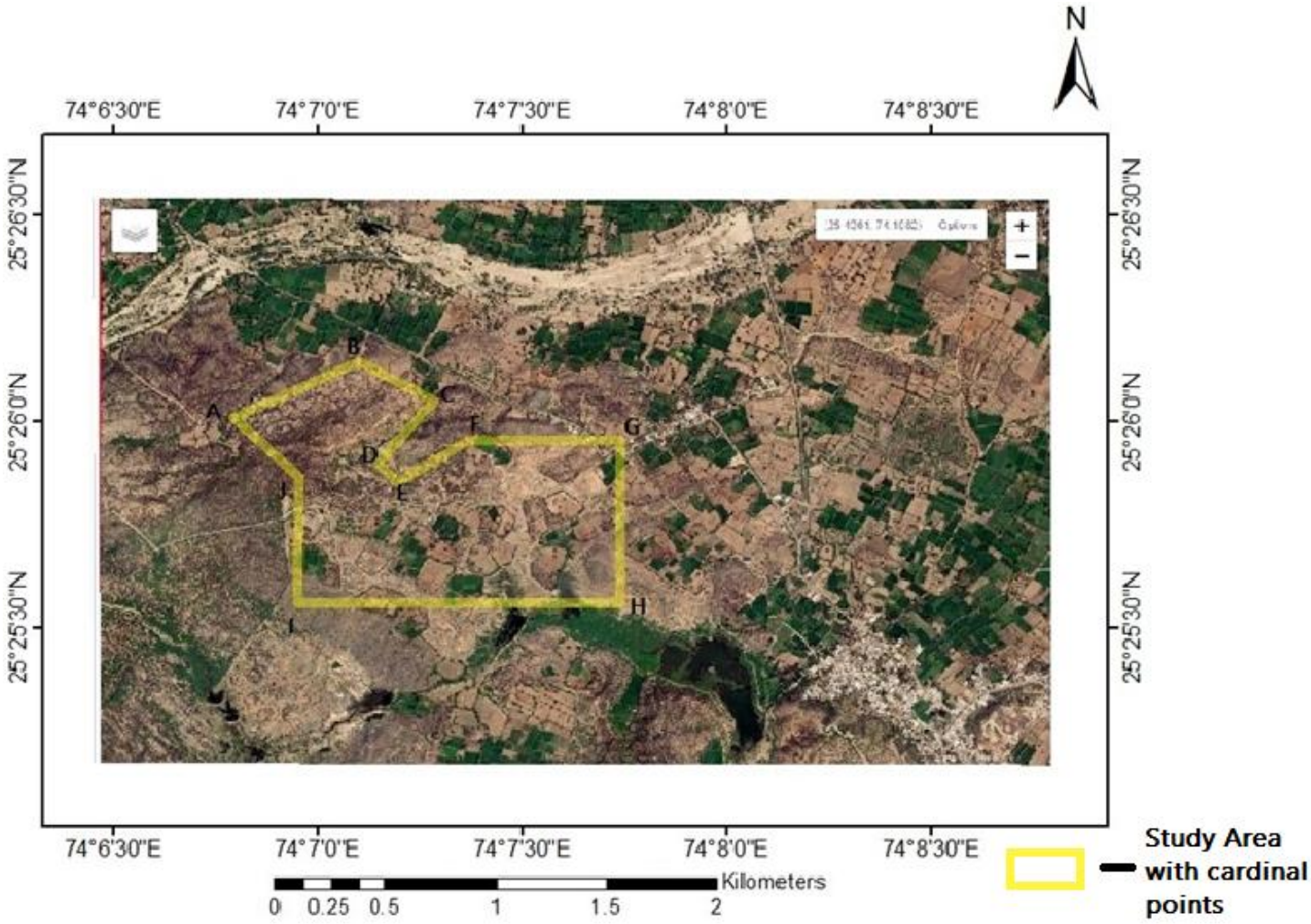

Fig 4.1 Location map of Borana block

4.4 Mineral(s) under investigation or granted under licence or lease

Mineral under investigation is REE.

CHAPTER 5 – PHYSIOGRAPHY AND ENVIRONMENT

5.1 Relief of the area with minimum and maximum elevation, drainage pattern, natural water courses, reservoirs, etc.

The highest elevation in the Borana Block is about 568 m above mean sea level (MSL), and the lowest elevation is about 548m. Relatively higher elevations are observed in the western part of the block. Based on a 1meter contour interval, both 2D and 3D elevation maps were generated to depict the topographic variation of the area. These are presented in Fig.5.1.

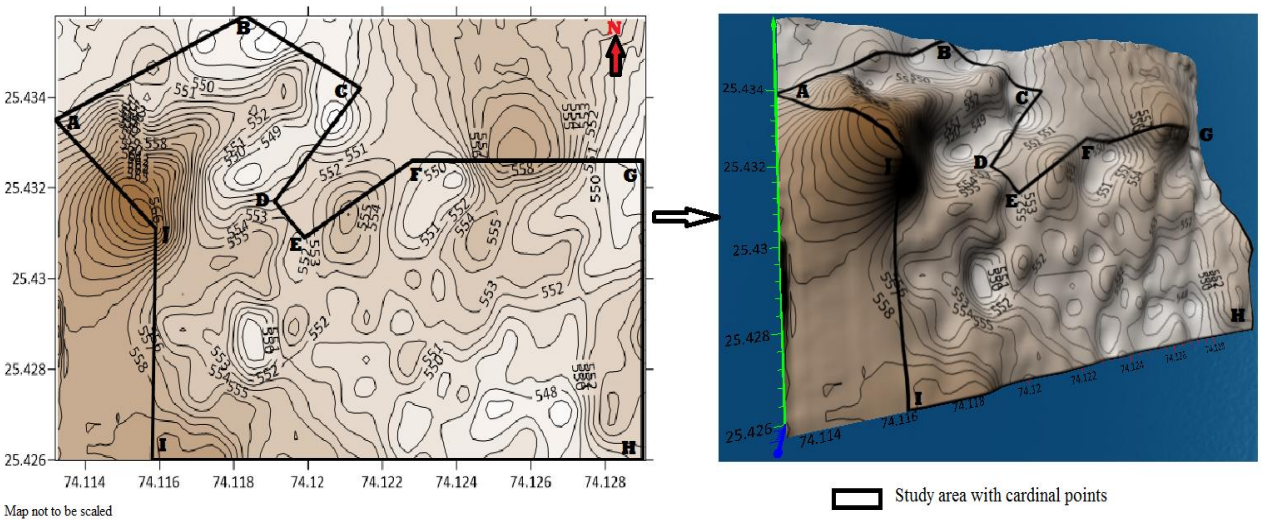

Fig 5.1 2D contour map and corresponding 3D elevation model of the Borana Block showing topographic variation and cardinal points with contour interval: 1m (source: Google earth pro).

Most of the proposed block is covered by private agricultural land. The area generally exhibits flat topography. The area has gentle undulating topography towards northwest regions with isolated ridges. It exhibits sub-dendritic to dendritic drainage patterns. Most of the Borana blocks have low dissected denudational hills and valleys. The geomorphological map of the Borana block is as shown

in Fig.5.2.

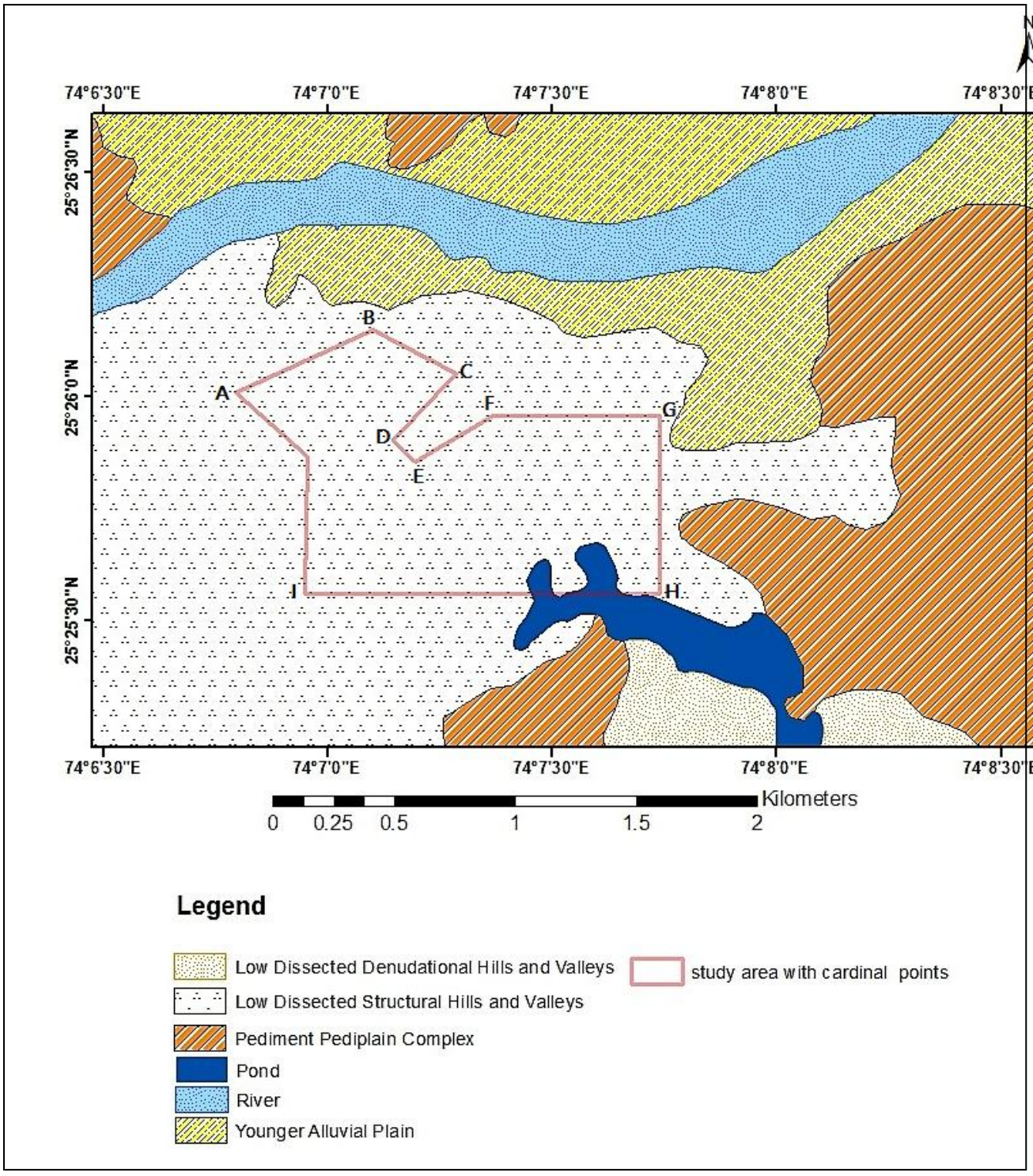

Fig 5.2 Geomorphological map of the Borana block (source: NGDR website)

5.2 Roads, railway track, electric transmission line, telephone line, etc., passing through the area or nearby

The investigated area is located at 75 kms North-West from the district headquarters Bhilwara and is connected by Pali – Bhilwara road. The block is located 6.40 km NW of Raipur town which is a small town and approximately at about 4 km south of Borana village. The area is covered under Survey of India Toposheet No. 45 K/03. Major villages are connected by metalled/unmetalled cart tracks. The nearest railway station is Bhilwara located at about 75 km towards east. Maharana Pratap Airport is the nearest Airport which is located about 143 km from the block.

5.3 Host population (local tribes), Human settlements within and nearby the area

Borana is a small rural village located in Rajasthan. The population of Borana and surrounding villages is around 1,500 to 2,000 people (as per 2011 Census) consisting mainly of local farming communities. The settlements are scattered with agriculture being the principal occupation. The density of population in the area is low to moderate typical of semi-arid regions of central Rajasthan.

5.4 Socio Demographic profile of the area and nearby

According to Census 2011, Borana has a population of 4,616 persons living in about 950 households. The village comprises 2,290 males and 2,326 females, with a sex ratio of 1,016 females per 1,000 males. Children in the age group of 0–6 years account for about 16% of the total population.

The overall literacy rate of the village is 58.49%. Male literacy is 73.51%, while female literacy is 44.16%. Government primary and secondary schools are available in and around the village. Higher education facilities are available at Raipur and Bhilwara.

5.5 Historical sites and archaeological monuments, places of worship, public utilities etc. within or near by

The Borana area lies near to Ajmer which is known for its rich historical and cultural background. While no major archaeological monuments are reported within the immediate vicinity of Borana village, several important historical and religious sites are located within a short distance. The nearby city of Ajmer (about 60–70 km away) is historically significant, housing the Ajmer Sharif Dargah, Taragarh Fort and Ana Sagar Lake, all which date back to the medieval period. Pushkar located about 70 km southeast of Borana is an ancient pilgrimage town famous for the Brahma Temple and the Pushkar Lake. The Beawar town about 25–30 km from Borana developed during the British period and serves as a regional commercial hub with colonial-era structures. Scattered old temples and village shrines can also be observed near Borana and adjoining villages indicating the area's long-standing human settlement and cultural continuity.

5.6 Forests, sanctuaries, national park and wild life sanctuaries; grazing land and gochar land within or near by the area with distance from periphery of the area explored.

No forests, sanctuaries, national park and wildlife sanctuaries; grazing land and gochar land within or near by the area with distance from periphery of the area explored exists.

5.7 Flora and Fauna within and nearby

The area's wildness is semi-arid to arid climatic conditions which results to very sparse vegetation. No exploitable forest is present in the area. The common vegetation mainly Dhok (Augisus pendula), Kher (Accaccacatochu), Thor, Cactus, Neem etc., are dominant in the block area. Rabi and Kharif seasons are practiced in the block area. Wheat, bajra, jowar and methi are the main crops grown and produced in the area. Regarding the population of wild animals, it is very sparce in the area. Chinkaras

are frequently seen in the protected forest of Chatawanmata area which falls northwest from the block. The animals found inside the borana block are hares, nilgai, jackals and foxes are common in the area.

5.8 Water bodies such as river, nala, stream, reservoir, etc., within or nearby

No major water body exists \ passes through the block but a Kothari river passes 2-3 km in the northern direction from the block flowing eastwards.

5.9 Climatic conditions:

(a) Temperature (annual) min 5°C max 46°C Avg 25-26

(b) Rain fall (annual) min 450mm max 850 mm Avg 640-650 mm

(c) Humidity (annual) min 25% max 85% Avg 55%

The area experiences dry weather with high temperature in the month of June and low in the month of December with the range of 45 degree maximum and 5 degrees minimum with scanty rainfall between July to September. The area witnesses' hot summer from March to June followed by a southwestern monsoon from July to September and a bracing winter from December to February. The annual average rainfall of the area is 682 mm.

5.10 Any other physiographic, social and environmental factor having potential to affect the viability of the project and assessment of resources and reserves.

No other physiographic, social and environmental factors exist having potential to affect the viability of the project and assessment of resources and reserves.

CHAPTER 6 – INFRASTRUCTURE

6.1 Local Infrastructure Details

The main settlements within the investigated block are Gujaro ka kheda towards northeast side. The area is well-connected by road networks to nearby towns and major highways. Borana village can be approached from Beawar or Ajmer via metalled roads. The nearest railway station is Bhilwara located at about 75 km towards east. Maharana Pratap Airport is the nearest Airport which is located about 143 km from the block. Groundwater is the primary source for drinking and domestic use, obtained through wells and borewells. Primary health centers and schools are available in nearby villages like Borana and surrounding hamlets.

CHAPTER 7 – GEOLOGY

7.1 Brief regional geology of the area outlining the broad geological, stratigraphical and structural framework.

The state of Rajasthan comprises a wide variety of litho-assemblages that include the Archean basement complex, Proterozoic Aravalli and Delhi fold belts and late Proterozoic Malani, Jalore and Siwana igneous suites. It is believed that the Aravalli and Delhi basins within the BGC (Basement Gneissic Complex) rocks were formed by ensialic rifting in two different periods. The rifting generated oceanic crust, and sediments were deposited in intra-continental rift and basin systems, resulting in fold belts (S Roy et al. 1992). This Meso- to Neo-archaean domain, which is characteristic of the southcentral cratonic region of Rajasthan, is traditionally known as the Banded Gneissic Complex (Gupta, 1934; Heron, 1953).

According to Bhattacharya and Kapoor (1988), the Sandmata Complex in the area is represented by augen gneiss and quartz-feldspathic gneiss with bands of enderbite, garnet-sillimanite gneiss and pyroxene granulite. Delhi Group of rocks delineating the western boundary of the Sandmata Complex is represented by quartzite, dolomite, mica schist, migmatites, meta greywacke, 'ignimbrite' and meta-basics. They are intruded by ultra-basics, pink granite and pegmatite. The Bhilwara Supergroup (Heron, 1953) includes the Mangalwar and Sandmata Complex. The present work was carried out in parts of the Mangalwar Complex of the Bhilwara Supergroup (Gupta et al., 1980). The stratigraphic succession proposed by Neogi and Raza (2017) is shown in Table 7.1.

Structurally, the area has undergone at least three phases of deformation. The regional gneissosity and schistosity prevailing in the area represent the earliest deformation phase (D1) preserved in migmatite gneiss and schist, respectively. The second phase of deformation is represented by mesoscopic tight to isoclinal folds. The tight to isoclinal folds are observed both in migmatite and migmatite gneiss in the area. Similarly, the third phase of deformation (D3) is represented by kinking observed in amphibolite, and warps observed in migmatite gneiss represent the third phase of deformation. The Regional geological map of the Mangalwar Complex is as shown on Fig.7.1.

Table 7.1: Regional Lithotectonic stratigraphic succession of the area

(After Neogi and Raza, 2017)

<table>
<tr><td rowspan="3">Mangalwar Complex</td><td></td><td>Pegmatite
Monzonite/Syenite/Alkali-feldspar syenite
Amphibolite dyke
Gabbro</td><td rowspan="2">Leucocratic granite
Porphyritic augen gneiss (granodiorite)
Porphyritic augen gneiss (Granite)</td></tr>
<tr><td rowspan="2">Ran Igneous Complex</td><td>Anjana granite</td></tr>
<tr><td colspan="2">Amet Granite</td></tr>
<tr><td>Sawadri Group</td><td colspan="2">Migmatite intermixed with augen-gniess
Migmatite gneiss Quartzite, Chert
Mica schist and migmatite
Amphibolite/Metabasic rock. Ultrabasic rock</td></tr>
<tr><td colspan="4">Tectonic contact</td></tr>
<tr><td colspan="2">Sandmata Complex</td><td colspan="2">Norite, Gabbro-gneiss
Garnet-cordierite-sillimanite Gneiss
Two-pyroxene granulite, Garnet- sillimanite gneiss with leptynite bands</td></tr>
</table>

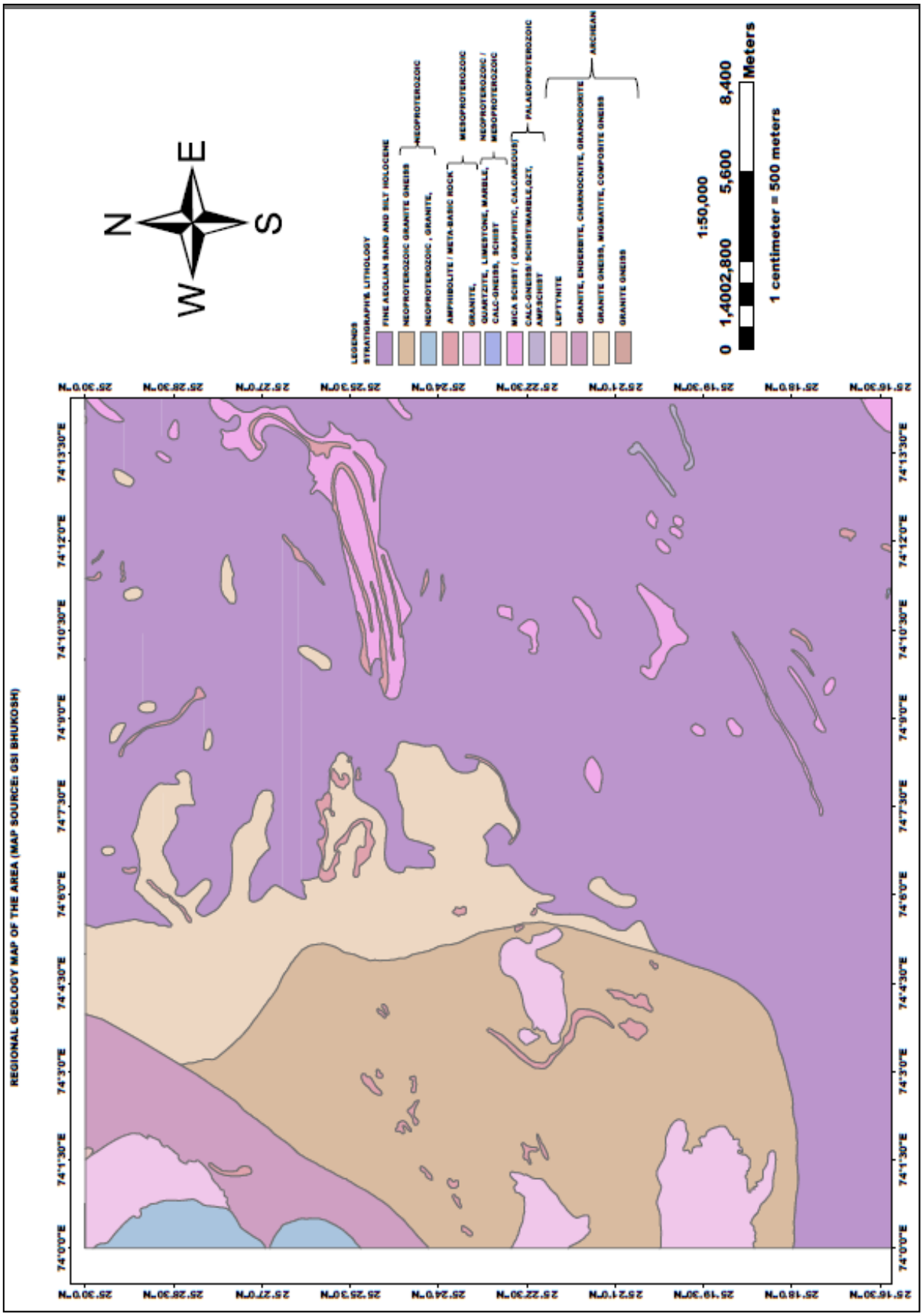

Fig 7.1 Regional geology map of the Mangalwar Complex

7.2 Local geological setting detailing the common rock types, controls of mineralization, details of old workings if any, surface exposures, etc., of the area under study also of adjoining nearby areas, if the information is likely to have an impact on the area under study.

The local area comprises the Archaean basement rocks belonging to the Mangalwar Complex of the Bhilwara Supergroup (Gupta et al., 1997). The various litho-units mapped in this area include amphibolites, migmatite gneiss and syenites which are intruded by the pegmatites. These show a complex structural history characterized by progressive deformation. Various planar and linear structures related to the S2 deformation among the three different phases of folding deformation are well preserved in the area. The overall trend of the structural fabric in the area is NNE-SSW. The 1:2,000 scale geological map was prepared which is shown in Plate-2. Table 7.2 shows the lithostratigraphy of the block based on the field relationship as proposed by the GSI (FSP: 2018-19).

Table 7.2: Lithostratigraphy of the proposed block (After GSI FSP:2018-19)

Mangalwar Complex		Pegmatite Syenite/alkai feldspar syenite
	Ran Igneous Complex	Ametgranite
	Sawadri Group	Migmatite Gneiss Quartzite Mica Schist and migmatite Amphibolite

7.2.1 Outcrop mapping

During large scale mapping (LSM) outcrop mapping was conducted in the study area. The area generally exhibits flat topography. The area has gentle undulating topography towards northwest regions with isolated ridges. The highest elevation in the area is 568 m above mean sea level. Outcrop map of the

investigated area, Borana block is given in Plate-1.

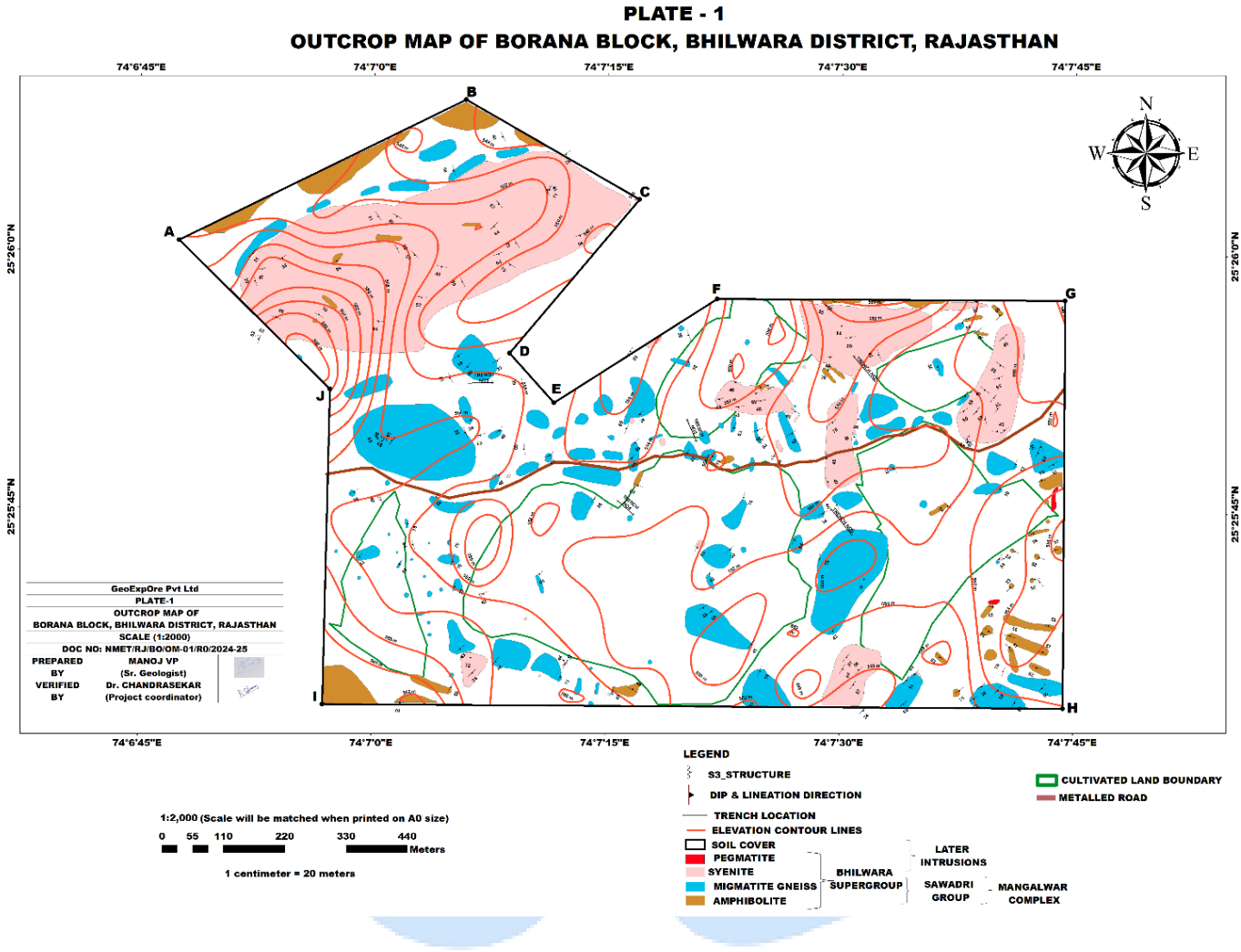

7.2.2 Geological Mapping

To achieve the goals of the preliminary exploration for this project GeoExpOre Pvt. Ltd conducted detailed geological mapping and structural mapping of approximately 1.14 square kilometers on a 1:2,000 scale started from 11.07.2024 to 31.08.2024. This study was executed with the highest precision, ensuring meticulous accuracy. The mapped area is represented by major rock types such as migmatite gneiss and the intrusive syenite/alkali syenites. The other minor rock types encountered during detailed mapping are small intrusions of amphibolite, quartz veins and pegmatite. The study area geographically coordinates: A) 25.4333N, 74.1130E B) 25.4355N, 74.1180E C) 25.4333N, 74.1211E D) 25.4316N, 74.1188E E) 25.4308N, 74.1197E F) 25.4325N, 74.1227E G) 25.4325N, 74.1288E H) 25.4258N, 74.1288E I)

25.4258N, 74.1155E J) 25.4308N, 74.1155E. Geological map of the investigated area is shown in Plate-2.

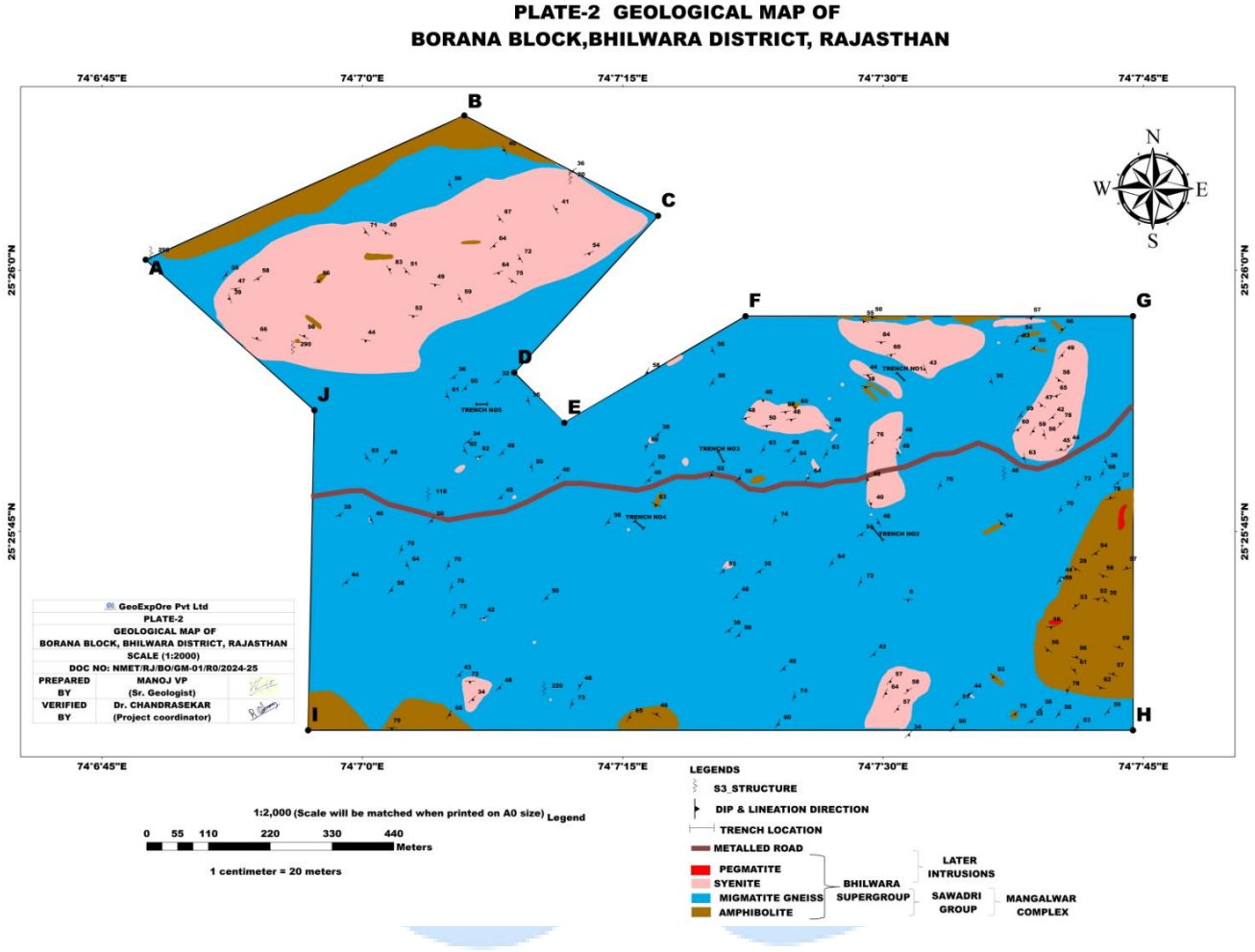

7.2.3 Description of Rock Types

7.2.3.1 Migmatite Gneiss

Migmatite gneiss covers most of the area investigated. Migmatites are formed by amalgamating the pre-existing gneisses with later intruded magma and consist of two main parts: the light-colored leucosome, consisting of quartz and feldspars, and the dark-colored paleosome, consisting of biotite, amphiboles, and at certain places, pyroxenes. Garnet may also be present as an accessory mineral. At times, the mafic minerals cumulate and occur within migmatites. The migmatite gneiss in the area near Borana village consists of dispersed grains of allanite with pleochroic haloes. In the central part of the migmatite gneiss several thin to thick epidote veins are found as fracture filling. Field photographs of Migmatite gneiss are shown on Fig.7.2.

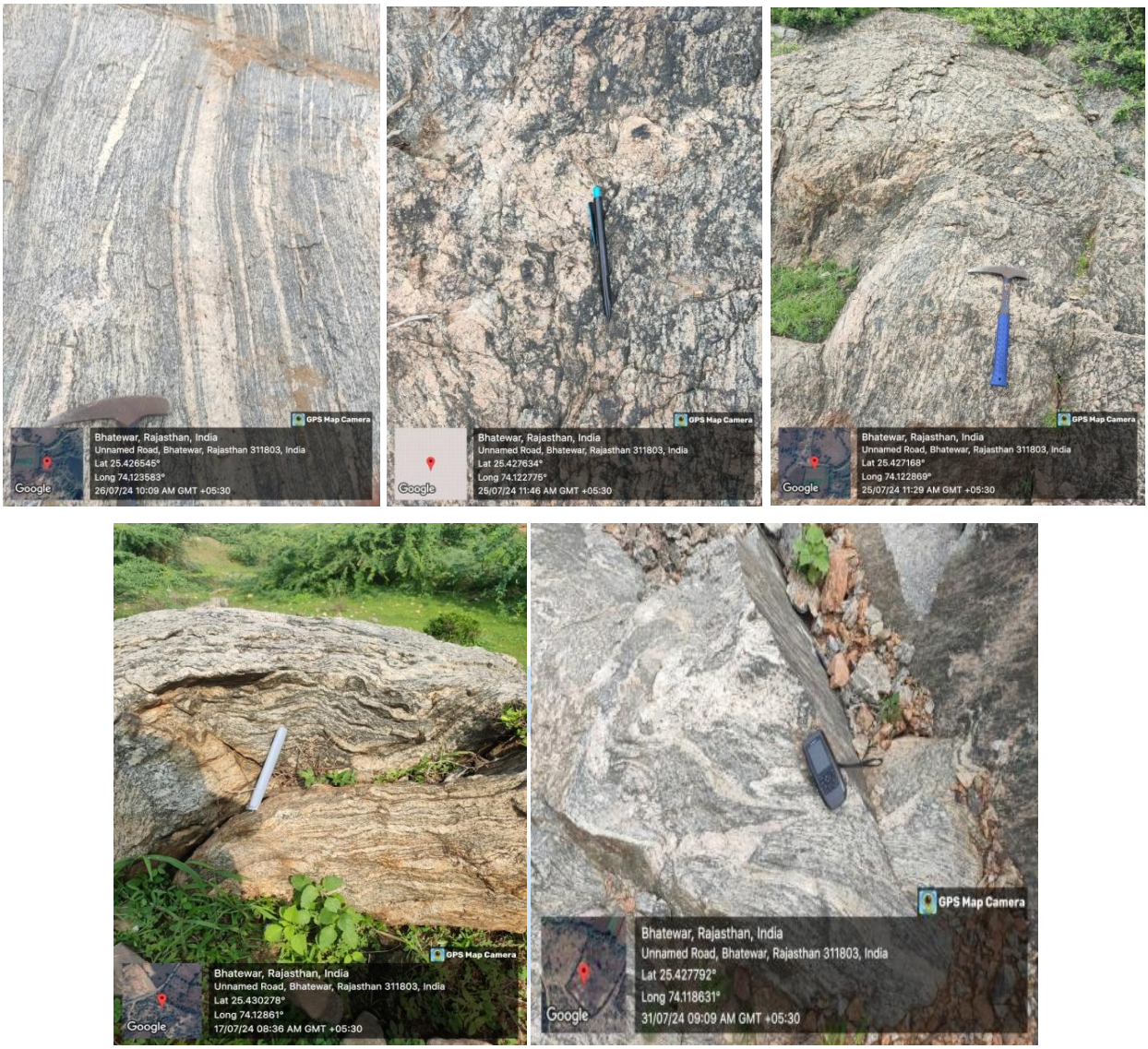

Fig 7.2 Field photographs of Migmatite Gneiss

7.2.3.2 Syenite/alkali syenite

The syenites in the area are the foliated younger intrusive bodies extending in the EW direction. Mineralogically, they are composed of alkali feldspar with small amounts of plagioclase and very limited amounts of quartz. The syenite/ alkali feldspar syenite is also marked with numerous crisscross epidote veins of varying size and consist of dispersed allanite grains. These allanite grains are dark in color, exhibit conchoidal fracture and expose pleochroic haloes developed due to the radiation damage in the immediately adjacent minerals. These syenite/alkali syenite were well exposed and in the southern parts of the Borana village. Field photographs of syenite are shown in Fig.7.3.

Fig 7.3 Field photographs of Syenite

7.2.3.3 Amphibolite

The Amphibolite in this area is found within the migmatite and syenite rocks which are dark green in color. It is hard and well foliated with fine to coarse grained and consists of hornblende and plagioclase predominantly. This amphibolite extends along NE-SW direction. These amphibolite bodies show a strong foliation and are banded parallel to the intrusive wall. In the southwestern part of the area shows a banding marked by quartz and epidote rich layers changing in their appearance. Field photographs of Amphibolite are shown in Fig.7.4.

Fig 7.4 Field photographs of Amphibolite

7.2.3.4 Pegmatite

Pegmatite veins were traced in the Northwestern part of the mapped area which trends NE-SW direction. The vein is about 5m length and 2m width. This Pegmatite vein consists of majority of quartz, and feldspar. Field photograph of Pegmatite is shown in Fig.7.5.

Fig 7.5 Field photograph of Pegmatites

7.2.4 Petrography

Twenty samples were sanctioned by TCC-NMEDT, 20 samples of different rock types of representative rock samples (14 BRS and 6 core samples) were petrologically investigated. The details of sample subjected for petrographic study are shown in Table-7.3

Table 7.3: Details of sample subjected for petrographic study

Sr No	Latitude	Longitude	Locality	Sample no	Rock type
1	25.42792	74.12515	Borana	RJBO/BRS-24/2024-25	Migmatite Gneiss
2	25.43066	74.12528	Borana	RJBO/BRS-36/2024-25	Migmatite Gneiss
3	25.43066	74.12528	Borana	RJBO/BRS-36/2024-25	Migmatite Gneiss
4	25.42749	74.11762	Borana	RJBO/BRS-93/2024-25	Migmatite Gneiss
5	25.42749	74.11762	Borana	RJBO/BRS-93/2024-25	Migmatite Gneiss
6	25.41959	74.12168	Borana	RJBO-02/CS-77(154mts)	Migmatite Gneiss
7	25.42903	74.12298	Borana	RJBO-03/CS-37(95mts)	Migmatite Gneiss
8	25.42633	74.12524	Borana	RJBO/BRS-25/2024-25	Syenite

Sr No	Latitude	Longitude	Locality	Sample no	Rock type
9	25.42633	74.12524	Borana	RJBO/BRS-25/2024-25	Syenite
10	25.43201	74.12812	Borana	RJBO/BRS-26/2024-25	Syenite
11	25.43362	74.11748	Borana	RJBO/BRS-107/2024-25	Syenite
12	25.43417	74.11658	Borana	RJBO/BRS-108/2024-26	Syenite
13	25.43093	74.12785	Borana	RJBO/BRS-29/2024-27	Syenite
14	25.43201	74.12812	Borana	RJBO/BRS-26/2024-25	Syenite
15	25.41959	74.12168	Borana	RJBO-02/CS-36(71mts)	Syenite
16	25.43037	74.12438	Borana	RJBO-04/CS-25(50mts)	Syenite
17	25.41959	74.12168	Borana	RJBO-04/CS-23(46mts)	Syenite
18	25.42956	74.12881	Borana	RJBO/BRS-07/2024-25	Amphibolite
19	25.43165	74.12574	Borana	RJB0-01/CS-25(75mts)	Amphibolite
20	25.42773	74.12768	Borana	RJBO/BRS-11/2024-25	Pegmatite

7.2.4.1 Migmatite gneiss

It is composed predominantly of K- feldspar, plagioclase, quartz, hornblende, biotite, muscovite, and allanite as accessory minerals. Light color bands are represented by K-feldspars (Kfs), plagioclase, and quartz (Qz), while dark color bands are biotite (Bt) and hornblende, exhibiting gneissic structure (Fig.7.6a&b). Euhedral to subhedral epidote and zoisite are distinctly formed in this rock. Distinct allanite grains (Aln) with radial cracks along the quartz and plagioclase (Pl+Qz) are well developed (Fig.7.6b).

In some samples Well-developed gneissic foliations are defined by biotite (Bt) and muscovite of this sample (Fig.7.7a). Polysynthetic lamellar twinning is well preserved in the plagioclases while quartz grains show undulose extinction. The quartz grains show sub-grain formations at places. Radial cracks are well developed in the quartz grains, indicative of the allanite occurring in the core of them.

Allanite (Aln) occurs as irregularly shaped, characterized by yellowish brown and high relief relative to their associated minerals (Fig.7.7b). Zircon (Zrn) and apatite (Ap) occupy the interstitial spaces within the quartz and plagioclase (Fig.7.7c.). Round to sub-rounded garnets is observed in association with plagioclase. These garnets are also called xenomorphic garnets (Grt) (Fig.7.7d). In some sample Cross-hatched twinning is seen in the microcline. Intergrowths of plagioclase (Pl) and quartz (Qz) exhibit

myrmekite texture (Fig.7.8a). Magnetite (Mt) occurs as anhedral, dominantly associated with biotite (Bt) (Fig. 7.8b). In some samples Sphene, epidote, monazite and opaques are accessories. An elongated monazite grain (Mnz) occurs in association with the hornblende (Hld) and plagioclase (Pl) and close to epidote (Ep) (Fig. 7.9).

In core sample number RJB-02/CS-77 (154 mts) it is coarse-grained rock with alternation of dark and light colour bands defined by pale-pink alkali feldspar-plagioclase-quartz and dark greenish-brown biotite–hornblende, respectively as this drill core sample was collected at 154 m depth (Fig. 7.10a). It has been traversed by quartz-carbonate veins. Crude foliation is defined by mafic minerals (Fig.7.10b). Under the microscope, it is observed that the rock developed a strong foliation and gneissose structure defined by alternating layers of dark (biotite-hornblende) and light color (plagioclase, K-feldspar, quartz) minerals (Fig. 7.10c).

The felsic minerals are inequigranular. K-feldspar mainly comprises of microcline which is easily distinguished by cross-hatched twinning. A few quartz grains included in the microcline are seen at places. Sericitization of microcline and plagioclase as the alteration product is recorded at places. At places, the subgrain formation of plagioclase (Pl) has taken place, which clearly indicates the deformation and metamorphism (Fig 7.10d). Biotite is often associated with muscovite, and it occurs as a platy form preferred orientation that defines foliation in the rock. Biotite shows a yellowish-brown color in the transmitted light. Hornblende showing trichroism from bluish green to dark green through yellowish green under plane polarized light. Euhedral zircon grains (Zrn) occur along the intergranular spaces of quartz. (Fig 7.10e).

In core sample number RJBO-03/CS-37(95mts) it is a coarse-grained rock. Rock shows alternations of mesocratic and leucocratic bands defined by gneissose structure. Mesocratic bands are made up of biotite, while plagioclase, K-feldspar, and quartz are in the leucocratic bands (Fig. 7.11a). The rock is biotite gneiss. A petrography study reveals that the sample displays gneissic texture defined by dark and light color bands, which are represented by biotite and plagioclase, microcline, orthoclase and quartz, respectively. Allanite (Alt), titanite (Tit), zoisite, epidote (Ep) and opaques are observed as accessories. The rock is coarse to medium grained.

Biotite (Bt) occurs as platy, showing preferred orientations that define gneissic foliation. But it is poorly developed. It defines the mafic band in the rock (Fig 7.11b). Polysynthetic lamellar twinning is well preserved in the plagioclases. Number of blebs of plagioclases included within the later plagioclases.

Intergrowths of plagioclase and quartz exhibit myrmekite texture are seen at places. The plagioclases have been partially replaced by sericites indicate hydrothermal fluid activity.

The quartz grains show sub-grain formations, suggesting strain-induced deformation. Zoisite-epidote veins are cross-cutting all the mineral phases. Cluster of titanite (Tit) are observed along the grain boundary between biotite, quartz and plagioclase (Fig. 7.11c). Primary allanite (Aln) is observed to show a yellowish green color and weak pleochroism. Six grains with variable sizes are distributed randomly over this rock (Fig. 7.11d).

Allanite occurs as a prominent accessory mineral in the migmatite gneiss from the drill core sample of Borehole 3 at a depth of 95 m. Based on measurements from photomicrographs, the allanite grain shows a length of approximately 1.96 mm and a width of about 0.71 mm which is as shown in the fig (7.11e) and also allanite grain shows a length of approximately 0.40 mm and a width of about 0.64 mm which is as shown in the fig (7.11f).

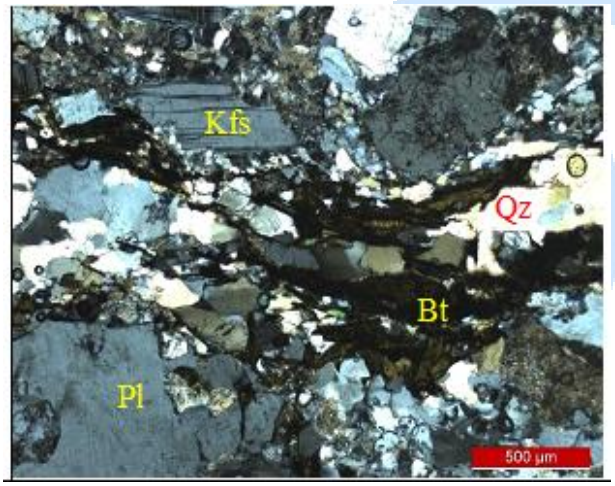

Fig 7.6a Photomicrograph showing dark and light colour bands of biotite, hornblende and K-feldspars, quartz, plagioclase respectively under CPL (Sample no. RJBO/BRS24/24-25).

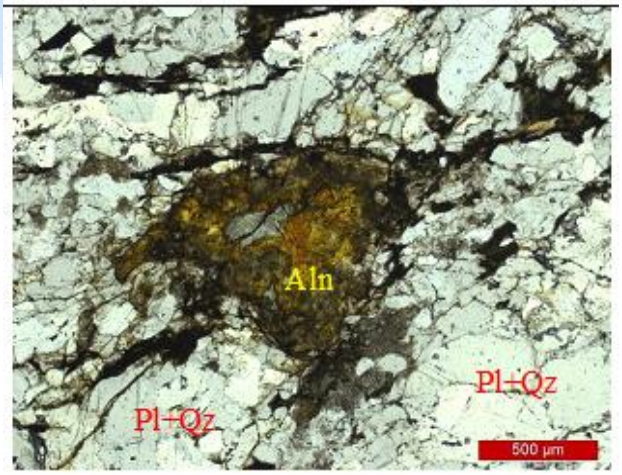

Fig 7.6b Photomicrograph showing Allanite (Aln) with radial cracks under CPL (Sample no. RJBO/BRS-24/24-25).

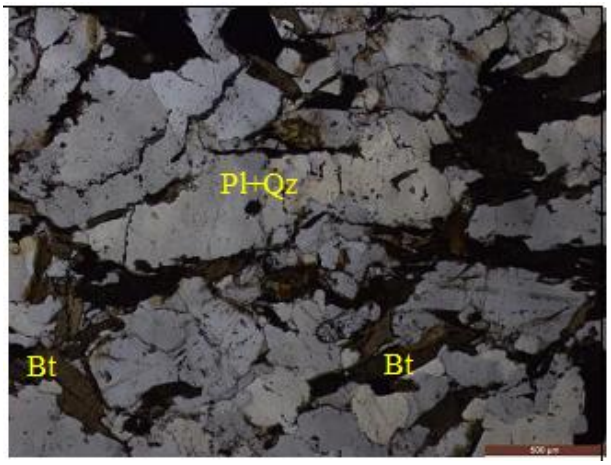

Fig 7.7a Photomicrograph showing biotite foliation defined by biotite (Bt) under PPL (sample no. RJBO/BRS93/2024-25).

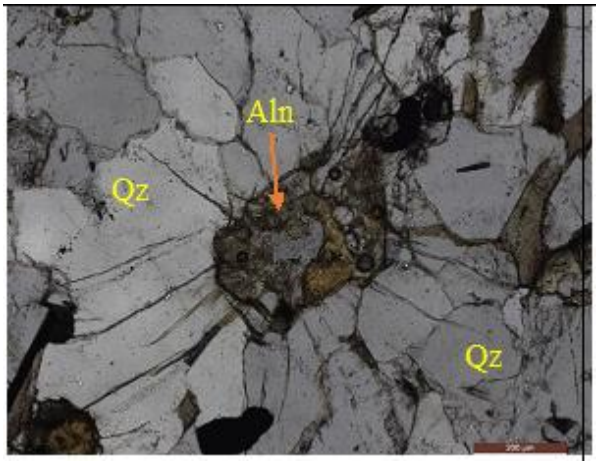

Fig 7.7b Photomicrograph showing irregular shaped allanite (Aln) with radial cracks developed the surrounding quartz grains under PPL (sample no. RJBO/BRS93/2024-25)

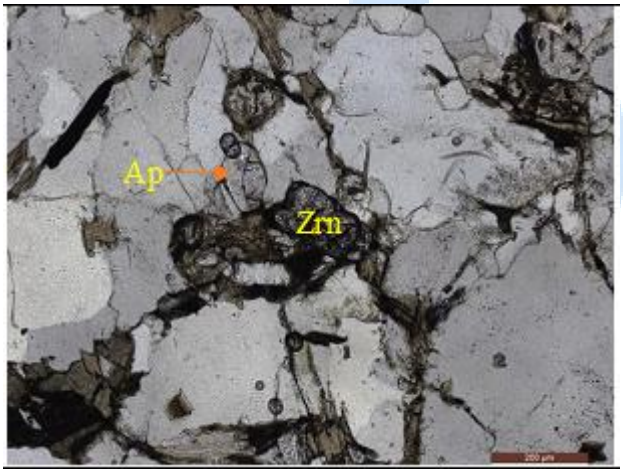

Fig 7.7c Photomicrograph showing Zircon (Zrn) and Apatite (Ap) under PPL (sample no. RJBO/BRS93/2024-25).

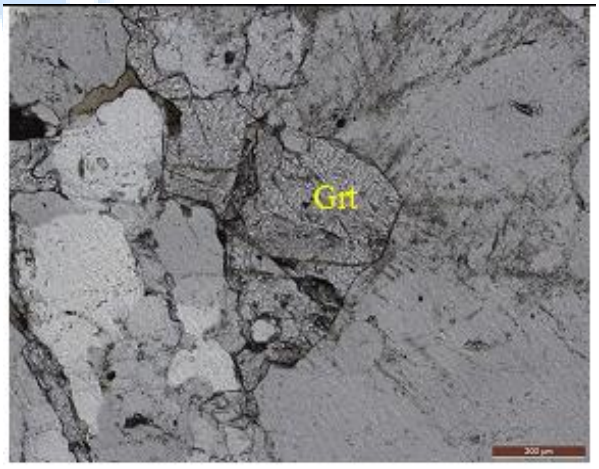

Fig 7.7d Photomicrograph showing xenomorphic garnet (Grt) under PPL (RJBO/BRS93/2024-25).

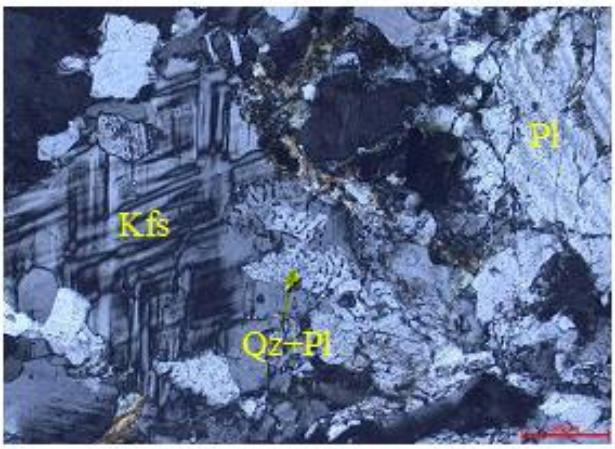

Fig 7.8a Photomicrograph showing mineral assemblages and intergrowth of plagioclase and quartz exhibits myrmekite texture under CPL (sample no. RJBO/BRS36/2024-25).

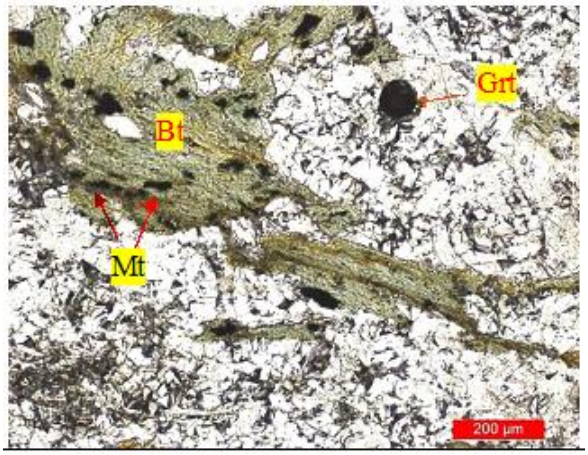

Fig 7.8b Photomicrograph showing schistosity defined by biotite and magnetite (opaques) are seen under PPL (sample no. RJBO/BRS36/202425).

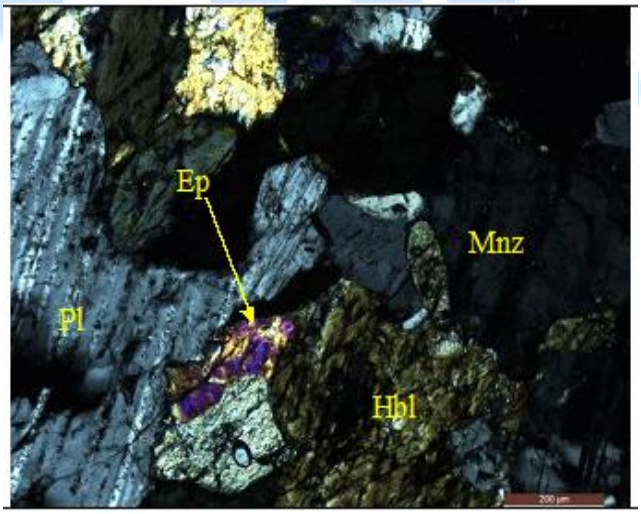

Fig 7.9 Photomicrograph of an elongated monazite grain associated with hornblende and plagioclase and close to epidote seen in cross polarized light (sample no. RJBO/BRS25/2024-25).

Fig 7.10a Hand sample of drill core sample of migmatite gneiss (RJBO-02/CS-77)

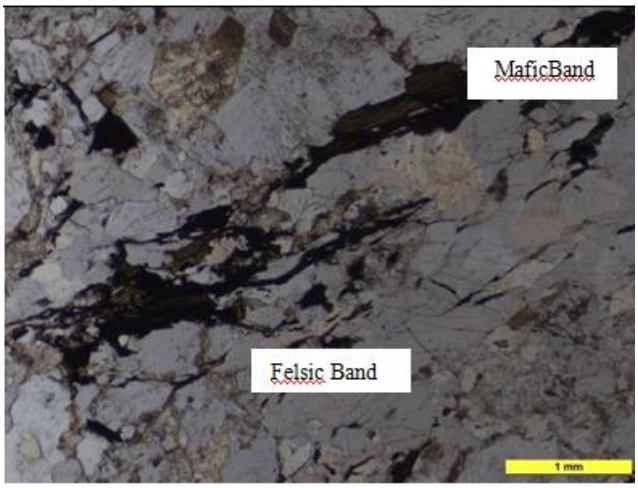

Fig 7.10b Photomicrograph displays alternations of mafic and felsic bands/layers, mafic band composed of Biotite-hornblende and felsic band composed of quartz-plagioclase under plane polar view (RJBO-02/CS-77)

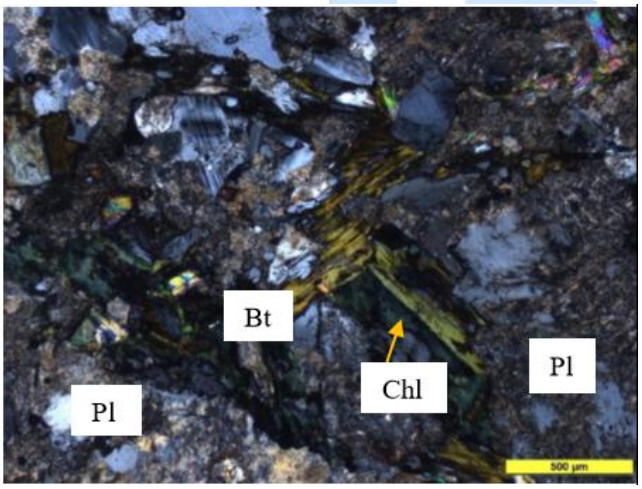

Fig 7.10c Photomicrograph showing alteration of biotite by chlorite under cross polar view (RJBO-02/CS-77)

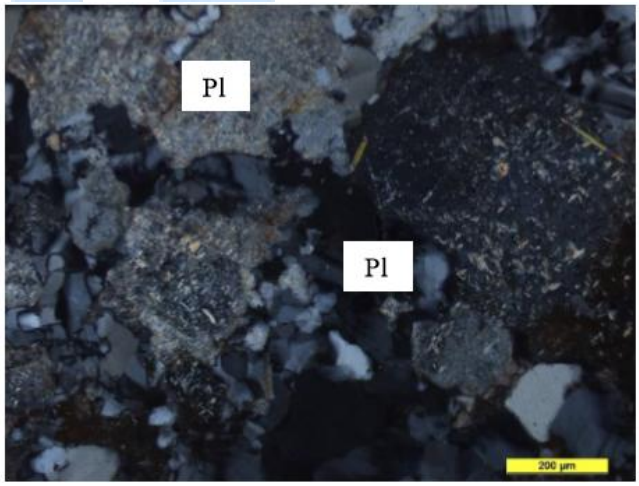

Fig 7.10d Photomicrograph of plagioclase (Pl) showing sub grain formation due to metamorphic activity under cross polar view (RJBO-02/CS-77)

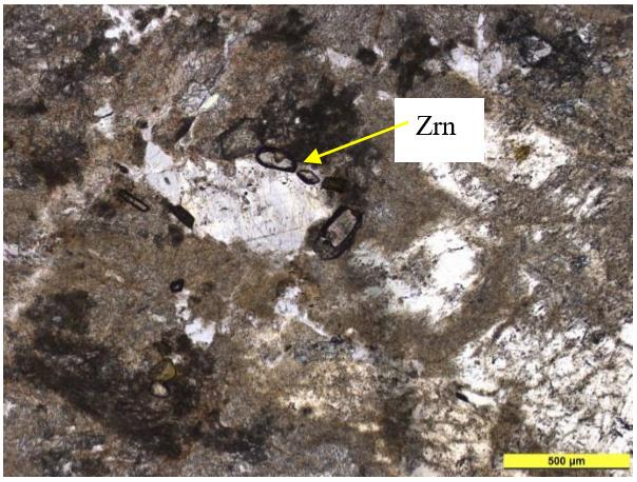

Fig 7.10e Photomicrograph cluster of zircon (Zrn) grains under plane polar view (RJBO-02/CS-77)

Fig. 7.11a Drill core sample of migmatite gneiss (RJBO-03/CS-37)

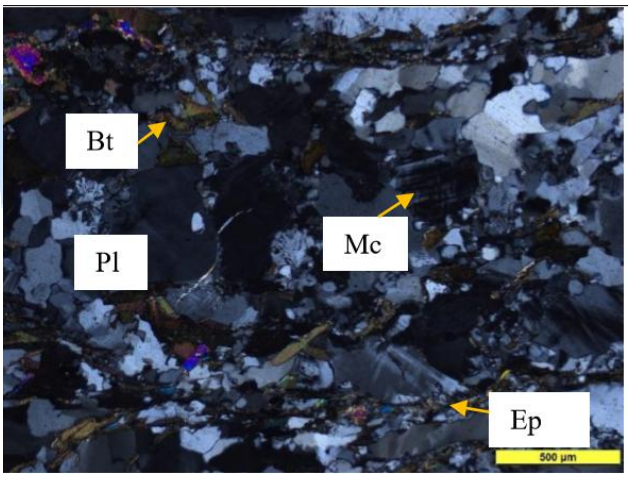

Fig 7.11b Photomicrograph displays epidote (Ep) veins along with major minerals like biotite (Bt), plagioclase (Pl) and microcline (Mc) under cross polarized light (RJBO-03/CS-37)

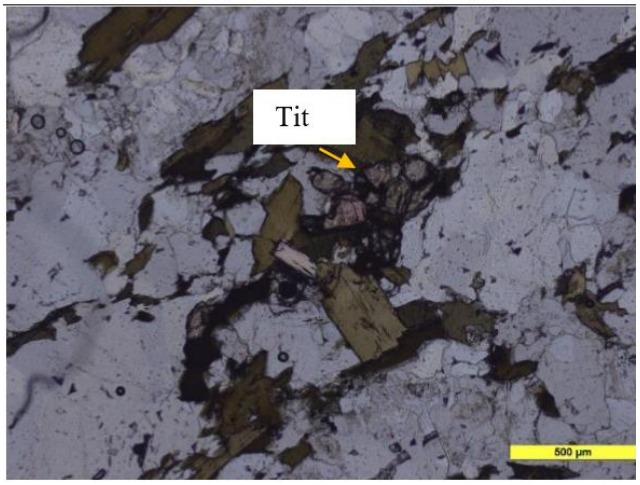

Fig 7.11c Photomicrograph showing cluster of titanite along the boundary of plagioclase and biotite under plane polarized light (RJBO-03/CS-37)

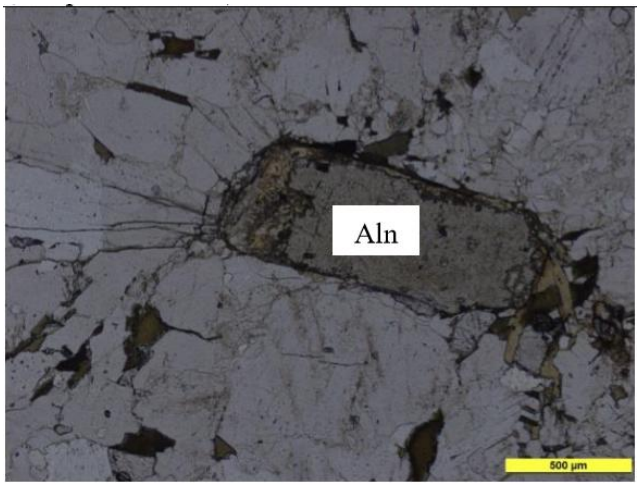

Fig 7.11d Photomicrograph showing a long prismatic allanite (Aln) with radial cracks under plane polar view (RJBO-03/CS-37)

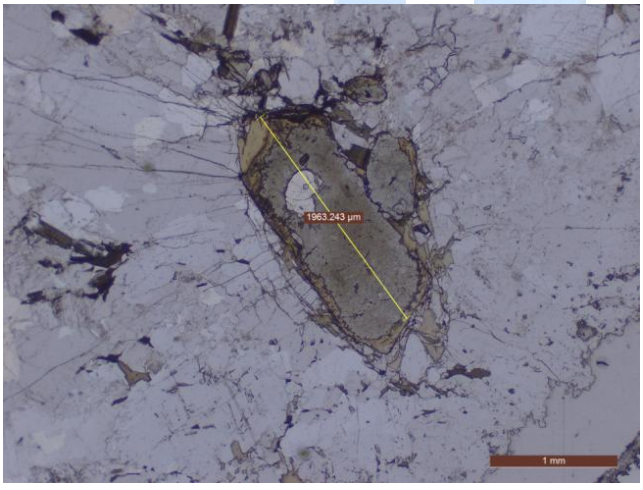

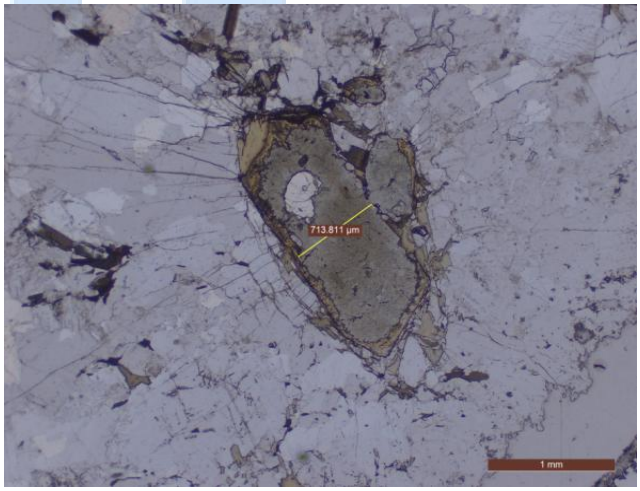

Fig 7.11e Photomicrograph showing Allanite grain in Migmatite Gneiss from Borehole 3 at 95 m depth

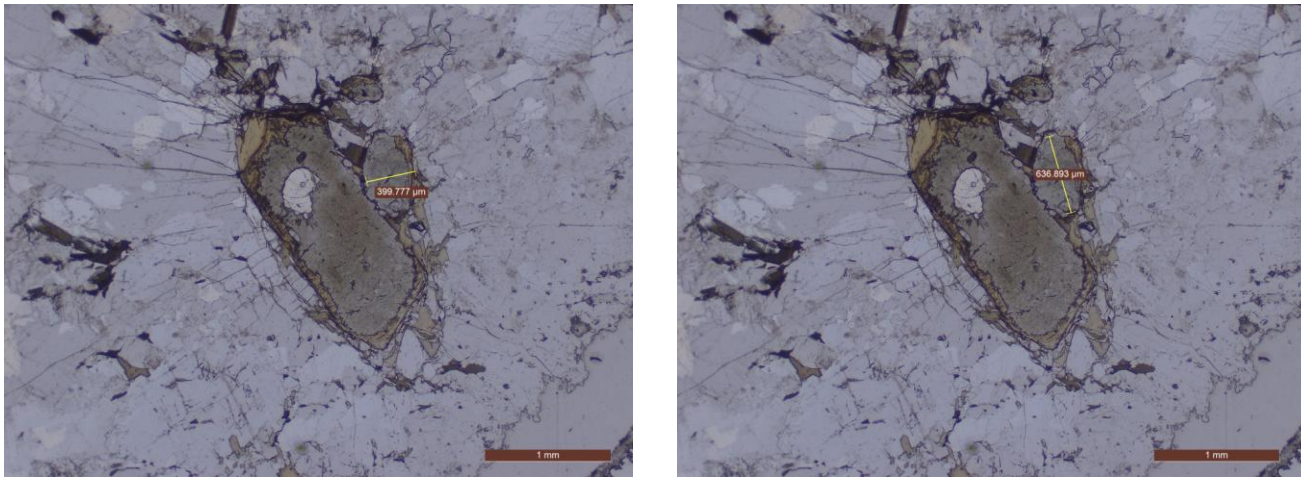

Fig 7.11f Photomicrograph showing Allanite grain in Migmatite Gneiss from Borehole 3 at 95 m depth

7.2.4.2 Syenite

It is composed of quartz (Qz) and K-feldspar as essential minerals and epidote, zoisite (Zo), and muscovite as accessory minerals (Fig.7.12a). Epidote veins are cross cutting all the mineral phases. These veins consist predominantly of epidote crystals in the form of aggregates that show higher-order interference color (Fig.7.12b). Xenomorphic garnet (Grt) is also noticed at places (Fig.7.12c). Allanite with radial cracks is observed for REE mineralization. It is a long prismatic crystal that is subhedral in some places (Fig.7.12d).

The vein consists predominantly of epidote and zoisite crystals in the form of aggregates that show higher-order interference color and bluish color for zoisite (Figs.7.13a). Allanite marginally altering to epidote, as seen by the higher interference color along the edges of the crystal (Fig. 7.13b). Subhedral to euhedral monazite grains are associated with the K-feldspars (Fig. 6.14a). An elongated allanite grain shows a yellowish-brown color with the development of radial cracks (Fig. 7.14b). It is associated marginally with magnetite and K-feldspars (Kfs).

A subhedral allanite (Aln) is associated marginally with epidote and subsequently plagioclase and orthoclase (Fig.7.15a). Vein of epidote-zoisite cross-cutting the rock (Fig. 7.15b), whereas the independent epidote grains are occurring in the interstitial to intergranular K-feldspars. The number of monazite (Mnz) grains is observed in this sample. These are occurring as granular forms associated with

K-feldspars (Kfs) (Fig.7.15c).

In drill core sample number RJBO-02/CS-36 (71mts) sample is distinguished by coarse-grained, pale pink rock. Alkali feldspar and plagioclase make up most of it (Fig. 7.16a). The alkali feldspar is dominated by orthoclase and microcline (Mc) and is characterized by subhedral to euhedral forms (Fig.7.16b). While the microcline displays crosshatched twinning, orthoclase often displays Carlsbad twinning. Besides, plagioclase exhibits polysynthetic twinning. It is easy to discern between their dual planes. This rock has undergone dynamic recrystallization during metamorphism and deformation, as evidenced by the formation of feldspar subgrain.

Hydrothermal alteration products like sericitization are often found in both alkali feldspar and plagioclase. Sub-hypidiomorphic texture is recorded. Epidote veins crosscut the rock. These veins predominantly consist of epidote crystals in the form of aggregates that show higher-order interference color. Zoisite is present as independent grains and as well as in the interstitial spaces of alkali feldspar. Chlorite, sericite, epidote and Zoisite are the typical features of the hydrothermal process whereas the subgrain formation/ mosaic texture depicts the metamorphic character. Zircon (Zrn) (Fig. 7.16c) and titanite formed as clusters.

The drill core sample number RJBO-04/CS-25 (50mts) is a coarse-grained rock and pale pink to greenish color, composed predominantly of plagioclase and alkali feldspar. Multiple epidote veins traversed into it (Fig. 7.17a). Due to occurrence of the epidote veins the rock appeared as pinkish green color. Photomicrograph shows myrmekite texture along with plagioclase (Pl) and microcline (Mc); subgrain formation of Plagioclase (Pl) in the alkali feldspar syenite under cross polar view (Fig 7.17b).

Petrographically, the rock is mainly composed of plagioclase and K-feldspar, and its accessory minerals are quartz, epidote, zoisite, chlorite, and carbonate. It is coarse-grained and inequigranular in texture. K-feldspar is dominated by microcline. Subgrain formation of plagioclase and K-feldspar that form during deformation results from recrystallization, which occurs when temperature increases. Sericitization in the K-feldspars and plagioclase are seen at places. The rock is highly deformed and sericitized. Quartz occurred in a minor amount. Sub-hypidiomorphic texture is also recorded in this rock. Photomicrograph showing granular Monazite (Mz) grains associated with plagioclase under Cross polar view (Sample no. RJB-4 (50mts) (Fig 7.17c). Petrographic study indicates the presence of a significant amount of allanite and monazite grains. In drill core sample of Borehole 4 at depth of 50 m depth shows allanites. The measured grain size ranges from approximately 4.03mm to 1.33 mm as shown in (Fig 7.17d).

Zoisite- epidote veins are cross-cutting all the mineral phases. These veins consist predominantly of epidote (Ep) crystals in the form of aggregates that show higher-order interference color (Fig. 7.18a). Later vein of carbonate, which is cross cutting the earlier vein (Fig 7.18a). Carbonate, chlorite, epidote and zoisite are the typical features of the hydrothermal process, whereas the subgrain formation depicts the metamorphic character. Titanite clusters display high relief and 2nd order interference colour at places. The irregular nature of allanite grains (Aln) is characterized by a yellowish brown and high relief relative to their associated minerals (Fig 7.18b).

The sample is a coarse-grained, inequigranular alkali-feldspar syenite of pale pink to greenish colour, composed predominantly of plagioclase and K-feldspar, with minor quartz and accessory epidote, zoisite, chlorite, and carbonate. In hand specimen, the rock appears pinkish green due to the presence of multiple epidote veins traversing the sample (Fig. 7.19a). Under the microscope, the rock is seen to consist mainly of plagioclase, K-feldspar(K-fel) (dominated by microcline), quartz (Qz), andepidote ((Ep), along with accessory phases (Fig. 7.19b). The rock is highly deformed and sericitized and shows subgrain formation in plagioclase and K-feldspar, as well as sub-hypidiomorphic texture. Zoisite–epidote veins are seen cross-cutting all mineral phases, and a later carbonate vein (Cal) is observed cutting across the earlier epidote vein (Fig. 7.19c).

Allanite (Aln) occurs as irregular grains showing yellowish brown colour and high relief relative to associated minerals (Fig. 7.19d). Cluster of monazites (Mnz) along the chlorite is recorded. These are granular in nature with high relief (Fig 7.19e). Based on the mineral assemblages, the rock may thus be classified as alkali feldspar syenite.

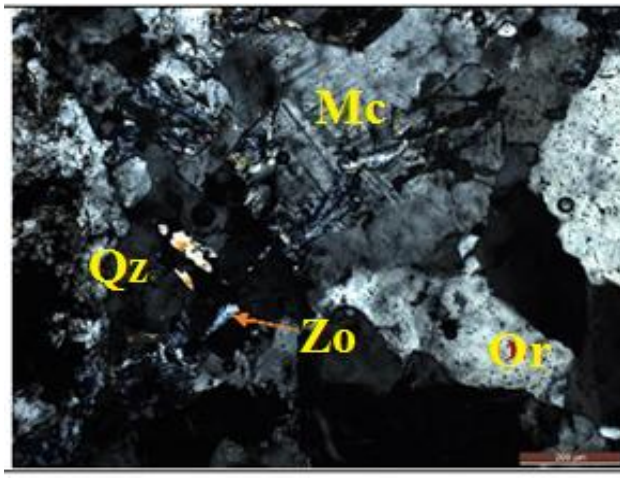

Fig 7.12a A Photomicrograph of syenite showing different mineral assemblages like microcline, quartz, orthoclase and zoisite under XPL (Sample no RJBO/BRS-107/2024-25).

Fig 7.12b Photomicrograph showing epidote vein cross cutting under XPL (Sample no. RJBO/BRS-107/2024-25).

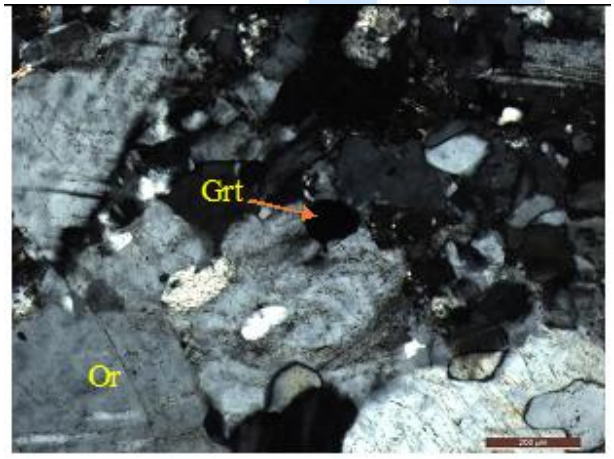

Fig 7.12c Photomicrograph showing of xenomorphic garnet in syenite (Sample no. RJBO/BRS-107/2024-25).

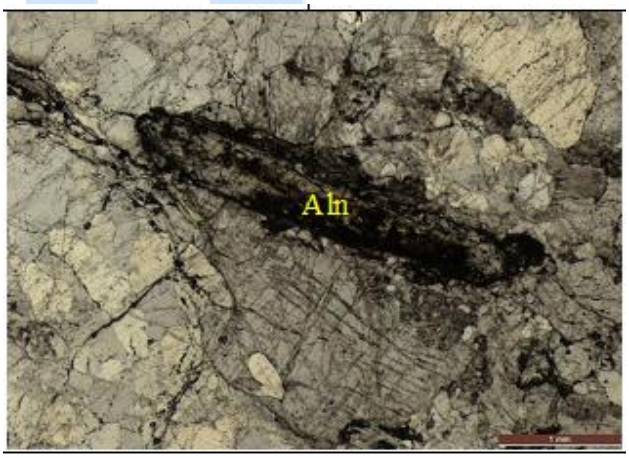

Fig 7.12d Photomicrograph along prismatic allanite with radial cracks in syenite under PPL (Sample no. RJBO/BRS-107/2024-25).

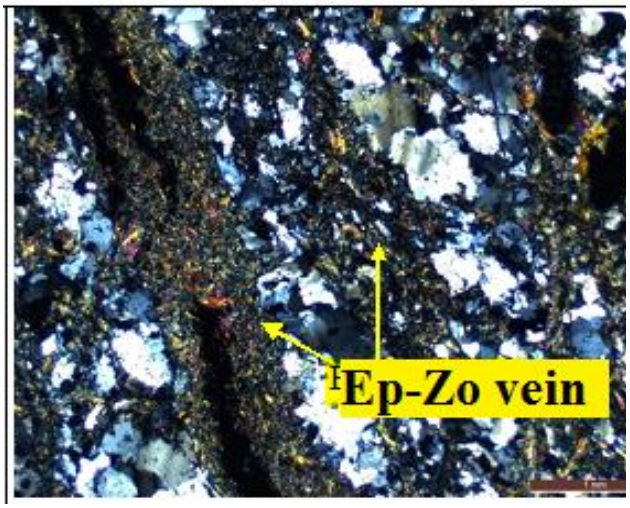

Fig 7.13a Photomicrograph showing epidote (ep)- zoisite (zo) veins intruded into the syenite under the cross-polar view (Sample no. RJBO/BRS-108/24-25).

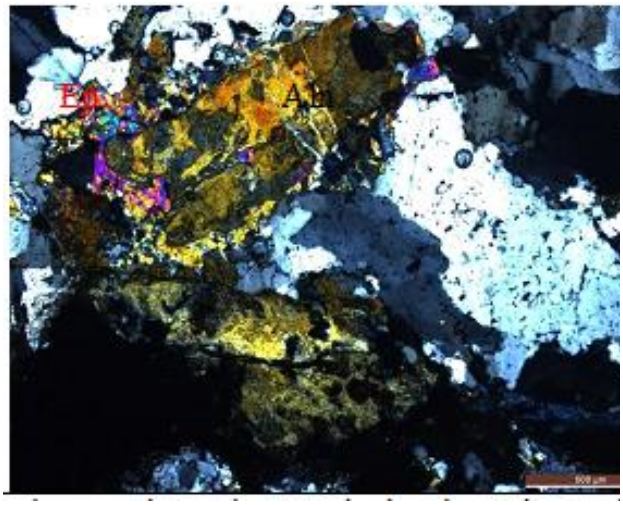

Fig 7.13b Photomicrograph showing a large allanite (aln) crystal altered marginally by epidote (ep) under the cross-polar view (Sample no. RJBO/BRS-108/24-25).

Fig 7.14a Photomicrograph showing Monazite (Mnz) associated with K-feldspars (Kfs) under cross-polar view (Sample no. RJBO/BRS-29/24-25).

Fig 7.14b Photomicrograph showing an elongated allanite (aln) with distinct radial cracks associated with K-feldspars (k-spar) and magnetite (mag), under plane polar view (Sample no. RJBO/BRS-29/24-25).

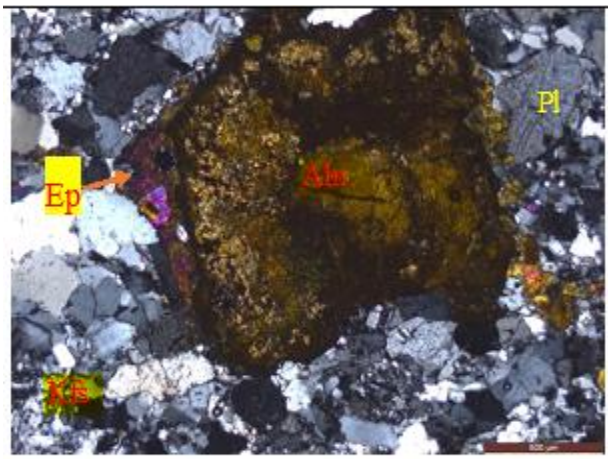

Fig 7.15a Photomicrograph showing a large subhedral allanite marginally associated with epidote embedded in the ground mass of K-feldspars under cross polar view (Sample no. RJBO/BRS26/24-25).

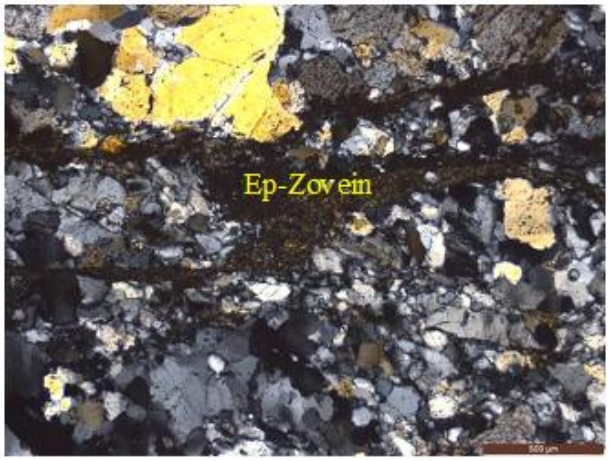

Fig 7.15b Photomicrograph showing epidote (ep)- zoisite (zo) veins traversed into syenite under cross polarized light (Sample no. RJBO/BRS26/24-25).

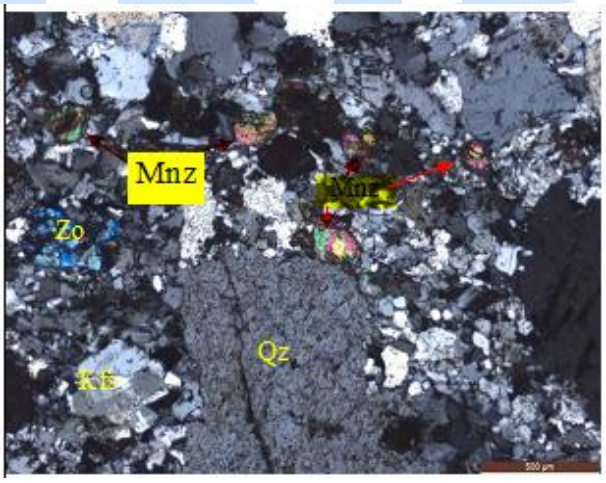

Fig 7.15c Photomicrograph showing granular monazite grains associated with K-feldspars and quartz in syenite under cross polar view (Sample no. RJBO/BRS26/24-25).

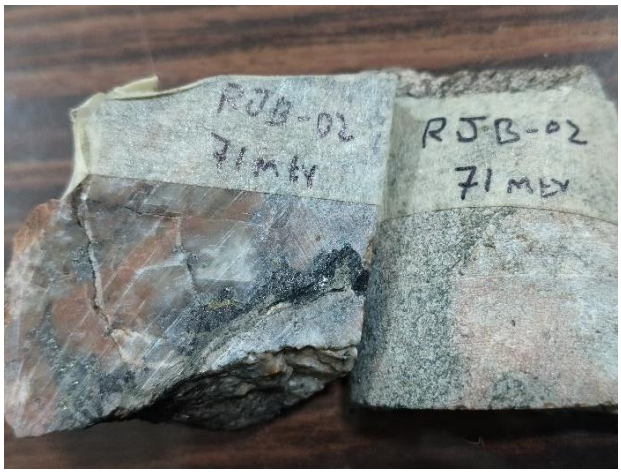

Fig 7.16a Drill core sample of alkali feldspar syenite (RJBO-02/CS-36)

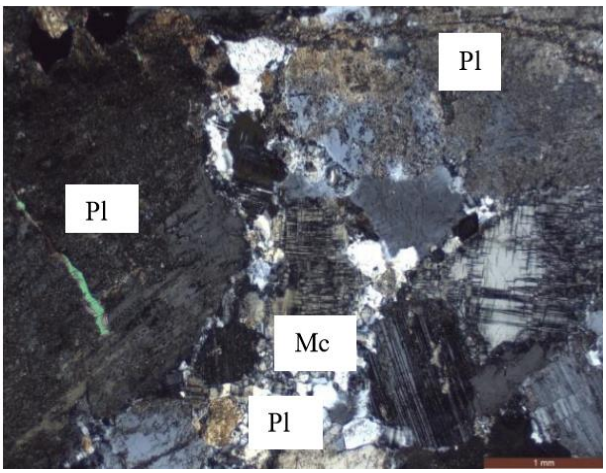

Fig 7.16b Photomicrograph of syenite showing assemblage of plagioclase (Pl), and microcline (Mc) displaying Sub-hypidiomorphic texture under cross polar view (RJBO-02/CS-36)

Fig 7.16c Photomicrograph showing clusters of zircon (zrn) grains under plane polar view (RJBO-02/CS-36)

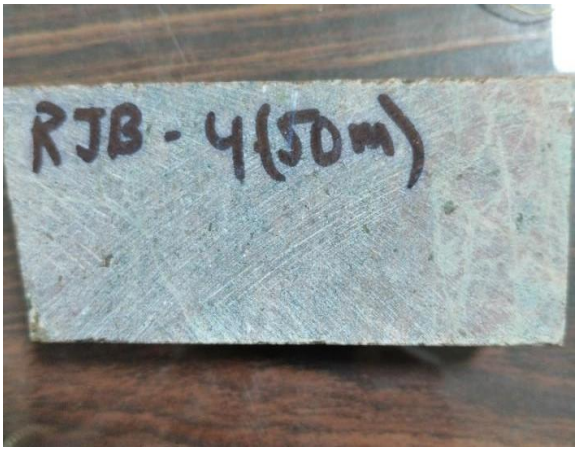

Fig 7.17a Hand sample of drill core sample of Alkali feldspar syenite (RJBO-04/CS-25)

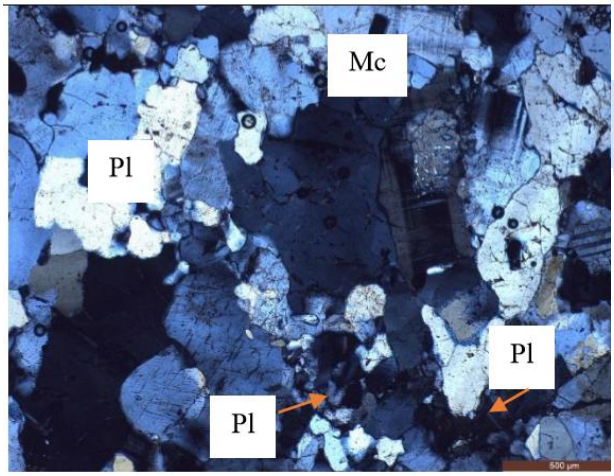

Fig 7.17b. Photomicrograph showing myrmekite texture along with plagioclase and microcline; subgrain formation of Plagioclase (Pl) in the alkali feldspar syenite under cross polar view (RJBO-04/CS-25)

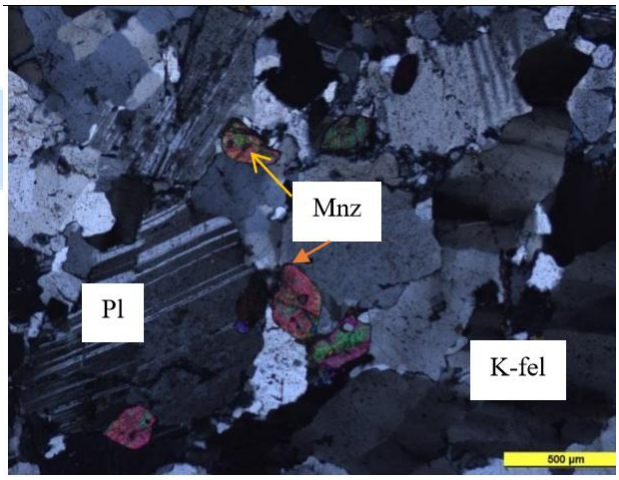

Fig 7.17c Photomicrograph showing granular Monazite (Mz) grains associated with plagioclase under Cross polar view (RJBO-04/CS-25)

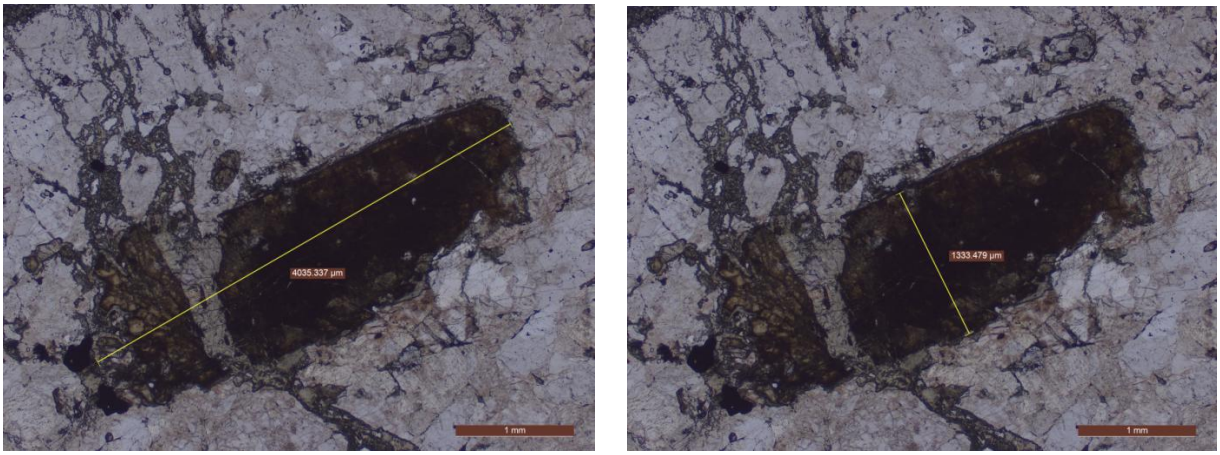

Fig 7.17d Photomicrograph showing Allanite grain in Syenite from Borehole 4 at 50 m depth

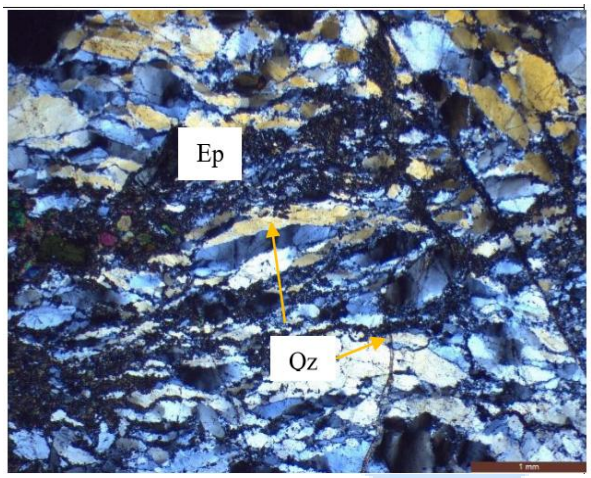

Fig 7.18a Photomicrograph showing ribbon quartz (Qz) with epidote (Ep) veins under Cross Polar view (Sample no. RJBO/BRS-24/24-25)

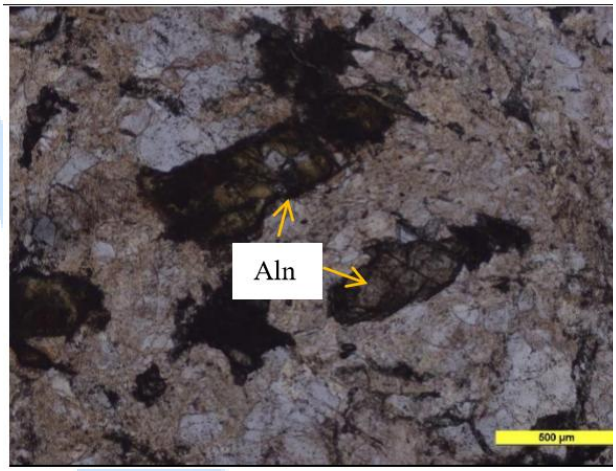

Fig 7.18b Photomicrograph showing primary allanite (Aln) under plane polar view (Sample no. RJB-4 (50mts).

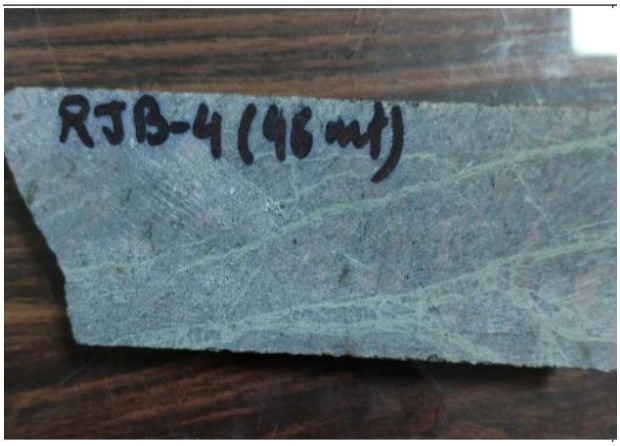

Fig 7.19a Drill core sample of alkali feldspar syenite (RJBO-04/CS-23)

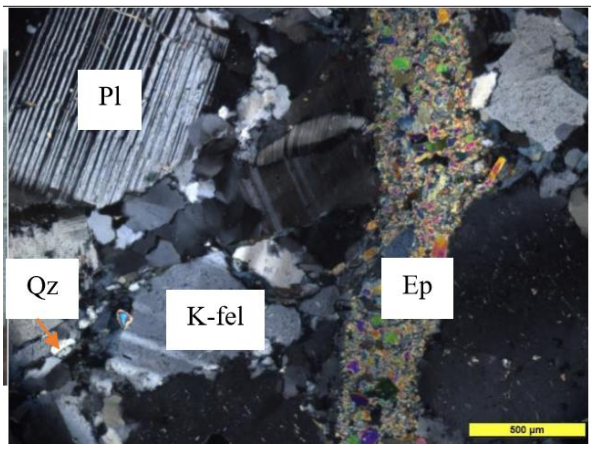

Fig 7.19b Photomicrograph alkali-feldspar syenite showing mineral assemblages such as plagioclase (Pl) and epidote (Ep) vein which intruded the syenite at earlier stage under CPL (RJBO-04/CS-23)

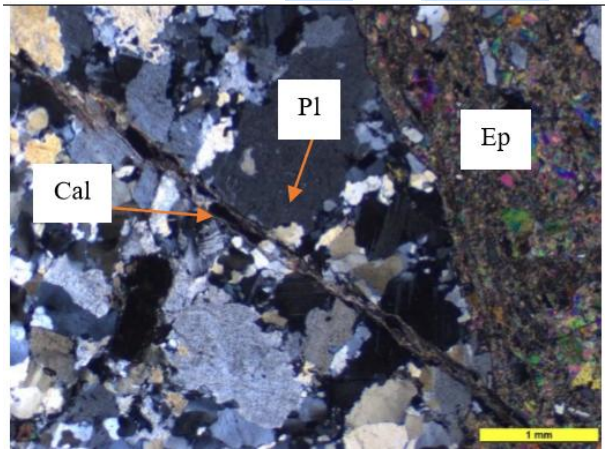

Fig 7.19c Photomicrograph showing a late-stage epidote and carbonate veins are cross-cutting the alkali feldspar syenite under CPL (RJBO-04/CS-23)

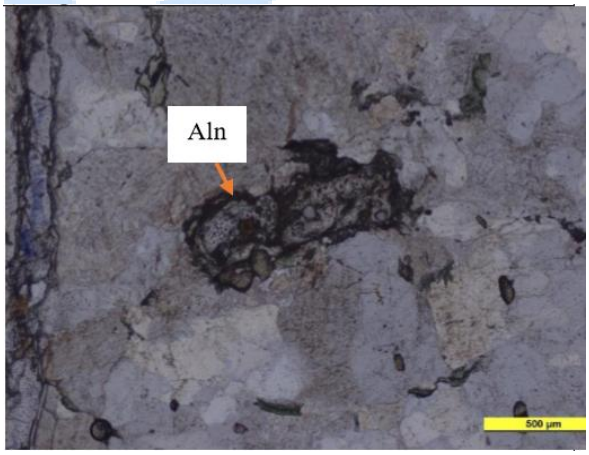

Fig 7.19d Photomicrograph showing primary allanite (Aln) rimmed by epidote (Ep) and plagioclase (Pl) under plane polarized light (RJBO-04/CS-23)

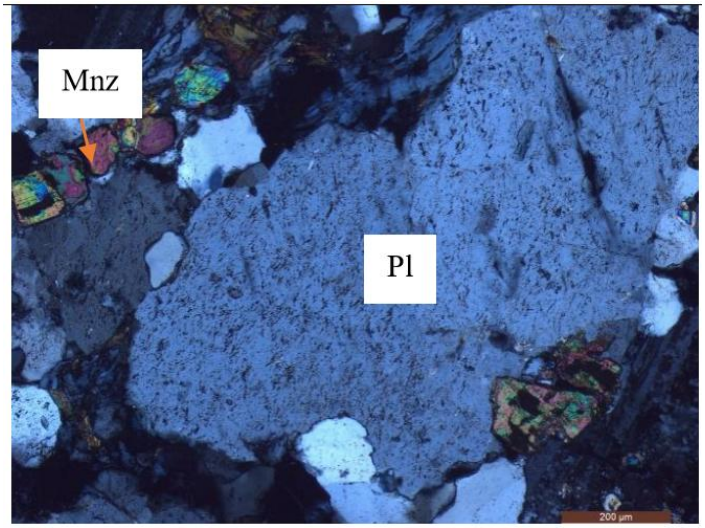

Fig 7.19e Photomicrograph showing cluster of Monazite (Mnz) and plagioclase (Pl) under cross polarized light (RJBO-04/CS-23)

7.2.4.3 Amphibolite

Petrographic study reveals that the rock mainly consists of hornblende (Hbl) and plagioclase (Pl). Epidote (Ep) and opaques occur as accessories (Fig.7.20a). The rock shows granulose texture. The plagioclase minerals are sericitized and few plagioclases (Pl) even occur as inclusion withinhornblende ((Hbl) (Fig.7.20b). The plagioclase mostly shows polysynthetic lamellar twinning. The hornblende occurs as elongated, prismatic crystals and is associated with plagioclases, epidote, and opaques. The higher iron content leads to more pronounced blue tones in the bluish hornblende. The hornblende shows both basal and prismatic sections. In plane polarized light, hornblende shows distinct trichroism that is dark green, yellowish green, and pale yellowish green.

The drill core sample number RJB0-01/CS-25(75mts) appears as a dark greenish to light-green-colored medium-grained rock exhibiting saccharoidal texture. A quartz vein crosscuts the alkali amphibolite. The primary sulphides dominated by pyrite and chalcopyrite were recorded. The rock consists predominantly of amphiboles and plagioclase (Fig.7.21a). Under microscopic examination, the sample is divided into two distinct portions. The first contains large, preferentially oriented amphibole crystals(K-amp) (Fig. 7.21b), while the second is dominated by

epidote-zoisite. In the first portion, amphibole phenocrysts are embedded within a fine-grained matrix (pseudo-amphibole) and calcite (Cal).

Large quartz crystals are also present; these are mostly deformed and recrystallized, exhibiting a metamorphic texture characterized by sharp boundaries and triple junctions between grains. Accessory calcite displays characteristic rhombohedral cleavage, twinkling, and twinning, with secondary quartz observed along the cleavage planes. The second portion consists of fine-grained amphiboles exhibiting a polygonal mosaic texture. Under cross-polarized light, these amphiboles show strong pleochroism (ranging from bluish to yellowish green) and two sets of perfect cleavage (Fig. 7.21c). Epidote-zoisite and clinopyroxene occur as accessory minerals.

A few euhedral to subhedral clinopyroxene grains, identified by their yellowish-to-purple interference colors and inclined extinction, are located along the boundaries of the alkali amphiboles (Fig. 7.21d). Zoned epidote is also present. Along the contact zones of the alkali amphiboles, clusters of titanite (Ttn) appear in pseudo-forms associated with amphibole, carbonate, and ilmenite; individual euhedral or wedge-shaped titanite (Ttn) crystals are also observed (Fig. 7.21e). Based on this petrographic study, the rock may thus be classified as an alkali amphibolite. The suspected alkali amphiboles tentatively identified as riebeckite or arfvedsonite composition which will be confirmed via Electron Probe Micro-Analyzer (EPMA) analysis.

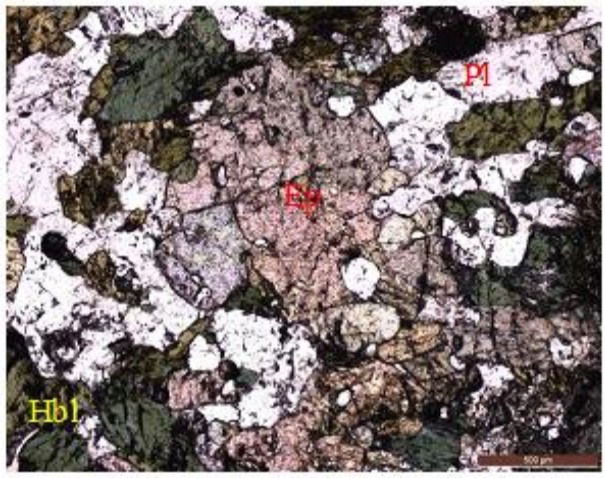

Fig 7.20a Photomicrograph of amphibolite showing assemblage of plagioclase (Pl), hornblende (Hbl) and epidote (Ep) exhibiting granulose texture under plane polar view (Sample no. RJBO/BRS-7/24-25)

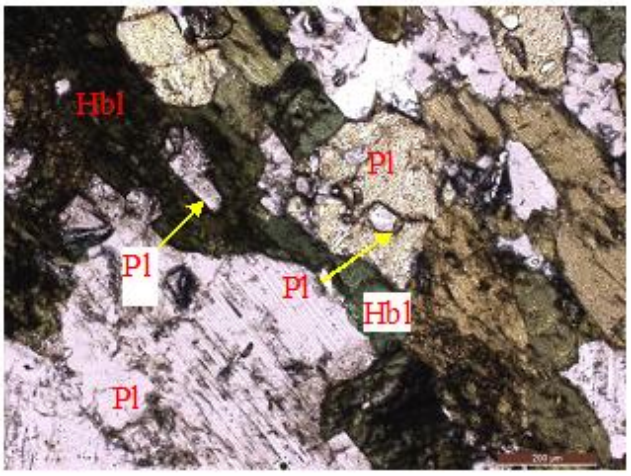

Fig 7.20b Photomicrograph showing minor plagioclase inclusion in hornblende and secondary plagioclase under plane polar view (Sample no. RJBO/BRS-7/24-25)

Fig 7.21a Drill core sample of alkali amphibolite (RJB0-01/CS-25) (75mts)

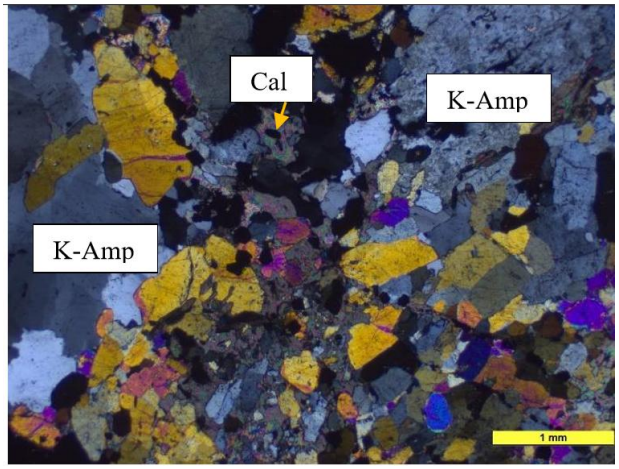

Fig 7.21b Photomicrograph of Alkali amphibolite showing mineral assemblages (K-Amp) under cross polar view (RJB0-01/CS-25) (75mts)

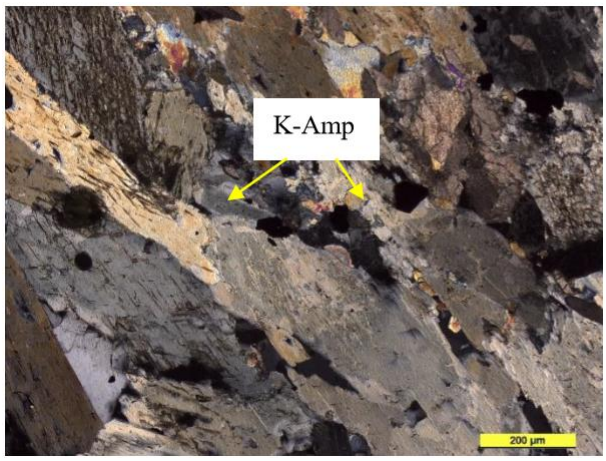

Fig 7.21c Photomicrograph showing yellow to bluish grey alkali amphiboles under cross polar view (RJB0-01/CS-25) (75mts)

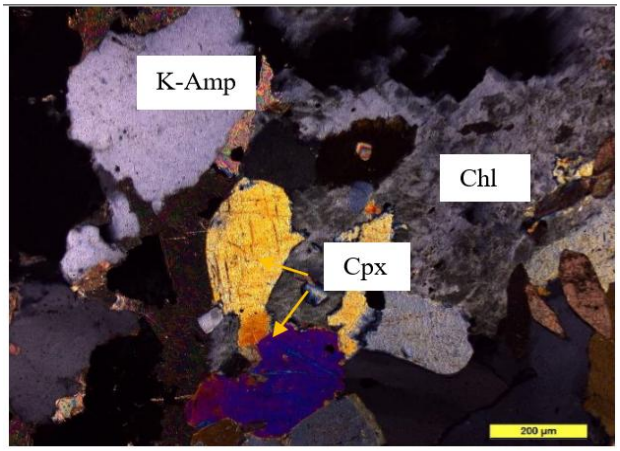

Fig 7.21d Photomicrograph showing Clinopyroxene (cpx) along with alkali amphiboles and titanite under cross polar view (RJB0-01/CS-25) (75mts)

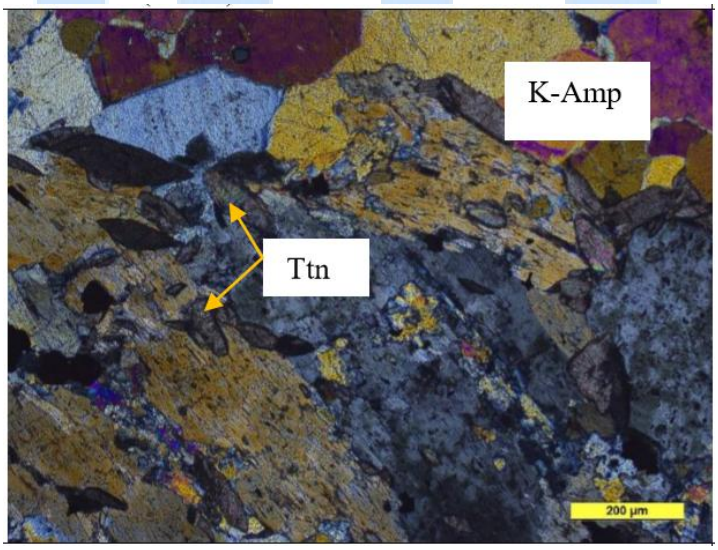

Fig 7.21e Photomicrograph showing cluster of titanite (Ttn) along the boundary of alkali amphiboles under cross polar view (RJB0-01/CS-25) (75mts)

7.2.4.4 Pegmatite

Petrographically, the sample is composed chiefly of plagioclase, K-feldspar (Kfs), quartz (Qz)muscovite (Ms), epidote (Ep) as accessories (Fig 7.22a). The modal proportion of plagioclases is more than the quartz. Several plagioclase inclusions have been observed within the interstitial plagioclase. Sericite alteration of plagioclases is seen at places. Polygonal mosaic texture with the sharp contact and triple junction is seen between the plagioclases (Fig.7.22b). Muscovite is observed as platy forms associated with plagioclase (Pl) and quartz(z). Euhedral to subhedral epidote (Ep) occurs in the intergranular spaces to the plagioclase (Pl) anquartz (z(Qz) (Fig 7.22c). The rock can be identified as Aplite but from the field observations it is confirmed as Pegmatite.

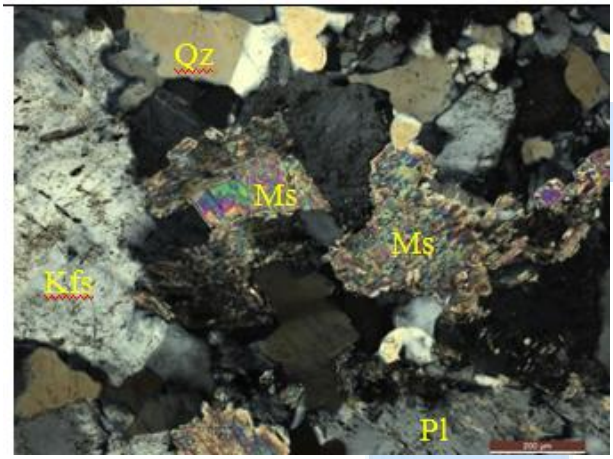

Fig 7.22a Photomicrograph of Pegmatite showing mineral assemblages under CPL (Sample no. RJBO/BRS-11/24-25).

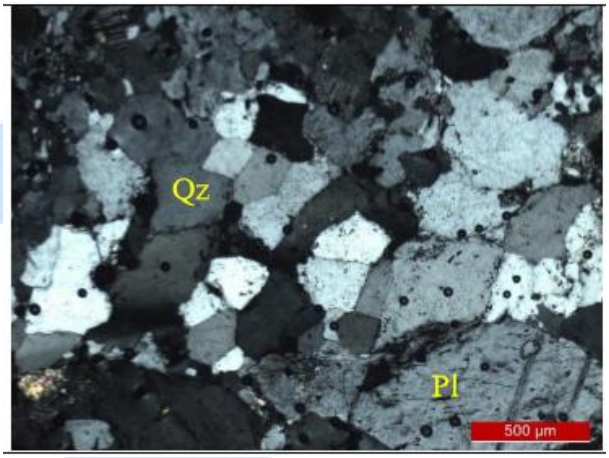

Fig 7.22b Photomicrograph of Polygonal mosaic texture in Pegmatite under CPL (Sample no. RJBO/BRS-11/24-25).

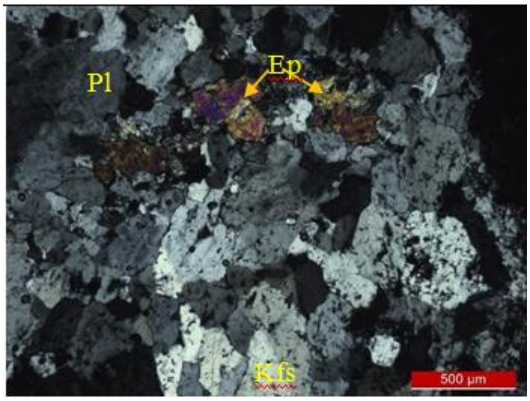

Fig 7.22c Photomicrograph showing epidotes in Pegmatite under CPL (Sample no. RJBO/BRS-11/24-25).

7.2.5 Ore microscopy

The detailed descriptions of polished rock sections of different rock types are enumerated below:

7.2.5.1 Migmatite Gneiss

In reflected light most of the opaques are the magnetite. Magnetite occurring in the form of veinlets and grains, which are commonly associated with biotite (Fig. 7.23). Magnetite occurs as anhedral, dominantly associated with biotite (Fig. 7.24). Hematite slightly transforms magnetite into goethite (Fig.7.25) due to hydrothermal alteration.

The drill core sample number RJBO-02/CS-77(154mts) under reflected light, the opaques are classified as magnetite, chalcopyrite and pyrite. Chalcopyrite occurs as disseminations and stringers while pyrite forms as euhedral crystal (Fig 7.26a). In RJBO-02/CS-77(154mts) most of the opaques are classified as magnetite. Magnetite occurs as euhedral as well as vein type, dominantly associated with biotite (Fig.7.26b).

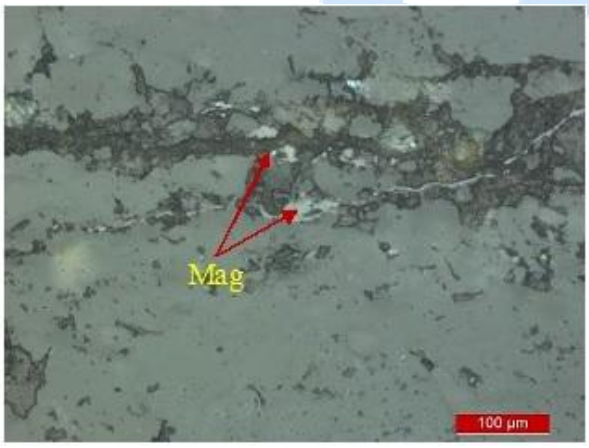

Fig 7.23 Photomicrograph showing magnetite (Mag) veinlet and discrete magnetite associated with biotite under reflected light (Sample no. RJBO/BRS-24/24-25)

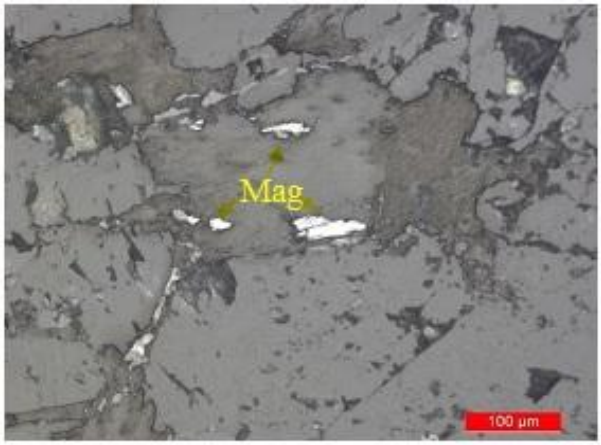

Fig 7.24 Photomicrograph showing discrete/ disseminated magnetite grains in the biotite gneiss, under reflected light (sample no. RJBO/BRS36/2024-25)

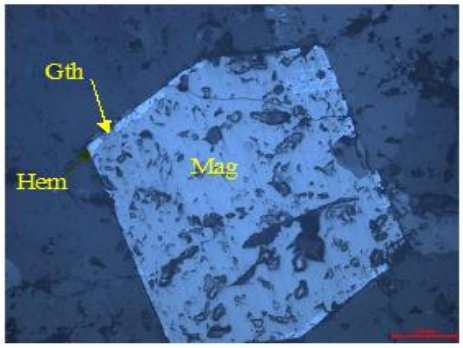

Fig 7.25 Photomicrograph showing a euhedral magnetite replaced by hematite and subsequently by goethite at the margin under reflected light (sample no. RJBO/BRS25/2024-25).

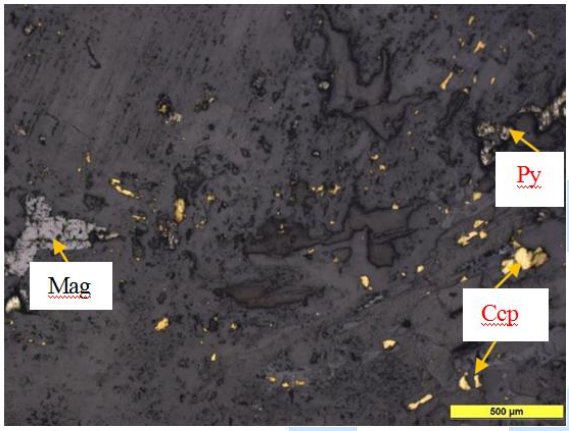

Fig 7.26a Photomicrograph showing disseminated chalcopyrite (Ccp), and pyrite (Py) under reflected light (RJBO-02/CS-77) (154mts)

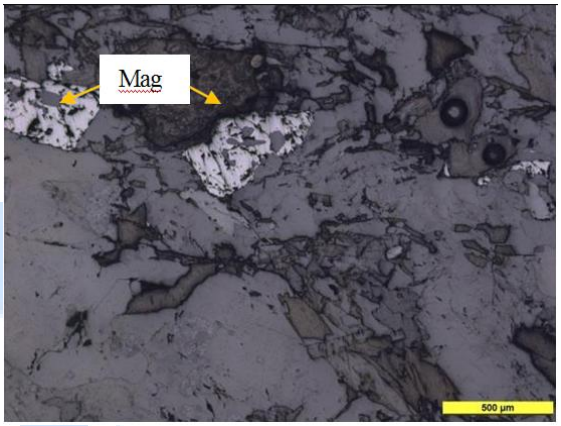

Fig 7.26b Photomicrograph showing magnetite (Mag) under reflected light (RJBO-02/CS-77) (154mts)

7.2.5.2 Syenite

In reflected light, it is observed that they are classified as magnetite, hematite, and goethite, where the hematite and goethite are the alteration products of magnetite. Magnetite's primary oxide phase manifests as irregular and subhedral to euhedral forms. It has a low reflectance and a pinkish to greyish tinge. Hematite, which exhibits moderate reflectivity, takes the place of magnetite (Fig.7.27a). In contrast, hematite-goethite alternations that occur as colloform structure (Fig. 7.27b), produced due to oxidation in the surficial environment.

The drill core sample number RJBO-02/CS-36(71mts) showing pyrite. Chalcopyrite and magnetite in association with silicates under reflected light (Fig.7.28). RJBO-04/CS-25(50mts) under reflected light, sulfide mineralization is represented by pyrite. The discrete nature of pyrite grains shows euhedral to subhedral forms (Fig.7.29).

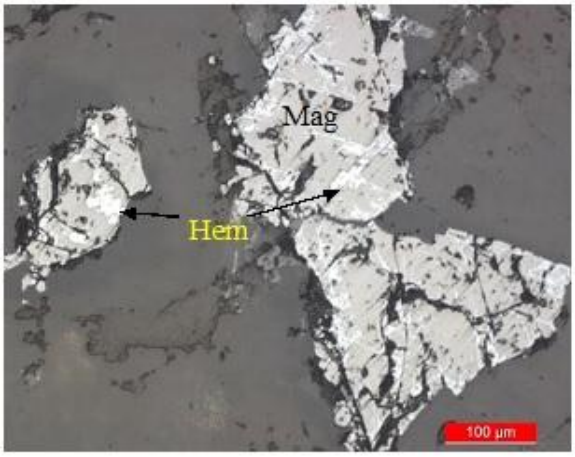

Fig 7.27a Photomicrograph showing Pinkish to grey tinge of irregularly shaped magnetite (Mag) replaced marginally by hematite (Hem) under reflected light (Sample no. RJBO/BRS29/24-25).

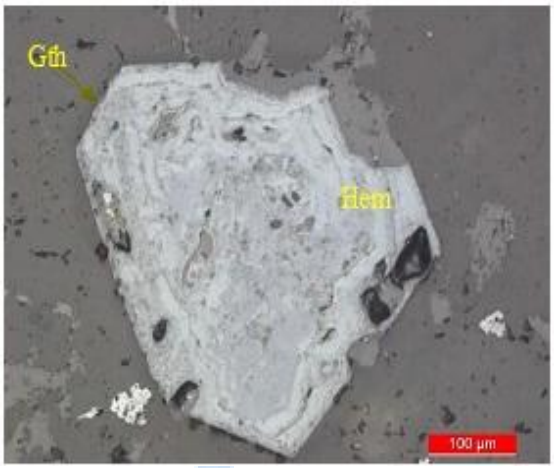

Fig 7.27b Photomicrograph showing magnetite replaced by hematite (Hem) and goethite (Gth) exhibits colloform structure under reflected light (Sample no. RJBO/BRS-29/24-25)

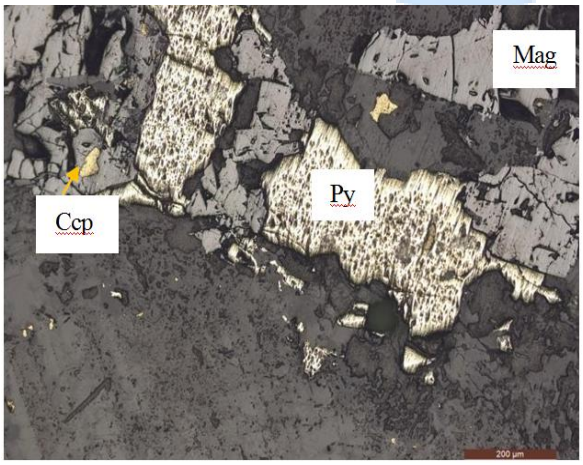

Fig 7.28 Photomicrograph showing pyrite. Chalcopyrite and magnetite in association with silicates under reflected light (RJBO-02/CS-36) (71mts)

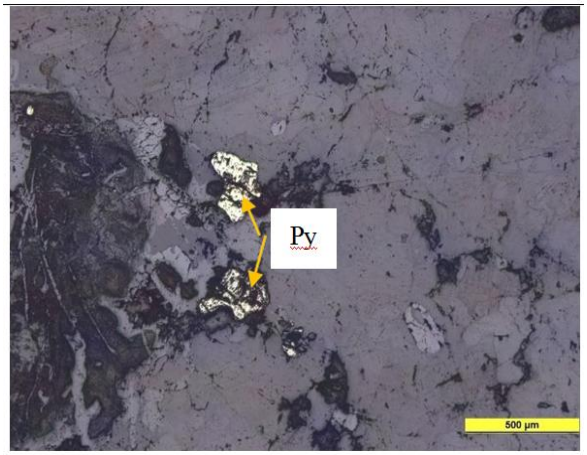

Fig 7.29 Photomicrograph showing euhedral pyrite (Py) under reflected light (RJBO-04/CS-25) (50mts)

7.2.5.3 Amphibolite

In reflected light, it is observed that in amphibolite opaques are hematite, which are euhedral to subhedral (Fig.7.30a) and show moderate reflectivity with blood-red internal reflection and are associated with hornblendes.

The drill core sample number RJB0-01/CS-25(75mts) under reflected light, the opaque mineral assemblage consists of chalcopyrite, pyrite, magnetite. Chalcopyrite occurs both in vein form and as euhedral crystals. Pyrite is found as euhedral grains associated with quartz, chalcopyrite (Fig.7.30b). Magnetite is primarily associated with pyrite and chalcopyrite.

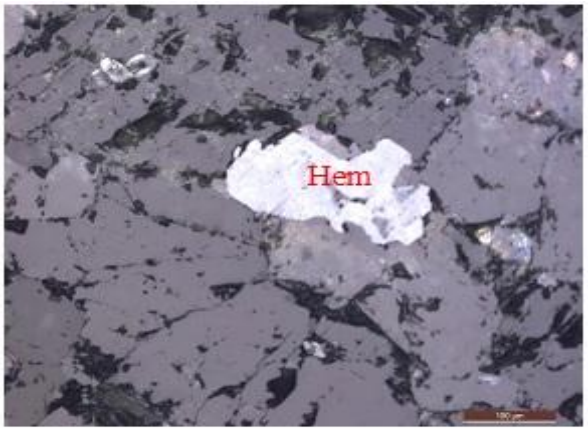

Fig 7.30a Photomicrograph showing subhedral hematite (Hem), associated with silicates under reflected light (RJB0-01/CS-25(75mts)

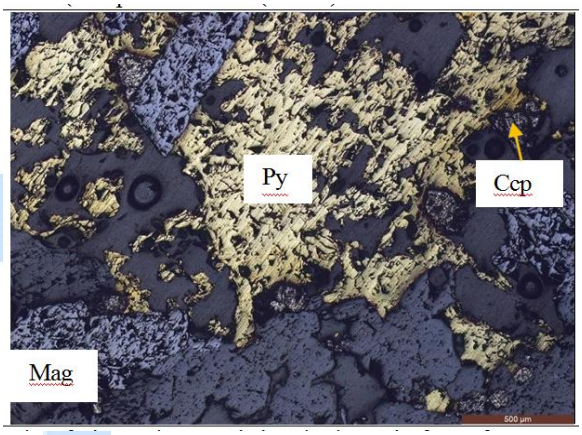

Fig 7.30b Photomicrograph showing irregular form of pyrite (Py), chalcopyrite (Ccp) and magnetite (Mag) associated with alkali amphiboles under reflected light (Sample no. RJB-1 (75mts). RJB0-01/CS-25(75mts)

7.3 Structural details of the area such as dip, strike, folds, faults, etc.

The block is devoid of primary structures as the area has experienced multiple stages of deformation. The litho-units in the area exhibit metamorphic planar structures like gneissic banding and foliation. The gneissic banding trending ENE-WSW is observed in the migmatite gneiss. Foliation trending NW-SW is well exhibited in the rocks observed in the block. The foliations are defined by the

reorientation of mineral grains parallel to the foliation plane. In migmatite, syenite/alkali syenite and amphibolites, it is observed that S2, S3 and S4 planes are well preserved.

The S2 planar fabric is dominantly observed in all rocks. It is very penetrative and defined by the re-orientation of mineral grains parallel to the foliation plane. It parallels the S1 gneissic band in most places and is preserved as crenulation cleavage in different rocks. The S3 planar fabric is developed only in a few places as a fracture plane. The trend of S3 depends on the regional geometry of the area, mainly NW-SE to NNW-SSE. The S4 planar fabric also occurs as fracture planes and is preserved in the form of vertically spaced cleavage perpendicular to the S1 in NNW-SSE to N-S direction.

The linear structures observed in the block include mineral lineation and joints. The mineral lineation is prominently observed in migmatite gneisses and mica schist, wherein sillimanite, amphibole, and micas are linearly arranged. The lineations are always parallel to the local orientation of fold axes, and most of them are parallel to the axes of F2 folds. Many of the amphibole mineral lineations are however, parallel to the axes of the F3 set of folds. Two to three sets of prominent joints have been noticed in the area in gneiss.

7.3.1 Detailed Structural Disposition

The structural elements observed in the area can be divided into planar structures, linear structure and joints, etc.

7.3.1.1 Planar Structure:

The planar structures observed in the study area can be described under the following headings.

7.3.1.1.1 Gneissic Banding

In the migmatite gneiss, the gneissic banding is well preserved and clearly defined by prominent color banding resulting from the segregation of mafic and felsic layers (Fig. 7.31). Variations in the trend of this planar fabric are very frequent, reflecting that the rock has undergone multiple phases of deformation after the development of the gneissic fabric.

7.3.1.2 Linear structures

The linear structures observed in the field area fall under the following categories.

7.3.1.2.1 Mineral lineation

In the migmatite gneiss, this lineation is defined by the preferred linear alignment of minerals such as amphibole and mica, which are oriented parallel to one another, giving rise to a prominent mineral lineation.

7.3.1.2.2 Joints

Vertical joints are observed in most of the rock types of the area. Two to three prominent sets of joints have been identified in the gneiss (Fig.7.32). These joint sets are consistently observed in the majority of the migmatite gneiss exposures across the study area.

7.3.1.2.3 Folds

The Area shows a tight, asymmetric, inclined fold developed in banded gneiss/migmatite (Fig. 7.33). Quartz veins within migmatite gneiss show ptygmatic folding (Fig.7.35). This indicates that the quartz veins behaved more rigidly during deformation and were squeezed into complex shapes. Presence of chevron folds were also noticed within migmatite gneiss (Fig.7.34) Their presence suggests strong compressive stress and repeated deformation events. Overall, these structures show that the rocks in the area have undergone intense, multi-phase deformation.

7.3.1.2.4 Faults

High-angle Fault seen in quartz vein within amphibolite (Fig.7.36).

7.3.1.2.5 Epidote veins

Epidote veins are prominently developed in the block area and are observed to crosscut the migmatite gneiss and syenites (Fig 7.37). These veins occur as thin to thick fracture fillings at several locations. The veins extend discontinuously over short distances.

Fig 7.31 Gneissic bandings

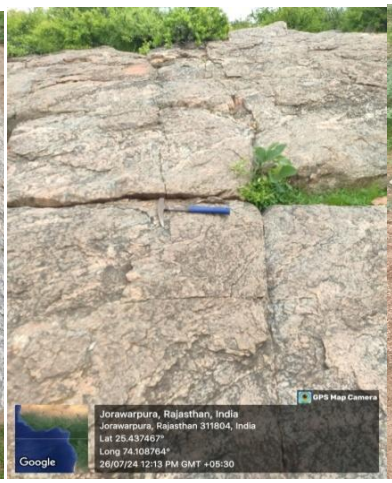

Fig 7.32 Set of joints

Fig 6.41 Folding

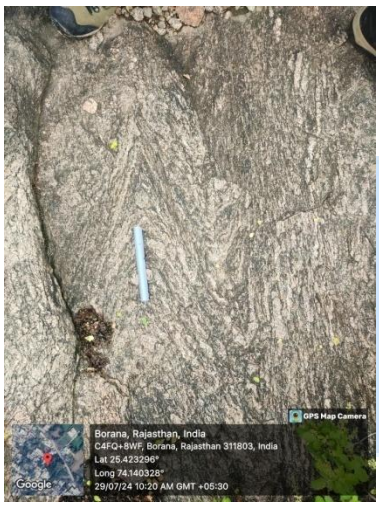

Fig 7.34 Chevron fold**.**

Fig 7.35 Ptygmatic fold

Fig 7.36 Faulting

Fig 7.37 Epidote veins cross-cutting

7.3.2 Detailed Structural Disposition and its Relationship with Mineralization

The structural pattern played a significant role in the localization and remobilization of mineralization. The prominent structural features observed in the area include Gneissic foliation and banding, Mineral lineation, Foliation-parallel and cross-cutting intrusive contacts, Fractures, joints, Epidote–zoisite vein networks. These structures show systematic orientations and provide important conduits for late-stage hydrothermal fluids responsible for REE mineralization.

REE mineralization in the area is predominantly represented by allanite and monazite, spatially and genetically associated with epidote–zoisite alteration. Structural control on mineralization is evident at multiple scales: Epidote–zoisite veins cross-cutting both migmatite gneiss and syenite represent a later hydrothermal event. Marginal alteration of allanite to epidote and association of monazite with K-feldspars indicate fluid-mediated REE remobilization

7.4 A discussion on the type of the deposit based on the style of mineralisation and minerals under investigation. Suggested exploration plan with spacing of the sampling points and depth of exploration commensurate with the stage of exploration.

Earlier works carried out by GSI have reported the anomalous value of REE in the Borana area and identified profuse amounts of allanite grains within the syenite/alkali feldspar syenite and migmatite gneiss of the Mangalwar Complex at Chatrawanmata temple near Borana and adjacent area. The G4 reconnaissance survey carried out by GSI during FS: 2018-19 has recommended taking up the detailed mapping within migmatite gneiss and syenite of Mangalwar complex near Chatrawan Mata temple, Borana area to delineate a probable zone for REE mineralization.

As per the report, REE mineralization is in the form of allanite crystals disseminated within migmatite gneiss and syenite. Further, it is interesting to note that minor indications of mineralization are also

observed by GSI during large-scale mapping in the area, such as epidotization within syenite and gem variety of epidote within syenite. Based on their field evidence, it is inferred that mineralization is of syngenetic origin and remobilized along weak planes due to later deformation. In some places, allanite crystals are aligned parallel to the S1 plane. Small pegmatite veins were developed due to reworking within migmatite gneiss, which contains allanite and magnetite grains. Surface evidence in the mapped area shows that mineralisation is structurally controlled at some places, especially by fault and brecciated brittle, deformed zones.

7.5 The extent and variability of the mineralisation expressed as length (in meter) (along strike or otherwise), plan width, and depth below surface to the upper and lower limits of the Mineral Resource.

According to the GSI report, about 19 nos. migmatite gneiss samples and 15 nos. of syenite that were analyzed have ΣREE values of more than 1500 ppm with a maximum of 2860 ppm within the proposed block. Five stream sediment samples in the GSI G4 area (out of 10 samples) have ΣREE values ranging from 1083 ppm to 1564 ppm. ΣREE values ranging from 1256 ppm to 2430 ppm in 23 numbers of trench samples in the GSI G4 area (out of 25 samples) over migmatite gneiss and syenite terrain of the Borana area is a clear indication of anomalous REE concentration in the area. Based on this recommendation, the proposed block has been identified as a REE mineral prospect.

Further, it is interesting to note that the gravity survey carried out during the National Geophysical mapping programme indicates a high-density body at shallow depth in toposheet no. 45K/3 near Borana and Raipur areas. The block is a part of the Borana area, which again justifies the objectives of the proposed study. Further, Dostal (2017) states that the alkali igneous rock deposits represent one of REE's most economically important resources. Many studies, including those by Guha et al. (2020), Balaram (2019), Baidya et al. (1999), Barakos et al. (2018), and others, have shown that migmatite gneisses that include allanite and monazite may be prospective REE mineralized zones. Thus, the presence of allanite and monazite in the migmatite gneiss of the proposed area, as per the GSI report, indicates the presence of REE prospects in the proposed block.

CHAPTER 8 - PREVIOUS EXPLORATION

8.1 Name and address of prospecting agency or permit holder or licensee involved in the exploration of the area with year and period of exploration (if more than one agency is involved details to be given separately for each agency)

1. The reconnaissance geological mapping around the Borana area was carried out by Hacket (1881).

2. Later, Bhattacharya and Guha (1989) carried out detailed mapping to reveal two distinct lithotectonic associations, viz., granulite-gneiss and greenstone-granite associations in the area. The granulite-gneiss (Sandmata Complex) sequence constituted of garnet-sillimanite gneiss, two-pyroxene granulite and cordierite-gedrite-sillimanite gneiss showing polymetamorphic characters and occurring as tectonic slivers within the amphibolite facies rocks of the Mangalwar Complex. The greenstone-granite sequence of the 'Mangalwar Complex' has been divided into 'Sawadri Group', 'Tanwan Group' and 'Asan Group'. The Sawadri and Tanwan Groups form the Archaean Greenstone Association, which is profusely and widely intruded and migmatised by oval or circular tonalitic trondhjemitic/granodioritic plutons of the Asan Group.

3. Mohanty and Guha (1990) studied high-grade sequence and associated rocks of the Sandmata Complex to understand the Archaean crustal evolution of the north-western Indian Shield in Rajasthan. The area was mapped on a 1:25,000 scale and brought out the lithostratigraphic succession of the area. Yadav and Garkhal (2007) carried out a gold investigation with the objective of assessing the gold potential in the South Delhi Fold Belt and Sandmata Complex. They mapped the Bhatewar-Borana-Raipur area on a 1:10,000 scale and brought out the geology of the area.

4. Neogi and Raza (2017) mapped the area on a 1:25,000 scale to work out the stratigraphic position and tectonic significance of the granite plutons and to locate potential zones of base metals, REE and other associated minerals. The litho-units exposed in the study area can be divided into viz. (i) Migmatite, amphibolite gneiss, quartzite, chert, meta basic rock, mica schist, ultramafics of the Mangalwar Complex, (ii) later intrusive granitoids, Anjana granite and Amet granite of Ran Igneous Complex, and, (iii) the alkali feldspar rich younger intrusive bodies of monzonite and syenite/alkali feldspar syenite within migmatite gneiss and granitoids. Profuse amounts of allanite grains have been reported by Neogi and Raza (2017) in FS: 2016-17 within the syenite/alkali feldspar syenite and migmatite gneiss of the Mangalwar Complex at Chatrawanmata temple near Borana. These allanite grains are dark black with conchoidal fractures and form haloes. Several syenite/alkali feldspar syenite bands extend in the east-west direction and are intrusive within the migmatite gneiss. The total thickness of the individual band varies from 100m to 200m.

8.2 Brief details of the exploration carried out (to be given separately for each agency)

Table 8.1 Brief Details of Exploration Carried Out

Agency/Author	Brief Details of Exploration Carried Out
Hacket (1881)	- Conducted the first reconnaissance geological mapping in and around the Borana area. - Established the preliminary geological framework of the region.
Bhattacharya & Guha (1989)	- Undertook detailed geological mapping. - Identified two major lithotectonic associations: **Sandmata Complex (granulite-gneiss association)** and **Mangalwar Complex (greenstone-granite association)**. - Characterized the lithology and metamorphic history of the Sandmata Complex. - Classified the Mangalwar Complex into Sawadri, Tanwan and

	Asan Groups, highlighting intrusive TTG plutons.
Mohanty & Guha (1990)	- Conducted geological mapping on a **1:25,000 scale**. - Investigated the high-grade rocks of the Sandmata Complex to understand the Archaean crustal evolution of the north-western Indian Shield. - Established the lithostratigraphic succession of the area.
Yadav & Garkhal (2007)	- Carried out a **gold investigation** targeting the South Delhi Fold Belt and Sandmata Complex. - Mapped the Bhatewar–Borana–Raipur area on a **1:10,000 scale**. - Assessed the gold potential and refined the local geology.
Neogi & Raza (2017) (GSI, FS 2016–17)	- Mapped the area on a **1:25,000 scale**. - Investigated the stratigraphic position and tectonic significance of granite plutons. - Explored the potential for **base metals, REE and associated minerals**. - Delineated major lithological units including the Mangalwar Complex, granitoids of the Ran Igneous Complex, and younger monzonite–syenite intrusions. - Reported abundant **allanite mineralization** within syenite/alkali feldspar syenite and migmatite gneiss near Chatrawanmata Temple, Borana. - Identified east–west trending syenite/alkali feldspar syenite bands (100–200 m thick), intrusive into migmatite gneiss, indicating favourable REE mineralization.

8.3 Reserves or resources estimated, if any, during the previous exploration campaign with quantity and grade under various categories

No reserves or resources were estimated during the previous exploration campaign.

CHAPTER 9 - AERIAL OR GROUND GEOPHYSICAL OR GEOCHEMICAL DATA

No Aerial or ground geophysical was carried out by GeoExpOre in the current study. Certain Geophysical and Geochemical studies were carried out previously by different agency, their details are as below.

9.1 Previous Geophysical Studies

The gravity and magnetic surveys conducted along the roads and cart tracks by GSI (Singh et al., 2014) in the Survey of India toposheets 45K/3, K/4, K/7, K/8 and K/12 were aimed at achieving a minimum station density of one station per 2.5 km² as per the National Geophysical Mapping Programme (NGPM). A total of 1402 gravity and magnetic stations were established in these toposheets. The minimum gravity value of -90gal was observed in the southeast part (toposheet 45K/12), while the maximum of 10gal was observed in the area's northwest part (toposheet 45K/3). The general trend of the Bouguer gravity contour is NE-SW, which follows the regional strike direction of geological formations. The E-W gravity high in part of toposheet 45K/3 near Borana and Raipur areas, which is the Sandmata Complex of Archaean Bhilwara Supergroup indicates a high-density body at shallow depth.

9.2 Previous Geochemical Investigations

The geochemical mapping in the area was initiated by Shekhawat and Garkhal (1990), covering an area of 12,100 sq. km involving about 18 SOI toposheets of scale 1: 50,000. They collected Soil and bedrock samples on a 5×5 km grid. The frequency of sample collection is one sample / 17 km^2, sample / 20 km^2, and one sample / 22 km^2 with respect to bedrock, soil, and stream sediments, respectively. The samples were analyzed for Fe, Ca, K, Na, Mg, Cu, Pb, Zn, Ni, Co, Cr, Cd, V, Hg, Mo and Se. As

and Au in selected samples.

No geochemical maps showing the dispersion of elements were prepared. Chishti and Mahadevappa (2004) carried out Geochemical mapping in toposheet Nos. 45K/3 and the southern part of toposheet 45K/6. They collected samples from three different media: stream sediment, soil and water. The density of stream sediment samples, which is the backbone of sampling, was kept at 1 sample per sq. km area. The geochemical distribution maps of oxides like Al_2O_3, SiO_2, MnO, TiO_2, and P_2O_5 and elements like Ni, Cr, and Sr show some definite patterns of their distribution, which are mainly dependent on lithology.

Sunil Kumar et al. (2016) upgraded and finalised the NGCM report of Geochemical Mapping in Toposheet Nos. 45 K/3, 4 & 7 districts Bhilwara and Rajsamand, Rajasthan. The elemental distribution maps for Y and Sc show medium to high concentrations in the GSI area of investigation.

CHAPTER 10 - EXPLORATION UNDERTAKEN DURING CURRENT INVESTIGATION

10.1 Objectives of Investigation

The present exploration work for Rare Earth Elements (REEs) and associated minerals in the Borana block, district Bhilwara, Rajasthan, aims to achieve the following objectives:

1. To carry out detailed large-scale geological mapping at a scale of 1:2000 in Borana block.
2. To collect a total of 200 samples, comprising 100 bedrock samples (BRS) and 100 trench samples (100 cubic meters), for the purpose of assessing REE distribution.
3. To conduct a Differential Global Positioning System (DGPS) survey at five locations, including one base station point and four borehole fixation points, to ensure precise spatial referencing of exploration data.
4. To execute core drilling operations up to a cumulative depth of 474 meters and to collect 235 core samples and analyze and evaluate subsurface mineralization patterns and continuity.
5. To collect, analyze petrological and petrochemical samples to characterize the mineralogical composition and ore-micrographic assemblages within the identified mineralized zones.
6. To submit report and recommendations in compliance with G3 level and suggestions for follow-up work to upgrade the project, if deemed necessary.

10.2 Basis for taking up investigation

Previous investigations carried out at Reconnaissance survey (G 4 stage) by the Geological Survey of India (GSI) and the encouraging results achieved forms the basis for this project. A reconnaissance survey for REE mineralization was conducted by GSI in F.S. 2018–19 in and around the Borana area,

which falls in the Bhilwara district of the Rajasthan State. (Das and Ahmad, 2019). The work was conducted in Toposheet No. 45K/03, covering an area of approximately 100 sq. km, which was mapped on a 1:12,500 scale. Systematic sampling and trenching were undertaken to evaluate the REE potential of the region

According to the analytical results of the 401-bedrock samples, the total REE values in migmatite gneiss range from 29.60 ppm to 3434.93 ppm, while in alkali syenite/syenite, they range from 83.03 ppm to 2336.27 ppm. The reconnaissance study revealed anomalous REE concentrations, indicating significant potential for mineralization. Based on these encouraging results, it was recommended that detailed geological mapping and higher-level investigations be undertaken to delineate the possible REE-bearing zones within the area. It was also recommended that the detailed mapping in higher level of investigation may be taken up within Migmatite Gneiss and Syenite of Mangalwar Complex near Chatrawan Mata temple, Borana area as well as south of Kemuniya village over Migmatite gneiss for identification and delineation of possible REE mineralized zone.

10.3 Details of Nature and Quantum of work Approved vs Achievement

10.3.1 Nature of work

The nature of the work and its flow pattern are shown in Table 10.1.

Table 10.1: Nature of Work

Sr. No.	Activities	1	2	3	4	5	6	7	8	9	10	11	12	13	14	15	16	17	18	19	20	21	22
		July-24	Aug-24	Sep-24	Oct-24	Nov-24	Dec-24	Jan-25	Feb-25	Mar-25	Apr-25	May-25	Jun-25	Jul-25	Aug-25	Sep-25	Oct-25	Nov-25	Dec-25	Jan-26	Feb-26	Mar-26	April -26
1	Geological Mapping (1:2000)																						
2	Trenching																						

3	Drilling																						
4	Geologist Days (field)																						
5	Sampling Days																						
6	Laboratory studies																						
7	Geologist Days HQ																						
8	Report writing																						

2.5.2 Quantum of work approved vs. achievement

The quantum of approved work and the achievements are shown in Table 10.2.

Table 10.2: Quantum of Approved Work vs Achievements

Sr. No.	Nature of Work	Target assigned	Target achieved
1	Topographical Survey – DGPS (sq.km)	5 Nos.	5 Nos.
2	Geological Mapping (LSM/DM) (Sq km).	1.14 (1:2000 scale)	1.14 (1:2000 scale)
3	Technological		
	a) Surface exploration –trenching (cu. m)	100 cu. m	100 cu m
	b) Sub-surface exploration – Drilling (mts)	474 mts	474.64 mts
4	Geochemical Survey		
	a) Bed Rock Survey (Nos)	100Nos	108Nos
	b) Trench Sample (Nos)	100 Nos.	100 Nos.
	c) Core Sample (Nos)	235 Nos	235Nos.
5	Petrographic/Mineralographic/Other studies		
	a) Petrographic (Nos)	20 Nos.	20Nos.
	b) Ore Microscopy (Nos)	20 Nos.	20 Nos.
	c) XRD*	20 Nos.	20 Nos.
	d) Bulk Density	5 Nos.	5 Nos.
	e) EPMA*	10 Hrs	10 Hrs
6	Chemical Analysis		
	a) Chemical Analysis – BRS	100 Nos.	100 Nos.
	b) Chemical Analysis – Trench	100 Nos.	100 Nos.
	c) Chemical Analysis – Core	235 Nos.	222 Nos.
	d) External Check samples (10% of Primary Samples)	42 Nos.	42 Nos.
	e) ICPMS 34 trace elements	20 Nos.	20 Nos.
	f) Whole Rock Analysis	10 Nos.	10 Nos.

*XRD interpretation and EPMA analyses results are awaited

2.5.3 Achievement

Under the approved G3 exploration program for the Borana block, the assigned field and laboratory targets were largely achieved in full. The team completed all 5 DGPS topographical survey points as targeted and carried out detailed geological mapping over 1.14 sq. km at 1:2,000 scale. In the technological component, 100 cu m of trenching was completed while 474.64 m of drilling was achieved against the proposed 474 m. Under geochemical survey, the team collected 108 bedrock samples against the target of 100 samples, whereas the targets for 100 trench samples and 235 core samples were achieved in full. In laboratory and mineralogical studies, the targets for 20 petrographic studies, 20 ore microscopic studies, 20 XRD analyses, and 5 bulk density determinations were fully achieved.

About chemical analysis, all targeted 100 bedrock samples and 100 trench samples were analyzed. Out of the 235 core samples collected, 222 samples were subjected to chemical analysis. The remaining 13 core samples represented amphibolitic lithology, which, based on field observations, petro-mineralogical character, and established geological understanding of the block, was considered non-prospective for significant REE mineralization in comparison to the felsic and syenitic host assemblages. Since amphibolite in the investigated area was not recognized as the principal host for REE enrichment, those samples were not prioritized for primary REE assay, and the analytical effort was focused on lithologies having greater exploration significance from the standpoint of REE concentration and continuity.

External check sampling was carried out in accordance with the prescribed 10% quality-control protocol. Since the total number of primary samples analyzed comprised 100 bedrock samples, 100 trench samples, and 222 core samples, the effective analytical population came to 422 samples. Accordingly, 42 samples were submitted for external check analysis, which satisfies the required 10% check-sample criterion on the analyzed primary sample set. In addition, the targets for 20 ICP-MS analyses for 34 trace elements and 10 whole-rock analyses were fully achieved. Overall, the program generated a substantial geological, geochemical, drilling, mineralogical, and analytical database for appraisal of REE and associated mineral potential in the Borana block.

10.4 Mode of operation of different work components and associated agency

GeoExpOre Pvt. Ltd. carried out exploration activity by detailed geological mapping and sample collections from outcrops and trenches on 1:2000 scale and associated works including the final G-3 stage report preparation. Chemical analysis of bed rock samples, trench samples and core samples were done by Shiva Analyticals (India) Limited, Bengaluru. Further petrographic studies were carried out through Geological Survey of India, Bengaluru and XRD, EPMA, Bulk density and external check for samples were analyzed at Indian institute of Science Bangalore.

10.5 Details of pitting, trenching, drilling, etc., with spacing and distribution of the sample points along with geographical co-ordinates.

10.5.1 Trenching

10.5.1.1 Trenching Methodology

Trenching was carried out in investigation to know the lateral extension of the REE and associated mineral bearing rock types in the submerged soil covered areas. A total of five trenches were excavated as detailed in Table 10.3. Trench's locations were selected based on prepared geochemical dispersion map shown in (Plate 4). Total five nos. of trenches were excavated to prove the strike extension and to expose the width of the mineralized rock. The trenches each 20 meters long, 1 meter deep and 1 meter wide were used to extrapolate the subsurface strike and depth of potential mineralized units for sampling. In total, 100 cubic meters of trenching was performed, yielding 50 trench samples collected from channels along the floor and walls of the trenches. Approximately 1 kilogram of sample was collected from every 2 meters of the suspected mineralized zones. The trench locations are depicted in the geological map (plate-2).

Trench samples collected from every trench and the individual sample width was kept based on lithology and mineralization. Total 50 numbers of trench samples were collected and the same was analyzed. Geochemical analysis of all trench samples was conducted using ICP-OES, preceded by acid digestion was performed by Shiva Analyticals, Bangalore. The geochemical data for all trenches is provided in Annexure-VIII b.

Table 10.3: Represents the location and bearing of the Trenches

Sr No	Trench Name	Latitude	Longitude	Direction	Length (m)	Width (m)	Depth (m)	Volume (cu.m)
1.	RJBO/T1/2024-25	25.43169	74.12522	NW-SE	20	1	1	20
		25.43158	74.12533					
2.	RJBO/T2/2024-25	25.42922	74.12483	NW-SE	20	1	1	20
		25.43028	74.125E					
3.	RJBO/T3/2024-25	25.43044	74.12236	NW-SE	20	1	1	20
		25.43028	74.12244					
4.	RJBO/T4/2024-25	25.42933	74.12103	NW-SE	20	1	1	20
		25.42922	74.12117					
5.	RJBO/T5/2024-25	25.43119	74.1185	NW-SE	20	1	1	20
		25.43119	74.11867					

10.5.1.2 Trench description

10.5.1.2.1 Trench 1-RJBO/T1/2024-25

Trench-1 was excavated at location from 25.43169N, 74.12522E to 25.43158N, 74.12533E. Trench-1 was selected on the basis of high REE concentrations reported from nearby BRS sample locations, supported further by the geochemical dispersion map prepared for the area (Plate 4), with the objective of assessing the lateral continuity of REE enrichment in the area. The trench was oriented along a N63°W direction and exposed a uniform lithological profile throughout the entire cross-section.

Along the full length of Trench-1, only syenite rock was encountered, showing no significant change in lithology. Representative samples collected from the exposed section were analyzed for REE concentrations. Geochemically, the REE distribution within Trench-1 is dominated by Light Rare

Earth Elements (LREEs), which constitute approximately 95.39 % of the total REE, while Heavy Rare Earth Elements (HREEs) account for the remaining 4.61 % with an LREE:HREE ratio of 20.70: 1. The average, maximum and minimum REE values obtained is shown in Table 10.4. The relative proportion of LREE and HREE is illustrated in the pie chart shown in Fig 10.1d. Fig.10.1a: (i) represent demarcated trench photographs before excavating (ii) represents trench during with the collection of composite samples and (iii) represents after excavation trench properly closed and backfilled. Fig 10.1b represents cross section of Trench-1. Fig. 10.1c represents cross section of Trench-1 with values.

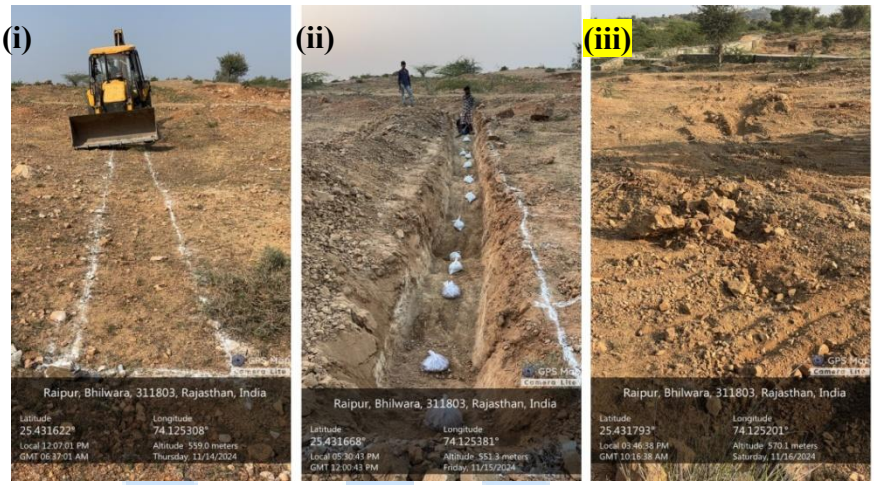

Fig 10.1a Trench no RJBO/T1/2024-25(i) represent demarcated trench photographs before excavating (ii) represents trench dug with the collection of composite samples and (iii) represents after excavation trench properly closed and backfilled

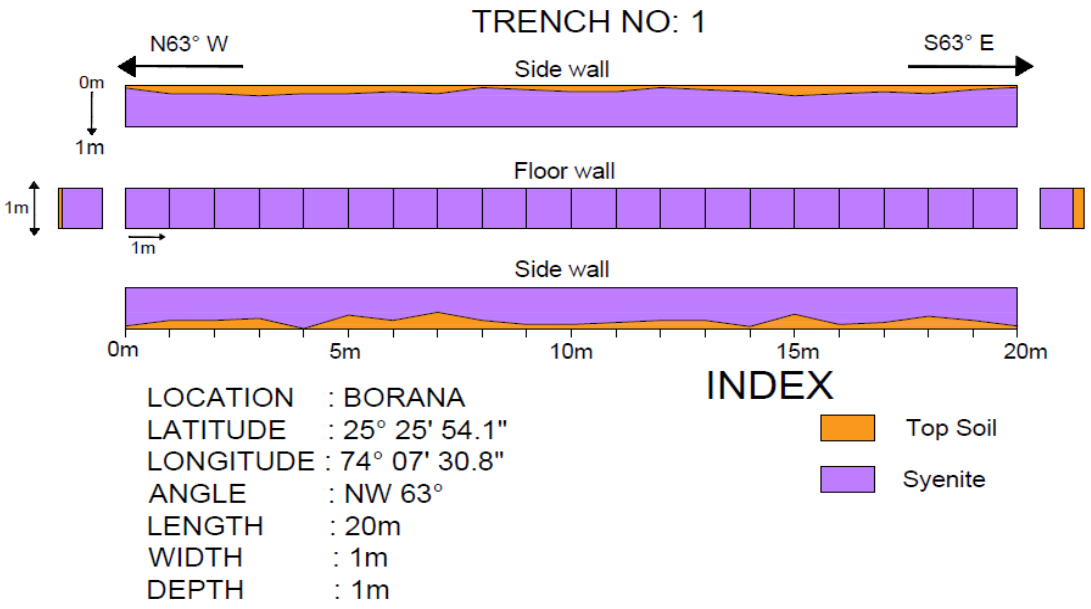

Fig 10.1b Cross section of Trench-1 (RJBO/T1/2024-25)

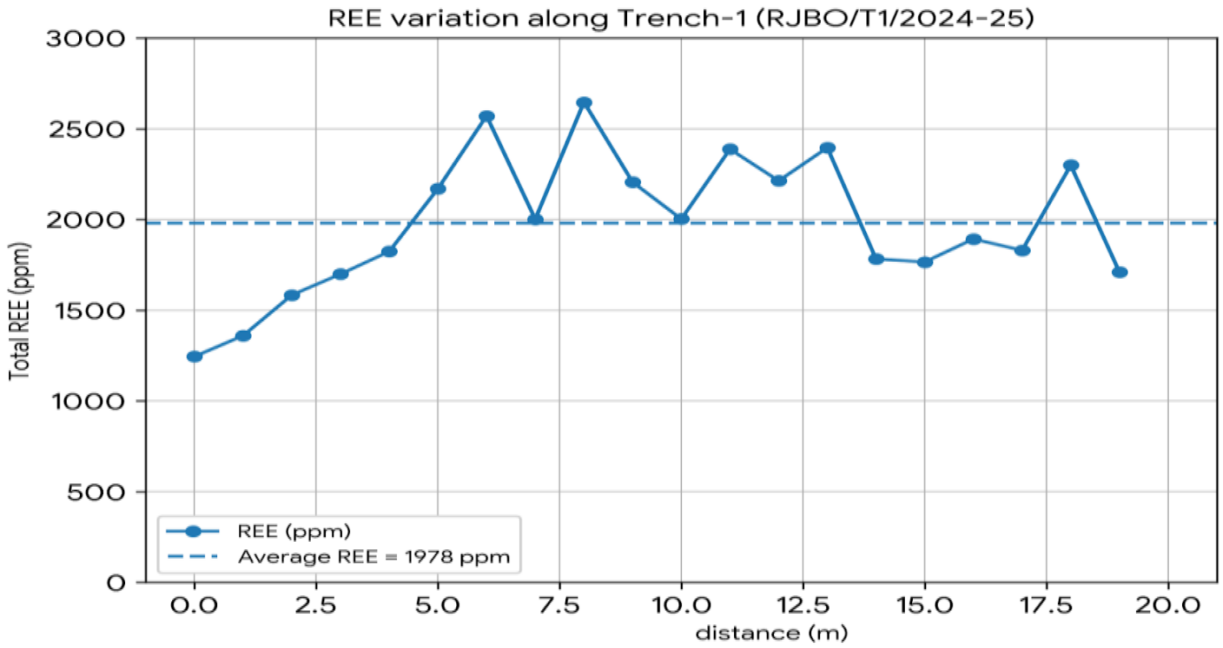

Fig 10.1c Cross section of Trench-1 with TREE vs distance along Trench (RJBO/T1/2024-25)

Table 10.4: The average, maximum and minimum REE values obtained from Trench-1 (RJBO/T1/2024-25)

	TREE	HREE	LREE
AVG	1978.462	91.163	1887.29
MIN	1243.99	73.53	1169.64
MAX	2645.85	114.92	2530.93

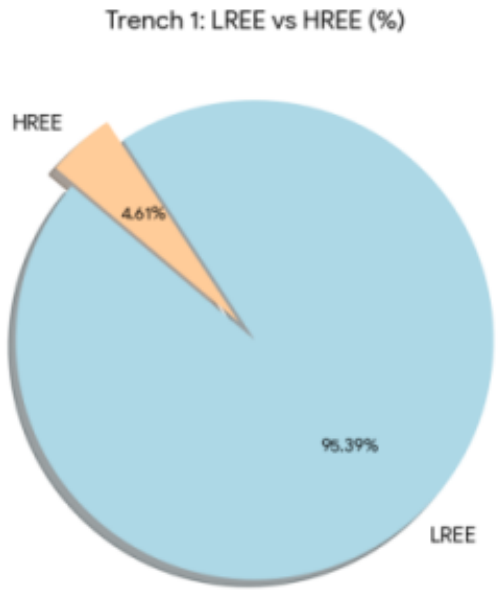

Fig 10.1d LREE and HREE proportion with its **ratio (LREE: HREE= 20.70: 1)** in Trench-1(RJBO/T1/2024-25)

10.5.1.2.2 Trench 2-RJBO/T2/2024-25

Trench-2 was excavated at a location from 25.42922N, 74.12483E to 25.43028N, 74.125E. The trench was oriented along a N64°W direction. Excavation of Trench-2 exposed two distinct lithologies along the trench cross-section, migmatite gneiss, quartz vein and syenite. Representative samples collected along the trench were analyzed for REE concentrations. The average, maximum and minimum REE values obtained from Trench-2 are presented in Table 10.5.

The REE distribution pattern of Trench-2 shows dominance of Light Rare Earth Elements (LREEs), which account for approximately 83.89% of the total REE content. Heavy Rare Earth Elements (HREEs) constitute the remaining 16.11% with an LREE–HREE proportion ratio of 5.82: 1 is depicted in the pie chart shown in Fig 10.2d. Fig. 10.2a (i) represent demarcated trench photographs before excavating (ii) represents trench dug with the collection of composite samples and (iii) represents after excavation trench properly closed and backfilled. Fig 10.2b Represents cross section of Trench-2. Fig. 10.2c Represents cross section of Trench-2 with REE (TREE) vs trench width plot.

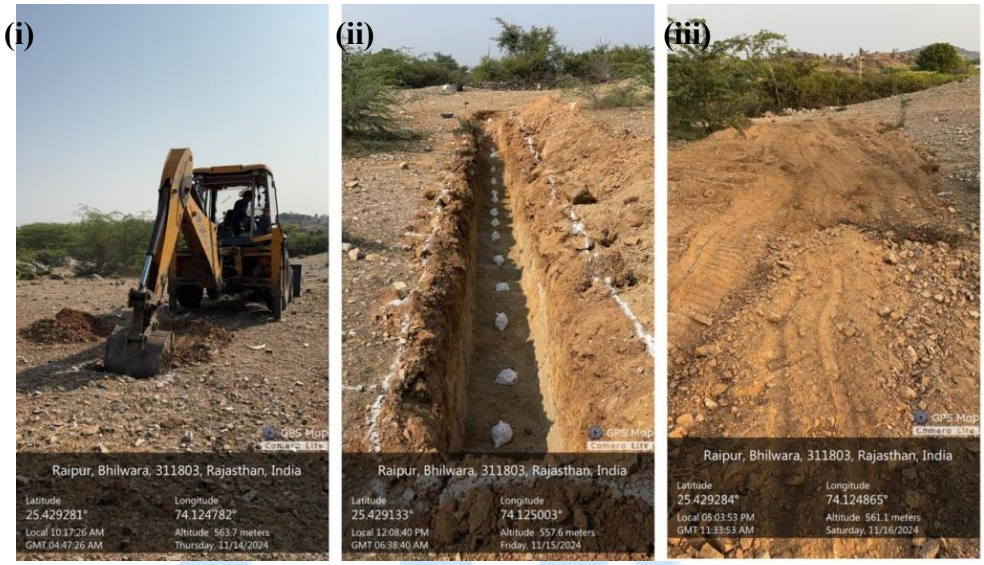

Fig 10.2a Trench no RJBO/T2/2024-25 (i) represent demarcated trench photographs before excavating (ii) represents trench dug with the collection of composite samples and (iii) represents after excavation trench properly closed and backfilled

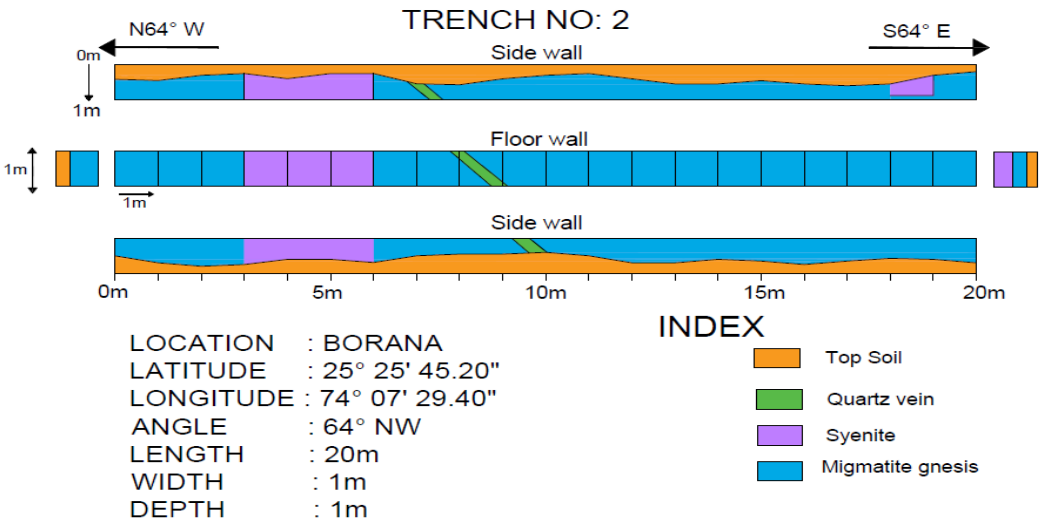

Fig 10.2b Cross section of Trench-2 (RJBO/T2/2024-25)

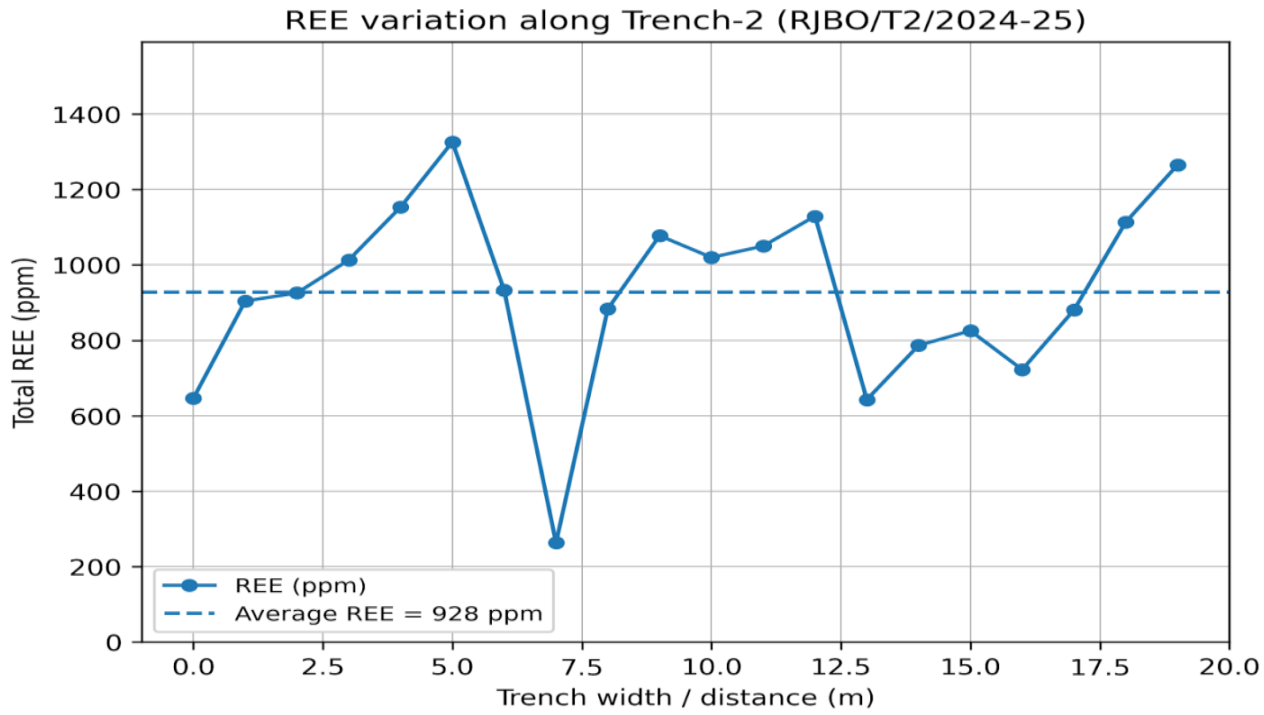

Fig 10.2c Cross section of Trench-2 with REE (TREE) vs trench width plot (RJBO/T2/2024-25)

Table 10.5: The average, maximum and minimum REE values obtained from Trench-2(RJBO/T2/2024-25)

	TREE	HREE	LREE
AVG	928.07	149.51	871.03
MIN	262.83	45.08	245.4
MAX	1326.27	203.91	1243.41

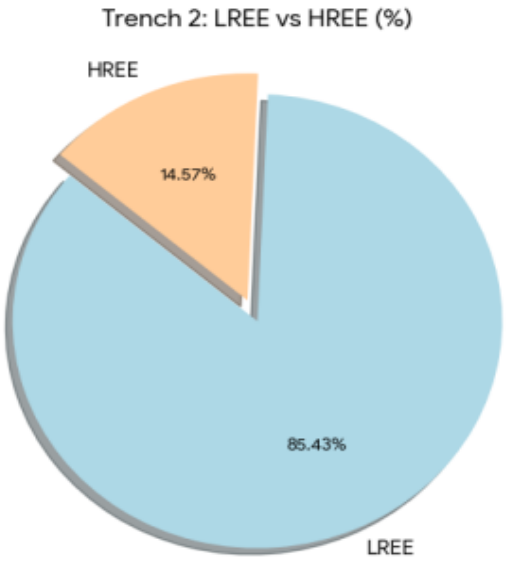

Fig 10.2d LREE and HREE proportion with **ratio (LREE: HREE= 5.87: 1**) in Trench-2 (RJBO/T25/2024-25)

10.5.1.2.3 Trench-3 RJBO/T3/2024-25

Trench-3 was excavated at a location from identified from 25.43044N, 74.12236E and 25.43028N, 74.12244E. The trench was oriented along a N56°W direction to examine the continuity of REE enrichment and to understand the lithological controls influencing REE distribution in the area.

Excavation revealed a lithological profile consisting of migmatite gneiss with occurrences of pegmatite vein exposed along the trench cross-section. The pegmatite veins occur as thin intrusion within the migmatite gneiss. Representative samples collected were analyzed for REE concentrations. The average, maximum and minimum REE values for Trench-3 are provided in Table 10.6.

Geochemically, Trench-3 shows a strong dominance of Light Rare Earth Elements (LREEs), which constitute approximately 94% of the total REE content, while Heavy Rare Earth Elements (HREEs) make up the remaining 6% with an LREE:HREE ratio of 15.68:1. The proportion of LREEs and HREEs is illustrated in the pie chart shown in Fig 10.3d.

Fig.10.3a (i) represent demarcated trench photographs before excavating (ii) represent trench dug with the collection of composite samples and (iii) represents after excavation trench properly closed and backfilled. Fig.10.3b represents cross section of Trench-3. Fig.10.3c represents cross section of Trench-3 with REE (TREE) vs trench width plot.

Fig 10.3a Trench no RJBO/T3/2024-25 (i) represent demarcated trench photographs before excavating (ii) represents trench dug with the collection of composite samples and (iii) represents after excavation trench properly closed and backfilled

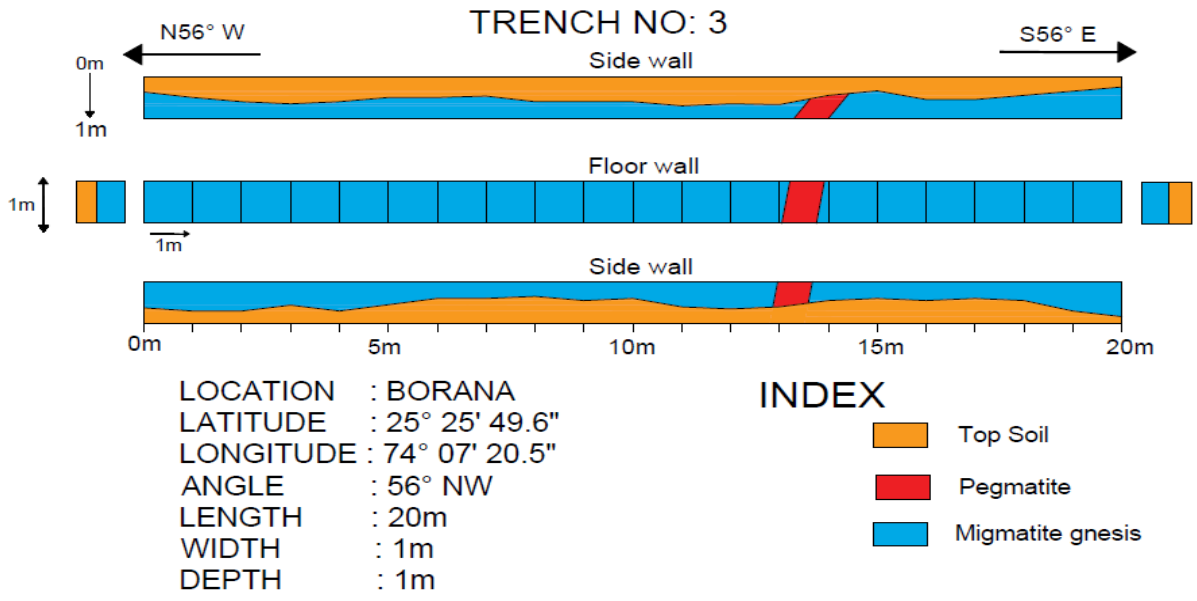

Fig 10.3b Cross section of Trench-3 (RJBO/T3/2024-25)

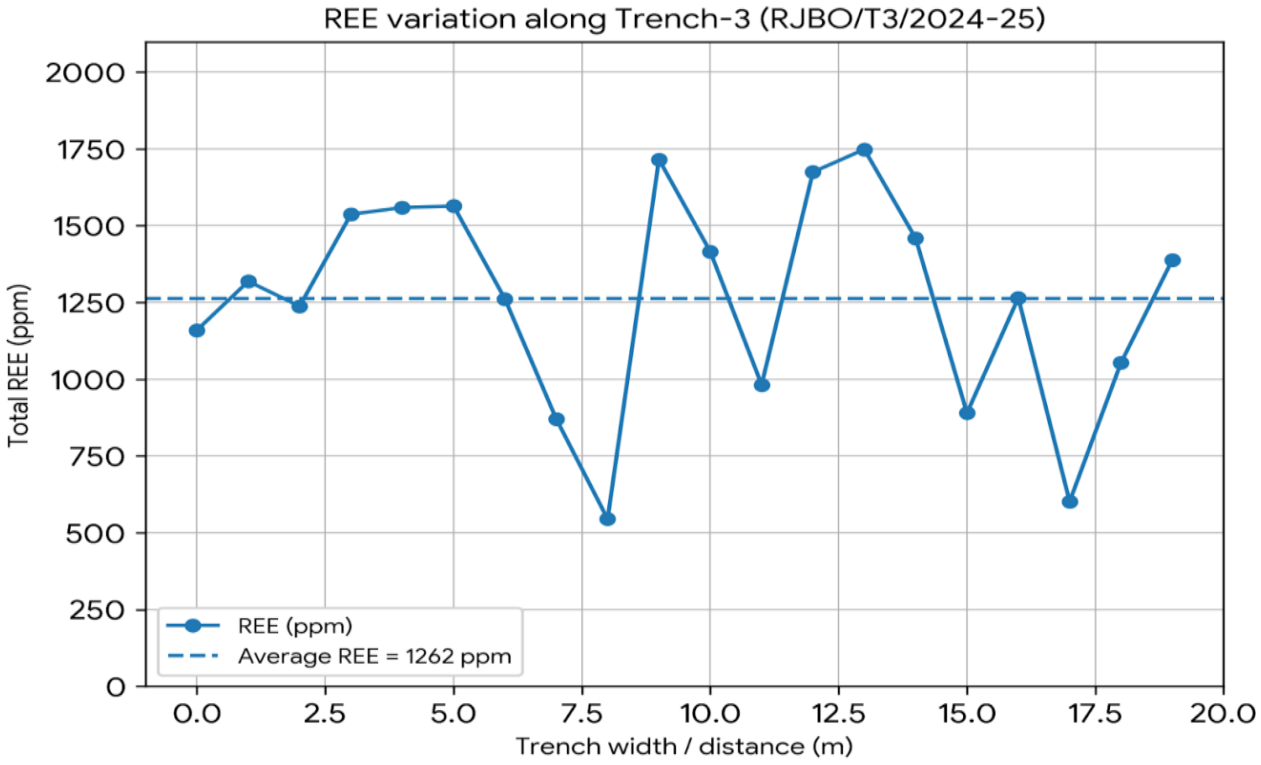

Fig 10.3c Cross section of Trench-3 with REE (TREE) vs trench width plot (RJBO/T3/2024-25)

Table 10.6: The average, maximum and minimum REE values obtained fromTrench-3(RJBO/T3/2024-25)

	TREE	HREE	LREE
AVG	1262.09	75.68	1186.41
MIN	544.75	37.17	507.58
MAX	1748.22	106.23	1641.99

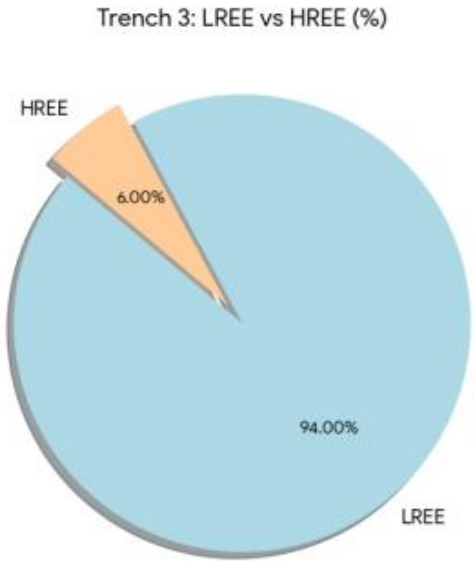

Fig 10.3d LREE and HREE proportion with **ratio (LREE: HREE= 15.68:1)** in Trench-3(RJBO/T3/2024-25)

10.5.1.2.4 Trench-4 RJBO/T4/2024-25

Trench-4 was excavated at a location 25.42933N, 74.12103E and 25.42922N, 74.12117E. The trench was aligned along a N62°W direction to assess the continuity of REE mineralization. Excavation of Trench-4 exposed two lithologies, consisting of syenite and migmatite gneiss throughout the trench cross-section. Representative samples collected from the trench were analyzed for REE content, and the average, maximum and minimum REE values for Trench-4 are summarized in Table 10.7.

Geochemically, Trench-4 exhibits a dominant presence of Light Rare Earth Elements (LREEs), constituting approximately 92.13% of the total REE concentration, while Heavy Rare Earth Elements (HREEs) account for 7.87% with an LREE:HREE ratio of 11.70 : 1. The LREE–HREE distribution is illustrated in the pie chart shown in Fig.10.4d. Fig.10.4a (i) represent demarcated trench photographs before excavating (ii) represents trench dug with the collection of composite samples and (iii) represents after excavation trench properly closed and backfilled. Fig.10.4b represents cross section

of Trench-4. Fig. 10.4c represents cross section of Trench-4 with REE (TREE) vs trench width plot.

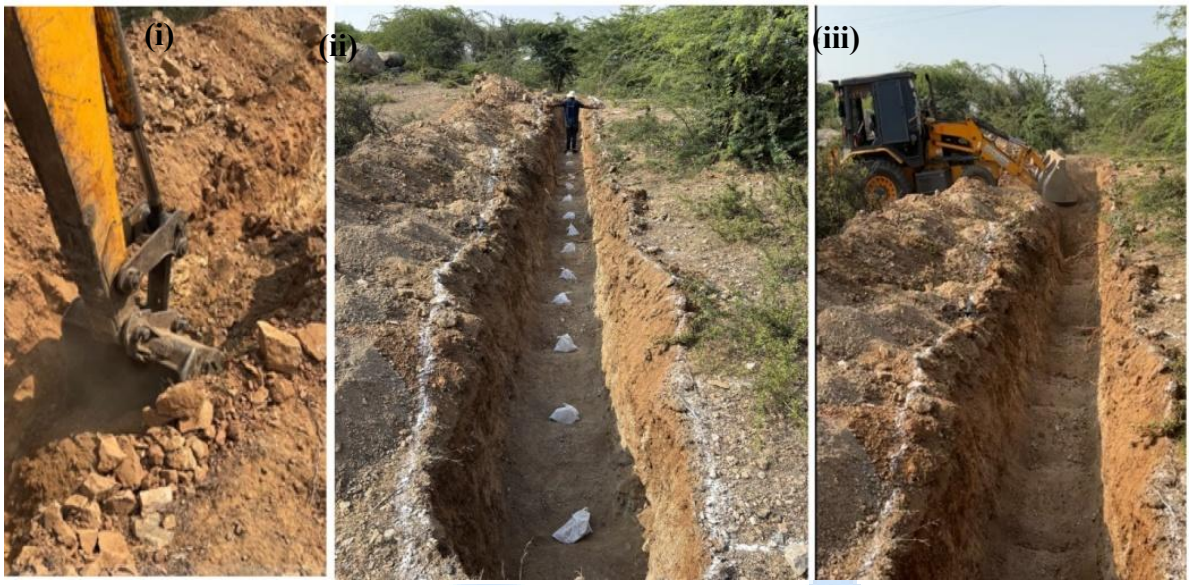

Fig 10.4a Trench no RJBO/T4/2024-25 (i) represent demarcated trench photographs before excavating (ii) represents trench dug with the collection of composite samples and (iii) represents after excavation trench properly closing and backfilling

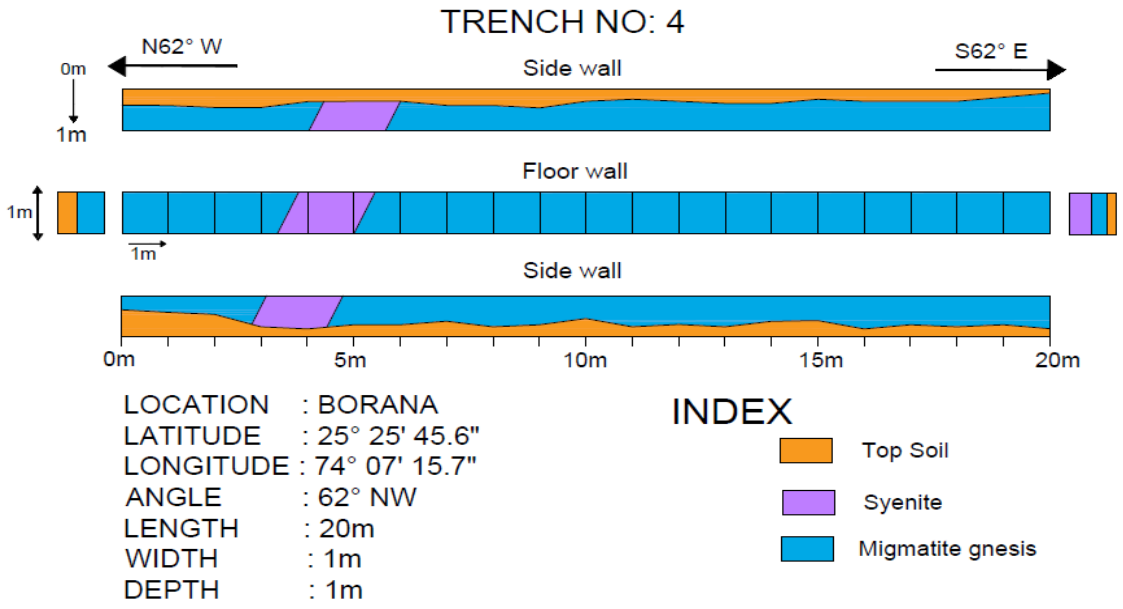

Fig 10.4b Cross section of Trench-4 (RJBO/T4/2024-25)

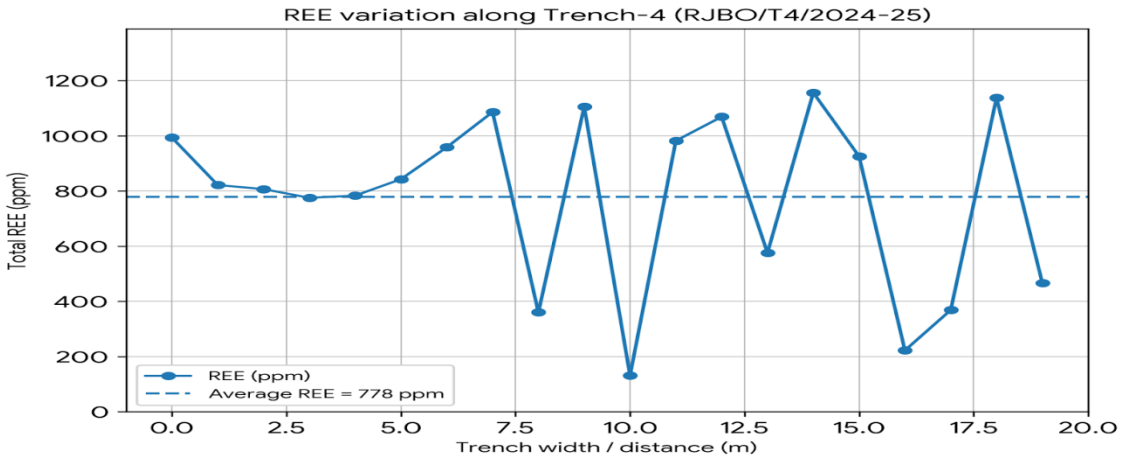

Fig 10.4c Cross section of Trench-4 with REE (TREE) vs trench width plot (RJBO/T4/2024-25)

Table 10.7: The average, maximum and minimum REE values obtained fromTrench-4(RJBO/T4/2024-25)

	LREE
AVG	717.09
MIN	117.58
MAX	1038.55

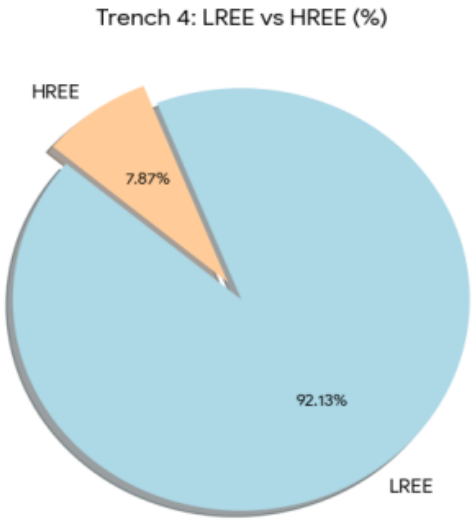

Fig 10.4d LREE and HREE proportion with **ratio (LREE: HREE= 11.70: 1)** in Trench-4 (RJBO/T4/2024-25)

10.5.1.2.5 Trench-5 RJBO/T5/2024-25

Trench-5 was excavated at a location 25.431194N, 74.1185E and 25.431194N, 74.118667E. The trench was aligned along a S73°W direction to assess the continuity of REE mineralization. Excavation of Trench-5 exposed migmatite gneiss consisting throughout the trench cross-section. Representative

samples collected from the trench were analyzed for REE content, and the average, maximum and minimum REE values for Trench-5 are summarized in Table 10.8.

Geochemically, Trench-5 exhibits a dominant presence of Light Rare Earth Elements (LREEs), constituting approximately 93.06% of the total REE concentration, while Heavy Rare Earth Elements (HREEs) account for 6.94% with an LREE:HREE ratio of 13.41 : 1. The LREE–HREE distribution is illustrated in the pie chart shown in Fig.10.5d. Fig.10.5a (i) represent demarcated trench photographs before excavating (ii) represents trench dug with the collection of composite samples and (iii) represents after excavation trench properly closed and backfilled. Fig.10.5b Represents cross section of Trench-5. Fig.10.5c Represents cross section of Trench-5 with REE (TREE) vs trench width plot.

Fig 10.5a Trench no RJBO/T5/2024-25 (i) represent demarcated trench photographs before excavating (ii) represents trench dug with the collection of composite samples and (iii) represents after excavation trench properly closing and backfilling

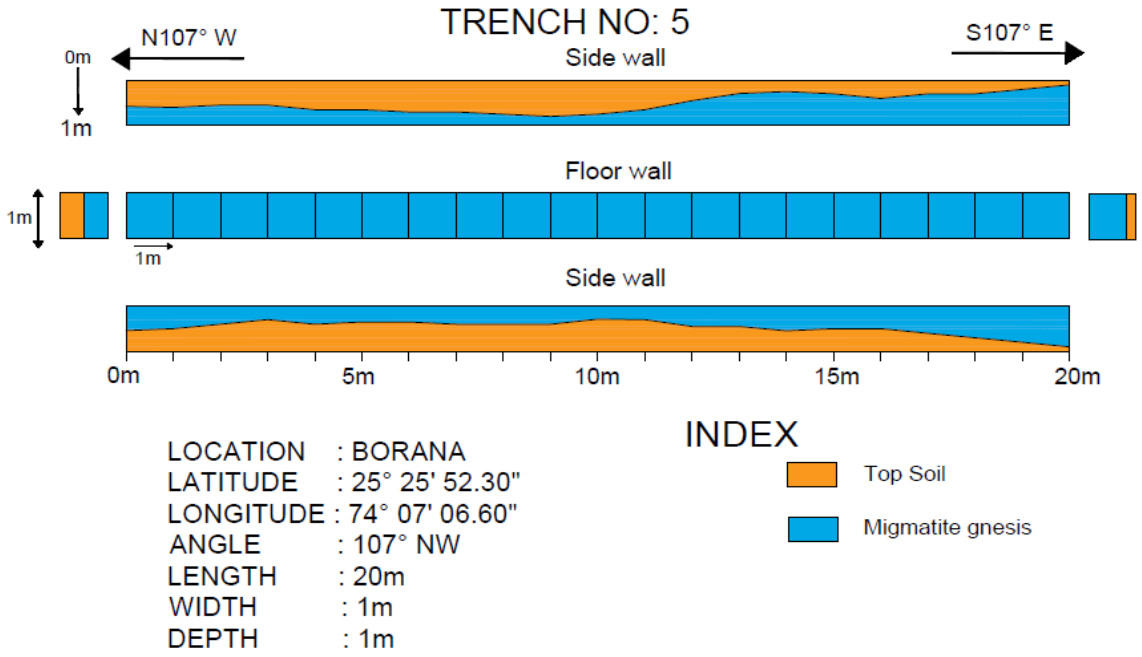

Fig 10.5b Cross section of Trench-5 (RJBO/T4/2024-25)

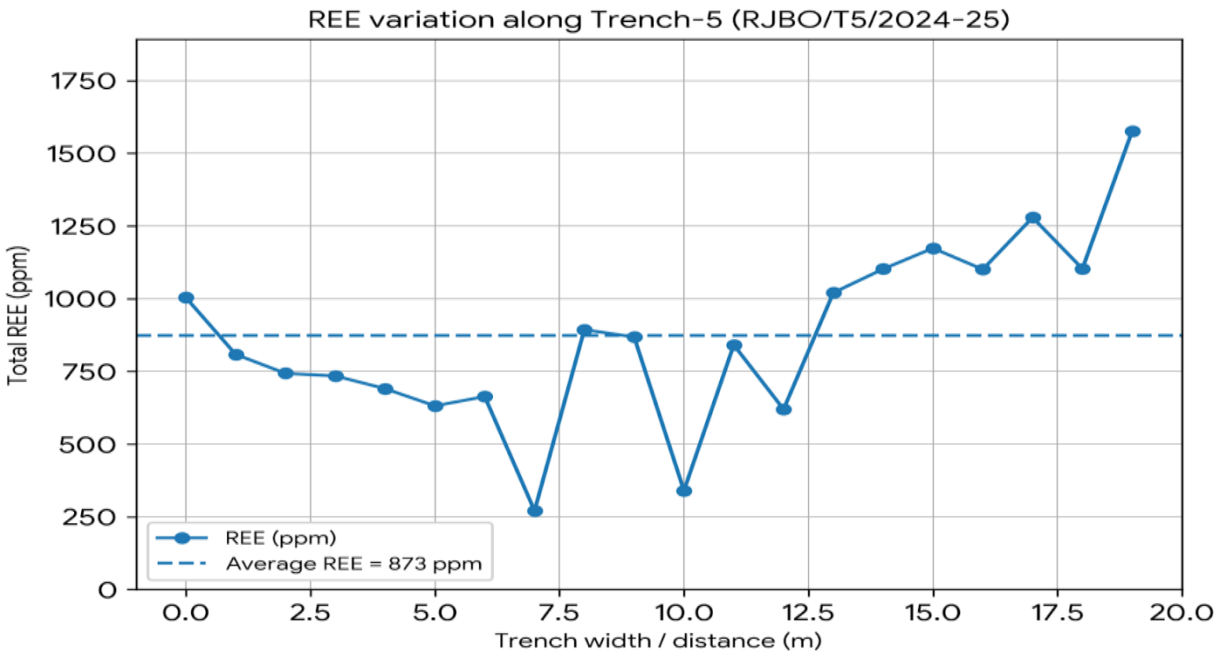

Fig 10.5c Cross section of Trench-5 with REE (TREE) vs trench width plot (RJBO/T5/2024-25)

Table 10.8: The average, maximum and minimum REE values obtained fromTrench-5(RJBO/T5/2024-25)

	TREE	HREE	LREE
AVG	872.93	60.59	812.344
MIN	270.63	19.3	251.33
MAX	1576.22	100.76	1475.46

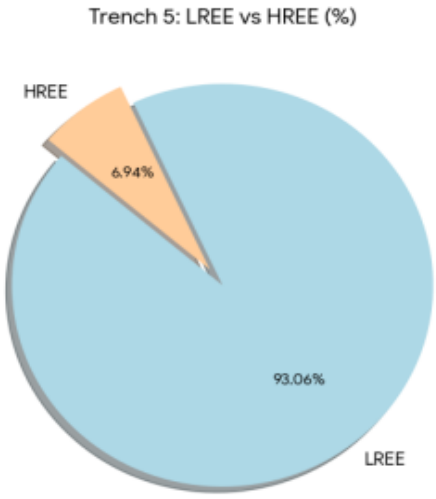

Fig 10.5d LREE and HREE proportion with **ratio (LREE: HREE= 13.41: 1)** in Trench-5 (RJBO/T5/2024-25)

10.5.2 Drilling

As per the MEMC Rules, 2015, for exploration at the G3 stage, grid spacing of boreholes is about 200 m. As the block was carried out at about 200 x 200 m grid pattern along Northeast-Southwest direction with spacing of 200 m interval. A total of four inclined boreholes of 45° inclination (BH-01 to BH-04), aggregating to 474.64 m of drilling were completed in the Borana Block to define the mineral resource under the Inferred category. The interval for drill core samples has been identified during the

logging. The sampling was carried out mostly at one-meter intervals.

10.6 Data spacing for reporting of exploration results:

The current borehole grid spacing of 200m has provided preliminary understanding of the deposit's geometry.

CHAPTER 11 - LOCATION OF DATA POINT

11.1 Accuracy and quality of surveys used to locate drill holes (collar and down-hole surveys, azimuth, inclination, coordinates of bore holes etc), trenches, mine workings and other locations used in mineral resource estimation.

Differential Global Positioning System (DGPS) survey was carried out in Borana Block to establish accurate ground control for the proposed drilling programme. A total of five DGPS points were surveyed and fixed, including one base point and four borehole fixation points. Hence assuring the accuracy and quality of surveys used to locate drill holes.

Code	Original Latitude	Original Longitude	Original Altitude	Antenna Height (m)	Northing (mts)	Easting (mts)	Elevation (m)
TBM-1	25°25'54.1206"	74°07'33.4274"	508.389	1.8	2813038.591	412108.584	555.53

Table 11.1 Co-ordinates of the base station for DGPS Survey

11.2 Quality and adequacy of topographic control.

Block boundary co-ordinates, the surface features, contour points and borehole pints were surveyed by DGPS.

CHAPTER 12 - SAMPLING TECHNIQUE

12.1 Nature and quality of sampling (eg. cut channels, random chips, etc.) and measures taken to ensure sample representation.

In order to assess the REE & associated mineral potential in the investigated area, a total of 108 number of bedrock samples (BRS), 100 number of trenching samples, 222 number of core samples, 20 number of petrological samples, 20 number of XRD samples, 20 number of ICPMS samples for 34 trace elements, 5 samples for bulk density, 4 samples for EPMA, 10 samples for whole rock elemental analysis and 10% of external check samples (bedrock samples, trench samples and core samples were selected. These samples were submitted in their respective laboratories for analysis. (Shiva Analytical Lab, Bangalore, GSI Bangalore and IISc Bangalore).

12.1.1 Bed rock sampling

A total of 108 nos. of bedrock samples were collected from different rock units (59 nos. from migmatite gneiss, 45 nos. from syenite, 1 no. from pegmatite, 2 nos. from amphibolite and 1 no. from the quartz vein). Samples were collected to target the main mineralized zones and samples were collected based on availability of desired rock type exposed in the investigated area. Most samples contributed from migmatite gneiss and syenites, as the mineralization in the area have been reported from the earlier and recent GSI G4 investigation.

Surface evidence of mineralization such as dispersion of allanite grains, epidotization, small crystals of magnetite in both migmatite and syenites were used as the target to get best mineralized samples. BRS samples have also been collected in between the BRS samples collected by GSI during their G4 study to establish the continuity of the mineralized zones. The quantity of samples collected varies from 1-1.5 kgs and the same was handed over to Shiva Analytical Bangalore with a request to analyze

the samples for REE for 14 elements by ICPMS method. The sample location map is shown in Plate-3.

PLATE - 3

SAMPLE LOCATION SHOWN ON GEOLOGICAL MAP OF BORANA BLOCK,BHILWARA DISTRICT, RAJASTHAN

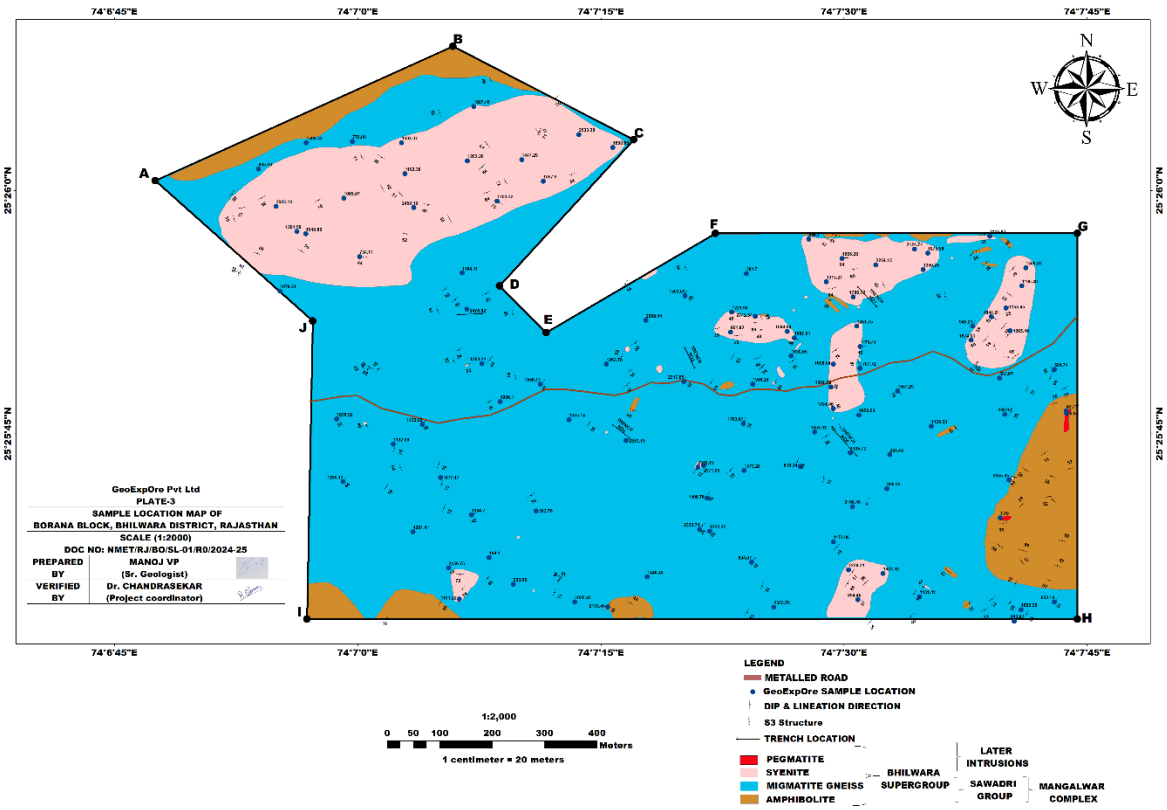

12.1.2 Trench sampling

Trenching was carried out in investigation to know the lateral extension of the REE and associated mineral rock types in the submerged soil covered areas. In total, five nos. of trenches were excavated. The dimensions of the trench are 20m in length, 1m width and 1m depth. These trench locations are depicted in the geological map (Plate-2). Samples were collected mostly from NNW to SSE direction for every trench and the individual sample width was kept based on lithology and mineralization. In total, 50 nos. of trench samples were collected and the same was analyzed at chemical lab Shiva Analytical, Bangalore.

12.1.3 Core sampling

A total of 222 nos. of samples were collected from four boreholes for every one meters interval. The collected samples were submitted for chemical analysis at Shiva Lab Bangalore.

12.1.4 External check sampling

To check the reliability of the analysis 10 % of the bedrock samples, 10 % of trench samples and 10% of core samples already analyzed were selected with the different range of REE values and the same was subjected for chemical analysis and compared with the primary samples analyzed values (Annexure VII a & VII b).

CHAPTER 13 - DRILLING TECHNIQUE AND DRILL SAMPLING EMPLOYED

13.1 Drill type (eg. core, reverse circulation, open-hole hammer, rotary air blast, auger, Bangka, sonic, etc.) and details (eg. core diameter, triple or standard tube).

Diamond Drill type was deployed for Inclined boreholes at 45 degree inclination. The wet drilling has been carried out with NQ size diameter (Core diameter: ~63.5 mm, Hole diameter: ~96 mm). A maximum 3 m run was deployed in single run of drilling. The depth wise drill core was sequentially preserved in the core box.

13.2 Whether core and chip sample recoveries have been properly recorded and results assessed.

The core samples have been recorded properly and the detailed borehole wise run wise lithologs and summarized lithologs for boreholes are given in Annexure-X. The run wise lithologs of drilled core as well as the cuttings from boreholes have helped in discerning the physical characters like colour, shape, size and nature of the mineralisation as well as texture, structural features and identification of different litho units.

13.3 Measures taken to maximize sample recovery and ensure representative nature of the samples.

The entire core drilling has been done by NQ size diamond drill bit with single barrel wire line, wet core drilling method to optimize sample recovery.

13.4 Whether a relationship exists between sample recovery and grade and whether sample bias could have occurred due to preferential loss or gain of fine or coarse material.

The drilling programme in the Borana Block yielded generally good core recovery, and no significant relationship was observed between sample recovery and REE grade. Core recovery was consistently monitored and recorded during drilling, with recovered core lengths measured against drilled intervals. The recovered core was systematically logged, photographed, and sampled according to standard geological procedures.

No evidence of sample bias due to preferential loss or gain of fine- or coarse-grained material was identified. The lithologies encountered, comprising predominantly syenite, migmatite gneiss, amphibolite, pegmatite, and associated weathered zones, exhibited competent core recovery over most of the drilled intervals. Any minor reduction in recovery within highly weathered or fractured zones was localized and did not correspond with anomalously high or low REE grades.

Sampling was carried out on recovered core over predetermined geological intervals without selective exclusion or inclusion of material. Standard sample preparation procedures, including crushing, splitting, and pulverization, were adopted at the laboratory to ensure representative samples for geochemical analysis. Accordingly, it is considered that sample recovery did not materially influence the reported assay results, and no significant sampling bias arising from differential recovery of fine or coarse material is expected.

13.5 Logging: -Whether core and chip samples have been logged to a level of detail to support appropriate Mineral Resource estimation, mining studies and metallurgical studies.

The diamond drill cores were geologically and geotechnically logged in sufficient detail to support the G3-stage Mineral Resource estimation. Logging included lithology, weathering, alteration, structures, mineralization, core recovery, and RQD, wherever applicable. Core was systematically photographed and sampled based on geological boundaries following standard procedures. The quality and level of logging are considered adequate to establish geological continuity and support the current stage of resource estimation.

13.6 Exploration Systematic Drilling

The core drilling in the block was executed by GeoExpOre Pvt. Ltd. The wet drilling has been carried out with NQ size diameter (Core diameter: ~63.5 mm, Hole diameter: ~96 mm). A maximum 3 m run was deployed in single run of drilling. The depth wise drill core was sequentially preserved in the core box. Average core recovery of all the 4 boreholes is 85.43%. Drilling site photographs are shown in Fig.13.1. The borehole details are tabulated in Table 13.1.

Table 13.1 Borehole Details

Sr. No.	BH No	Easting	Northing	RL in (m)	Depth (m)
1	BH-01	74° 07' 32.6900"	25° 25' 53.9427"	507.092	85m
2	BH-02	74° 07' 18.0708"	25° 25' 10.5262"	504.521	154.64m
3	BH-03	74° 07' 22.7573"	25° 25' 44.5360"	507.692	150m
4	BH-04	74°07'27.79"	25° 25' 49.35"	509.358	85m

Fig 13.1 Drilling site photographs

13.6.1 Drill Core Logging

The drill cores were logged to determine the run details, recovery factors, mineralization details and lithology. The lithological domains were initially defined based on the visual inspection of the features and later revised based on the chemical analysis results. Logging was qualitative in nature, i.e. based on lithology. Four litho units have been identified including migmatite gneiss, syenite, pegmatite and amphibolite.

During core logging, REE mineralization was observed predominantly represented by allanite seen both in syenite and migmatite gneiss and sulfides were observed. Drill core recovery with REE mineralization photographs are shown in Fig. 13.2. Drill cores showing Albitization and Epidotization Fig.13.3. Drill core shows Sulfides mineralization. Fig.13.4.

The detailed litho logs and summarized litho logs of all the boreholes are presented in Annexure X. The data was used for cross sections and further resource estimation The individual transverse cross sections for all the four boreholes are shown in Plate 6 to Plate 9.

Fig 13.2 Drill core recovery with REE mineralization

Fig 13.3 Drill core showing Albitization and Epidotization

Fig 13.4 Drill core showing Sulfides mineralization

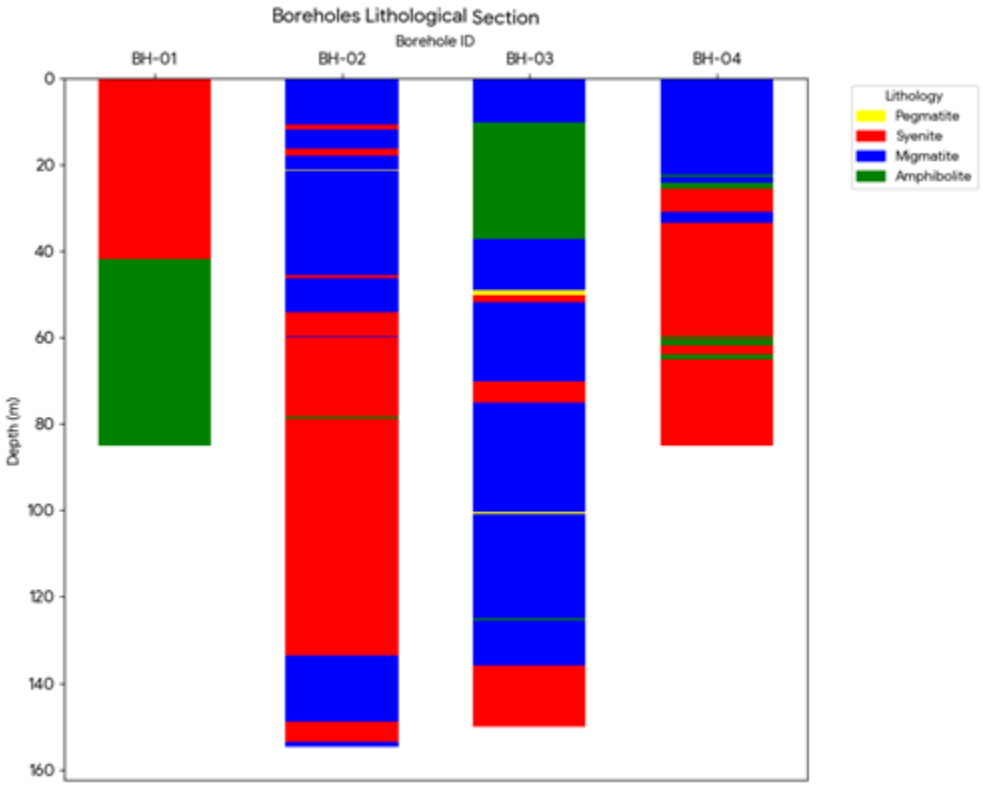

Fig 13.5 Boreholes Lithology Section

13.6.2 Drill Core Sampling

The interval for drill core samples has been identified during the logging. The sampling was carried out mostly at one-meter intervals. For sampling purposes, the drill core was vertically split into two equal halves. One half was retained in the core box for future reference and other half for further lab studies. Though 235 samples were to be analyzed as per NQT, only total of 222 nos. of primary core samples were sampled and sent to the laboratory to analyze REE content as rest samples belonged to amphibolite which were expected to be REE barren. A total of 222 half-core samples were crushed and ground to finer than 100 mesh. Representative samples were collected as per standard sampling procedures and were subjected to ICP-MS analysis.

13.7 Drill Core Preservation

The drill cores are preserved in Aluminum boxes and labelled with relevant details like borehole

number, box number, run interval from top to bottom etc.. They were then transported to core facility near Rayagada OMC office for further inspection, sampling and preservation purposes. At the core facility, all the core boxes were photographed. The recovery details including total recovered length and recovery percentage for each run are recorded in the Borehole logs. The core box photographs showing various lithounits are presented in Fig 13.6.

Fig 13.6a Borehole-3 from 40 m to 45 m

Fig 13.6b Borehole-1 from 25 m to 30 m

Fig 13.6c Borehole-2 from 65 m to 70 m

Fig13.6d Borehole-3 from 55 m to 60 m.

Fig 13.6: Photograph showing drill core boxes with appropriate labelling.

13.8 Discussion on the analysis results of handheld X-ray fluorescence (XRF), if used in the investigation.

No, handheld XRF was not used in the investigations.

CHAPTER 14 - SUB-SAMPLING TECHNIQUES AND SAMPLE PREPARATION

14.1 If core, whether cut or sawn and whether quarter, half or all core taken.

Core has been split into two equal halves by hydraulic core splitter in such a way that the core is uniformly split into two equal halves. The whole quantity of half portion of the sample as marked while logging is crushed to (-) 200 mesh size and about 500g representative sample of (-) 200 mesh was drawn by coning and quartering method of gradual size reduction with the help of crusher and pulveriser. Out of 500gm, 100gm each were drawn for Primary Chemical analysis.

14.2 If non-core, whether riffled, tube sampled, rotary split, etc., and whether sampled wet or dry.

It is not non-core.

14.2.1 For all sample types, the nature, quality and appropriateness of the sample preparation technique.

Quality of the sample preparation is maintained by proper cleaning, maintenance of the equipment and proper crushing, sieving and coning and quartering of samples. For sample preparation, proper technique and expertise has been used.

14.3 Quality control procedures adopted for all sub-sampling stages to maximize representation of samples.

The primary core samples have been collected from entire length intersected in the boreholes drilled and the samples have been prepared at shiva lab Bengaluru. The standard sampling procedure in supervision of qualified sampling technician has been adopted to control the quality of samples. Similarly external check samples have also been prepared under the supervision of qualified sampling technician following the standard sampling procedure and analysed at IISc lab Bengaluru.

14.4 Measures taken to ensure that the sampling is representative of the in-situ material collected.

All the primary samples have been marked and prepared from mineralised cores. During the preparation of primary samples, the mineralised cores have been studied meticulously and samples have been marked properly.

14.5 Whether sample sizes are appropriate to the grain size of the material being sampled.

All samples have been prepared (-) 200 mesh size.

CHAPTER 15 - QUALITY OF ASSAY DATA AND LABORATORY TESTS

15.1 EPMA Analysis

The Electron Microprobe Analysis (EPMA) of slides from different rocks were carried out from EPMA Lab, IISc Bangalore. Thin-cum-polished sections from different rock units (BRS and Core samples) were sent for analysis. The samples were analyzed for REE and silicate minerals to get information regarding the chemical composition of the minerals and mineral association. The details of samples sent for EPMA analysis are given below in Table 15.1.

Table 15.1: Details of Samples collected for EPMA study in Borana block

SL.NO	SAMPLE NO	LATITUDE	LONGITUDE	ROCK TYPE
1	RJBO/BRS-93	25.42749	74.11762	Migmatite gneiss
3	RJB-03(95mts)	25.4290	74.1230	Migmatite gneiss
2	RJBO/BRS-26	25.43201	74.12812	Syenite
4	RJB-04(50mts)	25.4304	74.1244	Syenite
5	RJB-01(75mts)	25.4290	74.1230	Amphibolite

The analytical results of EPMA received for all samples have been given in Annexure-V. The EPMA result indicates the presence of minerals as **monazite** and **zircon** within migmatite gneiss. **Zircon** in syenite. **Chalcopyrite**, **pyrite** and **magnetite** are within amphibolites samples.

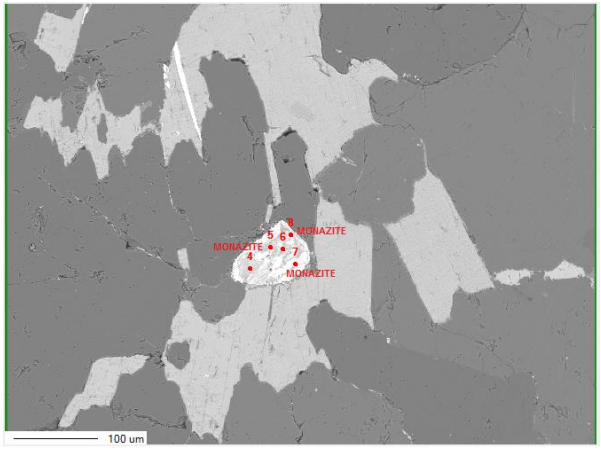

Fig 15.1a BSE image of monazite within migmatite gneiss in sample no RJBO/BRS-93

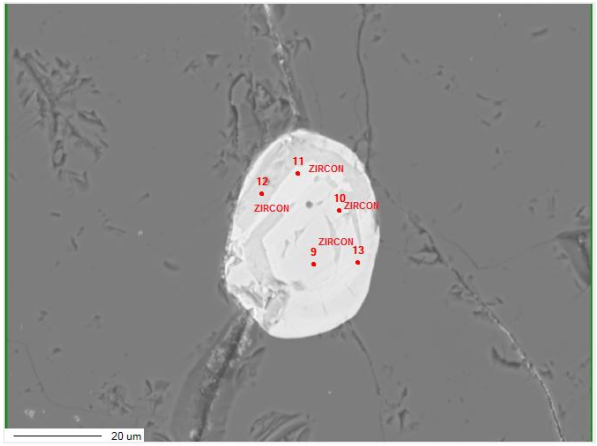

Fig 15.1b BSE image of zircon within migmatite gneiss in sample no RJBO/BRS-93

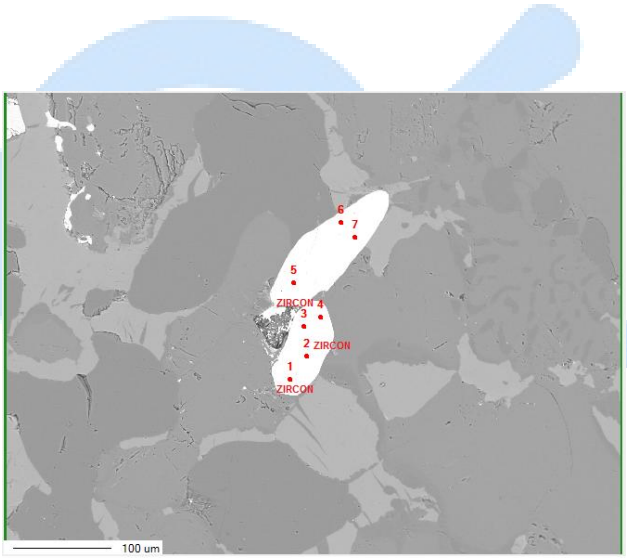

Fig 15.2 BSE image of zircon within migmatite gneiss in sample no RJB-03(95mts)

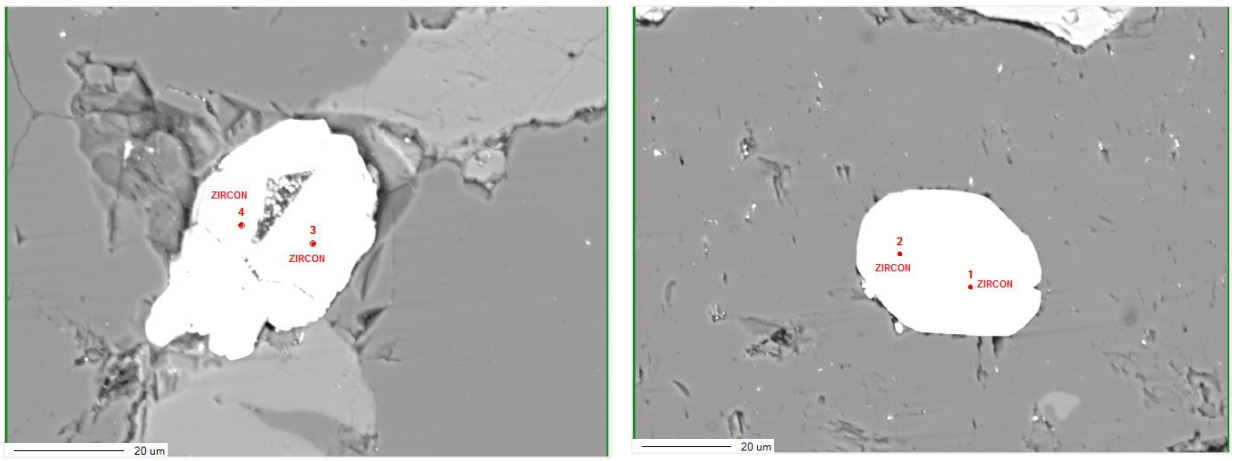

Fig 15.3a & Fig 15.3b BSE image of zircon within syenite in sample no RJBO/BRS-26

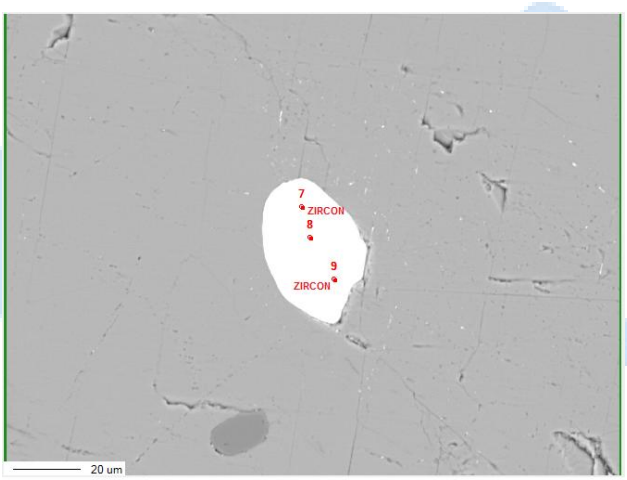

Fig 15.4 BSE image of zircon within syenite in sample no RJB-04(50mts)

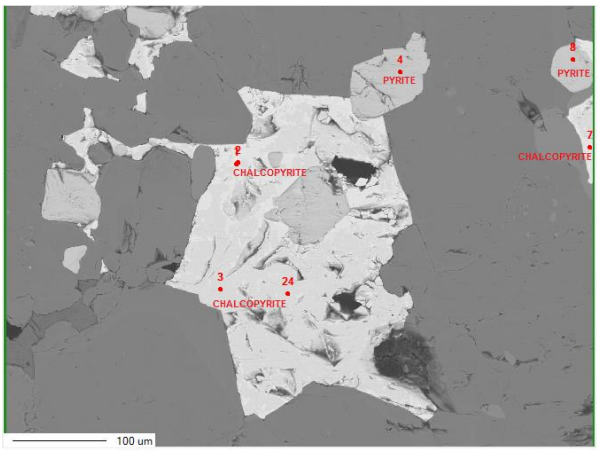

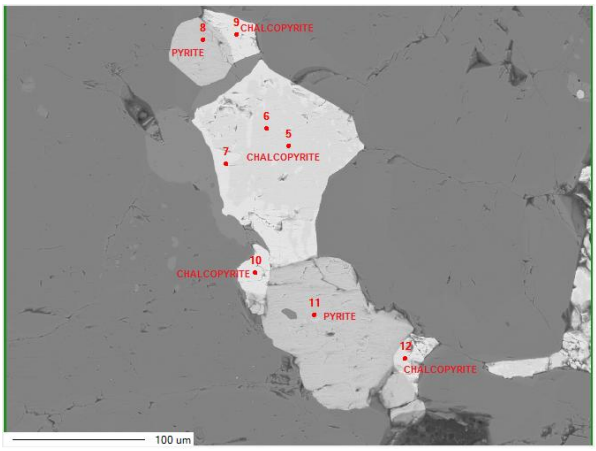

Fig 15.5a & Fig 15.5b BSE image of chalcopyrite and pyrite within amphibolite in sample no BRS-03(75 mts)

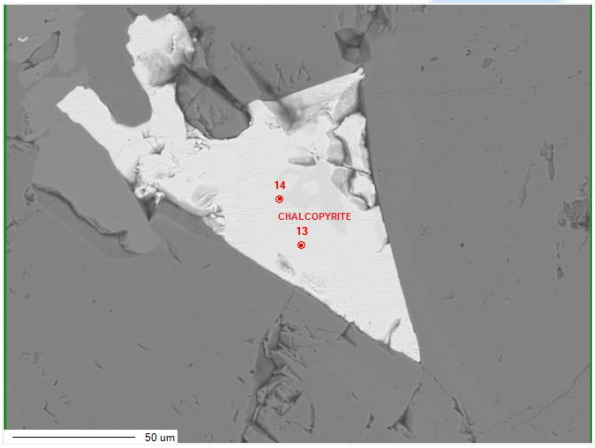

Fig 15.6a BSE image of chalcopyrite within amphibolite in sample no BRS-03(75 mts)

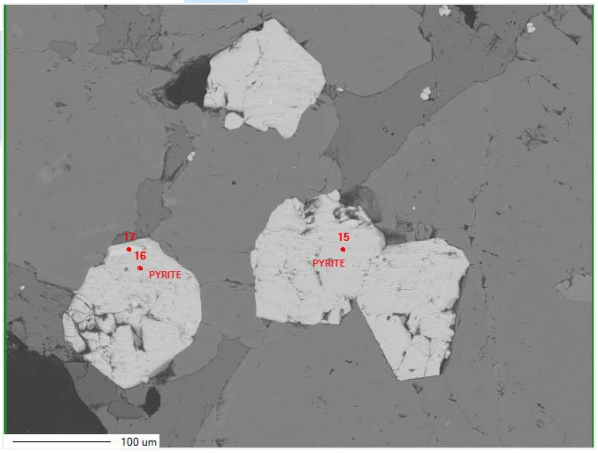

Fig 15.6b BSE image of pyrite within amphibolite in sample no BRS-03(75 mts)

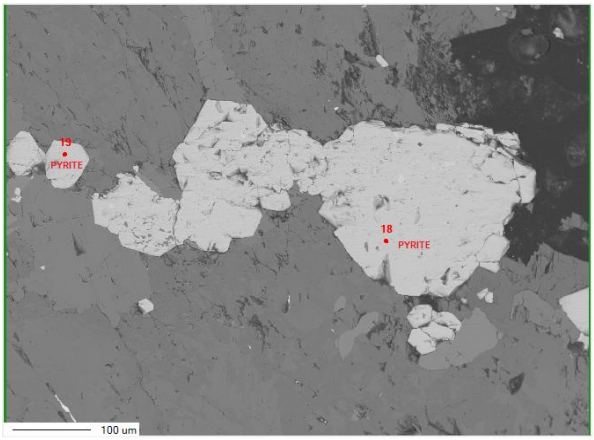

Fig 15.7a BSE image of pyrite within amphibolite in sample no BRS-03(75 mts)

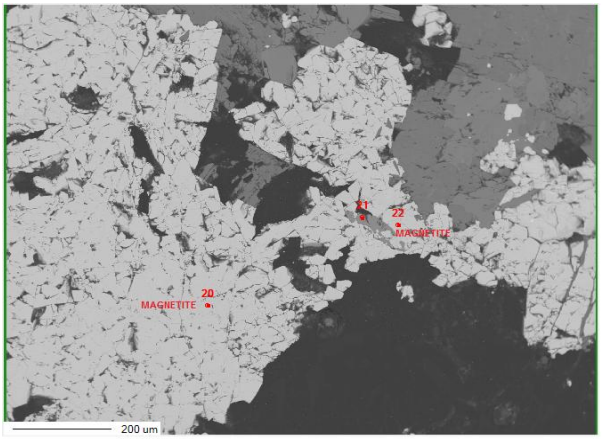

Fig 15.7b BSE image of magnetite within amphibolite in sample no BRS-03(75 mts)

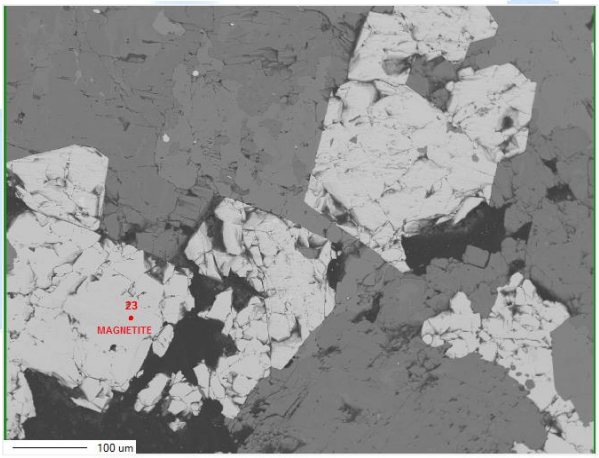

Fig 15.8 BSE image of magnetite within amphibolite in sample no BRS-03(75 mts)

15.2 XRD Analysis

For the XRD analysis twenty nos. of samples collected from mineralized patches to identify and confirm mineral assembly. The collected chip samples were submitted to Indian Institute of Science, Bangalore.

Table 15.2: Details of Samples analyzed for XRD in Borana block

Mineral Phases		
SL.NO	**SAMPLE NUMBER**	**MINERAL PHASES IDENTIFIED**
1	RJBO/BRS-03	Albite, Microcline, Nepheline, Orthoclase, Epidote, Augite.
2	RJBO/BRS-47	Orthoclase, Albite, Microcline, Orthopyroxene, Feldspar, Monazite
3	RJBO/BRS-49	Quartz, K-feldspar, Albite
4	RJBO/BRS-61	Quartz, Orthoclase, Microcline, Biotite, Amphibole, Apatite
5	RJBO/BRS-105	Quartz, Plagioclase feldspar, K-feldspar, Biotite.
6	RJBO/T1-01	Quartz, Albite, Microcline, Biotite, Orthoclase.
7	RJBO/T2-06	Albite, Quartz, Orthoclase, Clinopyroxene, Paracostibite, Zircon.
8	RJBO/T3-13	Quartz, K-feldspar, Albite, Muscovite, Biotite, Apatite, Zircon
9	RJBO/T4-11	Quartz, Albite, Microcline, Clinopyroxene, Garnet
10	RJBO/T5-08	Quartz, Microcline, Albite, Oligoclase, Muscovite, Biotite, Garnet
11	RJBO-01/CS-14	Feldspar, Orthoclase, Microcline, Sodalite, Apatite
12	RJBO-04/CS-11	Quartz, Microcline, Orthoclase, Plagioclase, Biotite, Muscovite, Garnet, Allanite, Monazite, Zircon
13	RJBO-03/CS-31	Quartz, K-feldspar, Plagioclase, Biotite, Muscovite, Garnet, Allanite, Monazite, Zircon
14	RJBO-03/CS-30	Quartz, Microcline, Plagioclase, Biotite, Muscovite, Garnet, Allanite, Monazite, Zircon
15	RJBO-03/CS-50	Quartz, Albite, Microcline, Zinnwaldite, Enstatite

16	RJBO-02/CS-63	Quartz, Orthoclase, Microcline, Albite, Nepheline, Monazite-Ce,
17	RJBO-02/CS-61	Quartz, Microcline, Orthoclase, Albite, Nepheline
18	RJBO-01 48 mtr	Quartz, Hornblende, Plagioclase Feldspar, Biotite, Epidote, Clinozoisite, Titanite, Magnetite, Ilmenite
19	RJBO-01 44 mtr	Quartz, Hornblende, Feldspar, Epidote, Titanite, magnetite
20	RJBO-01/CS-25	Clinopyroxene, Actinolite, Chlorite, Epidote, Ilmenite.

15.3 Whole Rock Elemental Analysis

Whole rock analysis of eight representative Bed Rock Samples (BRS) and two Core Samples is presented in Annexure VI. The whole rock analysis was conducted in Shiva Analytics Bengaluru using the Wavelength Dispersive Spectroscopy (WDXRF) method. The detection limit of all parameters except for Na_2O is 0.05% and with Na_2O having a detection limit of 0.08%.

The BRS sample analysis included 8 rock samples: three syenite samples, three migmatite gneiss samples, one amphibolite sample and one pegmatite sample. The core sample analysis included two rock samples: one migmatite gneiss and one syenite sample. Results of BRS samples were plotted for various geochemical plots using GCD kit 4.1 version software.

In **Migmatite gneiss rock BRS sample** major oxides are as follows: silica (SiO_2) ranges from around 69.25 wt.% to 74.01 wt.%. While alumina (Al_2O_3) is about 12.19 wt.% to 13.64 wt.%. The calcium oxide (CaO) content is relatively low from 1.75 wt. % to 2.93 wt.%. The total alkali content ($K_2O + Na_2O$) is about 5 wt.% to 8.46 wt. %. Iron oxide (Fe_2O_3) content is 4.09 wt.% to 4.7 wt.% and magnesium oxide (MgO) remains low at 0.23 wt.% to 0.4 wt.%.

In **Syenite rock BRS sample** major oxides are as follows: Silica (SiO_2) ranges from 61.97 to 69.55 wt.%, while alumina (Al_2O_3) varies between 13.30 and 16.48 wt.%. The calcium oxide (CaO) content ranges from 2.18 to 10.51 wt.%. The total alkali content ($K_2O + Na_2O$) varies from 2.54 to 8.22 wt.%. The iron oxide (Fe_2O_3) content ranges from 2.10 to 6.48 wt.% and magnesium oxide (MgO) shows relatively low values between 0.00 and 0.32 wt.%.

In **Amphibolites rock BRS sample** major oxides are as follows: silica (SiO_2) is 48.61 wt.%, while alumina (Al_2O_3) is 14.60 wt.%. The calcium oxide (CaO) content is 12.03 wt.%. The total alkali content ($K_2O + Na_2O$) is 2.29 wt.%. The iron oxide (Fe_2O_3) content is 13.76 wt.% and magnesium oxide (MgO) is 6.19 wt.%. These values reflect a mafic composition.

In **Pegmatite rock BRS sample** major oxides are as follows: silica (SiO_2) ranges 74.34 wt.%, while alumina (Al_2O_3) is 14.55 wt.%. The calcium oxide (CaO) content is 2.36 wt.%. The total alkali content ($K_2O + Na_2O$) is 6.76 wt.%. The iron oxide (Fe_2O_3) is 1.02 wt.% and magnesium oxide (MgO) is 0.08 wt.%. These values indicate a highly siliceous composition.

15.4 Trace Elemental Analysis

Thirty-four trace elements of twenty representative samples were analyzed. In twenty samples five BRS samples, six trench samples and nine core samples were analyzed is presented in Annexure VII. The trace elemental analysis was conducted in Shiva Analytics Bengaluru using ICPMS method. Results were plotted for various geochemical plots using GCD kit 4.1 version software.

In **Migmatite gneiss rock sample** Nb ranging from 42.11–106.50 ppm, Zr from 114–357 ppm, Rb from 11.28–225.48 ppm, and Sr from 120–497 ppm. Ba ranges between 26–1036 ppm, and Mn between 331–604 ppm. Ta varies from 3.60–7.29 ppm, Ga from 17.23–31.58 ppm, Be from 1.40–3.65 ppm, Co from 1.56–7.29 ppm, Pb from 8–37 ppm, Sn from 0.76–4.22 ppm, and Mo from <0.5–4.38 ppm, Cr ranges from <10–90 ppm, V from 11–41 ppm, Zn from <5–56 ppm, and Cu is mostly <5 ppm. Ni is consistently <5 ppm. Ag, Cd, In, Re, Sb, Te, Tl and W are generally

<0.5 ppm.

In **Syenite rock sample**, Ba ranging from 236–1084 ppm, Rb from 65.81–220.03 ppm, Sr from 116–590 ppm, Nb from 21.60–57.19 ppm, and Zr from 44–233 ppm. Mn varies between 122–569 ppm. Ta ranges from 2.44–7.01 ppm, Ga from 20.71–45.63 ppm, Be from 1.38–4.16 ppm, Co from 0.52–4.86 ppm, Pb from 5–41 ppm, Sn from 0.71–4.52 ppm, and Mo from 0.55–5.18 ppm. Cr ranges between <10–177 ppm, V between 6–21 ppm, Zn between <5–48 ppm, Cu is mostly <5 ppm except one value of 13 ppm, and Ni is <5 ppm in all samples. Ag, Cd, In, Re, Sb, Te, Tl and W are generally <0.5 ppm.

Amphibolites rock sample contain Co at 43.09 ppm, Cr 46 ppm, Ni 61 ppm, V 290 ppm, Cu 163 ppm, Mn 1580 ppm, Zn 87 ppm, and Sr 111 ppm. Ba is 24 ppm, Nb 0.81 ppm, Rb 9.31 ppm, Ta <0.5 ppm, Zr **7** ppm, Ga 16.26 ppm, Be <0.5 ppm, Sn <0.5 ppm, Mo <0.5 ppm, Pb <5 ppm, and Cs <0.5 ppm. Ag, Cd, In, Re, Sb, Te, Tl and W are <0.5 ppm.

Pegmatite rock sample contained Cr at 302 ppm, Bi 1.43 ppm, Co 0.67 ppm, Mo 0.85 ppm, and Rb 1.11 ppm. All other analyzed trace elements including Nb, Ni, Pb, Sr, Ta, Zr, Zn, Cu, Mn, Ga, Be, Sn, V and others are reported as <5 ppm or <0.5 ppm.

15.5 Rare Earth Elemental Analysis

Rare Earth elemental analysis of representative bedrock samples (108nos), trench samples (100 nos) and core samples (222 nos.) are presented in Annexure VIII respectively. The Rare Earth elemental analysis was conducted in Shiva Analytics Bengaluru using ICPMS method.

15.5.1 Rare Earth elemental analysis in migmatite gneiss

The **migmatite gneiss bedrock samples** show total REE values ranging from 194.1 to 2853.19 ppm. The average REE is about 1376.459ppm.

The **migmatite gneiss trench samples** show total REE values ranging from 130.82–1748.22 ppm.

The average REE is about 956.449ppm.

The **migmatite gneiss core samples** show total REE values ranging from 411.51–3081.88 ppm. The average REE is about 1235.059ppm.

15.5.2 Rare Earth elemental analysis in syenite

The **bedrock syenite samples** show total REE values ranging from 778.08 to 2742.54 ppm. The average REE is about 1552.94ppm.

The **syenite trench samples** show total REE values ranging from 904.23–2645.85 ppm. The average REE is about 1775.281ppm.

The **syenite core samples** show total REE values ranging from 333.63 to 3397.12 ppm. The average REE is about 1423.71 ppm.

15.5.3 Rare Earth elemental analysis in amphibolite

The amphibolite bedrock samples show total REE values ranging from 42.71 ppm.

15.5.4 Rare Earth elemental analysis in pegmatite

The pegmatite bedrock samples show total REE values ranging from 5.04 to 7.49 ppm.

15.6 Bivariate Geochemical Relationships of Total Rare Earth Elements (TREE) and Selected Major and Trace Elements

To evaluate the mineralogical controls and petrogenetic processes governing REE enrichment, bivariate plots of Total Rare Earth Elements (TREE) against selected major oxides (P_2O_5, CaO, TiO_2, Fe_2O_3, Na_2O, K_2O) and trace elements (Th, U, Zr, Nb, and Y) were constructed. These

elemental correlation diagrams provide insights into the roles of accessory minerals.

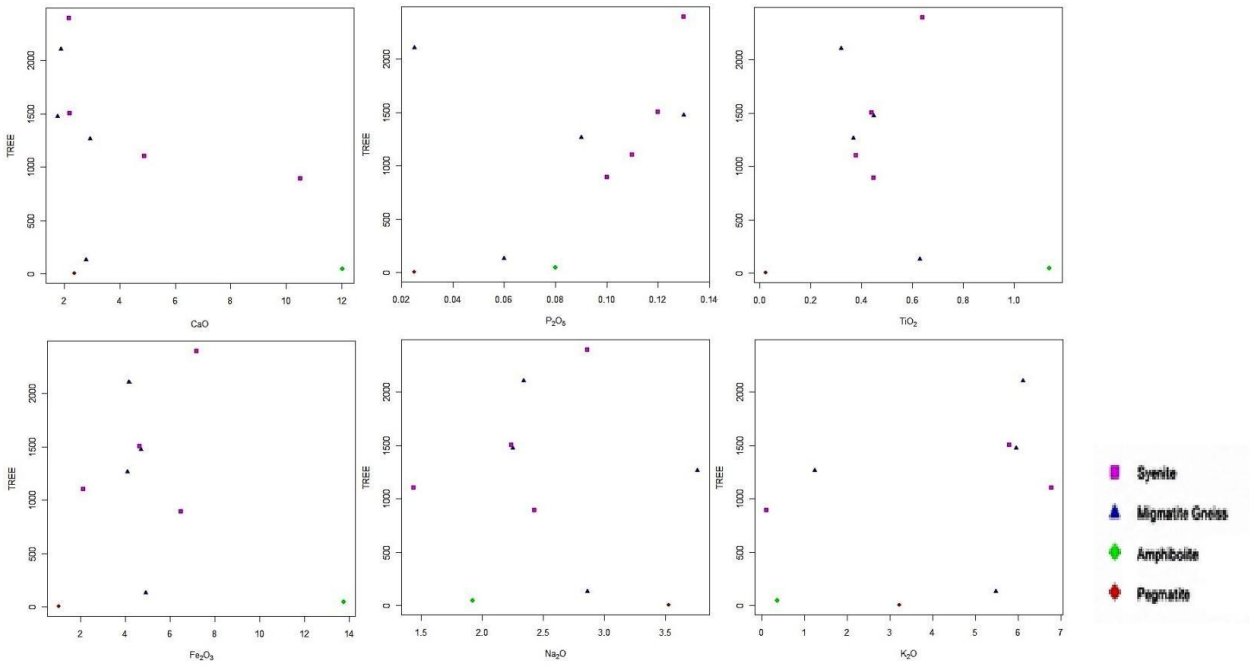

Fig 15.9 Bivariate geochemical relationships between Total Rare Earth Elements (TREE) and selected major oxides elements

TREE vs CaO

The TREE–CaO plot shows a weak negative to scattered relationship, suggesting that Ca-bearing minerals were not the principal controls on REE enrichment. The high TREE values at low to moderate CaO indicate that REEs are mainly concentrated in accessory minerals such as monazite and allanite rather than in major Ca-rich phases.

TREE vs P_2O_5

The TREE–P_2O_5 plot exhibits an overall positive relationship, indicating that phosphate minerals, particularly apatite and monazite, contributed to REE enrichment. The increase in TREE with increasing P_2O_5 suggests an important role of phosphate phases in concentrating REEs.

TREE vs TiO_2

The TREE–TiO_2 plot shows a weak positive relationship with considerable scatter, suggesting that

Ti-bearing minerals such as titanite may have contributed locally to REE enrichment, although they were not the dominant REE hosts.

TREE vs Fe_2O_3

The TREE–Fe_2O_3 plot displays a scattered and weak positive trend, indicating limited control of Fe-bearing minerals on REE distribution. The association may reflect minor contributions from allanite and Fe-rich accessory phases.

TREE vs Na_2O

The TREE–Na_2O plot shows a broadly positive but scattered relationship, suggesting enrichment of REEs during sodic magmatic differentiation. However, the wide scatter indicates that bulk-rock alkalinity alone did not control REE concentrations.

TREE vs K_2O

The TREE–K_2O plot exhibits a weak positive relationship, indicating progressive enrichment of incompatible elements during potassic magmatic evolution. The scatter suggests that REEs are primarily hosted by accessory minerals rather than directly related to K-bearing phases.

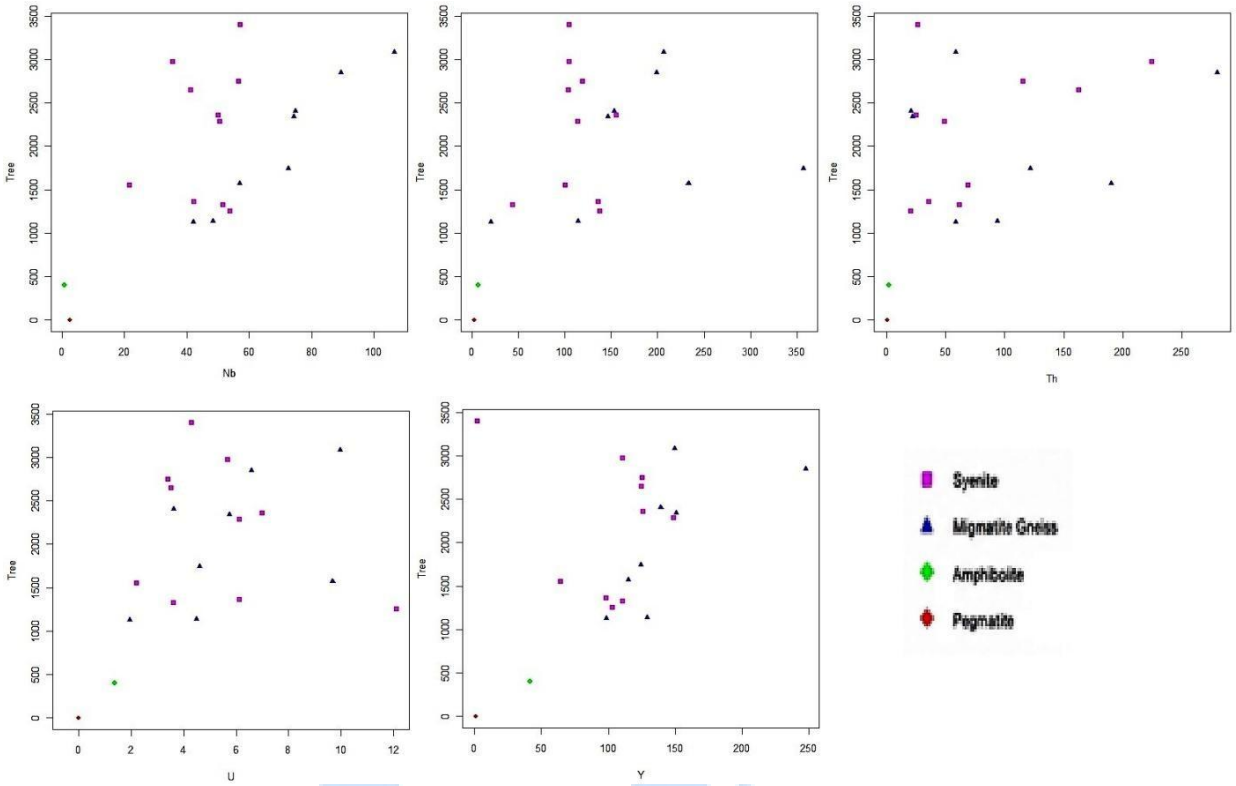

Fig 15.10 Bivariate geochemical relationships between Total Rare Earth Elements (TREE) and selected Trace elements.

TREE vs Nb

The TREE–Nb plot shows a moderate positive correlation, indicating that REEs and Nb behaved as incompatible elements and became progressively enriched during magmatic differentiation. This relationship suggests evolved magmatic processes favourable for REE–Nb enrichment.

TREE vs Zr

The TREE–Zr plot displays a scattered positive relationship, suggesting that zircon fractionation and magmatic differentiation influenced REE enrichment. However, the large scatter indicates that zircon was not the sole host of REEs.

TREE vs Th

The TREE–Th plot exhibits a weak to moderate positive correlation, indicating that Th-bearing accessory minerals, particularly monazite, played an important role in REE enrichment. The

scatter further suggests contributions from additional REE-bearing phases such as allanite and apatite.

TREE vs U

The TREE–U plot shows a weak positive relationship, suggesting partial co-enrichment of REEs and U during magmatic evolution. The scattered distribution indicates that U-bearing minerals had only a subordinate role in controlling REE concentrations.

TREE vs Y

The TREE–Y plot exhibits a moderate positive correlation, indicating that Y and REEs behaved similarly during magmatic differentiation. This relationship suggests the involvement of Y-bearing accessory minerals such as xenotime and zircon and reflects enrichment of incompatible elements in evolved melts.

15.7 Discussion

15.7.1 Detailed Interpretation of Chemical Analytical data

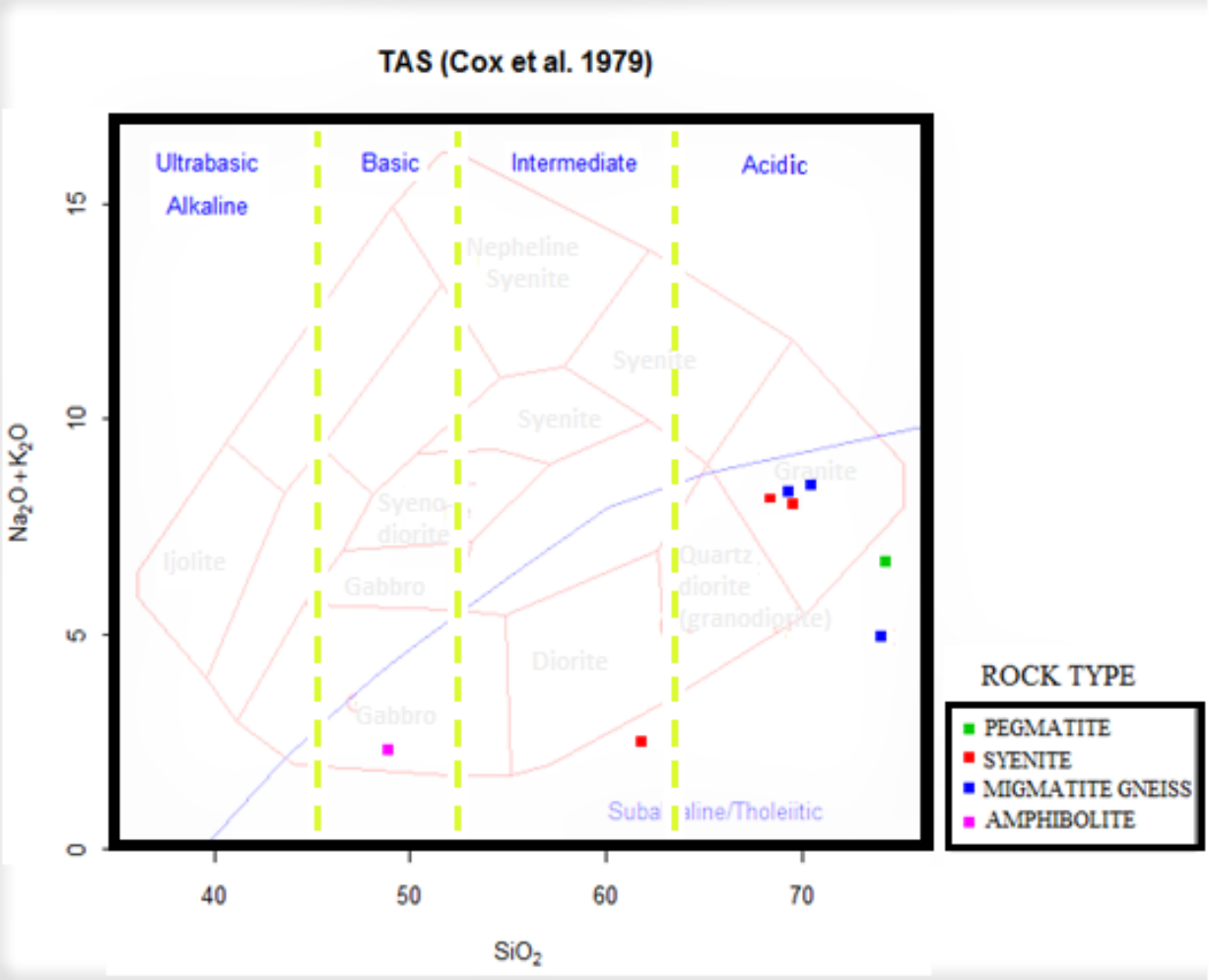

Fig 15.11 TAS diagram for Borana block

The geochemical classification has been carried out using the Total Alkali–Silica (TAS) diagram after Cox et al. (1979) (Fig.15.11), wherein SiO_2 (wt.%) is plotted against total alkalis (Na_2O + K_2O, wt.%). The TAS diagram provides a standardized framework for chemical classification of igneous rocks. The plotted data indicates that the samples span a compositional range from basic to acidic, with most of the samples occupying the intermediate to acidic fields. The diagram also demarcates the alkaline and subalkaline (tholeiitic–calc-alkaline) domains, enabling interpretation of magmatic affinity.

Syenite samples do not plot strictly within the syenite field in the TAS diagram. This is because the TAS classification is based on whole-rock chemistry, whereas syenite is defined mineralogically. Minor variations in SiO_2 and total alkali contents, caused by magmatic differentiation, transitional compositions, or silica saturation, can shift syenitic compositions into adjacent fields.

The migmatite gneiss samples plot mainly within the granite to quartz diorite/granodiorite fields, indicating felsic to intermediate compositions. Their chemical disposition supports an origin involving partial melting and anatexis of pre-existing crustal rocks, followed by variable degrees of differentiation.

The amphibolite samples plot in the gabbro field, characterized by low silica and low total alkalis, pointing towards a mafic protolith.

The pegmatite samples plot in the acidic field with high SiO_2 content and elevated alkalis.

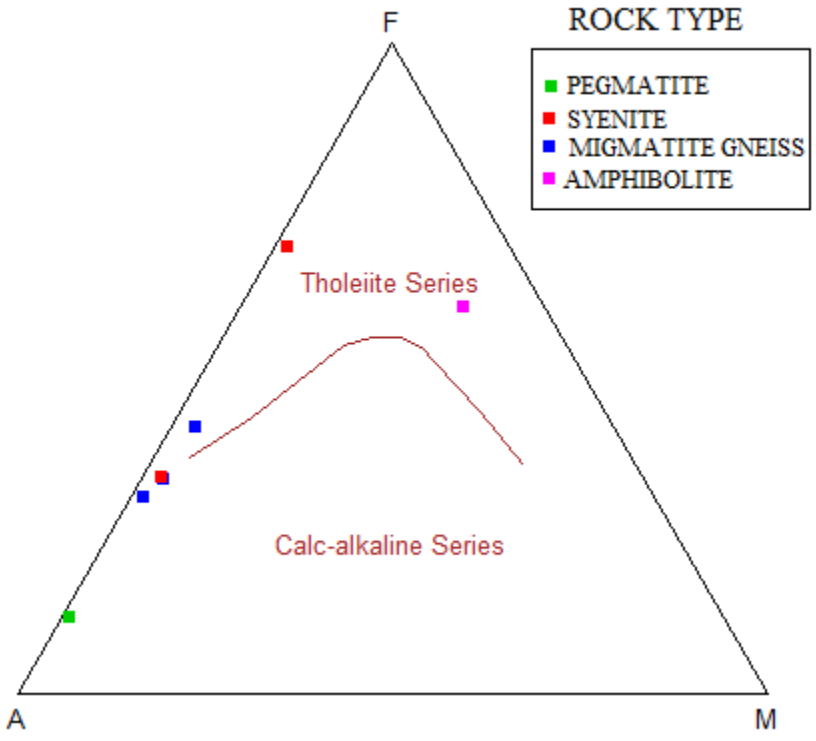

Fig 15.12 AFM diagram for Borana block

The AFM ternary diagram (A = $Na_2O + K_2O$, F = FeO total, M = MgO) is used to distinguish between tholeiitic and calc-alkaline magma series and to infer magmatic evolution trends. In the present study, the plotted data points represent pegmatite, syenite, migmatite gneiss and amphibolite samples (Fig.15.12).

Overall, the AFM diagram indicates a dominantly calc-alkaline magmatic suite with minor tholeiitic influence**,** supporting a complex magmatic evolution involving fractional crystallization and crustal interaction.

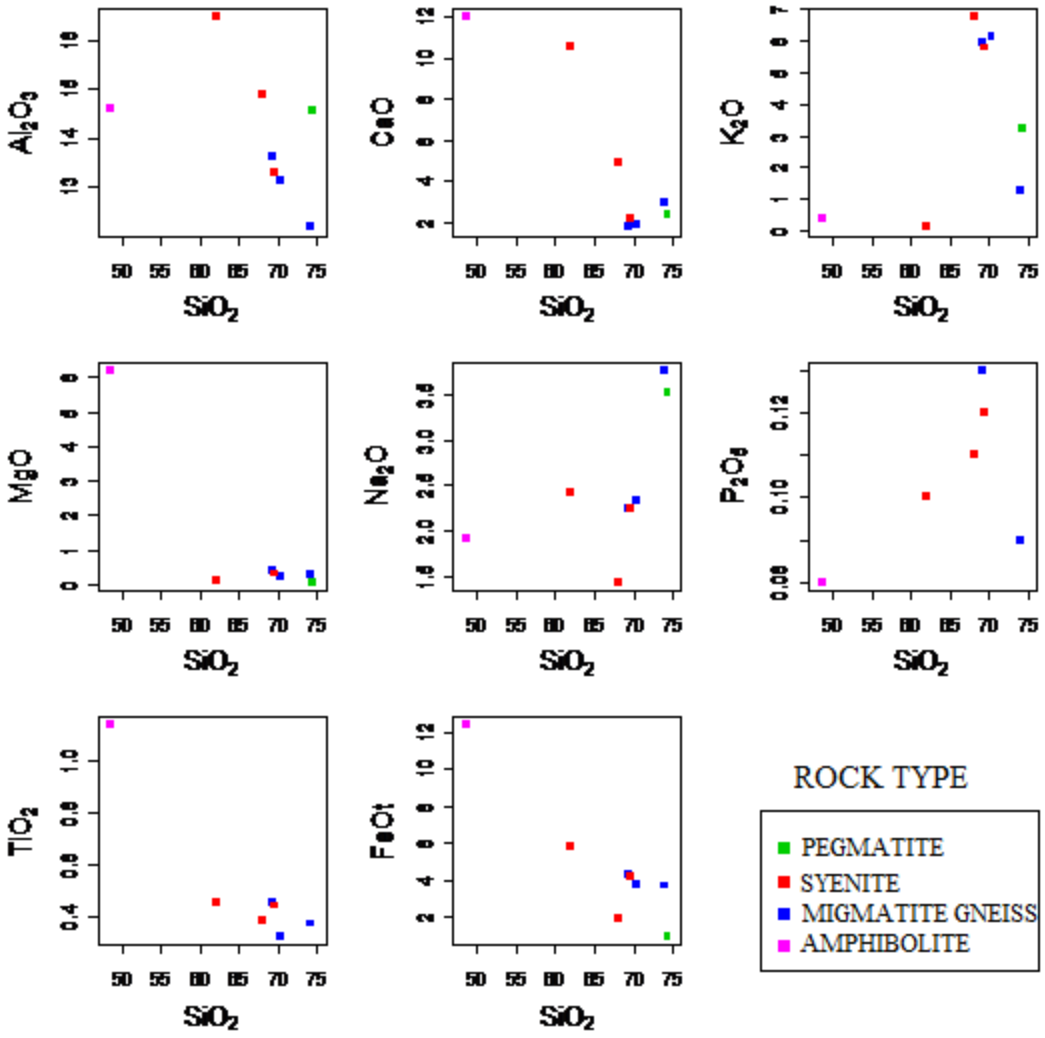

Fig 15.13 Harker bivariant diagrams SiO2 vs different elements for different rock types of Borana block

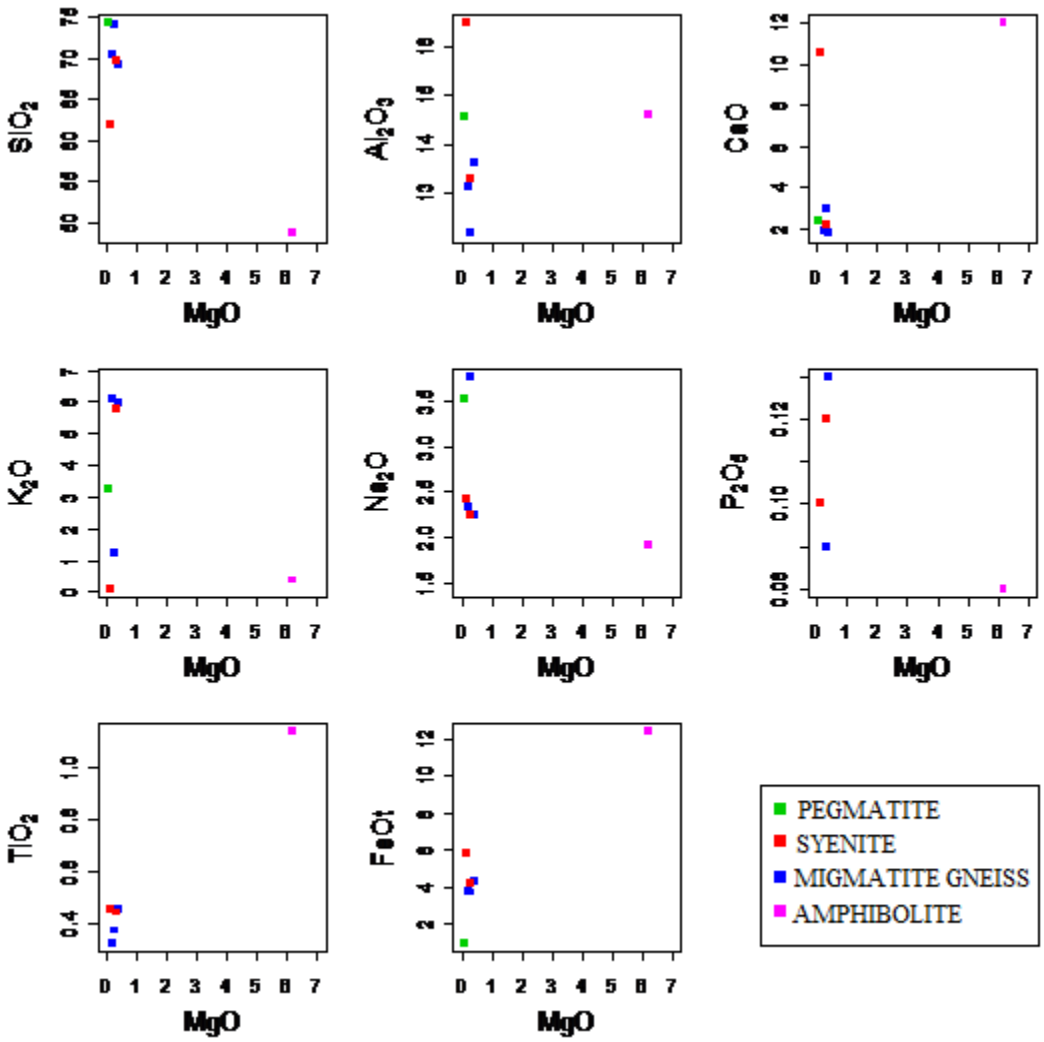

Fig 15.14 Harker bivariant diagrams SiO2 vs different elements for different rock types of Borana block

Harker variation diagrams depicting major oxides (Al_2O_3, CaO, K_2O, MgO, Na_2O, P_2O_5, TiO_2 and FeOt) plotted against SiO_2 have been prepared to evaluate the magmatic differentiation trends of various rock types in the study area. A systematic decrease in CaO, MgO, FeOt and TiO_2 with increasing SiO_2 is observed, that primarily indicates magmatic differentiation, specifically through progressive fractional crystallization. Al_2O_3 shows a moderate decrease with increasing SiO_2, suggesting fractional removal of plagioclase feldspar during magma evolution. Na_2O and K_2O

generally increase with SiO_2, reflecting progressive enrichment of alkalis in the evolved melts and dominance of alkali feldspar in felsic compositions. P_2O_5 exhibits a slight decreasing trend with increasing SiO_2, indicating early crystallization of apatite, whereas minor scatter in some plots may be attributed to alteration and metamorphic overprinting.

Overall, the Harker diagrams suggest that the rock suite represents a cogenetic magmatic sequence derived from a common parental magma through fractional crystallization, with limited chemical scatter due to post-magmatic processes.

Harker variation diagrams depicting major oxides (Al_2O_3, CaO, K_2O, MgO, Na_2O, P_2O_5, TiO_2 and FeOt) plotted against MgO have been prepared to evaluate the role of mafic mineral fractionation during magmatic evolution. A clear negative correlation of SiO_2 with MgO is observed, indicating that silica enrichment is associated with decreasing MgO content due to fractional crystallization of Mg-rich minerals. Amphibolite samples plot at higher MgO and lower SiO_2, representing the least evolved mafic compositions, whereas syenite, migmatite gneiss and pegmatite samples plot at low MgO values, reflecting evolved felsic compositions.

Oxides such as CaO, FeOt and TiO_2 show a systematic decrease with decreasing MgO, suggesting removal of clinopyroxene, amphibole and Fe–Ti oxide phases during magma evolution. Al_2O_3 displays moderate variation, indicating plagioclase fractionation at intermediate stages.

Na_2O and K_2O generally show enrichment at low MgO values, reflecting progressive concentration of alkalis in the evolved melts and dominance of alkali feldspar in felsic rocks. P_2O_5 decreases with decreasing MgO, indicating early crystallization of apatite.

Overall, the MgO variation diagrams suggest that the rock suite represents a genetically related magmatic sequence, evolving from a mafic parental magma through fractional crystallization. The observed trends are consistent with petrographic observations and support a multi-stage magmatic evolution of the study area.

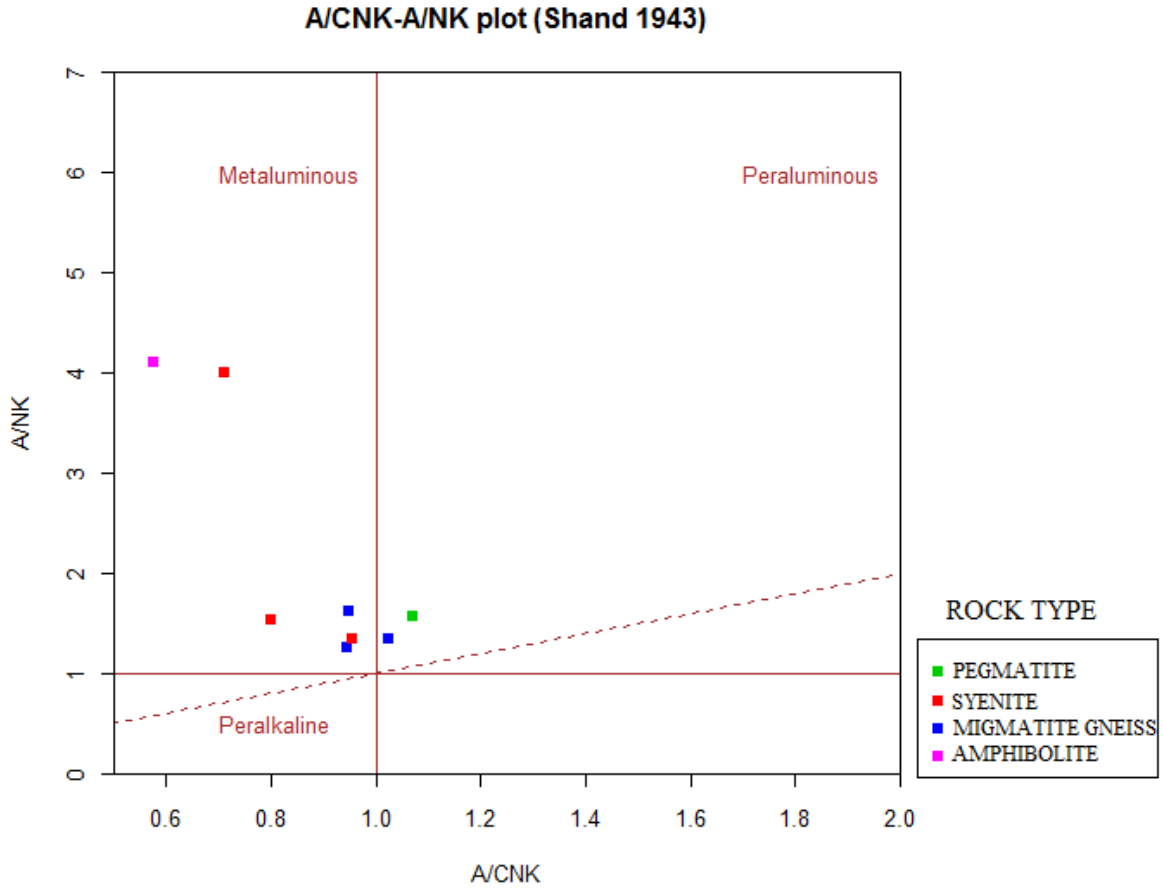

Fig 15.15 A/NK-A/CNK diagram for different rock types of Borana block (After Shand, 1943)

The alumina saturation characteristics of the rocks from the study area have been evaluated using the A/CNK–A/NK plot after Shand (1943), where A = Al_2O_3, C = CaO, N = Na_2O and K = K_2O (molar proportions). This diagram is widely used to distinguish peralkaline, metaluminous and peraluminous rock types and to infer magmatic affinity and source characteristics. The majority of the syenite and migmatite gneiss samples plot in the metaluminous field. This suggests dominance of feldspar- and mafic mineral–bearing assemblages and derivation from relatively alkali- and mantle-influenced magmas.

The pegmatite samples plot close to the metaluminous–peraluminous boundary, reflecting evolved felsic compositions and minor enrichment in alumina due to advanced fractional crystallization. The amphibolite samples plot distinctly in the metaluminous field with higher A/NK values,

consistent with a mafic protolith and dominance of plagioclase and amphibole. A few samples plot near the peralkaline field, indicating local enrichment of alkalis relative to alumina, possibly due to alkaline magmatism or post-magmatic alkali metasomatism.

Overall, the A/CNK–A/NK diagram indicates that the rock suite is predominantly metaluminous in nature, with limited peralkaline tendency.

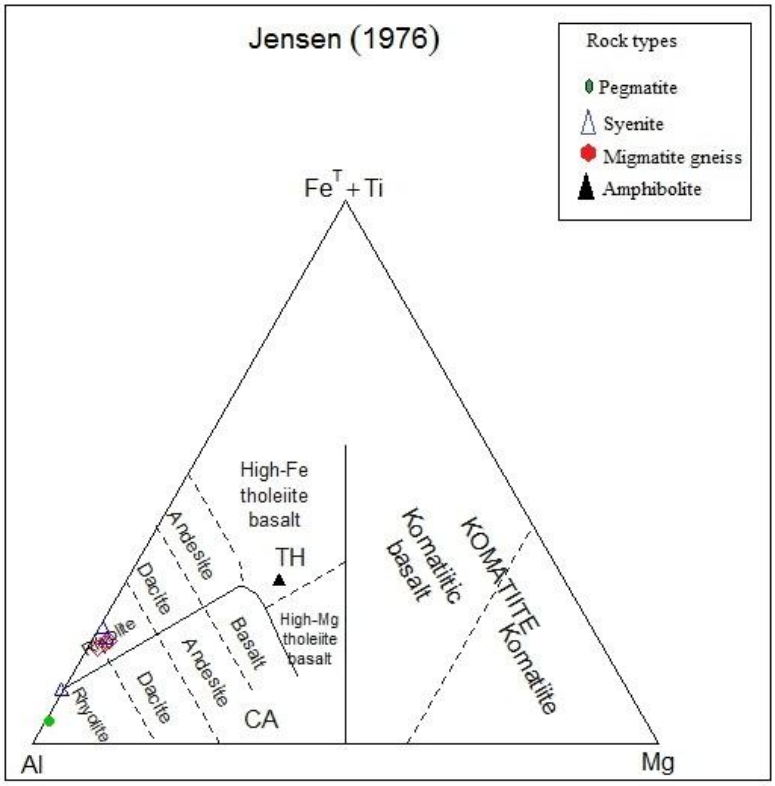

Fig 15.16 Fe(t) + Ti - Al - Mg ternary plot for different rock types of Borana block (Jensen, 1976)

The Jensen (1976) ternary diagram based on Fe(t) + Ti - Al - Mg is used to classify mafic to ultramafic rocks and to distinguish between tholeiitic, calc-alkaline and komatiitic magma series. This discrimination is particularly useful for metamorphosed mafic rocks where primary textures and mineralogical features are obscured.

In the present study, the syenite, migmatite gneiss and pegmatite samples plot towards the Al-rich corner and fall within the andesitic–dacitic-rhyolite fields, reflecting their evolved, felsic to intermediate compositions. Their distribution indicates magmatic differentiation and significant

crustal involvement. The amphibolite samples plot dominantly within the tholeiitic basalt field, with some samples showing affinity towards high-Fe and high-Mg tholeiitic basalt. This indicates derivation from a tholeiitic mafic parental magma, consistent with their mafic whole-rock chemistry and field occurrence. The position of these samples confirms that the amphibolites represent metamorphosed basaltic protoliths.

None of the sample's plot in the komatiitic basalt or komatiite fields, suggesting absence of ultramafic magmatism in the study area. Overall, the Jensen diagram indicates that the magmatic suite comprises dominantly tholeiitic mafic rocks with associated calc-alkaline to evolved felsic derivatives, supporting a polyphase magmatic evolution involving differentiation and crustal reworking.

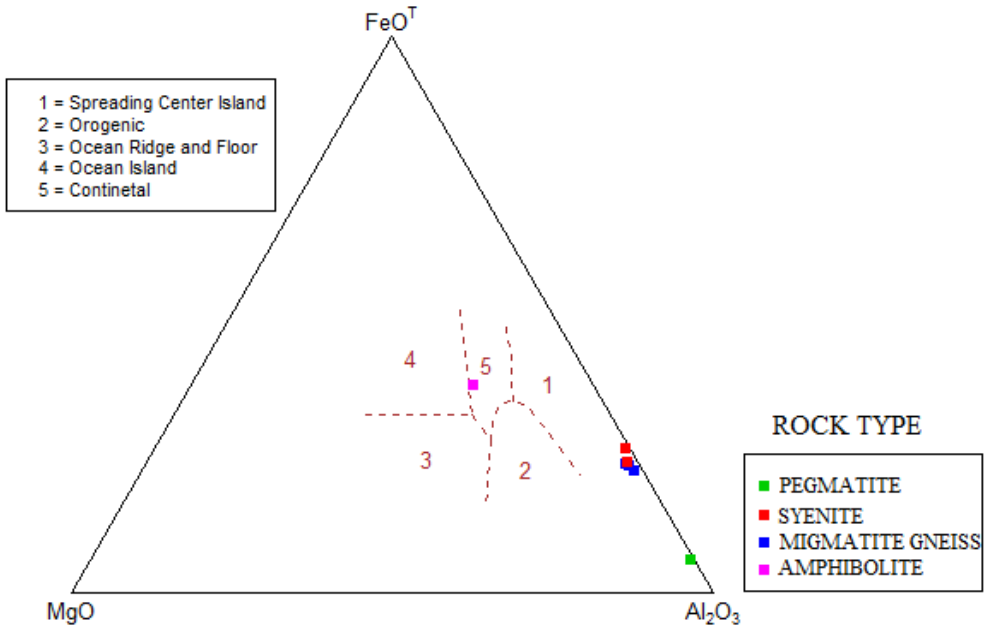

Fig 15.17 FeOT-MgO-Al2O3 ternary plot for different rock types of Borana block. (after Pearce et al., 1977)

The FeOT–MgO–Al_2O_3 ternary diagram has been used to evaluate the tectonic affinity of the igneous and metamorphosed rocks in the study area. The diagram discriminates between magmatic

suites generated in different tectonic environments, namely spreading centre island, orogenic, ocean ridge and floor, ocean island and continental settings.

The plotted data indicates that most of the samples cluster close to the spreading centre island field, with some samples plotting near the boundary between spreading centre island and orogenic fields. This distribution suggests that the parental magmas were derived predominantly from mantle sources in an extensional or spreading-related tectonic regime.

Amphibolite sample plots within or close to the ocean island to continental field, indicating derivation from a mantle-derived basaltic magma with possible crustal interaction prior to metamorphism. This supports interpretation of amphibolite as a metamorphosed mafic protolith.

Overall, the FeOT–MgO–Al_2O_3 diagram indicates that the magmatic suite of the area is best interpreted as having originated in a spreading centre or extensional tectonic setting, followed by emplacement, differentiation and metamorphic reworking within an orogenic continental framework.

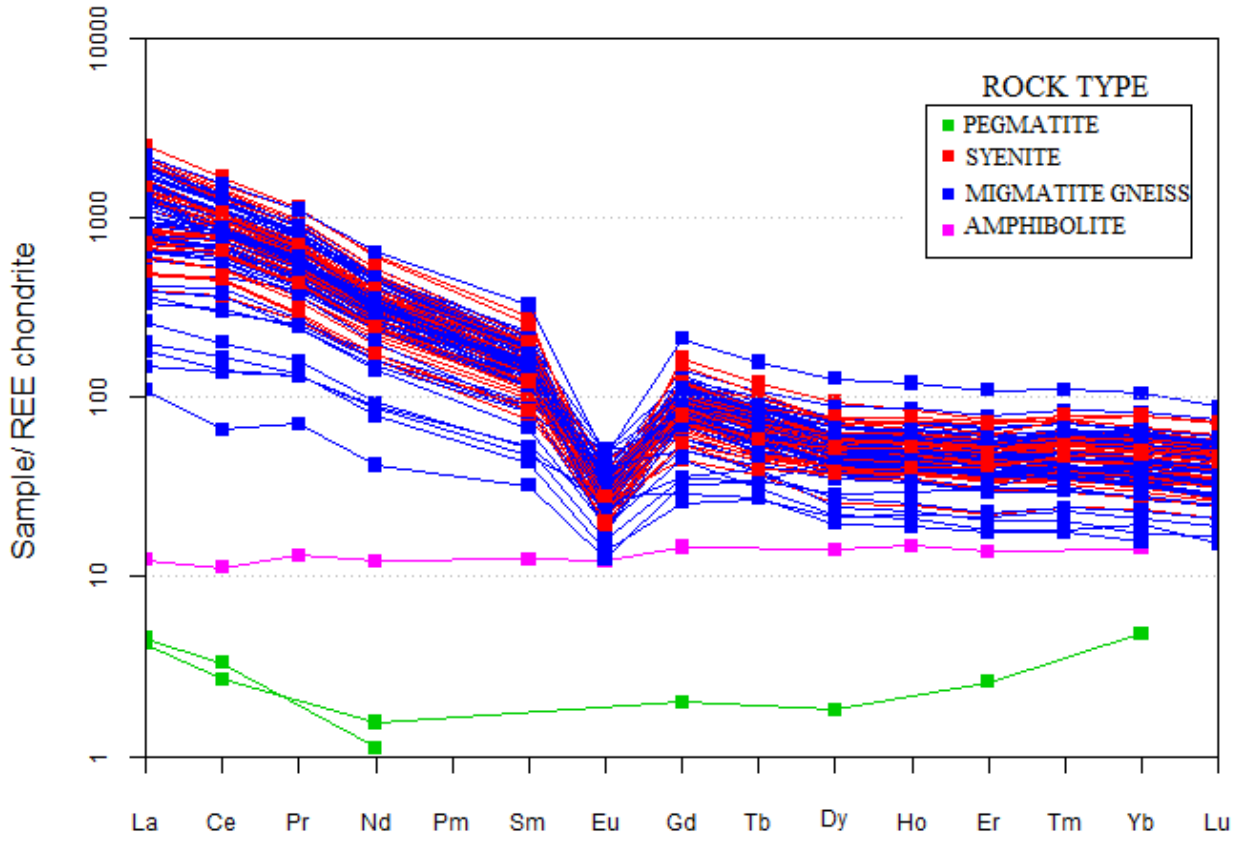

Fig 15.18 Chondrite normalized pattern for different BRS of Borana block (Nakamura, 1974)

Chondrite-normalized Rare Earth Element (REE) patterns of different bedrock suites (BRS) from the Borana block have been plotted using chondrite values of Nakamura (1974) to evaluate REE enrichment, fractionation trends and magmatic processes. The patterns reveal distinct REE behaviors among migmatite gneiss, syenite, pegmatite, and amphibolite.

The syenite and migmatite gneiss samples display strong enrichment of LREEs (La–Sm) relative to HREEs, with chondrite-normalized values reaching several hundred to over a thousand times chondritic abundance up to 2971.05 ppm. The systematic decrease from LREE to HREE indicates pronounced LREE/HREE fractionation, characteristic of evolved alkaline to calc-alkaline magmas. A well-defined negative Eu anomaly is observed in most syenite and migmatite gneiss samples, indicating fractionation of plagioclase and/or alkali feldspar during magma evolution.

The pegmatite samples show comparatively lower overall REE abundances but display a relatively flat to gently increasing HREE pattern from Dy to Lu. This suggests formation from highly evolved residual melts, with selective depletion of LREEs and relative HREE enrichment in late-stage magmatic fluids. The amphibolite samples show low total REE contents with near-flat patterns and minimal LREE–HREE fractionation, indicating derivation from a mafic basaltic protolith with limited magmatic differentiation. The absence of a significant Eu anomaly in amphibolites suggests negligible plagioclase fractionation prior to metamorphism.

Overall, the chondrite-normalized REE patterns indicate that the rock suites of the Borana block represent a cogenetic, compositionally evolved magmatic system, wherein mafic protoliths were followed by progressive differentiation and crustal involvement leading to syenite, migmatite gneiss and pegmatite emplacement. The strong LREE enrichment and distinct Eu anomalies in syenite and migmatite gneiss are significant from an exploration perspective and highlight the REE mineralization potential of the area

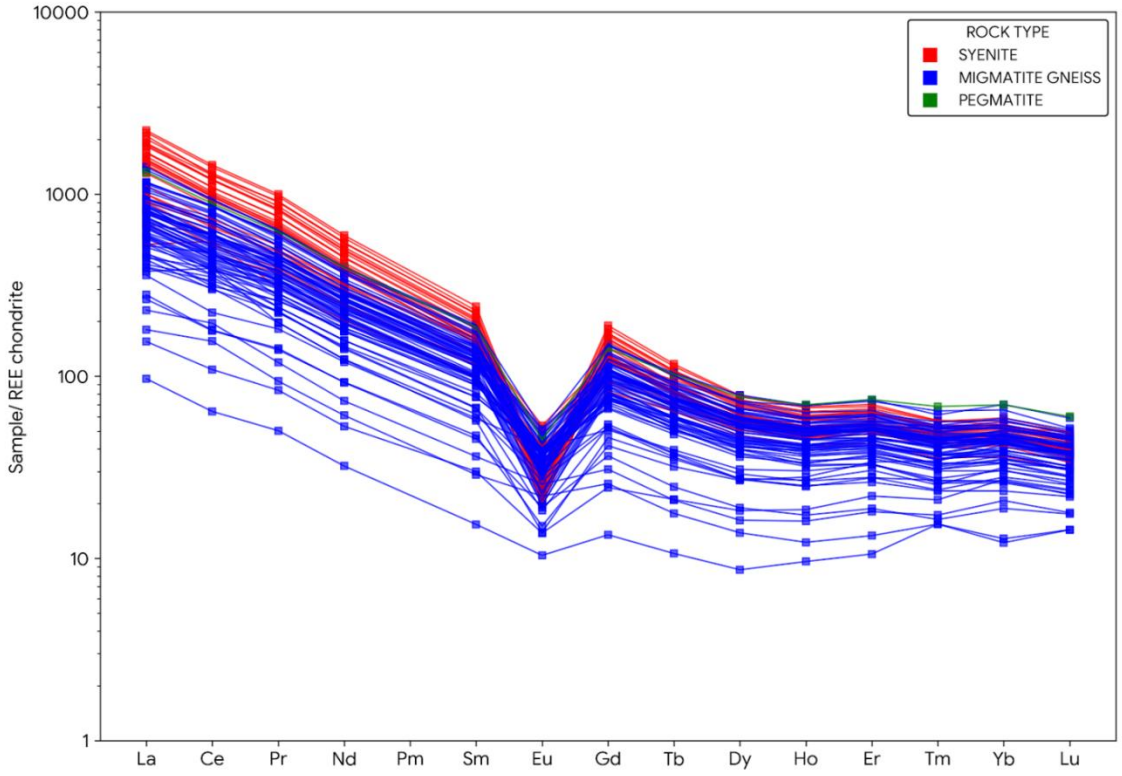

Fig 15.19 Chondrite normalized pattern for different trench samples of Borana block (Nakamura, 1974)

Chondrite-normalized Rare Earth Element (REE) patterns for trench samples from the Borana block have been plotted using Nakamura (1974**)** normalization values to assess REE distribution, fractionation behavior and mineralization characteristics.

The trench samples, representing syenite, migmatite gneiss and pegmatite, exhibit overall enrichment in LREEs (La–Sm) relative to HREEs (Gd–Lu), as indicated by steeply fractionated patterns in the LREE segment and comparatively flatter HREE trends. The syenite samples show the highest degree of REE enrichment, with chondrite-normalized concentrations reaching up to 2645.85 ppm, reflecting derivation from evolved, alkali-rich magmas**.**

A prominent negative Eu anomaly is consistently observed across most trench samples, indicating plagioclase and/or alkali feldspar fractionation during magma evolution. The coherence of Eu anomalies among samples suggests a common magmatic control rather than localized alteration.

The migmatite gneiss samples show similar REE patterns to syenite but with slightly lower absolute abundances, suggesting partial melting and anatectic processes with inheritance of REE signatures from source rocks. The pegmatite samples display relatively lower total REE contents and comparatively flat HREE patterns, consistent with crystallization from highly evolved, residual melts during late-stage magmatism.

Overall, the chondrite-normalized REE patterns of trench samples indicate a genetically related, compositionally evolved magmatic system, characterized by strong LREE enrichment and feldspar-controlled Eu depletion. These REE characteristics highlight the REE enrichment potential of the Borana block and support the continuity of mineralization across different trenches

15.7.2 REE Scenario from Reference Analytical Data

The reference analytical data from bedrock, trench, core, petrography, and trace-element datasets collectively define a coherent LREE-dominant REE system in the Borana block. In the core assay dataset, 222 unique core intervals yield a mean TREE of 1267.29 ppm, a median of 1273.87 ppm, and a maximum of 3398.03 ppm. Of these intervals, 188 are at or above 1000 ppm TREE. The average LREE proportion is 85.25%, which confirms that the mineralization is strongly dominated by LREE.

Lithology-wise, mineralization is clearly selective. Syenite returns the highest mean TREE values and the largest number of mineralized intervals, whereas migmatite gneiss also sustains a substantial population of mineralized intervals and hosts several high-grade zones. Amphibolite remains uniformly low in REE content and should be treated as a low-priority host. Petrographic studies independently support this interpretation by repeatedly identifying allanite and monazite in syenite and gneiss, commonly associated with epidote-zoisite alteration, deformation textures, and local magnetite-sulfide assemblages. The selected trace-element dataset further strengthens the interpretation by showing enrichment of Nb, Zr, Rb, Ba, Ga, and Ta in felsic REE-bearing samples, while amphibolite shows a mafic signature with elevated Co, Cu, V, Mn, Ni, and Cr and poor REE prospectivity.

The external/check datasets support the reliability of the analytical pattern. The phase-1 bedrock and trench check set records a maximum TREE of 2708.34 ppm, including high values in samples such as RJBO/T1-09 and RJBO/BRS-03. The phase-2 core check set reaches 3927.75 ppm, with repeated high-grade intervals in samples such as G3051-14 and G3051-186. These repeat analyses indicate that the high-grade REE values are reproducible and are not isolated analytical artefacts.

15.8 Check analysis of at least 10% of samples should be analyzed from third party National Accreditation Board for Testing and Calibration Laboratories (NABL) accredited or Department of Science and Technology (DST) or Bureau of Indian Standards (BIS) recognized laboratories or government laboratories for assessing the acceptable levels of accuracy.

The primary samples from mineralized zones have been analyzed for REE Analysis, Whole rock analysis, 34 Trace Elements and 13 major elements in Shiva Labs Bangalore.

10% of BRS samples, trench samples and core samples were analyzed from different labs as well for cross check of sample results. This was done in IISc Bangalore**.** The samples result of both labs is provided in table below. Most of the values are falling within the acceptable limit between the two labs. Few points were excluded due to their nugget effect. Since majority of samples fall within acceptable limits and no systematic drift is observed, the primary laboratory data is considered reliable.

Table 15.3: Check Samples Borana

Sample Type	Total REE By Shiva Labs	Total REE By IISc Lab	Error Percentage (%)
BRS	2645.85	2574.83	2.68
	1243.99	1211.64	2.60
	1326.27	1363.30	-2.79
	642.78	647.81	-0.78
	1748.22	1624.16	7.10
	1674.31	1536.56	8.23
	1137.73	1095.31	3.73
	130.82	133.26	-1.87

	1173.36	1179.00	-0.48
	270.63	289.12	-6.83
Trench	2971.05	1296.46	56.37
	2853.19	2330.44	18.33
	2742.54	2522.02	8.04
	2533.28	2256.95	10.91
	2476.92	1453.64	41.32
	1956.63	1548.12	20.88
	1887.01	2290.87	-21.40
	1862.25	1909.31	-2.53
	194.10	137.34	29.23
	42.71	36.78	13.88
Core Samples	3397.12	3728.79	-9.76
	3081.88	3492.55	-13.32
	2401.46	2824.66	-17.63
	2343.02	2622.85	-11.94
	2357.60	1992.15	15.50
	2283.82	1992.30	12.76
	2211.37	2262.50	-2.31
	2143.02	2071.09	3.36
	2125.15	2281.39	-7.35
	417.00	32.25	92.27
	104.47	38.76	62.90
	104.38	36.62	64.92
	102.87	40.78	60.36
	102.43	44.44	56.60
	403.93	41.22	89.79
	1306.34	1292.33	1.07
	1292.96	1352.95	-4.64

	1286.67	1441.38	-12.03
	1279.91	1248.75	2.43
	1280.36	1334.09	-4.20
	1273.87	1334.36	-4.75
	1269.34	1369.46	-7.89

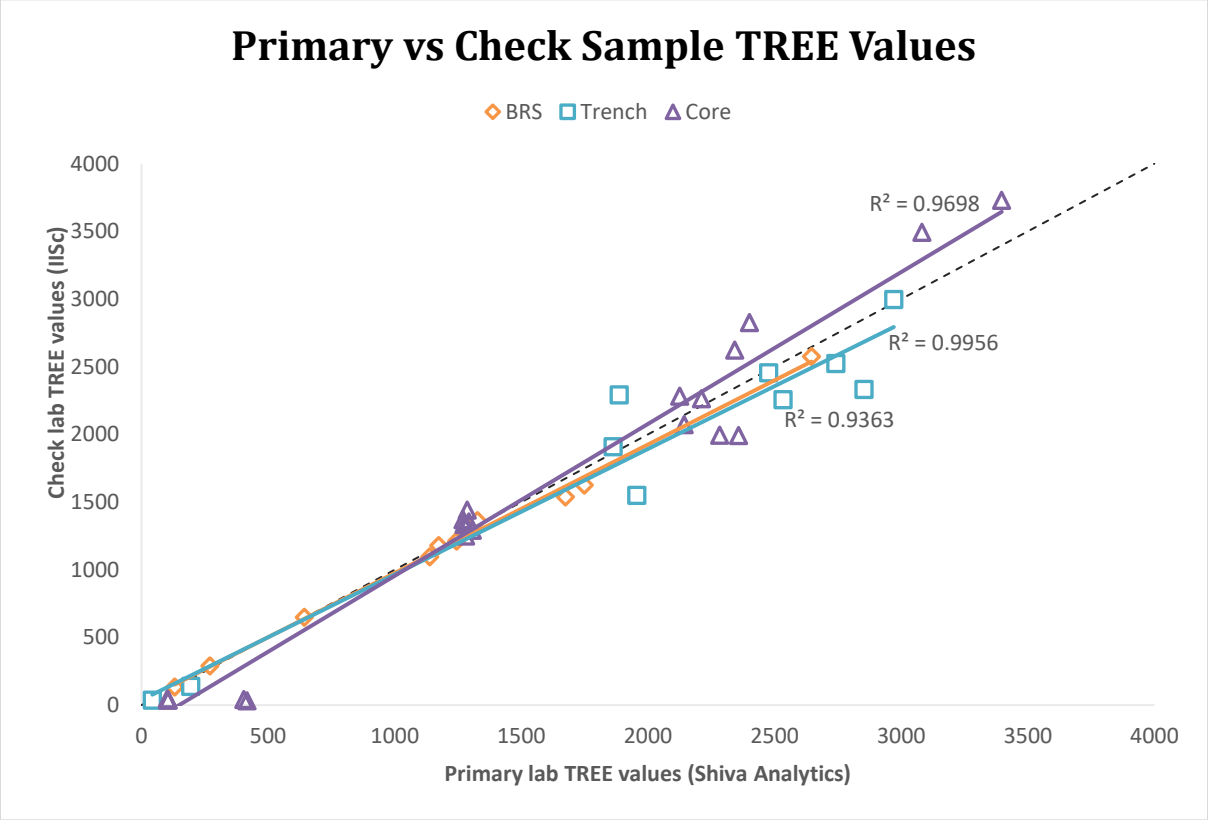

Fig 15.20 Comparison of BRS, Trench and Check Sample Total REE values between Shiva Analytical Labs and Indian Institute of Science (IISc) Bengaluru

Note: More than 80% of the samples are falling within the acceptable limit of 93% confidence level. The samples gave more errors due to nugget effects and have been eliminated for comparison studies. The purpose of reproducibility of the results has been established between the labs.

15.9 Integration of Geology, Geophysics and Geochemical Exploration and the Interpretation

Preliminary exploration (G3) for REE and associated mineralization was carried out in and around the Borana block in toposheet 45 K/3 covering the villages such as Borana, Borana Ka Khera, and Gujjaron Ka Khera of Raipur tahsil, Bhilwara District, Rajasthan to evaluate the REE and associated mineralization in an area of 1.14 Sq. km. No geophysical work was carried out as it is not in the scope of work.

To understand the geochemical signatures classification scheme and petrogenetic history of different rock types, 108 numbers of bedrock samples (BRS) and 100 of trench samples were collected. The samples were analyzed at M/s Shiva Analytical India Ltd., Bangalore which were analyzed by ICPMS method for 14 REE elements. The integration of Geochemical data on Geology has been attempted through preparation of total REE concentration for the major litho-units like migmatite gneiss and syenite by preparing geochemical dispersion maps which are shown in Plate 4. Later borehole location selection on outcrop map was prepared and borehole location selection on geochemical dispersion map with BRS and trench values was prepared Plate 5.

The integrated geological and analytical evidence shows that the Borana REE system is both lithologically selective and structurally prepared. Allanite- and monazite-bearing syenite and migmatite gneiss are repeatedly associated with epidote-zoisite alteration, brittle-fracture filling, and deformation-related remobilization. This relationship supports a model in which REE concentration was established in evolved felsic host rocks and subsequently enhanced or redistributed along favourable structural planes.

The surface and subsurface datasets are mutually reinforcing. Bedrock anomalies are reproduced in trench samples and continue into borehole intersections within the same host lithologies. The strongest and most persistent mineralization occurs in syenite and migmatite gneiss, whereas amphibolite is geochemically distinct and largely barren with respect to REE enrichment. Accordingly, the principal exploration domains for follow-up work should remain the syenite bodies and mineralized migmatite-gneiss corridors outlined in the current dispersion map and drill sections. The geochemical anomaly

defined by the 1500–1750 ppm contour occurs in both the syenite and migmatite gneiss units. The identified anomaly zones are described below.

In Syenite

1. **Zone I:** The anomaly extends for approximately 200 m with an average width of 100 m in the northwestern part.
2. **Zone II:** The anomaly measures about 170 m × 50 m and is located in the eastern-central part.
3. **Zone III:** The anomaly extends for approximately 160 m with an average width of 100 m in the north-central part.

In Migmatite Gneiss

1. **Zone I:** The main anomaly extends for approximately 1 km with an average width of 300 m in the central part, trending towards the northeastern side.
2. **Zone II:** The anomaly extends for about 200 m with an average width of 150 m in the central-eastern part.
3. **Zone III:** The anomaly measures approximately 100 m × 80 m and is located in the western part.
4. **Zone IV**: The anomaly measures about 100 m × 200 m and occurs in the northern part.
5. **Zone V**: The anomaly extends for approximately 140 m with an average width of 50 m in the northwestern part.
6. **Zone VI**: The anomaly measures approximately 70 m × 70 m and is located in the northwestern part.

PLATE - 4

GEOCHEMICAL DISPERSION MAP OF BORANA BLOCK, BHILWARA DISTRICT, RAJASTHAN

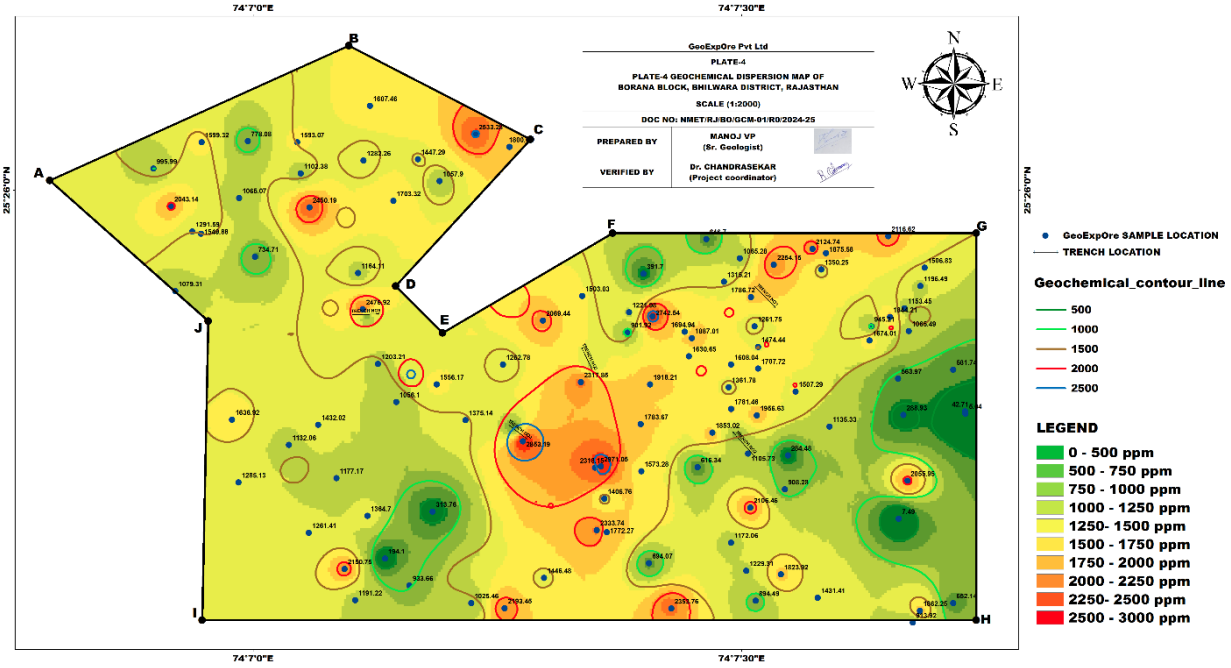

PLATE - 5

BOREHOLE SELECTION ON GEOCHEMICAL DISPERSION MAP OF BORANAN BLOCK, BHILWARA DISTRICT, RAJASTHAN

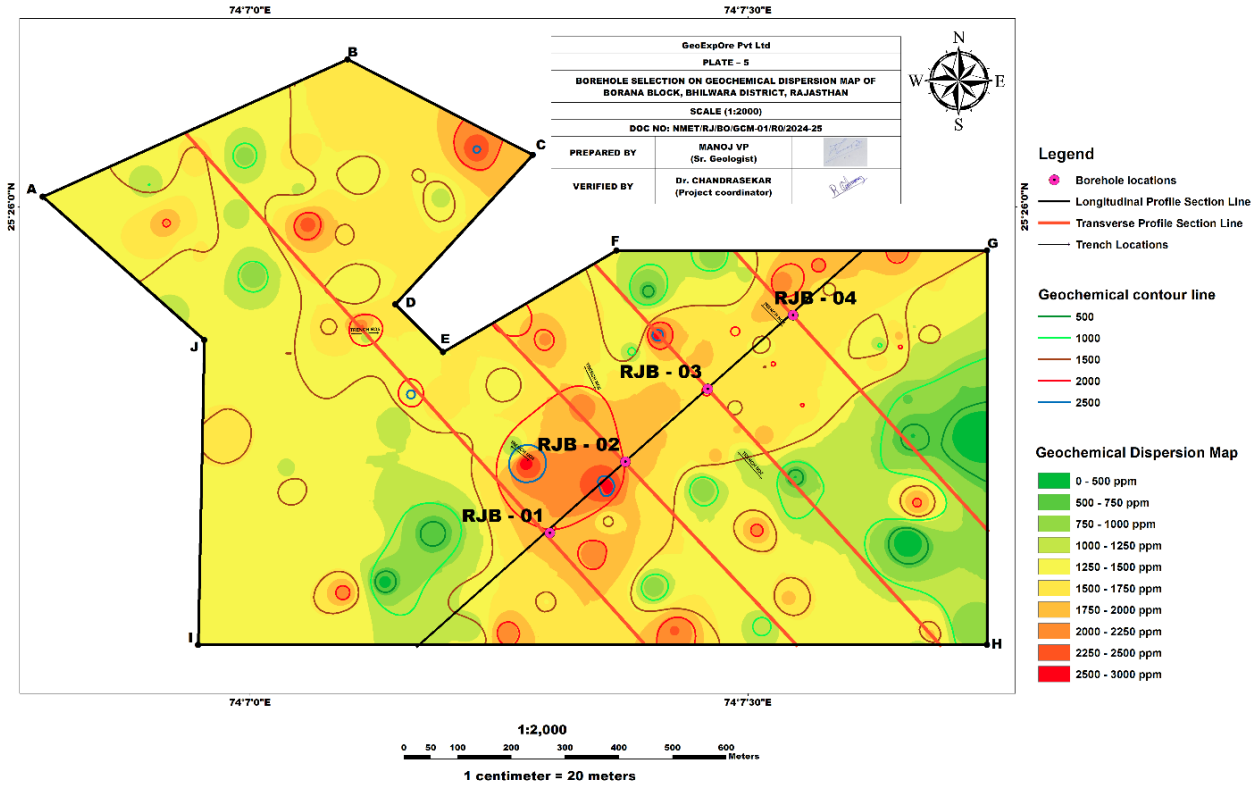

15.10 Mineral Prospect

15.10.1 Mineralization

The present G3 exploration was undertaken to investigate REE and associate mineral occurrences in the Borana Block, with migmatite gneiss and syenite constituting the principal host lithologies.

15.10.2 Surface indication of mineralization

In the area investigated, the REE mineralization was traced in the migmatite gneiss and syenite in the form of allanite grains with metallic to vitreous luster in conchoidal fractures. Numerous syenite/feldspar syenite bands extending in east-west directions were observed, which are intrusive

with in the migmatite gneiss which exhibit epidotization with small allanite crystals. This syenite band varies from few mts to hundreds of mts in thickness with the dispersion of allanite grains. Apart from the dispersion of allanite in both migmatite and syenites, medium to big crystals of Magnetite were noticed along the fractures. Epidote veins were also observed as intrusive veins and veinlet in the fractures plan in both migmatite gneiss and syenites.

15.10.3 Mode of occurrence

The REE mineralization occurs as dispersed grains in both migmatite gneiss as well as in syenites. With the field evidence, it may be inferred that mineralization is syngenetic in origin and remobilized along weak planes due to later deformation. At some places the allanite crystals are aligned parallel to S1 plane.

15.10.4 Strike length and width of anomalies identified based on geology and geochemical exploration

The geochemical dispersion map of the Borana Block delineates several well-defined anomaly zones characterized by elevated elemental concentrations. These anomaly zones show measurable strike continuity and lateral spread, which have been interpreted by correlating geochemical values with surface geology and trench locations.

The most prominent anomaly occurs in the central to south-central part of the block, where high-value contours form a coherent zone of significant areal extent. This anomaly trends consistently across multiple sample locations and overlaps with exposures of syenite and migmatite gneiss, as shown on the geological map. The anomaly exhibits appreciable strike length and moderate to broad width, indicating persistence of anomalous values over a sizeable surface area. Secondary anomaly zones are identified in the north-western and northeastern parts of the block; these zones are relatively discontinuous but display sufficient lateral continuity to warrant further investigation.

The persistence of elevated values both laterally and along strike suggests that these anomaly zones may extend to depth. Based on the areal extent, continuity, and intensity of anomalies, the central, south-central, north-western and northeastern parts of the block anomaly zones are considered suitable targets for future drilling, with proposed drill orientations designed to test the vertical continuity of mineralization beneath the anomalous surface zones.

15.10.5 Genesis of mineralization

The genesis of REE mineralization in the Borana block is interpreted to be linked to felsic to alkaline magmatic activity and subsequent localization within favorable host lithologies, principally syenite/alkali feldspar syenite and migmatite gneiss. The geochemical character of mineralized lithologies, together with the confirmed occurrence of REE-bearing accessory minerals such as allanite, monazite suggests that REE enrichment is primarily related to magmatic differentiation and concentration of incompatible elements within evolved intrusive phases.

The syenite/alkali feldspar syenite bodies, which intrude the migmatitic basement, are interpreted to represent the principal magmatic phase responsible for REE enrichment in the area. These intrusive bodies appear to have acted as favorable sites for crystallization of REE-bearing accessory minerals, particularly those enriched in light rare earth elements. The associated migmatite gneiss also hosts significant REE mineralization, which may reflect either primary enrichment within felsic leucocratic domains or secondary redistribution during high-grade metamorphism and deformation.

The mineralization is essentially disseminated to weakly structure-influenced, rather than vein-type or massive in character. Although local fractures, foliation planes, and intrusive contacts appear to have influenced mineral distribution and continuity, the available evidence indicates that mineralization is fundamentally lithology controlled. Thus, the Borana prospect is considered to represent an intrusive-associated LREE mineralized system developed within a high-grade metamorphic basement terrain affected by younger syenitic intrusive activity.

CHAPTER 16 - MOISTURE

All the analysis of borehole core samples has been carried out with in-situ moisture.

CHAPTER 17 – BULK DENSITY

Bulk density analysis of representative samples was carried out at the Indian Institute of Science, Bangalore, using the water displacement method to determine the specific gravity and bulk density of the samples. In this procedure, the weight of an empty beaker (M1), beaker with sample (M2), beaker with sample and water (M3), and beaker with water only (M4) were measured. The weight of the sample was calculated as the difference between M2 and M1, while the displaced water weight was determined from the difference between M3 and M4. The specific gravity (G) of each sample was calculated using the relation G = (M2 − M1) / {(M2 − M1) − (M3 − M4)} and the bulk density was obtained by multiplying the specific gravity with the density of water (1 g/cc). Five representative samples (BRS-105, BRS-07, BRS-61, G3051-14, and G3051-186) were analysed, yielding bulk density values ranging from 1.998 g/cc to 3.146 g/cc. These bulk density values are important parameters for resource and reserve estimation, as they are used to convert volumetric estimates of mineralized zones into tonnage. The results are provided in table below.

Table 17.1: Bulk Density Analysis

Sample ID	Rock type	M1- Empty Beaker wt (mg)	M2- EB+Sample wt (mg)	M3- EB+Sample+ Water wt (mg)	Clean EB wt (mg)	M4- EB+Water wt (mg)	Sample wt (g) {M2-M1}	Displaced Water wt by Sample(mg) {M3-M4}	Specific Gravity (G)	Bulk Density (g/cc)
BRS-105	Migmatite Gneiss	24700.3	26194.6	84050.7	24718.1	83135	1494.3	915.7	2.583	**2.583**
BRS-07	Amphibolite	24665.2	26387.9	84219.5	24685.9	83257.2	1722.7	962.3	2.266	**2.266**
BRS-61	Senite	24729.6	25881.6	83820.7	24720.8	83245.3	1152	575.4	1.998	**1.998**
G3051-14	Syenite	24710.5	25736.1	83799.7	24704.3	83100.1	1025.6	699.6	3.146	**3.146**
G3051-186	Migmatite Gneiss	24703.3	26037.2	84035.7	24702.6	83127.6	1333.9	908.1	3.133	**3.133**

CHAPTER 18 – BENEFICIATION STUDIES AS MAY BE REQUIRED

Beneficiation studies have not been carried out in the present level of exploration.

CHAPTER 19 – RESOURCE ESTIMATION TECHNIQUES

19.1 Discussion on sufficient data density to assure continuity of mineralisation and synthesis adequate data base for estimation procedure used.

Resource estimation is based on geological and geochemical data obtained from **four diamond drill boreholes**. Mineralized zones were delineated using **1000 ppm and 1200 ppm ΣREE cut-off grades**. Geological correlation of boreholes and longitudinal sections were used to establish continuity of the principal REE-bearing horizon. The discontinuous upper mineralized band in RJB-3 was excluded as it lacked lateral continuity.

19.2 Whether previous exploration data has been used and integrated with the current exploration data for assessment of the updated resources.

The estimation is based only on geological and geochemical data generated from the current drilling programme.

19.3 The nature and appropriateness of the estimation technique(s) applied and key assumptions,vincluding treatment of extreme grade values, domaining, interpolation parameters, maximum distance of extrapolation from data points

The volumetric (block) method on longitudinal sections was adopted. Each borehole was assigned an influence area of 200 m × 200 m, extending vertically through the mineralized interval. A uniform bulk density of 2.71 t/m³ was used. Resource estimation was carried out separately for 1000 ppm and 1200 ppm ΣREE cut-off grades. Average REE grades from laboratory analyses were used. No information is provided regarding domaining, interpolation, treatment of extreme grades or extrapolation distance.

19.4 The basis for the classification of the mineral resources into varying confidence classes.

The estimated REE resource has been classified as an **Inferred Mineral Resource (G3 level)** based on the available drilling data and geological continuity interpreted from four boreholes.

19.5 The assumptions made regarding recovery of by-products.

Separate estimates of **Scandium (Sc)** and **Yttrium (Y)** were calculated as additional resources. No assumptions regarding metallurgical recovery or recovery of by-products are discussed.

19.6 Detailed description of the method used and the assumptions made to estimate tonnages and grades (section, polygon, inverse distance, geostatistical, or other method).

The volumetric (block) method was adopted for the estimation of REE resources on longitudinal section. In this method, the influence area of each borehole is considered as a rectangular block measuring 200m × 200 m, extending vertically up to the depth of REE mineralization encountered in the drilling. A uniform bulk density of 2.71 t/m³ was applied for the calculation of ore tonnage. The average REE grades were derived from laboratory geochemical analyses and are expressed in parts per million (ppm). For the estimation of REE metal contained, these values were converted into percentage (%).

The following parameters and formulae were used for the estimation:

- Volume (m³) = Length × Width × Thickness
- Ore Tonnage (t) = Volume × Bulk Density
- REE Grade (%) = REE (ppm) / 10,000
- Contained REE Metal (t) = Ore Tonnage × REE Grade (%) / 100

The Longitudinal section on inclined plane (45°) is as shown in Fig.19.1

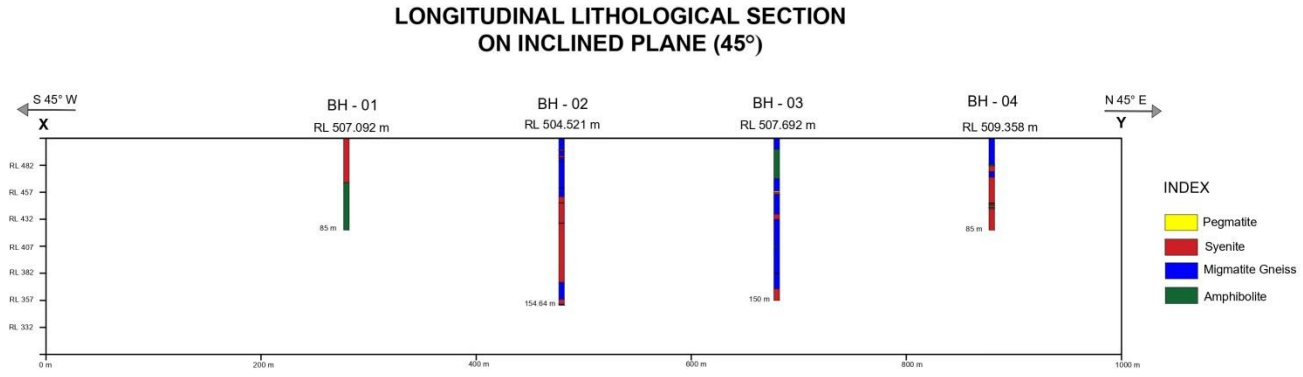

Fig 19.1 The Longitudinal section on inclined plane (45°)

19.7 Description of how the geological interpretation was used to control the resource estimates.

Geological interpretation from drill-hole correlation and longitudinal sections was used to delineate continuous mineralized zones. The **upper mineralized band in RJB-3 was excluded** because it was thin, discontinuous, comparatively low grade, and lacked lateral continuity, thereby restricting the resource estimate to the principal continuous REE-bearing horizon.

19.8 Discussion of basis for using or not using grade cutting or capping. If any computer software was used for estimation of resources then name of the software with the version and method chosen, description of programmes and parameters used.

Mineralized zones were defined using **1000 ppm and 1200 ppm ΣREE cut-off grades**. **No grade capping or top-cutting has been mentioned. No computer software, version, or estimation program has been reported.**

19.9 Geostatistical methods are extremely varied and should be described in detail. The method chosen should be justified. The geostatistical parameters, including the variogram, and their compatibility with the geological interpretation should be discussed. Experience gained in applying geo-statistics to similar deposits should be taken into account.

The resource estimation employed a **volumetric block method** and no geostatistical analysis (variogram, kriging, inverse distance weighting, etc.) has been described.

19.10 Data verification or validation procedures used, including peer review report.

No validation procedure, QA/QC verification, or peer review report is described.

CHAPTER 20 – REPORTING OF RESOURCES

The resource estimation of the study area was carried out to evaluate the quantity and grade of Rare Earth Element (REE) mineralization encountered in the drilled boreholes. The estimation is based on the geological and geochemical data obtained from four boreholes drilled within the study area. Core samples collected at regular depth intervals were analyzed for REE concentrations using ICP-OES after acid digestion. The geochemical dataset includes concentrations of individual REE elements from La to Lu along with Y, Th and U. The total rare earth element content (ΣREE) was calculated by summing the individual REE concentrations.

Based on the ΣREE values, mineralized zones were identified using cut-off grades of 1000 ppm and 1200 ppm separately. Bulk density determined from laboratory measurements was used for the estimation of ore tonnage. The resource estimation was carried out by integrating the thickness of mineralized zones, average grade, and bulk density to determine the total tonnage and containing REE metal in the study area. The results of the estimation provide an understanding of the distribution, grade variation, and potential economic significance of the REE mineralization.

Based on the ΣREE values obtained from the geochemical analysis, the depth-wise distribution of total rare earth elements in the Borana boreholes was examined (Fig 20.1). Histograms showing the distribution of total REE concentrations were plotted to understand the frequency and range of ΣREE values within the drilled samples. The histogram analysis indicates that most of the samples fall within the range of 1000 ppm to 1400 ppm ΣREE (Fig 20.2). Considering this distribution pattern, cut-off grades of 1000 ppm and 1200 ppm ΣREE were selected for the delineation of mineralized zones. Resource estimation was subsequently carried out separately for both cut-off grades to evaluate the variation in tonnage, grade, and contained REE metal.

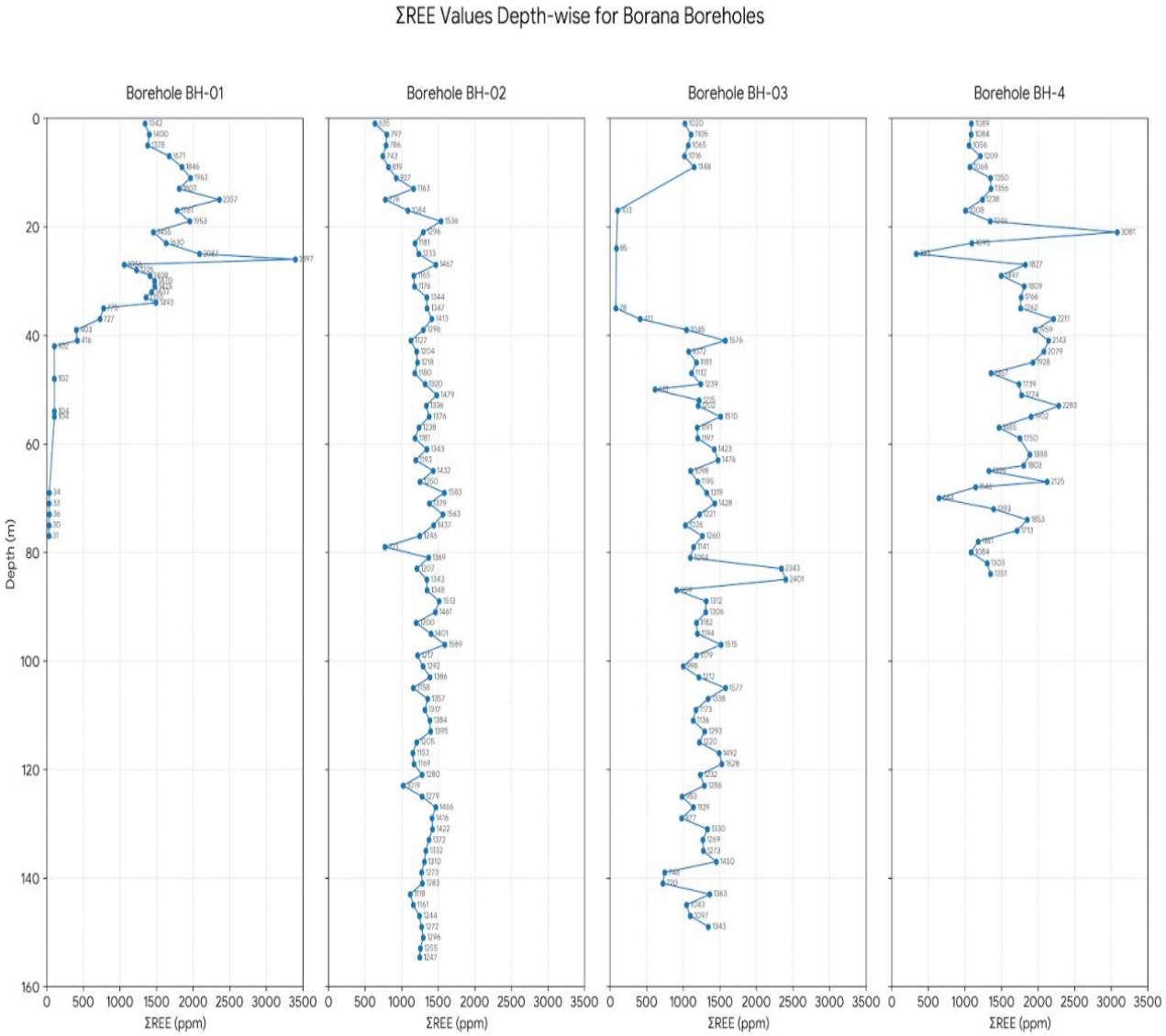

Fig 20.1 ΣREE values depth wise for Borana Boreholes

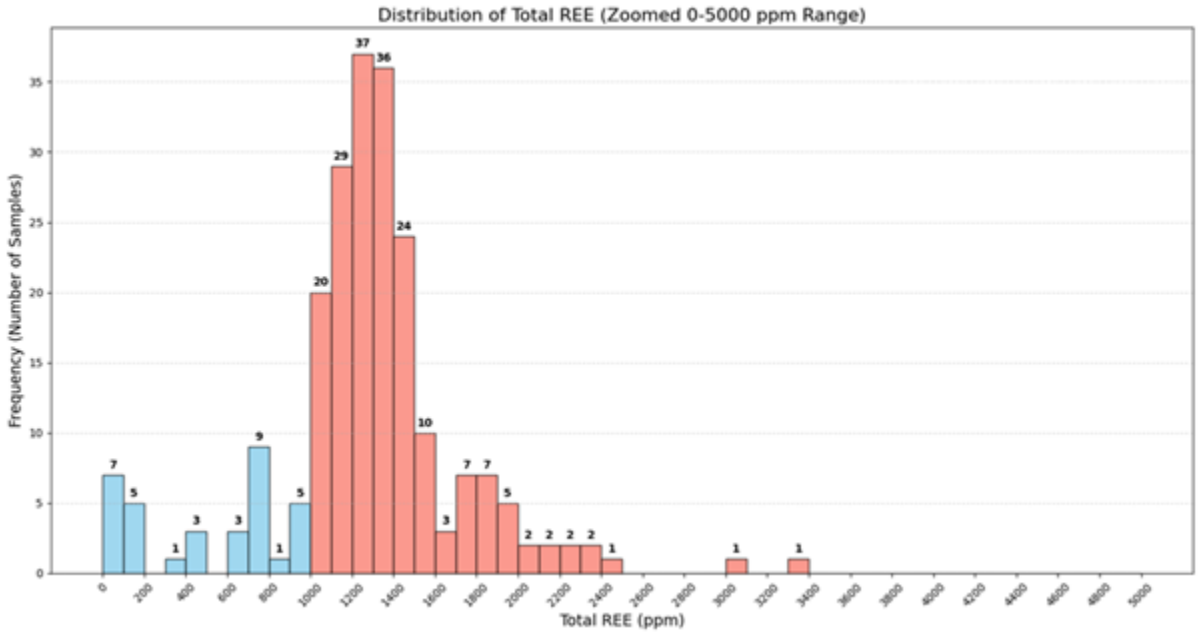

Fig 20.2 Histogram showing distribution of total REE

20.1 REE Resource Estimation (1000 ppm Cut-off Grade)

For the 1000 ppm ΣREE cut-off grade, borehole sections were prepared which are shown below

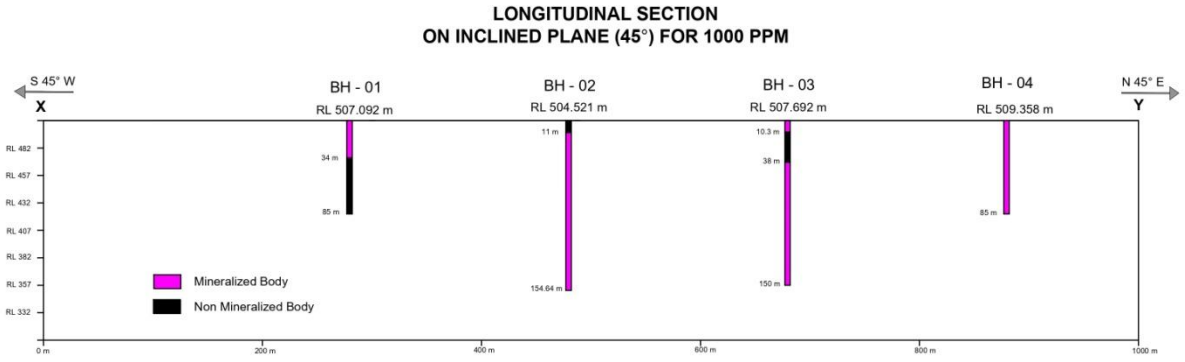

Fig 20.3 Longitudinal section on inclined plane (45°) for 1000ppm showing mineralized and non-mineralized bodies

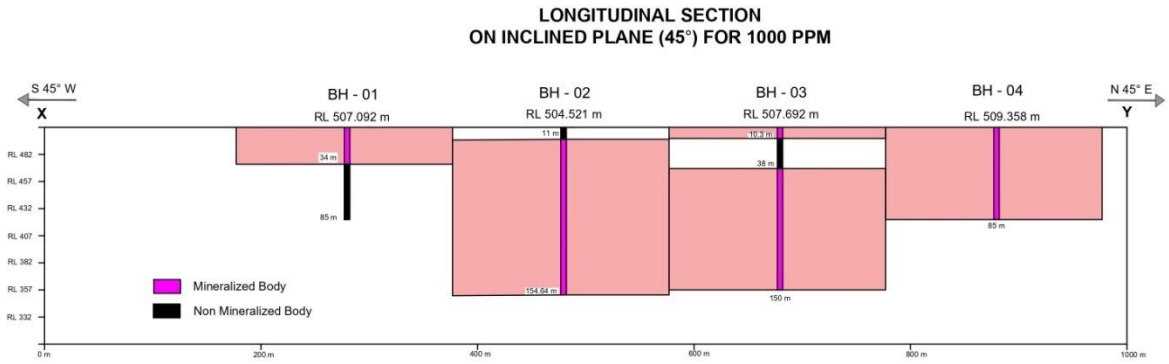

Fig 20.4 Longitudinal section on inclined plane (45°) for 1000ppm showing mineralized and non-mineralized bodies of entire area

Table 20.1: Ore resource estimation for 1000 ppm cut-off

BH-ID	Length (M)	Width (M)	Thickness (M)	Volume (M3)	Bulk Density (t/m3)	Tonnage (t)	REE Concentration	REE total in tonnes(t)
RJB-1	200	200	24.04	961600	2.71	2605936	(0.1681462%)	4381.782
RJB-2	200	200	101.55	4062000	2.71	11008020	(0.1284993%)	14,145.228
RJB-3	200	200	7.28	291200	2.71	789152	(0.1071618%)	845.669
			79.18	3167200	2.71	8583112	(0.1253060%)	10755.154
RJB4	200	200	60.09	2403600	2.71	6513756	(0.1544096%)	10057.864
						29499976 (29.49) million tonnes (Mt)		**40185.697 Tonnes Additional resource: (Sc + Y) = (221.59 t+2337.75 t) = 2559.34Tonnes**

In **RJB-1**, the estimated contained REE metal for Borehole RJB-1 is 4381.782 tonnes. Out of this, LREE constitutes approximately 4172.764 tonnes**,** while HREE accounts for about 209.017 tonnes. **RJB-2** shows the highest REE content among the drilled boreholes, with a total contained REE of 14,145.228 tonnes**.** The estimated LREE content is 13,221.824 tonnes, whereas HREE constitutes about 923.403 tonnes. In **RJB-3**, two mineralized zones were identified in Borehole RJB-3. Upper Zone (Thickness: 7.28 m). The estimated REE metal contained is 845.669 tonnes, consisting of

794.321 tonnes of LREE and 51.344 tonnes of HREE. Lower Zone (Thickness: 79.18 m). The lower zone contains 10,755.154 tonnes of total REE, of which 10,130.104 tonnes correspond to LREE, and 625.049 tonnes correspond to HREE. In **RJB-4,** the estimated contained REE metal in Borehole RJB-4 is 10,057.864 tonnes, comprising 9,612.974 tonnes of LREE and 444.890 tonnes of HREE.

Subsequent review of the geological sections, drill hole correlations, and geochemical data indicated that the upper mineralized band intersected in **BH RJB-03** represents a thin, discontinuous, and comparatively low-grade mineralized horizon, which lacks lateral continuity with the principal REE-bearing zone delineated across the block. As the horizon does not satisfy the criteria for defining a continuous mineralized body under G3 level resource estimation, it has been excluded from the final resource calculation. Accordingly, the resource estimation has been revised considering only the laterally persistent and geologically correlatable mineralized horizon, resulting in a more representative estimate of the REE resource.

Table 20.2: Resource Estimation

Parameter	**Resource Estimate**
Total Ore Volume (m^3)	10,594,400
Total Ore Tonnage (Mt)	28.71
Average TREE Grade (%)	0.14409
Contained TREE (t)	39,340.028

20.1.1 Overall REE Resource

The cumulative REE resource estimated from all four boreholes amounts to **39,340.028 tonnes** of total REE. The estimated resource is categorized as Inferred Resource.

Table 20.3: Different elements metal resource of all four boreholes:

Element	BH-1 Metal Content (Tonnes)	BH-2 Metal Content (Tonnes)	BH-3 upper zone Metal Content (Tonnes)	BH-3 lower zone Metal Content (Tonnes)	BH-4 Metal Content (Tonnes)
Lanthanum (La)	874.28	3,379.018	209.44	2,650.53	2,549.84
Cerium (Ce)	1,727.34	6,783.829	406.52	5,178.78	4,736.01
Praseodymium (Pr)	373.42	542.369	30.89	407.33	472.21
Neodymium (Nd)	948.70	2,124.260	125.41	1,608.78	1,581.83
Samarium (Sm)	103.49	341.402	20.05	263.52	225.86
Europium (Eu)	145.53	50.981	2.01	21.16	51.29
Gadolinium (Gd)	71.24	269.187	15.64	200.42	162.94
Terbium (Tb)	8.66	40.707	2.25	29.74	21.82
Dysprosium (Dy)	50.21	220.594	12.29	155.74	108.76
Holmium (Ho)	7.86	38.847	2.11	26.41	17.85
Erbium (Er)	35.50	163.418	8.90	103.68	66.46
Thulium (Tm)	4.74	21.621	1.14	12.01	5.27
Ytterbium (Yb)	27.37	149.414	8.00	87.54	56.86
Lutetium (Lu)	3.42	19.618	1.01	9.51	0.78
Scandium (Sc)	17.78	87.530	4.59	70.35	41.34
Yttrium (Y)	184.83	1,155.055	61.48	784.40	151.99
Thorium (Th)	40.59	214.926	8.11	145.83	197.37
Uranium (U)	12.64	113.456	2.37	51.70	37.16

20.2 REE Resource Estimation (1200 ppm Cutoff Grade)

For the 1200 ppm ΣREE cut-off grade, borehole sections were prepared which are shown below

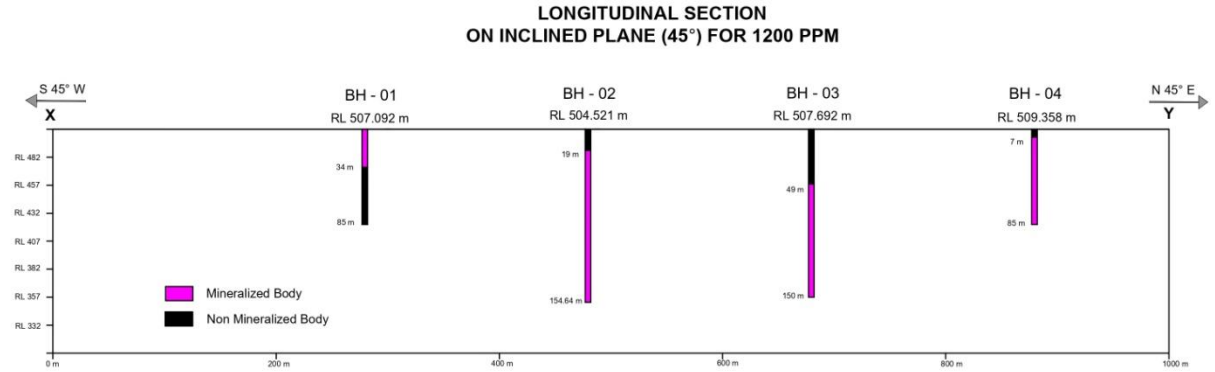

Fig 20.5 Longitudinal section on inclined plane (45°) for 1200ppm showing mineralized and non-mineralized bodies

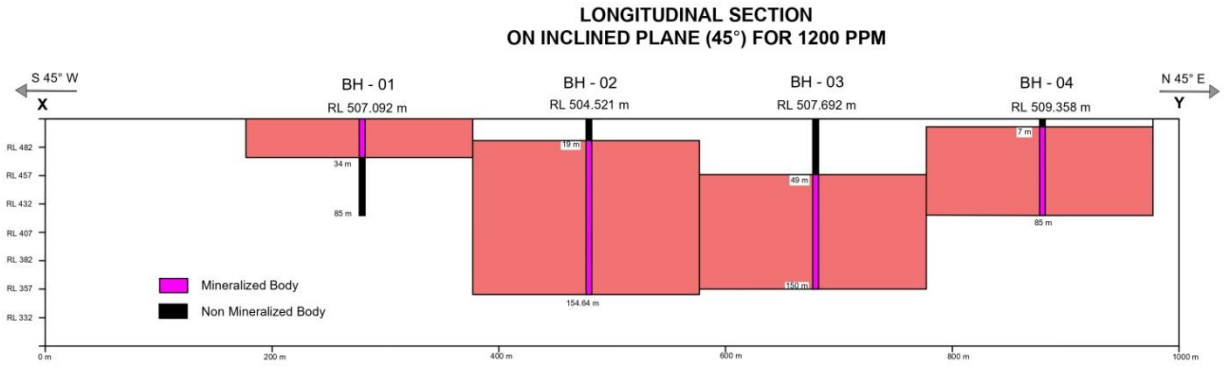

Fig 20.6 Longitudinal section on inclined plane (45°) for 1200ppm showing mineralized and non-mineralized bodies of entire area

Table 20.4: Ore resource estimation for 1200 ppm cut-off

BH-ID	Length (M)	Width (M)	Thickness (M)	Volume (M3)	Bulk Density (T/M3)	Tonnage (T)	REE Concentration	REE Total In Tonnes(T)
RJB-1	200	200	24.04	961600	2.71	2605936	(0.1681462%)	4381.782
RJB-2	200	200	95.89	3835600	2.71	10394476	(0.130219%)	13535.582
RJB-3	200	200	71.407	2856280	2.71	7740519	(0.1258371731%)	9740.450
RJB4	200	200	55.146	2205840	2.71	5977826.4	(0.157915425%)	9439.909
						26718757.4 (26.71 million tonnes (Mt).)		37097.723 Tonnes Additional resources: (Sc + Y) = (370.81t+ 3921.05t) = 4291.86 Tonnes

20.2.1 Overall REE Resource

The results of REE Resource Estimation Based on 1200 ppm Cut-off Grade:

In RJB-1, the estimated contained REE metal for Borehole RJB-1 is 4381.782 tonnes. Out of this, LREE contributes approximately 4172.782 tonnes, while HREE accounts for about 209.017 tonnes. **RJB-2** contains a total REE of 13,535.582 tonnes. Among this, LREE constitutes approximately 12,657.175 tonnes, whereas HREE contributes about 878.406 tonnes. In **RJB-3** the estimated REE metal contained is 9,740.450 tonnes. The LREE component is approximately 9,176.547 tonnes, while HREE accounts for about 563.902 tonnes. **RJB-4** contains an estimated 9,439.909 tonnes of total REE, consisting of 9,024.939 tonnes of LREE and 414.967 tonnes of HREE.

The Overall REE Resource: The cumulative REE resource estimated from all four boreholes at a 1200 ppm cut-off grade amounts to 37,097.723 tonnes of total REE. Of this, LREE constitutes approximately 35,031.443 tonnes (94.43%), while HREE accounts for about 2,066.292 tonnes (5.57%). The results indicate that the REE mineralization within the study area is predominantly enriched in Light Rare Earth Elements (LREE) with comparatively lower concentrations of Heavy Rare Earth Elements (HREE). The estimated resource is categorized as Inferred Resource.

Table 20.5: Different elements metal resource of all four boreholes:

Element	BH-1 Metal Content (Tonnes)	BH-2 Metal Content (Tonnes)	BH-3 Metal Content (Tonnes)	BH-4 Metal Content (Tonnes)
Lanthanum (La)	1,093.49	3,232.09	2,402.13	2,392.80
Cerium (Ce)	2,028.77	6,494.31	4,685.85	4,446.15
Praseodymium (Pr)	222.42	520.41	370.83	446.15
Neodymium (Nd)	731.32	2,034.20	1,459.65	1,481.02
Samarium (Sm)	118.00	326.37	239.08	210.21
Europium (Eu)	12.58	49.79	19.01	49.66
Gadolinium (Gd)	76.75	257.20	181.24	151.87
Terbium (Tb)	10.02	38.76	26.94	20.32
Dysprosium (Dy)	45.24	209.85	140.99	101.35
Holmium (Ho)	7.47	36.90	23.86	16.63
Erbium (Er)	17.89	155.01	93.23	61.9
Thulium (Tm)	2.51	20.49	10.71	6.47
Ytterbium (Yb)	13.15	141.62	78.54	53.09
Lutetium (Lu)	1.98	18.59	8.40	3.78
Scandium (Sc)	38.70	164.81	125.96	37.91
Yttrium (Y)	220.51	2,153.05	1,395.50	527.40
Thorium (Th)	10.74	214.06	89.48	184.53
Uranium (U)	483.00	406.84	259.60	35.51

CHAPTER 21 - SUMMARY AND RECOMMENDATIONS

21.1 Summary

Based on detailed geological mapping, trenching, drilling, petrographic, and geochemical investigations carried out during the G3 level exploration in the Borana Block, the following conclusions are drawn:

1. **Targets Assigned vs Targets Achieved**: The G3-stage preliminary investigation for Rare Earth Element (REE) and associated mineralization in the Borana Block of Bhilwara District, Rajasthan, was carried out successfully, with all planned activities meeting their respective targets. The assigned area of 1.14 km² was fully covered and geologically mapped at a 1:2000 scale, along with DGPS-based survey (5 nos). Technological operations, including trenching (100 cubic meters) and drilling (474.64 meters), were effectively completed. Furthermore, geochemical studies were accomplished, with bedrock sampling (108 samples), while trench sampling (100 samples) and core sampling (222samples) achieved the assigned goals. Overall, the project objectives were efficiently fulfilled, for evaluating the REE mineralization potential of the study area.
2. **Geology and Mineralization:** The block area comprises Archaean basement rocks belonging to the Mangalwar Complex of the Bhilwara Supergroup (Gupta et al., 1997). The litho-units mapped in the area include syenite, migmatite gneiss, pegmatite and amphibolite, which exhibit a complex structural history marked by progressive deformation. The study in the Borana block where REE mineralization occurs in the form of allanite crystals and monazite is disseminated within the syenite and migmatite gneiss.
3. **Significant REE Mineralization**: The Borana Block hosts appreciable rare earth element (REE) mineralization, predominantly within syenite/alkali syenite and migmatite gneiss of the Mangalwar Complex. Syenite samples display relatively higher REE enrichment.

Bedrock syenite samples range from **778.08 ppm to 2742.54 ppm** with an average of **1552.94 ppm** (n-45). Trench samples show values between **904.23 and 2645.85 ppm**, averaging **1775.28 ppm**(n-26), while core samples range from **333.63 ppm to 3397.12 ppm**, with an average of **1423.71 ppm** (n-112), indicating substantial enrichment in Syenite. The migmatite gneiss bedrock samples exhibit total REE concentrations ranging from **194.10 to 2853.19 ppm**, with an average value of **1376.46 ppm**(n-59). Trench samples from migmatite gneiss show REE values between **130.82 and 1748.22 ppm**, averaging **956.45 ppm** (n-74). Core samples record a wider range of **411.51 to 3081.88 ppm**, with an average of **1235.06 ppm** (n-98).

4. **Lithological Control on REE Distribution:** Analytical data from BRS, trench, and core samples indicate that syenite generally records higher average REE concentrations compared to migmatite gneiss, although both lithologies significantly contribute to the overall resource potential.
5. **Target Delineation through Geochemical Dispersion:** The geochemical dispersion map prepared using BRS and trench sample data effectively delineated high anomalous REE zones. These **anomalous zones** were utilized for the scientific selection of borehole locations, ensuring focused and efficient subsurface exploration. The 1000 ppm contour has been used as a threshold to define priority targets, with the principal anomaly showing an approximate strike length of 900 m and a width of 500 m.
6. **Petrography and REE-bearing Minerals**: Petrographic studies indicate that migmatite gneiss and syenite act as the principal host rocks for REE mineralization, with **allanite and monazite** identified as the dominant REE-bearing phases. Allanite occurs as irregular to prismatic grains exhibiting radial cracks and pleochroic haloes, whereas monazite occurs as granular to elongated grains. Syenite shows intense alteration and deformation with abundant REE minerals, suggesting it as a major contributor to REE enrichment, while migmatite gneiss also hosts significant REE phases. Overall, the petrographic characteristics indicate that REE mineralization is primarily controlled by **magmatic processes**, subsequently modified by **deformation and hydrothermal activity**.
7. **Geochemical Characteristics and Magmatic Evolution**: Geochemical studies indicate that the rock suite of the Borana Block ranges from **mafic to felsic composition**, with most samples plotting in the intermediate to acidic domain. The AFM diagram suggests a

dominantly **calc-alkaline affinity** with minor tholeiitic influence, reflecting a complex magmatic evolution. Harker variation trends show a systematic decrease of **CaO, MgO, FeOt, and TiO_2** with increasing SiO_2, confirming **fractional crystallization** as the principal magmatic process. Enrichment of **Na_2O and K_2O** in evolved rocks reflects alkali enrichment during differentiation. Alumina saturation indices indicate predominantly **metaluminous character** with minor peralkaline tendency, suggesting mantle-derived magmas with crustal interaction. Amphibolites represent tholeiitic mafic protoliths, while syenite and migmatite gneiss correspond to evolved felsic derivatives. Tectonic discrimination diagrams suggest that the magmatism is related to a **spreading/extensional tectonic setting**, later modified by crustal reworking and metamorphism. Overall, the geochemical data indicates a **cogenetic magmatic suite** derived from a mafic parental magma, evolving through fractional crystallization and crustal interaction.

8. **Continuity and Extent of Mineralization:** Trenching and drilling have established both **lateral and vertical continuity** of REE mineralization within the identified zones. The current borehole grid spacing of **200 m** has provided a preliminary understanding of the deposit geometry. The mineralized orebody within both **syenite and migmatite gneiss remains open in all directions**, indicating significant potential for extension. This warrants **further detailed drilling** to delineate the full extent and upgrade the resource category.
9. **Resource Estimation (Inferred Category):** Based on the integration of geological, geochemical, and drilling data, the REE resource has been estimated. Based on combined syenite and migmatite total REE values, resource has been calculated. The Resource is under the **Inferred Resource category**. The resources at different cut-off grades are summarized below:

Cut-off Grade	Tonnage (Mt)	Total REE (tonnes)	Average REE Concentration
1000 ppm	28.71	39,340	**1440 ppm (0.144%)**
1200 ppm	26.71	37,098	**1455 ppm (0.145%)**

The average REE values in ppm highlight the low to moderate grade nature of mineralization.

10. The identified anomaly zones are described below.

In Syenite

iv) Zone I: The anomaly extends for approximately 200 m with an average width of 100 m in the northwestern part.

v) Zone II: The anomaly measures about 170 m × 50 m and is located in the eastern-central part.

vi) Zone III: The anomaly extends for approximately 160 m with an average width of 100 m in the north-central part.

In Migmatite Gneiss

vii) Zone I: The main anomaly extends for approximately 1 km with an average width of 300 m in the central part, trending towards the northeastern side.

viii) Zone II: The anomaly extends for about 200 m with an average width of 150 m in the central-eastern part.

ix) Zone III: The anomaly measures approximately 100 m × 80 m and is located in the western part.

x) Zone IV: The anomaly measures about 100 m × 200 m and occurs in the northern part.

xi) Zone V: The anomaly extends for approximately 140 m with an average width of 50 m in the northwestern part.

xii) Zone VI: The anomaly measures approximately 70 m × 70 m and is located in the northwestern part.

21.2 Recommendations

Based on the encouraging results obtained from the G3 level exploration in the Borana Block, the following recommendations are proposed for further advancement of the project:

1. **Detailed Exploration (G2 Level)**: It is recommended to upgrade the exploration to **G2 level.** Drilling carried out each borehole at 200 m intervals indicates that the ore body remains open both along strike and in the dip direction. This warrants further exploration through systematic and closely spaced drilling on a 50 m × 50 m grid, which will help in accurately delineating the geometry, thickness, and continuity of the ore body. As the mineralization is open in all directions, such detailed investigation will enable the conversion of presently inferred resources into indicated resources and ultimately facilitate the establishment of mineable reserves.
2. **Detailed Geological and Structural Studies:** Integrated geological and structural mapping at a larger scale is recommended to better understand the **controls of mineralization**, including lithological contacts, deformation patterns, and structural features influencing REE concentration. This will aid in refining exploration targets and optimizing drilling locations.
3. **Detailed Petrological and Mineralogical studies:** Detailed petrological and mineralogical studies are recommended to better characterize the host rocks and REE-bearing phases, which will help in understanding the mode of occurrence, distribution, and controls of mineralization in the study area.
4. **Geochemical and Mineralogical Characterization:** Advanced geochemical and mineralogical investigations, including **REE deportment studies**, are recommended to understand the distribution of REE within different mineral phases. This will support process design and improve recovery efficiency.
5. **Detailed Resource Estimation and Classification:** A refined resource estimation should be carried out following internationally accepted standards such as **JORC/UNFC guidelines**, incorporating updated drilling data and geological modeling. This will help in upgrading the current **inferred resource** to higher confidence categories and in assessing the economic viability of the deposit.
6. **Beneficiation Studies:** Comprehensive **beneficiation studies** are required to establish an efficient process flow sheet for REE recovery from the host rocks. Emphasis should be placed on the recovery of REE from **allanite and monazite**, including studies on mineral liberation, grinding characteristics, and separation techniques.

7. **Pre-feasibility Studies:** Based on the upgraded resource, preliminary feasibility studies may be undertaken to assess the viability of mining and processing of REE from the Borana Block.

CHAPTER 22 – PLATES AND MAPS

PLATE - 1

OUTCROP MAP OF BORANA BLOCK, BHILWARA DISTRICT, RAJASTHAN

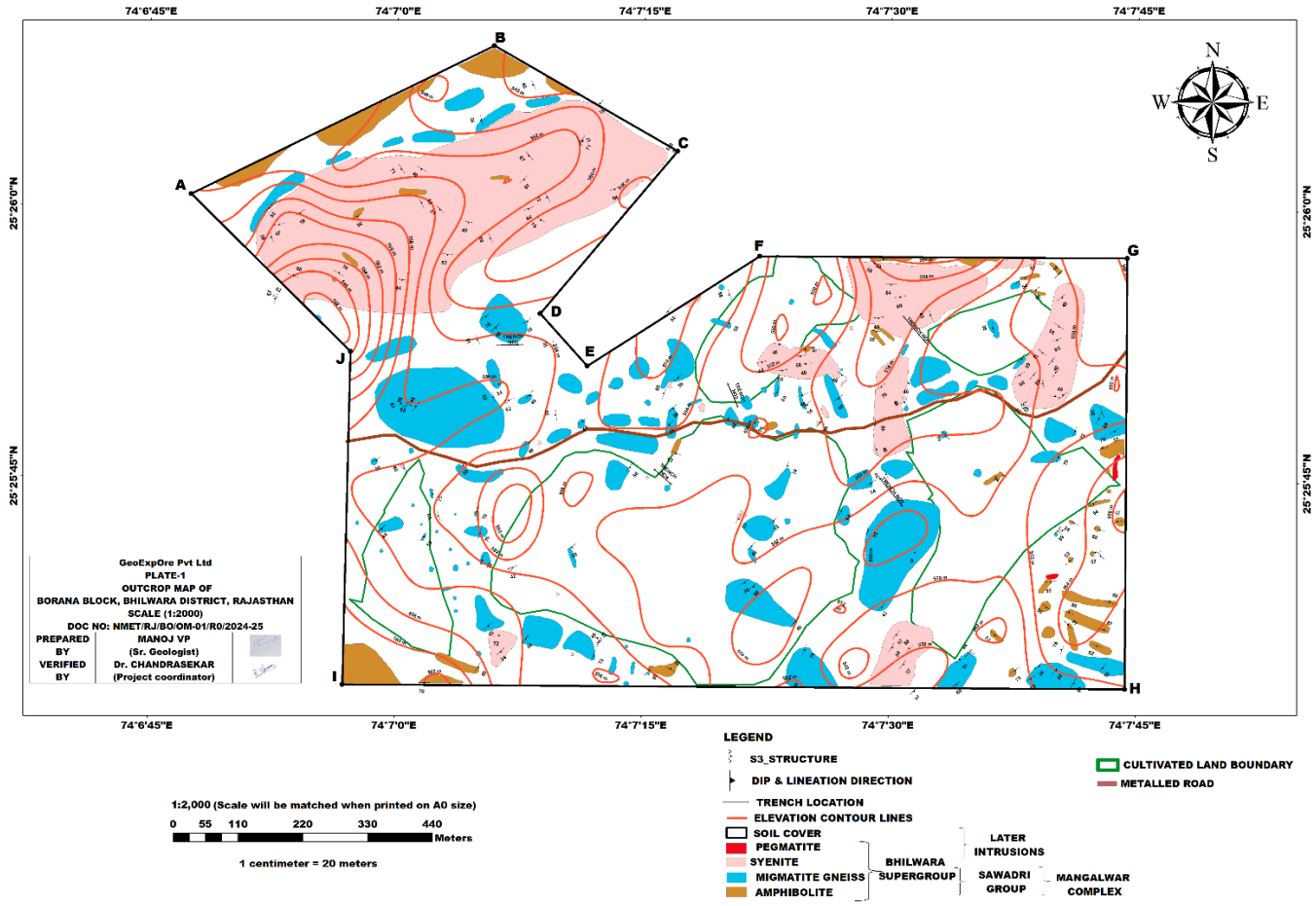

PLATE-2
GEOLOGICAL MAP OF BORANA BLOCK,BHILWARA DISTRICT, RAJASTHAN

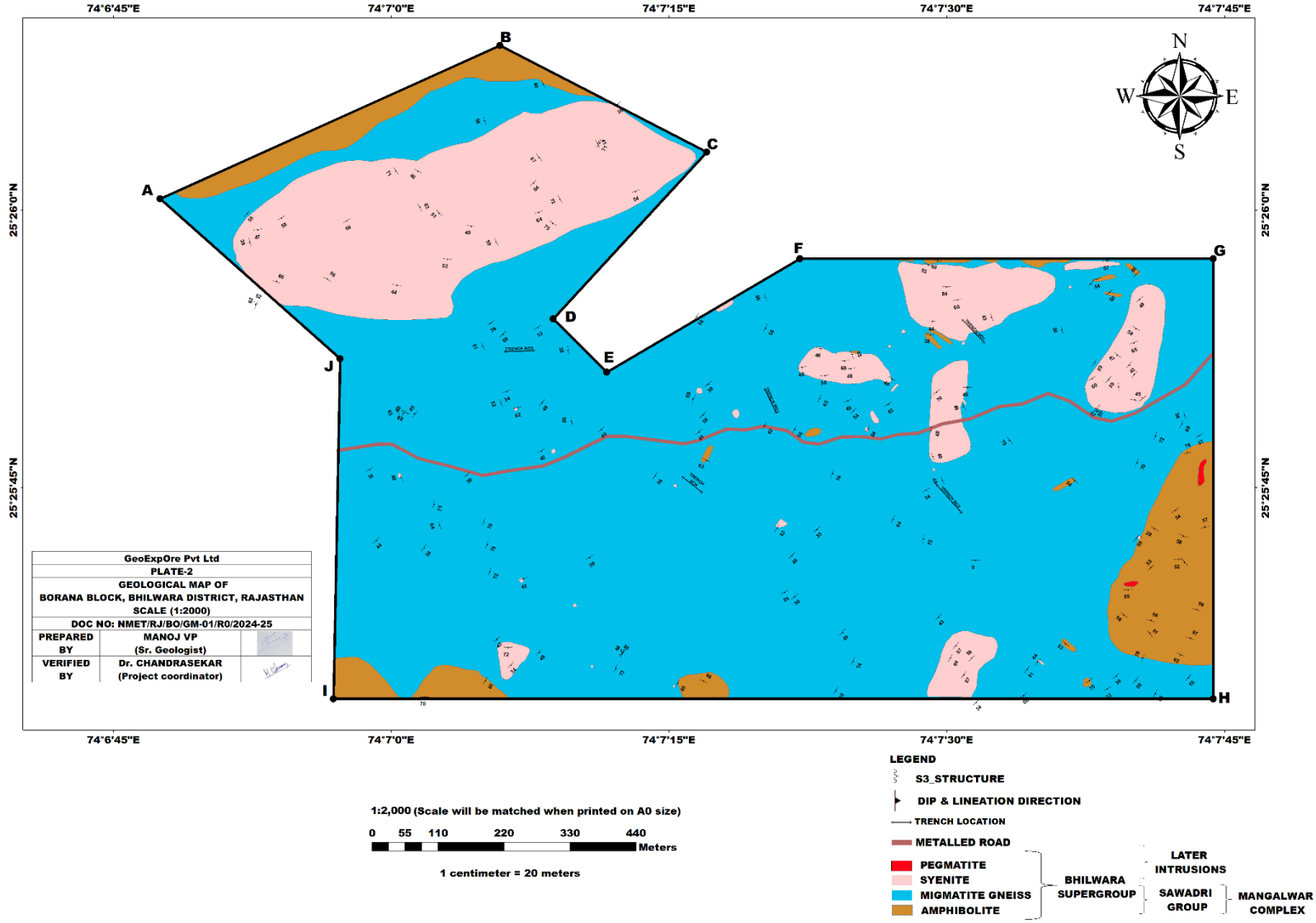

PLATE - 3

SAMPLE LOCATION SHOWN ON GEOLOGICAL MAP OF BORANA BLOCK,BHILWARA DISTRICT, RAJASTHAN

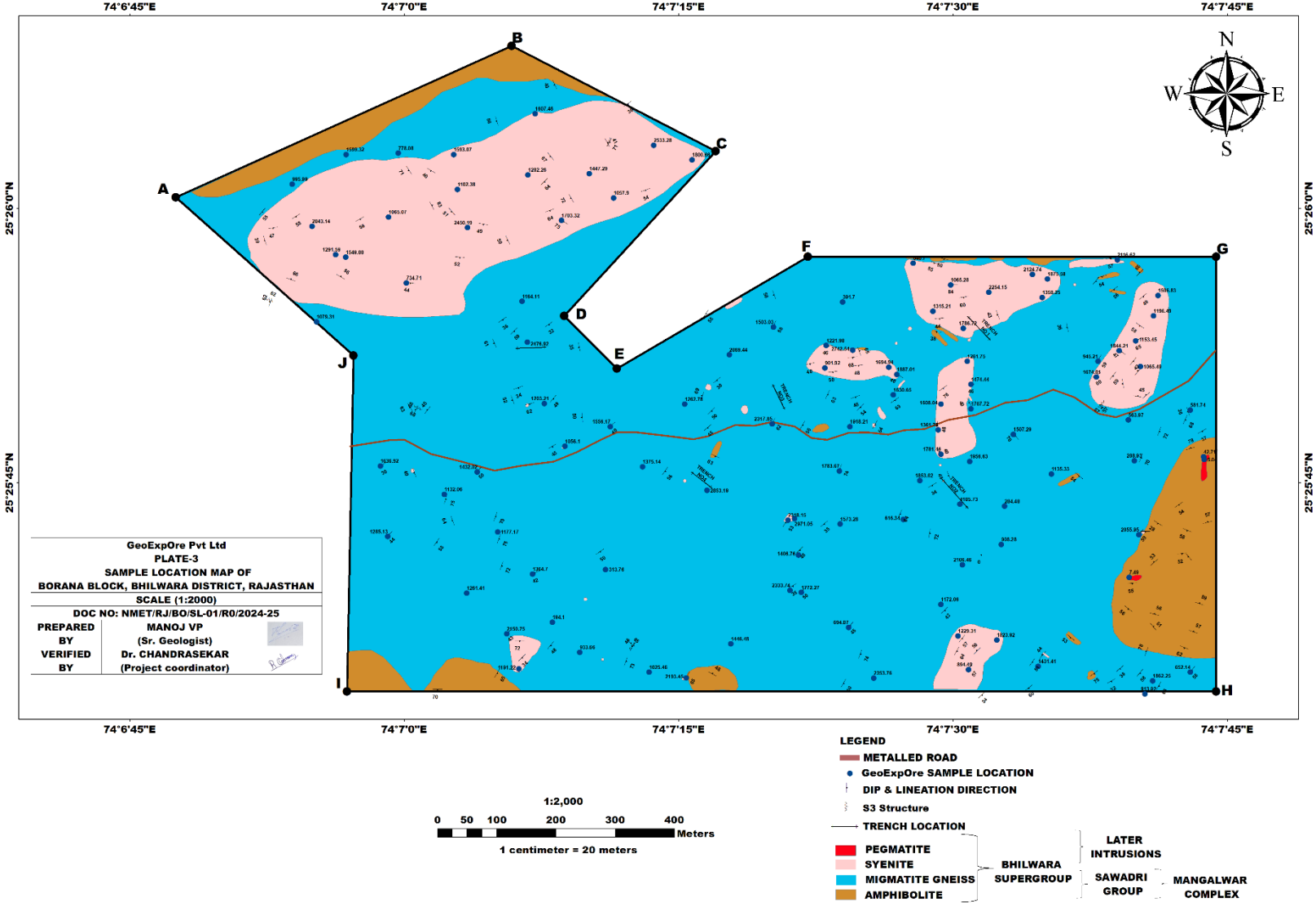

PLATE - 4

GEOCHEMICAL DISPERSION MAP OF BORANA BLOCK, BHILWARA DISTRICT, RAJASTHAN

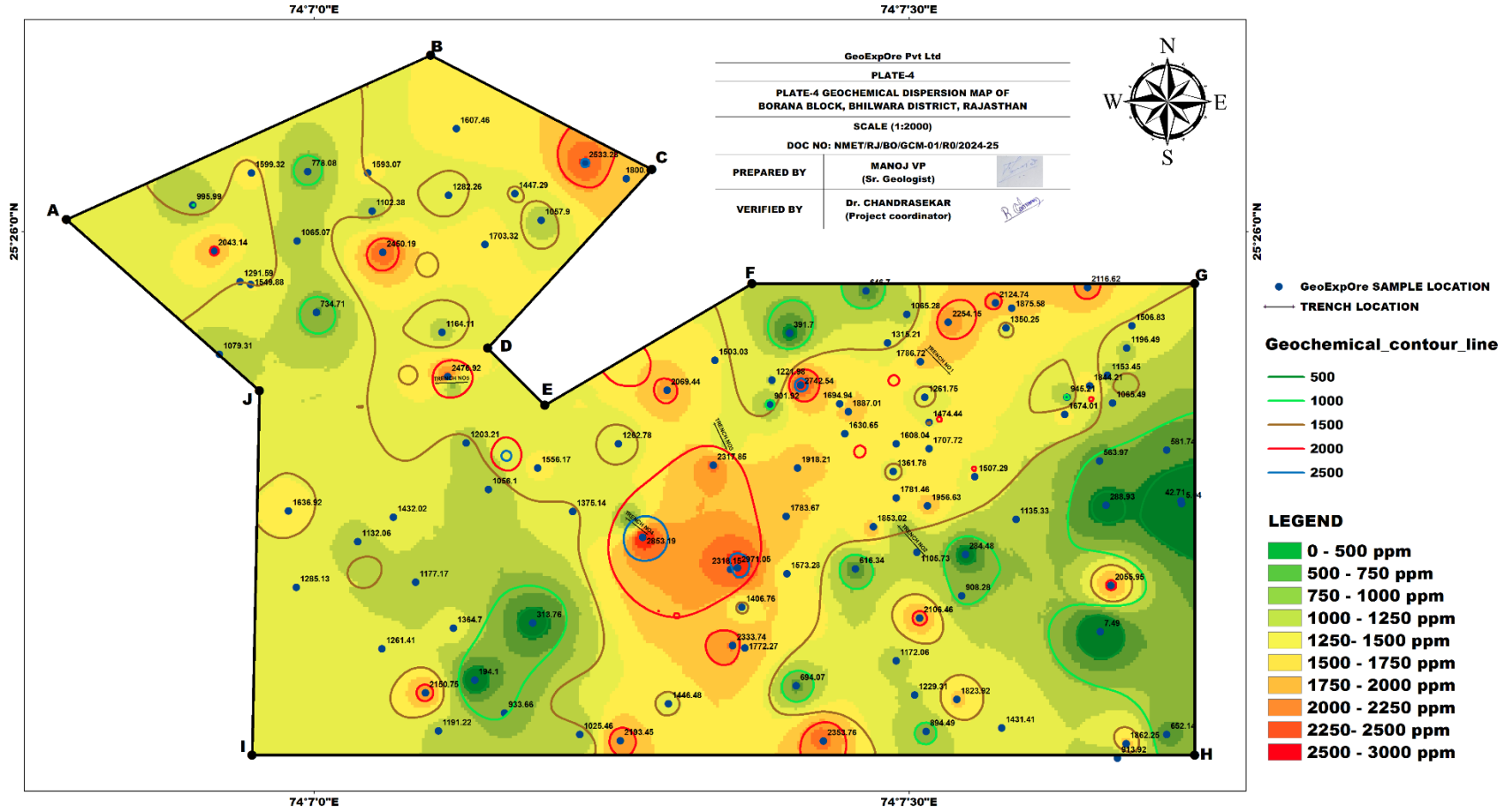

PLATE - 5

BOREHOLE SELECTION ON GEOCHEMICAL DISPERSION MAP OF BORANAN BLOCK, BHILWARA DISTRICT, RAJASTHAN

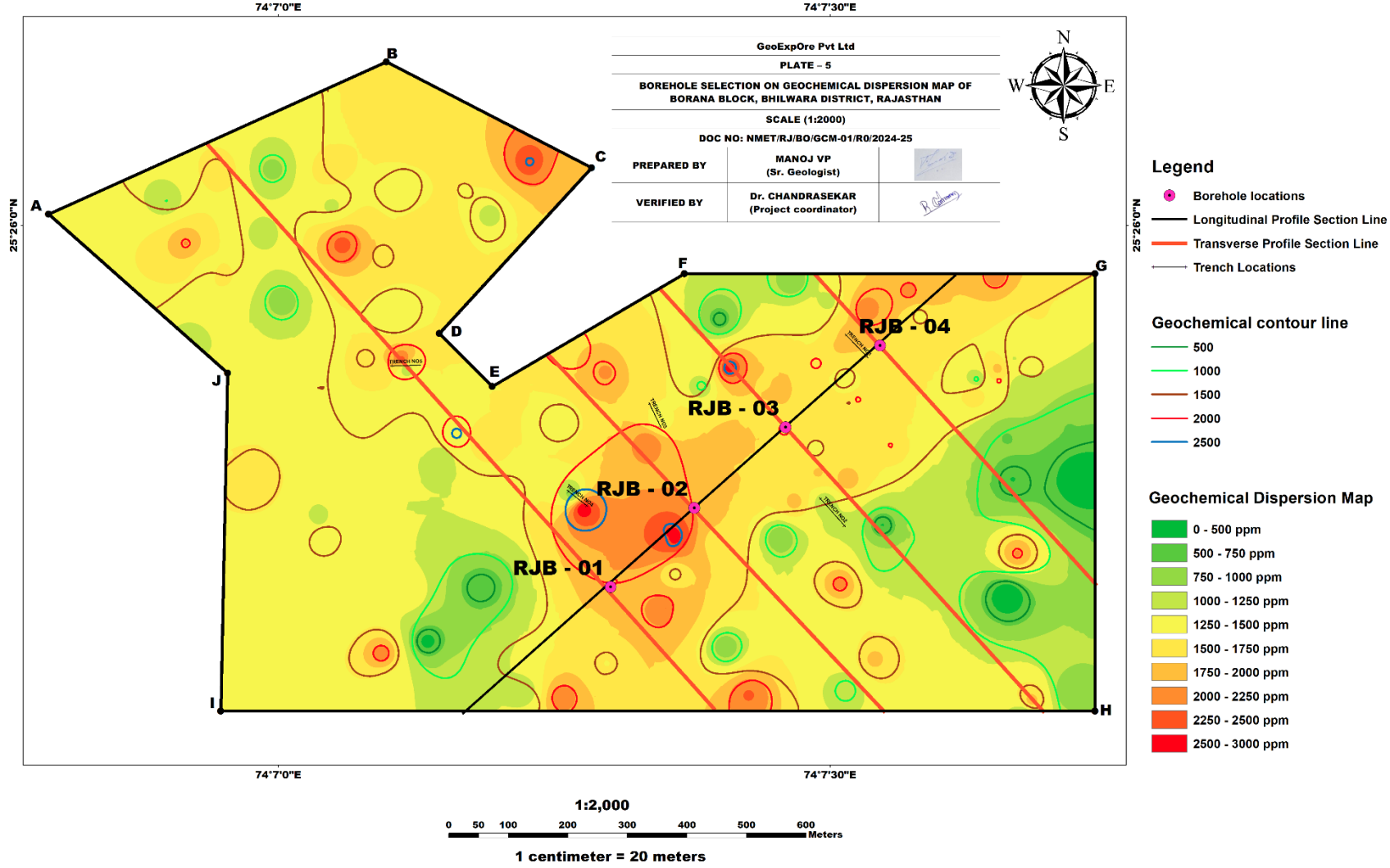

PLATE-6

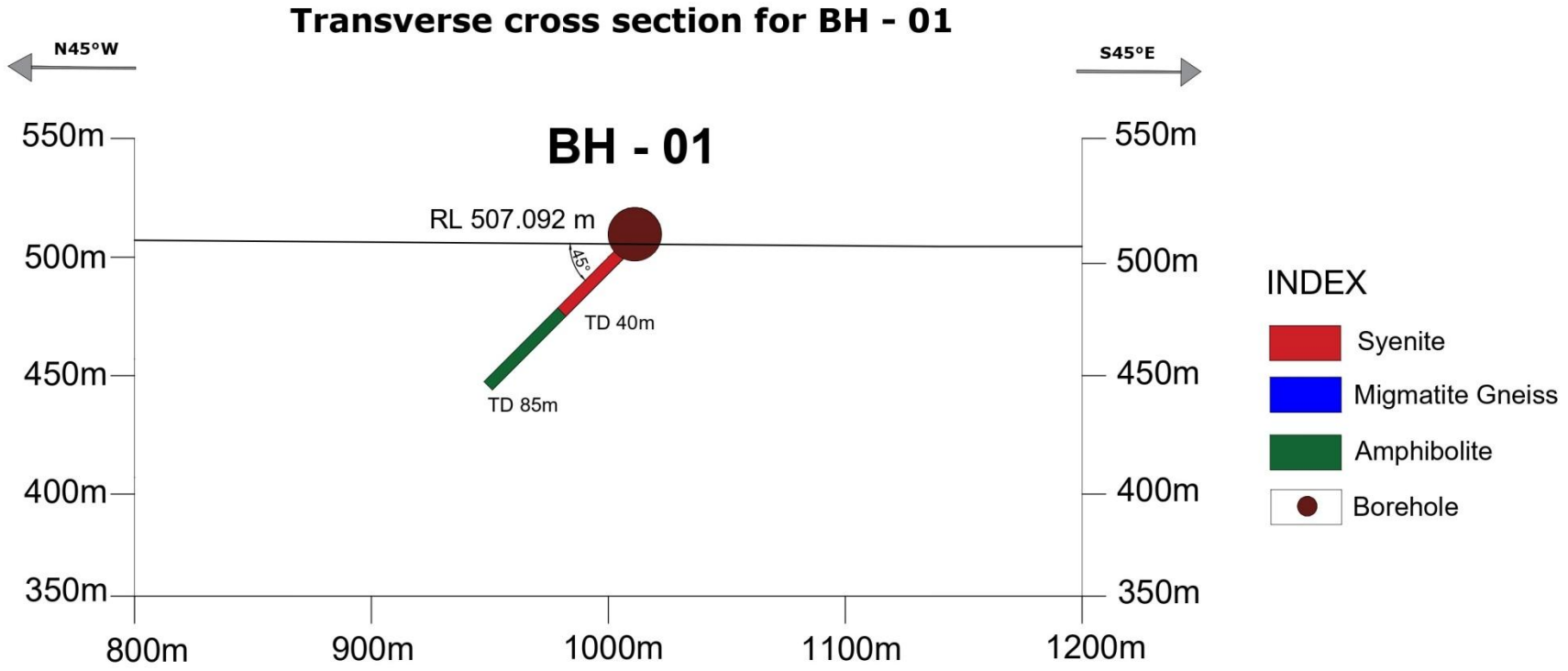
Transverse cross section for BH - 01
N45°W
S45°E
BH - 01
RL 507.092 m
45°
TD 40m
TD 85m
550m
500m
450m
400m
350m
800m
900m
1000m
1100m
1200m
INDEX
Syenite
Migmatite Gneiss
Amphibolite
Borehole

PLATE-7

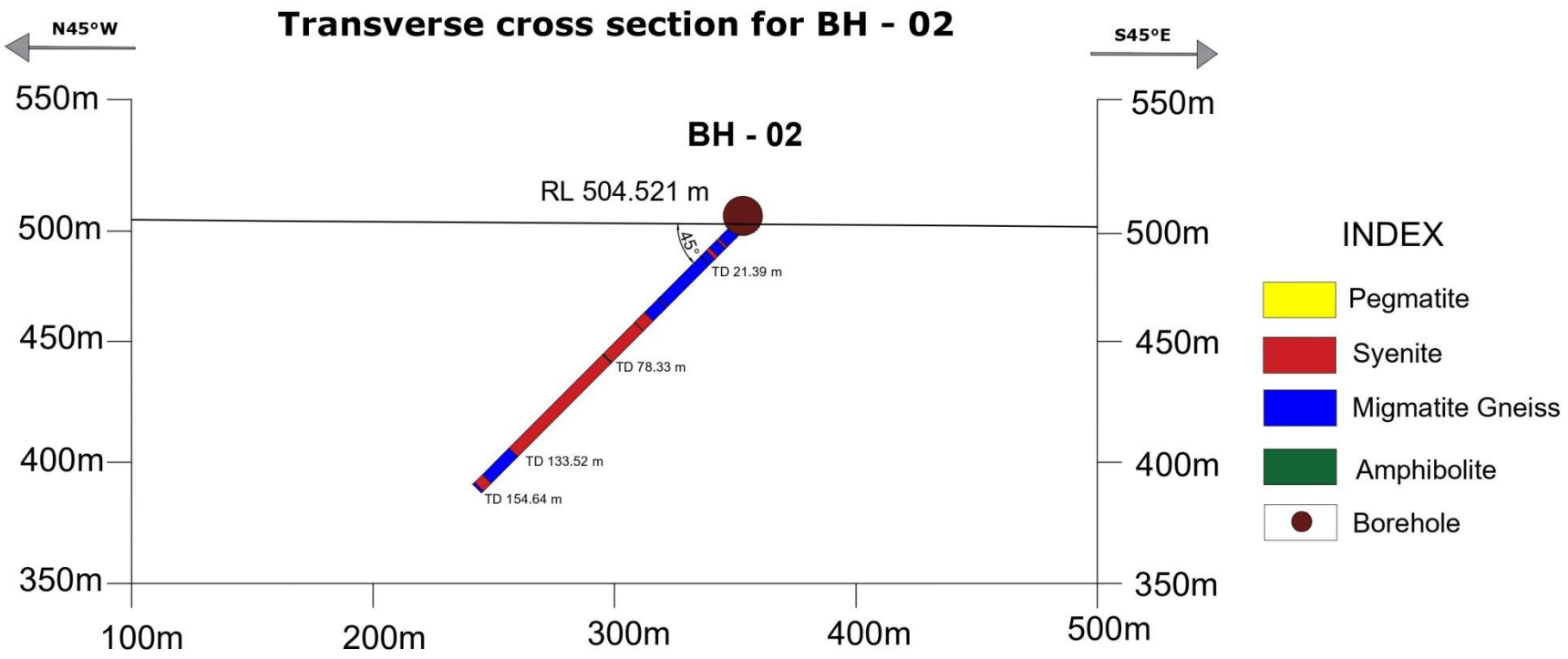
Transverse cross section for BH - 02
N45°W
S45°E
BH - 02
RL 504.521 m
45°
TD 21.39 m
TD 78.33 m
TD 133.52 m
TD 154.64 m
550m
500m
450m
400m
350m
100m
200m
300m
400m
500m
INDEX
Pegmatite
Syenite
Migmatite Gneiss
Amphibolite
Borehole

PLATE-8

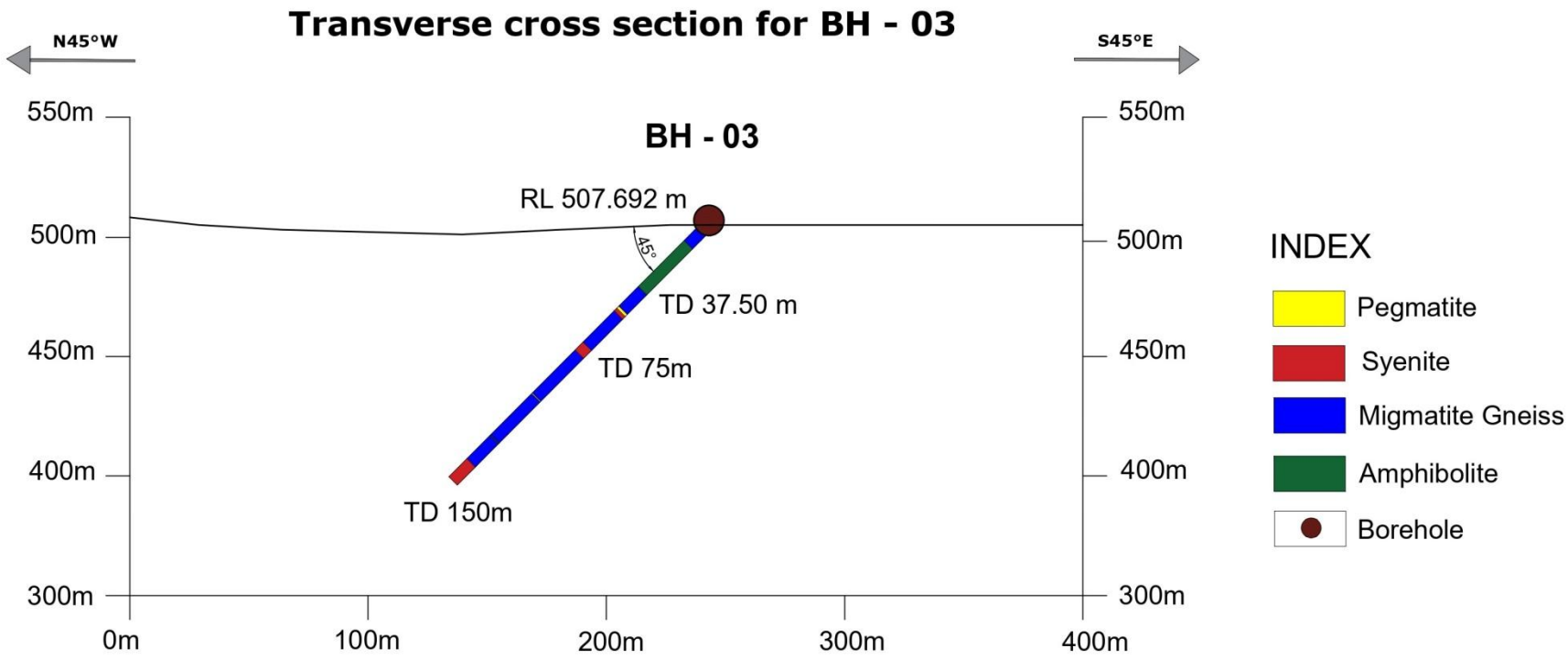
Transverse cross section for BH - 03
N45°W
S45°E
BH - 03
RL 507.692 m
45°
TD 37.50 m
TD 75m
TD 150m
550m
500m
450m
400m
300m
0m
100m
200m
300m
400m
INDEX
Pegmatite
Syenite
Migmatite Gneiss
Amphibolite
Borehole

PLATE-9

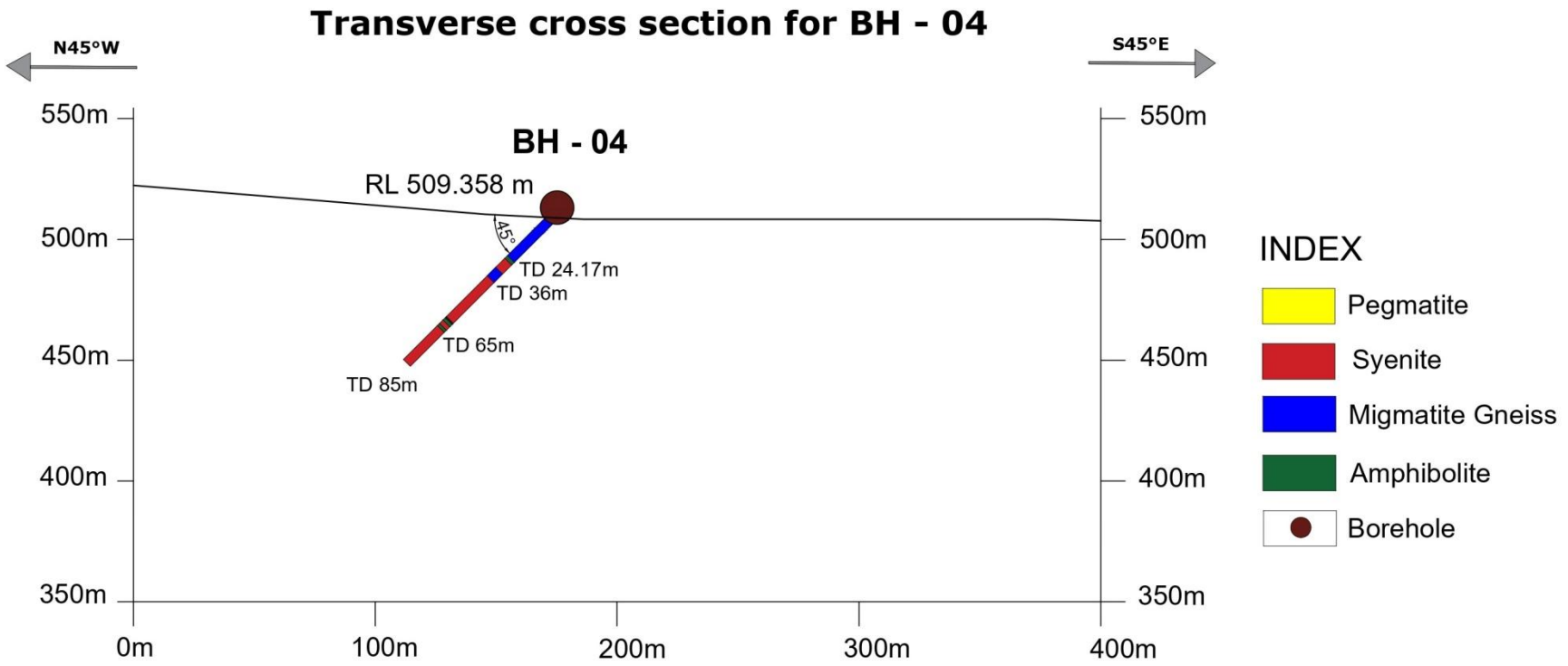
Transverse cross section for BH - 04
N45°W
S45°E
550m
500m
450m
400m
350m
BH - 04
RL 509.358 m
45°
TD 24.17m
TD 36m
TD 65m
TD 85m
0m
100m
200m
300m
400m
INDEX
Pegmatite
Syenite
Migmatite Gneiss
Amphibolite
Borehole

PLATE-10

LONGITUDINAL LITHOLOGICAL SECTION ON INCLINED PLANE (45°)

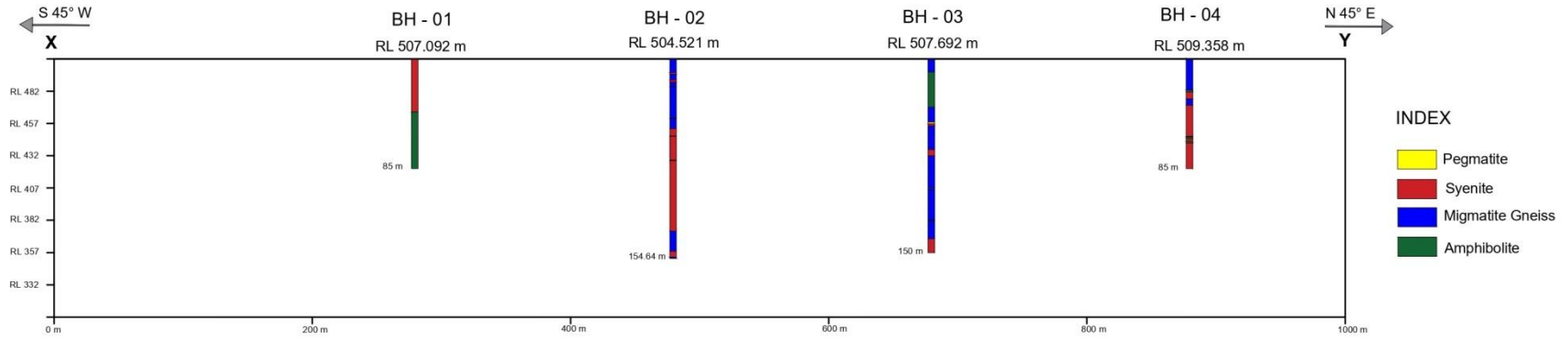

PLATE-11

LONGITUDINAL SECTION
ON INCLINED PLANE (45°) SHOWING MINERALIZED BODY FOR 1000 PPM

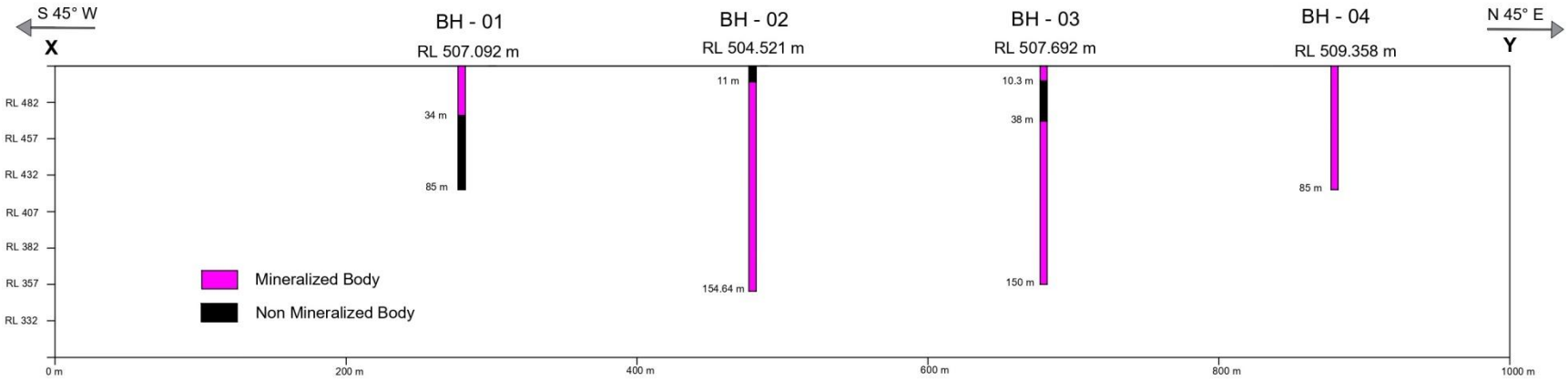

PLATE-12

LONGITUDINAL SECTION
ON INCLINED PLANE (45°) SHOWING MINERALIZED BODY WITH AREA OF INFLUENCE FOR 1000 PPM

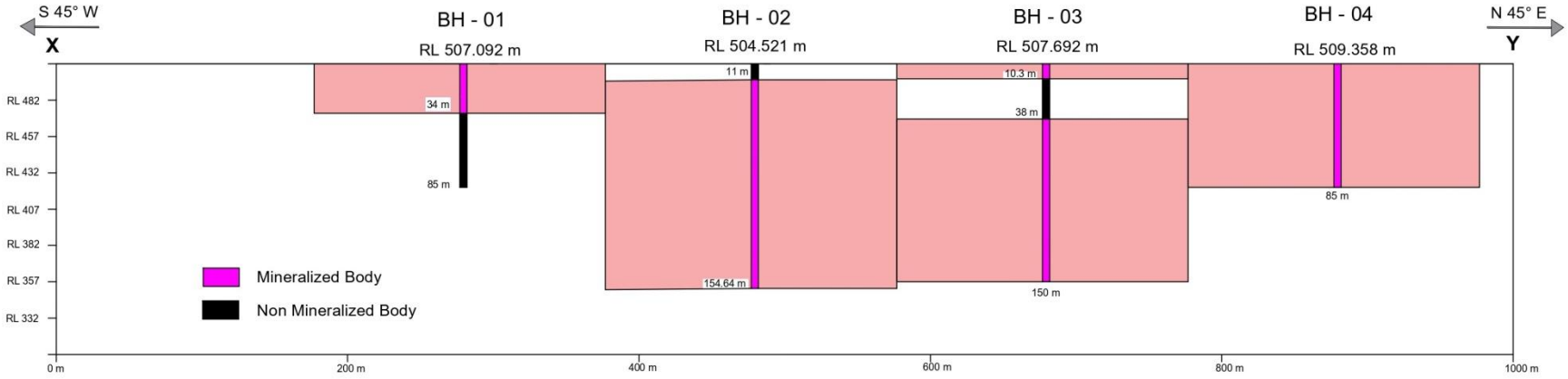

PLATE-13

LONGITUDINAL SECTION
ON INCLINED PLANE (45°) SHOWING MINERALIZED BODY FOR 1200 PPM

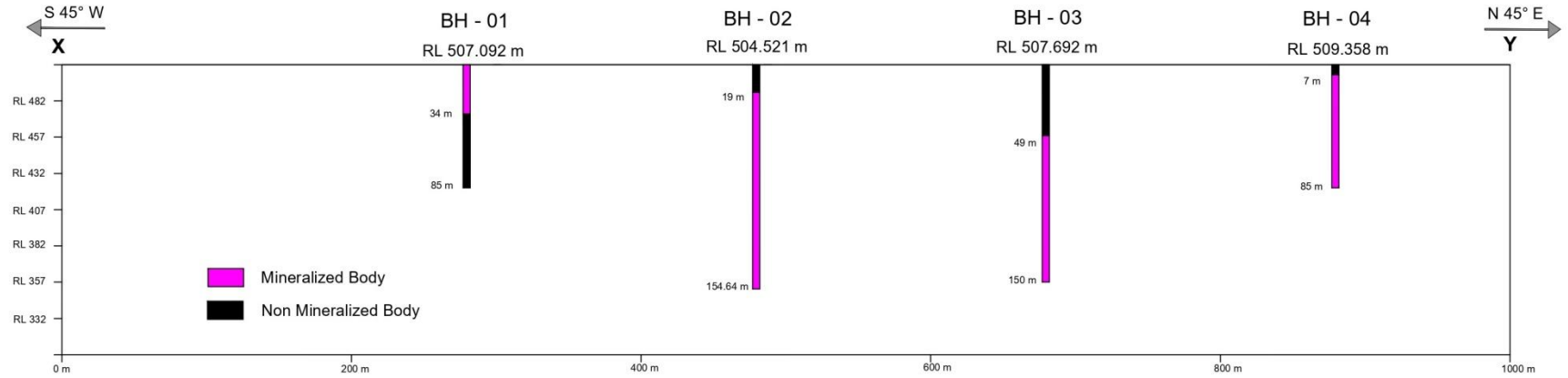

PLATE-14

ON INCLINED PLANE (45°) SHOWING MINERALIZED BODY WITH AREA OF INFLUENCE FOR 1200 PPM

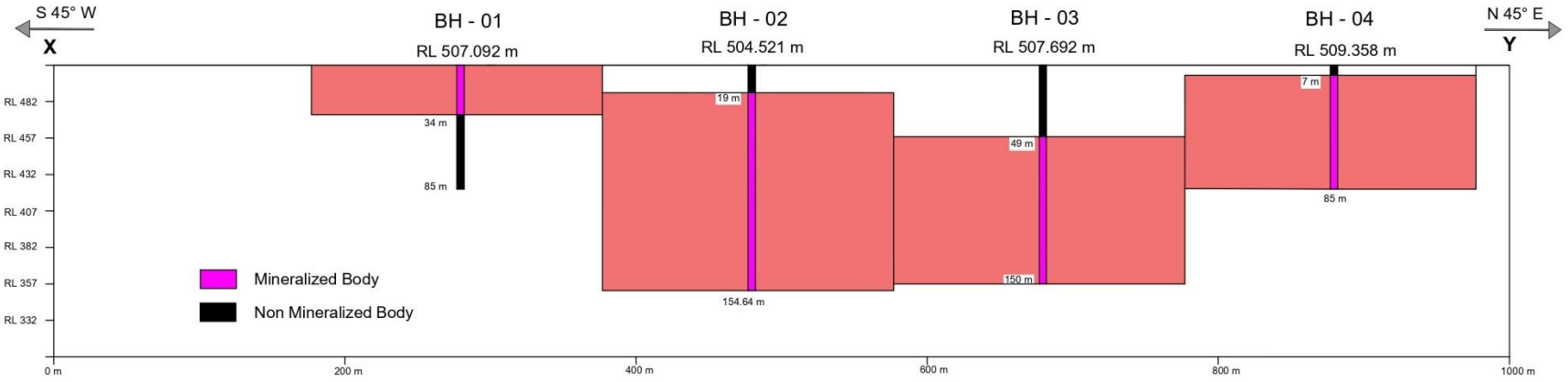

CHAPTER 23 – ANNEXURES OR ENCLOSURES TO THE REPORT

23.1 Annexure I – Sample Description

SAMPLE NO	LAT	LONG	ELIVATION	SAMPLE TYPE	LITHOLOGY
RJBO/BRS-01/2024-25	25.430920	74.124030	568 m	BRS	SYENITE
RJBO/BRS-02/2024-25	25.430810	74.124150	568 m	BRS	SYENITE
RJBO/BRS-03/2024-25	25.431180	74.123480	560 m	BRS	SYENITE
RJBO/BRS-04/2024-25	25.431250	74.123080	557 m	BRS	SYENITE
RJBO/BRS-05/2024-25	25.430910	74.123060	562 m	BRS	SYENITE/GNEISS
RJBO/BRS-06/2024-25	25.430270	74.128610	570 m	BRS	MIGMATITE GNEISS
RJBO/BRS-07/2024-25	25.429560	74.128810	567 m	BRS	AMPHIBOLITE
RJBO/BRS-08/2024-25	25.429520	74.128820	569 m	BRS	QUARTZ & FELDSPAR VEIN
RJBO/BRS-09/2024-25	25.426290	74.128610	559 m	BRS	MIGMATITE GNEISS
RJBO/BRS-10/2024-25	25.426160	74.128040	555 m	BRS	MIGMATITE GNEISS
RJBO/BRS-11/2024-25	25.427730	74.127680	564 m	BRS	PEGMATITE
RJBO/BRS-12/2024-25	25.431170	74.127530	562 m	BRS	SYENITE
RJBO/BRS-13/2024-25	25.432550	74.127500	564 m	BRS	SYENITE
RJBO/BRS-14/2024-25	25.429500	74.127760	559 m	BRS	MIGMATITE GNEISS
RJBO/BRS-15/2024-25	25.428230	74.125740	558 m	BRS	MIGMATITE GNEISS
RJBO/BRS-16/2024-25	25.426380	74.126300	558 m	BRS	MIGMATITE GNEISS
RJBO/BRS-17/2024-25	25.425960	74.127920	557 m	BRS	SYENITE
RJBO/BRS-18/2024-25	25.431010	74.127210	564 m	BRS	MIGMATITE GNEISS

RJBO/BRS-19/2024-25	25.432260	74.126440	565 m	BRS	SYENITE
RJBO/BRS-20/2024-25	25.432330	74.126210	566 m	BRS	SYENITE
RJBO/BRS-21/2024-25	25.431980	74.126360	564 m	BRS	SYENITE
RJBO/BRS-22/2024-25	25.432060	74.125550	563 m	BRS	SYENITE
RJBO/BRS-23/2024-25	25.429490	74.125260	567 m	BRS	MIGMATITE GNEISS
RJBO/BRS-24/2024-25	25.427920	74.125150	556 m	BRS	MIGMATITE GNEISS
RJBO/BRS-25/2024-25	25.426330	74.125240	560 m	BRS	SYENITE
RJBO/BRS-31/2024-25	25.432200	74.116700	566 m	BRS	SYENITE
RJBO/BRS-40/2024-25	25.429200	74.124500	566 m	BRS	MIGMATITE GNEISS
RJBO/BRS-41/2024-25	25.426200	74.123800	559 m	BRS	MIGMATITE GNEISS
RJBO/BRS-42/2024-25	25.427500	74.122700	563 m	BRS	MIGMATITE GNEISS
RJBO/BRS-43/2024-25	25.428600	74.122500	565 m	BRS	SYENITE
RJBO/BRS-44/2024-25	25.430500	74.124100	567 m	BRS	MIGMATITE GNEISS
RJBO/BRS-45/2024-25	25.432500	74.124400	567 m	BRS	SYENITE
RJBO/BRS-46/2024-25	25.430370	74.118800	573 m	BRS	MIGMATITE GNEISS
RJBO/BRS-47/2024-25	25.431300	74.118540	568 m	BRS	MIGMATITE GNEISS
RJBO/BRS-48/2024-25	25.433860	74.119480	568 m	BRS	MIGMATITE GNEISS
RJBO/BRS-49/2024-25	25.434290	74.120460	561 m	BRS	SYENITE
RJBO/BRS-50/2024-25	25.434070	74.121040	561 m	BRS	SYENITE
RJBO/BRS-51/2024-25	25.433840	74.118550	570 m	BRS	SYENITE
RJBO/BRS-52/2024-25	25.433200	74.116430	572 m	BRS	SYENITE
RJBO/BRS-53/2024-25	25.432590	74.115780	580 m	BRS	AMPHIBOLITE
RJBO/BRS-54/2024-25	25.432630	74.115630	578 m	BRS	SYENITE

RJBO/BRS-55/2024-25	25.433060	74.115270	572 m	BRS	MIGMATITE GNEISS
RJBO/BRS-56/2024-25	25.433700	74.114970	567 m	BRS	MIGMATITE GNEISS
RJBO/BRS-57/2024-25	25.434150	74.115790	571 m	BRS	MIGMATITE GNEISS
RJBO/BRS-58/2024-25	25.434150	74.117420	570 m	BRS	MIGMATITE GNEISS
RJBO/BRS-59/2024-25	25.434770	74.118660	567 m	BRS	SYENITE
RJBO/BRS-60/2024-25	25.429344	74.123281	569m	BRS	MIGMATITE GNEISS
RJBO/BRS-61/2024-25	25.428622	74.122597	566m	BRS	SYENITE
RJBO/BRS-62/2024-25	25.427533	74.122531	566m	BRS	MIGMATITE GNEISS
RJBO/BRS-63/2024-25	25.426203	74.120956	563m	BRS	MIGMATITE GNEISS
RJBO/BRS-64/2024-25	25.426592	74.119336	565m	BRS	MIGMATITE GNEISS
RJBO/BRS-65/2024-25	25.426872	74.118228	564	BRS	MIGMATITE GNEISS
RJBO/BRS-66/2024-25	25.428378	74.127828	562	BRS	MIGMATITE GNEISS
RJBO/BRS-67/2024-25	25.433040	74.117630	569 m	BRS	SYENITE
RJBO/BRS-68/2024-25	25.433150	74.119060	559 m	BRS	SYENITE CONTACT
RJBO/BRS-69/2024-25	25.433490	74.119850	561 m	BRS	SYENITE CONTACT
RJBO/BRS-70/2024-25	25.431920	74.118460	563 m	BRS	MIGMATITE GNEISS
RJBO/BRS-71/2024-25	25.430020	74.119800	567 m	BRS	MIGMATITE GNEISS
RJBO/BRS-72/2024-25	25.427850	74.119730	561 m	BRS	MIGMATITE GNEISS
RJBO/BRS-73/2024-25	25.426340	74.118410	573 m	BRS	SYENITE
RJBO/BRS-74/2024-25	25.427780	74.118620	563 m	BRS	SYENITE
RJBO/BRS-75/2024-25	25.431610	74.115340	576 m	BRS	MIGMATITE GNEISS
RJBO/BRS-76/2024-25	25.429420	74.116310	564 m	BRS	MIGMATITE GNEISS
RJBO/BRS-77/2024-25	25.428350	74.116420	570 m	BRS	MIGMATITE GNEISS

RJBO/BRS-78/2024-25	25.429720	74.119110	570 m	BRS	SYENITE
RJBO/BRS-79/2024-25	25.430360	74.120930	574 m	BRS	MIGMATITE GNEISS
RJBO/BRS-80/2024-25	25.431110	74.121610	573 m	BRS	MIGMATITE GNEISS
RJBO/BRS-81/2024-25	25.430060	74.122260	570 m	BRS	MIGMATITE GNEISS
RJBO/BRS-82/2024-25	25.430020	74.123440	549 m	BRS	MIGMATITE GNEISS
RJBO/BRS-83/2024-25	25.429330	74.117780	562 m	BRS	MIGMATITE GNEISS
RJBO/BRS-26/2024-25	25.432010	74.128120	574 m	BRS	SYENITE
RJBO/BRS-27/2024-25	25.431700	74.128050	572 m	BRS	SYENITE
RJBO/BRS-28/2024-25	25.431320	74.127780	569 m	BRS	SYENITE
RJBO/BRS-29/2024-25	25.430930	74.127850	566 m	BRS	SYENITE
RJBO/BRS-30/2024-25	25.430770	74.127180	569 m	BRS	SYENITE
RJBO/BRS-32/2024-25	25.432170	74.124970	570 m	BRS	SYENITE
RJBO/BRS-33/2024-25	25.431770	74.124700	564 m	BRS	SYENITE
RJBO/BRS-34/2024-25	25.431510	74.125160	566 m	BRS	SYENITE
RJBO/BRS-35/2024-25	25.431010	74.125220	567 m	BRS	SYENITE
RJBO/BRS-36/2024-25	25.430660	74.125280	573 m	BRS	MIGMATITE GNEISS
RJBO/BRS-37/2024-25	25.430360	74.124820	569 m	BRS	SYENITE
RJBO/BRS-38/2024-25	25.429970	74.124780	214 m	BRS	SYENITE
RJBO/BRS-39/2024-25	25.429600	74.124820	556 m	BRS	SYENITE
RJBO/BRS-84/2024-25	25.430290	74.125280	557 m	BRS	MIGMATITE GNEISS
RJBO/BRS-85/2024-25	25.428840	74.125110	584 m	BRS	MIGMATITE GNEISS
RJBO/BRS-86/2024-25	25.428610	74.124250	566 m	BRS	MIGMATITE GNEISS
RJBO/BRS-87/2024-25	25.427320	74.124820	562 m	BRS	MIGMATITE GNEISS

RJBO/BRS-88/2024-25	25.426840	74.125080	562 m	BRS	SYENITE
RJBO/BRS-89/2024-25	25.426780	74.125670	561 m	BRS	SYENITE
RJBO/BRS-90/2024-25	25.426970	74.123420	561 m	BRS	MIGMATITE GNEISS
RJBO/BRS-91/2024-25	25.426290	74.120390	570 m	BRS	MIGMATITE GNEISS
RJBO/BRS-92/2024-25	25.427050	74.118920	571 m	BRS	MIGMATITE GNEISS
RJBO/BRS-93/2024-25	25.427490	74.117620	574 m	BRS	MIGMATITE GNEISS
RJBO/BRS-94/2024-25	25.428420	74.118090	574 m	BRS	MIGMATITE GNEISS
RJBO/BRS-95/2024-25	25.428990	74.117280	575 m	BRS	MIGMATITE GNEISS
RJBO/BRS-96/2024-25	25.430120	74.127670	578 m	BRS	MIGMATITE GNEISS
RJBO/BRS-97/2024-25	25.429300	74.126500	579 m	BRS	MIGMATITE GNEISS
RJBO/BRS-98/2024-25	25.429900	74.125920	582 m	BRS	MIGMATITE GNEISS
RJBO/BRS-99/2024-25	25.428810	74.125790	582 m	BRS	MIGMATITE GNEISS
RJBO/BRS-100/2024-25	25.426720	74.121630	572 m	BRS	MIGMATITE GNEISS
RJBO/BRS-101/2024-25	25.428070	74.122660	575 m	BRS	MIGMATITE GNEISS
RJBO/BRS-102/2024-25	25.428540	74.123290	574 m	BRS	MIGMATITE GNEISS
RJBO/BRS-103/2024-25	25.431530	74.122280	578 m	BRS	MIGMATITE GNEISS
RJBO/BRS-104/2024-25	25.431910	74.123330	569 m	BRS	MIGMATITE GNEISS
RJBO/BRS-105/2024-25	25.429050	74.121270	571 m	BRS	MIGMATITE GNEISS
RJBO/BRS-106/2024-25	25.429410	74.120290	571 m	BRS	MIGMATITE GNEISS
RJBO/BRS-107/2024-25	25.433620	74.117480	575 m	BRS	SYENITE
RJBO/BRS-108/2024-25	25.434170	74.116580	576 m	BRS	SYENITE

23.2 Annexure II- Petrography Report

23.2.1 BRS Petrography Report

Report on Petrography/Mineragraphy studies of Mangalwar Complex suite of rocks, Borana block, Bhilwara District, Rajasthan

1. Introduction

On a payment basis, Dr. R. Chandrasekaran, Project Coordinator, GeoExpOre Pvt. Ltd, Bangalore, has submitted 14 samples for the preparation of thin and thin polished sections followed by complete petrography/mineragraphy studies at the Petrology laboratory, NCEGR, RSAS, GSI, Bangalore. Among these samples, four samples were made in duplicate for thin and thin polished sections for ore mineral studies. All thin and thin polished sections were examined under transmitted light and reflected light in a petrological microscope (Model: Leica DM2700P) for mineral content, textures, and other optical properties of REE-bearing minerals and their associated silicates, carbonates, and oxides. Numerous digital photomicrographs of the thin sections were taken using an attached digital camera.

The detailed descriptions of the thin, and thin polished sections of different rock types are enumerated below:

2. Sample Preparation

Selection and isolation have been done for the different types of rocks, such as granitoid, syenite, and pegmatite. Using a mixture of epoxy and hardener, these samples were mounted on thin-section slides measuring 46 x 25 mm, and the sections were left overnight. After that, the mounted sections were ground using several carborundum grinding media fractions until the specimen fractions were visible. This is followed by polishing using diamond and chrome paste.

3. Petrography/mineragraphy description of rocks

i) Sample no. RJBO/BRS-07/202024-25 (Amphibolite)

The sample number RJBO/BRS-7/2024-25 in the hand specimen is a medium-grained, dark- colored rock exhibiting a sacchoroidal texture. The rock consists predominantly of amphibole and plagioclase (Fig.1a).

Petrographic study reveals that the rock mainly consists of hornblendes and plagioclase. Epidote, sphene and opaques are as accessories (Fig. 1b). The rock shows granulose texture. The plagioclase minerals are sericitized and few plagioclases even occur as inclusion within hornblende (Fig. 1c). The

plagioclase mostly shows polysynthetic lamellar twinning. The hornblende occurs as elongated, prismatic crystals and is associated with plagioclases, epidote, and opaques. The higher iron content leads to more pronounced blue tones in the bluish hornblende. The hornblende shows both basal and prismatic sections. In plane polarized light, hornblende shows distinct trichroism, viz., dark green, yellowish green, and pale yellowish green.

In reflected light, it is observed that the opaques are hematite, which are euhedral to subhedral (Fig. 1d), and show moderate reflectivity with blood-red internal reflection and are associated with hornblendes.

Fig. 1a. Hand sample of Amphibolite (Sample no. RJBO/BRS-7/24-25).

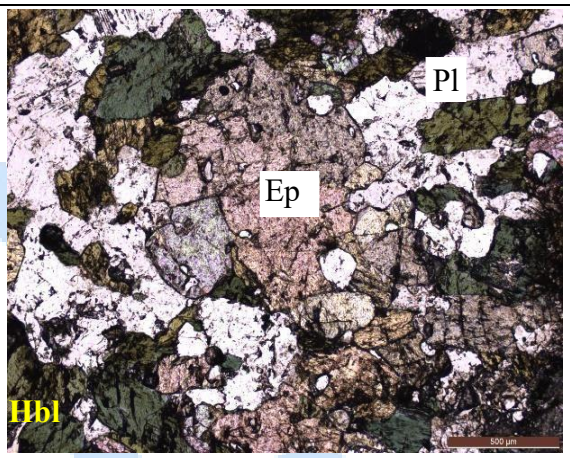

Fig. 1b. Photomicrograph of amphibolite showing assemblage of plagioclase (Pl), hornblende (Hbl), and epidote (Ep) exhibiting granulose texture under plane polar view (Sample no. RJBO/BRS-7/24-25).

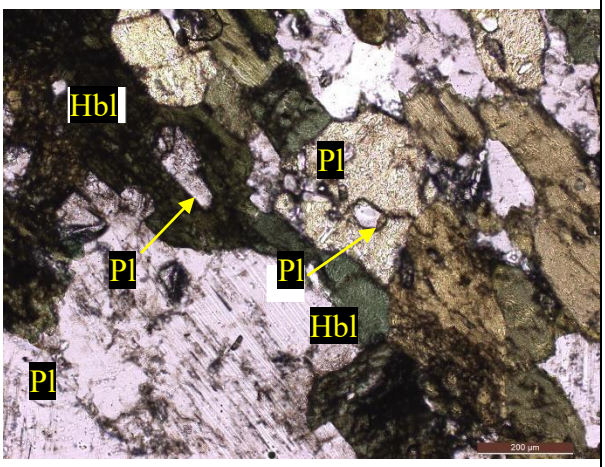

Fig. 1c. Photomicrograph showing minor plagioclase inclusion in hornblende and secondary plagioclase under plane polar view (Sample no. RJBO/BRS-7/24-25).

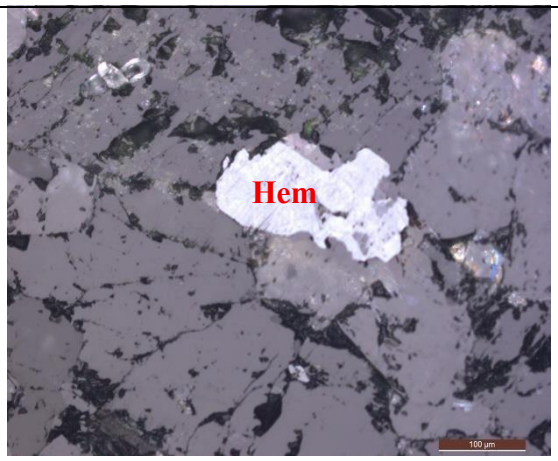

Fig. 1d. Photomicrograph showing subhedral hematite (Hem), associated with silicates under reflected light (Sample no. RJBO/BRS-7/24-25).

ii) Sample no. RJBO/BRS-24/2024-25 (Augen hornblende-biotite gneiss)

In hand specimen, the sample RJBO/BRS-24/24-25 is characterized by alternations of dark and light color bands/layers (Fig. 2a). The leucocratic bands show K-feldspar and quartz, while mesocratic bands/layers are attributed to the biotite. In contrast, the thickness of the leucocratic bands is more than the mesocratic layers/bands. K-feldspars show augen shapes and some are stretched along the long axis. Euhedral allanite grains are visible.

Under microscope, the sample (RJBO/BRS-24/24-25) is composed predominantly of K- feldspar, plagioclase, quartz, and hornblende, biotite, muscovite, and allanite as accessory minerals. Light color bands are represented by K-feldspars, plagioclase, and quartz, while dark color bands are in biotite and hornblende, exhibiting gneissic structure (Fig. 2b & c). The nature of the quartz grains is inequigranular. At places, the sub-grain formation of quartz grains has taken place, which clearly indicates the deformation and metamorphism. K-feldspar comprises microcline and orthoclase, which are easily distinguished by cross-hatched twinning and Carlsbad twinning, respectively. Biotite, along with muscovite, occurs in a platy form, showing preferred orientations that define foliation. Biotite shows a yellowish-green color in the transmitted light and a 2nd order interference color in cross-polarized light. Hornblende showing trichroism from bluish green to dark green through yellowish green under cross polarized light while white green to dark green in plane polarized light. It is occurring along the gneissosity plane with biotite and at places indivisible grain also. Sericitization of

microcline as the alteration products is recorded at places. Euhedral to subhedral epidote and zoisite are distinctly formed in this rock. Distinct allanite grains with radial cracks along the quartz and plagioclase are well developed (Fig. 2c), which needs to be confirmed in SEM/EPMA methods for REE potentiality.

Under reflected light, the opaques are classified as magnetite occurring in the form of veinlets and grains, which are commonly associated with the biotite (Fig. 2d).

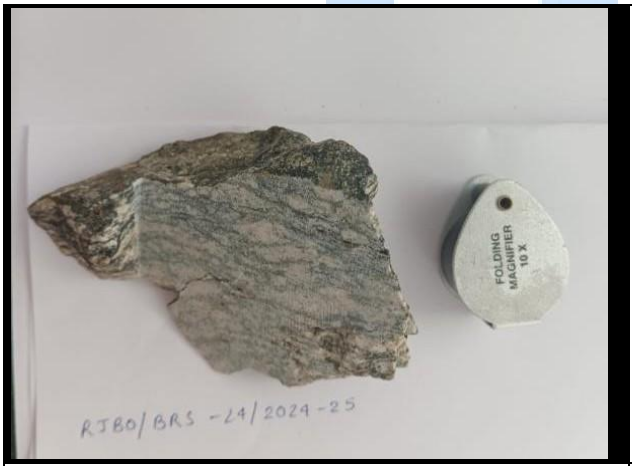

Fig. 2a. Hand sample of Augen gneiss (Hbl-Bt gneiss) (Sample no. RJBO/BRS-24/24-25).

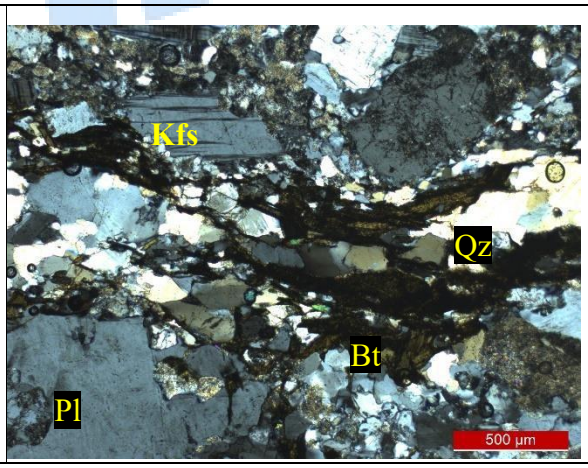

Fig. 2b. Photomicrograph showing dark and light colour bands defined by biotite, hornblende and K- feldspars, quartz, plagioclase respectively in the augen gneiss under CPL (Sample no. RJBO/BRS-24/24-25).

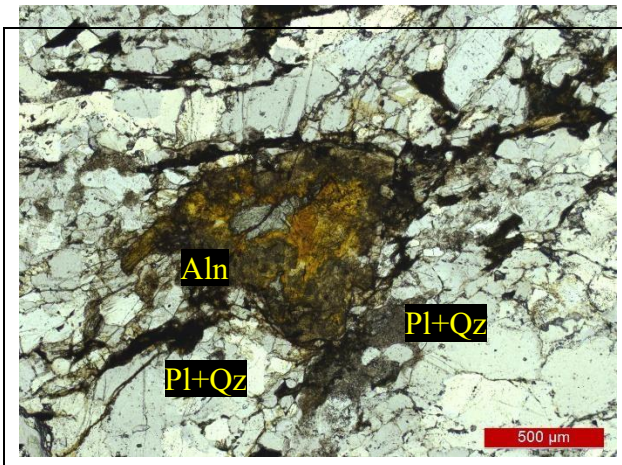

Fig. 2c. Photomicrograph showing Allanite (Aln) with radial cracks under CPL (Sample no. RJBO/BRS-24/24-25).

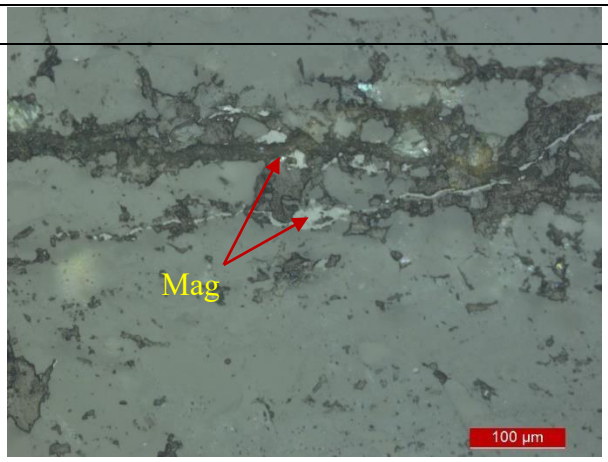

Fig. 2d. Photomicrograph showing magnetite (Mag) veinlet and discrete magnetite associated with biotite under reflected light (Sample no. RJBO/BRS-24/24-25).

iii)**Sample no. RJBO/BRS-93/2024-25 (Garnet-biotite Gneiss)**

The sample (RJBO/BRS-93/2024-25) in the hand specimen has a banded structure, with leucocratic and mesocratic layers consisting of multiple minerals alternately. It can be medium to coarse foliated, as the layers are sub-parallel to each other. The most common minerals in this rock are quartz and plagioclase, with traces of biotite and garnet. (Fig. 3a).

Petrographically, the rock is mainly composed of quartz and plagioclase, with accessories of biotite, muscovite, garnet, apatite, zircon, magnetite, and allanite. Well-developed gneissic foliations are defined by biotite and muscovite of this sample (Fig. 3b). Polysynthetic lamellar twinning is well preserved in the plagioclases while quartz grains show undulose extinction. The quartz grains show sub-grain formations at places. Radial cracks are well developed in the quartz grains, indicative of the allanite occurring in the core of them. Allanite occurs as irregularly shaped, characterized by yellowish brown and high relief relative to their associated minerals (Fig. 3c). Zircon and apatite occupy the interstitial spaces within the quartz and plagioclase (Fig. 3d.). Zircon exhibits a tetragonal shape and shows very high relief with a pale yellow to grey color in plane polarized light. Apatite is having a rounded to oval shape with moderate relief. Round to sub-rounded garnets are observed in association with plagioclase. These garnets are also called xenomorphic garnets (Fig. 3e).

Petrography studies indicate that the sample contains a significant amount of allanite grains, which need to be confirmed in SEM/EPMA methods for REE potentiality.

Fig.3a. Hand sample of Garnet-biotite gneiss (Sample no. RJBO/BRS93/2024-25).

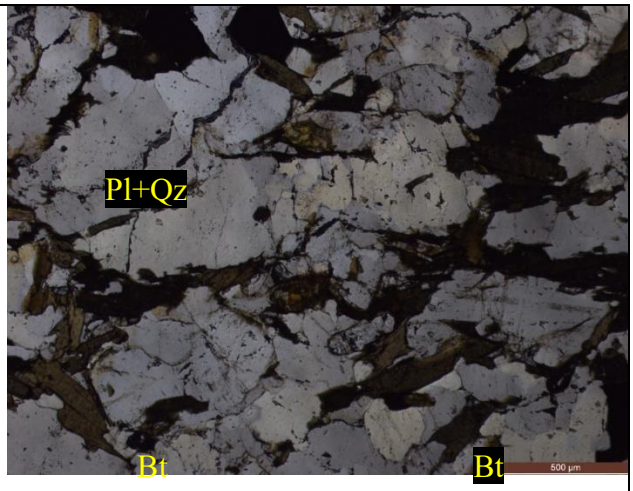

Fig.3b.Photomicrograph of garnet-biotite gneiss showing foliation defined by biotite (Bt) under PPL (sample no. RJBO/BRS93/2024-25).

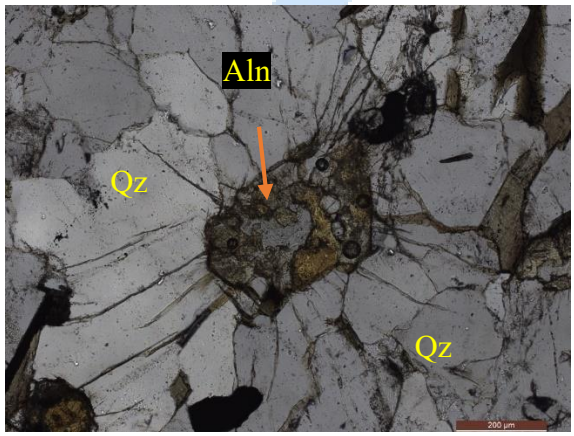

Fig 3c. Photomicrograph showing irregular shaped allanite (Aln) with radial cracks developed the surrounding quartz grains in Garnet Biotite Gneiss under plane polarized light (sample no. RJBO/BRS93/2024-25).

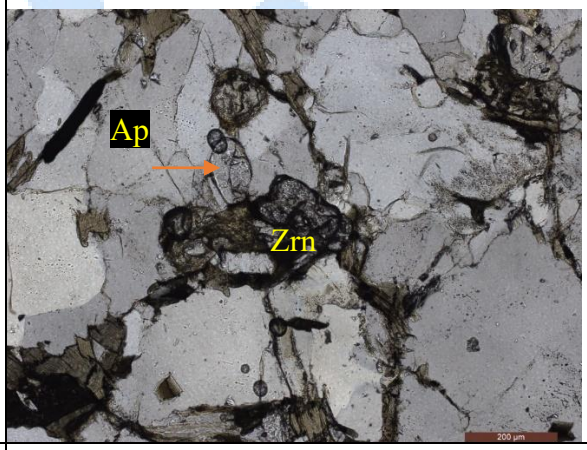

Fig 3d. Photomicrograph showing Zircon (Zrn) and Apatite (Ap) in garnet-biotite gneiss under PPL (sample no. RJBO/BRS93/2024-25).

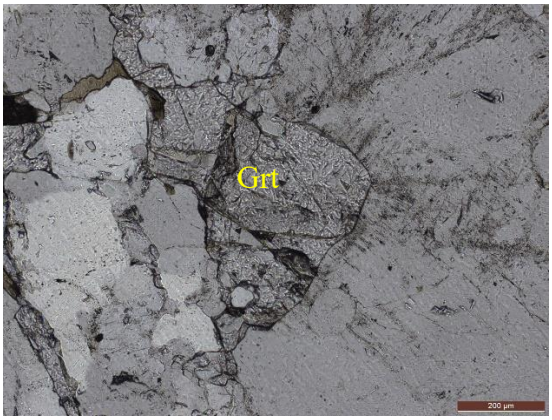

Fig 3e. Photomicrograph showing xenomorphic garnet (Grt) in garnet biotite gneiss under PPL (RJBO/BRS93/2024-25).

iv) Sample no. RJBO/BRS-36/2024-25 (Biotite Gneiss)

In hand specimen, it is a coarse-grained rock. The rock shows alternations of mesocratic and leucocratic bands defined by gneissose structure. Mesocratic bands are made up of biotite, while plagioclase, K-feldspar, and quartz are in the leucocratic bands (Fig. 4a).

Petrographic study reveals that the dark and light color bands are represented by biotite and plagioclase, microcline, and quartz, respectively (Fig. 4b). Zoisite, chlorite, and opaques are the accessories. Two variants of plagioclases are observed, such as inclusion and equant crystalline. Number of blebs of plagioclases as the inclusions occurring within the later plagioclases. Polysynthetic lamellar twinning is well preserved in the plagioclases. Cross-hatched twinning is seen in the microcline. Intergrowths of plagioclase and quartz exhibit myrmekite texture (Fig. 4b). The plagioclase in the rock has undergone sericitization. Biotite occurs as platy, showing preferred orientations that define foliation. It shows a yellowish-green color in the transmitted light (Fig. 4c). The quartz grains show sub-grain formations, suggesting strain-induced deformation.

In reflected light, most of the opaques are the magnetite (Fig. 4d). Magnetite occurs as anhedral, dominantly associated with biotite (Fig. 4c).

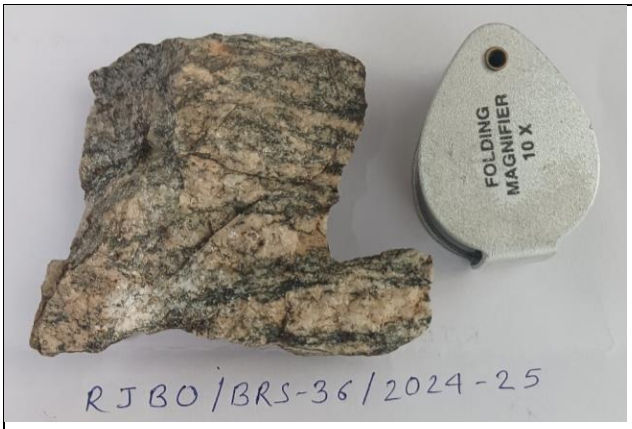

Fig. 4a. Hand sample of Biotite Gneiss (Sample no. RJBO/BRS-36/24-25).

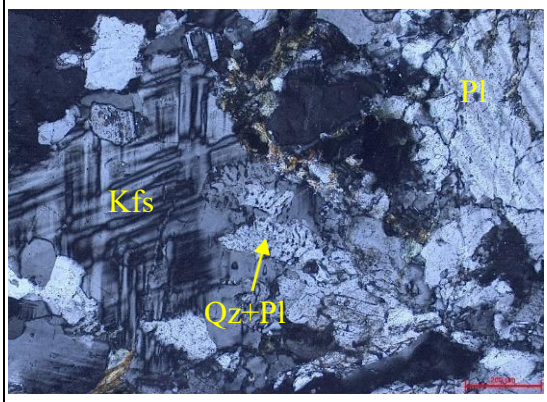

Fig. 4b. Photomicrograph showing mineral assemblages in the biotite gneiss, and intergrowth of plagioclase and quartz exhibits myrmekite texture under cross polarized light (sample no. RJBO/BRS36/2024-25).

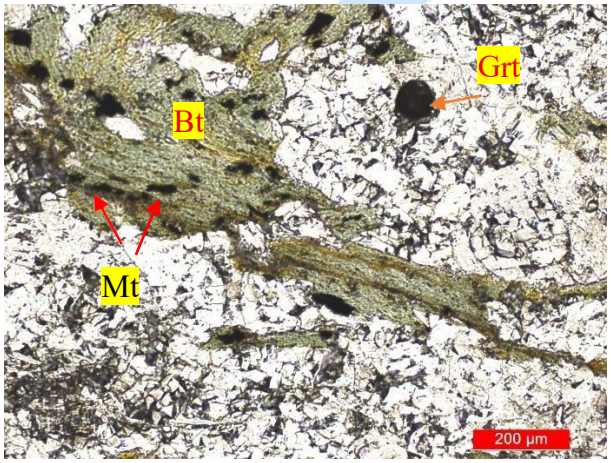

Fig. 4c. Photomicrograph showing schistosity defined by biotite, where chlorite alterations and clusters of magnetite (opaques) are seen in the biotite under plane polar view (sample no. RJBO/BRS36/2024- 25).

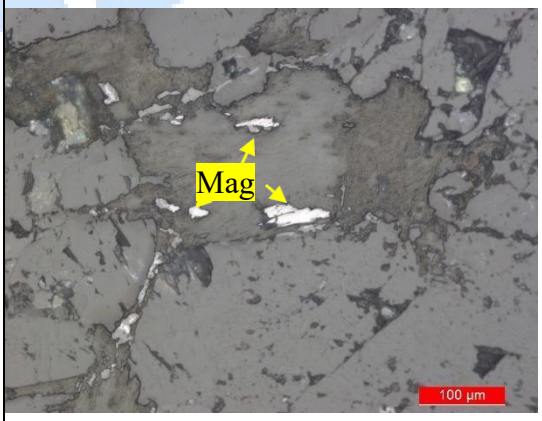

Fig. 4d. Photomicrograph showing discrete/ disseminated magnetite grains in the biotite gneiss, under reflected light (sample no. RJBO/BRS36/2024-25).

v) Sample no. RJBO/BRS-25/2024-25 (Hornblende Gneiss)

In hand specimen, the sample shows alterations of mesocratic and leucocratic bands defined by gneissose structure. Mesocratic bands are made up of hornblende, while plagioclase and quartz are in

the leucocratic bands (Fig. 5a).

Under microscope, the dark bands are represented by greenish hornblende showing trichroism from bluish green to dark green through yellowish green. The majority of plagioclase occurs in the light color bands, and quartz is less common (Fig. 5b). Sphene, epidote, monazite, and opaques are accessories. An elongated monazite grain occurs in association with the hornblende and plagioclase and close to the epidote (Fig. 5c). Granulose texture with sharp contact and triple junctions is seen among the plagioclases, indicating metamorphism.

Reflected light was used to examine the opaques; most of the opaques are categorized as magnetite. It is euhedral and has low reflectivity, with a grey to pale-pink tint. Hematite slightly transforms magnetite into goethite (Fig. 5d) due to hydrothermal alteration.

Petrography studies revealed that the number of monazite grains has been identified in this sample, which needs to be confirmed in SEM/EPMA methods for REE potentiality.

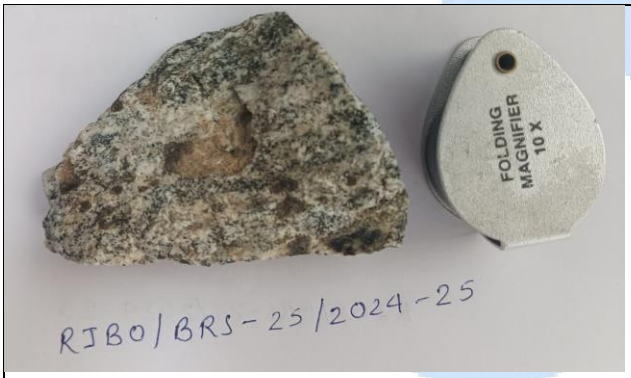

Fig. 5a. Hand sample of Hornblende Gneiss (Sample no. RJBO/BRS-25/24-25).

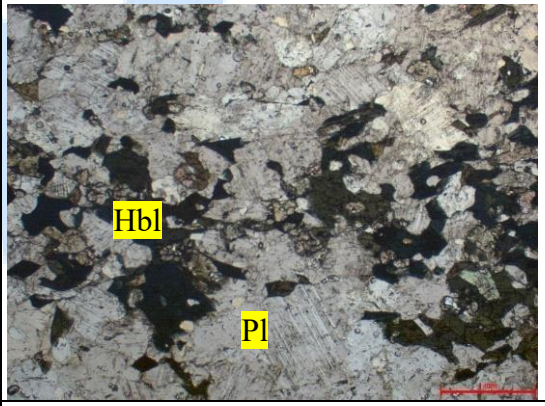

Fig. 5b. Photomicrograph showing dark and light colour bands, represented by hornblende and plagioclases, respectively, exhibit gneissic structure under plane polarized light (sample no. RJBO/BRS25/2024-25)

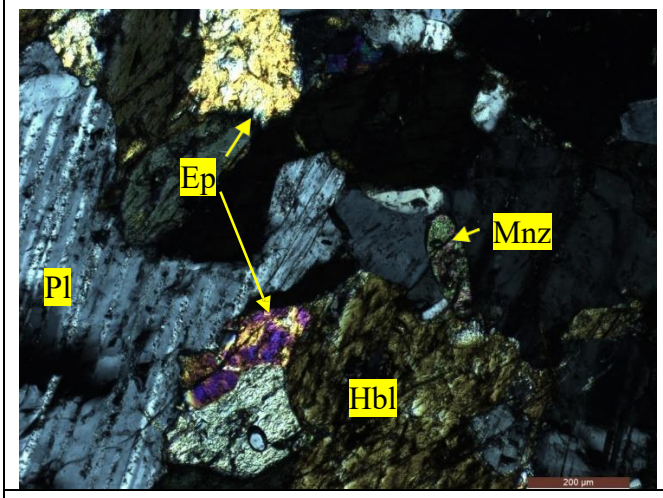

Fig. 5c. Photomicrograph an elongated monazite grain associated with hornblende and plagioclase and close to epidote in the hornblende gneiss under cross polarized light (sample no. RJBO/BRS25/2024-25).

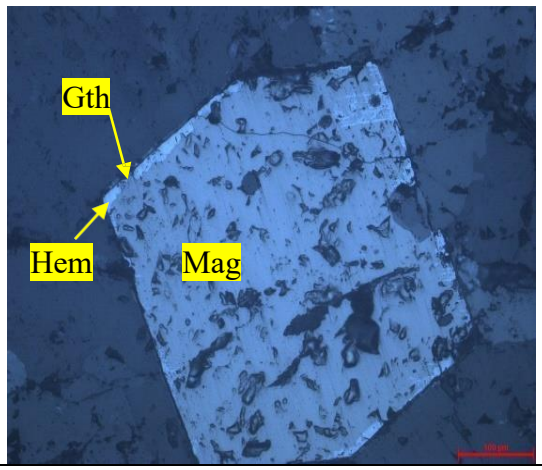

Fig. 5d. Photomicrograph showing a euhedral magnetite replaced by hematite and subsequently by goethite at the margin, under reflected light (sample no. RJBO/BRS25/2024-25).

vi) Sample no. RJBO/BRS-107/2024-25 (Alkali Feldspar Syenite)

In hand specimen, the sample (RJBO/BRS-107/2024-25) appears as a pale pink, coarse- grained rock. It is mostly composed of alkali feldspar and traces of quartz, garnet, and epidote (Fig. 6a). Epidote veins are transgressed into it.

In thin section, the sample RJBO/BRS-107/24-25 is composed of quartz and K-feldspar as essential minerals and epidote, zoisite, and muscovite as accessory minerals (Fig. 6b). K-feldspar comprises orthoclase and microcline. Their twin planes are clearly distinguished. Sub-grain formation of quartz and K-feldspar that form during deformation as the result of recrystallization of quartz, which occurs when temperature increases. At places, sericitization in the K-feldspars is seen. Granophyric texture is observed. Epidote veins are cross cutting all the mineral phases. These veins consist predominantly of epidote crystals in the form of aggregates that show higher- order interference color (Fig. 6c). Zoisite is present as independent grains and occurs in the interstitial spaces of alkali feldspar and quartz. According to the mineral assemblages, the rock may thus be classified as an alkali syenite or an alkali feldspar syenite. Allanite with radical cracks is observed for REE mineralization. It is a long prismatic crystal that is subhedral in some places (Fig. 6d). Xenomorphic garnet is also noticed at places (Fig. 6e).

The rock has a considerable amount of REE-bearing minerals, such as allanite, according to petrographic investigations; SEM and EPMA studies are advised to corroborate the REE potentiality of the rock.

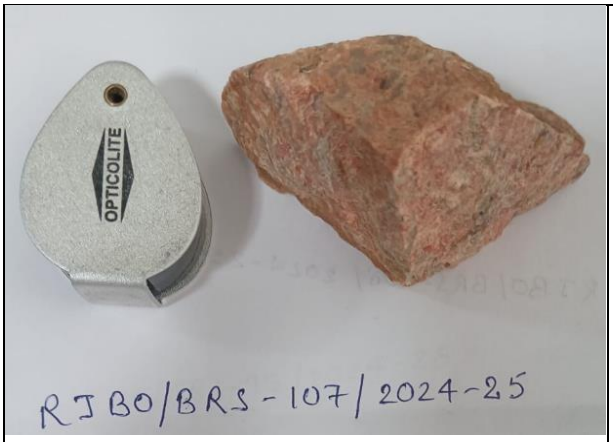

Fig. 6a. Hand sample of Alkali Feldspar Syenite (Sample no. RJBO/BRS-107/2024-25).

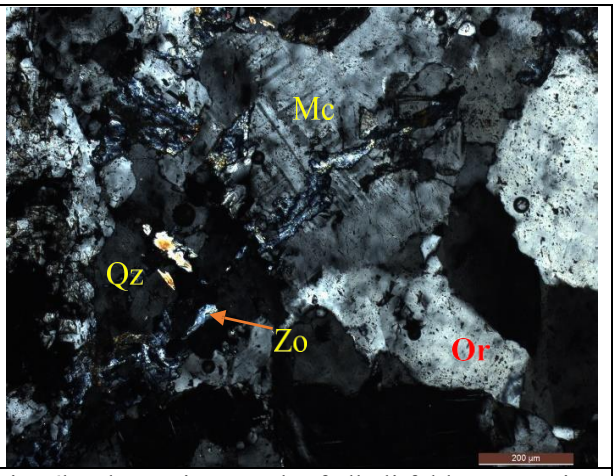

Fig. 6b. Photomicrograph of alkali feldspar syenite showing different mineral assemblages under XPL (Sample no RJBO/BRS-107/2024-25).

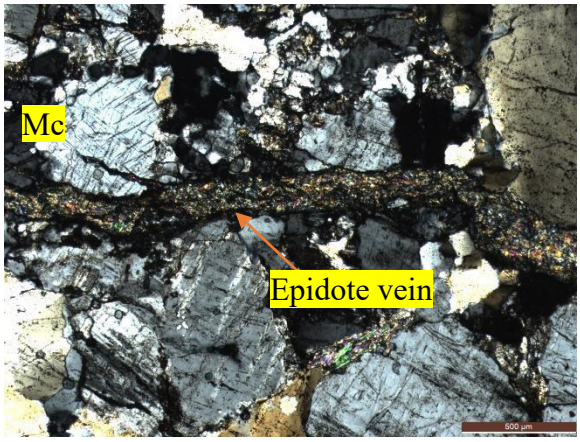

Fig. 6c. Photomicrograph showing epidote vein crosscutting the alkali feldspar syenite under XPL (Sample no. RJBO/BRS-107/2024-25).

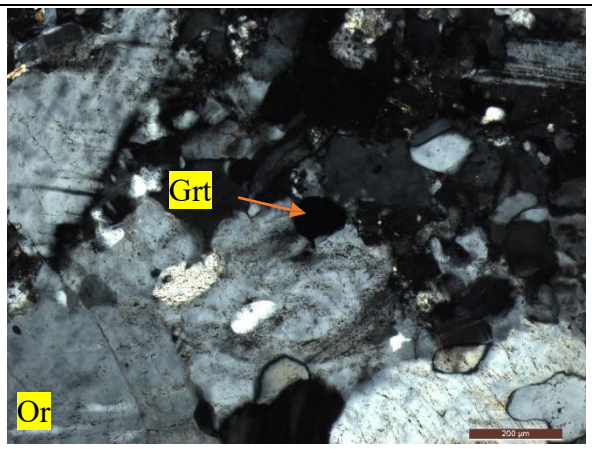

Fig. 6d. Photomicrograph showing of xenomorphic garnet in alkali feldspar syenite (Sample no. RJBO/BRS-107/2024-25).

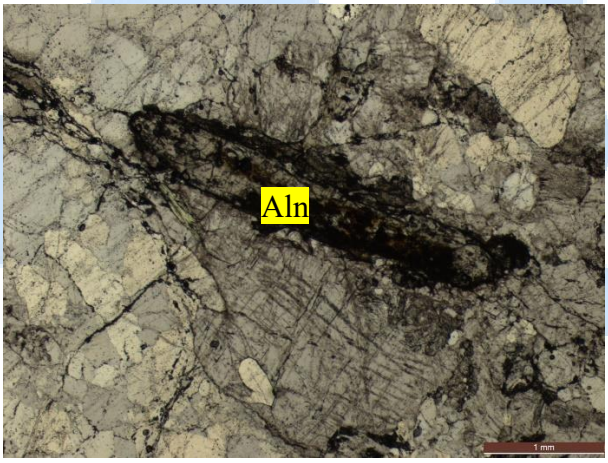

Fig. 6e. Photomicrograph showing a long prismatic allanite with radial cracks in alkali feldspar syeniteunder PPL (Sample no. RJBO/BRS-107/2024-25).

vii) Sample no. RJBO/BRS-108/2024-25 (Alkali Feldspar Syenite)

In hand specimen, the sample is a coarse-grained, flesh red-colored rock with several epidote veins cutting across the rock. The rock mainly consists of alkali feldspar and traces of quartz (Fig. 7a). Under microscope, the rock mainly consists of alkali feldspar and quartz, with allanite, muscovite, zircon, and epidote as accessories. Accordingly, the rock may thus be classified as alkali feldspar syenite. The rock exhibits both inequigranular and sub-hypidiomorphic textures. The alkali feldspars mostly show Carlsbad twinning and first-order grey color in cross-polarized light. Alkali feldspars are classified mostly as orthoclase. Two generations of epidote-zoisite veins are cross-cutting the rock.

The vein consists predominantly of epidote and zoisite crystals in the form of aggregates that show higher-order interference color and bluish color for zoisite (Figs. 7b & 7c). Epidote and zoisite are also present as independent grains and occur in the interstitial spaces of alkali feldspar. The quartz clearly exhibits undulatory extinction and sub-grain development, which are signs of strain-induced deformation. Zircon occurs as an accessory phase and is present as a prismatic bipyramidal grain, exhibiting high relief, high-order interference colors, and parallel extinction.

Allanite occurs as elongated minerals with a yellowish-brown color and exhibits high relief with distinct radial cracks (Fig. 7d). In cross-polarized light, it shows medium-high birefringence with interference colors masked by the crystal color. It is also marginally altering to epidote, as seen by the higher interference color along the edges of the crystal (Fig. 7e).

Petrography studies reveal that the rock contains significant amounts of REE-bearing minerals, i.e., allanite, and it is suggested to confirm in SEM and EPMA studies.

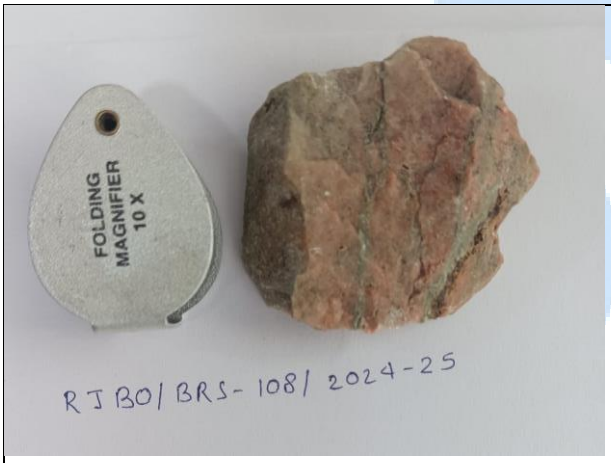

Fig. 7a. Hand sample of Alkali feldspar syenite (Sample no. RJBO/BRS-108/24-25).

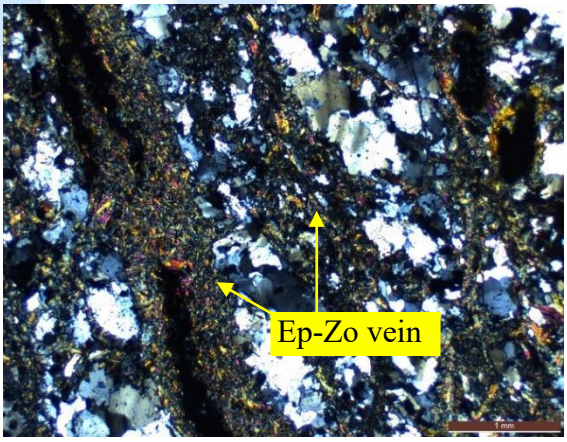

Fig. 7b. Photomicrograph showing epidote (ep)- zoisite (zo) veins intruded into the alkali feldspar syenite under the cross-polar view (Sample no. RJBO/BRS-108/24-25).

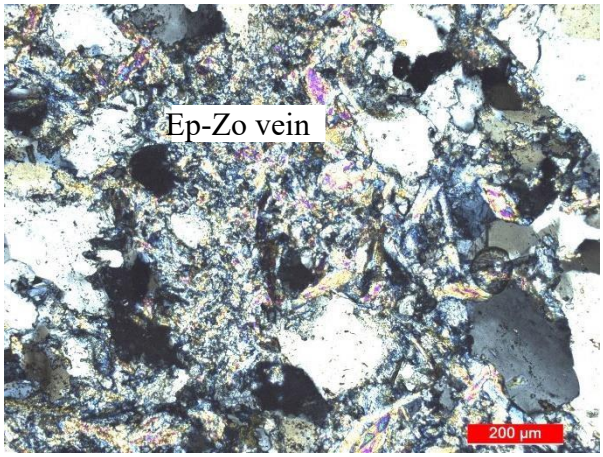

Fig. 7c. Photomicrograph showing magnified view of epidote (ep)-zoisite (zo) veins intruded into the alkali feldspar syenite under the cross-polar view (Sample no. RJBO/BRS-108/24-25).

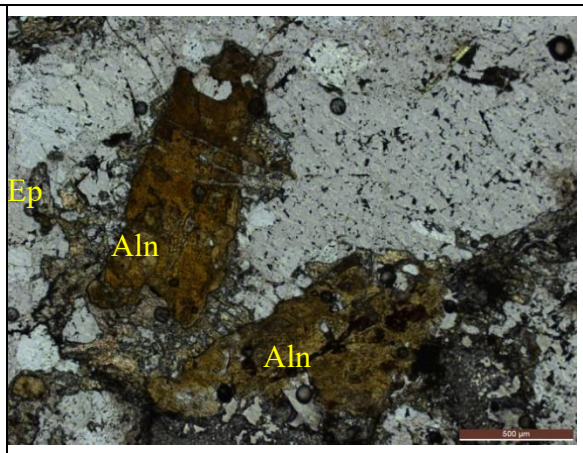

Fig. 7d. Photomicrograph showing a larger allanite (aln) crystals altered marginally by epidote (ep) under plane-polar view (Sample no. RJBO/BRS-108/24-25).

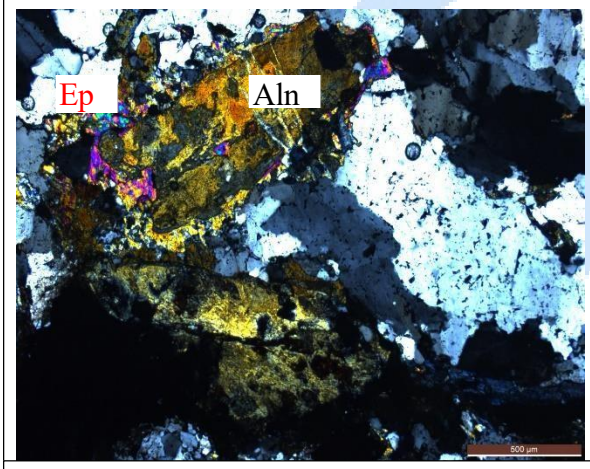

Fig. 7e. Photomicrograph showing a large allanite (aln) crystal altered marginally by epidote (ep) under the cross-polar view.

viii) Sample no. RJBO/BRS-29/2024-25 (Alkali feldspar syenite)

In hand specimen, the sample is a coarse-grained, flesh-red-colored rock. Epidote veins are crosscutting it. It mainly consists of alkali feldspar and trace amounts of quartz (Fig. 8a).

Petrographically, the rock is chiefly composed of alkali feldspars and quartz. The accessory minerals are plagioclase, hornblende, muscovite, chlorite, apatite, allanite, monazite, zircon, and epidote. The alkali feldspar comprises orthoclase and microcline. Accordingly, the rock may thus be classified as

alkali feldspar syenite. The K-feldspars are highly sericitized at places. Aggregates of epidote crystals are attributed to forming the epidote vein. Subhedral to euhedral monazite grains are associated with the K-feldspars (Fig. 8b). An elongated allanite grain shows a yellowish- brown color with the development of radial cracks (Fig. 8c). It is associated marginally with magnetite and K-feldspars.

The opaques were studied under the reflected light. Accordingly, they are classified as magnetite, hematite, and goethite, where the hematite and goethite are the alteration products of magnetite. Magnetite's primary oxide phase manifests as irregular and subhedral to euhedral forms. It has a low reflectance and a pinkish to greyish tinge. Hematite, which exhibits moderate reflectivity, takes the place of magnetite (Fig. 8d). In contrast, hematite-goethite alternations that occur as colloform structure (Fig. 8e) produced owing to oxidation in the surficial environment.

Petrography studies reveal that the rock contains significant amounts of REE-bearing minerals, i.e., allanite and monazite, and it is suggested to confirm in SEM and EPMA studies.

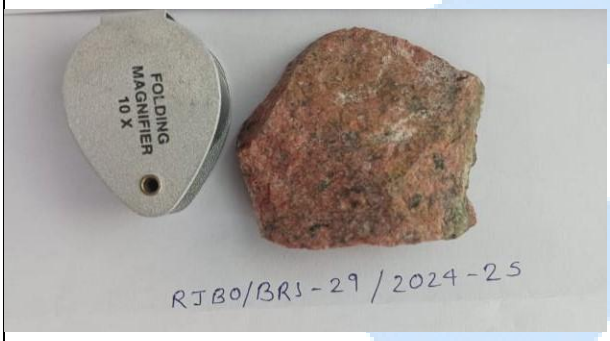

Fig. 8a. Hand sample of alkali feldspar syenite (Sample no. RJBO/BRS-29/24-25).

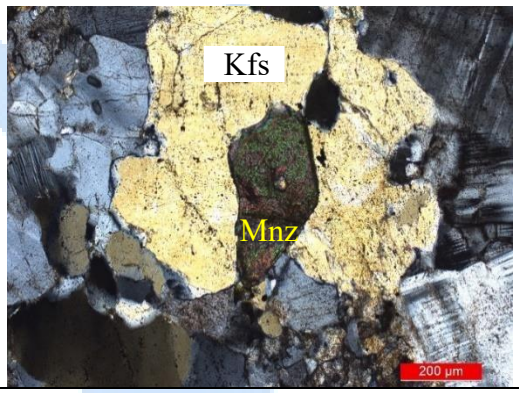

Fig. 8b. Photomicrograph showing Monazite (Mnz) associated with K-feldspars (Kfs) undercross-polar view (Sample no. RJBO/BRS- 29/24-25).

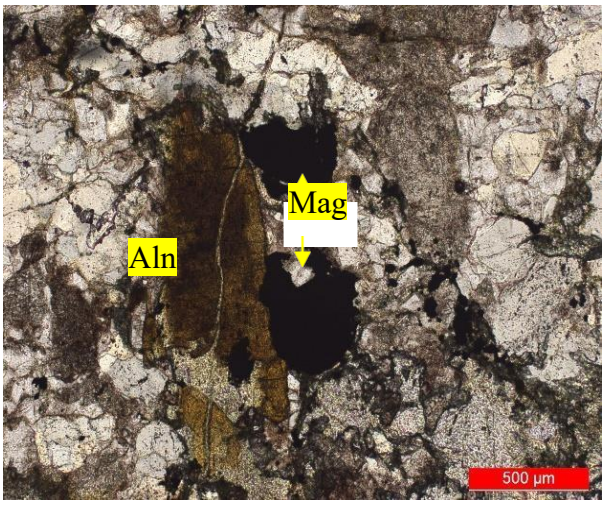

Fig.8c. Photomicrograph showing an elongated allanite (aln) with distinct radial cracks associated with K-feldspars (k-spar) and magnetite (mag), under plane polar view (Sample no. RJBO/BRS-29/24-25).

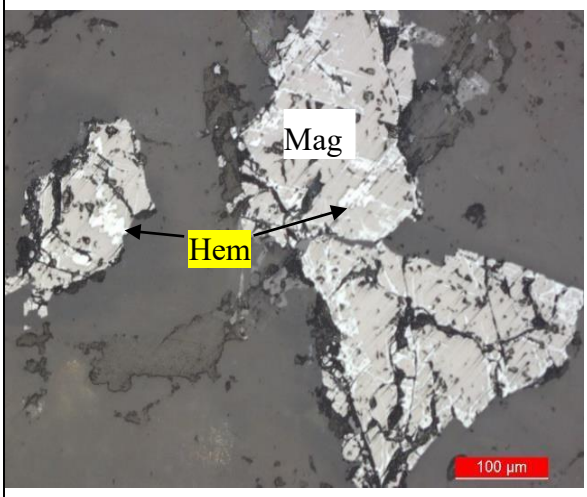

Fig. 8d. Photomicrograph showing Pinkish to grey tinge of irregularly shaped magnetite (Mag) replaced marginally by hematite (Hem) under reflected light (Sample no. RJBO/BRS-29/24-25).

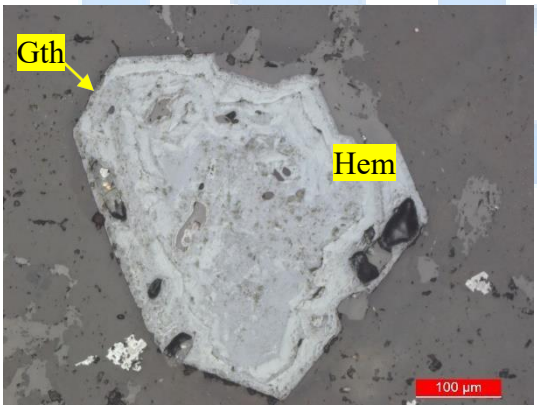

Fig. 8e. Photomicrograph showing magnetite replaced by hematite (Hem) and goethite (Gth) exhibits Colloform structure under reflected light (Sample no. RJBO/BRS-29/24-25).

ix)Sample no. RJBO/BRS-26/2024-25 (Alkali feldspar syenite)

In hand specimen, the sample is a flesh red, coarse-grained rock, intruded by several epidote veins. The rock consists predominantly of alkali feldspar and trace amounts of quartz (Fig. 9a).

In thin section, the rock mainly consists of alkali feldspar, with quartz, epidote, zoisite, sphene, hornblende, monazite, and allanite as accessory minerals. Accordingly, the rock name may thus be categorized as alkali feldspar syenite. Both sub-hypidiomorphic and inequigranular textures are present in this sample. The laths of plagioclase are randomly oriented in a fine groundmass of quartz and K-feldspar. Epidote occurs as veins and independent grains. Vein of epidote-zoisite cross-cutting the rock (Fig. 9c), whereas the independent epidote grains are occurring in the interstitial to intergranular K-feldspars. A subhedral allanite is associated marginally with epidote and subsequently plagioclase and orthoclase (Fig. 9b). The number of monazite grains is observed in this sample. These are occurring as granular forms associated with K-feldspars (Fig. 9d).

Petrography studies suggest that the rock is more promising for REE mineralization, which needs to be confirmed in SEM/EPMA methods.

Fig. 9a. Hand sample of alkali feldspar syenite (Sample no. RJBO/BRS-26/24-25).

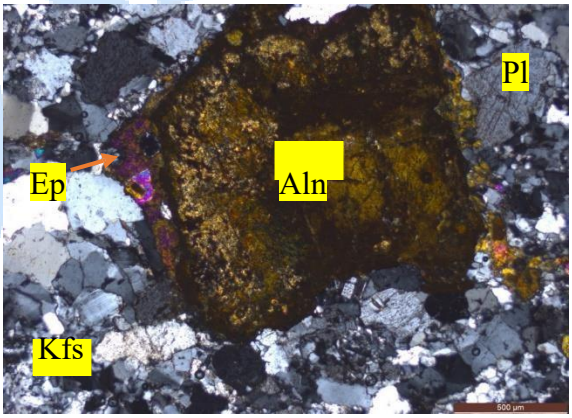

Fig. 9b. Photomicrograph showing a large subhedral allanite marginally associated with epidote embedded in the ground mass of K-feldspars under cross polar view (sample no. RJBO/BRS26/2024-25).

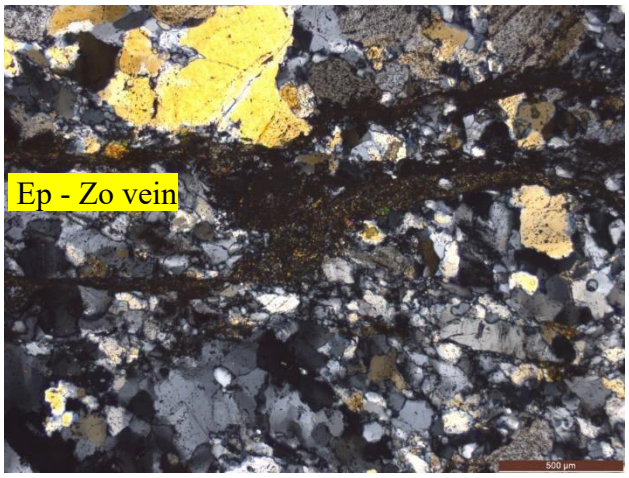

Fig. 9c. Photomicrograph showing epidote (ep)-zoisite (zo) veins traversed into alkali feldspar syenite under crosspolarized light (sample no.JBO/BRS26/2024-25).

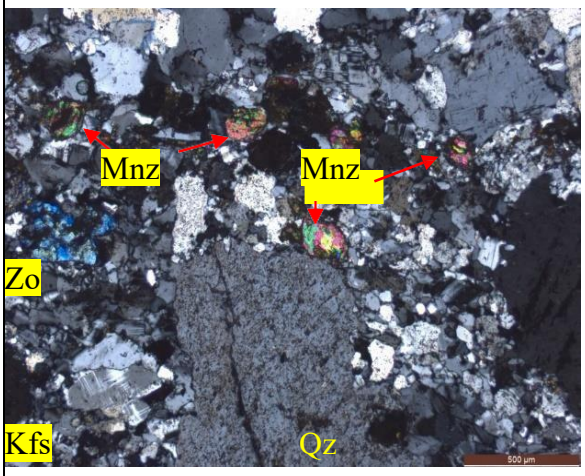

Fig. 9d. Photomicrograph showing granular monazite grains associated with K-feldspars and quartz in the alkali feldspar syenite under cross polar view (sample no. RJBO/BRS26/2024-25).

x) Sample no. RJBO/BRS-11/2024-25 (Aplite)

In hand specimen, the sample (RJBO/BRS-11/2024-25) is defined as a light-colored, medium- grained rock composed primarily of plagioclase and quartz as accessory. The grain size is smaller than those of pegmatite, as the average grain size in pegmatite is 8 to 10 cm. Hence, the rock may thus be categorized as Aplite (Fig. 10a). Petrographically, the sample is composed chiefly of plagioclase, K-feldspar, quartz, muscovite, and epidote as accessories (Fig. 10b). The modal proportion of plagioclase is more than the quartz. Several plagioclase inclusions have been observed within the interstitial plagioclase. Sericite alteration of plagioclases is seen at places. Polygonal mosaic texture with the sharp contact and triple junction is seen between the plagioclases (Fig. 10c). Muscovite is observed as platy forms associated with plagioclase and quartz. Euhedral to subhedral epidote occurs in the intergranular spaces to the plagioclase and quartz (Fig. 10d).

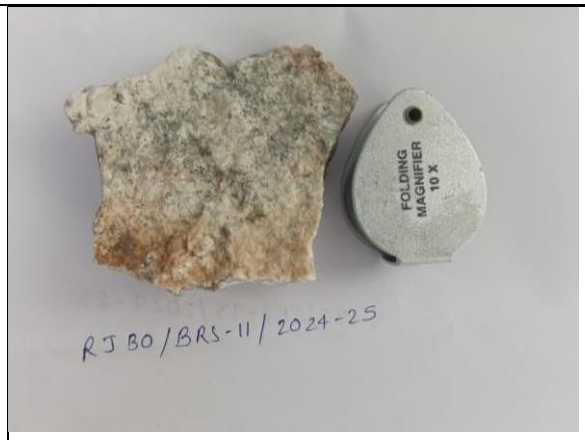

Fig. 10a. Hand sample of Aplite (Sample no. RJBO/BRS-11/24-25).

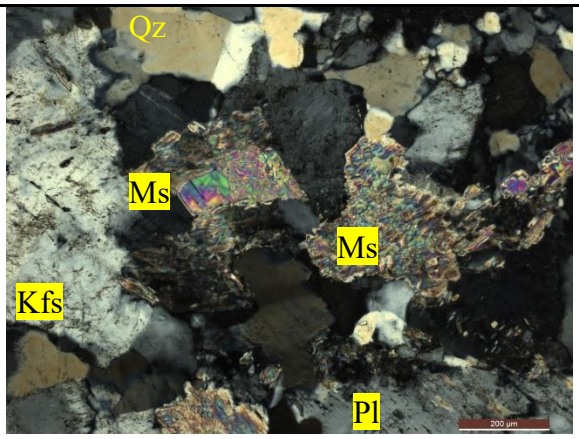

Fig. 10b. Photomicrograph of aplite showing mineral assemblages under CPL (Sample no. RJBO/BRS-11/24-25).

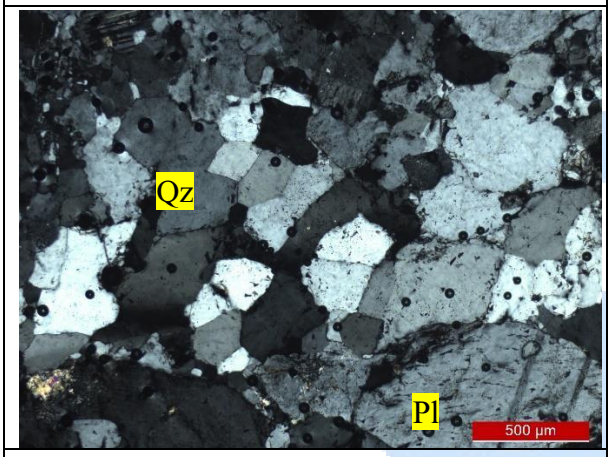

Fig. 10c. Photomicrograph of Polygonal mosaictexture in aplite under CPL (Sample no. RJBO/BRS-11/24-25).

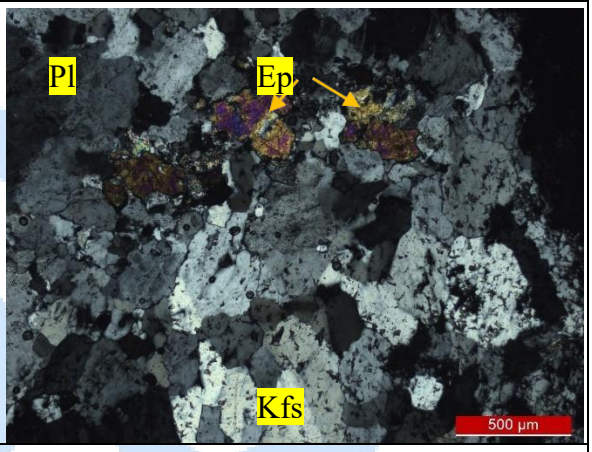

Fig. 10d. Photomicrograph showing epidotes inaplite under CPL (Sample no. RJBO/BRS-11/24-25).

4. Recommendations

Petrography studies indicate that the sample numbers include RJBO/BRS-24/24-25, RJBO/BRS-25/2024-25, RJBO/BRS-26/2024-25, RJBO/BRS-29/2024-25, RJBO/BRS-93/2024-25, RJBO/BRS-107/2024-25, and RJBO/BRS-108/2024-25 contain significant amounts of allanite and monazite grains, which warrant REE mineralization. It implies that to determine the REE potentiality, the REE-bearing minerals need to be confirmed in SEM/EPMA methods.

23.2.2 Core Petrography Report

भारतसरकार

GOVERNMENTOFINDIA

भारतीयभूवैज्ञानिकसवेक्षण

GEOLOGICALSURVEYOFINDIA

Report on Petrography studies of syenites and Granitoids of the Borana block, Bhilwara District, Rajasthan

1. Introduction

M/s GeoExpOre Pvt. Ltd., Banagalore has submitted 06 nos. of drill core samples for the preparation of thin polished sections to determine the petrography andminerals of the syenite and granitoids of the Borana block, Bhilwara dist., Rajasthan on a payment basis. All thin cum polished sections were examined under both the transmitted light and reflected light in a petrological microscope (Model: Leica DM2700P) for mineral content, textures, and other optical properties. Numerous digital photomicrographs of the thin sections were taken using an attached digital camera. The detailed descriptions of the thin, polished sections of different rock types are recorded, which are given below:

2. Sample Preparation

Selection and isolation have been done for the syenite, granite, magmatic gneiss and amphibolite rock. Using a mixture of epoxy and hardener, these samples were mounted on thin-section slides measuring 46 x 25 mm, and the sections were left overnight. After that, the mounted sections were ground using several carborundum grinding media fractions until the specimen fractions were visible. This is followed by polishing using diamond and chrome paste.

3. Petrography description of rocks

i)Sample no. RJB-01(75mts) (Alkali Amphibolite)

The hand specimen, RJB-01(75m) appears as a dark greenish to light-green-colored medium-grained rock exhibiting saccharoidal texture. A quartz vein cross-cut the alkali amphibolite. The primary sulphides dominated by pyrite and chalcopyrite were recorded. The rock consists predominantly of amphiboles and plagioclase (Fig.1a).

Under microscopic examination, the sample is divided into two distinct portions. The first contains large, preferentially oriented amphibole crystals (Fig. 1b), while the second is dominated by epidote-zoisite. In the first

portion, amphibole phenocrysts are embedded within a fine-grained matrix (pseudo-amphibole) and calcite. Large quartz crystals are also present; these are mostly deformed and recrystallized, exhibiting a metamorphic texture characterized by sharp boundaries and triple junctions between grains. Accessory calcite displays characteristic rhombohedral cleavage, twinkling, and twinning, with secondary quartz observed along the cleavage planes.

The second portion consists of fine-grained amphiboles exhibiting a polygonal mosaic texture. Under cross-polarized light, these amphiboles show strong pleochroism (ranging from bluish to yellowish-green) and two sets of perfect cleavage (Fig. 1c). Epidote-zoisite and clinopyroxene occur as accessory minerals. A few euhedral to subhedral clinopyroxene grains, identified by their yellowish-to-purple interference colors and inclined extinction, are located along the boundaries of the alkali amphiboles (Fig. 1d). Zoned epidote is also present. Along the contact zones of the alkali amphiboles, clusters of titanite appear in pseudo-forms associated with amphibole, carbonate, and ilmenite; individual euhedral or wedge-shaped titanite crystals are also observed (Fig. 1e).

Based on this petrographic study, the rock may thus be classified as an alkali amphibolite. The suspected alkali amphiboles tentatively identified as riebeckite or arfvedsonite composition which will be confirmed via Electron Probe Micro-Analyzer (EPMA) analysis. Under reflected light, the opaque mineral assemblage consists of chalcopyrite, pyrite, magnetite, and ilmenite. Chalcopyrite occurs both in vein form and as euhedral crystals. Pyrite is found as euhedral grains associated with quartz, chalcopyrite, and ilmenite (Fig. 1f). Magnetite is primarily associated with pyrite and chalcopyrite, while ilmenite exhibits an elongated, skeletal morphology.

Fig.1a. Hand sample of drill core sample of alkali-amphibolite (Sample no. RJB-1 (75mts).

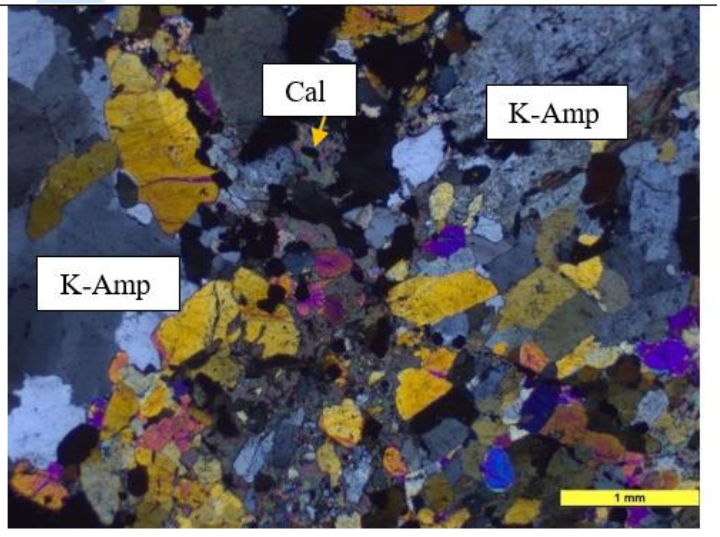

Fig. 1b. Photomicrograph of Alkali amphibolite showing mineral assemblages (K-Amp) under cross polar view (Sample no. RJB-1 (75mts).

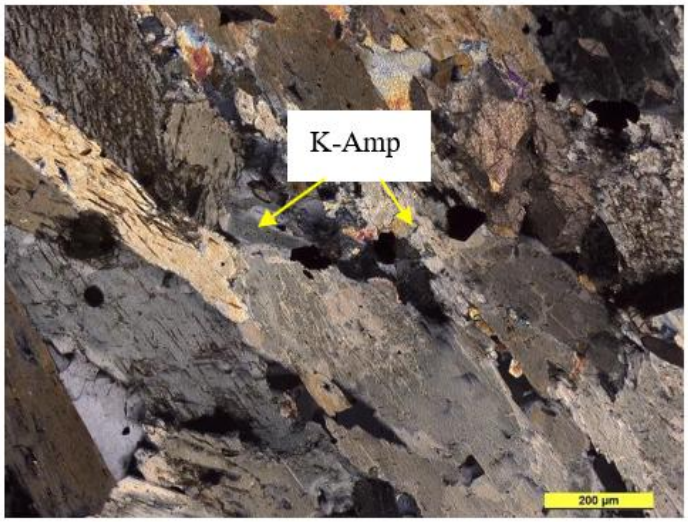

Fig. 1c. Photomicrograph showing yellow to bluish grey alkali amphiboles under cross polar view (Sample no. RJB-1 (75mts).

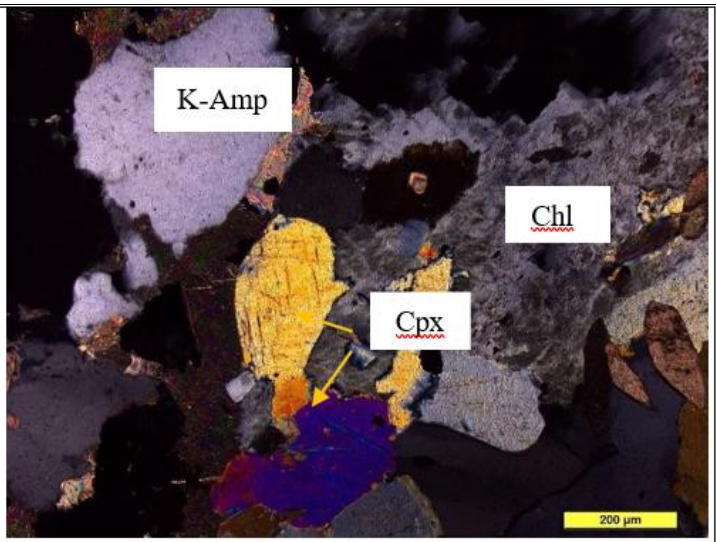

Fig. 1d. Photomicrograph showing Clinopyroxene (cpx) along with alkali amphiboles and titanite under cross polar view (Sample no. RJB-1 (75mts).

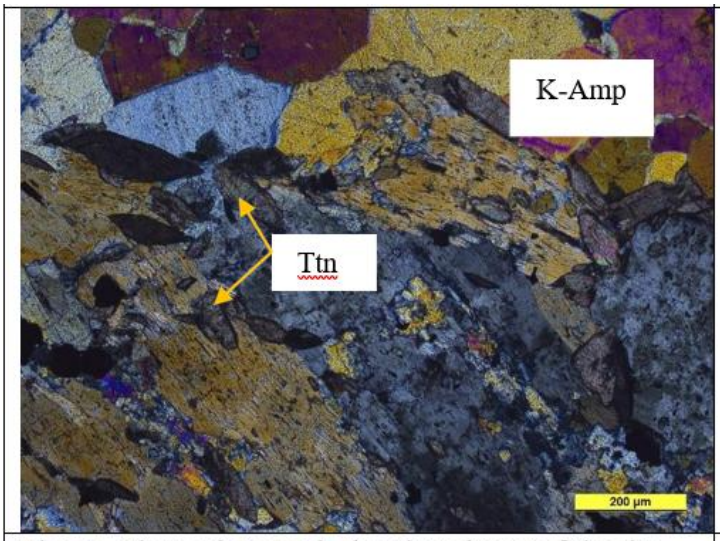

Fig. 1e. Photomicrograph showing cluster of titanite (Ttn) along the boundary of alkali amphiboles under cross polar view (Sample no. RJB-1 (75mts).

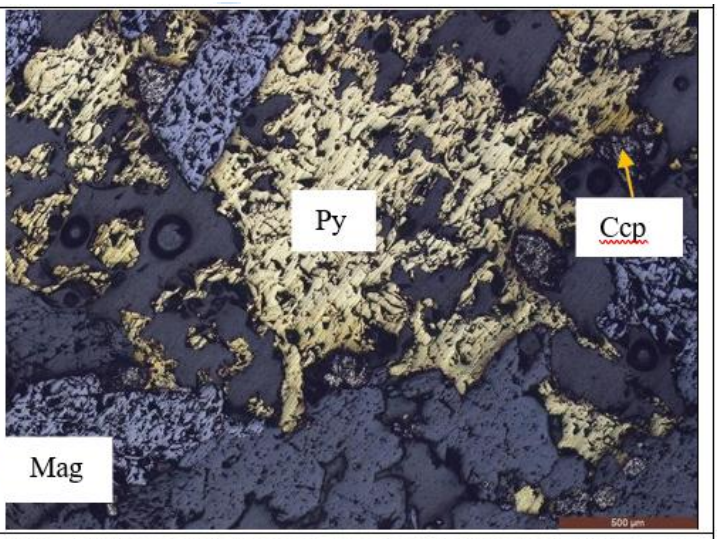

Fig. 1f. Photomicrograph showing irregular form of pyrite (Py), chalcopyrite (Ccp) and magnetite (Mag) associated with alkali amphiboles under reflected light (Sample no. RJB-1 (75mts).

ii)Sample no. RJB-02 (71 mts) (Alkali feldspar syenite)

The drill core sample RJB-02 was collected at 71m depth to understand the petrography characterization. The hand sample is distinguished by coarse-grained, pale pink rock. Alkali feldspar and plagioclase make up most of it (Fig. 2a). It was traversed by many epidote veins.

Petrographic study suggests that the sample RJB-02 is composed of alkali feldspar and plagioclase as essential minerals and epidote, zoisite, chlorite, muscovite, zircon and opaques as accessory phases. (Fig.2b). The alkali feldspar is dominated by orthoclase and microcline and is characterized by subhedral to euhedral forms.

While the microcline displays cross-hatched twinning, orthoclase often displays Carlsbad twinning. Besides, plagioclase exhibits polysynthetic twinning. It is easy to discern between their dual planes. This rock has undergoneunderg dynamic recrystallization during metamorphism and deformation, as evidenced by the formation of feldspar subgrains.

Hydrothermal alteration products like sericitization are often found in both alkali feldspar and plagioclase. Sub-hypidiomorphic textures are recorded. Epidote veins crosscut the rock. These veins predominantly consist of epidote crystals in the form of aggregates that show higher-order interference color. Zoisite are present as independent grains and as well as in the interstitial spaces of alkali feldspar. Chlorite, sericite, epidote and Zoisite are the typical features of the hydrothermal process whereas the subgrain formation/ mosaic texture depicts the metamorphic character. Zircon (Fig. 2c) and titanite formed as clusters.

In reflected light, it is observed that opaques are classified as chalcopyrite, pyrite and magnetite. Chalcopyrite occurs as stringers and idimorphic crystals. Pyrite occurs as fine-grained disseminations and and mostly associated with chalcopyrite and magnetite (Fig. 2d).

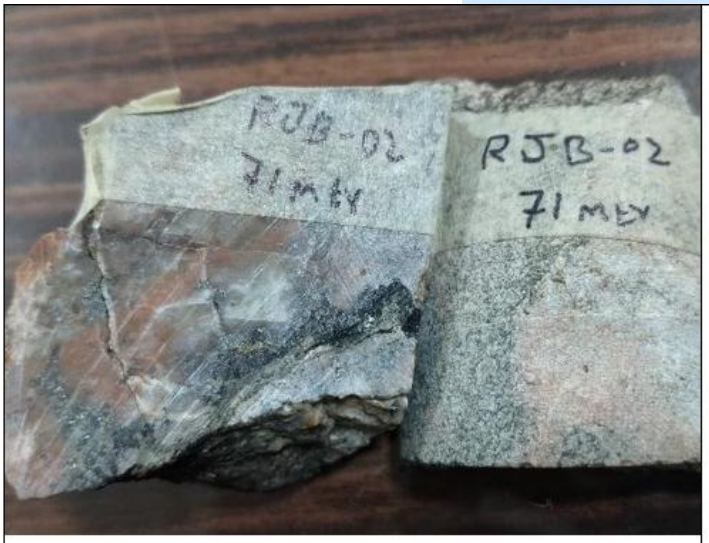

Fig.2a. Hand sample of drill core sample of alkali-feldspar syenite (Sample no. RJB2 (71mts).

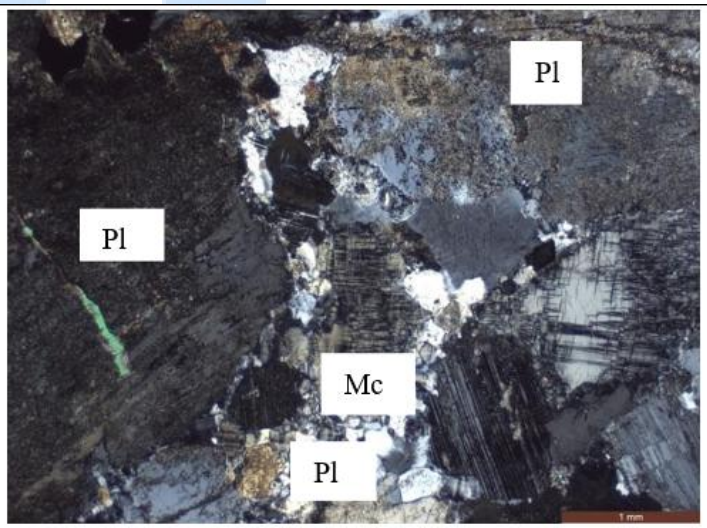

Fig. 2b. Photomicrograph of syenite showing assemblage of plagioclase (Pl), and microcline (Mc) displaying Sub-hypidiomorphic texture under cross polar view (Sample no. RJB-2 (71mts).

Fig. 2c. Photomicrograph showing clusters of zircon (zrn) grains under plane polar view (Sample no. RJB2 (71mts).

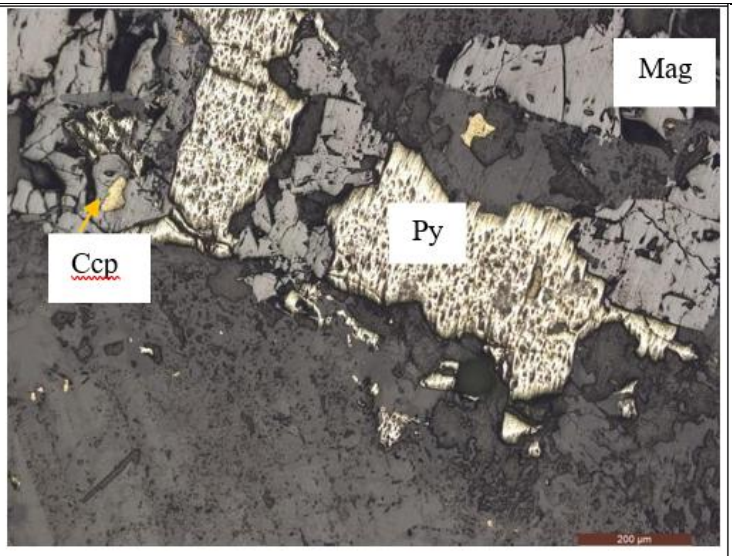

Fig. 2d. Photomicrograph showing pyrite. Chalcopyrite and magnetite in association with silicates under reflected light (Sample no. RJB2 (71mts).

iii)Sample no. RJB-02 (154 mts) (Biotite-hornblende Gneiss)

The sample (RJB-02) is coarse-grained rock with alternation of dark and light colour bands defined by pale-pink alkali feldspar-plagioclase-quartz and dark greenish-brown biotite-hornblende, respectively as this drill core sample was collected at 154 m depth (Fig. 3a). It has been traversed by quartz-carbonate veins. Crude foliation is developed defined by mafic minerals (Fig.3a).

Under the microscope, it is observed that the rock developed a strong foliation and gneissose structure defined by alternating layers of dark (biotite-hornblende) and light color (plagioclase, K-feldspar, quartz) minerals (Fig. 3b-c). The felsic minerals are inequigranular. K-feldspar mainly comprises of microcline which is easily distinguished by cross-hatched twinning. A few quartz grains included in the microcline are seen at places. Sericitization of microcline and plagioclase as the alteration product is recorded at places. At places, the sub¬grain formation of plagioclase has taken place, which clearly indicates the deformation and metamorphism (Fig 3d). Biotite is often associated with muscovite, and it occurs as a platy form preferred orientations that define foliation in the rock. Biotite shows a yellowish-brown color in the transmitted light. Hornblende showing trichroism from bluish green to dark green through yellowish green under plane polarized light. Euhedral zircon grains occur along the intergranular spaces of quartz. (Fig 3e).

Under reflected light, the opaques are classified as magnetite, chalcopyrite and pyrite. Chalcopyrite occurs as disseminations and stringers while pyrite forms as euhedral crystal. According to the mineral assemblages, the rock may thus be classified as biotite-hornblende gneiss.

Fig.3a. Hand sample of drill core sample of Biotite Hornblende Gneiss (Sample no. RJB-2 (154mts).

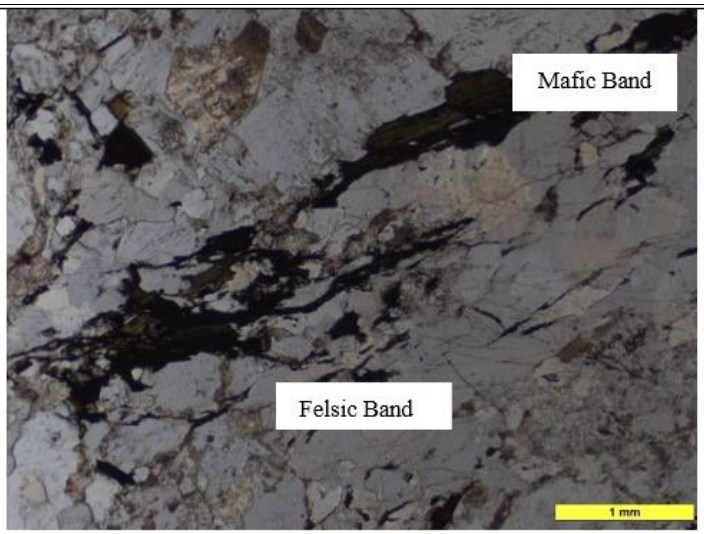

Fig. 3b. Photomicrograph Bt-Hbl gneiss displays alternations of mafic and felsic bands/layers defined by biotite-hornblende and quartz-plagioclase mafic band composed of Biotite-hornblende and felsic band composed of quartz-plagioclase under plane polar view (Sample no. RJB-2 (154mts).

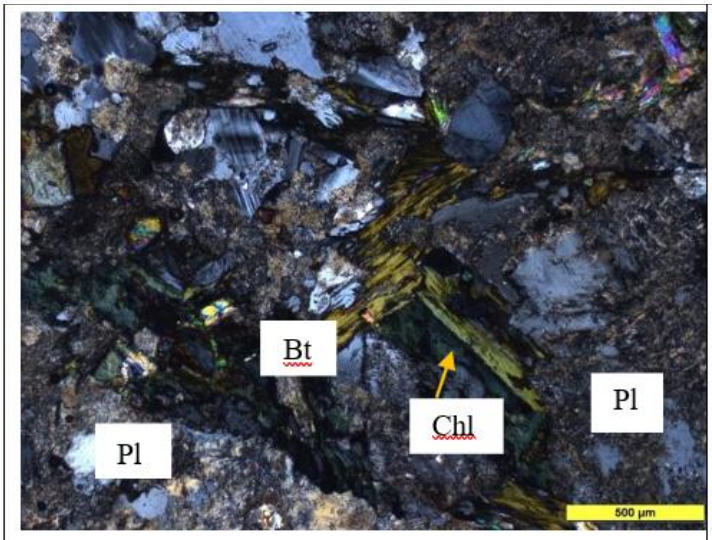

Fig. 3b. Photomicrograph showing alteration of biotite by chlorite under cross polar view (Sample no. RJB-2 (154mts).

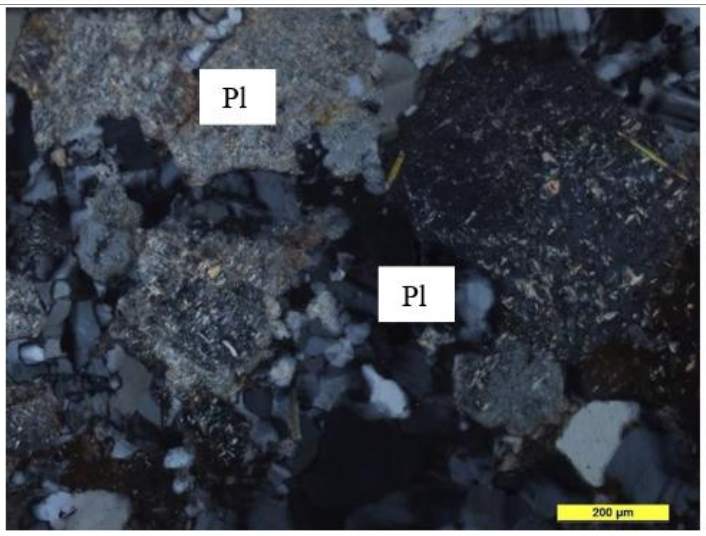

Fig. 3b. Photomicrograph of plagioclase (Pl) showing subgrain formation due to metamorphic activity under cross polar view (Sample no. RJB-2 (154mts).

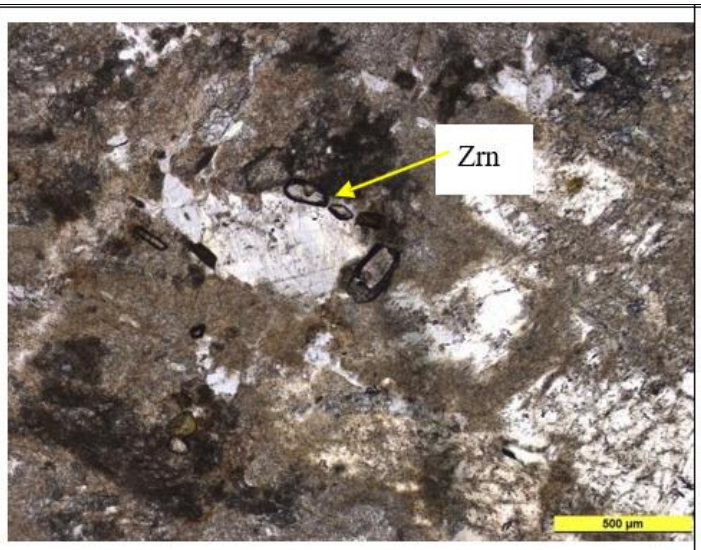

Fig. 3e. Photomicrograph cluster of zircon (Zrn) grains under plane polar view (Sample no. RJB-3 (75mts).

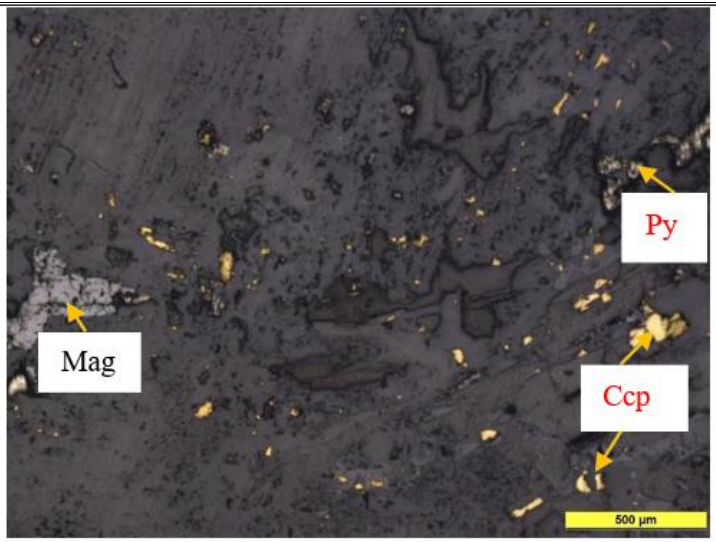

Fig. 3f. Photomicrograph showing disseminated chalcopyrite (Ccp), and pyrite (Py) under reflected light (Sample no. RJBO/BRS-7/24-25).

iv) Sample no. RJB-04 (50mts) (Alkali Feldspar Syenite)

The drill core sample (RJB-04) was collected at 50 m depth. In hand specimen, the sample RJB-04 is characterized by pale pink, coarse-grained rock. It is composed primarily of alkali feldspar, plagioclase and quartz. The rock is traversed by multiple epidote veins.

(Fig.4a). Based on the observation made through the thin polished section, the drill core sample has two portions, where one has alkali-feldspar syenite and the other is ribbon quartz.

Under the microscope the first portion of the rock consists predominantly of quartz, plagioclase, K-feldspar, and allanite, monazite, epidote, sphene chlorite and opaque as accessories. The second one is dominated by quartz grains. Quartz grains stretched, elongated and deformed indicate high-temperature plastic deformation (Fig. 4d). Sericitization of plagioclases is seen in places. The fine quartz and plagioclase inclusions are found within the microcline. Intergrowths of plagioclase and quartz exhibit myrmekite texture. Epidote-zoisiteveins cross-cutting the rock. Allanite and Monazite are the significant REE bearing minerals observed in the samples (Fig 4c and e). In the section seven grains of allanite have been recognized. They are often associated with rim of epidote. Cluster of titanite is recorded in this section.

Under reflected light, sulfide mineralization is represented by pyrite. The discrete nature of pyrite grains shows euhedral to subhedral forms. (Fig 4f).

Petrographic study indicates the presence of a significant amount of allanite and monazite grains which need to be confirmed in SEM/EPMA methods for REE potentiality.

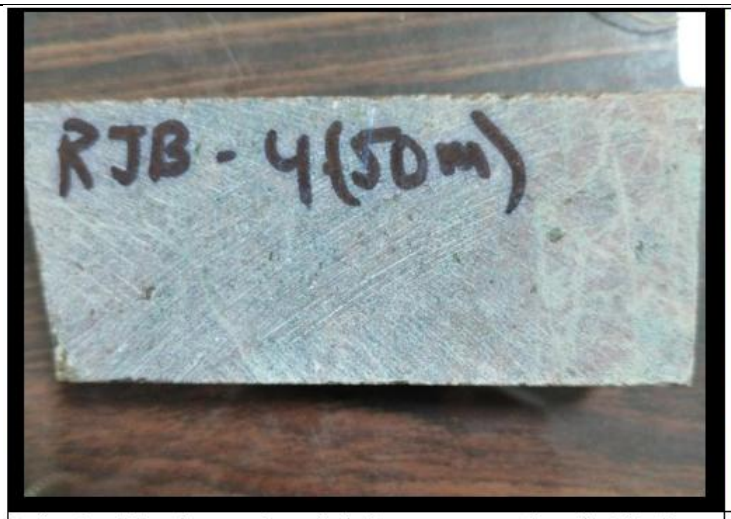

Fig.4a. Hand sample of drill core sample of Alkali-feldspar syenite. (Sample no. RJB-4 (50mts).

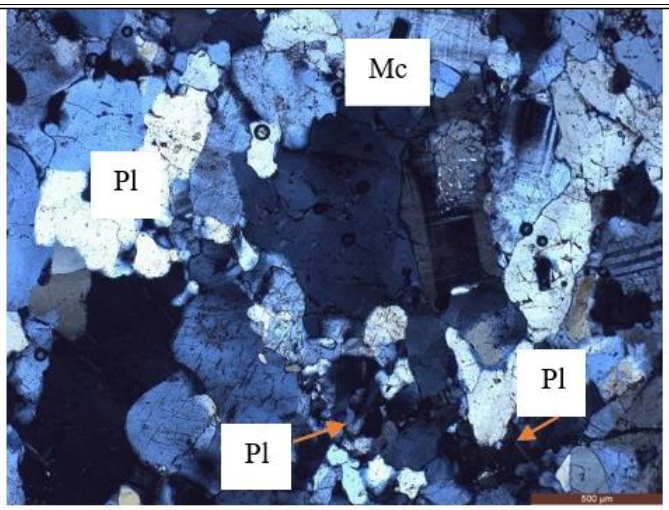

Fig.4b. Photomicrograph showing myrmekite texture along with plagioclase and microcline; subgrain formation of Plagioclase (Pl) in the alkali feldspar syenite under cross polar view (Sample no. RJB-4 (50mts).

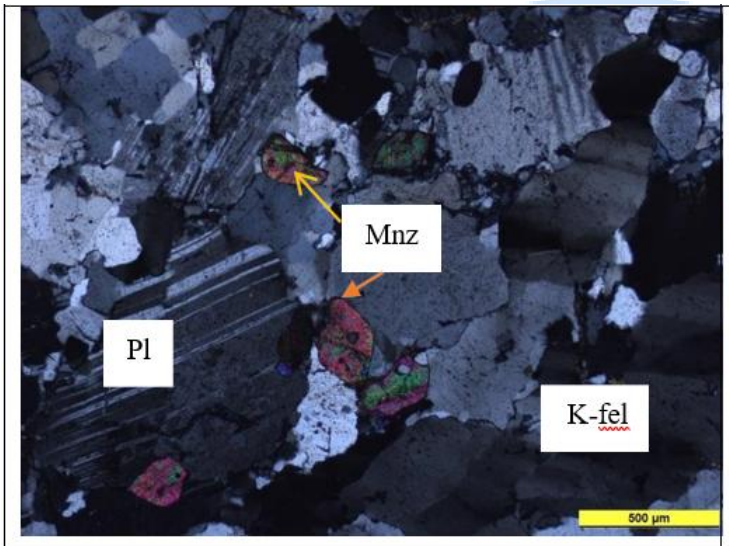

Fig.4c. Photomicrograph showing granular Monazite (Mnz) grains associated with plagioclase under Cross polar view (Sample no. RJB-4 (50mts).

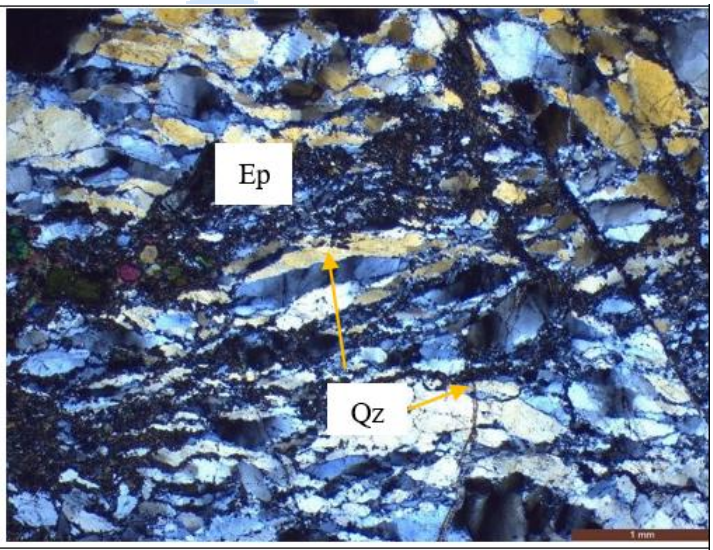

Fig.4d. Photomicrograph showing ribbon quartz (Qz) with epidote (Ep) veins under Cross Polar view (Sample no. RJBO/BRS-24/24-25).

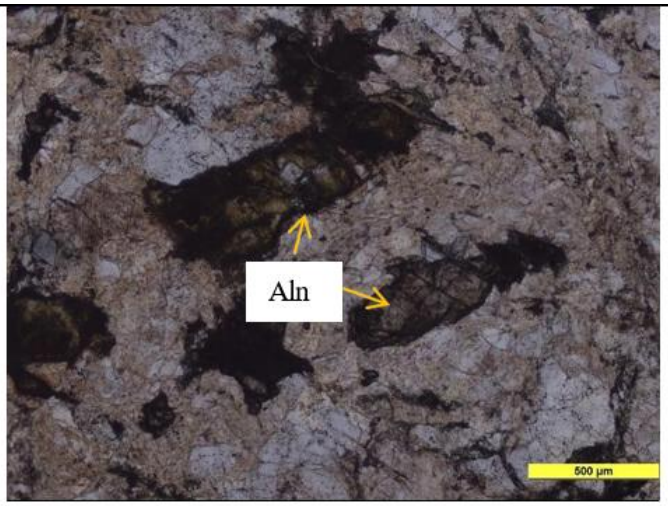

Fig.4e. Photomicrograph showing primary allanite (Aln) under plane polar view (Sample no. RJB-4 (50mts).

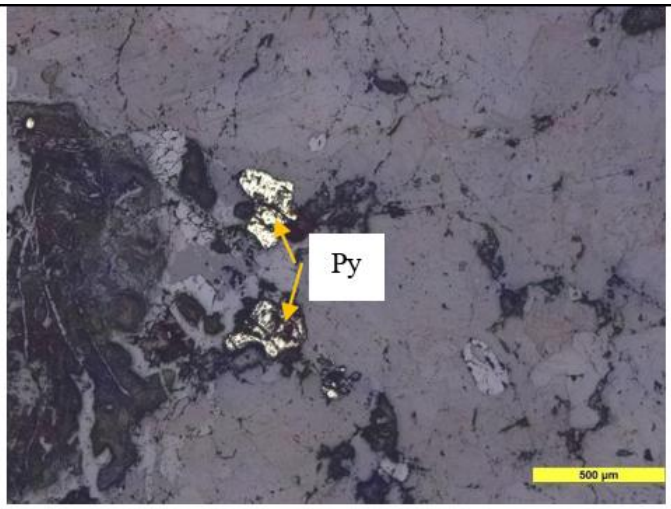

Fig.4f. Photomicrograph showing euhedral pyrite (Py) under reflected light (Sample no. RJB-4 (50mts).

v) Sample no. RJB-4 (96m) (Alkali feldspar Syenite)

The sample is a coarse-grained rock and pale pink to greenish colour, composed predominantly of plagioclase and alkali feldspar. Multiple epidote veins traversed into it. Due to occurrence of the epidote veins the rock appeared as pinkish green colour (Fig. 5a).

Petrographically, the rock is mainly composed of plagioclase and K-feldspar, and its accessory minerals are quartz, epidote, zoisite, chlorite, and carbonate. It is coarse-grained and inequigranular in texture. K-feldspar is dominated by microcline. Subgrain formation of plagioclase and K-feldspar that form during deformation results from recrystallization, which occurs when temperature increases. Sericitization in the K-feldspars and plagioclase are seen at places. The rock is highly deformed and sericitized. Quartz occurred in a minor amount. Sub-hypidiomorphic texture is also recorded in this rock. Zoisite- epidote veins are cross-cutting all the mineral phases. These veins consist predominantly of epidote crystals in the form of aggregates that show higher-order interference color (Fig. 5c). Later vein of carbonate, which is cross cutting the earlier vein (Fig 5c). Carbonate, chlorite, epidote and zoisite are the typical features of the hydrothermal process, whereas the subgrain formation depicts the metamorphic character. Titanite clusters display high relief and 2nd order interference colour at places. The irregular nature of allanite grains is characterized by a yellowish brown and high relief relative to their associated minerals (Fig 5d). Cluster of monazites along the chlorite is recorded. These are granular in nature with high relief (Fig 5e). Based on the mineral assemblages, the rock may thus be classified as alkali feldspar syenite.

Petrographic study indicates the presence of a significant amount of allanite and monazite grains, which need to be confirmed in SEM/EPMA methods for REE potentiality.

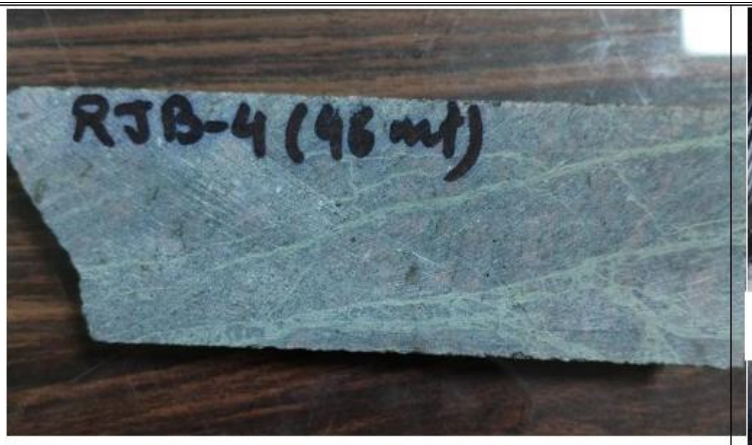

Fig.5a. Hand sample of drill core sample of alkali-feldspar syenite (Sample no. RJB-04).

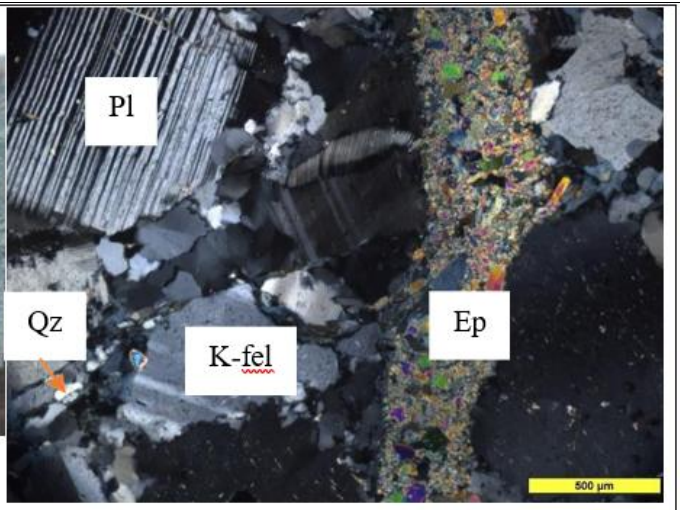

Fig.5b.Photomicrograph alkali-feldspar syenite showing mineral assemblages such as plagioclase (Pl) and epidote (Ep) vein which intruded the syenite at earlier stage under CPL (Sample no. RJB-04).

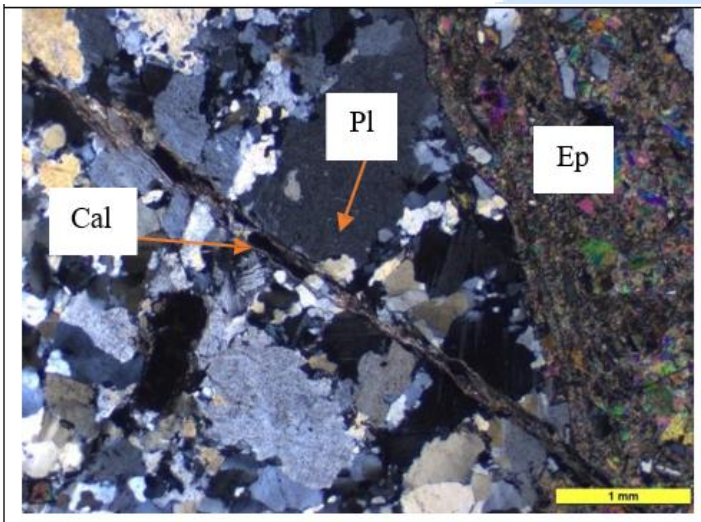

Fig 5c. Photomicrograph showing a late stage epidote and carbonate veins are cross-cutting the alkali feldspar syenite under CPL.

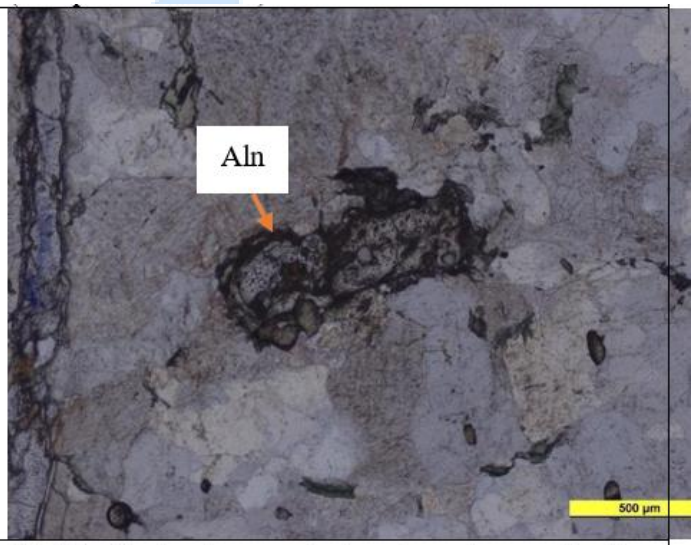

Fig 5d.: Photomicrograph showing primary allanite (Aln) rimmed by epidote (Ep) and plagioclase (Pl) under plane polarized light (Sample no. RJB-04).

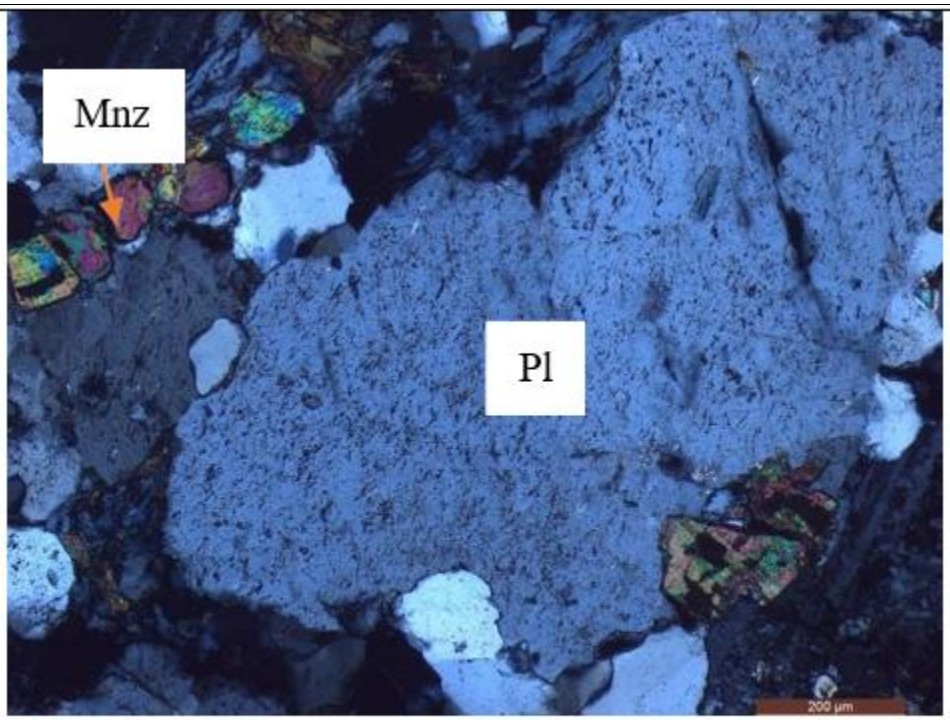

Fig 5e.: Photomicrograph showing cluster of Monazite (Mnz) and plagioclase (Pl) under cross polarized light (Sample no. RJB-04).

vi) Sample no. RJB-3 (95m) (Biotite gneiss)

The hand sample (drill core-RJB-03) was collected at 95m depth. The sample RJB-03 is a coarse-grained rock. Rock shows alternations of mesocratic and leucocratic bands defined by gneissose structure. Mesocratic bands are made up of biotite, while plagioclase, K-feldspar, and quartz are in the leucocratic bands (Fig. 6a). The rock is biotite gneiss.

A petrography study reveals that the sample displays gneissic texture defined by dark and light color bands, which are represented by biotite and plagioclase, microcline, orthoclase and quartz, respectively. Allanite, titanite, zoisite, epidote and opaques are observed as accessories. The rock is coarse to medium grained. Biotite occurs as platy, showing preferred orientations that define gneissic foliation. But it is poorly developed. It defines the mafic band in the rock (Fig 6b). Polysynthetic lamellar twinning is well preserved in the plagioclases. Number of blebs of plagioclases included within the later plagioclases. Intergrowths of plagioclase and quartz exhibit myrmekite texture are seen at places. The plagioclases have been partially replaced by sericites indicate hydrothermal fluid activity. The quartz grains show sub-grain formations, suggesting strain-induced deformation (Fig. 6c). Zoisite-epidote veins are cross-cutting all the mineral phases. Cluster of titanite are observed along the grain boundary between biotite, quartz and plagioclase (Fig. 6d). Primary allanite is observed to show a yellowish green color

and weak pleochroism. Six grains with variable sizes are distributed randomly over this rock (Fig. 6e).

In reflected light, most opaques are classified as magnetite. Magnetite occurs as euhedral as well as vein type, dominantly associated with biotite (Fig. 6f).

Petrographic study indicates the presence of a significant amount of allanite grains which need to be confirmed in SEM/EPMA methods for REE potentiality.

Fig. 6a Drill core sample of Biotite gneiss (sample no. RJB-3)

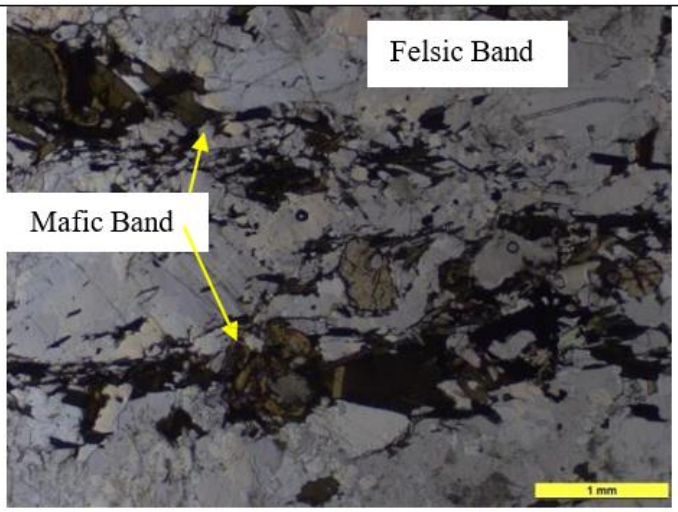

Fig. 6b. Photomicrograph of biotite gneiss showing alternations of mafic and felsic band defining gneissosity under plane polarized light (Sample no. RJB-3).

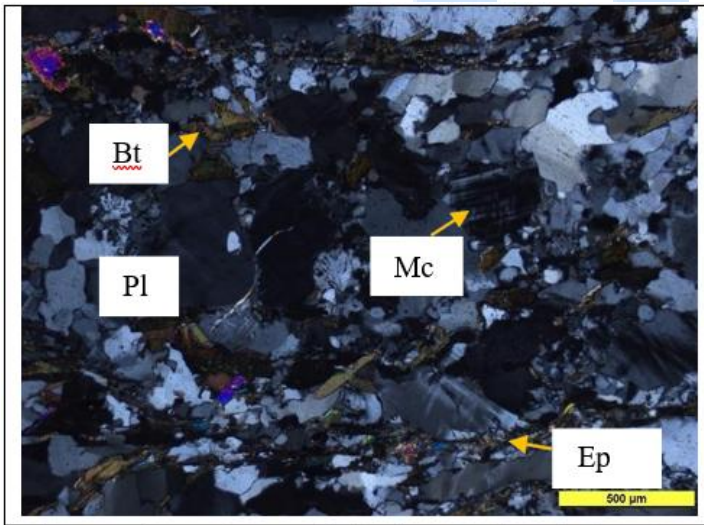

Fig. 6c. Photomicrograph displays epidote (Ep) veins along with major minerals like biotite (Bt), plagioclase (Pl) and microcline (Mc) under cross polarized light (Sample no. RJB-3).

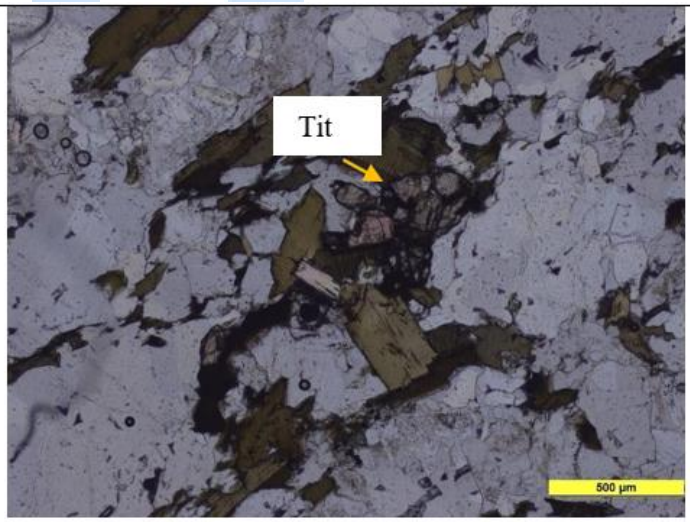

Fig. 6d. Photomicrograph showing cluster of titanite along the boundary of plagioclase and biotite under plane polarized light (Sample no. RJB-3).

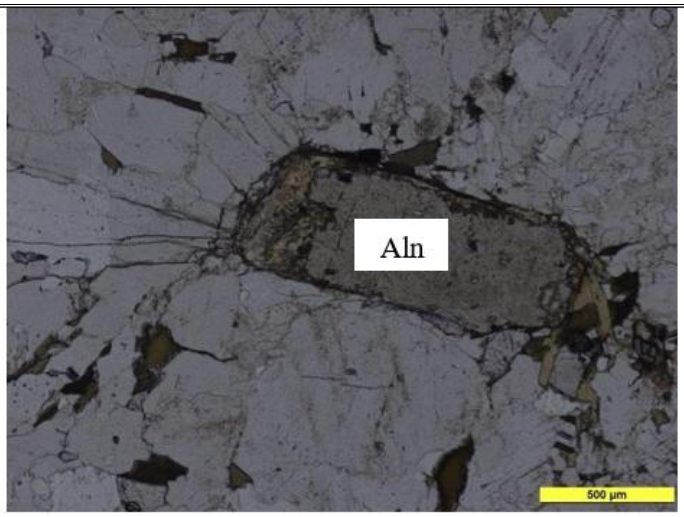

Fig. 6e. Photomicrograph showing a long prismatic allanite (Aln) with radial cracks under plane polar view (Sample no. RJB-3).

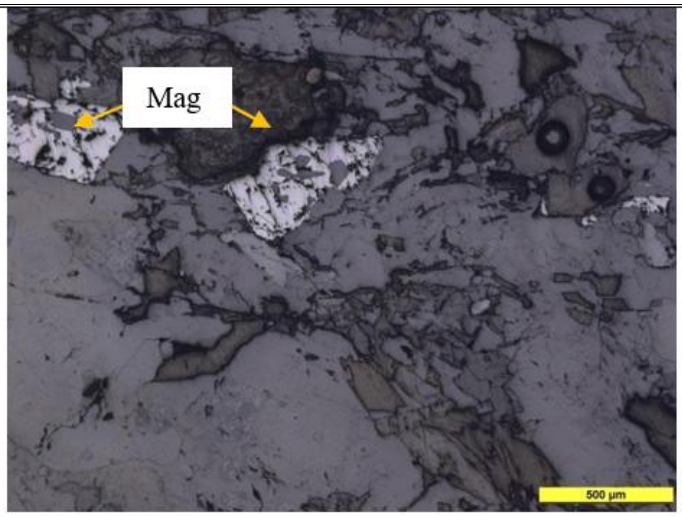

Fig. 6f. Photomicrograph showing a long prismatic allanite (Aln) with magnetite (Mg) in biotite gneiss, under reflected light (Sample no. RJB-3.

23.3 Annexure III- XRD

The samples from Borana Block, Bhilwara District, Rajasthan were characterized for their mineralogy using X-Ray Diffraction (XRD) at Room Temperature using a Bruker D8 Advance, at the Department of Inorganic and Physical Chemistry, Indian Institute of Science, Bengaluru. The analyses were performed for 2Θ range 5° to 65°. The resolution as better than 0.0001° and the X-ray source as 2.2 KW Cu anode.

SR.NO.	SAMPLE NUMBER	MINERAL PHASES IDENTIFIED
1	RJBO/BRS-03	Albite, Microcline, Nepheline, Orthoclase, Epidote, Augite.
2	RJBO/BRS-47	Orthoclase, Albite, Microcline, Orthopyroxene, Feldspar, Monazite
3	RJBO/BRS-49	Quartz, K-feldspar, Albite
4	RJBO/BRS-61	Quartz, Orthoclase, Microcline, Biotite, Amphibole, Apatite
5	RJBO/BRS-105	Quartz, Plagioclase feldspar, K-feldspar, Biotite.
6	RJBO/T1-01	Quartz, Albite, Microcline, Biotite, Orthoclase.
7	RJBO/T2-06	Albite, Quartz, Orthoclase, Clinopyroxene, Paracostibite, Zircon.
8	RJBO/T3-13	Quartz, K-feldspar, Albite, Muscovite, Biotite, Apatite, Zircon
9	RJBO/T4-11	Quartz, Albite, Microcline, Clinopyroxene, Garnet
10	RJBO/T5-08	Quartz, Microcline, Albite, Oligoclase, Muscovite, Biotite, Garnet
11	RJBO-01/CS-14	Feldspar, Orthoclase, Microcline, Sodalite, Apatite
12	RJBO-04/CS-11	Quartz, Microcline, Orthoclase, Plagioclase, Biotite, Muscovite, Garnet, Allanite, Monazite, Zircon
13	RJBO-03/CS-31	Quartz, K-feldspar, Plagioclase, Biotite, Muscovite, Garnet, Allanite, Monazite, Zircon
14	RJBO-03/CS-30	Quartz, Microcline, Plagioclase, Biotite, Muscovite, Garnet, Allanite, Monazite, Zircon
15	RJBO-03/CS-50	Quartz, Albite, Microcline, Zinnwaldite, Enstatite
16	RJBO-02/CS-63	Quartz, Orthoclase, Microcline, Albite, Nepheline, Monazite-Ce,
17	RJBO-02/CS-61	Quartz, Microcline, Orthoclase, Albite, Nepheline
18	RJBO-01 48 mtr	Quartz, Hornblende, Plagioclase Feldspar, Biotite, Epidote, Clinozoisite, Titanite, Magnetite, Ilmenite
19	RJBO-01 44 mtr	Quartz, Hornblende, Feldspar, Epidote, Titanite, magnetite
20	RJBO-01/CS-25	Clinopyroxene, Actinolite, Chlorite, Epidote, Ilmenite.

23.4 Annexure IV- Bulk Density

Sample ID	M1- Empty Beaker wt (mg)	M2- EB+Sample wt (mg)	M3- EB+Sample+Water wt (mg)	Clean EB wt (mg)	M4- EB+Water wt (mg)	Sample wt (g) {M2-M1}	Displaced Water wt by Sample(mg) {M3-M4}	Specific Gravity (G)	Bulk Density (g/cc)
BRS-105	24700.3	26194.6	84050.7	24718.1	83135	1494.3	915.7	2.583	**2.583**
BRS-07	24665.2	26387.9	84219.5	24685.9	83257.2	1722.7	962.3	2.266	**2.266**
BRS-61	24729.6	25881.6	83820.7	24720.8	83245.3	1152	575.4	1.998	**1.998**
G3051-14	24710.5	25736.1	83799.7	24704.3	83100.1	1025.6	699.6	3.146	**3.146**
G3051-186	24703.3	26037.2	84035.7	24702.6	83127.6	1333.9	908.1	3.133	**3.133**

23.5 Annexure V- EPMA

Sample: RJB/BRS-93 (MIGMATITE GNEISS)

No.	Displacement	Pr2O3	Nd2O3	Gd2O3	Yb2O3	Lu2O3	Ho2O3	Tb2O3	Er2O3	Dy2O3	La2O3	Ce2O3	Sm2O3	Eu2O3	Tm2O3	Total	Comment	Type	P
1	0	0.289	0.034	0	0.036	0	0	0.067	0	0	0	0	0.08	0.051	0.002	0.559	C1ZR	Zircon	
2	0.0098	0	0.054	0	0.046	0.15	0.201	0.045	0.16	0.056	0.034	0.053	0	0	0	0.799	C1ZR	Zircon	
3	0.0184	0.121	0	0	0.038	0.017	0	0	0.222	0	0	0.011	0.007	0	0	0.416	C1ZR	Zircon	
4	1.5763	0.373	1.406	0.566	0.109	0.098	0	0	0.208	0.187	2.529	4.351	0.288	0	0	10.115	C1	MONAZITE	P1
5	1.6112	0.229	1.037	0.457	0	0.15	0.128	0	0	0.248	1.951	3.963	0.189	0	0.062	8.414	C1	MONAZITE	P2
6	1.6199	0.369	1.567	0.802	0	0	0	0	0.116	0.334	2.016	4.617	0.258	0	0	10.079	C1	MONAZITE	P3
7	1.6191	0.551	2.065	1.077	0.091	0	0	0	0.067	0.228	3.771	6.996	0.459	0	0.044	15.349	C1	MONAZITE	P4
8	1.6391	0.3	1.5	0.507	0	0	0	0	0.037	0.181	1.891	3.965	0.283	0	0	8.664	C1	MONAZITE	P5
9	11.7124	0	0.006	0	0.056	0.02	0.101	0	0	0.086	0	0.007	0.039	0	0.074	0.389	C2	Zircon	P2
10	11.726	0	0	0.104	0	0.132	0	0.019	0	0	0.061	0	0	0	0.115	0.431	C2	Zircon	P3
11	11.7282	0.04	0.123	0.146	0.191	0.175	0	0.027	0	0.285	0	0.784	0.049	0	0	1.82	C2	Zircon	P4
12	11.7199	0	0.232	0.712	0.816	0.149	0	0	0.768	0.722	0.022	4.049	0.016	0	0.041	7.527	C2	Zircon	P5
13	11.718	0.081	0	0	0.099	0.04	0	0	0	0.102	0	0.087	0.018	0	0	0.427	C2	Zircon	P6

Sample: RJB-03(95mts) (MIGMATITE GNEISS)

No.	Displacement	Pr2O3	Nd2O3	Gd2O3	Yb2O3	Lu2O3	Ho2O3	Tb2O3	Er2O3	Dy2O3	La2O3	Ce2O3	Sm2O3	Eu2O3	Tm2O3	Total	Comment	Type	P
1	0	0.110	0.025	0.000	0.105	0.000	0.131	0.000	0.000	0.000	0.004	0.009	0.051	0.000	0.000	0.435	C1	Zircon	P1
2	0.0297	0.025	0.015	0.011	0.018	0.052	0.069	0.129	0.000	0.144	0.000	0.049	0.028	0.000	0.098	0.638	C1	Zircon	P2
3	0.0570	0.000	0.000	0.017	0.000	0.000	0.000	0.065	0.000	0.032	0.000	0.073	0.000	0.000	0.120	0.307	C1	Zircon	P3
4	0.0713	0.000	0.067	0.000	0.000	0.101	0.000	0.032	0.087	0.000	0.048	0.000	0.000	0.003	0.076	0.414	C1	Zircon	P4
5	0.1000	0.043	0.027	0.075	0.374	0.024	0.000	0.000	0.500	0.266	0.000	0.086	0.019	0.000	0.057	1.471	C1	UNKNOWN	P1
6	0.1699	0.000	0.071	0.194	0.322	0.048	0.000	0.000	0.318	0.340	0.000	0.040	0.041	0.008	0.000	1.382	C1	UNKNOWN	P2
7	0.1606	0.112	0.065	0.028	0.404	0.077	0.083	0.000	0.349	0.392	0.000	0.100	0.047	0.000	0.079	1.736	C1	UNKNOWN	P3

Sample: RJBO/BRS-26 (SYENITE)

No.	Displacement	Pr2O3	Nd2O3	Gd2O3	Yb2O3	Lu2O3	Ho2O3	Tb2O3	Er2O3	Dy2O3	La2O3	Ce2O3	Sm2O3	Eu2O3	Tm2O3	Total	Comment	Type	P
1	0	0.073	0.042	0	0	0.097	0.057	0.039	0.243	0.044	0.045	0.027	0.019	0	0.057	0.743	C1	Zircon	P1
2	0.0178	0.007	0	0	0.018	0.002	0	0.098	0	0	0.045	0	0	0.013	0	0.183	C1	Zircon	P2
3	0.7734	0.03	0.087	0	0	0.061	0.053	0	0	0	0.023	0.047	0	0	0	0.301	C1	Zircon	P3
4	0.7806	0	0	0.072	0	0	0	0.109	0	0	0	0	0	0.035	0.057	0.273	C1	Zircon	P4

Sample: RJB-04(50mts) (SYENITE)

No.	Displacement	Pr2O3	Nd2O3	Gd2O3	Yb2O3	Lu2O3	Ho2O3	Tb2O3	Er2O3	Dy2O3	La2O3	Ce2O3	Sm2O3	Eu2O3	Tm2O3	Total	Comment	Type	P
1	0	0	0	0.026	0.016	0.026	0	0	0.006	0	0	0	0.026	0	0	0.1	C1	UNKNOWN	P1
2	0.0529	0.014	0.01	0.039	0.078	0.037	0	0.032	0.085	0.105	0	0	0.01	0	0.036	0.446	C1	UNKNOWN	P2
3	0.0894	0	0	0.015	0	0	0	0.103	0.057	0.194	0	0.046	0	0	0	0.415	C1	UNKNOWN	P3
4	0.1061	0.007	0.01	0.056	0	0.06	0	0.083	0	0.099	0	0	0.007	0	0.014	0.336	C1	UNKNOWN	P4
5	0.1352	0.015	0.013	0	0.061	0	0.021	0	0	0	0	0	0	0.044	0.092	0.246	C1	Zrn	P5
6	0.1123	0.007	0.042	0.079	0.007	0.158	0	0.141	0.063	0.156	0	0.055	0.005	0.013	0.046	0.772	C1	Zrn	P6
7	3.1257	0.084	0	0	0	0.124	0	0.122	0.058	0.038	0	0	0.07	0.013	0	0.509	C1	Zrn	P7
8	3.1351	0.014	0	0.053	0	0.073	0.154	0.083	0	0	0	0.029	0	0	0	0.406	C1	Zrn	P8
9	3.1483	0	0.004	0	0	0	0	0	0.209	0	0.02	0.062	0	0.012	0	0.307	C1	Zrn	P9

Sample: RJB-01(75mts) (AMPHIBOLITE)

No.	Displacement	S	Fe	Co	Ni	Cu		Zn	As	Pb	Total	Comment	Type	P
1	0.0000	33.705	28.125	0.050	0.044	33.453		0.021	0.000	0.400	95.798	C1	CHALCOPYRITE	P1
2	0.0030	33.591	28.840	0.074	0.000	32.955		0.091	0.000	0.376	95.927	C1	CHALCOPYRITE	P2
3	0.1354	33.020	27.760	0.111	0.053	32.204		0.000	0.000	0.273	93.421	C1	CHALCOPYRITE	P3
4	0.2028	51.284	42.829	1.740	0.000	0.000		0.000	0.000	0.579	96.432	C1	PYRITE	P4
5	0.4291	32.918	28.123	0.030	0.000	31.666		0.002	0.000	0.414	93.153	C1	CHALCOPYRITE	P5
6	0.4136	32.769	28.425	0.070	0.000	32.650		0.091	0.000	0.387	94.392	C1	CHALCOPYRITE	P6
7	0.3808	33.113	28.049	0.070	0.000	33.158		0.000	0.000	0.404	94.794	C1	CHALCOPYRITE	P7
8	0.3797	49.926	42.411	0.700	0.022	0.134		0.000	0.000	0.553	93.746	C1	PYRITE	P8
9	0.4056	32.878	28.302	0.078	0.000	33.305		0.000	0.000	0.311	94.874	C1	CHALCOPYRITE	P9
10	0.4077	33.260	28.624	0.084	0.000	32.296		0.000	0.102	0.349	94.715	C1	CHALCOPYRITE	P10
11	0.4575	52.659	43.007	0.564	0.035	0.000		0.000	0.032	0.536	96.833	C1	PYRITE	P11
12	0.5319	31.967	28.637	0.056	0.008	32.568		0.015	0.053	0.325	93.629	C1	CHALCOPYRITE	P12
13	0.4812	33.332	28.476	0.093	0.042	32.850		0.000	0.000	0.494	95.287	C1	CHALCOPYRITE	P13
14	0.4694	33.603	28.904	0.091	0.000	33.585		0.000	0.000	0.418	96.601	C1	CHALCOPYRITE	P14
15	3.7985	52.622	43.897	0.474	0.000	0.010		0.000	0.000	0.653	97.656	C1	PYRITE	P15
16	3.8900	51.703	43.019	0.549	0.000	0.000		0.000	0.021	0.522	95.814	C1	PYRITE	P16
17	3.8766	52.501	42.121	3.103	0.000	0.003		0.025	0.000	0.519	98.272	C1	PYRITE	P17
18	2.5743	52.660	44.100	0.281	0.000	0.050		0.045	0.000	0.476	97.612	C1	PYRITE	P18
19	2.9006	52.746	43.901	0.225	0.016	0.022		0.000	0.014	0.496	97.420	C1	PYRITE	P19
20	3.6292	0.000	63.455	0.113	0.032	0.000		0.020	0.094	0.017	63.731	C1	MAGNETITE	P20
21	3.8019	0.000	0.139	0.000	0.020	0.000		0.020	0.000	0.007	0.186	C1	BADPOINT	P21
22	3.7872	0.001	61.632	0.071	0.002	0.062		0.000	0.000	0.000	61.768	C1	MAGNETITE	P22
23	3.7980	0.012	63.318	0.116	0.000	0.000		0.000	0.004	0.000	63.450	C1	MAGNETITE	P23

23.6 Annexure VI- Whole Rock Analyses

Annexure VI: Details of Whole Rock Analysis in Borana Block, Bhilwara District, Rajasthan															
Sr. No	Sample no.	Rock type	SiO2	Al2O3	CaO	Cr2O3	Fe2O3	K2O	MgO	MnO	Na2O	P2O5	SO3	TiO2	V2O5	LOI
1	RJBO/BRS24/2024-25	Migmatite Gneiss	70.34	13.12	1.87	<0.05	4.16	6.12	0.23	<0.05	2.34	<0.05	<0.05	0.32	<0.05	1.28
2	RJBO/BRS36/2024-25	Migmatite Gneiss	69.25	13.64	1.75	<0.05	4.70	5.95	0.40	<0.05	2.25	0.13	<0.05	0.45	<0.05	1.26
3	RJBO/BRS93/2024-25	Migmatite Gneiss	74.01	12.19	2.93	<0.05	4.09	1.24	0.29	<0.05	3.76	0.09	<0.05	0.37	<0.05	0.86
4	RJBO-04/CS-11	Migmatite Gneiss	66.54	14.96	2.78	<0.05	4.91	5.48	0.32	<0.05	2.86	0.06	<0.05	0.63	<0.05	1.25
5	RJBO/BRS25/2024-25	Syenite	61.97	16.48	10.51	<0.05	6.48	0.11	0.14	<0.05	2.43	0.10	<0.05	0.45	<0.05	1.12
6	RJBO/BRS26/2024-25	Syenite	69.55	13.30	2.18	<0.05	4.63	5.79	0.32	<0.05	2.24	0.12	<0.05	0.44	<0.05	1.20
7	RJBO/BRS107/2024-25	Syenite	68.05	14.90	4.89	<0.05	2.10	6.78	<0.05	<0.05	1.44	0.11	<0.05	0.38	<0.05	1.05
8	RJB0-01/CS-14	Syenite	64.49	14.83	2.16	<0.05	7.19	5,76	0.56	<0.05	2.86	0.13	<0.05	0.64	<0.05	1.09
9	RJBO/BRS07/2024-25	Amphibolite	48.61	14.60	12.03	<0.05	13.76	0.37	6.19	0.16	1.92	0.08	<0.05	1.14	<0.05	0.97
10	RJBO/BRS11/2024-25	Pegmatite	74.34	14.55	2.36	<0.05	1.02	3.23	0.08	<0.05	3.53	<0.05	<0.05	<0.05	<0.05	0.71

* All the values are in %

23.7 Annexure VII- Details of 34 Trace Elemental Analyses in Borana Block, Bhilwara District, Rajasthan

Sr. No.	ROCK ID	ROCK NAME	Trace Elements															
			Ag	As	B	Ba	Be	Bi	Co	Cd	Cr	Cs	Cu	Ga	Ge	Hf	Li	In	Mn
1	BRS-61	SYENITE	<1	7	<5	1084	3.35	<0.5	1.68	<0.5	177	<0.5	<5	31.87	<0.5	1.67	<0.5	<0.5	220
2	BRS-03	SENITE	<1	16	<5	39	1.94	0.81	2.01	<0.5	34	<0.5	<5	45.63	0.82	1.22	<0.5	<0.5	569
3	BRS-53	SYENITE	<1	6	<5	294	1.38	<0.5	0.52	<0.5	86	<0.5	<5	27.20	<0.5	1.64	<0.5	<0.5	122
4	T1-9	SYENITE	<1	21	<5	340	2.79	1.02	2.73	<0.5	110	0.58	11	26.25	0.87	1.21	<0.5	<0.5	287
5	T2-6	SENITE	<1	9	<5	649	2.52	<0.5	4.21	<0.5	<10	<0.5	<5	20.71	<0.5	1.37	<0.5	<0.5	235
6	T5-29	SYENITE	<1	9	<5	980	3.72	<0.5	4.35	<0.5	84	2.70	<5	26.81	0.63	1.41	7.14	<0.5	448
7	G3051-14	SYENITE	<1	28	<5	778	3.21	1.24	4.86	<0.5	49	1.14	13	33.68	1.25	1.92	3.09	<0.5	384
8	G3051-08	SYENITE	<1	21	<5	281	2.73	1.15	2.83	<0.5	58	0.60	<5	27.27	0.83	1.46	2.84	<0.5	265
9	G3O51-202	SYENITE	<1	16	<5	236	3.93	<0.5	2.97	<0.5	<10	<0.5	<5	28.29	0.75	1.31	<0.5	<0.5	221
10	G3051-200	SYENITE	<1	14	<5	330	2.28	<0.5	1.57	<0.5	58	<0.5	<5	25.93	0.68	1.09	<0.5	<0.5	253
11	G3051-108	SYENITE	<1	9	<5	850	4.16	<0.5	3.11	<0.5	<10	1.36	<5	22.95	0.51	1.82	4.27	<0.5	351
12	BRS-105	MIGMATITE GNEISS	<1	17	<5	26	1.40	<0.5	1.56	<0.5	90	<0.5	<5	27.33	0.91	2.07	<0.5	<0.5	365
13	T2-13	MIGMATITE GNEISS	<1	6	<5	554	2.12	<0.5	7.29	<0.5	41	<0.5	<5	24.56	<0.5	1.41	2.76	<0.5	391

14	T3-14	MIGMATITE GNEISS	<1	11	<5	107	2.24	<0.5	6.15	<0.5	88	<0.5	<5	25.86	0.60	2.25	<0.5	<0.5	432
15	T4-19	MIGMATITE GNEISS	<1	7	<5	109	1.60	<0.5	5.12	<0.5	<10	<0.5	<5	17.23	<0.5	1.96	1.83	<0.5	331
16	G3051-186	MIGMATITE GNEISS	<1	29	<5	346	3.65	<0.5	3.87	<0.5	65	1.40	<5	31.58	1.09	1.03	1.49	<0.5	367
17	G3051-140	MIGMATITE GNEISS	<1	19	<5	1036	3.10	1.24	4.64	<0.5	56	1.44	<5	28.22	0.95	1.20	12.80	<0.5	604
18	G3051-139	MIGMATITE GNEISS	<1	18	<5	767	3.06	<0.5	5.20	<0.5	<10	1.11	<5	30.21	1.03	2.71	15.58	<0.5	566
19	G3051-30	AMPHIBOLITE	<1	<5	<5	24	<0.5	<0.5	43.09	<0.5	46	<0.5	163	16.26	<0.5	0.96	6.83	<0.5	1580
20	BRS-08	PEGMATITE	<1	<5	<5	<5	<0.5	1.43	0.67	<0.5	302	<0.5	<5	<0.5	<0.5	<0.5	<0.5	<0.5	<100

Sr. No.	ROCK ID	ROCK NAME	Trace Elements															
			Mo	Nb	Ni	Pb	Re	Rb	Sb	Se	Sn	Sr	Ta	Te	Tl	V	W	Zn	Zr
1	BRS-61	SYENITE	0.63	35.53	<5	13	<0.5	188.75	<0.5	2.61	3.17	264	4.37	<0.5	<0.5	17	0.78	<5	105
2	BRS-03	SENITE	<0.5	56.81	<5	30	<0.5	65.81	<0.5	3.70	1.57	590	6.33	<0.5	<0.5	16	<0.5	<5	119
3	BRS-53	SYENITE	0.55	21.60	<5	19	<0.5	141.81	<0.5	1.53	0.71	437	2.44	<0.5	<0.5	6	<0.5	<5	101
4	T1-9	SYENITE	1.72	41.43	<5	26	<0.5	220.03	<0.5	3.80	<0.5	127	3.46	<0.5	<0.5	7	<0.5	20	104
5	T2-6	SENITE	<0.5	51.72	<5	<5	<0.5	193.91	<0.5	3.50	1.09	162	5.59	<0.5	<0.5	21	<0.5	8	44

6	T5-29	SYENITE	0.76	57.00	<5	41	<0.5	154.09	<0.5	2.92	4.52	122	4.73	<0.5	<0.5	13	<0.5	41	233
7	G3051-14	SYENITE	3.59	57.19	<5	37	<0.5	104.54	<0.5	5.45	2.50	157	5.14	<0.5	<0.5	21	<0.5	48	105
8	G3051-08	SYRNITE	1.06	50.07	<5	24	<0.5	113.91	<0.5	3.22	3.08	139	6.69	<0.5	<0.5	9	<0.5	23	156
9	G3O51-202	SYENITE	2.92	50.57	<5	13	<0.5	119.52	<0.5	3.83	0.85	226	7.01	<0.5	<0.5	7	<0.5	5	114
10	G3051-200	SYENITE	5.18	42.46	<5	12	<0.5	107.16	<0.5	3.21	2.65	348	4.82	<0.5	<0.5	9	<0.5	<5	136
11	G3051-108	SYENITE	3.34	53.87	<5	39	<0.5	125.16	<0.5	3.57	2.99	116	6.10	<0.5	<0.5	11	<0.5	40	138
12	BRS-105	MIGMATITE GNEISS	<0.5	89.45	<5	24	<0.5	11.28	<0.5	5.13	4.22	497	7.29	<0.5	<0.5	12	<0.5	<5	199
13	T2-13	MIGMATITE GNEISS	0.54	42.11	<5	8	<0.5	75.86	<0.5	2.67	2.49	317	4.46	<0.5	<0.5	41	<0.5	37	20
14	T3-14	MIGMATITE GNEISS	<0.5	72.59	<5	17	<0.5	52.35	<0.5	3.06	1.24	300	5.91	<0.5	<0.5	11	<0.5	45	357
15	T4-19	MIGMATITE GNEISS	0.99	48.39	<5	8	<0.5	43.90	<0.5	2.54	1.31	243	3.60	<0.5	<0.5	14	<0.5	35	114
16	G3051-186	MIGMATITE GNEISS	4.38	106.50	<5	37	<0.5	140.42	<0.5	3.54	2.59	120	5.98	<0.5	<0.5	12	0.56	37	206
17	G3051-140	MIGMATITE GNEISS	3.12	74.80	<5	27	<0.5	132.67	<0.5	4.79	<0.5	127	5.78	<0.5	<0.5	18	0.51	56	153
18	G3051-139	MIGMATITE GNEISS	2.16	74.31	<5	16	<0.5	225.48	<0.5	5.11	0.76	156	5.07	<0.5	<0.5	17	<0.5	53	146
19	G3051-30	AMPHIBOLITE	<0.5	0.81	61	<5	<0.5	9.31	<0.5	0.58	<0.5	111	<0.5	<0.5	<0.5	290	<0.5	87	7
20	BRS-08	PEGMATITE	0.85	<5	<5	<5	<0.5	1.11	<0.5	<0.5	<0.5	<5	<0.5	<0.5	<0.5	<5	<0.5	<5	<5

* All the values are in ppm

23.8 Annexure VIII- REE Analysis

23.8.1 Details of REE elemental analyses of BRS samples in Borana Block, Bhilwara District, Rajasthan

S.N.	Sample ID	Lithology	Lab Id	Sc	Y	La	Ce	Pr	Nd	Sm	Eu	Gd	Tb	Dy	Ho	Er	Tm	Yb	Lu	Th	U	ΣLREE	ΣHREE	ΣREE	Σ Th + U	Σ Sc + Y
1	RJBO/BRS-01/2024-25	SYENITE	G9187-1	2.1	78.6	482.97	839.44	73.08	211.66	26.79	1.64	21.86	2.32	13.89	2.74	8.42	1.15	7.89	1.09	134.99	6.13	1635.58	59.36	1694.94	141.12	80.7
2	RJBO/BRS-02/2024-25	SYENITE	G9187-2	1.98	79.58	545.29	930.02	81.56	237.08	29.99	1.62	23.99	2.79	14.98	2.85	7.96	1.07	6.85	0.96	201.13	7.19	1825.56	61.45	1887.01	208.32	81.56
3	RJBO/BRS-03/2024-25	SYENITE	G9187-3	3.45	125.53	719.58	1319.79	125.86	393.05	57.37	1.91	45.85	5.7	32.34	5.99	16.76	2.19	14.21	1.94	115.45	3.41	2617.56	124.98	2742.54	118.86	128.98
4	RJBO/BRS-04/2024-25	SYENITE	G9187-4	10.6	138.07	278.4	581	57.54	181.19	29.04	2.09	23.84	3.53	24.59	5.2	16.29	2.28	14.88	2.11	134.23	12.89	1129.26	92.72	1221.98	147.12	148.67
5	RJBO/BRS-05/2024-25	SYENITE/GNEISS	G9187-5	3.43	79.06	195.98	452.68	41.6	131.96	21.14	1.67	17.95	2.3	14.47	2.89	8.71	1.23	8.15	1.19	284.72	7.77	845.03	56.89	901.92	292.49	82.49
6	RJBO/BRS-06/2024-25	MIGMATITE GNEISS	G9187-6	13.27	58.81	121.56	259.07	28.45	102.39	18.16	3.91	16.45	2.05	12.64	2.42	6.84	0.96	5.98	0.86	28.85	1.96	533.54	48.2	581.74	30.81	72.08
7	RJBO/BRS-07/2024-25	AMPHIBOLITE	G9187-7	42.55	24.61	4.1	9.71	1.48	7.73	2.55	0.94	4.03	0	4.85	1.04	3.12	0	3.16	0	3.42	0	26.51	16.2	42.71	3.42	67.16
8	RJBO/BRS-08/2024-25	QUARTZ & FELDSPAR VEIN	G9187-8	0	1.06	1.49	2.85	0	0.7	0	0	0	0	0	0	0	0	0	0	0.58	0	5.04	0	5.04	0.58	1.06
9	RJBO/BRS-09/2024-25	MIGMATITE GNEISS	G9187-9	15.14	60.83	131.17	310.03	30.03	108.9	19.21	3.92	16.36	2.25	12.96	2.49	7.03	0.92	6.03	0.84	23.65	1.78	603.26	48.88	652.14	25.43	75.97
10	RJBO/BRS-10/2024-25	MIGMATITE GNEISS	G9187-10	16.78	115.08	461.12	890.02	83.9	280.64	41.96	3.9	34.46	4.75	26.58	4.95	14.32	1.88	12.08	1.69	73.03	2.6	1761.54	100.71	1862.25	75.63	131.86
11	RJBO/BRS-11/2024-25	PEGMATITE	G9187-11	1.38	4.9	1.4	2.31	0	0.97	0	0	0.55	0	0.62	0	0.58	0	1.06	0	1.76	0.74	4.68	2.81	7.49	2.5	6.28
12	RJBO/BRS-12/2024-25	SYENITE	G9187-12	7.75	79.74	521.33	905.9	78.71	234.26	31.6	2.02	27.31	3.02	16.88	3.17	9.43	1.25	8.22	1.11	104.97	4.71	1773.82	70.39	1844.21	109.68	87.49

13	RJBO/BRS-13/2024-25	SYENITE	G9187-13	4.04	101.53	574.44	1035.58	93.24	285.68	40.76	2.39	32.22	4.01	20.6	3.91	11.11	1.48	9.84	1.36	358.75	9.03	2032.09	84.53	2116.62	367.78	105.57
14	RJBO/BRS-14/2024-25	MIGMATITE GNEISS	G9187-14	8.05	33.65	59.69	122.39	14.86	54.66	9.69	2.2	8.06	1.31	6.79	1.33	3.98	0.53	3.44	0	12.61	0.81	263.49	25.44	288.93	13.42	41.7
15	RJBO/BRS-15/2024-25	MIGMATITE GNEISS	G9187-15	17.22	108.8	160.29	411.2	44.65	169.81	32.25	3.86	26.67	3.95	23.68	4.49	12.69	1.77	11.37	1.6	39.48	2.97	822.06	86.22	908.28	42.45	126.02
16	RJBO/BRS-16/2024-25	MIGMATITE GNEISS	G9187-16	13.93	126.62	339.38	677.6	65.17	213.54	34.75	2.76	29.43	4.17	25.51	5.04	15.05	2.13	14.83	2.05	104.8	7.68	1333.2	98.21	1431.41	112.48	140.55
17	RJBO/BRS-17/2024-25	SYENITE	G9187-17	9.44	74.11	199.48	446.84	41.44	139.82	23.3	3.12	19.24	2.98	15.9	3.02	8.79	1.18	7.76	1.05	42.4	1.84	854	59.92	913.92	44.24	83.55
18	RJBO/BRS-18/2024-25	MIGMATITE GNEISS	G9187-18	11.46	98.23	192.32	458.22	43.58	148.03	26.28	2.72	21.55	3.32	19.07	3.81	11.56	1.67	11.55	1.53	73.29	3.12	871.15	74.06	945.21	76.41	109.69
19	RJBO/BRS-019/2024-25	SYENITE	G9187-19	3.06	81.69	518.44	917.77	83.43	251.47	35.09	2.01	26.54	3.52	16.29	2.93	8.57	1.12	7.3	1.1	323.94	10.81	1808.21	67.37	1875.58	334.75	84.75
20	RJBO/BRS-020/2024-25	SYENITE	G9187-20	3	94.51	603.26	1041.2	92.96	275.53	36.33	2.02	28.83	3.67	17.32	3.26	9.62	1.24	8.38	1.12	324.65	10.07	2051.3	73.44	2124.74	334.72	97.51
21	RJBO/BRS-21/2024-25	SYENITE	G9187-21	2.76	94.58	314.34	675.41	62.39	192.95	28.67	2.2	23.1	3.18	18.14	3.62	11.2	1.61	11.8	1.64	74.27	4.97	1275.96	74.29	1350.25	79.24	97.34
22	RJBO/BRS-22/2024-25	SYENITE	G9187-22	7.17	108.23	649.63	1090.36	95.96	286.66	38.91	2.44	32.29	3.96	21.98	4.29	12.52	1.75	11.79	1.61	128.03	5.76	2163.96	90.19	2254.15	133.79	115.4
23	RJBO/BRS-23/2024-25	MIGMATITE GNEISS	G9187-23	2.66	109.49	527.33	944.44	88.08	273.52	40.11	1.74	30.93	3.91	19.27	3.69	10.67	1.46	10.1	1.38	460.46	13.47	1875.22	81.41	1956.63	473.93	112.15
24	RJBO/BRS-24/2024-25	MIGMATITE GNEISS	G9187-24	3.48	86.76	598.72	1030.46	92.35	273.59	36.77	1.76	28.78	3.76	17.26	3.13	9.15	1.22	8.33	1.18	139.35	4.68	2033.65	72.81	2106.46	144.03	90.24
25	RJBO/BRS-25/2024-25	SYENITE	G9187-25	11.79	69.07	202.91	453.26	38.9	124.32	19.85	3.52	16.95	2.15	13.31	2.64	7.5	1.04	7.18	0.96	43.98	3.73	842.76	51.73	894.49	47.71	80.86
26	RJBO/BRS-26/2024-25	SYENITE	G9187-71	9.8	109.72	364.39	749.56	66.1	207.72	32.53	2.6	26.54	3.4	20.79	4.18	12.55	1.79	12.88	1.8	140.5	8.26	1422.9	83.93	1506.83	148.76	119.52
27	RJBO/BRS-27/2024-25	MIGMATITE GNEISS	G9187-72	10.62	105.17	261.19	599.56	55.56	173.38	27.12	2.38	23.05	3.33	20.04	3.93	11.91	1.67	11.73	1.64	139.06	5	1119.19	77.3	1196.49	144.06	115.79
28	RJBO/BRS-28/2024-25	MIGMATITE GNEISS	G9187-73	7.22	94.4	237.61	595.1	52.52	167.93	27.65	2.19	22.28	3.21	17.89	3.56	10.43	1.48	10.16	1.44	130.36	8.82	1083	70.45	1153.45	139.18	101.62

29	RJBO/BRS-29/2024-25	MIGMATITE GNEISS	G9187-74	6.38	80.01	226.52	548.54	48.76	152.59	23.91	2.21	19.42	2.86	15.57	3.1	9.53	1.4	9.76	1.32	244.3	20.52	1002.53	62.96	1065.49	264.82	86.39
30	RJBO/BRS-30/2024-25	SYENITE	G9187-75	9.2	89.85	416.96	830.15	75.08	235.66	37.25	2.24	29.24	3.85	19.47	3.49	9.6	1.23	8.6	1.19	201.34	4.71	1597.34	76.67	1674.01	206.05	99.05
31	RJBO/BRS-31/2024-25	MIGMATITE GNEISS	G9187-26	7.43	45.66	161.35	387.36	32.12	100.27	15.21	2.01	12.34	1.72	8.89	1.74	5.02	0.73	5.23	0.72	69.05	3.29	698.32	36.39	734.71	72.34	53.09
32	RJBO/BRS-32/2024-25	SYENITE	G9187-76	6.27	94.42	216.79	557.11	48.11	150.21	24.28	1.96	19.56	2.94	16.6	3.34	10.32	1.5	11.04	1.52	130.71	8.99	998.46	66.82	1065.28	139.7	100.69
33	RJBO/BRS-33/2024-25	MIGMATITE GNEISS	G9187-77	8.07	88.31	279.47	689.64	59.92	185.25	29.36	2	23.83	3.19	17.56	3.33	9.55	1.35	9.43	1.33	227.53	11.38	1245.64	69.57	1315.21	238.91	96.38
34	RJBO/BRS-34/2024-25	MIGMATITE GNEISS	G9187-78	7.36	125.52	461.12	896.55	75.75	227.88	32.16	2.22	27.09	3.47	20.17	4.25	13.87	2.25	17.46	2.48	196.82	10.53	1695.68	91.04	1786.72	207.35	132.88
35	RJBO/BRS-35/2024-25	MIGMATITE GNEISS	G9187-79	10.26	99.73	260.22	651.42	57.61	182.11	29.25	2.34	26.13	3.02	19.85	3.94	11.66	1.66	11	1.54	113.29	7.9	1182.95	78.8	1261.75	121.19	109.99
36	RJBO/BRS-36/2024-25	SYENITE	G9187-80	9.77	109.47	366.32	723.06	64.65	203.17	31.49	2.57	26.2	3.63	20.75	4.19	12.36	1.74	12.52	1.79	125.7	6.9	1391.26	83.18	1474.44	132.6	119.24
37	RJBO/BRS-37/2024-25	SYENITE	G9187-81	14.54	102.51	405.43	783.36	70.83	226.91	36.14	3.27	27.89	3.65	20.78	3.93	11.64	1.62	11.07	1.52	96.31	2.69	1525.94	82.1	1608.04	99	117.05
38	RJBO/BRS-38/2024-25	SYENITE	G9187-82	9.56	111.66	280.58	698.89	62.21	197.98	33.13	2.57	27.33	3.63	21.95	4.45	12.92	1.82	12.64	1.68	123.88	5.47	1275.36	86.42	1361.78	129.35	121.22
39	RJBO/BRS-39/2024-25	SYENITE	G9187-83	11.1	143.29	435.78	866.15	78.7	250.26	40.32	2.37	32.97	4.08	26.71	5.42	16.39	2.4	17.48	2.43	200.42	13.29	1673.58	107.88	1781.46	213.71	154.39
40	RJBO/BRS-040/2024-25	AMPHIBOLITE	G9187-27	7.07	75.13	520.74	908.89	80.15	240.9	32.72	2.37	26.87	3.42	16.01	3	8.59	1.05	7.32	0.99	117.23	3.94	1785.77	67.25	1853.02	121.17	82.2
41	RJBO/BRS-041/2024-25	SYENITE	G9187-28	7.79	83.38	672.96	1151.55	101.95	305.95	40.73	2.48	33.54	3.92	18.28	3.29	9.28	1.17	7.58	1.08	153	5.19	2275.62	78.14	2353.76	158.19	91.17
42	RJBO/BRS-042/2024-25	MIGMATITE GNEISS	G9187-29	6.38	80.82	499.54	869.57	75.7	226.14	31.18	1.97	25.12	3.28	16.64	3.15	9.28	1.25	8.33	1.12	101.8	5.19	1704.1	68.17	1772.27	106.99	87.2
43	RJBO/BRS-043/2024-25	MIGMATITE GNEISS	G9187-30	7.78	97.26	663.8	1126.81	100.54	299.36	39.9	2.38	32.16	4.24	20.95	3.87	11.31	1.49	9.97	1.37	134.82	3.66	2232.79	85.36	2318.15	138.48	105.04
44	RJBO/BRS-044/2024-25	MIGMATITE GNEISS	G9187-31	10.77	136.34	431.67	761.5	71.72	228.22	36.64	2.47	30.77	4.27	24.71	5.12	15.26	2.13	14.3	1.87	112.71	11.79	1532.22	98.43	1630.65	124.5	147.11

45	RJBO/BRS-045/2024-25	MIGMATITE GNEISS	G9187-32	4.91	62.73	132.62	317.01	30.14	100.31	18.45	1.68	14.96	2.14	12.21	2.46	6.86	0.9	6.11	0.85	111.59	7.85	600.21	46.49	646.7	119.44	67.64
46	RJBO/BRS-046/2024-25	SYENITE	G9187-33	7.35	100.29	265.72	594.03	55.86	179.83	31.04	2.26	25.74	3.72	19.97	3.82	10.34	1.27	8.47	1.14	118.58	4.1	1128.74	74.47	1203.21	122.68	107.64
47	RJBO/BRS-047/2024-25	MIGMATITE GNEISS	G9187-34	8.02	119.98	710.99	1183.45	108.36	325.07	44.63	2.37	36.8	4.41	24.91	4.66	14.08	1.93	13.45	1.81	137.7	5.22	2374.87	102.05	2476.92	142.92	128
48	RJBO/BRS-048/2024-25	SYENITE	G9187-35	4.46	75.36	416.41	695.43	62.7	186.83	25.45	1.61	20.46	2.56	13.45	2.69	8.35	1.21	8.95	1.19	105.45	4.52	1388.43	58.86	1447.29	109.97	79.82
49	RJBO/BRS-049/2024-25	MIGMATITE GNEISS	G9187-36	4.47	95.36	709.76	1256.83	109.92	327.58	43.72	2.05	34.23	4.06	19.39	3.64	10.29	1.32	9.29	1.2	213.59	5.57	2449.86	83.42	2533.28	219.16	99.83
50	RJBO/BRS-050/2024-25	MIGMATITE GNEISS	G9187-37	1.79	79.47	518.53	881.22	78.69	229.86	29.61	1.58	24.18	2.53	13.56	2.6	8.01	1.12	8.05	1.12	150.64	7.12	1739.49	61.17	1800.66	157.76	81.26
51	RJBO/BRS-051/2024-25	MIGMATITE GNEISS	G9187-38	2.46	75.51	295.59	651.5	60.3	184.77	27.71	1.63	21.41	2.69	14.99	2.86	8.5	1.16	8.05	1.1	171.22	6.01	1221.5	60.76	1282.26	177.23	77.97
52	RJBO/BRS-052/2024-25	MIGMATITE GNEISS	G9187-39	15.55	64.83	251.87	536.28	47.59	150.48	22.22	2.06	18.76	2.23	13.95	2.66	7.98	1.03	7.05	0.91	51.44	2.01	1010.5	54.57	1065.07	53.45	80.38
53	RJBO/BRS-053/2024-25	MIGMATITE GNEISS	G9187-40	8.99	64.22	441.14	756.59	65.39	199.39	26.91	2.62	21.98	2.82	14.32	2.7	7.65	0.99	6.49	0.89	69.43	2.19	1492.04	57.84	1549.88	71.62	73.21
54	RJBO/BRS-054/2024-25	SYENITE	G9187-41	8.54	95.79	292.57	640.37	60.16	190.37	30.47	2.42	24.69	3.36	18.32	3.69	11.04	1.53	11.06	1.54	141.57	9.46	1216.36	75.23	1291.59	151.03	104.33
55	RJBO/BRS-055/2024-25	SYENITE CONTACT	G9187-42	10.04	151.44	519.35	961.09	92.61	298.1	47.43	3	39.13	5.08	30.33	6.08	17.65	2.54	18.2	2.55	132.91	7.91	1921.58	121.56	2043.14	140.82	161.48
56	RJBO/BRS-056/2024-25	SYENITE CONTACT	G9187-43	10.82	89.35	217.1	493.18	45.56	148.14	23.88	2.42	19.98	2.52	16.63	3.35	10.2	1.46	10.17	1.4	97.14	5.79	930.28	65.71	995.99	102.93	100.17
57	RJBO/BRS-057/2024-25	MIGMATITE	G9187-44	2.44	83.33	440.63	785.68	69.15	207.3	28.1	2.16	24.89	3	15.83	3.08	8.85	1.22	8.34	1.09	121.7	4.98	1533.02	66.3	1599.32	126.68	85.77
58	RJBO/BRS-058/2024-25	MIGMATITE	G9187-45	8.55	101.29	442.68	763	68.6	209.47	30.37	2.03	25.36	3.15	18.47	3.86	11.97	1.65	10.95	1.51	95.07	7.1	1516.15	76.92	1593.07	102.17	109.84
59	RJBO/BRS-059/2024-25	MIGMATITE	G9187-46	12.17	125.99	402.74	763.62	70.7	229.11	39.61	2.59	32.12	4.62	26.06	4.98	14	1.94	13.51	1.86	113.6	10.38	1508.37	99.09	1607.46	123.98	138.16
60	RJBO/BRS-060/2024-25	SYENITE	G9187-47	10.67	108.69	472.12	852.44	78.31	248.76	38.14	2.98	32.9	4.18	23.14	4.32	12.28	1.63	11	1.47	238.78	9.77	1692.75	90.92	1783.67	248.55	119.36

61	RJBO/BRS-61/2024-25	SYENITE	G9187-48	7.44	110.61	835.53	1467.75	127.71	382.11	51.93	2.54	40.85	5.03	24.97	4.63	13	1.71	11.75	1.54	225.09	5.68	2867.57	103.48	2971.05	230.77	118.05
62	RJBO/BRS-62/2024-25	MIGMATITE GNEISS	G9187-49	5.48	111.06	642.2	1145.97	101.66	307.19	43.08	2.1	34.89	4.2	21.55	4.14	12.05	1.64	11.51	1.56	287.07	8.7	2242.2	91.54	2333.74	295.77	116.54
63	RJBO/BRS-63/2024-25	MIGMATITE GNEISS	G9187-50	6.28	85.69	634.46	1061.19	95.65	280.76	38.86	2.39	32.19	3.72	19.56	3.54	10.12	1.27	8.6	1.14	136.99	3.72	2113.31	80.14	2193.45	140.71	91.97
64	RJBO/BRS-64/2024-25	MIGMATITE GNEISS	G9187-51	3.83	45.65	211.55	495.72	41.68	125.46	17.37	1.52	15.56	1.8	9.46	1.79	5.14	0.73	5.16	0.72	68.38	2.84	893.3	40.36	933.66	71.22	49.48
65	RJBO/BRS-65/2024-25	SYENITE	G9187-52	5.38	93.98	573.88	1082.25	94.21	279.4	38.25	1.92	30.32	3.71	19.91	3.61	10.79	1.47	9.72	1.31	214.99	6.49	2069.91	80.84	2150.75	221.48	99.36
66	RJBO/BRS-66/2024-25	MIGMATITE GNEISS	G9187-53	5.59	85.88	549.47	1033.95	91.01	266.24	36.17	1.81	29.85	3.4	18.45	3.46	10.06	1.4	9.43	1.25	143.6	5.1	1978.65	77.3	2055.95	148.7	91.47
67	RJBO/BRS-67/2024-25	MIGMATITE GNEISS	G9187-54	10.04	143.69	652.06	1236.45	105.37	307.43	41.07	2.44	33.71	4.04	24.23	5.17	16.01	2.4	17.39	2.42	166.32	16.17	2344.82	105.37	2450.19	182.49	153.73
68	RJBO/BRS-68/2024-25	MIGMATITE GNEISS	G9187-55	6.67	93.51	443.53	857.12	73.26	218.17	30.85	1.76	25.06	3.32	19.56	3.83	11.62	1.67	11.93	1.64	92.92	4.2	1624.69	78.63	1703.32	97.12	100.18
69	RJBO/BRS-69/2024-25	MIGMATITE GNEISS	G9187-56	12.33	78.3	218.57	560.12	47.5	147.73	23.68	2.03	19.18	2.66	14.64	2.78	8.45	1.19	8.19	1.18	104.06	5.6	999.63	58.27	1057.9	109.66	90.63
70	RJBO/BRS-70/2024-25	MIGMATITE GNEISS	G9187-57	2.81	75.42	236.06	613.33	54.5	168.95	24.77	1.71	20.27	2.84	16.47	3.34	9.79	1.35	9.46	1.27	59.14	3.96	1099.32	64.79	1164.11	63.1	78.23
71	RJBO/BRS-71/2024-25	SYENITE	G9187-58	4.41	71.85	427.79	784.13	66.13	191.93	25.59	1.32	20.51	2.66	14.36	2.81	8.41	1.21	8.16	1.16	89.57	2.53	1496.89	59.28	1556.17	92.1	76.26
72	RJBO/BRS-72/2024-25	SYENITE	G9187-59	2.96	44.43	66.43	144.81	15.14	49.39	8.75	1.07	7.1	1.28	7.43	1.55	4.81	0.7	4.65	0.65	92.17	4.86	285.59	28.17	313.76	97.03	47.39
73	RJBO/BRS-73/2024-25	SYENITE	G9187-60	10.43	105.77	240.66	601.81	55.24	180.43	30.08	2.68	24.6	3.71	20.58	4.09	12.13	1.73	11.83	1.65	105.08	3.9	1110.9	80.32	1191.22	108.98	116.2
74	RJBO/BRS-74/2024-25	SYENITE	G9187-61	10.47	104.39	283.13	701.41	63.12	201.54	32.05	2.87	25.9	3.49	20.28	4.03	11.73	1.7	11.8	1.65	128.62	6.25	1284.12	80.58	1364.7	134.87	114.86
75	RJBO/BRS-75/2024-25	SYENITE	G9187-62	9.21	86.49	218.14	563.53	48.85	155.32	25.15	2.33	20.66	2.76	16.48	3.3	9.85	1.44	10.13	1.37	109.85	5.74	1013.32	65.99	1079.31	115.59	95.7
76	RJBO/BRS-76/2024-25	SYENITE	G9187-63	8.13	125.2	404.36	796.9	72.43	231.23	36.79	2.44	30.27	4.11	23.66	4.63	13.62	1.87	12.87	1.74	203.43	10.17	1544.15	92.77	1636.92	213.6	133.33

77	RJBO/BRS-77/2024-25	SYENITE	G9187-64	7.39	108.23	269.05	654.07	59.58	189.03	30.29	2.11	26.64	3.48	20.84	4.02	11.73	1.62	11.16	1.51	189.09	10.43	1204.13	81	1285.13	199.52	115.62
78	RJBO/BRS-78/2024-25	SYENITE	G9187-65	5.41	95.22	220.97	543.44	47.39	149.88	23.36	1.73	19.63	2.71	17.16	3.47	10.99	1.66	12.07	1.64	133.02	8.94	986.77	69.33	1056.1	141.96	100.63
79	RJBO/BRS-79/2024-25	SYENITE	G9187-66	7.72	113.51	263.68	646.83	58.01	182.85	29.37	2.12	23.91	3.35	19.96	4	12.49	1.76	12.66	1.79	128.04	7.39	1182.86	79.92	1262.78	135.43	121.23
80	RJBO/BRS-80/2024-25	MIGMATITE GNEISS	G9187-67	3.32	101.39	552.74	1056.05	88.71	257.68	33.18	1.83	26.46	3.09	17.36	3.57	11.55	1.74	13.52	1.96	195.37	6.81	1990.19	79.25	2069.44	202.18	104.71
81	RJBO/BRS-81/2024-25	SYENITE	G9187-68	6.58	106.09	630.36	1161.45	99.67	294.72	39.91	2.13	31.96	4.06	21.72	4.21	12.36	1.7	12.02	1.58	131.2	4.43	2228.24	89.61	2317.85	135.63	112.67
82	RJBO/BRS-82/2024-25	SYENITE	G9187-69	3.42	83.58	505.19	957.99	86.74	260.54	36.82	2.04	28.36	3.02	16.25	2.9	8.37	1.15	7.71	1.13	329.28	9.02	1849.32	68.89	1918.21	338.3	87
83	RJBO/BRS-83/2024-25	SYENITE	G9187-70	7.72	105.82	319.84	729	65.44	201.96	31.19	2.47	25.65	3.41	20.83	4.05	12.51	1.82	12.16	1.69	204.41	8.09	1349.9	82.12	1432.02	212.5	113.54
84	RJBO/BRS-84/2024-25	MIGMATITE GNEISS	G9187-84	2.46	81.25	440.35	880.31	74.82	220.03	29.56	1.36	23.51	2.85	14.58	2.79	8.27	1.07	7.26	0.96	414.26	12.37	1646.43	61.29	1707.72	426.63	83.71
85	RJBO/BRS-85/2024-25	MIGMATITE GNEISS	G9187-85	11.6	75.28	215.13	561.52	53.37	181.33	28.34	3.59	22.42	2.92	16.41	3.06	8.59	1.05	7.07	0.93	49.42	1.7	1043.28	62.45	1105.73	51.12	86.88
86	RJBO/BRS-86/2024-25	MIGMATITE GNEISS	G9187-86	7.04	36.04	128.92	322.98	27.63	89.08	13.61	1.49	12.55	1.46	7.61	1.47	4.13	0.54	4.35	0.52	33.2	0.84	583.71	32.63	616.34	34.04	43.08
87	RJBO/BRS-87/2024-25	MIGMATITE GNEISS	G9187-87	10.25	73.68	260.13	600.96	53.81	169.75	25.23	2.75	20.65	2.68	14.92	2.86	8.35	1.12	7.79	1.06	59.51	2.52	1112.63	59.43	1172.06	62.03	83.93
88	RJBO/BRS-88/2024-25	SYENITE	G9187-88	5.21	67.91	280.65	647	55.81	163.43	22.9	1.47	22.3	2.26	12.95	2.59	7.79	1.16	7.94	1.06	84.22	4.76	1171.26	58.05	1229.31	88.98	73.12
89	RJBO/BRS-89/2024-25	SYENITE	G9187-89	6.03	87.79	485.15	915.57	78.97	235.94	32.85	2.06	26.8	3.32	18.3	3.47	10.01	1.36	8.96	1.16	127.73	4.43	1750.54	73.38	1823.92	132.16	93.82
90	RJBO/BRS-90/2024-25	MIGMATITE GNEISS	G9187-90	5.51	71.64	139.1	349.33	31.19	101.98	17.08	1.74	14.11	1.86	13.18	2.73	8.98	1.36	10.09	1.34	70.35	8.39	640.42	53.65	694.07	78.74	77.15
91	RJBO/BRS-91/2024-25	MIGMATITE GNEISS	G9187-91	7.75	76.48	218.17	525.68	47.27	150.02	23.36	1.92	19.16	2.34	15.01	2.97	8.66	1.25	8.52	1.13	96.1	5.49	966.42	59.04	1025.46	101.59	84.23
92	RJBO/BRS-92/2024-25	MIGMATITE GNEISS	G9187-92	0.77	62.84	36.21	57.08	7.95	26.39	6.55	0.97	9.07	1.58	15.54	3.54	11.49	1.96	13.95	1.82	85.75	16.64	135.15	58.95	194.1	102.39	63.61

93	RJBO/BRS-93/2024-25	MIGMATITE GNEISS	G9187-93	9.57	92.83	263.87	652.06	58.33	182.99	30.41	2.03	25.01	3.01	17.95	3.53	9.95	1.4	9.59	1.28	120.28	6.51	1189.69	71.72	1261.41	126.79	102.4
94	RJBO/BRS-94/2024-25	MIGMATITE GNEISS	G9187-94	6.7	83.49	251.77	606.3	54.08	170.28	26.83	2.09	22.45	2.92	17.23	3.25	9.22	1.21	8.45	1.09	123.19	5.65	1111.35	65.82	1177.17	128.84	90.19
95	RJBO/BRS-95/2024-25	MIGMATITE GNEISS	G9187-95	8.37	95.77	234.62	584.95	51.82	161.85	26.41	2.24	21.28	2.89	17.19	3.55	10.9	1.59	11.24	1.53	122.01	10.34	1061.89	70.17	1132.06	132.35	104.14
96	RJBO/BRS-96/2024-25	MIGMATITE GNEISS	G9187-96	10.88	58.22	110.72	266.66	27.38	94.41	16.67	3.16	14.01	1.99	11.98	2.33	6.62	0.9	6.28	0.86	31.9	1.8	519	44.97	563.97	33.7	69.1
97	RJBO/BRS-97/2024-25	MIGMATITE GNEISS	G9187-97	10.21	72.78	252.82	588.64	50.78	157.23	23.71	2.55	19.53	2.41	14.84	2.93	8.59	1.2	8.81	1.29	52.2	3.04	1075.73	59.6	1135.33	55.24	82.99
98	RJBO/BRS-98/2024-25	MIGMATITE GNEISS	G9187-98	6.56	69.31	414.12	753.65	63.61	188.46	25.82	2.22	21.49	2.58	14.9	2.87	8.13	1.08	7.38	0.98	69.74	2.42	1447.88	59.41	1507.29	72.16	75.87
99	RJBO/BRS-99/2024-25	MIGMATITE GNEISS	G9187-99	8.25	40.37	49.1	119.61	14.75	56.91	10.78	1.85	9.89	1.87	8.39	1.62	4.66	0.61	3.86	0.58	7.76	1.11	253	31.48	284.48	8.87	48.62
100	RJBO/BRS-100/2024-25	MIGMATITE GNEISS	G9187-100	8	96.05	346.57	728.01	65.5	200.94	29.38	2.69	23.62	3.83	18.73	3.65	10.78	1.47	9.84	1.47	187.81	7.8	1373.09	73.39	1446.48	195.61	104.05
101	RJBO/BRS-101/2024-25	MIGMATITE GNEISS	G9187-101	10.49	89.05	310.4	726.9	63.45	199.6	30.16	2.76	25.31	3.27	17.77	3.37	10.32	1.49	10.48	1.48	200.71	10.78	1333.27	73.49	1406.76	211.49	99.54
102	RJBO/BRS-102/2024-25	MIGMATITE GNEISS	G9187-102	11.19	123.55	400.75	748.28	68.15	223.11	35.86	3.09	31.27	4.03	23.21	4.54	13.5	2	13.6	1.89	138.48	5.56	1479.24	94.04	1573.28	144.04	134.74
103	RJBO/BRS-103/2024-25	MIGMATITE GNEISS	G9187-103	11.72	113.77	395.44	706.02	65.34	211.19	32.52	2.88	28.96	3.99	21.47	4.27	13.03	1.89	14.16	1.87	114.19	4.48	1413.39	89.64	1503.03	118.67	125.49
104	RJBO/BRS-104/2024-25	MIGMATITE GNEISS	G9187-104	4.36	60.48	86.94	174.39	17.85	58.54	10.48	1.25	9.8	1.63	9.87	2.09	7.1	1.22	9.25	1.29	228.66	9.56	349.45	42.25	391.7	238.22	64.84
105	RJBO/BRS-105/2024-25	MIGMATITE GNEISS	G9187-105	22.58	247.43	734.59	1346.75	124.66	405.35	66.25	3.65	58.47	7.36	43.43	8.39	24.68	3.33	23.25	3.03	280.07	6.57	2681.25	171.94	2853.19	286.64	270.01
106	RJBO/BRS-106/2024-25	MIGMATITE GNEISS	G9187-106	8.16	114.06	304.94	695.8	61.82	194.9	30.32	2.36	27.05	3.44	20.89	4.05	12.51	1.86	13.33	1.87	199.29	10.92	1290.14	85	1375.14	210.21	122.22
107	RJBO/BRS-107/2024-25	SYENITE	G9187-107	7.97	96.74	235.49	563.49	48.29	156.49	24.95	2.16	21.82	2.72	17.85	3.66	11.09	1.62	11.16	1.59	122.64	6.32	1030.87	71.51	1102.38	128.96	104.71
108	RJBO/BRS-108/2024-25	SYENITE	G9187-108	6.94	78.87	165	395.55	33.53	109.69	17.08	1.57	15.29	1.86	13.01	2.83	9.28	1.42	10.48	1.49	98.06	7.51	722.42	55.66	778.08	105.57	85.81

23.8.2 Details of REE elemental analyses of Trench no 1 samples in Borana Block, Bhilwara District, Rajasthan

S.N.	SAMPLE ID	Lithology	Sc	Y	La	Ce	Pr	Nd	Sm	Eu	Gd	Tb	Dy	Ho	Er	Tm	Yb	Lu	Th	U	ΣLREE	ΣHREE	ΣREE	Σ Th + U	Σ Sc + Y
1	RJBO/T1-1/2024-25	SYENITE	7.31	92.98	328.63	565.97	58.67	187.59	26.8	1.98	26.48	3.24	16.3	3.31	10.78	1.59	10.93	1.72	85.21	3.15	1169.64	74.35	1243.99	88.36	100.29
2	RJBO/T1-2/2024-25	SYENITE	6.18	89.91	364.08	628.58	63.52	199.88	27.59	1.98	28.11	3.33	16.86	3.29	10.15	1.39	9.13	1.27	91.87	2.97	1285.63	73.53	1359.16	94.84	96.09
3	RJBO/T1-3/2024-25	SYENITE	7.06	92.6	427.67	739.12	73.55	230.17	31.34	2.17	31.67	3.68	17.91	3.43	10.63	1.4	9.01	1.28	92.85	3.64	1504.02	79.01	1583.03	96.49	99.66
4	RJBO/T1-4/2024-25	SYENITE	6.51	95.81	471.53	787.94	78.56	243.28	32.77	2.18	33.01	3.87	18.4	3.6	10.79	1.42	9.64	1.39	94.74	3.47	1616.26	82.12	1698.38	98.21	102.32
5	RJBO/T1-5/2024-25	SYENITE	5.19	90.21	512.53	852.58	83.64	257.56	33.87	1.97	33.65	3.92	18.05	3.45	10.41	1.31	8.66	1.17	102.21	3.05	1742.15	80.62	1822.77	105.26	95.4
6	RJBO/T1-6/2024-25	SYENITE	6.04	107.99	601.32	1031.07	98.91	299.15	39.57	2.16	40.05	4.67	21.63	4.11	12.51	1.62	10.55	1.44	124.74	3.48	2072.18	96.58	2168.76	128.22	114.03
7	RJBO/T1-7/2024-25	SYENITE	6.37	124.12	717.21	1213.36	118.38	361.31	46.43	2.2	47.16	5.32	24.92	4.82	14.31	1.85	11.33	1.63	143.59	2.96	2458.89	111.34	2570.23	146.55	130.49
8	RJBO/T1-8/2024-25	SYENITE	5.48	98.94	558.83	941.78	91.46	281.3	36.93	1.75	37	4.23	19.7	3.77	11.59	1.52	9.81	1.36	110.58	2.55	1912.05	88.98	2001.03	113.13	104.42
9	RJBO/T1-9/2024-25	SYENITE	5.93	124.89	735.64	1248.64	121.6	373.65	49.16	2.24	49.2	5.48	25.24	4.89	14.7	1.85	11.88	1.68	163.09	3.51	2530.93	114.92	2645.85	166.6	130.82
10	RJBO/T1-10/2024-25	SYENITE	5.57	109.39	608.88	1039.98	100.53	312.34	41.54	1.9	41.78	4.7	22.11	4.2	13.09	1.69	10.74	1.49	132.06	3.03	2105.17	99.8	2204.97	135.09	114.96
11	RJBO/T1-11/2024-25	SYENITE	5.21	98.3	553.4	941.74	92.02	283.97	37.7	1.81	38.49	4.28	19.87	3.81	11.7	1.56	10.05	1.41	127.07	3.55	1910.64	91.17	2001.81	130.62	103.51
12	RJBO/T1-12/2024-25	SYENITE	5.66	113.01	660.19	1126.17	110.13	338.66	44.81	2.1	44.22	5.03	23.38	4.39	13.38	1.7	11.23	1.57	154.48	4.37	2282.06	104.9	2386.96	158.85	118.67
13	RJBO/T1-13/2024-25	SYENITE	5.99	107.77	622.8	1037.72	100.93	308.6	40.81	1.76	41.15	4.77	22.44	4.3	13.16	1.66	10.77	1.52	128.1	3.32	2112.62	99.77	2212.39	131.42	113.76
14	RJBO/T1-14/2024-25	SYENITE	5.85	122.03	687.23	1100.58	111.18	341.33	44.47	2.08	44.71	5.04	23.94	4.58	13.88	1.83	12.34	1.72	137.71	3.59	2286.87	108.04	2394.91	141.3	127.88
15	RJBO/T1-15/2024-25	SYENITE	4.87	89.24	498.77	839.47	80.68	247.36	32.41	1.52	32.45	3.79	18.1	3.53	10.96	1.48	9.68	1.37	109.52	2.9	1700.21	81.36	1781.57	112.42	94.11
16	RJBO/T1-16/2024-25	SYENITE	5.55	91.62	489.79	833.15	79.86	245.76	32.31	1.55	32.68	3.88	18.74	3.68	11.12	1.43	9.65	1.38	101.17	2.55	1682.42	82.56	1764.98	103.72	97.17

17	RJBO/T1-17/2024-25	SYENITE	5.2	94.85	528.82	888.71	85.94	264.89	34.69	1.71	35.24	4.11	19.67	3.83	11.4	1.58	9.74	1.39	109.4	2.76	1804.76	86.96	1891.72	112.16	100.05
18	RJBO/T1-18/2024-25	SYENITE	4.84	94.98	505.14	869.36	81.96	253.31	33.72	1.67	33.53	3.9	18.74	3.66	11.21	1.54	9.91	1.46	108.79	3.16	1745.16	83.95	1829.11	111.95	99.82
19	RJBO/T1-19/2024-25	SYENITE	6.53	109.49	624.93	1098.75	104.57	321.88	42.4	2.13	43.36	4.93	22.91	4.3	13.49	1.69	11.03	1.61	144.95	3.82	2194.66	103.32	2297.98	148.77	116.02
20	RJBO/T1-20/2024-25	SYENITE	4.69	86.7	475.11	806.84	77.74	237.7	30.66	1.61	31.55	3.78	18.05	3.51	10.81	1.44	9.51	1.33	101.37	3.18	1629.66	79.98	1709.64	104.55	91.39

23.8.3 Details of REE elemental analyses of Trench no 2 samples in Borana Block, Bhilwara District, Rajasthan

S.N.	SAMPLE ID	Lithology	Sc	Y	La	Ce	Pr	Nd	Sm	Eu	Gd	Tb	Dy	Ho	Er	Tm	Yb	Lu	Th	U	ΣLREE	ΣHREE	ΣREE	Σ Th + U	Σ Sc + Y
1	RJBO/T2-1/2024-25	MIGMATITE	9.98	68.86	130.68	288.99	31.51	116.11	19.88	2.67	19.01	2.75	14.47	2.82	8.35	1.07	7.02	0.99	27.23	1.77	599.84	125.34	646.32	29	78.84
2	RJBO/T2-2/2024-25	SYENITE	12.78	81.47	174.31	475.9	37.43	127.64	20.49	2.54	21.3	3.01	16.28	3.33	10.09	1.45	9.18	1.28	46.24	2.59	851.09	147.4	904.23	48.883	94.25
3	RJBO/T2-3/2024-25	SYENITE	11.77	86.43	226.68	402.19	45.13	153.63	24.56	3.18	24.32	3.3	17.13	3.47	10.44	1.38	8.97	1.23	51.53	2.47	867.14	156.68	925.61	54	98.2
4	RJBO/T2-4/2024-25	SYENITE	9.38	72.67	265.42	453.12	47.76	156.58	23.43	3.15	23.72	3.01	15.17	2.98	8.98	1.15	7.6	1.07	50.54	2.27	958.84	136.34	1013.14	52.81	82.05
5	RJBO/T2-5/2024-25	SYENITE	12.08	85.35	295.63	516.98	53.57	180.22	27.59	3.7	27.79	3.59	18.49	3.59	10.52	1.39	9.14	1.26	56.24	2.92	1089.77	161.11	1153.46	59.16	97.43
6	RJBO/T2-6/2024-25	SYENITE	10.24	110.8	328.12	603.63	60.12	204.85	32.32	4.13	32.36	4.48	23.64	4.61	13.33	1.74	11.36	1.58	61.67	3.62	1243.41	203.91	1326.27	65.29	121.04
7	RJBO/T2-7/2024-25	MIGMATITE	8.24	80.47	235.07	415.2	43.32	146.9	22.98	2.88	22.93	3.08	15.87	3.24	9.67	1.36	8.86	1.33	46.39	2.58	874.58	146.82	932.69	48.97	88.71
8	RJBO/T2-8/2024-25	QUARTZ	2.82	24.82	70.98	108.33	12.92	43.02	6.51	0.81	6.67	0.96	5.06	0.99	2.87	0.5	2.71	0.5	12.58	1.04	245.4	45.08	262.83	13.62	27.64
9	RJBO/T2-9/2024-25	MIGMATITE	14.19	79.92	215.88	380.45	43.05	149.18	24.12	2.92	24.18	3.28	16.8	3.26	9.62	1.33	8.14	1.21	44.55	1.88	829.78	147.74	883.42	46.43	94.11
10	RJBO/T2-10/2024-25	MIGMATITE	13.06	89.56	255.74	485.47	50.3	176.92	28.99	3.51	27.87	3.72	18.58	3.62	10.73	1.43	9.32	1.33	55.68	2.44	1013.98	166.16	1077.53	58.12	102.62
11	RJBO/T2-11/2024-25	MIGMATITE	12.83	88.74	241.54	456.01	48.17	168.54	27.14	3.36	26.64	3.54	18.9	3.66	10.55	1.39	9.13	1.27	48.56	2.1	957.59	163.83	1019.84	50.66	101.57
12	RJBO/T2-12/2024-25	MIGMATITE	11.78	86.84	259.41	469.16	49.23	168.94	26.27	3.26	26.58	3.48	17.87	3.52	10.5	1.4	9.14	1.28	53.16	1.77	988.05	160.62	1050.04	54.93	98.62

13	RJBO/T2-13/2024-25	MIGMATITE	13.77	98.46	262.56	510.7	53.21	185.68	29.86	3.63	30.47	3.93	20.38	4.02	11.87	1.59	10.09	1.4	58.49	1.93	1059.42	182.22	1129.39	60.42	112.23
14	RJBO/T2-14/2024-25	MIGMATITE	10.8	58.93	156.29	269.59	31.8	112.76	18.67	2.3	18.1	2.34	12.81	2.47	7.42	0.98	6.32	0.93	29.03	1.31	602.23	110.3	642.78	30.34	69.73
15	RJBO/T2-15/2024-25	MIGMATITE	10.76	72.46	192.82	327.33	39.13	139.09	23.19	2.75	21.87	3.02	15.23	3.04	8.99	1.2	7.78	1.06	38.22	1.61	735.08	134.66	786.5	39.83	83.22
16	RJBO/T2-16/2024-25	MIGMATITE	12.01	82.66	195.37	351.96	40.13	141.44	24.15	2.91	23.65	3.32	17.27	3.41	10.09	1.4	9	1.24	39.92	1.99	767.97	152.04	825.34	41.91	94.67
17	RJBO/T2-17/2024-25	MIGMATITE	9.91	64.98	175.3	312.81	34.56	121.65	19.84	2.48	19.76	2.59	13.67	2.65	7.92	1.08	6.99	0.97	38.14	1.67	676.55	120.61	722.27	39.81	74.89
18	RJBO/T2-18/2024-25	MIGMATITE	12.88	94.84	212.59	378.41	41.5	145.11	24.66	3.03	24.7	3.62	19.17	3.77	11.44	1.55	9.74	1.33	44.07	2.06	818.18	170.17	880.62	46.13	107.72
19	RJBO/T2-19/2024-25	SYENITE/MIGMATITE	12.97	92.53	276.69	494.85	52.48	180.38	27.97	3.42	28.21	3.7	19.05	3.73	11.17	1.47	9.37	1.31	59.91	1.84	1048.76	170.53	1113.8	61.75	105.5
20	RJBO/T2-20/2024-25	SYENITE	14.28	101.75	301.26	586.15	55.87	200.04	31.43	3.87	31.46	4.24	21.49	4.14	12.1	1.61	10.26	1.44	68.1	2.46	1192.9	188.49	1265.36	70.56	116.03

23.8.4 Details of REE elemental analyses of Trench no 3 samples in Borana Block, Bhilwara District, Rajasthan

S.N.	SAMPLE ID	Lithology	Sc	Y	La	Ce	Pr	Nd	Sm	Eu	Gd	Tb	Dy	Ho	Er	Tm	Yb	Lu	Th	U	ΣLREE	ΣHREE	ΣTREE	Σ Th + U	Σ Sc + Y
1	RJBO/T3-1/2024-25	MIGMATITE	7.1	94.57	279.01	555.69	51.89	170.29	25.77	2.14	26.35	3.36	17.75	3.6	11.06	1.5	9.82	1.4	86.46	4.49	1084.79	74.84	1159.63	90.95	101.67
2	RJBO/T3-2/2024-25	MIGMATITE	8.22	92.92	310.62	645.6	59.32	194.5	29.5	2.23	28.29	3.56	18.35	3.56	10.81	1.49	9.4	1.32	108.87	4.87	1241.77	76.78	1318.55	113.74	101.14
3	RJBO/T3-3/2024-25	MIGMATITE	8.59	101.36	297.42	590.43	55.7	182.91	28.12	2.42	27.78	3.58	18.85	3.82	11.89	1.7	11.28	1.63	99.25	4.84	1157	80.53	1237.53	104.09	109.95
4	RJBO/T3-4/2024-25	MIGMATITE	9.78	102.22	371.61	738.98	69.83	230.42	34.23	2.52	34.41	4.16	20.33	3.98	12.29	1.67	10.77	1.55	124.38	6.03	1447.59	89.16	1536.75	130.41	112
5	RJBO/T3-5/2024-25	MIGMATITE	9.61	106.7	380.89	739.98	71.78	235.62	35.69	2.38	35.15	4.35	21.27	4.22	12.89	1.73	11.24	1.62	113.42	3.57	1466.34	92.47	1558.81	116.99	116.31
6	RJBO/T3-6/2024-25	MIGMATITE	7.88	110.37	379.25	749.29	71.71	233.21	35.06	2.5	34.17	4.26	21.53	4.28	13.02	1.82	11.99	1.68	118.71	4.59	1471.02	92.75	1563.77	123.3	118.25
7	RJBO/T3-7/2024-25	MIGMATITE	6.65	87.43	310.92	606.61	56.58	183.5	27.09	2.21	27.74	3.47	17.29	3.41	10.53	1.45	9.11	1.27	95.09	3.39	1186.91	74.27	1261.18	98.48	94.08
8	RJBO/T3-8/2024-25	MIGMATITE	5.33	57.07	218.96	407.56	40.64	131.22	19.85	1.52	19.66	2.41	12.01	2.3	6.94	0.86	5.57	0.78	70.01	2.76	819.75	50.53	870.28	72.77	62.4
9	RJBO/T3-9/2024-25	MIGMATITE	3.56	46.83	130.07	263.12	24.07	77.67	11.58	1.07	11.94	1.65	8.75	1.78	5.82	0.87	5.54	0.82	39.8	2.09	507.58	37.17	544.75	41.89	50.39
10	RJBO/T3-10/2024-25	MIGMATITE	7.74	103.05	446.57	804.09	77.43	249.6	38.88	2.95	38.51	4.73	22.92	4.22	12.68	1.58	9.81	1.3	126.24	4.62	1619.52	95.75	1715.27	130.86	110.79
11	RJBO/T3-11/2024-25	MIGMATITE	7.43	93.2	349.72	681.51	63.95	206.39	30.31	2.29	30.88	3.84	19.21	3.69	11.13	1.43	9.57	1.29	104.36	4	1334.17	81.04	1415.21	108.36	100.63
12	RJBO/T3-12/2024-25	MIGMATITE	6.76	86.5	246.03	445.53	45.47	149.27	23.35	1.78	23.57	3.1	16.89	3.42	10.77	1.52	9.74	1.48	75.03	4.35	911.43	70.49	981.92	79.38	93.26

13	RJBO/T3-13/2024-25	PEGMATITE/QUARTZ	10.84	132.35	435.09	766.58	75.94	249.48	37.82	3.45	36.88	4.81	24.74	5.01	15.64	2.21	14.57	2.09	120.57	6.65	1568.36	105.95	1674.31	127.22	143.19
14	RJBO/T3-14/2024-25	MIGMATITE	8.72	124.38	463.53	811.02	76.8	250.81	37.35	2.48	38.13	4.89	25.4	4.98	15.29	2.09	13.65	1.8	121.64	4.6	1641.99	106.23	1748.22	126.24	133.1
15	RJBO/T3-15/2024-25	MIGMATITE	4.92	101.12	361.11	695.03	66.37	215.34	32.5	2.12	32.05	4.05	20.09	3.94	11.98	1.7	10.87	1.55	109.43	4.42	1372.47	86.23	1458.7	113.85	106.04
16	RJBO/T3-16/2024-25	MIGMATITE	5.13	72.78	227.29	403.9	41.48	135.05	20.64	1.96	20.82	2.63	13.99	2.73	8.52	1.21	8.2	1.19	69.2	3.88	830.32	59.29	889.61	73.08	77.91
17	RJBO/T3-17/2024-25	MIGMATITE	7.3	91.3	308.72	614.35	56.21	181.36	26.82	2.07	27.76	3.51	17.27	3.52	10.95	1.45	9.29	1.32	99.66	4.44	1189.53	75.07	1264.6	104.1	98.6
18	RJBO/T3-18/2024-25	MIGMATITE	3.58	46.86	150.79	279.72	27.72	90.21	13.64	1.41	13.65	1.76	8.77	1.8	5.51	0.76	4.9	0.76	51.01	2.95	563.49	37.91	601.4	53.96	50.44
19	RJBO/T3-19/2024-25	MIGMATITE	5.06	60.19	259	506.62	48.88	157.95	23.96	2.33	22.69	2.76	12.77	2.35	6.91	0.84	5.43	0.79	100.72	4.64	998.74	54.54	1053.28	105.36	65.25
20	RJBO/T3-20/2024-25	MIGMATITE	5.69	80.75	338.67	671.95	63.51	207.49	31.3	2.56	29.68	3.58	17.11	3.2	9.37	1.2	7.41	1.07	120.32	5.42	1315.48	72.62	1388.1	125.74	86.44

23.8.5 Details of REE elemental analyses of Trench no 4 samples in Borana Block, Bhilwara District, Rajasthan

S.N.	SAMPLE ID	Lithology	Sc	Y	La	Ce	Pr	Nd	Sm	Eu	Gd	Tb	Dy	Ho	Er	Tm	Yb	Lu	Th	U	ΣLREE	ΣHREE	ΣTREE	Σ Th + U	Σ Sc + Y
1	RJBO/T4-1/2024-25	MG/SYN	8.65	106.12	232.86	454.02	45.81	154.12	24.89	2.48	25.17	3.49	19.06	4.04	12.56	1.84	11.67	1.67	88.96	3.64	914.18	79.5	993.68	92.6	114.77
2	RJBO/T4-2/2024-25	MIGMATITE	5.81	73.93	198.34	371.42	39.02	130.36	20.98	1.77	21.22	2.74	14.23	2.91	8.57	1.14	7.73	1.11	84.27	4.56	761.89	59.65	821.54	88.83	79.74
3	RJBO/T4-3/2024-25	MIGMATITE	6.61	75.08	194.55	363.56	38.16	128.12	20.16	1.6	20.87	2.81	14.94	2.96	8.75	1.2	7.98	1.11	76.05	4.04	746.15	60.62	806.77	80.09	81.69
4	RJBO/T4-4/2024-25	MIGMATITE	7.89	78.49	187.21	342.77	36.82	124.29	20.26	1.51	20.57	2.84	14.91	3.02	9.63	1.32	8.84	1.21	67.05	3.59	712.86	62.34	775.2	70.64	86.38
5	RJBO/T4-5/2024-25	MIGMATITE	7.35	78.4	190.76	346.58	37.47	124.37	20.17	1.71	20.6	2.83	14.62	2.96	9.48	1.34	9.03	1.31	81.66	3.4	721.06	62.17	783.23	85.06	85.75
6	RJBO/T4-6/2024-25	MG/SYN	7.16	85.85	204.29	376.33	39.79	132.97	21.35	1.93	21.18	2.86	15.71	3.22	10.11	1.49	10.1	1.41	78.03	3.47	776.66	66.08	842.74	81.5	93.01
7	RJBO/T4-7/2024-25	MIGMATITE	8.31	95.48	233.75	424.79	45.88	153.32	24.19	2.2	24.46	3.32	17.68	3.56	11.34	1.66	10.85	1.59	92.27	5.91	884.13	74.46	958.59	98.18	103.79
8	RJBO/T4-8/2024-25	MIGMATITE	9.01	91.68	255.02	511.56	48.62	164.81	26.54	2.32	26.39	3.53	18.2	3.67	11.4	1.62	10.89	1.6	96.32	5.37	1008.87	77.3	1086.17	101.69	100.69
9	RJBO/T4-9/2024-25	MIGMATITE	3.43	33.47	92.06	154.78	17.34	58.22	9.2	1.47	9.47	1.16	6.1	1.24	3.94	0.53	3.93	0.61	32.98	2.14	333.07	26.98	360.05	35.12	36.9
10	RJBO/T4-10/2024-25	MIGMATITE	9.13	95.63	282.46	483.05	53.6	176.08	27.73	3.96	28.45	3.59	18.68	3.72	11.34	1.45	10.09	1.5	95.63	4.49	1026.88	78.82	1105.7	100.12	104.76
11	RJBO/T4-11/2024-25	MIGMATITE	1.05	18.09	31.87	55.41	6.13	20.25	3.12	0.8	3.49	0.5	2.79	0.69	2.22	0.5	2.55	0.5	11.04	0.86	117.58	13.24	130.82	11.9	19.14

12	RJBO/T4-12/2024-25	MIGMATITE	9.6	90.94	245.24	437.19	46.6	152.74	24.4	3.04	24.98	3.18	16.93	3.47	10.74	1.4	10.54	1.58	81.99	3.95	909.21	72.82	982.03	85.94	100.54
13	RJBO/T4-13/2024-25	MIGMATITE	8.58	90.48	272.21	473.36	51.15	168.01	25.58	2.82	27.43	3.43	17.58	3.51	10.82	1.45	10	1.45	92.96	4.16	993.13	75.67	1068.8	97.12	99.06
14	RJBO/T4-14/2024-25	MIGMATITE	4.58	49.41	143.4	259.43	27.64	88.84	13.52	2.2	14.11	1.78	9.36	1.91	5.85	0.77	5.84	0.88	52.31	3.17	535.03	40.5	575.53	55.48	53.99
15	RJBO/T4-15/2024-25	MIGMATITE	11.12	106.03	289.73	510.05	55.39	182.39	28.98	3.81	29.99	4.07	20.6	4.19	12.66	1.6	11.14	1.65	98.26	4.04	1070.35	85.9	1156.25	102.3	117.15
16	RJBO/T4-16/2024-25	MIGMATITE	8.58	104.76	224.16	399.88	44.38	149.56	24.21	2.74	26.15	3.59	18.85	3.99	12.7	1.69	11.75	1.72	76.85	3.73	844.93	80.44	925.37	80.58	113.34
17	RJBO/T4-17/2024-25	MIGMATITE	2.09	36.66	51	94.07	10.23	33.43	6.09	1.06	6.35	0.99	5.89	1.33	4.62	0.68	5.68	0.83	21.82	1.24	195.88	26.37	222.25	23.06	38.75
18	RJBO/T4-18/2024-25	MIGMATITE	2.98	54.81	87.04	153.96	17.05	58.47	9.6	1.16	10.76	1.5	8.63	2.01	7.11	1.11	8.8	1.29	34.15	1.8	327.28	41.21	368.49	35.95	57.79
19	RJBO/T4-19/2024-25	MIGMATITE	9.87	129.12	279.46	491.37	54.2	181.04	29.99	2.49	32.18	4.37	23.45	4.94	15.58	1.99	14.62	2.05	93.67	4.49	1038.55	99.18	1137.73	98.16	138.99
20	RJBO/T4-20/2024-25	MIGMATITE	4.91	56.57	117.71	193.57	22.18	75.54	11.93	3.12	13.14	1.85	9.91	2.17	6.84	0.89	6.38	0.89	38.6	2.21	424.05	42.07	466.12	40.81	61.48

23.8.6 Details of REE elemental analyses of Trench no 5 samples in Borana Block, Bhilwara District, Rajasthan

S.N.	SAMPLE ID	Lithology	Sc	Y	La	Ce	Pr	Nd	Sm	Eu	Gd	Tb	Dy	Ho	Er	Tm	Yb	Lu	Th	U	ΣLREE	ΣHREE	ΣTREE	Σ Th + U	Σ Sc + Y
1	RJBO/T5-1/2024-25	MIGMATITE	10.91	96.43	236.48	457.21	46.1	156.37	25.61	3.72	26.99	3.53	18.55	3.74	11.53	1.46	10.56	1.57	70.75	4.46	925.49	77.93	1003.42	75.21	107.34
2	RJBO/T5-2/2024-25	MIGMATITE	9	72.74	171.63	412.07	33.53	110.97	18.07	3.01	20.05	2.54	13.82	2.86	9.02	1.12	8.19	1.2	55.41	3.58	749.28	58.8	808.08	58.99	81.74
3	RJBO/T5-3/2024-25	MIGMATITE	8.67	68.38	178.66	335.1	34.82	115.95	19.65	2.8	19.33	2.56	13.36	2.67	8.22	1.05	7.65	1.12	55.56	3.26	686.98	55.96	742.94	58.82	77.05
4	RJBO/T5-4/2024-25	MIGMATITE	9.32	77.27	167.78	340.71	33	110.58	18.2	2.96	19.92	2.74	14.47	2.98	9.29	1.21	9.02	1.31	53.61	4.02	673.23	60.94	734.17	57.63	86.59
5	RJBO/T5-5/2024-25	MIGMATITE	9.39	70.2	147.23	339.35	29.23	98.82	16.47	2.89	18.58	2.48	13.17	2.8	8.77	1.14	8.16	1.22	47.24	3.9	633.99	56.32	690.31	51.14	79.59
6	RJBO/T5-6/2024-25	MIGMATITE	8.39	70.02	135.32	302.5	27.22	91.83	15.61	3	17.38	2.37	13.29	2.81	8.82	1.18	8.49	1.3	44.76	4.68	575.48	55.64	631.12	49.44	78.41
7	RJBO/T5-7/2024-25	MIGMATITE	7.4	61.7	153.96	311.79	29.27	99.33	15.58	3.14	17.14	2.26	11.63	2.4	7.64	1	6.95	1.09	45	3.37	613.07	50.11	663.18	48.37	69.1
8	RJBO/T5-8/2024-25	MIGMATITE	3.05	23.55	59.26	134.65	11.47	38.41	5.85	1.69	6.66	0.83	4.45	0.88	2.8	0.5	2.68	0.5	16.26	1.11	251.33	19.3	270.63	17.37	26.6
9	RJBO/T5-9/2024-25	MIGMATITE	7	67.51	221.57	417.5	41.65	133.5	19.97	2.87	20.69	2.54	12.79	2.6	8.06	1.03	7.34	1.07	88.24	3.93	837.06	56.12	893.18	92.17	74.51
10	RJBO/T5-10/2024-25	MIGMATITE	5.89	78.92	215.61	392.1	40.74	133.16	20.32	2.8	21.2	2.78	14.44	2.98	9.74	1.29	9.38	1.35	89.35	4.91	804.73	63.16	867.89	94.26	84.81
11	RJBO/T5-11/2024-25	MIGMATITE	2.36	32.06	75.93	169.15	14.53	46.1	7.36	1.97	7.99	0.98	5.22	1.15	3.79	0.56	4.34	0.62	32.11	2.74	315.04	24.65	339.69	34.85	34.42

12	RJBO/T5-12/2024-25	MIGMATITE	5.76	64.23	201.88	402.84	37.88	122.89	18.8	2.49	19.87	2.43	12.18	2.39	7.77	1	7.28	1.06	78.02	3.1	786.78	53.98	840.76	81.12	69.99
13	RJBO/T5-13/2024-25	MIGMATITE	5.6	49.37	124.03	338.02	24.02	78.04	12.55	2.06	13.47	1.69	8.84	1.93	6.4	0.82	6.6	0.98	67.02	3.61	578.72	40.73	619.45	70.63	54.97
14	RJBO/T5-14/2024-25	MIGMATITE	7.29	73.74	225.16	521.49	43.76	142.6	21.35	2.57	22.84	2.79	14.02	2.88	9.27	1.23	9.01	1.3	99.74	3.97	956.93	63.34	1020.27	103.71	81.03
15	RJBO/T5-15/2024-25	MIGMATITE	8	84.16	265.05	522.42	51.41	164.13	24.67	3.06	25.95	3.2	15.84	3.2	10.22	1.36	9.82	1.47	106.2	5.16	1030.74	71.06	1101.8	111.36	92.16
16	RJBO/T5-16/2024-25	MIGMATITE	7.79	85.64	284.03	547.21	55.59	180.18	27.54	2.96	28.16	3.53	17.47	3.35	10.74	1.3	9.88	1.42	99.92	4.98	1097.51	75.85	1173.36	104.9	93.43
17	RJBO/T5-17/2024-25	MIGMATITE	8.03	84.36	268.63	514.47	51.78	164.86	25.65	2.87	26.58	3.26	16.43	3.19	10.51	1.37	9.54	1.34	131.89	8.37	1028.26	72.22	1100.48	140.26	92.39
18	RJBO/T5-18/2024-25	MIGMATITE	9.07	94.75	307.3	604.58	60.08	192.01	29.57	3.28	30.58	3.77	19.35	3.71	11.72	1.48	10	1.42	151.35	7.8	1196.82	82.03	1278.85	159.15	103.82
19	RJBO/T5-19/2024-25	MIGMATITE	8.37	85.31	265.58	522.47	51.49	162.57	24.87	3	25.31	3.19	16.92	3.34	10.9	1.48	10.33	1.44	121.58	5.8	1029.98	72.91	1102.89	127.38	93.68
20	RJBO/T5-20/2024-25	MIGMATITE	9.61	114.84	383.32	734.77	73.9	241.11	38.43	3.93	38.92	4.74	23.12	4.53	13.63	1.74	12.32	1.76	190.39	9.68	1475.46	100.76	1576.22	200.07	124.45

23.8.7 REE elemental analyses of Core samples, BH-1 in Borana Block, Bhilwara District, Rajasthan

From(m)	To (m)	Sample ID	Lithology	Sc	Y	La	Ce	Pr	Nd	Sm	Eu	Gd	Tb	Dy	Ho	Er	Tm	Yb	Lu	Th	U	ΣLREE	ΣHREE	ΣTREE	Σ Th + U	Σ Sc + Y
1	2	RJBO-01/CS-01	Syenite	5.14	79.74	361.83	667.75	47.64	178.41	24.17	1.54	19.68	2.98	13.99	2.32	10.2	1.25	9.23	1.11	7.27	2.58	1281.34	60.76	1342.1	9.85	84.88
3	4	RJBO-01/CS-02	Syenite	5.26	81.6	372.39	701.61	49.3	188.63	24.82	1.6	20.3	3	14.42	2.45	10.73	1.29	8.93	1.21	7.9	2.56	1338.35	62.35	1400.7	10.46	86.86
5	6	RJBO-01/CS-03	Syenite	4.81	80.89	369.79	684.3	49.28	184.3	26.5	1.53	20.96	2.93	14.69	2.37	10.75	1.25	8.64	1.2	8.44	2.77	1315.7	62.79	1378.49	11.21	85.7
7	8	RJBO-01/CS-04	Syenite	4.95	93.95	432.77	843.31	60.48	232.05	30.79	1.9	24.12	3.42	16.07	2.61	11.62	1.29	9.93	1.21	19.53	4.09	1601.3	70.27	1671.57	23.62	98.9
9	10	RJBO-01/CS-05	Syenite	8.01	93.78	487.2	931.55	65.77	247.76	34.91	2.08	27.92	3.87	18.08	2.99	12.31	1.43	9.29	1.19	15.97	2.86	1769.27	77.08	1846.35	18.83	101.79
11	12	RJBO-01/CS-06	Syenite	7.01	95.35	519.01	990.16	70.68	266.72	35.87	2.03	29.1	4.1	18.31	2.91	12.55	1.28	9.24	1.1	13.39	2.68	1884.47	78.59	1963.06	16.07	102.36
13	14	RJBO-01/CS-07	Syenite	3.36	79.21	479.81	921.06	64.93	241.93	32.21	1.76	25.69	3.41	14.44	2.29	10.16	1.12	7.87	1.02	18.73	4.24	1741.7	66	1807.7	22.97	82.57
15	16	RJBO-01/CS-08	Syenite	3.35	126.25	626.99	1190.69	85.09	312.3	42.95	1.9	34.51	4.75	21.55	3.5	16.27	1.91	13.46	1.73	25.33	7	2259.92	97.68	2357.6	32.33	129.6
17	18	RJBO-01/CS-09	Syenite	2.16	91.72	472.45	903.19	64.13	238.89	31.73	1.5	25.56	3.46	15.89	2.55	10.79	1.25	8.71	1.11	20.49	6.69	1711.89	69.32	1781.21	27.18	93.88
19	20	RJBO-01/CS-10	Syenite	2.44	98.45	520.03	993.19	69.65	258.39	34.4	1.56	27.04	3.85	17.32	2.78	12.37	1.49	9.9	1.29	21.18	7.12	1877.22	76.04	1953.26	28.3	100.89

21	22	RJBO-01/CS-11	Syenite	1.38	79.17	385.61	737.52	52.08	192.14	27.1	1.19	21.25	2.97	13	2.2	9.73	1.17	8.23	1.09	16.83	6.01	1395.64	59.66	1455.3	22.84	80.55
23	24	RJBO-01/CS-12	Syenite	0.96	80.38	424.52	831.22	58.73	221.53	29.87	1.48	22.91	3.16	14.01	2.3	10.4	1.17	8.12	1.11	20.35	6.15	1567.35	63.18	1630.53	26.5	81.34
25	25	RJBO-01/CS-13	Syenite	4.15	106.17	540.93	1060.18	75.94	284.42	39.64	1.91	30.89	4.21	19.01	3.09	13.44	1.56	10.68	1.41	32.58	8.6	2003.02	84.29	2087.31	41.18	110.32
26	26	RJBO-01/CS-14	Syenite	14.89	2.05	16.03	153.87	842.67	1620.29	151.6	430.09	62.36	3	50.69	6.99	30.76	5.23	21.13	2.41	26.64	4.29	3214.55	182.57	3397.12	30.93	16.94
27	27	RJBO-01/CS-15	Syenite	7.25	71.63	271.97	523.19	37.63	145.15	22.01	2.04	17.77	2.58	13.33	2.09	9.39	1.07	7.34	0.9	7.6	4.07	1001.99	54.47	1056.46	11.67	78.88
28	28	RJBO-01/CS-16	Syenite	7.63	0.98	7.6	74.59	294.76	568.45	41.54	163.65	23.79	2.1	19.19	2.78	13.82	2.35	9.5	1.11	7.8	3.22	1150.59	74.64	1225.23	11.02	8.61
29	29	RJBO-01/CS-17	Syenite	11.19	88.27	358.36	697.02	51.11	201.21	29.92	2.51	23.03	3.54	16.97	2.65	11.5	1.4	9.2	1.17	9.32	4.7	1340.13	69.46	1409.59	14.02	99.46
30	30	RJBO-01/CS-18	Syenite	10.7	1.37	11.04	97.85	344.87	673.39	48.98	197.92	30.33	2.47	24.42	3.64	18.46	3.06	12.84	1.47	9.72	5.02	1374.05	96.69	1470.74	14.74	12.07
31	31	RJBO-01/CS-19	Syenite	11.81	100.79	363.34	725.44	53.92	218.4	32.59	2.67	25.34	3.82	19.55	3.13	13.32	1.63	11.12	1.49	14.64	5.27	1396.36	79.4	1475.76	19.91	112.6
32	32	RJBO-01/CS-20	Syenite	10.51	1.42	11.78	95.35	331.69	656.71	49.36	194.04	30.19	2.71	23.74	3.61	17.87	2.98	12.35	1.55	13.48	4.93	1338.93	95	1433.93	18.41	11.93
33	33	RJBO-01/CS-21	Syenite	12.09	105.75	333.5	655.39	49.04	202.8	31.31	2.81	24.88	3.83	19.22	3.21	13.87	1.62	12.02	1.5	9.36	5.27	1274.85	80.15	1355	14.63	117.84
34	0	RJBO-01/CS-22	Syenite	11.02	1.44	13.97	104.21	333.15	675.34	51.46	210.88	33.83	2.94	25.98	3.91	19.41	3.2	13.32	1.56	16.13	6.59	1389.01	104.15	1493.16	22.72	12.46
35	36	RJBO-01/CS-23	Syenite	13.12	73.23	179.98	365.86	28.4	123.02	20.9	2.9	15.86	2.58	13.7	2.44	9.55	1.17	8.01	1.04	4.09	3.06	721.06	54.35	775.41	7.15	86.35
37	38	RJBO-01/CS-24	Syenite	13.44	60.98	173.65	345.68	26.45	111.89	19.43	3.2	14.53	2.29	11.82	1.95	7.85	0.97	6.6	0.77	3.29	1.99	680.3	46.78	727.08	5.28	74.42
39	40	RJBO-01/CS-25	Syenite	11.64	41.41	67.63	204.41	15.58	69.18	12.92	3.06	9.91	1.44	7.77	1.31	5.24	0.63	4.34	0.51	1.75	1.36	372.78	31.15	403.93	3.11	53.05
41	42	RJBO-01/CS-26	Syenite	16.64	41.63	69.97	210.34	15.98	72.87	13.39	3.09	10.16	1.55	8.25	1.37	5.25	0.6	4.18	<0.5	1.6	1.15	385.64	31.36	417	2.75	58.27
42	44	RJBO-01 44 mtr	Amphibolite	3.09	<0.5	43.26	24.86	3.51	7.97	1.26	7.35	2.69	0.8	2.67	<0.5	4.23	0.8	3.03	<0.5	<0.5	<0.5	88.21	14.22	102.43	0	3.09
48	50	RJBO-01 48 mtr	Amphibolite	3.14	<0.5	44.82	25.32	2.99	7.04	1.15	7.05	2.56	0.81	2.69	<0.5	4.43	0.82	3.19	<0.5	<0.5	<0.5	88.37	14.5	102.87	0	3.14
54	55	RJBO-01 54 mtr	Amphibolite	3.35	<0.5	46.94	25.91	2.32	6.08	1.08	7.04	2.72	0.85	2.75	<0.5	4.45	0.88	3.36	<0.5	<0.5	<0.5	89.37	15.01	104.38	0	3.35
55	58	RJBO-01 55 mtr	Amphibolite	3.35	<0.5	44.61	26.97	2.23	6.18	1.11	7.16	2.74	0.89	2.91	0.5	4.75	0.88	3.54	<0.5	<0.5	<0.5	88.26	16.21	104.47	0	3.35
69	70	RJBO-01/CS-22	Amphibolite	55.15	27.23	1.97	5.69	1	6.74	2.42	0.82	2.81	0.58	4.52	0.89	3.5	0.52	3.48	<0.5	<0.5	<0.5	18.64	16.3	34.94	0	82.38
71	72	RJBO-01/CS-23	Amphibolite	52.94	25.95	1.7	5.31	0.91	6.5	2.51	0.84	2.63	0.55	4.65	0.86	3.39	<0.5	3.23	<0.5	<0.5	<0.5	17.77	15.31	33.08	0	78.89
73	74	RJBO-01/CS-24	Amphibolite	56.43	26.21	2.49	6.89	1.09	6.89	2.51	0.84	2.87	0.54	4.48	0.88	3.48	<0.5	3.33	<0.5	<0.5	<0.5	20.71	15.58	36.29	0	82.64

75	76	RJBO-01/CS-25	Amphibolite	47.67	25.2	2.01	6.31	0.86	5.81	2.07	0.7	2.41	<0.5	3.83	0.75	3.05	<0.5	2.78	<0.5	<0.5	<0.5	17.76	12.82	30.58	0	72.87
77	78	RJBO-01/CS-26	Amphibolite	52.62	24.23	1.72	5.27	0.87	6.03	2.24	0.82	2.51	0.51	4.06	0.82	3.11	<0.5	3.15	<0.5	<0.5	<0.5	16.95	14.16	31.11	0	76.85

23.8.8 REE elemental analyses of Core samples, BH-2 in Borana Block, Bhilwara District, Rajasthan

From (m)	To(m)	Sample ID	Lithology	Sc	Y	La	Ce	Pr	Nd	Sm	Eu	Gd	Tb	Dy	Ho	Er	Tm	Yb	Lu	Th	U	LREE	HREE	TREE	Σ Th + U	Σ Sc + Y
1	2	RJBO-02/CS-01	Migmatite gneiss	9.93	62.06	150.65	311.33	22.3	88.48	15.44	1.69	12.27	1.97	11.14	1.96	8.09	1.08	7.7	0.97	6.61	3.09	589.89	45.18	635.07	9.7	71.99
3	4	RJBO-02/CS-02	Migmatite gneiss	6.44	64.23	196.14	390.25	28.45	113.1	18.51	1.65	15.1	2.2	12.1	2.05	8.59	1.04	6.99	0.95	9.38	4.12	748.1	49.02	797.12	13.5	70.67
5	6	RJBO-02/CS-03	Migmatite gneiss	7.1	66.5	190.37	385.53	28.18	113.09	18.39	1.76	14.52	2.35	12.36	2.15	8.57	1.1	7.58	0.98	9.48	4.28	737.32	49.61	786.93	13.76	73.6
7	8	RJBO-02/CS-04	Migmatite gneiss	5.2	64.32	183.03	360.95	26.41	106.39	17.67	1.5	13.8	2.08	11.07	2.13	8.57	1.13	7.48	0.96	9.45	4.25	695.95	47.22	743.17	13.7	69.52
9	10	RJBO-02/CS-05	Migmatite gneiss	5.57	77.12	200.9	393.54	29.32	118.71	19.72	1.67	15.4	2.43	13.93	2.35	9.84	1.26	9.33	1.13	9.2	3.85	763.86	55.67	819.53	13.05	82.69
11	12	RJBO-02/CS-06	Migmatite gneiss	5.64	95.43	228.15	435.95	34.1	138.55	22.75	1.78	18.18	2.91	15.74	2.88	12.21	1.57	10.9	1.42	10.09	5.61	861.28	65.81	927.09	15.7	101.07
13	14	RJBO-02/CS-07	Migmatite gneiss	7.62	114.44	278.55	557.27	42.16	172.49	28.43	2.09	22.7	3.7	20.35	3.49	15.35	1.84	13.64	1.77	18.39	7.5	1080.99	82.84	1163.83	25.89	122.06
15	16	RJBO-02/CS-08	Migmatite gneiss	4.89	95.26	185.73	360.91	27.28	114.62	19	1.69	15.22	2.61	15.09	2.99	13.71	1.98	13.89	1.85	8.4	11.1	709.23	67.34	776.57	19.5	100.15
17	18	RJBO-02/CS-09	Migmatite gneiss	7.37	104.96	260.04	521.89	38.55	157.83	27.32	1.99	21.68	3.45	18.67	3.32	13.44	1.94	12.32	1.66	18.52	7.4	1007.62	76.48	1084.1	25.92	112.33
19	20	RJBO-02/CS-10	Migmatite gneiss	7.97	121	373.25	751	55.67	224.02	35.92	2.45	28.55	4.35	23.22	4.07	16.32	2.06	14.25	1.79	24.04	6.55	1442.31	94.61	1536.92	30.59	128.97
21	22	RJBO-02/CS-11	Migmatite gneiss	7.05	113.31	316.32	629.8	46.36	188.38	29.85	2.26	24.07	3.72	20.1	3.51	14.9	1.95	13.5	1.68	19.24	5.77	1212.97	83.43	1296.4	25.01	120.36
23	24	RJBO-02/CS-12	Migmatite gneiss	7.48	103.37	284.1	571.24	42.98	172.88	28.67	2.16	23.16	3.43	18.93	3.22	14.04	1.8	12.94	1.65	17.67	5.86	1102.03	79.17	1181.2	23.53	110.85
25	26	RJBO-02/CS-13	Migmatite gneiss	7.74	108.96	300	602.59	44.56	177.55	28.73	2	22.41	3.4	18.36	3.34	14.03	1.85	13.1	1.73	19.59	9.12	1155.43	78.22	1233.65	28.71	116.7
27	28	RJBO-02/CS-14	Migmatite gneiss	9.08	123.11	361.2	713.92	52.18	210.08	34.57	2.36	27.36	4.09	21.98	3.89	16.43	2.14	15.01	2.03	22.24	11.18	1374.31	92.93	1467.24	33.42	132.19
29	30	RJBO-02/CS-15	Migmatite gneiss	5.95	107.4	283.65	563.02	41.86	168.99	27.99	1.95	22.1	3.37	18.4	3.31	14.17	1.84	13.32	1.78	17.07	11.6	1087.46	78.29	1165.75	28.67	113.35
31	32	RJBO-02/CS-16	Migmatite gneiss	7.37	134.61	283.98	563.43	41.81	165.7	27.07	2.2	21.95	3.58	21.04	3.96	18.06	2.53	18.79	2.67	16.56	16.61	1084.19	92.58	1176.77	33.17	141.98
33	34	RJBO-02/CS-17	Migmatite gneiss	7.34	115.04	328.21	651.48	48.95	195.98	32.16	2.11	24.94	3.79	20.16	3.57	15.25	2	13.85	1.85	17.76	9.2	1258.89	85.41	1344.3	26.96	122.38
35	36	RJBO-02/CS-18	Migmatite gneiss	7.68	113.95	327.88	650.59	48.42	196.35	33.63	2.1	26.91	3.84	20.73	3.79	15.08	2.07	14.61	1.86	18.41	9.44	1258.97	88.89	1347.86	27.85	121.63

37	38	RJBO-02/CS-19	Migmatite gneiss	8.58	121.69	339.38	686.68	51.24	207.84	34.35	2.39	26.64	4.25	22.04	4.07	15.75	2.22	14.29	2.06	23.6	12.09	1321.88	91.32	1413.2	35.69	130.27
39	40	RJBO-02/CS-20	Migmatite gneiss	6.71	104.45	314.32	628.38	46.58	191.77	31.16	2.18	24.52	3.69	19.55	3.4	14.3	1.77	12.97	1.77	19.65	10.46	1214.39	81.97	1296.36	30.11	111.16
41	42	RJBO-02/CS-21	Migmatite gneiss	5.43	98.51	275.91	548.26	40.52	163.16	26.6	1.91	20.12	3.15	16.06	3.04	12.76	1.84	12.79	1.72	17.8	10.23	1056.36	71.48	1127.84	28.03	103.94
43	44	RJBO-02/CS-22	Migmatite gneiss	5.73	103.19	292.29	586.37	43.3	173.76	29.49	2.11	22.91	3.43	18.11	3.13	13.69	1.74	12.75	1.68	17.87	9.19	1127.32	77.44	1204.76	27.06	108.92
45	46	RJBO-02/CS-23	Migmatite gneiss	6.58	112.09	297.41	589.51	43.33	173.78	28.86	2.11	23.33	3.5	19.49	3.47	15.17	2.05	14.21	1.95	17.58	9.84	1135	83.17	1218.17	27.42	118.67
47	48	RJBO-02/CS-24	Migmatite gneiss	5.16	101.48	290	576.12	41.96	168.38	26.82	2.04	21.26	3.28	17.66	3.07	13.17	1.77	13.23	1.82	18.14	12.27	1105.32	75.26	1180.58	30.41	106.64
49	50	RJBO-02/CS-25	Migmatite gneiss	5.28	110.88	322.01	644.1	47.25	190.52	29.51	2.3	24.67	3.69	19.38	3.38	14.84	2.06	14.6	2.08	20.69	12.67	1235.69	84.7	1320.39	33.36	116.16
51	52	RJBO-02/CS-26	Migmatite gneiss	7.4	123.17	361.81	723.5	52.79	210.87	33.83	2.61	26.93	4.16	21.94	3.88	16.23	2.18	16.4	2.24	22.88	12.91	1385.41	93.96	1479.37	35.79	130.57
53	54	RJBO-02/CS-27	Migmatite gneiss	7.15	119.27	324.54	646.9	48.12	192.87	31.66	2.23	24.87	4.01	21.41	3.83	15.97	2.28	16.13	2.13	21.41	12.35	1246.32	90.63	1336.95	33.76	126.42
55	56	RJBO-02/CS-28	Syenite	6.15	108.28	337.15	672.7	49.66	199.19	31.09	2.35	24.69	3.71	20.15	3.35	15.11	1.89	13.83	1.87	21.81	12.31	1292.14	84.6	1376.74	34.12	114.43
57	58	RJBO-02/CS-29	Syenite	6.27	98.53	304.12	605.11	44.13	176.96	28.7	2.08	22.47	3.42	18.38	3.29	14.05	1.92	12.57	1.73	19.31	9.47	1161.1	77.83	1238.93	28.78	104.8
59	60	RJBO-02/CS-30	Syenite	5.68	97.9	289.7	572.11	42.3	172.86	28.67	2.08	21.67	3.34	17.56	3.12	12.83	1.73	12.18	1.62	19.98	9.7	1107.72	74.05	1181.77	29.68	103.58
61	62	RJBO-02/CS-31	Syenite	5.85	108.01	328.42	654.99	48.4	193.12	31.97	2.23	24.87	3.69	19.65	3.42	14.55	1.98	14.3	1.83	21.56	10.31	1259.13	84.29	1343.42	31.87	113.86
63	64	RJBO-02/CS-32	Syenite	5.48	94.16	293.26	585.05	42.69	169.6	27.13	2.13	22.08	3.21	16.77	3.03	12.66	1.74	12.26	1.65	18.68	10.81	1119.86	73.4	1193.26	29.49	99.64
65	66	RJBO-02/CS-33	Syenite	10.22	99.49	349.34	698.54	51.44	211.38	33.7	2.51	26.69	3.86	20.26	3.54	14.44	1.82	12.86	1.64	20.44	8.41	1346.91	85.11	1432.02	28.85	109.71
67	68	RJBO-02/CS-34	Syenite	8.42	92.59	302.45	608.72	45.61	186.18	29.8	2.61	23.18	3.47	17.89	3.08	12.8	1.64	11.65	1.47	19.78	10.3	1175.37	75.18	1250.55	30.08	101.01
69	70	RJBO-02/CS-35	Syenite	11.5	110.66	382.94	775.51	57.31	233.9	37.61	2.81	29.91	4.4	22.12	3.9	15.78	1.97	13.33	1.68	21.45	8.84	1490.08	93.09	1583.17	30.29	122.16
71	72	RJBO-02/CS-36	Syenite	10.72	100.3	340.39	670.71	49.49	203.04	32.24	2.48	25.25	3.81	19.53	3.42	14	1.81	11.98	1.74	19.11	8.95	1298.35	81.54	1379.89	28.06	111.02
73	74	RJBO-02/CS-37	Syenite	10.75	105.68	383.41	767.75	56.36	226.28	37.78	2.72	29.03	4.14	21.36	3.68	14.5	1.88	12.91	1.68	20.03	8.06	1474.3	89.18	1563.48	28.09	116.43
75	76	RJBO-02/CS-38	Syenite	9.57	100.46	354.55	703.51	52	208.42	32.61	2.64	25.99	3.94	20.46	3.45	14.24	1.69	12.44	1.58	18.22	7.31	1353.73	83.79	1437.52	25.53	110.03
77	78	RJBO-02/CS-39	Syenite	8.98	89.93	306.65	605.89	44.4	181.12	29.93	2.47	23.99	3.4	17.62	3.11	13.05	1.71	11.46	1.42	17.49	7.64	1170.46	75.76	1246.22	25.13	98.91
79	80	RJBO-02/CS-40	Syenite	10.63	61.97	187.62	372.29	27.72	114.27	18.77	2.02	14.76	2.26	11.98	2.03	8.56	1.05	7.46	0.94	7.45	5.59	722.69	48.98	771.67	13.04	72.6
81	82	RJBO-02/CS-41	Syenite	9.47	99.92	331.99	663.48	49.55	204.68	33.29	2.66	26.35	3.85	19.82	3.44	13.96	1.76	12.73	1.6	17.8	7.67	1285.65	83.46	1369.11	25.47	109.39

83	84	RJBO-02/CS-42	Syenite	8.55	86.09	296.19	586.46	43.9	178.87	28.74	2.5	22.6	3.3	16.78	2.95	12.03	1.49	10.73	1.29	17.47	8.31	1136.66	71.17	1207.83	25.78	94.64
85	86	RJBO-02/CS-43	Syenite	10.78	106.01	323.01	646.71	48.43	202.95	32.91	2.66	26.12	3.99	21.04	3.73	14.98	1.87	13.61	1.74	17.74	9.04	1256.67	87.08	1343.75	26.78	116.79
87	88	RJBO-02/CS-44	Syenite	10.47	111.56	326.83	650.35	47.47	197.88	33.37	2.82	26.22	3.97	21.76	3.78	16.31	1.99	13.9	1.79	17.71	7.9	1258.72	89.72	1348.44	25.61	122.03
89	90	RJBO-02/CS-45	Syenite	10.23	111.3	369.15	733.4	54.46	225.52	36.54	2.82	28.54	4.44	22.29	3.87	15.87	1.86	13.36	1.75	19.62	8.2	1421.89	91.98	1513.87	27.82	121.53
91	92	RJBO-02/CS-46	Syenite	10.23	100.49	356.8	717.39	52.74	212.41	35.29	2.66	27.18	3.98	20.27	3.6	14.04	1.74	12.04	1.52	19.13	8.19	1377.29	84.37	1461.66	27.32	110.72
93	94	RJBO-02/CS-47	Syenite	8.52	80.41	293.73	588.78	43.18	174.29	28.81	2.37	22.37	3.31	15.97	2.83	11.43	1.45	10.2	1.26	17.54	13.98	1131.16	68.82	1199.98	31.52	88.93
95	96	RJBO-02/CS-48	Syenite	10.21	88.78	342.77	683.18	50.19	209.19	33.77	2.3	25.88	3.85	18.87	3.14	13.22	1.67	11.67	1.5	20.59	9.31	1321.4	79.8	1401.2	29.9	98.99
97	98	RJBO-02/CS-49	Syenite	9.6	106.51	375.69	781.33	58.77	238.05	37.35	2.69	28.88	4.84	24.23	3.9	15.81	2.05	13.81	1.89	19.29	11.23	1493.88	95.41	1589.29	30.52	116.11
99	100	RJBO-02/CS-50	Syenite	8.77	92.76	297.63	589.85	43.31	177.88	29.53	2.16	23.45	3.48	18.59	3.22	13.13	1.79	12.25	1.55	15.6	8.13	1140.36	77.46	1217.82	23.73	101.53
101	102	RJBO-02/CS-51	Syenite	6.66	94.93	312.53	634.07	46.61	188.34	30.3	2.26	23.74	3.52	19	3.27	13.92	1.72	12.1	1.58	21.72	11.05	1214.11	78.85	1292.96	32.77	101.59
103	104	RJBO-02/CS-52	Syenite	7.65	103.56	336.34	680.65	50.23	201.01	32.63	2.4	25.38	3.88	19.92	3.49	14.62	1.89	12.65	1.63	22.5	9.99	1303.26	83.46	1386.72	32.49	111.21
105	106	RJBO-02/CS-53	Syenite	6.33	100.46	282.14	560.26	41.31	167.89	27.47	2.25	21.59	3.35	18.15	3.35	14.2	1.87	13.31	1.67	17.57	9.42	1081.32	77.49	1158.81	26.99	106.79
107	108	RJBO-02/CS-54	Syenite	7.71	117.23	324.54	651.81	48.38	198.38	33.43	2.41	26.65	4.18	24.13	4.14	17.65	2.32	17.12	2.2	18.76	11.97	1258.95	98.39	1357.34	30.73	124.94
109	110	RJBO-02/CS-55	Syenite	10.93	105.3	317.03	632.44	47.65	196.67	34.47	2.3	26.69	3.98	20.9	3.69	14.7	1.93	12.86	1.7	19.59	9.34	1230.56	86.45	1317.01	28.93	116.23
111	112	RJBO-02/CS-56	Syenite	7.98	96.58	335.49	678.79	50.29	203.75	33.15	2.52	25.19	3.74	19.59	3.21	13.61	1.73	12.08	1.58	22.02	11.2	1303.99	80.73	1384.72	33.22	104.56
113	114	RJBO-02/CS-57	Syenite	7.37	100.57	342.02	685.29	50.3	201.13	32.95	2.35	25.14	3.68	19.31	3.31	14.09	1.79	12.65	1.6	22.08	12.2	1314.04	81.57	1395.61	34.28	107.94
115	116	RJBO-02/CS-58	Syenite	7.23	97.52	298.73	584.33	43.55	174.68	27.54	2.15	22.06	3.35	17.38	3.16	13.22	1.81	11.62	1.51	18.95	9.19	1130.98	74.11	1205.09	28.14	104.75
117	118	RJBO-02/CS-59	Syenite	5.02	84.46	279.3	565.11	41.43	170.04	27.07	2.17	20.87	3.09	16.11	2.77	11.9	1.55	10.61	1.37	21.89	11.26	1085.12	68.27	1153.39	33.15	89.48
119	120	RJBO-02/CS-60	Syenite	5.52	84.76	284.1	571.23	42.97	172.01	27.1	2.09	21.41	3.13	16.15	2.8	11.8	1.63	11.2	1.42	19.2	9.95	1099.5	69.54	1169.04	29.15	90.28
121	122	RJBO-02/CS-61	Syenite	3.77	91.73	311.84	627.24	46.26	190.33	29.12	2.15	22.72	3.32	16.99	3.06	12.67	1.69	11.47	1.5	24.06	13.1	1206.94	73.42	1280.36	37.16	95.5
123	124	RJBO-02/CS-62	Syenite	5.03	80.34	244.11	500.26	36.43	148.52	23.55	1.91	18.71	2.92	15.06	2.64	11.66	1.48	11.06	1.48	15.87	10.29	954.78	65.01	1019.79	26.16	85.37
125	126	RJBO-02/CS-63	Syenite	8.8	99.3	312.68	625.75	45.33	185.15	28.92	2.3	23.9	3.5	19.12	3.31	13.96	1.81	12.59	1.59	19.64	11.1	1200.13	79.78	1279.91	30.74	108.1
127	128	RJBO-02/CS-64	Syenite	11.73	103.36	355.78	718.1	53.34	217.56	34.14	2.42	26.51	4.02	20.56	3.55	14.67	1.78	12.32	1.56	21.47	8.99	1381.34	84.97	1466.31	30.46	115.09

129	130	RJBO-02/CS-65	Syenite	10.95	108.52	342.64	686.64	51.11	209.69	34.74	2.47	27.69	4.08	21.97	3.71	15.3	1.95	13.09	1.76	22.44	9.17	1327.29	89.55	1416.84	31.61	119.47
131	132	RJBO-02/CS-66	Syenite	8.62	103.76	338.31	693	51.81	215.29	35	2.26	26.7	4.07	20.9	3.71	15	1.89	13	1.62	20.95	9.49	1335.67	86.89	1422.56	30.44	112.38
133	134	RJBO-02/CS-67	Migmatite gneiss	8.54	102.32	327.95	668.97	49.16	203.38	34.37	2.33	26.3	3.93	20.55	3.54	14.48	1.93	13.44	1.83	21.69	10.24	1286.16	86	1372.16	31.93	110.86
135	136	RJBO-02/CS-68	Migmatite gneiss	8.6	136.91	312.54	635.9	47.39	196.39	33.05	2.34	27.38	4.44	25.67	4.69	19.65	2.65	17.66	2.29	30.17	19.07	1227.61	104.43	1332.04	49.24	145.51
137	138	RJBO-02/CS-69	Migmatite gneiss	7.81	155.84	305.77	620.56	46.26	188.1	34.25	2.27	27.87	4.62	28.01	5.06	21.18	3.04	20.66	2.82	19.51	13.09	1197.21	113.26	1310.47	32.6	163.65
139	140	RJBO-02/CS-70	Migmatite gneiss	7.89	145.03	292.31	602.21	45.77	189.08	33.7	2.36	26.63	4.45	26.68	4.92	20.39	2.83	19.18	2.49	19.5	11.21	1165.43	107.57	1273	30.71	152.92
141	142	RJBO-02/CS-71	Migmatite gneiss	8.51	141.26	298.29	603.22	45.43	188.98	34.49	2.29	28.41	4.57	27.65	5.09	20.15	2.86	19.35	2.6	24.12	13.8	1172.7	110.68	1283.38	37.92	149.77
143	144	RJBO-02/CS-72	Migmatite gneiss	7.74	135.34	260.52	524.62	39.53	164.29	28.86	2.11	23.55	3.89	23.58	4.53	18.59	2.69	19.12	2.58	19.16	11.45	1019.93	98.53	1118.46	30.61	143.08
145	146	RJBO-02/CS-73	Migmatite gneiss	6.53	111.38	274.46	559.54	41.43	168.31	28.82	2.11	22.51	3.61	20.88	3.62	15.86	2.17	15.74	2.03	20.83	13.22	1074.67	86.42	1161.09	34.05	117.91
147	148	RJBO-02/CS-74	Migmatite gneiss	7.21	106.41	300.19	600.59	44.98	183.09	30.36	2.32	24.05	3.61	19.93	3.55	14.67	1.92	13.67	1.74	19.45	9.83	1161.53	83.14	1244.67	29.28	113.62
149	150	RJBO-02/CS-75	Syenite	8.88	128.29	300.26	607.93	45.48	186.6	32.16	2.31	26.08	4.24	24.92	4.5	18.47	2.34	15.27	1.96	22.82	13.79	1174.74	97.78	1272.52	36.61	137.17
151	152	RJBO-02/CS-76	Syenite	7.09	121.86	309.8	622.67	46.65	190.1	31.35	2.34	25.16	3.94	22.88	3.9	17.47	2.26	16.15	2.09	22.62	13.45	1202.91	93.85	1296.76	36.07	128.95
153	154	RJBO-02/CS-77	Syenite	6.85	103.36	297.66	603.82	45.86	187.63	31.87	2.31	24.87	3.65	20.17	3.53	15.5	2.06	14.53	1.81	20.84	12.11	1169.15	86.12	1255.27	32.95	110.21
154.6	-	RJBO-02/CS-78	Migmatite gneiss	15.22	2.03	8.22	105.37	268.28	546.31	41.13	172.81	30.8	2.11	24.94	3.96	22.1	3.81	15.31	2.17	20.48	14.77	1142.12	105.2	1247.32	35.25	17.25

23.8.9 REE elemental analyses of Core samples, BH-3 in Borana Block, Bhilwara District, Rajasthan

From (m)	To (m)	Sample ID	Lithology	Sc	Y	La	Ce	Pr	Nd	Sm	Eu	Gd	Tb	Dy	Ho	Er	Tm	Yb	Lu	Th	U	ΣLREE	ΣHREE	ΣREE	Σ Th + U	Σ Sc + Y
1	2	RJBO-03/CS-01	Migmatite gneiss	5.23	75.3	253.89	489.23	37.33	150.37	24.44	2.5	19.01	2.71	14.97	2.68	10.95	1.44	9.93	1.27	8.49	2.36	957.76	62.96	1020.72	10.85	80.53
3	4	RJBO-03/CS-02	Migmatite gneiss	5.71	84.13	271.71	533.33	40.13	163.48	25.75	2.46	20.06	3.06	16.52	2.68	12.51	1.6	11.23	1.42	13.89	3.62	1036.86	69.08	1105.94	17.51	89.84
5	6	RJBO-03/CS-03	Migmatite gneiss	5.55	80.65	265.5	505.79	38.99	159.94	26.11	2.64	20.07	2.9	16.03	2.79	11.68	1.52	10.55	1.36	9.57	2.94	998.97	66.9	1065.87	12.51	86.2
7	8	RJBO-03/CS-04	Migmatite gneiss	5.55	73.87	250.15	488.19	37.3	152.33	24.2	2.38	19.18	2.7	14.87	2.57	10.53	1.36	9.74	1.22	9.09	2.44	954.55	62.17	1016.72	11.53	79.42

9	10.3	RJBO-03/CS-05	Migmatite gneiss	7.04	75.59	285.73	559.14	41.97	168.48	26.53	2.74	20.78	2.9	15.5	2.67	10.74	1.33	9.21	1.12	10.37	3.63	1084.59	64.25	1148.84	14	82.63
37	38	RJBO-03/CS-06	Migmatite gneiss	27.35	41.26	68.64	212.77	15.86	66.23	12.39	1.83	9.58	1.44	8.57	1.53	5.78	0.76	5.48	0.65	3.89	2.63	377.72	33.79	411.51	6.52	68.61
39	40	RJBO-03/CS-07	Migmatite gneiss	7.2	68.14	257.91	509.49	37.43	154.29	24.36	2.36	18.89	2.76	14.13	2.45	10.19	1.24	9.07	1.08	9.03	4.78	985.84	59.81	1045.65	13.81	75.34
41	42	RJBO-03/CS-08	Migmatite gneiss	8.31	96.91	395.97	780.55	55.72	224.32	34.46	2.92	27.3	3.79	19.06	3.27	13.75	1.73	11.96	1.5	19.77	8.33	1493.94	82.36	1576.3	28.1	105.22
43	44	RJBO-03/CS-09	Migmatite gneiss	5.35	78.1	260.22	523	38.73	156.57	27.25	2.33	20.51	3.01	15.22	2.7	11.07	1.4	9.3	1.14	22.83	10.2	1008.1	64.35	1072.45	33.03	83.45
45	46	RJBO-03/CS-10	Migmatite gneiss	6.55	90.99	286.14	568.82	42.53	176.73	29.33	2.58	23.45	3.45	18.65	3.23	12.88	1.62	11.11	1.39	18.76	7.81	1106.13	75.78	1181.91	26.57	97.54
47	48	RJBO-03/CS-11	Migmatite gneiss	8.54	97.48	264.51	531.08	39.48	166.2	28.53	2.64	23.33	3.55	20.07	3.45	14.33	1.8	12.26	1.58	9.32	5.86	1032.44	80.37	1112.81	15.18	106.02
49	50	RJBO-03/CS-12	Migmatite gneiss	9.31	103.55	297.95	598.14	44.66	182.62	30.46	2.66	25.04	3.74	20.39	3.51	14.49	1.76	12.75	1.58	15.98	6.48	1156.49	83.26	1239.75	22.46	112.86
50	51	RJBO-03/CS-13	Syenite	3.62	49.51	148.25	296.64	21.62	87.89	14.78	1.66	11.16	1.72	9.99	1.77	7.73	1.08	7.79	0.98	6.34	7.59	570.84	42.22	613.06	13.93	53.13
52	52	RJBO-03/CS-14	Syenite	11.14	91.56	297.55	586.6	43.18	178.73	29.76	2.48	23.85	3.39	18.83	3.29	13.55	1.65	11.45	1.43	15.98	5.72	1138.3	77.44	1215.74	21.7	102.7
53	54	RJBO-03/CS-15	Migmatite gneiss	9.49	90.24	296.55	584.99	42.67	170.84	29.21	2.56	23.08	3.4	17.94	3.25	13.12	1.73	11.3	1.45	11.15	6.13	1126.82	75.27	1202.09	17.28	99.73
55	56	RJBO-03/CS-16	Migmatite gneiss	8.72	118.94	367.93	732.03	54.04	218.71	36.4	2.98	29.35	4.36	23.79	4.19	17.14	2.22	15.05	1.92	21.3	8.7	1412.09	98.02	1510.11	30	127.66
57	58	RJBO-03/CS-17	Migmatite gneiss	7.39	91.1	293.83	575.63	42.04	172.78	29.05	2.35	22.62	3.37	18.67	3.27	13.27	1.71	11.31	1.33	14.49	7.41	1115.68	75.55	1191.23	21.9	98.49
59	60	RJBO-03/CS-18	Migmatite gneiss	7.41	92.22	293.02	580.85	42.93	172.97	28.59	2.39	23.03	3.38	18.79	3.31	13.18	1.63	11.55	1.43	16.13	7.33	1120.75	76.3	1197.05	23.46	99.63
61	62	RJBO-03/CS-19	Migmatite gneiss	9	106.03	343.58	693.65	50.84	208.47	35.21	2.84	27.14	4.05	22.19	3.79	15.55	1.91	12.81	1.64	21.17	8.55	1334.59	89.08	1423.67	29.72	115.03
63	64	RJBO-03/CS-20	Migmatite gneiss	8.85	114.93	357.87	711.36	54.17	218.33	37.48	2.8	28.81	4.3	23.64	4.02	16.46	2.01	13.72	1.77	20.03	7.03	1382.01	94.73	1476.74	27.06	123.78
65	66	RJBO-03/CS-21	Migmatite gneiss	7.39	88.39	266.49	527.46	39.75	162.16	27.8	2.42	21.67	3.48	18.3	3.14	12.68	1.55	10.62	1.41	9.61	6.49	1026.08	72.85	1098.93	16.1	95.78
67	68	RJBO-03/CS-22	Migmatite gneiss	7.51	99.08	290.15	571.78	42.41	176.84	30.04	2.62	23.48	3.48	19.82	3.6	14.82	1.95	13.05	1.57	11.3	6.21	1113.84	81.77	1195.61	17.51	106.59
69	70	RJBO-03/CS-23	Migmatite gneiss	6.68	97.29	322.32	646.6	47.24	190.67	30.52	2.63	24.27	3.61	19.42	3.35	13.61	1.7	11.62	1.46	18.51	7.58	1239.98	79.04	1319.02	26.09	103.97
71	72	RJBO-03/CS-24	Syenite	8.69	95.81	346.84	698.49	51.34	211.57	34.19	2.38	25.97	3.77	20.58	3.58	14.56	1.76	12.22	1.54	21.55	10.34	1344.81	83.85	1428.66	31.89	104.5
73	74	RJBO-03/CS-25	Syenite	6.04	90.66	300.66	593.22	43.81	178.57	28.88	2.52	22.51	3.22	17.29	3.04	12.88	1.66	12.28	1.44	10.28	7.13	1147.66	74.18	1221.84	17.41	96.7
75	76	RJBO-03/CS-26	Syenite	5.58	77.42	248.92	498.64	37.08	151.42	25.88	2	19.39	2.79	15.15	2.63	10.53	1.44	9.76	1.32	8.93	7.77	963.94	63.01	1026.95	16.7	83
77	78	RJBO-03/CS-27	Migmatite gneiss	5.48	81.82	308.25	615.09	46.23	189.15	29.79	2.25	22.99	3.35	16.81	2.83	11.76	1.4	9.85	1.22	10.31	7.8	1190.76	70.21	1260.97	18.11	87.3

79	80	RJBO-03/CS-28	Migmatite gneiss	7.15	85.23	275.71	551.03	40.8	172.4	27.32	2.33	22.35	3.21	17.38	2.89	12.04	1.54	10.68	1.37	9.54	5.79	1069.59	71.46	1141.05	15.33	92.38
81	82	RJBO-03/CS-29	Migmatite gneiss	4.2	75.08	267.1	533.91	39.25	163.72	25.02	2.47	20	2.86	15.69	2.58	10.79	1.37	8.97	1.2	17.47	8.99	1031.47	63.46	1094.93	26.46	79.28
83	84	RJBO-03/CS-30	Migmatite gneiss	19.91	150.6	566.85	1140.91	85.71	353.16	58.15	2.92	45.26	6.7	34.31	5.5	22.43	2.47	16.49	2.16	21.94	5.73	2207.7	135.32	2343.02	27.67	170.51
85	86	RJBO-03/CS-31	Migmatite gneiss	26.12	139.19	585.01	1180.55	88.21	355.24	59.82	3.09	45.97	6.45	31.38	5.41	20.69	2.33	15.37	1.94	20.32	3.62	2271.92	129.54	2401.46	23.94	165.31
87	88	RJBO-03/CS-32	Migmatite gneiss	5.69	57.59	218.02	441.38	33.06	137.98	23.37	1.97	17.98	2.49	13.36	2.15	8.91	1.11	7.13	0.89	8.49	5.81	855.78	54.02	909.8	14.3	63.28
89	90	RJBO-03/CS-33	Migmatite gneiss	8.39	89.36	306.08	641.5	48.6	201.68	33.23	2.46	25.33	3.71	19.37	3.32	13.62	1.66	10.82	1.36	17.37	6.81	1233.55	79.19	1312.74	24.18	97.75
91	92	RJBO-03/CS-34	Migmatite gneiss	10.55	85.02	321.59	635.11	47.41	192.6	31.89	2.31	24.44	3.59	18.8	3.18	12.82	1.48	9.91	1.21	9.47	5	1230.91	75.43	1306.34	14.47	95.57
93	94	RJBO-03/CS-35	Migmatite gneiss	5.41	79.25	290.73	576.78	42.62	173.83	27.25	2.47	21.84	3.17	16.88	2.82	11.6	1.37	9.61	1.21	8.96	4.89	1113.68	68.5	1182.18	13.85	84.66
95	96	RJBO-03/CS-36	Migmatite gneiss	6.54	77.52	293.48	586.08	42.85	173.53	28.04	2.38	20.87	3.07	16.14	2.77	11.56	1.52	10.61	1.34	9.3	6.91	1126.36	67.88	1194.24	16.21	84.06
97	98	RJBO-03/CS-37	Migmatite gneiss	8.34	94.56	375.92	745.19	54.92	221.29	34.77	2.85	26.72	3.88	19.75	3.36	13.24	1.58	11.12	1.3	10.46	4.48	1434.94	80.95	1515.89	14.94	102.9
99	100	RJBO-03/CS-38	Migmatite gneiss	6.21	80.98	289.84	575.15	42.8	173.26	27.14	2.65	22.16	3.24	16.48	2.97	12.12	1.38	9.42	1.13	9.39	5.67	1110.84	68.9	1179.74	15.06	87.19
101	102	RJBO-03/CS-39	Migmatite gneiss	4.89	63.08	247.39	491.33	36.42	143.87	22.74	2.06	17.86	2.57	13.34	2.22	9.34	1.07	7.41	0.88	7.41	4.23	943.81	54.69	998.5	11.64	67.97
103	104	RJBO-03/CS-40	Migmatite gneiss	6.94	80.05	302.5	591.07	43.66	176.95	27.62	2.33	22.07	3.15	16.52	2.69	11.46	1.42	9.71	1.13	9.43	5.66	1144.13	68.15	1212.28	15.09	86.99
105	106	RJBO-03/CS-41	Migmatite gneiss	9.61	88.68	387.76	785.34	57.48	225.25	35.81	3.29	28.87	4.03	20.69	3.31	13.2	1.46	10.03	1.26	10.45	4.38	1494.93	82.85	1577.78	14.83	98.29
107	108	RJBO-03/CS-42	Migmatite gneiss	9.76	90.57	341.99	638.7	55.27	202.46	31.53	2.79	23.05	3.42	16.92	2.79	10.02	0.99	8.34	0.64	19.99	5.11	1272.74	66.17	1338.91	25.1	100.33
109	110	RJBO-03/CS-43	Migmatite gneiss	10.12	96.65	289.77	549.71	48.45	183.69	30.78	2.77	22.17	3.39	17.93	3.02	10.73	1.09	9.17	0.66	16.64	5.2	1105.17	68.16	1173.33	21.84	106.77
111	112	RJBO-03/CS-44	Migmatite gneiss	10.86	97.09	278.67	530.15	47.29	178.81	30.78	2.64	21.77	3.49	18.51	3.03	10.86	1.07	8.81	0.61	15.72	4.05	1068.34	68.15	1136.49	19.77	107.95
113	114	RJBO-03/CS-45	Migmatite gneiss	12.73	99.1	325.27	609.74	52.83	198.9	33.15	2.76	23.67	3.76	19.37	3.16	10.86	1.08	8.49	0.64	17.63	3.91	1222.65	71.03	1293.68	21.54	111.83
115	116	RJBO-03/CS-46	Migmatite gneiss	8.73	93.74	308.5	576.11	50.36	186.02	30.54	2.66	21.54	3.47	17.33	2.89	10.42	1.04	8.74	0.66	18.87	5.51	1154.19	66.09	1220.28	24.38	102.47
117	118	RJBO-03/CS-47	Migmatite gneiss	10.34	115.05	370.01	709.44	61.83	229.18	37.29	2.96	26.66	4.28	21.58	3.56	12.95	1.33	10.99	0.82	27.44	5.61	1410.71	82.09	1492.8	33.05	125.39
119	120	RJBO-03/CS-48	Migmatite gneiss	12.16	115.24	381.61	723.15	63.18	235.62	39.4	2.71	28.17	4.32	21.74	3.55	12.47	1.26	10.36	0.8	24.16	4.97	1445.67	82.67	1528.34	29.13	127.4
121	122	RJBO-03/CS-49	Migmatite gneiss	10.13	98.34	309.9	582.01	50.18	187.58	30.71	2.51	22.47	3.58	18.09	3.09	11.01	1.12	9.28	0.7	18.34	5.49	1162.89	69.34	1232.23	23.83	108.47
123	124	RJBO-03/CS-50	Migmatite gneiss	6.93	98.29	322.37	611.4	53.08	195.99	31.66	2.51	22.74	3.65	18.47	3.08	10.85	1.08	9.12	0.67	18.38	4.39	1217.01	69.66	1286.67	22.77	105.22

125	126	RJBO-03/CS-51	Migmatite gneiss	12.24	82.05	246.47	462	39.87	149.89	24.97	2.29	18.34	2.82	15.12	2.5	9.11	0.96	8.05	0.62	14.45	4.21	925.49	57.52	983.01	18.66	94.29
127	128	RJBO-03/CS-52	Migmatite gneiss	7.47	96.42	283.83	533.39	46.45	175.82	29.08	2.45	21.67	3.39	17.65	3.02	10.99	1.14	9.67	0.74	16.83	7	1071.02	68.27	1139.29	23.83	103.89
129	130	RJBO-03/CS-53	Migmatite gneiss	4.99	92.59	236.99	449.92	39.87	156.8	27.45	2.23	20.05	3.17	17.44	2.85	10.42	1.07	8.92	0.66	28.41	6.13	913.26	64.58	977.84	34.54	97.58
131	132	RJBO-03/CS-54	Migmatite gneiss	7.23	100.29	333.51	630.54	54.17	205.4	32.66	2.48	24	3.55	18.18	3.08	11.44	1.18	9.99	0.75	21.18	4.86	1258.76	72.17	1330.93	26.04	107.52
133	134	RJBO-03/CS-55	Migmatite gneiss	7.19	91.84	320.74	602.61	51.7	193.99	31.19	2.26	22.67	3.36	16.46	2.78	10.46	1.07	9.32	0.73	19.99	6.53	1202.49	66.85	1269.34	26.52	99.03
135	136	RJBO-03/CS-56	syenite	5.25	93.58	321.18	603.23	51.64	196.52	31.01	2.11	23	3.25	16.92	2.81	10.88	1.11	9.49	0.72	20.54	5.33	1205.69	68.18	1273.87	25.87	98.83
137	138	RJBO-03/CS-57	syenite	3.26	102.53	369.92	692.66	58.95	219.88	34.55	2.2	25.42	3.72	18.41	3.05	11.11	1.1	9.23	0.7	39.6	6.13	1378.16	72.74	1450.9	45.73	105.79
139	140	RJBO-03/CS-58	syenite	3.09	72.72	184.07	346.05	30.25	117.06	20.35	1.58	14.9	2.29	12.78	2.17	8.14	0.85	7.03	0.53	21.72	4.57	699.36	48.69	748.05	26.29	75.81
141	142	RJBO-03/CS-59	syenite	3.72	60.42	178.08	336.59	29.52	112.05	19.21	1.59	13.72	2.03	10.62	1.81	7.02	0.77	6.65	0.5	20.08	3.56	677.04	43.12	720.16	23.64	64.14
143	144	RJBO-03/CS-60	syenite	7.37	94.76	345.7	650.17	55.87	209.34	33.08	2.45	23.55	3.45	16.95	2.81	10.06	1	8.26	0.62	33.91	4.94	1296.61	66.7	1363.31	38.85	102.13
145	146	RJBO-03/CS-61	syenite	9.34	75.44	264.09	493.09	42.78	161.13	26.33	2.2	18.82	2.82	13.87	2.31	8.2	0.81	6.86	0.53	24.86	4.22	989.62	54.22	1043.84	29.08	84.78
147	148	RJBO-03/CS-62	syenite	8.28	83.9	276.83	520.82	44.83	167.34	27.01	2.18	19.54	2.88	14.42	2.44	9.3	0.97	8.4	0.66	18.93	4.52	1039.01	58.61	1097.62	23.45	92.18
149	150	RJBO-03/CS-63	syenite	7.79	92.2	339.63	641.1	55.02	205.77	33.16	2.27	23.58	3.42	16.72	2.74	9.99	0.98	8.07	0.6	27.99	3.87	1276.95	66.1	1343.05	31.86	99.99
17	18	RJBO-03/CS-64	Amphibolite	29.52	23.98	16.16	35.71	4.87	24.11	5.6	1.39	4.35	0.7	4.49	0.75	2.69	<0.5	2.46	<0.5	1.36	0.83	87.84	15.44	103.28	2.19	53.5
35	36	RJBO-03/CS-65	Amphibolite	29.08	17.98	11.56	26.23	3.63	18.81	4.41	1.2	3.49	0.53	3.51	0.6	2.16	<0.5	1.9	<0.5	0.52	0.5	65.84	12.19	78.03	1.02	47.06
24	25	RJBO-03/CS-66	Amphibolite	28.7	19.32	12.84	29.03	4	20.42	4.78	1.29	3.76	0.59	3.85	0.65	2.36	<0.5	2.01	<0.5	0.57	0.58	72.36	13.22	85.58	1.15	48.02

23.8.10 REE elemental analyses of Core samples, BH-4 in Borana Block, Bhilwara District, Rajasthan

From (m)	To(m)	Sample ID	Lithology	Sc	Y	La	Ce	Pr	Nd	Sm	Eu	Gd	Tb	Dy	Ho	Er	Tm	Yb	Lu	Th	U	ΣLREE	ΣHREE	ΣREE	Σ Th + U	Σ Sc + Y
1	2	RJBO-04/CS-01	Migmatite gneiss	7.11	71.17	274.99	505.01	45.71	179.32	28.37	2.12	19.92	2.71	13.32	2.15	8.16	0.77	6.6	<0.5	20.44	2.42	1035.52	53.63	1089.15	22.86	78.28
3	4	RJBO-04/CS-02	Migmatite gneiss	6.22	74.3	274.06	503.62	45.55	177	27.95	2.04	19.73	2.71	13.33	2.17	8.22	0.81	6.79	0.51	22.36	2.55	1030.22	54.27	1084.49	24.91	80.52
5	6	RJBO-04/CS-03	Migmatite gneiss	5.92	71.97	267.2	491.59	44.37	171.5	27.43	1.97	19.28	2.61	12.85	2.12	8.01	0.8	6.63	<0.5	25.4	2.7	1004.06	52.3	1056.36	28.1	77.89
7	8	RJBO-04/CS-04	Migmatite gneiss	7.61	75.21	299.58	571.17	50.79	196.31	31.48	2.19	21.68	3.02	14.43	2.31	8.62	0.84	7	0.51	28.6	3.1	1151.52	58.41	1209.93	31.7	82.82

9	10	RJBO-04/CS-05	Migmatite gneiss	6.32	71.23	265.63	503.59	44.14	172.11	27.75	2.15	19.19	2.74	13.03	2.13	8	0.79	6.77	<0.5	19.34	3.41	1015.37	52.65	1068.02	22.75	77.55
11	12	RJBO-04/CS-06	Migmatite gneiss	9.51	86.77	335.73	643.5	56.37	212.28	34.2	2.52	23.75	3.38	16.49	2.72	9.69	0.95	7.96	0.55	30.92	4.78	1284.6	65.49	1350.09	35.7	96.28
13	14	RJBO-04/CS-07	Migmatite gneiss	10.09	78.15	336.34	640.64	57.25	219.81	36.13	2.29	24.78	3.43	16.11	2.57	9.06	0.85	6.91	<0.5	30.89	3.25	1292.46	63.71	1356.17	34.14	88.24
15	16	RJBO-04/CS-08	Migmatite gneiss	9.8	70.76	305.27	589.31	51.97	199.35	32.89	2.41	22.24	3.06	14.54	2.34	8.27	0.81	6.52	<0.5	33.8	4.05	1181.2	57.78	1238.98	37.85	80.56
17	18	RJBO-04/CS-09	Migmatite gneiss	8.56	67.15	250.88	476.1	41.68	159.96	26.63	2.16	18.13	2.54	12.67	2.04	7.65	0.8	6.93	<0.5	20.69	3.5	957.41	50.76	1008.17	24.19	75.71
19	20	RJBO-04/CS-10	Migmatite gneiss	2.16	65.76	356.09	660.26	54.38	196.74	26.79	1.57	19.37	2.52	11.51	1.88	7.42	0.77	6.74	<0.5	21.4	3.57	1295.83	50.21	1346.04	24.97	67.92
21	22	RJBO-04/CS-11	Migmatite gneiss	3.26	149.55	771.73	1439.49	150.62	549.99	55.9	2.39	40.77	5.41	23.99	4.11	17.06	1.87	17.19	1.36	58.67	9.97	2970.12	111.76	3081.88	68.64	152.81
23	24	RJBO-04/CS-12	Migmatite gneiss	11.46	55.71	289.04	535.93	44.61	159.68	22.61	1.45	16.67	2.16	9.93	1.55	6.1	0.62	5.5	<0.5	18.08	3.67	1053.32	42.53	1095.85	21.75	67.17
25	26	RJBO-04/CS-13	syenite	24.77	32.22	62.5	169.7	13.95	55.4	9.39	1.33	7.02	0.97	5.72	0.97	3.56	<0.5	3.12	<0.5	5.3	1.96	312.27	21.36	333.63	7.26	56.99
27	28	RJBO-04/CS-14	syenite	1.69	84.74	488.09	904.4	75.1	260.49	35.27	1.65	25.48	3.38	14.94	2.39	8.87	0.85	6.8	<0.5	42.91	5.41	1765	62.71	1827.71	48.32	86.43
29	30	RJBO-04/CS-15	syenite	1.35	77.19	402.78	742.97	60.87	206.04	28.69	1.43	21.02	2.83	12.6	2.12	8.07	0.81	7.07	<0.5	33.08	6	1442.78	54.52	1497.3	39.08	78.54
31	32	RJBO-04/CS-16	syenite	1.44	86.33	486.22	897.46	73.03	253.43	34.04	1.57	25.3	3.33	14.91	2.43	9.1	0.9	7.65	0.54	40.59	7.18	1745.75	64.16	1809.91	47.77	87.77
33	34	RJBO-04/CS-17	syenite	1.69	92.86	478.65	871.57	70.96	244.84	33.5	1.54	24.74	3.41	15.53	2.57	9.57	0.94	8.14	0.59	37.38	7.13	1701.06	65.49	1766.55	44.51	94.55
35	36	RJBO-04/CS-18	syenite	1.51	85.92	472.94	868.75	70.88	249.33	34.26	1.43	24.92	3.4	15.24	2.47	9.43	0.93	7.99	0.57	37.17	7.22	1697.59	64.95	1762.54	44.39	87.43
37	38	RJBO-04/CS-19	syenite	2.11	111.46	590.62	1089.28	89.71	312.3	43.36	1.87	32.02	4.24	19.14	3.17	12.42	1.24	11.2	0.8	47.33	10.35	2127.14	84.23	2211.37	57.68	113.57
39	40	RJBO-04/CS-20	syenite	2.69	97.18	516.16	958.73	84.58	284.16	39.92	1.72	28.6	3.81	17.48	2.82	10.54	1.05	8.96	0.66	39.71	8.18	1885.27	73.92	1959.19	47.89	99.87
41	42	RJBO-04/CS-21	syenite	2.63	99.41	558.59	1039.95	97.88	324.23	42.67	1.8	30.65	4.16	18.52	3.02	11.02	1.07	8.86	0.6	41.42	6.91	2065.12	77.9	2143.02	48.33	102.04
43	44	RJBO-04/CS-22	syenite	3.69	111.46	542.9	1015.25	83.89	309.39	43.24	1.83	31.53	4.04	18.93	3.15	12.51	1.27	11.08	0.79	45.56	10.36	1996.5	83.3	2079.8	55.92	115.15
45	46	RJBO-04/CS-23	syenite	2.32	92.87	511.3	945.67	78.76	279.82	39.72	1.73	28.31	3.79	16.9	2.67	9.99	0.95	8.28	0.58	40.33	6.45	1857	71.47	1928.47	46.78	95.19
47	48	RJBO-04/CS-24	syenite	5.43	95.56	342.03	640.56	55.26	211.08	34.21	1.68	24.73	3.5	17.88	3.02	11.54	1.16	9.93	0.72	20.31	5.19	1284.82	72.48	1357.3	25.5	100.99
49	50	RJBO-04/CS-25	syenite	4.24	98.69	446.04	842.31	70.92	259.68	39.88	1.69	29.05	3.96	19.46	3.11	11.53	1.15	9.74	0.75	36.04	6.12	1660.52	78.75	1739.27	42.16	102.93
51	52	RJBO-04/CS-26	syenite	4.08	98.68	543.47	866.27	63.02	193.07	30.01	1.66	29.03	3.39	17.66	3.37	11.04	1.48	9.69	1.34	25.44	6.77	1697.5	77	1774.5	32.21	102.76
53	54	RJBO-04/CS-27	syenite	3.73	148.71	689.52	1110.4	82.7	256.48	39.76	2.57	37.96	4.65	23.66	4.71	14.68	1.95	12.93	1.85	49.46	6.12	2181.43	102.39	2283.82	55.58	152.44

55	56	RJBO-04/CS-28	syenite	4.71	116.57	494.94	923.82	77.16	277.99	41.14	2.22	29.69	4.19	20.53	3.4	13.11	1.36	12.37	0.93	38.49	7.91	1817.27	85.58	1902.85	46.4	121.28
57	58	RJBO-04/CS-29	syenite	9.57	81.71	375.46	711.36	60.05	218.83	33.39	1.75	23.8	3.25	15.51	2.59	9.55	0.97	8.42	0.6	24.84	4.96	1400.84	64.69	1465.53	29.8	91.28
59	60	RJBO-04/CS-30	syenite	3.9	88.3	451.06	854.22	72.1	259.6	39.09	1.83	27.65	3.82	18.08	2.83	10.12	1.01	8.26	0.58	34.68	5.54	1677.9	72.35	1750.25	40.22	92.2
62	63	RJBO-04/CS-31	syenite	4.75	105.29	484.23	923.05	78.52	278.18	41.44	1.88	29.25	4.14	19.79	3.23	12.14	1.21	10.29	0.74	37.32	6.28	1807.3	80.79	1888.09	43.6	110.04
64	64	RJBO-04	syenite64 mtr	7.17	<0.5	4.7	75.35	452.87	842.5	70.77	257.95	38.12	1.57	27.32	3.59	16.27	2.51	9.03	0.85	42.49	8.2	1704.14	99.26	1803.4	50.69	7.17
65	66	RJBO-04/CS-32	syenite	12.49	73.39	340.26	641.56	54.42	201.71	30.29	1.65	22.17	3.02	15.13	2.36	8.72	0.83	7.08	<0.5	17.54	3.43	1269.89	59.31	1329.2	20.97	85.88
67	0	RJBO-04/CS-33	syenite	5.2	103.83	558.33	1036.5	86.51	309.59	45.41	1.94	33.22	4.52	21.43	3.38	12.39	1.21	9.99	0.73	34.7	6.09	2038.28	86.87	2125.15	40.79	109.03
68	69	RJBO-04/CS-34	syenite	6.24	88.42	293.21	543.51	46.15	171.02	27.31	1.84	20.09	3	16.29	2.78	10.2	1.09	9.61	0.74	16.73	6.04	1083.04	63.8	1146.84	22.77	94.66
70	71	RJBO-04/CS-35	syenite	7.52	57.93	156.46	300.56	27.05	101.06	16.91	1.45	12.22	1.89	10.73	1.82	6.63	0.72	6.5	<0.5	9.28	6.04	603.49	40.51	644	15.32	65.45
72	73	RJBO-04/CS-36	syenite	6.75	81.85	366.91	669.34	55.53	203.46	31.1	1.9	22.98	3.19	16.46	2.66	9.77	0.99	8.45	0.61	15.65	5.15	1328.24	65.11	1393.35	20.8	88.6
74	75	RJBO-04/CS-37	syenite	6.02	93.87	486.8	905.3	75.46	268.17	39.37	1.81	28.58	4	18.93	3.04	11	1.07	9.25	0.67	29.68	4.86	1776.91	76.54	1853.45	34.54	99.89
76	77	RJBO-04/CS-38	syenite	6.79	95.17	444.33	836.33	70.08	247.84	37.07	1.74	26.75	3.86	18.71	3.1	11.46	1.14	9.94	0.69	30.28	4.82	1637.39	75.65	1713.04	35.1	101.96
78	79	RJBO-04/CS-39	syenite	9.46	92.39	290.58	559.05	48.75	181.82	30.97	2.32	21.97	3.38	17.78	2.95	10.53	1.08	9.66	0.71	27.91	6.18	1113.49	68.06	1181.55	34.09	101.85
80	81	RJBO-04/CS-40	syenite	10.21	91	266.68	507.79	44.53	168.92	28.77	2.19	20.6	3.17	17.01	2.84	10.27	1.1	9.96	0.74	22.49	6.67	1018.88	65.69	1084.57	29.16	101.21
82	83	RJBO-04/CS-41	syenite	8.99	92.32	328.27	616.7	52.66	200.26	32.73	2.37	23.89	3.46	18.38	3	10.85	1.12	9.48	0.7	23.56	5.93	1232.99	70.88	1303.87	29.49	101.31
84	85	RJBO-04/CS-42	syenite	11.76	133.21	324.88	623.22	55.17	213.15	38.57	2.84	28.32	4.37	24.84	4.1	15.44	1.6	13.97	1.05	24.69	8.86	1257.83	93.69	1351.52	33.55	144.97

23.9 Annexure IX- External Check Samples (IISc Lab)

Sample Name	Y	La	Ce	Pr	Nd	Sm	Eu	Gd	Tb	Dy	Ho	Er	Tm	Yb	Lu
RJBO/T1-09	133.51	716.87	1215.93	127.49	354.01	49.34	2.02	41.81	5.57	29.41	4.86	12.91	1.85	11.17	1.59
RJBO/T1-01	98.47	314.81	556.64	58.38	179.89	26.57	1.83	25.82	3.18	17.89	3.35	9.61	1.55	10.49	1.63
RJBO/T2-06	107.51	353.52	623.49	61.47	206.25	32.03	3.63	29.70	4.06	22.67	4.01	10.65	1.50	9.00	1.32
RJBO/T2-14	64.15	158.73	275.31	32.22	111.47	18.95	2.05	16.99	2.41	13.12	2.42	6.57	0.94	5.80	0.84
RJBO/T3-14	133.87	419.14	745.93	77.28	240.53	37.50	2.25	35.94	4.63	27.26	4.86	13.12	1.95	12.10	1.66
RJBO/T3-13	144.04	403.39	682.55	75.02	236.19	36.83	3.06	33.34	4.55	25.42	4.97	13.93	2.06	13.34	1.89
RJBO/T4-19	134.54	267.84	490.44	52.32	167.31	28.13	2.13	25.73	3.92	22.78	4.60	13.20	2.03	13.02	1.85
RJBO/T4-11	16.78	33.06	58.42	6.43	20.52	3.33	0.44	3.01	0.44	2.78	0.55	1.71	0.27	1.99	0.30
RJBO/T5-16	90.03	286.11	561.96	55.31	175.97	27.41	1.97	25.09	3.16	17.92	3.18	9.00	1.41	9.17	1.34
RJBO/T5-08	26.27	63.34	146.22	12.48	40.69	6.71	0.80	6.43	0.85	4.80	0.91	2.58	0.38	2.57	0.37
RJBO/BRS-61	123.84	315.26	599.97	62.67	196.71	31.71	2.62	31.00	3.84	21.56	4.22	12.15	1.82	11.23	1.70
RJBO/BRS-105	258.93	574.99	1029.92	112.88	371.61	62.27	3.51	56.58	8.27	46.15	9.00	25.35	3.80	22.77	3.32
RJBO/BRS-03	161.94	658.87	1203.90	119.29	355.55	52.85	1.63	47.00	6.13	34.54	6.16	17.32	2.39	14.30	2.10
RJBO/BRS-49	139.41	596.83	1058.60	109.10	336.44	46.03	2.26	42.08	5.08	26.69	4.58	13.59	1.94	11.91	1.83
RJBO/BRS-47	107.47	365.07	680.35	68.46	219.52	34.02	2.15	31.51	4.09	21.58	3.91	11.07	1.52	9.06	1.33
RJBO/BRS-23	93.54	399.27	729.65	76.23	231.96	33.85	1.31	34.00	3.41	17.87	2.97	8.49	1.13	6.96	1.02
RJBO/BRS-02	116.47	630.63	1114.07	108.68	311.07	38.95	1.69	35.93	3.95	20.58	3.46	10.34	1.36	8.80	1.35
RJBO/BRS-10	115.42	483.01	884.88	93.12	298.86	45.17	3.69	40.99	5.21	26.14	4.49	11.95	1.54	9.01	1.26
RJBO/BRS-92	66.56	19.47	43.70	4.09	13.99	3.96	0.84	6.00	1.61	13.25	3.44	10.81	1.89	12.45	1.83
RJBO/BRS-07	29.76	2.43	6.59	1.14	6.53	2.46	0.83	3.25	0.66	4.66	1.08	3.10	0.48	3.10	0.48

Sample ID	Y	La	Ce	Pr	Nd	Sm	Eu	Gd	Tb	Dy	Ho	Er	Tm	Yb	Lu	TREE
G3051-14	198.96	954.10	1688.23	172.30	663.89	69.91	3.34	76.11	8.03	41.18	7.77	21.78	2.91	16.93	2.33	3728.79
G3051-186	176.46	897.62	1601.92	164.07	626.17	58.00	2.56	61.40	5.79	28.54	5.53	17.59	2.71	17.97	2.69	3492.55
G3051-140	178.89	693.05	1259.10	135.01	518.07	63.18	3.00	65.45	7.16	36.37	6.70	18.42	2.47	14.63	2.04	2824.66
G3051-139	204.46	619.93	1153.24	127.33	486.73	64.49	3.11	67.99	7.85	41.67	7.81	21.14	2.83	16.45	2.31	2622.85
G3051-08	111.81	511.09	909.77	92.58	355.78	35.40	1.63	32.98	3.83	19.90	3.82	11.57	1.69	10.64	1.48	1992.15
G3051-202	157.01	493.00	894.94	95.33	361.56	41.31	2.33	37.47	4.73	25.06	4.91	14.35	2.07	13.25	1.96	1992.30
G3051-194	116.68	583.77	1036.28	105.47	406.02	39.65	1.72	36.45	4.06	20.10	3.81	11.45	1.65	10.52	1.55	2262.50
G3051-196	96.77	531.04	949.55	97.73	374.43	36.91	1.54	34.21	3.77	18.31	3.37	9.68	1.32	8.09	1.16	2071.09
G3051-208	118.66	581.77	1037.90	107.02	409.60	43.06	1.90	40.54	4.70	23.73	4.43	12.66	1.76	10.80	1.53	2281.39
G3051-31	25.20	2.17	5.87	1.10	4.74	2.21	0.79	2.99	0.60	4.34	0.97	2.76	0.44	2.83	0.43	32.25
G3051-221	32.46	2.79	7.27	1.33	5.76	2.60	0.91	3.55	0.71	5.14	1.16	3.28	0.51	3.24	0.50	38.76
G3051-220	28.64	2.66	6.90	1.26	5.39	2.43	0.87	3.36	0.68	4.79	1.10	3.11	0.49	3.10	0.48	36.62
G3051-219	29.93	3.86	8.40	1.42	6.16	2.60	0.89	3.54	0.69	4.87	1.11	3.16	0.49	3.09	0.47	40.78
G3051-218	30.08	4.67	10.00	1.62	6.93	2.69	0.91	3.59	0.69	4.93	1.11	3.19	0.49	3.14	0.48	44.44
G3051-30	32.22	3.09	7.90	1.44	6.25	2.76	0.97	3.75	0.74	5.30	1.19	3.43	0.53	3.36	0.51	41.22
G3051-143	102.58	323.47	546.93	64.20	247.58	31.66	2.23	27.66	3.67	19.67	3.80	10.48	1.44	8.40	1.16	1292.33
G3051-82	124.50	335.90	575.18	66.47	256.71	32.54	2.17	28.44	3.82	21.00	4.17	12.05	1.76	11.12	1.63	1352.95
G3051-159	109.52	366.30	614.22	70.49	274.00	33.83	2.30	29.36	3.82	20.33	3.89	10.95	1.52	9.06	1.29	1441.38
G3051-94	123.46	311.83	525.97	61.01	235.88	30.44	2.21	27.18	3.73	20.67	4.12	11.73	1.74	10.68	1.57	1248.75
G3051-92	116.97	336.14	565.81	65.40	253.45	30.86	2.16	27.06	3.57	19.80	3.93	11.50	1.74	11.04	1.63	1334.09
G3051-165	106.77	342.61	570.16	64.59	251.40	29.41	2.11	25.92	3.43	18.42	3.64	10.53	1.53	9.29	1.32	1334.36
G3051-164	104.11	350.99	585.52	66.71	258.49	30.58	2.22	26.92	3.48	18.43	3.60	10.25	1.51	9.39	1.37	1369.46

23.10 Annexure X- Logsheets

Logsheet for BH 1

BORE HOLE NO	RJB-01		
TOPOSHEET NO	45K/03		
LOCATION	LAT	25° 25' 53.9427"	
	LONG	74° 07' 32.6900"	
R L OF COLLAR	507.092		
BH. ANGLE	45		
AZIMUTH	N45°W	TOTAL DRILLING TARGET	85 m
INCLINATION	45	DRILL TYPE	Core Drilling
BH DEPTH	85		

FROM (m)	TO (m)	RUN (m)	RECOVERY (%)	CORE SIZE	RQD %	GRAIN SIZE	COLOUR	MINERALOGY	ROCK TYPE	DESCRIPTION
0.00	3.00	3.00	50.00%	NQ	0.00	medium to coarse	pinkish brown	allanite /magnetite & quartz	Weathered Syenite	Highly weathered syenite, predominantly of a reddish-brown in color, moderately compact sandy soil. The color is reddish-brown, indicative of iron oxide staining, possibly due to prolonged weathering.
3.00	5.00	2.00	50.00%	NQ	0.00	medium to coarse	pinkish brown	allanite /magnetite & quartz	Weathered Syenite	Highly weathered syenite, predominantly of a reddish-brown in color, moderately compact sandy soil. The color is reddish-brown, indicative of iron oxide staining.
5.00	5.55	0.55	54.55%	NQ	0.00	medium to coarse	pinkish brown	allanite /magnetite & quartz	Weathered Syenite	Highly weathered syenite, predominantly of a reddish-brown in color, moderately compact sandy soil. The color

										is reddish-brown, indicative of iron oxide staining.
5.55	6.00	0.45	55.56%	NQ	0.00	medium to coarse	pinkish black to white	allanite /magnetite & quartz	Syenite	The core consists of coarse- to medium-grained syenite with epidote veins, displaying a light grey to pinkish-grey color. The rock is predominantly composed of alkali feldspar, with minor plagioclase.
6.00	9.00	3.00	75.00%	NQ	11.00	medium to coarse	pinkish black to white	allanite /magnetite & quartz	Syenite	The core interval consists of a coarse- to medium-grained syenite with epidote vein, displaying a light grey to pinkish-grey colour. The rock is predominantly composed of alkali feldspar, with minor plagioclase.
9.00	10.00	1.00	60.00%	NQ	11.00	medium to coarse	pinkish black to white	allanite /magnetite & quartz	Syenite	The core consists of coarse- to medium-grained syenite with an epidote vein, displaying a light grey to pinkish-grey color. The rock is predominantly composed of alkali feldspar, with minor plagioclase.
10.00	12.00	2.00	85.00%	NQ	35.75	medium to coarse	pinkish black to white	allanite /magnetite & quartz	Syenite	The core consists of a coarse- to medium-grained syenite with epidote vein, displaying a light grey to pinkish-grey colour. The rock is predominantly composed of alkali feldspar, with minor plagioclase.
12.00	13.00	1.00	70.00%	NQ	10.00 %	medium to coarse	pinkish black to white	allanite /magnetite & quartz	Syenite	The core consists of a coarse- to medium-grained syenite with epidote vein, displaying a light grey to pinkish-grey colour. The rock is predominantly composed of alkali feldspar, with minor plagioclase.
13.00	13.60	0.60	66.67%	NQ	0.00%	medium to coarse	pinkish black to white	allanite /magnetite & quartz	Syenite	The core consists of a coarse- to medium-grained syenite with epidote vein, displaying a light grey to pinkish-grey colour. The rock is predominantly composed of alkali feldspar, with minor plagioclase.
13.60	15.00	1.40	85.71%	NQ	17.85 %	medium to coarse	pinkish black to white	allanite /magnetite & quartz	Syenite	The core consists of a coarse- to medium-grained syenite with epidote vein, displaying a light grey to pinkish-grey colour. The rock is predominantly composed of alkali feldspar, with minor plagioclase.
15.00	18.00	3.00	88.33%	NQ	51.67 %	medium to coarse	pinkish black to white	allanite /magnetite & quartz	Syenite	The core consists of a coarse- to medium-grained syenite with epidote vein, displaying a light grey to pinkish-grey colour. The rock is predominantly composed of alkali feldspar, with minor plagioclase.
18.00	20.00	2.00	97.50%	NQ	96.50 %	medium to coarse	pinkish black to white	allanite /magnetite & quartz	Syenite	The core consists of a coarse- to medium-grained syenite with epidote vein & allanite in dissiminated form, displaying a light grey to pinkish-grey colour. The rock is

										predominantly composed of alkali feldspar, with minor plagioclase.
20.00	21.00	1.00	95.00%	NQ	58.00 %	medium to coarse	pinkish black to white	allanite /magnetite & quartz	Syenite	The core consists of a coarse- to medium-grained syenite with epidote vein, displaying a light grey to pinkish-grey colour. The rock is predominantly composed of alkali feldspar, with minor plagioclase.
21.00	24.00	3.00	95.00%	NQ	78.00 %	medium to coarse	pinkish black to white	allanite /magnetite & quartz	Syenite	The core consists of a coarse- to medium-grained syenite with epidote vein, displaying a light grey to pinkish-grey colour. The rock is predominantly composed of alkali feldspar, with minor plagioclase.
24.00	25.00	1.00	97.00%	NQ	80.00 %	medium to coarse	pinkish black to white	allanite /magnetite & quartz	Syenite	The core consists of a coarse- to medium-grained syenite with epidote vein, displaying a light grey to pinkish-grey colour. The rock is predominantly composed of alkali feldspar, with minor plagioclase.
25.00	27.00	2.00	96.50%	NQ	75.50 %	medium to coarse	pinkish black to white	allanite /magnetite & quartz	Syenite	The core consists of a coarse- to medium-grained syenite with epidote vein, displaying a light grey to pinkish-grey colour. The rock is predominantly composed of alkali feldspar, with minor plagioclase.
27.00	30.00	3.00	94.00%	NQ	70.66 %	medium to coarse	pinkish black to white	allanite /magnetite & quartz	Syenite	The core consists of a coarse- to medium-grained syenite with epidote vein & allanite in dissiminated form, displaying a light grey to pinkish-grey colour. The rock is predominantly composed of alkali feldspar, with minor plagioclase.
30.00	33.00	3.00	91.67%	NQ	58.67 %	medium to coarse	pinkish black to white	allanite /magnetite & quartz	Syenite	The core consists of coarse- to medium-grained syenite with epidote veins and disseminated allanite, displaying a light grey to pinkish-grey color. The rock is predominantly composed of alkali feldspar, with minor plagioclase.
33.00	35.00	2.00	97.50%	NQ	93.00 %	medium to coarse	pinkish black to white	allanite /magnetite & quartz	Syenite	The core consists of a coarse- to medium-grained syenite with epidote vein, displaying a light grey to pinkish-grey colour. The rock is predominantly composed of alkali feldspar, with minor plagioclase.
35.00	36.00	1.00	70.00%	NQ	43.00 %	medium to coarse	pinkish black to white	allanite /magnetite & quartz	Syenite	The core consists of a coarse- to medium-grained syenite with epidote vein, displaying a light grey to pinkish-grey colour. The rock is predominantly composed of alkali feldspar, with minor plagioclase.
36.00	39.00	3.00	91.67%	NQ	79.33	medium	pinkish black to	allanite /magnetite &	Syenite	The core consists of a coarse- to medium-grained syenite

					%	to coarse	white	quartz		with epidote vein, displaying a light grey to pinkish-grey colour. The rock is predominantly composed of alkali feldspar, with minor plagioclase.
39.00	40.00	1.00	96.00%	NQ	82.00 %	medium to coarse	pinkish black to white	allanite /magnetite & quartz	Syenite	The core consists of a coarse- to medium-grained syenite with epidote vein, displaying a light grey to pinkish-grey colour. The rock is predominantly composed of alkali feldspar, with minor plagioclase.
40.00	41.65	1.65	93.33%	NQ	83.03 %	medium to coarse	pinkish black to white	allanite /magnetite & quartz	Syenite	The core consists of a coarse- to medium-grained syenite with epidote vein, displaying a light grey to pinkish-grey colour. The rock is predominantly composed of alkali feldspar, with minor plagioclase.
41.65	42.00	0.35	94.29%	NQ	57.14 %	medium to coarse	pinkish gray to yellowish	allanite /magnetite & quartz	Syenite intermixed with Amphibolite	The core consists of a coarse- to medium-grained syenite & intermixed with amphibolite, displaying a light grey to pinkish-grey colour. The rock is predominantly composed of alkali feldspar, with minor plagioclase and ambhiboles.
42.00	45.00	3.00	95.33%	NQ	83.00 %	medium to coarse	Greenish gray & Pink	chlorite & epidote	Amphibolite	The core consists of amphibolite, dark greenish in color, massive in nature, and weakly foliated. It is primarily composed of hornblende and epidote, which impart a dark coloration and contribute to its dense, compact appearance.
45.00	48.00	3.00	95.00%	NQ	89.67 %	fine to medium	pinkish brown	chlorite & quartz	Amphibolite	The core consists of weakly fractured amphibolite, dark greenish in color, massive in nature, and weakly foliated. It is composed mainly of plagioclase and hornblende, which contribute to its dark coloration and dense, compact appearance.
48.00	50.00	2.00	94.50%	NQ	79.50 %	fine to medium	pinkish brown	chlorite & quartz	Amphibolite	The core consists of weakly fractured amphibolite, dark greenish in color, massive in nature, and weakly foliated. It is composed mainly of plagioclase and hornblende, which contribute to its dark coloration and dense, compact appearance.
50.00	51.00	1.00	85.00%	NQ	59.00 %	fine to medium	pinkish brown	chlorite & quartz	Amphibolite	The core consists of weakly fractured amphibolite, dark greenish in color, massive in nature, and weakly foliated. It is composed of plagioclase and hornblende, which impart a dark hue and contribute to its dense, compact appearance.
51.00	54.00	3.00	96.67%	NQ	94.66 %	fine to medium	pinkish brown	Quartz & Mica	Amphibolite	Weakly fractured amphibolite dark greenish in colour massive in nature with weakly foliated with consist of plagioclase & hornblend in dark colour and contributing to

										dense compact appearance.
54.00	55.00	1.00	96.00%	NQ	96.00 %	fine to medium	pinkish brown	Quartz & Mica	Amphibolite	Weakly fractured amphibolite dark greenish in colour massive in nature with weakly foliated with consist of plagioclase & hornblend in dark colour and contributing to dense compact appearance.
55.00	58.00	3.00	95.67%	NQ	78.00 %	fine to medium	pinkish brown	Quartz & Mica	Amphibolite	Weakly fractured amphibolite dark greenish in colour massive in nature with weakly foliated with consist of plagioclase & hornblend in dark colour and contributing to dense compact appearance.
58.00	60.00	2.00	95.00%	NQ	95.00 %	fine to medium	pinkish brown	Quartz & Mica	Amphibolite	Weakly fractured amphibolite dark greenish in colour massive in nature with weakly foliated with consist of plagioclase & hornblend in dark colour and contributing to dense compact appearance.
60.00	63.00	3.00	94.33%	NQ	94.33 %	fine to medium	pinkish brown	Quartz & Mica	Amphibolite	Weakly fractured amphibolite dark greenish in colour massive in nature with weakly foliated with consist of plagioclase & hornblend in dark colour with 3 cm thick quartz vein intruded at 62.75m run.
63.00	65.00	2.00	92.50%	NQ	92.00 %	fine to medium	pinkish brown	Quartz & Mica	Amphibolite	Weakly fractured amphibolite dark greenish in colour massive in nature with weakly foliated with consist of plagioclase & hornblend in dark colour and contributing to dense compact appearance.
65.00	66.00	1.00	93.00%	NQ	93.00 %	fine to medium	pinkish brown	Quartz & Mica	Amphibolite	Weakly fractured amphibolite dark greenish in colour massive in nature with weakly foliated with consist of plagioclase & hornblend in dark colour and contributing to dense compact appearance.
66.00	69.00	3.00	95.00%	NQ	95.00 %	fine to medium	pinkish brown	Quartz & Mica	Amphibolite	Weakly fractured amphibolite dark greenish in colour massive in nature with weakly foliated with consist of plagioclase & hornblend in dark colour and contributing to dense compact appearance.
69.00	70.00	1.00	96.00%	NQ	96.00 %	fine to medium	pinkish brown	Pyroxene Mica & Chalcopyrite	Amphibolite	The core consists of weakly fractured amphibolite with pyroxene and chlorite, dark greenish in color, massive in nature, and weakly foliated. It is composed of plagioclase and hornblende, contributing to its dark appearance. Disseminated chalcopyrite is present, along with a 1.5 cm thick quartz vein.
70.00	72.00	2.00	95.00%	NQ	95.00	fine to	pinkish brown	Pyroxene Mica &	Amphibolite	The core consists of weakly fractured amphibolite with

					%	medium		Chalcopyrite		pyroxene and chlorite, dark greenish in color, massive in nature, and weakly foliated. It comprises plagioclase and hornblende, contributing to its dark coloration and dense appearance. Disseminated chalcopyrite is also observed.
72.00	75.00	3.00	96.67%	NQ	96.67 %	fine to medium	pinkish brown	Pyroxene Mica & Chalcopyrite	Amphibolite	The core consists of weakly fractured amphibolite with pyroxene and chlorite, exhibiting a dark greenish color. It is massive in nature and weakly foliated. The rock is composed of plagioclase and hornblende, contributing to its dark, dense appearance. Disseminated chalcopyrite is also observed.
75.00	76.65	1.65	96.36%	NQ	96.36 %	fine to medium	pinkish brown	Mica & Quartz	Amphibolite	The core consists of weakly fractured amphibolite, dark greenish in color, massive in nature, and weakly foliated. It is composed of plagioclase and hornblende, which impart a dark hue and contribute to its dense, compact appearance.
76.65	78.00	1.35	98.52%	NQ	98.51 %	fine to medium	Yellowish green to gray	chlorite chalcopyrite amphibolite & mica	Amphibolite	The core consists of weakly fractured amphibolite with pyroxene and chlorite, dark greenish in color, massive in nature, and weakly foliated. It is composed of plagioclase and hornblende, contributing to its dark, compact appearance. Disseminated pyrite is also observed.
78.00	80.00	2.00	99.00%	NQ	98.00 %	fine to medium	Greenish black to white	Mica & Quartz	Amphibolite	The core consists of weakly fractured amphibolite, dark greenish in color, massive in nature, and weakly foliated. It is primarily composed of plagioclase and hornblende, which contribute to its dark coloration and dense, compact appearance.
80.00	81.00	1.00	94.00%	NQ	94.00 %	fine to medium	Greenish black to white	Mica & Quartz	Amphibolite	The core consists of weakly fractured amphibolite, dark greenish in color, massive in nature, and weakly foliated. It is composed of plagioclase and hornblende, which give the rock its dark coloration and contribute to its dense, compact appearance.

Log Sheet for BH 2

BORE HOLE NO	**RJB-02**		
TOPOSHEET NO	**45K/03**		
LOCATION	**LAT**	**25° 25' 10.5262"**	
	LONG	**74° 07' 18.0708"**	
RL OF COLLAR	**504.521**		
BH. ANGLE	**45°**		
AZIMUTH	**N45°W**		
INCLINATION	**45°**	**TOTAL DRILLING TARGET**	**154 m**
BH DEPTH	**154.64m**		

FROM (m)	TO (m)	RUN (m)	RECOVERY (%)	CORE SIZE	RQD %	GRAIN SIZE	COLOUR	MINERALOGY	ROCK TYPE	DESCRIPTION
0.00	3.00	3.00	50.00	NQ	0	Medium	Reddish-brown	quratz, Mica	Weathered Migmatite Gneiss	Highly weathered zone, predominantly of a reddish-brown in color, moderately compact sandy soil. The color is reddish-brown, indicative of iron oxide staining, possibly due to prolonged weathering.
3.00	6.00	3.00	50.00	NQ	0	Fine to medium grain	Reddish-brown	quratz, Mica	Weathered Migmatite Gneiss	Highly weathered zone, predominantly of a reddish-brown in color, moderately compact sandy soil. The color is reddish-brown, indicative of iron oxide staining, possibly due to prolonged weathering.
6.00	9.00	3.00	65.00	NQ	0	Fine to medium grain	Reddish-brown	quratz, Mica	Weathered Migmatite Gneiss	Highly weathered zone, predominantly of a reddish-brown in color, moderately compact sandy soil. The color is reddish-brown, indicative

										of iron oxide staining.
9.00	10.70	1.70	70.59	NQ	0	medium grain	Reddish	quratz, Mica	Weathered Migmatite Gneiss	Highly weathered zone, predominantly of a reddish-brown in color, moderately compact sandy soil with occasional gravel-sized fragments. The color is reddish-brown, indicative of iron oxide staining, possibly due to prolonged weathering.
10.70	11.25	0.55	81.82	NQ	0	medium grain	Black to white & redish	Allanite/magnetite	Weathered Syenite	Weathered syenites are observed. The rock is highly decomposed, with a friable to crumbly texture and variable coloration ranging from light brown to pale reddish grey, indicating oxidation.
11.25	11.86	0.61	73.77	NQ	0	medium grain	Black to white & redish	Allanite/magnetite	Migmatite gneiss and syenite intermix	The core run comprises migmatite interlayered with syenite. Migmatite displays alternating bands of leucosome and melanosome, with leucosome enriched in orthoclase feldspar. The syenite is coarse-grained, light pink to salmon in color, and dominated by alkali feldspar, primarily orthoclase and microcline.
11.86	12.00	0.14	85.71	NQ	0	medium grain	Black to white & redish	Allanite/magnetite	Migmatite gneiss	The core consists of migmatite characterized by alternating leucocratic and melanocratic bands. The leucocratic bands are dominated by coarse-grained orthoclase feldspar, appearing as pink to salmon-colored crystals, often forming megacrysts or intergrown aggregates. Orthoclase dominates the felsic bands.
12.00	12.35	0.35	94.29	NQ	34.28%	Fine to medium grain	Black to pinkish	Mica, Magnetite	Migmatite gneiss and syenite intermix	The core run comprises migmatite interlayered with syenite. Migmatite displays alternating bands of leucosome and melanosome, with leucosome enriched in orthoclase feldspar. The syenite is coarse-grained, light pink to salmon in color, and dominated by alkali feldspar, primarily orthoclase and microcline.
12.35	13.75	1.40	50.00	NQ	0	Fine to medium grain	Black to pinkish	Mica, Magnetite	Migmatite gneiss and syenite intermix	The core comprises migmatite intermixed with syenite, displaying alternating bands of leucosome and melanosome. The leucosome is notably enriched in orthoclase feldspar, while the

										syenite exhibits a coarse-grained texture and overall light pink to salmon coloration. The rock is dominated by alkali feldspar, primarily orthoclase and microcline.
13.75	14.09	0.34	73.53	NQ	0	Fine to medium grain	Black to pinkish	Allanite/magnetite	Migmatite gneiss	The core consists of migmatite with alternating leucocratic and melanocratic bands. The leucocratic bands are rich in coarse-grained orthoclase feldspar, appearing as pink to salmon-colored megacrysts or intergrown aggregates. Orthoclase is the dominant phase in the felsic layers.
14.09	14.77	0.68	60.29	NQ	0	Fine to medium grain	Black to white & redish	Allanite/magnetite	Migmatite Gneiss	The core comprises migmatite exhibiting alternating leucocratic (light-colored) and melanocratic (dark-colored) bands. The leucocratic bands are enriched in coarse-grained orthoclase feldspar, typically appearing as pink to salmon-colored crystals that often form large megacrysts or intergrown aggregates. Orthoclase is the dominant mineral phase within the felsic layers.
14.77	15.00	0.23	78.26	NQ	0	Fine to medium grain	pink to Black	Allanite/magnetite	Migmatite Gneiss	The core is of migmatite with well-defined alternating leucocratic (light-colored) and melanocratic (dark-colored) bands. The leucocratic zones are dominated by coarse-grained orthoclase feldspar, typically pink to salmon in color, often forming large megacrysts or intergrown aggregates. Orthoclase is the principal constituent of the felsic bands.
15.00	16.26	1.26	67.46	NQ	0	Fine to medium grain	Redish Black to white	–	Migmatite Gneiss	The core consists of migmatite with alternating leucocratic (light-colored) and melanocratic (dark-colored) bands. The leucocratic portions are rich in coarse-grained orthoclase feldspar, which appears as pink to salmon-colored crystals, often forming large megacrysts or intergrown aggregates. Orthoclase is the dominant mineral in the felsic bands.

16.26	17.32	1.06	85.85	NQ	18.86	Fine to medium grain	Redish Black to white	Epidote vein, Allanite/Magnetite	Syenite	The core interval consists of a coarse- to medium-grained syenite with epidote vein, displaying a light grey to pinkish-grey colour. The rock is predominantly composed of alkali feldspar, with minor plagioclase.
17.32	18.00	0.68	85.29	NQ	47.05	Fine to medium grain	Redish Black to white	Epidote vein, Allanite/Magnetite	Syenite	The core interval consists of a coarse- to medium-grained syenite with epidote vein, displaying a light grey to pinkish-grey colour. The rock is predominantly composed of alkali feldspar, with minor plagioclase.
18.00	19.60	1.60	95.00	NQ	50.00	Fine to medium grain	Redish Black to white	Allanite/magnetite	Migmatite Geniss	The run consists of migmatite with alternating leucocratic (light-colored) and melanocratic (dark-colored) bands. The leucocratic portions are enriched in coarse-grained orthoclase feldspar, appearing as pink to salmon-colored crystals, often forming large megacrysts or intergrown aggregates.
19.60	20.00	0.40	55.00	NQ	0.00	Fine to medium grain	Black to Yellow	Allanite/magnetite	Migmatite Geniss	The run consists of migmatite with alternating leucocratic (light-colored) and melanocratic (dark-colored) bands. The leucocratic portions are enriched in coarse-grained orthoclase feldspar, appearing as pink to salmon-colored crystals, often forming large megacrysts or intergrown aggregates.
20.00	20.54	0.54	59.26	NQ	0.00	Fine to medium grain	Black to Yellow	Allanite/magnetite	Migmatite Geniss	The run consists of migmatite with alternating leucocratic (light-colored) and melanocratic (dark-colored) bands. The leucocratic portions are enriched in coarse-grained orthoclase feldspar, appearing as pink to salmon-colored crystals, often forming large megacrysts or intergrown aggregates.
20.54	21.00	0.46	100.00	NQ	0.00	Fine to medium grain	pink to Black	Allanite/magnetite	Migmatite Geniss	The run consists of migmatite with alternating leucocratic (light-colored) and melanocratic (dark-colored) bands. The leucocratic portions are enriched in coarse-grained orthoclase feldspar, appearing as pink to salmon-colored

										crystals, often forming large megacrysts or intergrown aggregates.
21.00	21.29	0.29	93.10	NQ	16.00	Fine to medium grain	pink to Black	quratz, Mica	Migmatite Gneiss	The run comprises migmatite with alternating leucocratic (light-colored) and melanocratic (dark-colored) bands. The leucocratic portions are rich in coarse-grained orthoclase feldspar, which appears as pink to salmon-colored crystals, often forming large megacrysts or intergrown aggregates. Orthoclase is the dominant mineral phase in the felsic bands.
21.29	21.39	0.10	80.00	NQ	0.00	Fine to medium grain	pink to Black	Feldspar, Quartz, Mica	Pegmatite	The core interval consists of a coarse- to medium-grained pegmatite vein, exhibiting a light grey to pinkish-grey color. The rock is predominantly composed of alkali feldspar and quartz, with minor amounts of mica.
21.39	24.00	2.61	96.93	NQ	81.80	Fine to medium grain	pink to Black	Feldspar, Quartz, Mica	Migmatite Geniss	The core consists of migmatite with alternating leucocratic (light-colored) and melanocratic (dark-colored) bands. The leucocratic zones are dominated by coarse-grained orthoclase feldspar, appearing as pink to salmon-colored crystals, frequently forming large megacrysts or intergrown aggregates.
24.00	25.00	1.00	97.00	NQ	88.00	Fine to medium grain	pink to Black	Feldspar, Quartz, Mica	Migmatite Geniss	The core consists of migmatite with alternating leucocratic (light-colored) and melanocratic (dark-colored) bands. The leucocratic zones are dominated by coarse-grained orthoclase feldspar, appearing as pink to salmon-colored crystals, frequently forming large megacrysts or intergrown aggregates.
25.00	27.00	2.00	99.00	NQ	93.00	Fine to medium grain	pink to Black	Feldspar, Quartz, Mica	Migmatite Geniss	The core consists of migmatite with alternating leucocratic (light-colored) and melanocratic (dark-colored) bands. The leucocratic zones are dominated by coarse-grained orthoclase feldspar, appearing as pink to salmon-colored crystals, frequently forming large megacrysts or intergrown aggregates.

27.00	27.40	0.40	100.00	NQ	52.00	Fine to medium grain	Black to White	Feldspar, Quartz, Mica	Migmatite Geniss	The core consists of migmatite with alternating leucocratic (light-colored) and melanocratic (dark-colored) bands. The leucocratic zones are dominated by coarse-grained orthoclase feldspar, appearing as pink to salmon-colored crystals, frequently forming large megacrysts or intergrown aggregates.
27.40	28.89	1.49	97.32	NQ	94.96	Fine to medium grain	Black to White	Feldspar, Quartz, Mica	Migmatite Geniss	The core consists of migmatite with alternating leucocratic (light-colored) and melanocratic (dark-colored) bands. The leucocratic zones are dominated by coarse-grained orthoclase feldspar, appearing as pink to salmon-colored crystals, frequently forming large megacrysts or intergrown aggregates.
28.89	30.00	1.11	97.30	NQ	90.09	Fine to medium grain	Black to White	Feldspar, Quartz, Mica	Migmatite Geniss	The core consists of migmatite with alternating leucocratic (light-colored) and melanocratic (dark-colored) bands. The leucocratic zones are dominated by coarse-grained orthoclase feldspar, appearing as pink to salmon-colored crystals, frequently forming large megacrysts or intergrown aggregates.
30.00	30.39	0.39	94.87	NQ	92.30	Fine to medium grain	Black to White	Feldspar, Quartz, Mica	Migmatite Geniss	The core consists of migmatite with alternating leucocratic (light-colored) and melanocratic (dark-colored) bands. The leucocratic zones are dominated by coarse-grained orthoclase feldspar, appearing as pink to salmon-colored crystals, frequently forming large megacrysts or intergrown aggregates.
30.39	33.00	2.61	99.23	NQ	99.23	Fine to medium grain	Black to White	Feldspar, Quartz, Mica	Migmatite Geniss	The core consists of migmatite with alternating leucocratic (light-colored) and melanocratic (dark-colored) bands. The leucocratic zones are dominated by coarse-grained orthoclase feldspar, appearing as pink to salmon-colored crystals, frequently forming large megacrysts or intergrown aggregates.
33.00	33.53	0.53	98.11	NQ	86.07	Fine to medium	Black to	Feldspar, Quartz, Mica	Migmatite Geniss	The core consists of migmatite characterized by

						grain	White			alternating leucocratic (light-colored) and melanocratic (dark-colored) bands. The leucocratic zones are enriched in coarse-grained orthoclase feldspar, typically appearing as pink to salmon-colored crystals, often forming large megacrysts or intergrown aggregates. Orthoclase is the dominant mineral in the felsic bands.
33.53	35.00	1.47	95.24	NQ	87.07	Fine to medium grain	Black to Yellow	Feldspar, Quartz, Mica	Migmatite Geniss	The core consists of migmatite characterized by alternating leucocratic (light-colored) and melanocratic (dark-colored) bands. The leucocratic zones are enriched in coarse-grained orthoclase feldspar, typically appearing as pink to salmon-colored crystals, often forming large megacrysts or intergrown aggregates. Orthoclase is the dominant mineral in the felsic bands.
35.00	35.19	0.19	100.00	NQ	100.00	Fine to medium grain	Black to Yellow	Feldspar, Quartz, Mica	Migmatite Geniss	The core consists of migmatite characterized by alternating leucocratic (light-colored) and melanocratic (dark-colored) bands. The leucocratic zones are enriched in coarse-grained orthoclase feldspar, typically appearing as pink to salmon-colored crystals, often forming large megacrysts or intergrown aggregates. Orthoclase is the dominant mineral in the felsic bands.
35.19	36.00	0.81	100.00	NQ	100.00	Fine to medium grain	_	Feldspar, Quartz, Mica	Migmatite Geniss	The core consists of migmatite characterized by alternating leucocratic (light-colored) and melanocratic (dark-colored) bands. The leucocratic zones are enriched in coarse-grained orthoclase feldspar, typically appearing as pink to salmon-colored crystals, often forming large megacrysts or intergrown aggregates. Orthoclase is the dominant mineral in the felsic bands.
36.00	36.75	0.75	96.00	NQ	96.00	Fine to medium grain	_	Feldspar, Quartz, Mica	Migmatite Geniss	The core consists of migmatite with alternating leucocratic (light-colored) and melanocratic (dark-colored) bands. The leucocratic portions are rich in coarse-grained orthoclase feldspar, appearing as pink to salmon-colored crystals that

										often form large megacrysts or intergrown aggregates.
36.75	38.23	1.48	98.65	NQ	86.48	Fine to medium grain	Black to white	Feldspar, Quartz, Mica	Migmatite Geniss	The core consists of migmatite with alternating leucocratic (light-colored) and melanocratic (dark-colored) bands. The leucocratic portions are rich in coarse-grained orthoclase feldspar, appearing as pink to salmon-colored crystals that often form large megacrysts or intergrown aggregates.
38.23	39.00	0.77	97.40	NQ	96.10	Fine to medium grain	Black to white	Feldspar, Quartz, Mica	Migmatite Geniss	The core consists of migmatite with alternating leucocratic (light-colored) and melanocratic (dark-colored) bands. The leucocratic portions are rich in coarse-grained orthoclase feldspar, appearing as pink to salmon-colored crystals that often form large megacrysts or intergrown aggregates.
39.00	40.00	1.00	97.00	NQ	97.00	Fine to medium grain	Black, white, pink	Feldspar, Quartz, Mica	Migmatite Geniss	The core of migmatite with alternating leucocratic (light-colored) and melanocratic (dark-colored) bands. The leucocratic portions are rich in orthoclase feldspar, which appears as coarse-grained, pink to salmon-colored crystals, often forming large megacrysts or intergrown aggregates. Orthoclase dominates the felsic bands.
40.00	41.79	1.79	95.53	NQ	95.53	Fine to medium grain	pink	Quartz, Allanite/magnetite	Migmatite Geniss	The core consists of migmatite with alternating leucocratic (light-colored) and melanocratic (dark-colored) bands. The leucocratic portions are rich in orthoclase feldspar, which appears as coarse-grained, pink to salmon-colored crystals, often forming large megacrysts or intergrown aggregates. Orthoclase dominates the felsic bands.
41.79	42.00	0.21	95.24	NQ	95.23	Fine to medium grain	Black to White	Quartz, Allanite/magnetite	Migmatite Geniss	The core is consisting of migmatite with alternating leucocratic (light-colored) and melanocratic (dark-colored) bands. The leucocratic portions are rich in orthoclase

										feldspar, which appears as coarse-grained, pink to salmon-colored crystals, often forming large megacrysts or intergrown aggregates. Orthoclase dominates the felsic bands.
42.00	45.00	3.00	99.33	NQ	99.33	Fine to medium grain	Light to Dark	Quartz, Biotite	Migmatite Geniss	The core is consisting of migmatite with alternating leucocratic (light-colored) and melanocratic (dark-colored) bands. The leucocratic portions are rich in orthoclase feldspar, which appears as coarse-grained, pink to salmon-colored crystals, often forming large megacrysts or intergrown aggregates. Orthoclase dominates the felsic bands.
45.00	45.71	0.71	100.00	NQ	100.00	Fine to medium grain	Light to Dark	Quartz, Biotite	Migmatite Gneiss	The core is consisting of migmatite with alternating leucocratic (light-colored) and melanocratic (dark-colored) bands. The leucocratic portions are rich in orthoclase feldspar, which appears as coarse-grained, pink to salmon-colored crystals, often forming large megacrysts or intergrown aggregates. Orthoclase dominates the felsic bands.
45.71	46.19	0.48	97.92	NQ	97.12	medium grain	pink, white to black	Epidote, Sodalite	Syenite	The core interval consists of coarse- to medium-grained syenite with epidote veining, displaying a light grey to pinkish-grey color. The rock is predominantly composed of alkali feldspar, with minor amounts of plagioclase.
46.19	48.00	1.81	98.90	NQ	98.89	medium grain	Light to Dark and pink	Quartz, Biotite, Hornblende	Migmatite Gneiss	The core consists of migmatite with alternating leucocratic (light-colored) and melanocratic (dark-colored) bands. The leucocratic portions are enriched in coarse-grained orthoclase feldspar, which appears as pink to salmon-colored crystals, often forming large megacrysts or intergrown aggregates. Orthoclase is the dominant mineral in the felsic bands.
48.00	49.77	1.77	100.00	NQ	100.00	Fine to medium grain	Light to Dark	Quartz, Biotite, Hornblende	Migmatite Gneiss	The core consists of migmatite with alternating leucocratic (light-colored) and melanocratic (dark-colored) bands. The leucocratic portions

										are enriched in coarse-grained orthoclase feldspar, which appears as pink to salmon-colored crystals, often forming large megacrysts or intergrown aggregates. Orthoclase is the dominant mineral in the felsic bands.
49.77	50.00	0.23	86.96	NQ	0.00	Fine to medium grain	Light to Dark	Quartz, Biotite, Hornblende	Migmatite Gneiss	The core consists of migmatite with alternating leucocratic (light-colored) and melanocratic (dark-colored) bands. The leucocratic portions are rich in orthoclase feldspar, which appears as coarse-grained, pink to salmon-colored crystals, often forming large megacrysts or intergrown aggregates. Orthoclase dominates the felsic bands.
50.00	51.00	1.00	96.00	NQ	53.00	Fine to medium grain	Pinkish and black to white	Epidote, zeolite, orthoclase	Migmatite Gneiss intermixed with syenite	The core consists of migmatite intermixed with syenite. The rock displays alternating bands of leucosome (light-colored) and melanosome (dark-colored), with the leucosome notably enriched in orthoclase feldspar. The syenite exhibits a coarse-grained texture and an overall light-colored appearance. It is dominated by alkali feldspar, primarily orthoclase and microcline.
51.00	53.09	2.09	98.09	NQ	98.08	Fine to medium grain	Pinkish to black	Quartz, Biotite, Hornblende	Migmatite Gneiss	The core consists of migmatite with alternating leucocratic (light-colored) and melanocratic (dark-colored) bands. The leucocratic portions are rich in orthoclase feldspar, which appears as coarse-grained, pink to salmon-colored crystals, often forming large megacrysts or intergrown aggregates. Orthoclase dominates the felsic bands.
53.09	53.74	0.65	100.00	NQ	100.00	Fine to medium grain	Black and white	Epidote, zeolite, orthoclase	Migmatite Gneiss intermixed with syenite	The core consists of migmatite intermixed with syenite. The rock displays alternating bands of leucosome (light-colored) and melanosome (dark-colored), with the leucosome notably enriched in orthoclase feldspar. The syenite exhibits a coarse-grained texture and an overall

										light-colored appearance. It is dominated by alkali feldspar, primarily orthoclase and microcline.
53.74	54.00	0.26	88.46	NQ	84.46	Fine to medium grain	Pinkish and black to white	Epidote, zeolite, orthoclase	Migmatite Gneiss intermixed with syenite	The core consists of migmatite intermixed with syenite. The rock displays alternating bands of leucosome (light-colored) and melanosome (dark-colored), with the leucosome notably enriched in orthoclase feldspar. The syenite exhibits a coarse-grained texture and an overall light-colored appearance. It is dominated by alkali feldspar, primarily orthoclase and microcline.
54.00	54.12	0.12	100.00	NQ	100.00	Fine to medium grain	white to black	Quartz, Biotite, Hornblende	Migmatite Gneiss	The core shows melanocratic (dark-colored) bands of migmatite alternating with leucocratic (light-colored) portions. The leucocratic zones are enriched in coarse-grained orthoclase feldspar, typically appearing as pink to salmon-colored crystals, often forming large megacrysts or intergrown aggregates.
54.12	55.00	0.88	94.32	NQ	94.31	coarse to medium grain	Pink to Black	Quartz, Biotite, orthoclase and epidote	Syenite	The core interval consists of a coarse- to medium-grained syenite with epidote vein, displaying a light grey to pinkish-grey colour. The rock is predominantly composed of alkali feldspar, with minor plagioclase.
55.00	55.75	0.75	97.33	NQ	85.33	coarse to medium grain	pink to Black	epidote, Pyrite and Quartz	Syenite	The core interval consists of a coarse- to medium-grained syenite with epidote vein, displaying a light grey to pinkish-grey colour. The rock is predominantly composed of alkali feldspar, minor plagioclase with sulphide dissiminated staining along the fracture quartz veins also observed.
55.73	56.62	0.89	97.75	NQ	86.52	coarse to medium grain	pinkish, White to Black	Epidote, Quartz	Syenite	The core interval consists of a coarse- to medium-grained syenite with epidote vein, displaying a light grey to pinkish-grey colour. The rock is predominantly composed of alkali feldspar, minor plagioclase with sulphide

										disseminated staining along the fracture quartz veins also observed.
56.62	57.00	0.38	94.74	NQ	71.05	coarse to medium grain	pinkish, White to Black	Epidote, Quartz	Syenite	The core interval consists of a coarse- to medium-grained syenite with epidote vein, displaying a light grey to pinkish-grey colour. The rock is predominantly composed of alkali feldspar, minor plagioclase with sulphide dissiminated staining along the fracture quartz veins also observed.
57.00	58.50	1.50	93.33	NQ	72.66	coarse to medium grain	pinkish, White to Black	Epidote, Quartz	Syenite	The core interval consists of a coarse- to medium-grained syenite with epidote vein, displaying a light grey to pinkish-grey colour. The rock is predominantly composed of alkali feldspar, minor plagioclase with limonitization along the fracture quartz veins also observed.
58.50	59.00	0.50	100.00	NQ	100.00	coarse to medium grain	pinkish, White to Black	Quartz, Feldspar	Syenite	The core interval consists of a coarse- to medium-grained syenite with epidote vein, displaying a light grey to pinkish-grey colour. The rock is predominantly composed of alkali feldspar, minor plagioclase with limonitization along the fracture quartz veins also observed.
59.00	59.83	0.83	98.80	NQ	98.79	coarse to medium grain	pinkish, White to Black	Quartz, Feldspar	Syenite	The core interval consists of a coarse- to medium-grained syenite with epidote vein, displaying a light grey to pinkish-grey colour. The rock is predominantly composed of alkali feldspar, minor plagioclase with limonitization along the fracture quartz veins also observed.
59.83	60.00	0.17	58.82	NQ	58.82	coarse to medium grain	white to black	Quartz, Hornblende, Biotite	Migmatite Gneiss	The core features melanocratic (dark-colored) migmatite bands alternating with leucocratic (light-colored) zones. The leucocratic portions are rich in orthoclase feldspar, which occurs as coarse-grained, pink to salmon-colored crystals, often forming large megacrysts or intergrown aggregates.
60.00	61.25	1.25	98.40	NQ	98.40	coarse to medium grain	pink, white to black	Epidote, Quartz, Feldspar	Syenite	The core interval consists of a coarse- to medium-grained syenite with epidote vein,

										displaying a light grey to pinkish-grey colour. The rock is predominantly composed of alkali feldspar, minor plagioclase observed.
61.25	63.00	1.75	97.14	NQ	88.57	coarse to medium grain	pink, white to black	Epidote, Quartz, Feldspar	Syenite	The core interval consists of a coarse- to medium-grained syenite with epidote vein, displaying a light grey to pinkish-grey colour. The rock is predominantly composed of alkali feldspar, minor plagioclase observed.
63.00	65.00	2.00	96.50	NQ	79.00	coarse to medium grain	pinkish, White to grey	Epidote, Quartz, Feldspar	Syenite	The core interval consists of a coarse- to medium-grained syenite with epidote vein, displaying a light grey to pinkish-grey colour. The rock is predominantly composed of alkali feldspar, minor plagioclase observed.
65.00	66.00	1.00	97.00	NQ	97.00	coarse to medium grain	pinkish, White to grey	Allanite/magnetite and epidote	Syenite	The core interval consists of a coarse- to medium-grained syenite with epidote vein, displaying a light grey to pinkish-grey colour. The rock is predominantly composed of alkali feldspar, minor plagioclase observed.
66.00	69.00	3.00	97.67	NQ	97.66	coarse to medium grain	pinkish, White to grey	Allanite/magnetite and epidote	Syenite	The core interval consists of a coarse- to medium-grained syenite with epidote vein, displaying a light grey to pinkish-grey colour. The rock is predominantly composed of alkali feldspar, minor plagioclase observed.
69.00	69.04	0.04	100.00	NQ	100.00	coarse to medium grain	pinkish, White to grey	Allanite/magnetite, pyrite and epidote	Syenite	The core interval consists of a coarse- to medium-grained syenite with epidote vein with dissiminated sulphide staining, displaying a light grey to pinkish-grey colour. The rock is predominantly composed of alkali feldspar, minor plagioclase observed.
69.04	70.00	0.96	98.96	NQ	98.95	coarse to medium grain	pinkish, White to grey	Allanite/magnetite, Pyrite and epidote	Syenite	The core interval consists of coarse- to medium-grained syenite with epidote and quartz veins and disseminated pyrite. The rock displays a light grey to pinkish-grey color and is predominantly composed of alkali feldspar, with minor plagioclase observed.
70.00	70.33	0.33	93.94	NQ	93.33	coarse to	pinkish, White	Allanite/magnetite and	Syenite	The core interval consists of coarse- to medium-

						medium grain	to grey	epidote		grained syenite with epidote and quartz veins, along with disseminated pyrite. The rock displays a light grey to pinkish-grey color and is predominantly composed of alkali feldspar, with minor plagioclase also observed.
70.33	71.78	1.45	97.93	NQ	97.93	coarse to medium grain	pinkish, White to grey	Allanite/magnetite and epidote	Syenite	The core interval consists of a coarse- to medium-grained syenite with epidote vein, displaying a light grey to pinkish-grey colour. The rock is predominantly composed of alkali feldspar, minor plagioclase observed.
71.78	72.00	0.22	90.91	NQ	90.90	coarse to medium grain	pinkish, White to grey	Allanite/magnetite and epidote	Syenite	The core interval consists of a coarse- to medium-grained syenite with epidote vein, displaying a light grey to pinkish-grey colour. The rock is predominantly composed of alkali feldspar, minor plagioclase observed.
72.00	75.00	3.00	97.00	NQ	97.00	coarse to medium grain	pinkish, White to grey	Allanite/magnetite	Syenite	The core interval consists of a coarse- to medium-grained syenite with epidote vein, displaying a light grey to pinkish-grey colour. The rock is predominantly composed of alkali feldspar, minor plagioclase observed.
75.00	78.00	3.00	95.67	NQ	95.66	coarse to medium grain	pinkish, White to grey	Zeolite, Epidote, Allanite, Pyrite	Syenite	The core interval consists of a coarse- to medium-grained syenite with epidote vein, displaying a light grey to pinkish-grey colour. The rock is predominantly composed of alkali feldspar, minor plagioclase observed.
78.00	78.33	0.33	96.97	NQ	96.96	coarse to medium grain	pinkish, White to grey	Zeolite, Epidote, Allanite, Pyrite	Syenite	The core interval consists of a coarse- to medium-grained syenite with epidote vein, displaying a light grey to pinkish-grey colour. The rock is predominantly composed of alkali feldspar, minor plagioclase observed.
78.33	78.77	0.44	95.45	NQ	95.45	coarse to medium grain	greenish Black	Quartz, mica	Amphibolite	The core interval consists of a coarse- to medium-grained syenite with epidote vein, displaying a light grey to pinkish-grey colour. The rock is predominantly composed of alkali feldspar, minor plagioclase observed.
78.77	80.00	1.23	96.75	NQ	96.74	coarse to	pinkish to	Allanite/magnetite	Syenite	The core interval consists of a coarse- to

						medium grain	Black to White			medium-grained syenite with epidote vein, displaying a light grey to pinkish-grey colour. The rock is predominantly composed of alkali feldspar, minor plagioclase observed.
80.00	81.00	1.00	94.00	NQ	94.00	coarse to medium grain	pinkish to Black to White	Allanite/magnetite	Syenite	The core interval consists of a coarse- to medium-grained syenite with epidote vein, displaying a light grey to pinkish-grey colour. The rock is predominantly composed of alkali feldspar, minor plagioclase observed.
81.00	81.25	0.25	100.00	NQ	100.00	coarse to medium grain	pinkish to Black to White	Allanite/magnetite	Syenite	The core interval consists of a coarse- to medium-grained syenite with epidote vein, displaying a light grey to pinkish-grey colour. The rock is predominantly composed of alkali feldspar, minor plagioclase observed.
81.25	81.33	0.08	75.00	NQ	75.00	coarse to medium grain	pinkish to Black to White	Aersnopyrite Allanite/magnetite	Syenite	The core interval consists of a coarse- to medium-grained syenite with epidote vein with dissiminated sulphide staining, displaying a light grey to pinkish-grey colour. The rock is predominantly composed of alkali feldspar, minor plagioclase observed.
81.33	83.14	1.81	97.79	NQ	97.79	coarse to medium grain	pinkish to Black to White	Allanite/magnetite	Syenite	The core interval consists of a coarse- to medium-grained syenite with epidote vein with allanite & magnetite, displaying a light grey to pinkish-grey colour. The rock is predominantly composed of alkali feldspar, minor plagioclase observed.
83.14	84.00	0.86	97.67	NQ	97.67	coarse to medium grain	pinkish to Black to White	pyrite, Allanite	Syenite	The core interval consists of a coarse- to medium-grained syenite with epidote vein with allanite & magnetite, displaying a light grey to pinkish-grey colour. The rock is predominantly composed of alkali feldspar, minor plagioclase observed.
84.00	85.00	1.00	98.00	NQ	98.00	coarse to medium grain	pinkish to Black to White	Allanite/Magnetite	Syenite	The core interval consists of a coarse- to medium-grained syenite with epidote vein with allanite & magnetite, displaying a light grey to pinkish-grey colour. The rock is predominantly

										composed of alkali feldspar, minor plagioclase observed.
85.00	87.00	2.00	98.50	NQ	98.50	coarse to medium grain	pinkish to Black to White	Allanite/Magnetite	Syenite	The core interval consists of a coarse- to medium-grained syenite with epidote vein with allanite & magnetite, displaying a light grey to pinkish-grey colour. The rock is predominantly composed of alkali feldspar, minor plagioclase observed.
87.00	87.93	0.93	97.85	NQ	97.84	coarse to medium grain	pinkish to Black to White	Allanite/Magnetite	Syenite	The core interval consists of a coarse- to medium-grained syenite with epidote vein with allanite & magnetite, displaying a light grey to pinkish-grey colour. The rock is predominantly composed of alkali feldspar, minor plagioclase observed.
87.93	89.00	1.07	97.20	NQ	97.19	coarse to medium grain	pinkish to Black to White	Epidote, Allanite/Magnetite	Epidotic syenite	The core interval consists of a coarse- to medium-grained epidotic syenite with allanite & magnetite, displaying a light grey to pinkish-grey colour. The rock is predominantly composed of alkali feldspar, minor plagioclase observed.
89.00	89.17	0.17	100.00	NQ	82.35	coarse to medium grain	pinkish to Black to White	Allanite/Magnetite	Syenite	The core interval consists of a coarse- to medium-grained syenite with epidote vein with allanite & magnetite, displaying a light grey to pinkish-grey colour. The rock is predominantly composed of alkali feldspar, minor plagioclase observed.
89.17	90.00	0.83	93.98	NQ	93.97	coarse to medium grain	pinkish to Black to White	Epidote, Allanite/Magnetite	Syenite	The core interval consists of coarse- to medium-grained syenite with epidote veins containing allanite and magnetite. The rock exhibits a light grey to pinkish-grey color and is predominantly composed of alkali feldspar, with minor plagioclase also observed.
90.00	90.62	0.62	95.16	NQ	95.16	coarse to medium grain	pinkish to Black to White	Epidote, Allanite/Magnetite	Syenite	The core interval consists of a coarse- to medium-grained syenite with epidote vein with allanite & magnetite, displaying a light grey to pinkish-grey colour. The rock is predominantly composed of alkali feldspar, minor plagioclase

										observed.
90.62	92.40	1.78	96.63	NQ	68.53	coarse to medium grain	pinkish to Black to White	Allanite/Magnetite	Syenite	The core interval consists of a coarse- to medium-grained syenite with epidote vein with allanite & magnetite, displaying a light grey to pinkish-grey colour. The rock is predominantly composed of alkali feldspar, minor plagioclase observed.
92.40	93.00	0.60	93.33	NQ	80.00	coarse to medium grain	pinkish to Black to White	Epidote	Syenite	The core interval consists of a coarse- to medium-grained syenite with epidote vein with allanite & magnetite, displaying a light grey to pinkish-grey colour. The rock is predominantly composed of alkali feldspar, minor plagioclase observed.
93.00	93.36	0.36	97.22	NQ	58.33	coarse to medium grain	Dark black and pink	-	Syenite	The core interval consists of a coarse- to medium-grained syenite with epidote vein with allanite & magnetite, displaying a light grey to pinkish-grey colour. The rock is predominantly composed of alkali feldspar, minor plagioclase observed.
93.36	94.63	1.27	96.85	NQ	96.85	coarse to medium grain	light pinkish to Black to White	Allanite/Magnetite	Syenite	The core interval consists of a coarse- to medium-grained alkali rich syenite with epidote vein with allanite & magnetite, displaying a light grey to pinkish-grey colour. The rock is predominantly composed of alkali feldspar, minor plagioclase observed.
94.63	94.87	0.24	91.67	NQ	91.67	coarse to medium grain	light pinkish to Black to White	Allanite/Magnetite	Syenite	The core interval consists of a coarse- to medium-grained alkali rich syenite with epidote vein with allanite & magnetite, displaying a light grey to pinkish-grey colour. The rock is predominantly composed of alkali feldspar, minor plagioclase observed.
94.87	95.00	0.13	84.62	NQ	81.61	coarse to medium grain	pinkish Black	Allanite/Magnetite	Syenite	The core interval consists of a coarse- to medium-grained alkali rich syenite with epidote vein with allanite & magnetite, displaying a light grey to pinkish-grey colour. The rock is predominantly composed of alkali feldspar,

										minor plagioclase observed.
95.00	96.00	1.00	94.00	NQ	75.00	coarse to medium grain	pinkish Black	Allanite/Magnetite	Syenite	The core interval consists of a coarse- to medium-grained alkali rich syenite with epidote vein with allanite & magnetite, displaying a light grey to pinkish-grey colour. The rock is predominantly composed of alkali feldspar, minor plagioclase observed.
96.00	97.23	1.23	96.75	NQ	96.74	coarse to medium grain	pinkish Black to greenish	Epidote, Allanite/Magnetite	Syenite	The core interval consists of a coarse- to medium-grained alkali rich syenite with epidote vein with allanite & magnetite, displaying a light grey to pinkish-grey colour. The rock is predominantly composed of alkali feldspar, minor plagioclase observed.
97.23	98.46	1.23	98.37	NQ	98.37	coarse to medium grain	pinkish Black to greenish	Epidote, Allanite/Magnetite	Syenite	The core interval consists of coarse- to medium-grained, alkali-rich syenite with epidote veins containing allanite and magnetite. The rock displays a light grey to pinkish-grey color and is predominantly composed of alkali feldspar, with minor plagioclase.
98.46	98.83	0.37	94.59	NQ	0.00	coarse to medium grain	pinkish Black to greenish	Epidote, Allanite/Magnetite	Syenite	The core interval consists of coarse- to medium-grained, alkali-rich syenite with epidote veins containing allanite and magnetite. The rock displays a light grey to pinkish-grey color and is predominantly composed of alkali feldspar, with minor plagioclase.
98.83	99.00	0.17	70.59	NQ	58.82	coarse to medium grain	pinkish Black to greenish	Epidote, Allanite/Magnetite	Syenite	The core interval consists of coarse- to medium-grained, alkali-rich syenite with epidote veins containing allanite and magnetite. The rock displays a light grey to pinkish-grey color and is predominantly composed of alkali feldspar, with minor plagioclase.
99.00	100.00	1.00	95.00	NQ	95.00	coarse to medium grain	pinkish Black to greenish	Epidote, Allanite/Magnetite	Syenite	The core interval consists of a coarse- to medium-grained alkali rich syenite with epidote vein with allanite & magnetite, displaying a light grey to pinkish-grey colour. The rock is predominantly composed of alkali feldspar,

										minor plagioclase observed.
100.00	100.85	0.85	96.47	NQ	94.11	coarse to medium grain	pinkish Black to white	Epidote, Allanite/Magnetite	Syenite	The core interval consists of coarse- to medium-grained, alkali-rich syenite with epidote veins containing allanite and magnetite. The rock displays a light grey to pinkish-grey color and is predominantly composed of alkali feldspar, with minor plagioclase.
100.85	101.32	0.47	93.62	NQ	63.82	coarse to medium grain	pinkish Black to white	Epidote, Allanite/Magnetite	Syenite	The core interval consists of a coarse- to medium-grained alkali rich syenite with epidote vein with allanite & magnetite, displaying a light grey to pinkish-grey colour. The rock is predominantly composed of alkali feldspar, minor plagioclase observed.
101.32	102.00	0.68	92.65	NQ	0.00	coarse to medium grain	pinkish Black to white	Epidote, Allanite/Magnetite	Syenite	The core interval consists of a coarse- to medium-grained alkali rich syenite with epidote vein with allanite & magnetite, displaying a light grey to pinkish-grey colour. The rock is predominantly composed of alkali feldspar, minor plagioclase observed.
102.00	103.09	1.09	98.17	NQ	98.17	coarse to medium grain	pinkish Black to white	Allanite/Magnetite	lecocratic migmatite intermixed with Syenite	Leucocratic (light-colored) migmatite bands are intermixed with syenite. The leucocratic portions are rich in coarse-grained orthoclase feldspar. The rock is predominantly composed of alkali feldspar, with minor plagioclase.
103.09	105.00	1.91	97.91	NQ	97.90	coarse to medium grain	pinkish Black to white	Epidote, Allanite/Magnetite	Syenite	The core interval consists of coarse- to medium-grained, alkali-rich syenite with epidote veins containing allanite and magnetite. The rock displays a light grey to pinkish-grey color and is predominantly composed of alkali feldspar, with minor plagioclase.
105.00	105.14	0.14	92.86	NQ	92.86	coarse to medium grain	pinkish Black to white	Epidote, Allanite/Magnetite	Syenite	The core interval consists of coarse- to medium-grained, alkali-rich syenite with epidote veins containing allanite and magnetite. The rock displays a light grey to pinkish-grey color and is predominantly composed of alkali feldspar, with minor plagioclase.

105.14	108.00	2.86	98.95	NQ	95.80	coarse to medium grain	pinkish Black to white	Epidote, Allanite/Magnetite	Epidotic Syenite	The core interval consists of a coarse- to medium-grained alkali rich syenite with epidote vein with allanite & magnetite, displaying a light grey to pinkish-grey colour. The rock is predominantly composed of alkali feldspar, minor plagioclase observed.
108.00	108.90	0.90	98.89	NQ	98.88	coarse to medium grain	Pinkish grey to Black	Epidote, Allanite/Magnetite	Epidotic Syenite	The core interval consists of a coarse- to medium-grained alkali rich syenite with epidote vein with allanite & magnetite, displaying a light grey to pinkish-grey colour. The rock is predominantly composed of alkali feldspar, minor plagioclase observed.
108.9	110	1.10	92.73	NQ	83.63	coarse to medium grain	Pinkish grey to Black	Epidote, Allanite/Magnetite	Epidotic Syenite	The core interval consists of a coarse- to medium-grained alkali rich syenite with epidote vein with allanite & magnetite, displaying a light grey to pinkish-grey colour. The rock is predominantly composed of alkali feldspar, minor plagioclase observed.
110	110.79	0.79	98.73	NQ	98.73	coarse to medium grain	Pinkish grey to Black	Epidote, Allanite/Magnetite	Epidotic Syenite	The core interval consists of a coarse- to medium-grained alkali rich syenite with epidote vein with allanite & magnetite, displaying a light grey to pinkish-grey colour. The rock is predominantly composed of alkali feldspar, minor plagioclase observed.
110.79	112	1.21	94.21	NQ	94.21	coarse to medium grain	Pinkish grey to Black	Epidote, Allanite/Magnetite	Epidotic Syenite	The core interval consists of a coarse- to medium-grained alkali rich syenite with epidote vein with allanite & magnetite, displaying a light grey to pinkish-grey colour. The rock is predominantly composed of alkali feldspar, minor plagioclase observed.
112	114	2.00	97.00	NQ	91	coarse to medium grain	Pinkish grey to Black	Allanite/Magnetite	Alkali Syenite	The core interval consists of a coarse- to medium-grained alkali rich syenite with allanite & magnetite, displaying a light grey to pinkish-grey colour. The rock is predominantly composed of alkali feldspar, minor plagioclase observed.

114	114.4	0.40	97.50	NQ	97.50	coarse to medium grain	Pinkish grey to Black	Allanite/Magnetite	Alkali Syenite	The core interval consists of a coarse- to medium-grained alkali rich syenite with allanite & magnetite, displaying a light grey to pinkish-grey colour. The rock is predominantly composed of alkali feldspar, minor plagioclase observed.
114.40	115	0.60	93.33	NQ	93.33	coarse to medium grain	Pinkish grey to Black	Allanite/Magnetite	Alkali Syenite	The core interval consists of a coarse- to medium-grained alkali rich syenite with allanite & magnetite, displaying a light grey to pinkish-grey colour. The rock is predominantly composed of alkali feldspar, minor plagioclase observed.
115	116.09	1.09	97.25	NQ	97.24	coarse to medium grain	Pinkish grey to Black	Epidote, Allanite/Magnetite	Alkali Syenite	The core interval consists of a coarse- to medium-grained alkali rich syenite with epidote vein with allanite & magnetite, displaying a light grey to pinkish-grey colour. The rock is predominantly composed of alkali feldspar, minor plagioclase observed.
116.09	117	0.91	97.80	NQ	97.8	coarse to medium grain	Pinkish grey to Black	Epidote, Allanite/Magnetite	Alkali Syenite	The core interval consists of coarse- to medium-grained, alkali-rich syenite with epidote veins containing allanite and magnetite. The rock exhibits a light grey to pinkish-grey color and is predominantly composed of alkali feldspar, with minor plagioclase also observed.
117	117.5	0.50	96.00	NQ	80	coarse to medium grain	Pinkish grey to Black	Epidote, Allanite/Magnetite	Alkali Syenite	The core interval consists of a coarse- to medium-grained alkali rich syenite with epidote vein with allanite & magnetite, displaying a light grey to pinkish-grey colour. The rock is predominantly composed of alkali feldspar, minor plagioclase observed.
117.50	118.89	1.39	97.84	NQ	97.84	coarse to medium grain	Pinkish grey to Black	Epidote, Allanite/Magnetite	Alkali Syenite	The core interval consists of a coarse- to medium-grained alkali rich syenite with epidote vein with allanite & magnetite, displaying a light grey to pinkish-grey colour. The rock is predominantly composed of alkali feldspar, minor plagioclase observed.

118.89	120	1.11	93.69	NQ	76.57	coarse to medium grain	Pinkish grey to Black	Epidote, Allanite/Magnetite	Alkali Syenite	The core interval consists of a coarse- to medium-grained alkali rich syenite with epidote vein with allanite & magnetite, displaying a light grey to pinkish-grey colour. The rock is predominantly composed of alkali feldspar, minor plagioclase observed.
120.00	120.3	0.30	96.67	NQ	96.66	coarse to medium grain	Pinkish grey to Black	Allanite/Magnetite	Alkali Syenite	The core interval consists of a coarse- to medium-grained alkali rich syenite with allanite & magnetite, displaying a light grey to pinkish-grey colour. The rock is predominantly composed of alkali feldspar, minor plagioclase observed.
120.30	121.37	1.07	98.13	NQ	98.13	coarse to medium grain	Pinkish grey to Black	Allanite/Magnetite	Alkali Syenite	The core interval consists of a coarse- to medium-grained alkali rich syenite with allanite & magnetite, displaying a light grey to pinkish-grey colour. The rock is predominantly composed of alkali feldspar, minor plagioclase observed.
121.37	123.0	1.63	94.48	NQ	94.48	coarse to medium grain	Pinkish grey to Black	Allanite/Magnetite	Alkali Syenite	The core interval consists of a coarse- to medium-grained alkali rich syenite with allanite & magnetite, displaying a light grey to pinkish-grey colour. The rock is predominantly composed of alkali feldspar, minor plagioclase observed.
123.00	123.8	0.80	98.75	NQ	98.75	coarse to medium grain	Pinkish grey to Black	Allanite/Magnetite	Alkali Syenite	The core interval consists of a coarse- to medium-grained alkali rich syenite with allanite & magnetite, displaying a light grey to pinkish-grey colour. The rock is predominantly composed of alkali feldspar, minor plagioclase observed.
123.80	125.00	1.20	97.50	NQ	97.5	coarse to medium grain	Pinkish grey to Black	Allanite/Magnetite	Alkali Syenite	The core interval consists of a coarse- to medium-grained alkali rich syenite with allanite & magnetite, displaying a light grey to pinkish-grey colour. The rock is predominantly composed of alkali feldspar, minor plagioclase observed.

125.00	125.92	0.92	97.83	NQ	97.83	coarse to medium grain	Pinkish grey to Black	Allanite/Magnetite	Alkali Syenite	The core interval consists of a coarse- to medium-grained alkali rich syenite with allanite & magnetite, displaying a light grey to pinkish-grey colour. The rock is predominantly composed of alkali feldspar, minor plagioclase observed.
125.92	126.00	0.08	87.50	NQ	0	coarse to medium grain	Pinkish grey to Black	Allanite/Magnetite	Alkali Syenite	The core interval consists of a coarse- to medium-grained alkali rich syenite with allanite & magnetite, displaying a light grey to pinkish-grey colour. The rock is predominantly composed of alkali feldspar, minor plagioclase observed.
126.00	128.46	2.46	97.56	NQ	97.56	coarse to medium grain	Pinkish grey to Black	Allanite/Magnetite	Alkali Syenite	The core interval consists of a coarse- to medium-grained alkali rich syenite with allanite & magnetite, displaying a light grey to pinkish-grey colour. The rock is predominantly composed of alkali feldspar, minor plagioclase observed.
128.46	129.00	0.54	98.15	NQ	98.14	coarse to medium grain	Pinkish grey to Black	Allanite/Magnetite	Alkali Syenite	The core interval consists of a coarse- to medium-grained alkali rich syenite with allanite & magnetite, displaying a light grey to pinkish-grey colour. The rock is predominantly composed of alkali feldspar, minor plagioclase observed.
129.00	130.00	1.00	97.00	NQ	97.00	coarse to medium grain	Pinkish grey to Black	Allanite/Magnetite	Alkali Syenite	The core interval consists of a coarse- to medium-grained alkali rich syenite with allanite & magnetite, displaying a light grey to pinkish-grey colour. The rock is predominantly composed of alkali feldspar, minor plagioclase observed.
130.00	130.52	0.52	96.15	NQ	96.15	coarse to medium grain	Pinkish grey to Black	Allanite/Magnetite	Alkali Syenite	The core interval consists of a coarse- to medium-grained alkali rich syenite with allanite & magnetite, displaying a light grey to pinkish-grey colour. The rock is predominantly composed of alkali feldspar, minor plagioclase observed.

130.52	131.67	1.15	95.65	NQ	95.65	coarse to medium grain	Pinkish grey to Black	Allanite/Magnetite	Alkali Syenite	The core interval consists of a coarse- to medium-grained alkali rich syenite with allanite & magnetite, displaying a light grey to pinkish-grey colour. The rock is predominantly composed of alkali feldspar, minor plagioclase observed.
131.67	132.00	0.33	84.85	NQ	96.42	coarse to medium grain	Pinkish grey to Black	Allanite/Magnetite	Alkali Syenite	The core consists of coarse- to medium-grained, alkali-rich syenite containing allanite and magnetite. The rock displays a light grey to pinkish-grey color and is predominantly composed of alkali feldspar, with minor plagioclase.
132.00	132.55	0.55	94.55	NQ	60.0	coarse to medium grain	Pinkish grey to Black	Allanite/Magnetite	Alkali Syenite	The core consists of coarse- to medium-grained, alkali-rich syenite containing allanite and magnetite. The rock displays a light grey to pinkish-grey color and is predominantly composed of alkali feldspar, with minor plagioclase.
132.55	133.52	0.97	93.81	NQ	93.81	Medium to coarse grain	Pinkish grey to Black	Allanite/Magnetite	Alkali Syenite	The core consists of coarse- to medium-grained, alkali-rich syenite containing allanite and magnetite. The rock displays a light grey to pinkish-grey color and is predominantly composed of alkali feldspar, with minor plagioclase.
133.52	135.00	1.48	94.59	NQ	94.59	Medium to coarse grain	Ligth pinkish and black	Allanite/Magnetite	Migmatite Gneiss	The core consists of migmatite intermixed with syenite, exhibiting alternating bands of leucosome (light-colored) and melanosome (dark-colored). The leucosome is notably enriched in orthoclase feldspar, while the syenite displays a coarse-grained texture and an overall light-colored appearance. The rock is dominated by alkali feldspar, primarily orthoclase and microcline.
135.00	135.61	0.61	96.72	NQ	96.72	Medium to coarse grain	Ligth pinkish and black	Allanite/Magnetite	Migmatite Gneiss	The core consists of migmatite intermixed with syenite, exhibiting alternating bands of leucosome (light-colored) and melanosome

										(dark-colored). The leucosome is notably enriched in orthoclase feldspar, while the syenite displays a coarse-grained texture and an overall light-colored appearance. The rock is dominated by alkali feldspar, primarily orthoclase and microcline.
135.61	136.75	1.14	95.61	NQ	95.61	Medium to coarse grain	Ligth pinkish and black	Allanite/Magnetite	Migmatite Gneiss	The core consists of migmatite intermixed with syenite, exhibiting alternating bands of leucosome (light-colored) and melanosome (dark-colored). The leucosome is notably enriched in orthoclase feldspar, while the syenite displays a coarse-grained texture and an overall light-colored appearance. The rock is dominated by alkali feldspar, primarily orthoclase and microcline.
136.75	137.91	1.16	95.69	NQ	95.69	Medium to coarse grain	Ligth pinkish and black	Allanite/Magnetite	Migmatite Gneiss	The core consists of migmatite intermixed with syenite, exhibiting alternating bands of leucosome (light-colored) and melanosome (dark-colored). The leucosome is notably enriched in orthoclase feldspar, while the syenite displays a coarse-grained texture and an overall light-colored appearance. The rock is dominated by alkali feldspar, primarily orthoclase and microcline.
137.91	138.00	0.09	77.78	NQ	0	Medium to coarse grain	Ligth pinkish and black	Allanite/Magnetite	Migmatite Gneiss	The core consists of migmatite intermixed with syenite, exhibiting alternating bands of leucosome (light-colored) and melanosome (dark-colored). The leucosome is notably enriched in orthoclase feldspar, while the syenite displays a coarse-grained texture and an overall light-colored appearance. The rock is dominated by alkali feldspar, primarily orthoclase and microcline.
138.00	141.00	3.00	97.33	NQ	97.33	Medium to coarse grain	Ligth pinkish and black	Allanite/Magnetite	Migmatite Gneiss	The core consists of migmatite with alternating leucocratic (light-colored) and melanocratic (dark-colored) bands. The leucocratic zones are

										enriched in coarse-grained orthoclase feldspar, typically appearing as pink to salmon-colored crystals that often form large megacrysts or intergrown aggregates.
141.00	142.29	1.29	95.35	NQ	95.35	Medium to coarse grain	Ligth pinkish and black	Allanite/Magnetite	Migmatite Gneiss	The core consists of migmatite with alternating leucocratic (light-colored) and melanocratic (dark-colored) bands. The leucocratic zones are enriched in coarse-grained orthoclase feldspar, typically appearing as pink to salmon-colored crystals that often form large megacrysts or intergrown aggregates.
142.29	143.00	0.71	97.18	NQ	97.18	Medium to coarse grain	Ligth pinkish and black	Allanite/Magnetite	Migmatite Gneiss	The core consists of migmatite with alternating leucocratic (light-colored) and melanocratic (dark-colored) bands. The leucocratic zones are enriched in coarse-grained orthoclase feldspar, typically appearing as pink to salmon-colored crystals that often form large megacrysts or intergrown aggregates.
143.00	143.90	0.90	98.89	NQ	98.89	Medium to coarse grain	Ligth pinkish and black	Allanite/Magnetite	Migmatite Gneiss	The core consists of migmatite with alternating leucocratic (light-colored) and melanocratic (dark-colored) bands. The leucocratic zones are enriched in coarse-grained orthoclase feldspar, typically appearing as pink to salmon-colored crystals that often form large megacrysts or intergrown aggregates.
143.90	144.75	0.85	88.24	NQ	58.82	Medium to coarse grain	Ligth pinkish and black	Allanite/Magnetite	Migmatite Gneiss	The core consists of migmatite with alternating leucocratic (light-colored) and melanocratic (dark-colored) bands. The leucocratic zones are enriched in coarse-grained orthoclase feldspar, typically appearing as pink to salmon-colored crystals that often form large megacrysts or intergrown aggregates.
144.75	145.53	0.78	97.44	NQ	78.20	Medium to coarse grain	Ligth pinkish and black	Allanite/Magnetite	Migmatite Gneiss	The core consists of migmatite with alternating leucocratic (light-colored) and melanocratic (dark-colored) bands. The leucocratic zones are enriched with coarse-grained orthoclase feldspar.

145.53	147.00	1.47	99.32	NQ	99.32	Medium to coarse grain	Ligth pinkish and black	Allanite/Magnetite	Migmatite Gneiss	The core consists of migmatite with alternating leucocratic (light-colored) and melanocratic (dark-colored) bands. The leucocratic zones are enriched with coarse-grained orthoclase feldspar.
147.00	149.00	2.00	98.00	NQ	98.00	Medium to coarse grain	Ligth pinkish and black	Allanite/Magnetite	Migmatite Gneiss	The core consists of migmatite with alternating leucocratic (light-colored) and melanocratic (dark-colored) bands. The leucocratic zones are enriched with coarse-grained orthoclase feldspar.
149.00	150.00	1.00	98.00	NQ	98.00	Medium to coarse grain	pinkish and black	Epidote vein Allanite/Magnetite	Syenite	The core consists of coarse- to medium-grained, alkali-rich syenite with epidote veins containing allanite and magnetite. It displays a light grey to pinkish-grey color and is predominantly composed of alkali feldspar, with minor plagioclase.
150.00	150.13	0.13	92.31	NQ	92..31	Medium to coarse grain	pinkish and black	Epidote vein Allanite/Magnetite	Syenite	The core consists of coarse- to medium-grained, alkali-rich syenite with epidote veins containing allanite and magnetite. It displays a light grey to pinkish-grey color and is predominantly composed of alkali feldspar, with minor plagioclase.
150.13	150.54	0.41	95.12	NQ	95.12	Medium to coarse grain	pinkish and black	Epidote vein Allanite/Magnetite	Syenite	The core consists of coarse- to medium-grained, epidote-bearing syenite containing allanite and magnetite. It displays a light grey to pinkish-grey color and is predominantly composed of alkali feldspar, with minor plagioclase.
150.54	151.00	0.46	93.48	NQ	93.48	Medium to coarse grain	pinkish and black	Epidote vein Allanite/Magnetite	Syenite	The core consists of coarse- to medium-grained, epidote-bearing syenite containing allanite and magnetite. It displays a light grey to pinkish-grey color and is predominantly composed of alkali feldspar, with minor plagioclase.
151.00	151.69	0.69	98.55	NQ	98.55	Medium to coarse grain	pinkish and black	Epidote vein Allanite/Magnetite	Syenite	The core consists of coarse- to medium-grained, epidote-bearing syenite containing allanite and magnetite. It displays a light grey to pinkish-grey color and is predominantly composed of alkali feldspar, with minor plagioclase.
151.69	151.93	0.24	91.67	NQ	58.33	Medium to	Pinkish grey	Epidote vein	Syenite	The core consists of coarse- to medium-grained,

						coarse grain	to Black	Allanite/Magnetite		epidote-bearing syenite containing allanite and magnetite. It displays a light grey to pinkish-grey color and is predominantly composed of alkali feldspar, with minor plagioclase.
151.93	152.16	0.23	86.96	NQ	47.82	Medium to coarse grain	Pinkish grey to Black	Epidote vein Allanite/Magnetite	Syenite	The core consists of coarse- to medium-grained, epidote-bearing syenite containing allanite and magnetite. It displays a light grey to pinkish-grey color and is predominantly composed of alkali feldspar, with minor plagioclase.
152.16	152.47	0.31	90.32	NQ	90.32	Medium to coarse grain	Pinkish grey to Black	Epidote vein Allanite/Magnetite	Syenite	The core consists of coarse- to medium-grained, epidote-bearing syenite containing allanite and magnetite. It displays a light grey to pinkish-grey color and is predominantly composed of alkali feldspar, with minor plagioclase.
152.47	153	0.53	98.11	NQ	98.11	Medium to coarse grain	Pinkish grey to Black	Epidote vein Allanite/Magnetite	Syenite	The core consists of coarse- to medium-grained, epidote-bearing syenite containing allanite and magnetite. It displays a light grey to pinkish-grey color and is predominantly composed of alkali feldspar, with minor plagioclase.
153	153.61	0.61	96.72	NQ	96.72	Medium to coarse grain	Pinkish grey to Black	Epidote vein Allanite/Magnetite	Syenite	The core consists of coarse- to medium-grained, epidote-bearing syenite containing allanite and magnetite. It displays a light grey to pinkish-grey color and is predominantly composed of alkali feldspar, with minor plagioclase.
153.61	154	0.39	94.87	NQ	94.87	Medium to coarse grain	Pinkish grey to Black	Allanite/Magnetite	Migmatite Gneiss	The core consists of migmatite gneiss with alternating leucocratic (light-colored) and melanocratic (dark-colored) bands. The leucocratic zones are enriched with coarse-grained orthoclase feldspar.
154	154.64	0.64	98.44	NQ	98.44	Medium to coarse grain	Pinkish grey to Black	Allanite/Magnetite	Migmatite Gneiss	The core consists of migmatite gneiss with alternating leucocratic (light-colored) and melanocratic (dark-colored) bands. The leucocratic zones are enriched with coarse-grained orthoclase feldspar.

Log Sheet for BH 3

BORE HOLE NO	**RJB-03**		
TOPOSHEET NO	**45K/03**		
LOCATION	**LAT**	**25° 25' 44.5360"**	
	LONG	**74° 07' 22.7573"**	
RL OF COLLAR	**507.692**		
BH. ANGLE	**45°**		
AZIMUTH	**N45°W**	**TOTAL DRILLING TARGET**	**150 m**
INCLINATION	**45°**	**DRILL TYPE**	**Core Drilling**
BH DEPTH	**150**		

FROM (m)	TO (m)	RUN (m)	RECOVERY (%)	CORE SIZE	RQD %	GRAIN SIZE	COLOUR	MINERALOGY	ROCK TYPE	DESCRIPTION
0.00	3.00	3.00	76.67	HQ	0.00	Medium to coarse grain	greenish grey to Black	-	Weathered Migmatite Gneiss	Highly weathered zone, predominantly of a greenish grey in color, moderately compact sand of highly fractured migmatite gneiss observed.
3.00	6.00	3.00	81.00	HQ	0.00	Medium to coarse grain	greenish grey to Black	-	Weathered Migmatite Gneiss	Highly weathered zone, predominantly of a greenish grey in color, moderately compact sand with occasional gravel-sized fragments of highly fractured migmatite gneiss observed.
6.00	9.00	3.00	81.67	HQ	0.00	Medium to coarse grain	Greenish Black	-	Weathered Migmatite Gneiss	Highly weathered zone, predominantly of a greenish grey in color, moderately compact sand with occasional gravel-sized fragments of highly fractured migmatite gneiss observed.
9.00	10.00	1.00	95.00	NQ	11.00	Medium to coarse grain	Blackish grey to Black	Allanite/magnetite	Migmatite Gneiss	The core consists of migmatite gneiss with alternating leucocratic (light-colored) and melanocratic (dark-colored) bands. The leucocratic portions are rich in coarse-grained orthoclase feldspar, which appears as salmon-colored crystals, often forming large megacrysts or intergrown

										aggregates. Orthoclase is the dominant mineral in the felsic bands.
10.00	10.30	0.30	96.67	NQ	33.33	Medium to coarse grain	Blackish grey to Black	Allanite/magnetite	Migmatite Gneiss	The core consists of migmatite gneiss with alternating leucocratic (light-colored) and melanocratic (dark-colored) bands. The leucocratic portions are rich in coarse-grained orthoclase feldspar, which appears as salmon-colored crystals, often forming large megacrysts or intergrown aggregates. Orthoclase is the dominant mineral in the felsic bands.
10.30	12.00	1.70	95.88	NQ	62.94	Medium to coarse grain	Dark green to black in color	-	Amphibolite	Weakly fractured amphibolite dark greenish in colour massive in nature with weakly foliated with consist of plagioclase & hornblend in dark colour and contributing to dense compact appearance.
12.00	15.00	3.00	97.00	NQ	97.00	Medium to coarse grain	Dark green to black in color	-	Amphibolite	Weakly fractured amphibolite dark greenish in colour massive in nature with weakly foliated with consist of plagioclase & hornblend in dark colour and contributing to dense compact appearance.
15.00	16.10	1.10	96.36	NQ	0.83	Medium to coarse grain	Dark green to black in color	-	Amphibolite	Weakly fractured amphibolite dark greenish in colour massive in nature with weakly foliated with consist of plagioclase & hornblend in dark colour and contributing to dense compact appearance.
16.10	17.09	0.99	95.96	NQ	33.33	Medium to coarse grain	Dark green to black in color	-	Amphibolite	Weakly fractured amphibolite dark greenish in colour massive in nature with weakly foliated with consist of plagioclase & hornblend in dark colour and contributing to dense compact appearance.
17.09	18.00	0.91	97.80	NQ	80.80	Medium to coarse grain	Dark green to black in color	-	Amphibolite	Weakly fractured amphibolite dark greenish in colour massive in nature with weakly foliated with consist of plagioclase & hornblend in dark colour and contributing to dense compact appearance.
18.00	19.45	1.45	97.93	NQ	97.93	Medium to coarse grain	Dark green to black in color	-	Amphibolite	Weakly fractured amphibolite dark greenish in colour massive in nature with weakly foliated with consist of plagioclase & hornblend in dark colour and contributing to dense compact appearance.
19.45	20.00	0.55	94.55	NQ	94.55	Medium to coarse grain	Dark green to black in color	-	Amphibolite	Weakly fractured amphibolite dark greenish in colour massive in nature with weakly foliated with consist of plagioclase & hornblend in dark colour and contributing to

										dense compact appearance.
20.00	21.00	1.00	98.00	NQ	82.00	Medium to coarse grain	Dark green to black in color	-	Amphibolite	Weakly fractured amphibolite dark greenish in colour massive in nature with weakly foliated with consist of plagioclase & hornblend in dark colour and contributing to dense compact appearance.
21.00	22.16	1.16	95.69	NQ	89.65	Medium to coarse grain	Dark green to black in color	-	Amphibolite	Weakly fractured amphibolite dark greenish in colour massive in nature with weakly foliated with consist of plagioclase & hornblend in dark colour and contributing to dense compact appearance.
22.16	24.00	1.84	98.91	NQ	95.10	Medium to coarse grain	Dark green to black in color	-	Amphibolite	The core consists of weakly fractured amphibolite with pyroxene and chlorite, dark greenish in color, massive in nature, and weakly foliated. It is composed of plagioclase and hornblende, contributing to its dark, compact appearance.
24.00	24.21	0.21	85.71	NQ	85.71	Medium to coarse grain	Dark green to black in color	Epidote vein	Amphibolite	The core consists of weakly fractured amphibolite with pyroxene and chlorite, dark greenish in color, massive in nature, and weakly foliated. It is composed of plagioclase and hornblende, contributing to its dark, compact appearance.
24.21	25.00	0.79	98.73	NQ	98.73	Medium to coarse grain	Dark green to black in color	Arsenopyrite	Amphibolite	The core consists of weakly fractured amphibolite with pyroxene and chlorite, dark greenish in color, massive in nature, and weakly foliated. It is composed of plagioclase and hornblende, contributing to its dark, compact appearance. Disseminated pyrite is also observed.
25.00	25.67	0.67	98.51	NQ	91.04	Medium to coarse grain	Dark green to black in color	-	Amphibolite	Weakly fractured amphibolite dark greenish in colour massive in nature with weakly foliated with consist of plagioclase & hornblend in dark colour and contributing to dense compact appearance.
25.67	27.00	1.33	97.74	NQ	97.74	Medium to coarse grain	Dark green to black in color	-	Amphibolite	The core consists of weakly fractured amphibolite with pyroxene and chlorite, dark greenish in color, massive in nature, and weakly foliated. It is composed of plagioclase and hornblende, contributing to its dark, compact appearance. Disseminated pyrite is also observed.
27.00	29.58	2.58	99.22	NQ	99.22	Medium to coarse grain	Dark green to black in color	-	Amphibolite	The core consists of weakly fractured amphibolite with pyroxene and chlorite, dark greenish in color, massive in nature, and weakly foliated. It is composed of plagioclase

										and hornblende, contributing to its dark, compact appearance. Disseminated pyrite is also observed.
29.58	30.00	0.42	97.62	NQ	57.14	Medium to coarse grain	Dark green to black in color	-	Amphibolite	Weakly fractured amphibolite dark greenish in colour massive in nature with weakly foliated with consist of plagioclase & hornblend in dark colour along the fracture limonitization observed.
30.00	31.55	1.55	96.77	NQ	90.32	Medium to coarse grain	Dark green to black in color	-	Amphibolite	The core consists of weakly fractured amphibolite with pyroxene and chlorite, dark greenish in color, massive in nature, and weakly foliated. It is composed of plagioclase and hornblende, contributing to its dark, compact appearance. Disseminated pyrite is also observed.
31.55	33.00	1.45	98.62	NQ	98.62	Medium to coarse grain	Dark green to black in color	-	Amphibolite	The core consists of weakly fractured amphibolite with pyroxene and chlorite, dark greenish in color, massive in nature, and weakly foliated. It is composed of plagioclase and hornblende, contributing to its dark, compact appearance. Disseminated pyrite is also observed.
33.00	34.75	1.75	98.29	NQ	98.29	Medium to coarse grain	Dark green to black in color	-	Amphibolite	Weakly fractured amphibolite dark greenish in colour massive in nature with weakly foliated with consist of plagioclase & hornblend in dark colour and contributing to dense compact appearance.
34.75	35.00	0.25	92.00	NQ	0.00	Medium to coarse grain	Dark green to black in color	-	Amphibolite	Weakly fractured amphibolite dark greenish in colour massive in nature with weakly foliated with consist of plagioclase & hornblend in dark colour and contributing to dense compact appearance.
35.00	36.00	1.00	96.00	NQ	96.00	Medium to coarse grain	Dark green to black in color	-	Amphibolite	Weakly fractured amphibolite dark greenish in colour massive in nature with weakly foliated with consist of plagioclase & hornblend in dark colour and contributing to dense compact appearance.
36.00	37.32	1.32	97.73	NQ	91.66	Medium to coarse grain	Dark green to black in color	-	Amphibolite	Weakly fractured amphibolite dark greenish in colour massive in nature with weakly foliated with consist of plagioclase & hornblend in dark colour and contributing to dense compact appearance.
37.32	37.50	0.18	94.44	NQ	94.44	Medium to coarse grain	Dark green to black in color	-	Amphibolite Intermixed with migmatite	Weakly fractured amphibolite dark greenish in colour massive in nature with weakly foliated with consist of plagioclase & hornblend in dark colour and migmatite with alternating leucocratic (light-colored) and melanocratic

									gneiss	(dark-colored) bands.
37.50	39.00	1.50	92.67	NQ	45.33	Medium to coarse grain	Pinkish grey to white	-	Migmatite Gneiss	Highly fractured migmatite gneiss with alternating leucocratic (light-colored) and melanocratic (dark-colored) bands. The leucocratic portions are rich in coarse-grained orthoclase feldspar, which appears as salmon-colored crystals, often forming large megacrysts or intergrown aggregates. Orthoclase is the dominant mineral in the felsic bands.
39.00	40.00	1.00	94.00	NQ	57.00	Medium to coarse grain	Pinkish grey to white	Allanite/magnetite	Migmatite Gneiss	Highly fractured migmatite gneiss with alternating leucocratic (light-colored) and melanocratic (dark-colored) bands. The leucocratic portions are rich in coarse-grained orthoclase feldspar, which appears as salmon-colored crystals, often forming large megacrysts or intergrown aggregates. Orthoclase is the dominant mineral in the felsic bands.
40.00	42.00	2.00	94.00	NQ	84.00	Medium to coarse grain	Pinkish grey to white	Allanite/magnetite	Migmatite Gneiss	The core consists of migmatite gneiss with alternating leucocratic (light-colored) and melanocratic (dark-colored) bands. The leucocratic portions are rich in coarse-grained orthoclase feldspar, which appears as salmon-colored crystals, often forming large megacrysts or intergrown aggregates. Orthoclase is the dominant mineral in the felsic bands.
42.00	43.00	1.00	93.00	NQ	76.00	Medium to coarse grain	Pinkish grey to white	-	Migmatite Gneiss	The core consists of migmatite gneiss with alternating leucocratic (light-colored) and melanocratic (dark-colored) bands. The leucocratic portions are rich in coarse-grained orthoclase feldspar, which appears as salmon-colored crystals, often forming large megacrysts or intergrown aggregates. Orthoclase is the dominant mineral in the felsic bands.
43.00	45.00	2.00	98.00	NQ	94.00	Medium to coarse grain	Pinkish grey to white	pyrite	Migmatite Gneiss	The core consists of migmatite gneiss with alternating leucocratic (light-colored) and melanocratic (dark-colored) bands. The leucocratic portions are rich in coarse-grained orthoclase feldspar, which appears as salmon-colored crystals, often forming large megacrysts or intergrown aggregates. Orthoclase is the dominant mineral in the felsic bands.

45.00	48.00	3.00	97.33	NQ	97.33	Medium to coarse grain	Pinkish grey to white	Allanite/magnetite	Migmatite Gneiss	The core consists of migmatite gneiss with alternating leucocratic (light-colored) and melanocratic (dark-colored) bands. The leucocratic portions are rich in coarse-grained orthoclase feldspar, which appears as salmon-colored crystals, often forming large megacrysts or intergrown aggregates. Orthoclase is the dominant mineral in the felsic bands.
48.00	48.92	0.92	98.91	NQ	98.91	Medium to coarse grain	Pinkish grey to white	Allanite/magnetite	Migmatite Gneiss	The core consists of migmatite gneiss with alternating leucocratic (light-colored) and melanocratic (dark-colored) bands. The leucocratic portions are rich in coarse-grained orthoclase feldspar, which appears as salmon-colored crystals, often forming large megacrysts or intergrown aggregates. Orthoclase is the dominant mineral in the felsic bands.
48.92	49.00	0.08	100.00	NQ	100.00	Medium to coarse grain	Pinkish grey to white	Allanite/magnetite	Migmatite Gneiss intermixed with pegmatite	The core consists of migmatite gneiss with alternating leucocratic (light-colored) and melanocratic (dark-colored) bands with coarse grained pink coloured orthoclase & quartz & muscovite observed.
49.00	50.00	1.00	97.00	NQ	97.00	coarse grain	Pink, white & black	quartz & mica	pegmatite	Coarse grained Pegmatite with pink coloured orthoclase feldspar, quartz & muscovite observed.
50.00	50.15	0.15	93.33	NQ	93.33	coarse grain	Pink, white & black	quartz & mica	pegmatite	Coarse grained Pegmatite with pink coloured orthoclase feldspar, quartz & muscovite observed.
50.15	50.26	0.11	90.91	NQ	90.91	coarse grain	Pink, white & black	quartz & mica	pegmatite	Coarse grained Pegmatite with pink coloured orthoclase feldspar, quartz & muscovite observed.
50.26	51.00	0.74	98.65	NQ	98.65	Medium to coarse grain	Pinkish Black to white	epidote, allanite	Syenite	The core interval consists of a coarse- to medium-grained syenite with epidote vein, displaying a light grey to pinkish-grey colour. The rock is predominantly composed of alkali feldspar, with minor plagioclase.
51.00	51.87	0.87	98.85	NQ	98.85	Medium to coarse grain	Pinkish Black to white	epidote, allanite	Syenite	The core interval consists of a coarse- to medium-grained syenite with epidote vein, displaying a light grey to pinkish-grey colour. The rock is predominantly composed of alkali feldspar, with minor plagioclase.
51.87	54.00	2.13	98.12	NQ	98.12	Medium to coarse grain	Pinkish Black to grey	Allanite/magnetite	Migmatite Gneiss	The core consists of migmatite gneiss with alternating leucocratic (light-colored) and melanocratic (dark-colored) bands. The leucocratic portions are rich in coarse-grained

										orthoclase feldspar, which appears as salmon-colored crystals, often forming large megacrysts or intergrown aggregates. Orthoclase is the dominant mineral in the felsic bands.
54.00	55.00	1.00	97.00	NQ	82.00	Medium to coarse grain	greyish black to grey	Allanite/magnetite	Migmatite Gneiss	The core consists of migmatite gneiss with alternating leucocratic (light-colored) and melanocratic (dark-colored) bands. The leucocratic portions are rich in coarse-grained orthoclase feldspar, which appears as salmon-colored crystals, often forming large megacrysts or intergrown aggregates. Orthoclase is the dominant mineral in the felsic bands.
55.00	55.82	0.82	98.78	NQ	98.78	Medium to coarse grain	greyish black to grey	Quartz, biotite	Migmatite Gneiss	The core consists of migmatite gneiss with melanocratic (dark-colored) bands. The melanocratic portions are enriched in coarse-grained biotite & amphibole, appearing as grey to black-colored crystals, often forming large megacrysts or intergrown aggregates.
55.82	57.00	1.18	98.31	NQ	98.31	Medium to coarse grain	greyish black to grey	Quartz, biotite	Migmatite Gneiss	The core consists of migmatite gneiss with melanocratic (dark-colored) bands. The melanocratic portions are enriched in coarse-grained biotite & amphibole, appearing as grey to black-colored crystals, often forming large megacrysts or intergrown aggregates.
57.00	60.00	3.00	95.67	NQ	73.00	Medium to coarse grain	greyish black to grey	Quartz, biotite	Migmatite Gneiss	The core consists of migmatite gneiss with melanocratic (dark-colored) bands. The melanocratic portions are enriched in coarse-grained biotite & amphibole, appearing as grey to black-colored crystals, often forming large megacrysts or intergrown aggregates.
60.00	63.00	3.00	97.33	NQ	97.33	Medium to coarse grain	greyish black to grey	Quartz, biotite	Migmatite Gneiss	The core consists of migmatite gneiss with melanocratic (dark-colored) bands. The melanocratic portions are enriched in coarse-grained biotite & amphibole, appearing as grey to black-colored crystals, often forming large megacrysts or intergrown aggregates.
63.00	63.57	0.57	98.25	NQ	98.25	Medium to coarse grain	greyish black to grey	Quartz, biotite	Migmatite Gneiss	The core consists of migmatite gneiss with melanocratic (dark-colored) bands. The melanocratic portions are enriched in coarse-grained biotite & amphibole, appearing as grey to black-colored crystals, often forming large megacrysts or intergrown aggregates.

63.57	65.00	1.43	97.90	NQ	93.00	Medium to coarse grain	greyish black to grey	Quartz, biotite	Migmatite Gneiss	The core consists of migmatite gneiss with melanocratic (dark-colored) bands. The melanocratic portions are enriched in coarse-grained biotite & amphibole, appearing as grey to black-colored crystals, often forming large megacrysts or intergrown aggregates.
65.00	66.00	1.00	98.00	NQ	98.00	Medium to coarse grain	greyish black to grey	Quartz, biotite	Migmatite Gneiss	The core consists of migmatite gneiss with melanocratic (dark-colored) bands. The melanocratic portions are enriched in coarse-grained biotite & amphibole, appearing as grey to black-colored crystals, often forming large megacrysts or intergrown aggregates.
66.00	68.75	2.75	98.91	NQ	98.91	Medium to coarse grain	Ligth pinkish to Black & grey	Quartz, biotite	Migmatite Gneiss	The core consists of migmatite gneiss with melanocratic (dark-colored) bands. The melanocratic portions are enriched in coarse-grained biotite & amphibole, appearing as grey to black-colored crystals, often forming large megacrysts or intergrown aggregates.
68.75	69.00	0.25	96.00	NQ	96.00	Medium to coarse grain	Ligth pinkish to Black & grey	-	Migmatite Gneiss	The core consists of migmatite gneiss with alternating leucocratic (light-colored) and melanocratic (dark-colored) bands. The leucocratic portions are rich in coarse-grained orthoclase feldspar, which appears as salmon-colored crystals, often forming large megacrysts or intergrown aggregates. Orthoclase is the dominant mineral in the felsic bands.
69.00	69.74	0.74	98.65	NQ	98.65	Medium to coarse grain	Ligth pinkish to Black & grey	-	Migmatite Gneiss	The core consists of migmatite gneiss with alternating leucocratic (light-colored) and melanocratic (dark-colored) bands. The leucocratic portions are rich in coarse-grained orthoclase feldspar, which appears as salmon-colored crystals, often forming large megacrysts or intergrown aggregates. Orthoclase is the dominant mineral in the felsic bands.
69.74	70.25	0.51	92.16	NQ	74.50	Medium to coarse grain	Ligth pinkish to Black & grey	-	Migmatite Gneiss	The core consists of migmatite gneiss with alternating leucocratic (light-colored) and melanocratic (dark-colored) bands. The leucocratic portions are rich in coarse-grained orthoclase feldspar, which appears as salmon-colored crystals, often forming large megacrysts or intergrown aggregates. Orthoclase is the dominant mineral in the felsic bands.

70.25	72.00	1.75	94.29	NQ	80.57	Medium to coarse grain	Pinkish to Black	Allanite/magnetite	Syenite	The core interval consists of a coarse- to medium-grained syenite with epidote vein, displaying a light grey to pinkish-grey colour. The rock is predominantly composed of alkali feldspar, with minor plagioclase.
72.00	72.63	0.63	98.41	NQ	98.41	Medium to coarse grain	Pinkish to Black	Epidote Allanite/magnetite	Syenite	The core interval consists of a coarse- to medium-grained syenite with epidote vein, displaying a light grey to pinkish-grey colour. The rock is predominantly composed of alkali feldspar, with minor plagioclase.
72.63	72.82	0.19	94.74	NQ	94.73	coarse grain	Pinkish to Black	Epidote Allanite/magnetite	Syenite	The core interval consists of a coarse- to medium-grained syenite with epidote vein, displaying a light grey to pinkish-grey colour. The rock is predominantly composed of alkali feldspar, with minor plagioclase.
72.82	73.42	0.60	95.00	NQ	95.00	Medium to coarse grain	Pinkish to Black	Epidote Allanite/magnetite	Syenite	The core interval consists of a coarse- to medium-grained syenite with epidote vein, displaying a light grey to pinkish-grey colour. The rock is predominantly composed of alkali feldspar, with minor plagioclase.
73.42	75.00	1.58	98.73	NQ	98.73	Medium to coarse grain	Pinkish to Black	Zeosite, Epidote, Allanite/Magnetite	Syenite	The core interval consists of a coarse- to medium-grained syenite with epidote vein, displaying a light grey to pinkish-grey colour. The rock is predominantly composed of alkali feldspar, with minor plagioclase.
75.00	75.54	0.54	96.30	NQ	51.85	Medium to coarse grain	Ligth pinkish to Black & grey	Allanite/magnetite	Migmatite Gneiss	The core consists of migmatite gneiss with melanocratic (dark-colored) bands. The melanocratic portions are enriched in coarse-grained biotite & amphibole, appearing as grey to black-colored crystals, often forming large megacrysts or intergrown aggregates.
75.54	78.00	2.46	98.37	NQ	93.08	Medium to coarse grain	Ligth pinkish to Black & grey	Allanite/magnetite	Migmatite Gneiss	The core consists of migmatite gneiss with melanocratic (dark-colored) bands. The melanocratic portions are enriched in coarse-grained biotite & amphibole, appearing as grey to black-colored crystals, often forming large megacrysts or intergrown aggregates.
78.00	80.00	2.00	96.50	NQ	94.50	Medium to coarse grain	Ligth pinkish to Black & grey	Allanite/magnetite	Migmatite Gneiss	The core consists of migmatite gneiss with melanocratic (dark-colored) bands. The melanocratic portions are enriched in coarse-grained biotite & amphibole, appearing as grey to black-colored crystals, often forming large megacrysts or intergrown aggregates.
80.00	80.37	0.37	97.30	NQ	97.30	Medium to	Ligth pinkish	Allanite/magnetite	Migmatite	The core consists of migmatite gneiss with melanocratic

						coarse grain	to Black & grey		Gneiss	(dark-colored) bands. The melanocratic portions are enriched in coarse-grained biotite & amphibole, appearing as grey to black-colored crystals, often forming large megacrysts or intergrown aggregates.
80.37	81.00	0.63	92.06	NQ	92.06	Medium to coarse grain	Ligth to Black & grey	Tremolite, Allanite/Magnetite	Migmatite Gneiss	The core consists of migmatite gneiss with melanocratic (dark-colored) bands. The melanocratic portions are enriched in coarse-grained biotite & amphibole, appearing as grey to black-colored crystals, often forming large megacrysts or intergrown aggregates.
81.00	82.48	1.48	97.97	NQ	97.97	Medium to coarse grain	Ligth pinkish to Black & grey	Allanite/magnetite	Migmatite Gneiss	The core consists of migmatite gneiss with melanocratic (dark-colored) bands. The melanocratic portions are enriched in coarse-grained biotite & amphibole, appearing as grey to black-colored crystals, often forming large megacrysts or intergrown aggregates.
82.48	84.00	1.52	95.39	NQ	95.39	Medium to coarse grain	Ligth pinkish to Black & grey	Allanite/magnetite	Migmatite Gneiss	The core consists of migmatite gneiss with melanocratic (dark-colored) bands. The melanocratic portions are enriched in coarse-grained biotite & amphibole, appearing as grey to black-colored crystals, often forming large megacrysts or intergrown aggregates.
84.00	87.00	3.00	97.00	NQ	97.00	Medium to coarse grain	Ligth pinkish to Black & grey	Allanite/magnetite	Migmatite Gneiss	The core consists of migmatite gneiss with melanocratic (dark-colored) bands. The melanocratic portions are enriched in coarse-grained biotite & amphibole, appearing as grey to black-colored crystals, often forming large megacrysts or intergrown aggregates.
87.00	87.32	0.32	96.88	NQ	62.50	Medium to coarse grain	Ligth pinkish to Black & grey	Allanite/magnetite	Migmatite Gneiss	The core consists of migmatite gneiss with melanocratic (dark-colored) bands. The melanocratic portions are enriched in coarse-grained biotite & amphibole, appearing as grey to black-colored crystals, often forming large megacrysts or intergrown aggregates.
87.32	88.15	0.83	96.39	NQ	96.39	Medium to coarse grain	Ligth pinkish to Black & grey	Allanite/magnetite	Migmatite Gneiss	The core consists of migmatite gneiss with melanocratic (dark-colored) bands. The melanocratic portions are enriched in coarse-grained biotite & amphibole, appearing as grey to black-colored crystals, often forming large megacrysts or intergrown aggregates.
88.15	88.74	0.59	98.31	NQ	98.31	Medium to coarse grain	Ligth pinkish to Black &	Allanite/magnetite	Migmatite Gneiss	The core consists of migmatite gneiss with melanocratic (dark-colored) bands. The melanocratic portions are enriched

							grey			in coarse-grained biotite & amphibole, appearing as grey to black-colored crystals, often forming large megacrysts or intergrown aggregates.
88.74	90.00	1.26	94.44	NQ	94.44	Medium to coarse grain	Ligth pinkish to Black & grey	Allanite/magnetite	Migmatite Gneiss	The core consists of migmatite gneiss with melanocratic (dark-colored) bands. The melanocratic portions are enriched in coarse-grained biotite & amphibole, appearing as grey to black-colored crystals, often forming large megacrysts or intergrown aggregates.
90.00	91.88	1.88	97.87	NQ	97.87	Medium to coarse grain	Ligth pinkish to Black & grey	Allanite/magnetite	Migmatite Gneiss	The core consists of migmatite gneiss with melanocratic (dark-colored) bands. The melanocratic portions are enriched in coarse-grained biotite & amphibole, appearing as grey to black-colored crystals, often forming large megacrysts or intergrown aggregates.
91.88	93.00	1.12	98.21	NQ	98.21	Medium to coarse grain	Ligth pinkish to Black & grey	Allanite/magnetite	Migmatite Gneiss	The core consists of migmatite gneiss with melanocratic (dark-colored) bands. The melanocratic portions are enriched in coarse-grained biotite & amphibole, appearing as grey to black-colored crystals, often forming large megacrysts or intergrown aggregates.
93.00	95.35	2.35	97.87	NQ	97.87	Medium to coarse grain	Ligth pinkish to Black & grey	Pyrite, Allanite/magnetite	Migmatite Gneiss	The core consists of migmatite gneiss with melanocratic (dark-colored) bands. The melanocratic portions are enriched in coarse-grained biotite & amphibole, appearing as grey to black-colored crystals, often forming large megacrysts or intergrown aggregates.
95.35	96.00	0.65	89.23	NQ	73.75	Medium to coarse grain	Ligth pinkish to Black & grey	Allanite/magnetite	Migmatite Gneiss	The core consists of migmatite gneiss with melanocratic (dark-colored) bands. The melanocratic portions are enriched in coarse-grained biotite & amphibole, appearing as grey to black-colored crystals, often forming large megacrysts or intergrown aggregates.
96.00	99.00	3.00	97.33	NQ	97.33	Medium to coarse grain	Ligth pinkish to Black & grey	Allanite/magnetite	Migmatite Gneiss	The core consists of migmatite gneiss with melanocratic (dark-colored) bands. The melanocratic portions are enriched in coarse-grained biotite & amphibole, appearing as grey to black-colored crystals, often forming large megacrysts or intergrown aggregates.
99.00	99.55	0.55	98.18	NQ	98.18	Medium to coarse grain	Ligth pinkish to Black & grey	Allanite/magnetite	Migmatite Gneiss	The core consists of migmatite gneiss with melanocratic (dark-colored) bands. The melanocratic portions are enriched in coarse-grained biotite & amphibole, appearing as grey to

										black-colored crystals, often forming large megacrysts or intergrown aggregates.
99.55	100.33	0.78	97.44	NQ	97.43	Medium to coarse grain	Ligth pinkish to Black & grey	Allanite/magnetite	Migmatite Gneiss	The core consists of migmatite gneiss with melanocratic (dark-colored) bands. The melanocratic portions are enriched in coarse-grained biotite & amphibole, appearing as grey to black-colored crystals, often forming large megacrysts or intergrown aggregates.
100.33	100.75	0.42	92.86	NQ	92.86	coarse grain	Pinkish White to Black	Mica, Quartz, Feldspar	Pegmatite	Coarse grained Pegmatite with pink coloured orthoclase feldspar, quartz & mica observed.
100.75	101.48	0.73	94.52	NQ	94.52	Medium to coarse grain	Ligth pinkish to Black &grey	Allanite/magnetite	Migmatite Gneiss	The core consists of migmatite gneiss with melanocratic (dark-colored) bands. The melanocratic portions are enriched in coarse-grained biotite & amphibole, appearing as grey to black-colored crystals, often forming large megacrysts or intergrown aggregates.
101.48	102.00	0.52	90.38	NQ	90.38	Medium to coarse grain	Ligth pinkish to Black & grey	Allanite/magnetite	Migmatite Gneiss	The core consists of migmatite gneiss with melanocratic (dark-colored) bands. The melanocratic portions are enriched in coarse-grained biotite & amphibole, appearing as grey to black-colored crystals, often forming large megacrysts or intergrown aggregates.
102.00	103.24	1.24	98.39	NQ	98.39	Medium to coarse grain	Ligth pinkish to Black & grey	Allanite/magnetite	Migmatite Gneiss	The core consists of migmatite gneiss with melanocratic (dark-colored) bands. The melanocratic portions are enriched in coarse-grained biotite & amphibole, appearing as grey to black-colored crystals, often forming large megacrysts or intergrown aggregates.
103.24	103.42	0.18	77.78	NQ	0.00	Medium to coarse grain	pinkish to Black & grey	Allanite/magnetite	Migmatite Gneiss	The core consists of migmatite gneiss with melanocratic (dark-colored) bands. The melanocratic portions are enriched in coarse-grained biotite & amphibole, appearing as grey to black-colored crystals, often forming large megacrysts or intergrown aggregates.
103.42	104.00	0.58	96.55	NQ	96.55	Medium to coarse grain	pinkish to Black & grey	Allanite/magnetite	Migmatite Gneiss	The core consists of migmatite gneiss with melanocratic (dark-colored) bands. The melanocratic portions are enriched in coarse-grained biotite & amphibole, appearing as grey to black-colored crystals, often forming large megacrysts or intergrown aggregates.
104.00	105.00	1.00	97.00	NQ	65.00	Medium to	pinkish to	Allanite/magnetite	Migmatite	The core consists of migmatite gneiss with melanocratic

						coarse grain	Black & grey		Gneiss	(dark-colored) bands. The melanocratic portions are enriched in coarse-grained biotite & amphibole, appearing as grey to black-colored crystals, often forming large megacrysts or intergrown aggregates.
105.00	107.00	2.00	97.50	NQ	97.50	Medium to coarse grain	pinkish to Black & grey	Allanite/magnetite	Migmatite Gneiss	The core consists of migmatite gneiss with melanocratic (dark-colored) bands. The melanocratic portions are enriched in coarse-grained biotite & amphibole, appearing as grey to black-colored crystals, often forming large megacrysts or intergrown aggregates.
107.00	108.00	1.00	98.00	NQ	98.00	Medium to coarse grain	pinkish to Black & grey	Allanite/magnetite	Migmatite Gneiss	The core consists of migmatite gneiss with melanocratic (dark-colored) bands. The melanocratic portions are enriched in coarse-grained biotite & amphibole, appearing as grey to black-colored crystals, often forming large megacrysts or intergrown aggregates.
108.00	111.00	3.00	97.33	NQ	97.33	Medium to coarse grain	pinkish to Black & grey	Epidote, Allanite/magnetite	Migmatite Gneiss	The core consists of migmatite gneiss with melanocratic (dark-colored) bands. The melanocratic portions are enriched in coarse-grained biotite & amphibole, appearing as grey to black-colored crystals, often forming large megacrysts or intergrown aggregates.
111.00	111.81	0.81	97.53	NQ	97.53	Medium to coarse grain	Ligth pinkish to Black & grey	Allanite/magnetite	Migmatite Gneiss	The core consists of migmatite gneiss with melanocratic (dark-colored) bands. The melanocratic portions are enriched in coarse-grained biotite & amphibole, appearing as grey to black-colored crystals, often forming large megacrysts or intergrown aggregates.
111.81	112.23	0.42	92.86	NQ	92.86	Medium to coarse grain	Ligth pinkish to Black & grey	Allanite/magnetite	Migmatite Gneiss	The core consists of migmatite gneiss with melanocratic (dark-colored) bands. The melanocratic portions are enriched in coarse-grained biotite & amphibole, appearing as grey to black-colored crystals, often forming large megacrysts or intergrown aggregates.
112.23	114.00	1.77	98.87	NQ	98.87	Medium to coarse grain	Ligth pinkish to Black & grey	Allanite/magnetite	Migmatite Gneiss	The core consists of migmatite gneiss with melanocratic (dark-colored) bands. The melanocratic portions are enriched in coarse-grained biotite & amphibole, appearing as grey to black-colored crystals, often forming large megacrysts or intergrown aggregates.
114.00	114.66	0.66	98.48	NQ	98.48	Medium to coarse grain	Ligth pinkish to Black &	Allanite/magnetite	Migmatite Gneiss	The core consists of migmatite gneiss with melanocratic (dark-colored) bands. The melanocratic portions are enriched

							grey			in coarse-grained biotite & amphibole, appearing as grey to black-colored crystals, often forming large megacrysts or intergrown aggregates.
114.66	117.00	2.34	98.29	NQ	98.29	Medium to coarse grain	Ligth pinkish to Black & grey	Allanite/magnetite	Migmatite Gneiss	The core consists of migmatite gneiss with melanocratic (dark-colored) bands. The melanocratic portions are enriched in coarse-grained biotite & amphibole, appearing as grey to black-coloured crystals, often forming large megacrysts or intergrown aggregates.
117.00	118.48	1.48	98.65	NQ	98.65	Medium to coarse grain	Light pinkish to Black & grey	Allanite/magnetite	Migmatite Gneiss	The core consists of migmatite gneiss with melanocratic (dark coloured) bands. The melanocratic portions are enriched in coarse-grained biotite & amphibole, appearing as grey to black-coloured crystals, often forming large megacrysts or intergrown aggregates.
118.48	120.00	1.52	98.68	NQ	98.68	Medium to coarse grain	Light pinkish to Black & grey	Allanite/magnetite	Migmatite Gneiss	The core consists of migmatite gneiss with melanocratic (dark coloured) bands. The melanocratic portions are enriched in coarse-grained biotite & amphibole, appearing as grey to black-coloured crystals, often forming large megacrysts or intergrown aggregates.
120.00	123.00	3.00	98.67	NQ	98.67	Medium to coarse grain	Light pinkish to Black & grey	Allanite/magnetite	Migmatite Gneiss	The core consists of migmatite gneiss with melanocratic (dark coloured) bands. The melanocratic portions are enriched in coarse-grained biotite & amphibole, appearing as grey to black-coloured crystals, often forming large megacrysts or intergrown aggregates.
123.00	125.00	2.00	97.50	NQ	97.50	Medium to coarse grain	Light pinkish to Black & grey	Allanite/magnetite	Migmatite Gneiss	The core consists of migmatite gneiss with melanocratic (dark coloured) bands. The melanocratic portions are enriched in coarse-grained biotite & amphibole, appearing as grey to black-colored crystals, often forming large megacrysts or intergrown aggregates.
125.00	125.49	0.49	81.63	NQ	0.00	Medium to coarse grain	Light pinkish to Black & grey	-	Amphibolite	The core consists of migmatite gneiss with melanocratic (dark-colored) bands. The melanocratic portions are enriched in coarse-grained biotite & amphibole, appearing as grey to black-colored crystals, often forming large megacrysts or intergrown aggregates.
125.49	125.92	0.43	97.67	NQ	97.67	Medium to coarse grain	Light pinkish to Black & grey	Allanite/magnetite	Migmatite Gneiss	The core consists of migmatite gneiss with melanocratic (dark-colored) bands. The melanocratic portions are enriched in coarse-grained biotite & amphibole, appearing as grey to

										black-colored crystals, often forming large megacrysts or intergrown aggregates.
125.92	126.00	0.08	87.50	NQ	0.00	Medium to coarse grain	Light pinkish to Black & grey	Allanite/magnetite	Migmatite Gneiss	The core consists of migmatite gneiss with melanocratic (dark-colored) bands. The melanocratic portions are enriched in coarse-grained biotite & amphibole, appearing as grey to black-colored crystals, often forming large megacrysts or intergrown aggregates.
126.00	126.49	0.49	93.88	NQ	93.87	Medium to coarse grain	Light pinkish to Black & grey	Allanite/magnetite	Migmatite Gneiss	The core consists of migmatite gneiss with melanocratic (dark-colored) bands. The melanocratic portions are enriched in coarse-grained biotite & amphibole, appearing as grey to black-colored crystals, often forming large megacrysts or intergrown aggregates.
126.49	127.43	0.94	95.74	NQ	80.86	Medium to coarse grain	pinkish to Black & grey	Allanite/magnetite	Migmatite Gneiss	The core consists of migmatite gneiss with melanocratic (dark-colored) bands. The melanocratic portions are enriched in coarse-grained biotite & amphibole, appearing as grey to black-colored crystals, often forming large megacrysts or intergrown aggregates.
127.43	129.00	1.57	97.45	NQ	84.07	Medium to coarse grain	pinkish to Black & grey	Allanite/magnetite	Migmatite Gneiss	The core consists of migmatite gneiss with melanocratic (dark-colored) bands. The melanocratic portions are enriched in coarse-grained biotite & amphibole, appearing as grey to black-colored crystals, often forming large megacrysts or intergrown aggregates.
129.00	129.25	0.25	96.00	NQ	96.00	Medium to coarse grain	Ligth pinkish to Black & grey	Allanite/magnetite	Migmatite Gneiss	The core consists of migmatite gneiss with melanocratic (dark-colored) bands. The melanocratic portions are enriched in coarse-grained biotite & amphibole, appearing as grey to black-colored crystals, often forming large megacrysts or intergrown aggregates.
129.25	129.52	0.27	88.89	NQ	0.00	Medium to coarse grain	Ligth pinkish to Black & grey	Allanite/magnetite	Migmatite Gneiss	The core consists of migmatite gneiss with melanocratic (dark-colored) bands. The melanocratic portions are enriched in coarse-grained biotite & amphibole, appearing as grey to black-colored crystals, often forming large megacrysts or intergrown aggregates.
129.52	131.31	1.79	98.32	NQ	85.00	Medium to coarse grain	pinkish to Black & grey	Allanite/magnetite	Migmatite Gneiss	The core consists of migmatite gneiss with melanocratic (dark-colored) bands. The melanocratic portions are enriched in coarse-grained biotite & amphibole, appearing as grey to black-colored crystals, often forming large megacrysts or

										intergrown aggregates.
131.31	131.70	0.39	92.31	NQ	28.00	Medium to coarse grain	pinkish to Black & grey	Allanite/magnetite	Migmatite Gneiss	The core consists of migmatite gneiss with melanocratic (dark-colored) bands. The melanocratic portions are enriched in coarse-grained biotite & amphibole, appearing as grey to black-colored crystals, often forming large megacrysts or intergrown aggregates.
131.70	132.00	0.30	96.67	NQ	96.67	Medium to coarse grain	pinkish to Black & grey	Allanite/magnetite	Migmatite Gneiss	The core consists of migmatite gneiss with melanocratic (dark-colored) bands. The melanocratic portions are enriched in coarse-grained biotite & amphibole, appearing as grey to black-colored crystals, often forming large megacrysts or intergrown aggregates.
132.00	132.71	0.71	94.37	NQ	94.37	Medium to coarse grain	pinkish to Black & grey	Allanite/magnetite	Migmatite Gneiss	The core consists of migmatite gneiss with melanocratic (dark-colored) bands. The melanocratic portions are enriched in coarse-grained biotite & amphibole, appearing as grey to black-colored crystals, often forming large megacrysts or intergrown aggregates.
132.71	133.14	0.43	93.02	NQ	34.00	Medium to coarse grain	pinkish to Black & grey	Biotite, Quartz	Migmatite Gneiss	The core consists of migmatite gneiss with melanocratic (dark-colored) bands. The melanocratic portions are enriched in coarse-grained biotite & amphibole, appearing as grey to black-colored crystals, often forming large megacrysts or intergrown aggregates.
133.14	134.73	1.59	98.74	NQ	98.74	Medium to coarse grain	pinkish to Black & grey	Allanite/magnetite	Migmatite Gneiss	The core consists of migmatite gneiss with melanocratic (dark-colored) bands. The melanocratic portions are enriched in coarse-grained biotite & amphibole, appearing as grey to black-colored crystals, often forming large megacrysts or intergrown aggregates.
134.73	135.00	0.27	96.30	NQ	96.3	Medium to coarse grain	pinkish to Black & grey	Allanite/magnetite	Migmatite Gneiss	The core consists of migmatite gneiss with melanocratic (dark-colored) bands. The melanocratic portions are enriched in coarse-grained biotite & amphibole, appearing as grey to black-colored crystals, often forming large megacrysts or intergrown aggregates.
135.00	135.87	0.87	97.70	NQ	87.35	Medium to coarse grain	pinkish to Black & grey	Allanite/magnetite	Migmatite Gneiss	The core consists of migmatite gneiss with melanocratic (dark-colored) bands. The melanocratic portions are enriched in coarse-grained biotite & amphibole, appearing as grey to black-colored crystals, often forming large megacrysts or intergrown aggregates.

135.87	137.0	1.13	97.35	NQ	97.35	Medium to coarse grain	Reddish to Black & grey	Epidote, Allanite/magnetite	Intermix Migmatite Gneiss & syenite	The core interval consists of a coarse- to medium-grained syenite with epidote vein, displaying Reddish-Black & grey colour. The rock is predominantly composed of alkali feldspar, with minor plagioclase.
137.0	139.0	2.00	98.50	NQ	98.50	Medium to coarse grain	Reddish to Black & grey	Epidote, Allanite/magnetite	Intermix Migmatite Gneiss & syenite	The core interval consists of a coarse- to medium-grained syenite with epidote vein, displaying Reddish-Black & grey colour. The rock is predominantly composed of alkali feldspar, with minor plagioclase.
139.00	139.24	0.24	95.83	NQ	95.83	Medium to coarse grain	Reddish to Black & grey	-	Intermix Migmatite Gneiss & syenite	The core interval consists of a coarse- to medium-grained syenite with epidote vein, displaying Reddish-Black & grey colour. The rock is predominantly composed of alkali feldspar, with minor plagioclase.
139.24	140.0	0.76	96.05	NQ	89.47	Coarse grain	Reddish to Black & grey	Epidote	Syenite	The core interval consists of a coarse- to medium-grained syenite with epidote vein, displaying Reddish-Black & grey colour. The rock is predominantly composed of alkali feldspar, with minor plagioclase.
140.0	141.0	1.00	97.00	NQ	97.0	Coarse grain	Reddish to Black & grey	Epidote, Allanite/magnetite	Syenite	The core interval consists of a coarse- to medium-grained syenite with epidote vein, displaying Reddish-Black & grey colour. The rock is predominantly composed of alkali feldspar, with minor plagioclase.
141.0	141.73	0.73	98.63	NQ	98.63	Coarse grain	Reddish to Black & grey	Epidote, Allanite/magnetite	Syenite	The core interval consists of a coarse- to medium-grained syenite with epidote vein, displaying Reddish-Black & grey colour. The rock is predominantly composed of alkali feldspar, with minor plagioclase.
141.73	143.26	1.53	98.69	NQ	93.46	coarse grain to Medium Grain	Reddish to Black & grey	Epidote, Allanite/magnetite	Intermixed Migmatite Gneiss & syenite	The core interval consists of a coarse- to medium-grained Migmatite & syenite with epidote vein, displaying Reddish-Black & grey colour. The rock is predominantly composed of alkali feldspar, with minor plagioclase.
143.26	144.0	0.74	97.30	NQ	97.3	coarse grain to Medium Grain	Reddish to Black & grey	Zeosite, Epidote, Allanite/magnetite	Intermix Migmatite Gneiss & syenite	The core interval consists of a coarse- to medium-grained Migmatite & syenite with epidote vein, displaying Reddish-Black & grey colour. The rock is predominantly composed of alkali feldspar, with minor plagioclase.
144.00	145.81	1.81	99.45	NQ	99.45	Coarse grain	Reddish to Black & grey	Chalcopyrite, Epidote, Allanite/magnetite	Syenite	The core interval consists of a coarse- to medium-grained syenite with epidote vein, displaying Reddish-Black & grey colour. The rock is predominantly composed of alkali feldspar, with minor plagioclase.

145.81	147.0	1.19	98.32	NQ	98.31	Coarse grain	Pinkish to Grey & Black	Pyrite, Epidote, Allanite/magnetite	Syenite	The core interval consists of a coarse- to medium-grained syenite with epidote vein, displaying Reddish-Black & grey colour. The rock is predominantly composed of alkali feldspar, with minor plagioclase.
147.0	147.45	0.45	97.78	NQ	97.78	coarse grain to Medium Grain	Pinkish to Grey & Black	Pyrite, Epidote, Allanite/magnetite	Intermix ed Migmatite Gneiss & syenite	The core interval consists of a coarse- to medium-grained Migmatite & syenite with epidote vein, displaying Reddish-Black & grey colour. The rock is predominantly composed of alkali feldspar, with minor plagioclase.
147.45	148.0	0.55	96.36	NQ	96.36	Coarse grain	Pinkish to Grey & Black	Pyrite, Epidote, Allanite/magnetite	Syenite	The core interval consists of a coarse- to medium-grained syenite with epidote vein, displaying Reddish-Black & grey colour. The rock is predominantly composed of alkali feldspar, with minor plagioclase.
148.00	150.00	2.00	98.50	NQ	92.0	Coarse grain	Pinkish to Grey & Black	Epidote, Allanite/magnetite	Syenite	The core interval consists of a coarse- to medium-grained syenite with epidote vein, displaying Reddish-Black & grey colour. The rock is predominantly composed of alkali feldspar, with minor plagioclase.
0.00	3.00	3.00	76.67	HQ	0.00	Medium to coarse grain	greenish grey to Black	-	Weathered Migmatite Gneiss	Highly weathered zone, predominantly of a greenish grey in color, moderately compact sand of highly fractured migmatite gneiss observed.
3.00	6.00	3.00	81.00	HQ	0.00	Medium to coarse grain	greenish grey to Black	-	Weathered Migmatite Gneiss	Highly weathered zone, predominantly of a greenish grey in color, moderately compact sand with occasional gravel-sized fragments of highly fractured migmatite gneiss observed.
6.00	9.00	3.00	81.67	HQ	0.00	Medium to coarse grain	Greenish Black	-	Weathered Migmatite Gneiss	Highly weathered zone, predominantly of a greenish grey in color, moderately compact sand with occasional gravel-sized fragments of highly fractured migmatite gneiss observed.
9.00	10.00	1.00	95.00	NQ	11.00	Medium to coarse grain	Blackish grey to Black	Allanite/magnetite	Migmatite Gneiss	The core consists of migmatite gneiss with alternating leucocratic (light-colored) and melanocratic (dark-colored) bands. The leucocratic portions are rich in coarse-grained orthoclase feldspar, which appears as salmon-colored crystals, often forming large megacrysts or intergrown aggregates. Orthoclase is the dominant mineral in the felsic bands.
10.00	10.30	0.30	96.67	NQ	33.33	Medium to coarse grain	Blackish grey to Black	Allanite/magnetite	Migmatite Gneiss	The core consists of migmatite gneiss with alternating leucocratic (light-colored) and melanocratic (dark-colored) bands. The leucocratic portions are rich in coarse-grained orthoclase feldspar, which appears as salmon-colored

										crystals, often forming large megacrysts or intergrown aggregates. Orthoclase is the dominant mineral in the felsic bands.
10.30	12.00	1.70	95.88	NQ	62.94	Medium to coarse grain	Dark green to black in color	-	Amphibolite	Weakly fractured amphibolite dark greenish in colour massive in nature with weakly foliated with consist of plagioclase & hornblend in dark colour and contributing to dense compact appearance.
12.00	15.00	3.00	97.00	NQ	97.00	Medium to coarse grain	Dark green to black in color	-	Amphibolite	Weakly fractured amphibolite dark greenish in colour massive in nature with weakly foliated with consist of plagioclase & hornblend in dark colour and contributing to dense compact appearance.
15.00	16.10	1.10	96.36	NQ	0.83	Medium to coarse grain	Dark green to black in color	-	Amphibolite	Weakly fractured amphibolite dark greenish in colour massive in nature with weakly foliated with consist of plagioclase & hornblend in dark colour and contributing to dense compact appearance.
16.10	17.09	0.99	95.96	NQ	33.33	Medium to coarse grain	Dark green to black in color	-	Amphibolite	Weakly fractured amphibolite dark greenish in colour massive in nature with weakly foliated with consist of plagioclase & hornblend in dark colour and contributing to dense compact appearance.
17.09	18.00	0.91	97.80	NQ	80.80	Medium to coarse grain	Dark green to black in color	-	Amphibolite	Weakly fractured amphibolite dark greenish in colour massive in nature with weakly foliated with consist of plagioclase & hornblend in dark colour and contributing to dense compact appearance.
18.00	19.45	1.45	97.93	NQ	97.93	Medium to coarse grain	Dark green to black in color	-	Amphibolite	Weakly fractured amphibolite dark greenish in colour massive in nature with weakly foliated with consist of plagioclase & hornblend in dark colour and contributing to dense compact appearance.

Log Sheet for BH 4

BORE HOLE NO	**RJB-04**		
TOPOSHEET NO	**45K/03**		
LOCATION	**LAT**	**2525'49.35"**	
	LONG	**74°07'27.79"**	
RL OF COLLAR	**509.358m**		
BH. ANGLE	**45°**	**TOTAL DRILLING TARGET**	**85 m**
AZIMUTH	**N45°W**	**DRILL TYPE**	**Core Drilling**
INCLINATION	**45°**		
BH DEPTH	**85m**		

FROM (m)	TO (m)	RUN (m)	RECOVERY (%)	CORE SIZE	RQD %	GRAIN SIZE	COLOUR	MINERALOGY	ROCK TYPE	DESCRIPTION
0.00	3.00	3.00	2.50	HQ	0.00	Medium to Coarse grain	light grey to dark	-	Wearthered Migmatite Gneiss	Highly weathered zone, predominantly of a Light grey to dark in color, moderately compact sand of highly fractured migmatite gneiss observed.
3.00	6.00	3.00	2.40	HQ	0.00	Medium to Coarse grain	light grey to dark	-	Wearthered Migmatite Gneiss	Highly weathered zone, predominantly of a Light grey to dark in color, moderately compact sand of highly fractured migmatite gneiss observed.
6.00	9.00	3.00	2.50	HQ	0.00	Medium to Coarse grain	light grey to dark	-	Wearthered Migmatite Gneiss	Highly weathered zone, predominantly of a Light grey to dark in color, moderately compact sand of highly fractured migmatite gneiss observed.
9.00	9.40	0.40	0.30	HQ	0.00	Medium to Coarse grain	light grey to dark	-	Wearthered Migmatite Gneiss	Highly weathered zone, predominantly of a Light grey to dark in color, moderately compact sand of highly fractured migmatite gneiss observed.
9.40	10.0	0.60	0.50	HQ	0.00	Medium to	light grey	-	Wearthered	Highly weathered zone, predominantly of a Light grey to dark in

	0					Coarse grain	to dark		Migmatite Gneiss	color, moderately compact sand of highly fractured migmatite gneiss observed.
10.00	12.00	2.00	1.85	NQ	56.50	Medium to Coarse grain	light grey to dark	Allanite/Magnetite	Migmatite Gneiss	The core consists of migmatite gneiss with melanocratic (dark-colored) bands. The melanocratic portions are enriched in coarse-grained biotite & amphibole, appearing as grey to black-colored crystals, often forming large megacrysts or intergrown aggregates.
12.00	13.48	1.48	1.40	NQ	60.13	Medium to Coarse grain	light Pinkish to grey to Black	Allanite/Magnetite	Migmatite Gneiss	The core consists of migmatite gneiss with melanocratic (dark-colored) bands. The melanocratic portions are enriched in coarse-grained biotite & amphibole, appearing as grey to black-colored crystals, often forming large megacrysts or intergrown aggregates.
13.48	14.42	0.94	0.87	NQ	0.00	Medium to Coarse grain	light Pinkish to grey to Black	Allanite/Magnetite	Migmatite Gneiss	The core consists of migmatite gneiss with alternating leucocratic (light-colored) and melanocratic (dark-colored) bands. The leucocratic zones are enriched with coarse-grained orthoclase feldspar.
14.42	15.00	0.58	0.55	NQ	68.96	Medium to Coarse grain	light Pinkish to grey to Black	Allanite/Magnetite	Migmatite Gneiss	The core consists of migmatite gneiss with alternating leucocratic (light-colored) and melanocratic (dark-colored) bands. The leucocratic zones are enriched with coarse-grained orthoclase feldspar.
15.00	18.00	3.00	2.92	NQ	48.00	Medium to Coarse grain	light Pinkish to grey to Black	Epidote, Zeosite, Allanite/Magnetite	Migmatite Gneiss	The core consists of migmatite gneiss with alternating leucocratic (light-colored) and melanocratic (dark-colored) bands. The leucocratic zones are enriched with coarse-grained orthoclase feldspar.
18.00	20.29	2.29	2.25	NQ	56.33	Medium to Coarse grain	light Pinkish to grey to Black	Allanite/Magnetite	Migmatite Gneiss	The core consists of migmatite gneiss with alternating leucocratic (light-colored) and melanocratic (dark-colored) bands. The leucocratic zones are enriched with coarse-grained orthoclase feldspar.
20.29	21.00	0.71	0.69	NQ	69.01	Medium to Coarse grain	light Pinkish to grey to Black	Allanite/Magnetite	Migmatite Gneiss	The core consists of migmatite gneiss with alternating leucocratic (light-colored) and melanocratic (dark-colored) bands. The leucocratic zones are enriched with coarse-grained orthoclase feldspar.
21.00	22.28	1.28	1.27	NQ	99.22	Medium to Coarse grain	White to grey to Black	-	Migmatite Gneiss	The core consists of migmatite gneiss with alternating leucocratic (light-colored) and melanocratic (dark-colored) bands. The leucocratic zones are enriched with coarse-grained orthoclase feldspar.

22.28	22.89	0.61	0.59	NQ	96.72	Medium to Coarse grain	Greenish to Black	-	Amphibolite	Amphibolite dark greenish in colour massive in nature with weakly foliated with consist of plagioclase & hornblend in dark colour and contributing to dense compact appearance
22.89	24.00	1.11	1.07	NQ	45.04	Medium to Coarse grain	light Pinkish to grey to Black	Allanite/Magnetite	Migmatite Gneiss	The core consists of migmatite gneiss with alternating leucocratic (light-colored) and melanocratic (dark-colored) bands. The leucocratic zones are enriched with coarse-grained orthoclase feldspar.
24.00	24.17	0.17	0.16	NQ	94.12	Medium to Coarse grain	light Pinkish to grey to Black	Allanite/Magnetite	Migmatite Gneiss	The core consists of migmatite gneiss with alternating leucocratic (light-colored) and melanocratic (dark-colored) bands. The leucocratic zones are enriched with coarse-grained orthoclase feldspar.
24.17	25.71	1.54	1.51	NQ	83.11	Medium to Coarse grain	Greenish to Black	-	Amphibolite	Amphibolite dark greenish in colour massive in nature with weakly foliated with consist of plagioclase & hornblend in dark colour and contributing to dense compact appearance
25.71	26.72	1.01	0.99	NQ	85.14	Coarse grain to Medium	Pinkish to grey to Black	Epidote, Allanite/Magnetite	Syenite	The core consists of a coarse- to medium-grained syenite with epidote vein, displaying a light pinkish-grey colour. The rock is predominantly composed of alkali feldspar, with minor plagioclase.
26.72	27.00	0.28	0.26	NQ	75.00	Coarse grain to Medium	Pinkish to grey to Black	Epidote, Allanite/Magnetite	Syenite	The core consists of a coarse- to medium-grained syenite with epidote vein, displaying a pinkish-grey colour. The rock is predominantly composed of alkali feldspar, with minor plagioclase.
27.00	27.37	0.37	0.36	NQ	97.30	Coarse grain to Medium	Pinkish to grey to Black	Epidote, Allanite/Magnetite	Syenite	The core consists of a coarse- to medium-grained syenite with epidote vein, displaying a pinkish-grey colour. The rock is predominantly composed of alkali feldspar, with minor plagioclase.
27.37	28.00	0.63	0.60	NQ	20.63	Coarse grain to Medium	Pinkish to grey to Black	Zeosite, Epidote, Allanite/Magnetite	Syenite	The core consists of a coarse- to medium-grained syenite with epidote vein, displaying a pinkish-grey colour. The rock is predominantly composed of alkali feldspar, with minor plagioclase.
28.00	30.00	2.00	1.95	NQ	97.50	Coarse grain to Medium	Pinkish to grey to Black	Epidote, Allanite/Magnetite	Syenite	The core consists of a coarse- to medium-grained syenite with epidote vein, displaying a pinkish-grey colour. The rock is predominantly composed of alkali feldspar, with minor plagioclase.
30.00	31.00	1.00	0.98	NQ	98.00	Coarse grain to Medium	Pinkish to grey to	Epidote, Allanite/Magnetite	Syenite	The core consists of a coarse- to medium-grained syenite with epidote vein, displaying a pinkish-grey colour. The rock is

							Black			predominantly composed of alkali feldspar, with minor plagioclase.
31.00	33.00	2.00	1.97	NQ	98.50	Medium to Coarse grain	light Pinkish to grey to Black	Epidote, Allanite/Magnetite	Migmatite Gneiss	The core consists of migmatite gneiss with alternating leucocratic (light-colored) and melanocratic (dark-colored) bands. The leucocratic zones are enriched with coarse-grained orthoclase feldspar.
33.00	33.64	0.64	0.63	NQ	98.44	Medium to Coarse grain	light Pinkish to grey to Black	Epidote, Allanite/Magnetite	Migmatite Gneiss	The core consists of migmatite gneiss with alternating leucocratic (light-colored) and melanocratic (dark-colored) bands. The leucocratic zones are enriched with coarse-grained orthoclase feldspar.
33.64	35.82	2.18	2.17	NQ	99.54	Coarse grain to Medium	Pinkish to grey to Black	Epidote, Allanite/Magnetite	Intermixed migmatite gneiss & Syenite	The core consists of migmatite gneiss with alternating leucocratic (light-colored) and melanocratic (dark-colored) bands. The leucocratic zones are enriched with coarse-grained orthoclase feldspar.
35.82	36.00	0.18	0.18	NQ	100.00	Coarse grain to Medium	Pinkish to grey to Black	Epidote, Allanite/Magnetite	Intermixed migmatite gneiss & Syenite	The core consists of a coarse- to medium-grained syenite with epidote vein, displaying a pinkish-grey colour. The rock is predominantly composed of alkali feldspar, with minor plagioclase.
36.00	39.00	3.00	2.97	NQ	86.66	Coarse grain to Medium	Pinkish to grey to Black	Epidote, Allanite/Magnetite	Syenite	The core consists of a coarse- to medium-grained syenite with epidote vein, displaying a pinkish-grey colour. The rock is predominantly composed of alkali feldspar, with minor plagioclase.
39.00	41.20	2.20	2.16	NQ	98.18	Coarse grain to Medium	Pinkish to grey to Black	Zeosite, Epidote, Allanite/Magnetite	Syenite	The core consists of a coarse- to medium-grained syenite with epidote vein, displaying a pinkish-grey colour. The rock is predominantly composed of alkali feldspar, with minor plagioclase.
41.20	42.00	0.80	0.78	NQ	97.50	Coarse grain to Medium	Pinkish to grey to Black	Zeosite, Epidote, Allanite/Magnetite	Syenite	The core consists of a coarse- to medium-grained syenite with epidote vein, displaying a pinkish-grey colour. The rock is predominantly composed of alkali feldspar, with minor plagioclase.
42.00	43.69	1.69	1.66	NQ	98.22	Coarse grain to Medium	Pinkish to grey to Black	Zeosite, Epidote, Allanite/Magnetite	Syenite	The core consists of a coarse- to medium-grained syenite with epidote vein, displaying a pinkish-grey colour. The rock is predominantly composed of alkali feldspar, with minor plagioclase.
43.69	44.55	0.86	0.84	NQ	97.67	Coarse grain to Medium	Pinkish to grey to	Zeosite, Epidote, Allanite/Magnetite	Syenite	The core consists of a coarse- to medium-grained syenite with epidote vein, displaying a pinkish-grey colour. The rock is

							Black			predominantly composed of alkali feldspar, with minor plagioclase.
44.55	45.00	0.45	0.43	NQ	95.56	Coarse grain to Medium	Pinkish to grey to Black	Zeosite, Epidote, Allanite/Magnetite	Syenite	The core consists of a coarse- to medium-grained syenite with epidote vein, displaying a pinkish-grey colour. The rock is predominantly composed of alkali feldspar, with minor plagioclase.
45.00	45.66	0.66	0.65	NQ	98.48	Coarse grain to Medium	Pinkish to grey to Black	Zeosite, Epidote, Allanite/Magnetite	Syenite	The core consists of a coarse- to medium-grained syenite with epidote vein, displaying a pinkish-grey colour. The rock is predominantly composed of alkali feldspar, with minor plagioclase.
45.66	46.00	0.34	0.32	NQ	0.00	Coarse grain to Medium	Pinkish to grey to Black	Zeosite, Epidote, Allanite/Magnetite	Syenite	The core consists of a coarse- to medium-grained syenite with epidote vein, displaying a pinkish-grey colour. The rock is predominantly composed of alkali feldspar, with minor plagioclase.
46.00	47.05	1.05	1.04	NQ	99.05	Coarse grain to Medium	Greenish to Pinkish	Arsenopyrite, Zeosite, Epidote, Allanite/Magnetite	Epidiotic Syenite	The core consists of a coarse- to medium-grained epidiotic syenite with epidote vein, displaying a Greenish to pink colour. The rock is predominantly composed of epidotization, with minor feldspar.
47.05	48.00	0.95	0.93	NQ	97.89	Coarse grain to Medium	Pinkish to grey to Black	Zeosite, Epidote, Allanite/Magnetite	Epidiotic Syenite	The core consists of a coarse- to medium-grained syenite with epidote vein, displaying a pinkish-grey colour. The rock is predominantly composed of alkali feldspar, with minor plagioclase.
48.00	48.54	0.54	0.53	NQ	98.14	Coarse grain to Medium	Reddish to grey to Black	Epidote, Allanite/Magnetite	Syenite	The core consists of a coarse- to medium-grained syenite with epidote vein, displaying a pinkish-grey colour. The rock is predominantly composed of alkali feldspar, with minor plagioclase.
48.54	51.00	2.46	2.42	NQ	98.37	Coarse grain to Medium	Reddish to grey to Black	Chlocopyrite, Allaniteepidote	Syenite	The core consists of a coarse- to medium-grained syenite with epidote vein, displaying a pinkish-grey colour. The rock is predominantly composed of alkali feldspar, with minor plagioclase.
51.00	53.63	2.63	2.61	NQ	99.24	Coarse grain to Medium	Pinkish to grey to Black	Epidote, Allanite	Syenite	The core consists of a coarse- to medium-grained syenite with epidote vein, displaying a pinkish-grey colour. The rock is predominantly composed of alkali feldspar, with minor plagioclase.
53.63	54.00	0.37	0.35	NQ	94.59	Coarse grain to Medium	Pinkish to grey to	Zeosite, Epidote, Allanite/Magnetite	Syenite	The core consists of a coarse- to medium-grained syenite with epidote vein, displaying a pinkish-grey colour. The rock is

							Black			predominantly composed of alkali feldspar, with minor plagioclase.
54.00	57.00	3.00	2.96	NQ	98.67	Coarse grain to Medium	Pinkish to grey to Black	Zeosite, Epidote, Allanite/Magnetite	Syenite	The core consists of a coarse- to medium-grained syenite with epidote vein, displaying a pinkish-grey colour. The rock is predominantly composed of alkali feldspar, with minor plagioclase.
57.00	57.41	0.41	0.40	NQ	97.56	Coarse grain to Medium	Pinkish to grey to Black	Zeosite, Epidote, Allanite/Magnetite	Syenite	The core consists of a coarse- to medium-grained syenite with epidote vein, displaying a pinkish-grey colour. The rock is predominantly composed of alkali feldspar, with minor plagioclase.
57.41	59.86	2.45	2.42	NQ	98.78	Coarse grain to Medium	Pinkish to grey to Black	Epidote, Allanite/Magnetite	Syenite	The core consists of a coarse- to medium-grained syenite with epidote vein, displaying a pinkish-grey colour. The rock is predominantly composed of alkali feldspar, with minor plagioclase.
59.86	60.00	0.14	0.13	NQ	92.86	Fine to Coarse grained	Greenish to Black	Epidote	Amphibolite	Amphibolite dark greenish in colour massive in nature with weakly foliated with consist of plagioclase & hornblend in dark colour and contributing to dense compact appearance
60.00	60.19	0.19	0.18	NQ	94.74	Fine to Coarse grained	Greenish to Black	Epidote	Amphibolite	Amphibolite dark greenish in colour massive in nature with weakly foliated with consist of plagioclase & hornblend in dark colour and contributing to dense compact appearance
60.19	60.54	0.35	0.34	NQ	97.14	Coarse grain to Medium	Pinkish to grey to Black	Epidote, Allanite/Magnetite	Syenite	The core consists of a coarse- to medium-grained syenite with epidote vein, displaying a pinkish-grey colour. The rock is predominantly composed of alkali feldspar, with minor plagioclase.
60.54	61.89	1.35	1.33	NQ	98.52	Fine to Coarse grained	Greenish to Black	Epidote	Amphibolite	Amphibolite dark greenish in colour massive in nature with weakly foliated with consist of plagioclase & hornblend in dark colour and contributing to dense compact appearance
61.89	63.00	1.11	1.09	NQ	98.20	Coarse grain to Medium	Light Pinkish to grey to Black	Epidote, Allanite/Magnetite	Intermixed migmatite gneiss & Syenite	The core consists of a coarse- to medium-grained syenite with epidote vein, displaying a light pinkish-grey colour. The rock is predominantly composed of alkali feldspar, with minor plagioclase.
63.00	63.40	0.40	0.37	NQ	92.50	Coarse grain to Medium	Light Pinkish to grey to Black	Epidote, Allanite/Magnetite	Intermixed migmatite gneiss & Syenite	The core consists of a coarse- to medium-grained syenite with epidote vein, displaying a light pinkish-grey colour. The rock is predominantly composed of alkali feldspar, with minor plagioclase.
63.40	63.8	0.44	0.43	NQ	97.73	Coarse grain	Light	Allanite/Magnetite	Intermixed	The core consists of a coarse- to medium-grained syenite with

	4					to Medium	Pinkish to grey to Black		migmatite gneiss & Syenite	epidote vein, displaying a light pinkish-grey colour. The rock is predominantly composed of alkali feldspar, with minor plagioclase.
63.84	65.15	1.31	1.28	NQ	97.71	Fine to Coarse grained	Greenish to Black	-	Amphibolite	Amphibolite dark greenish in colour massive in nature with weakly foliated with consist of plagioclase & hornblend in dark colour and contributing to dense compact appearance
65.15	66.00	0.85	0.83	NQ	97.65	Coarse grain to Medium	Light Pinkish to grey to Black	Allanite/Magnetite	Intermixed migmatite gneiss & Syenite	The core consists of a coarse- to medium-grained syenite with epidote vein, displaying a light pinkish-grey colour. The rock is predominantly composed of alkali feldspar, with minor plagioclase.
66.00	69.00	3.00	2.93	NQ	85.00	Coarse grain to Medium	Light Pinkish to grey to Black	Allanite/Magnetite	Intermixed migmatite gneiss & Syenite	The core consists of a coarse- to medium-grained syenite with epidote vein, displaying a light pinkish-grey colour. The rock is predominantly composed of alkali feldspar, with minor plagioclase.
69.00	72.00	3.00	2.94	NQ	71.66	Coarse grain to Medium	Pinkish to grey to Black	Epidote, Allanite/Magnetite, Zeosite	Syenite	The core consists of a coarse- to medium-grained syenite with epidote vein, displaying a pinkish-grey colour. The rock is predominantly composed of alkali feldspar, with minor plagioclase.
72.00	75.00	3.00	2.95	NQ	69.66	Coarse grain to Medium	Pinkish to grey to Black	Epidote, Allanite/Magnetite, Zeosite	Syenite	The core consists of a coarse- to medium-grained syenite with epidote vein, displaying a pinkish-grey colour. The rock is predominantly composed of alkali feldspar, with minor plagioclase.
75.00	76.54	1.54	1.49	NQ	62.33	Coarse grain to Medium	Pinkish to grey to Black	Epidote, Allanite/Magnetite, Zeosite	Syenite	The core consists of a coarse- to medium-grained syenite with epidote vein, displaying a pinkish-grey colour. The rock is predominantly composed of alkali feldspar, with minor plagioclase.
76.54	77.43	0.89	0.83	NQ	0.00	Coarse grain to Medium	Pinkish to grey to Black	Epidote, Allanite	Syenite	The core consists of a coarse- to medium-grained syenite with epidote vein, displaying a pinkish-grey colour. The rock is predominantly composed of alkali feldspar, with minor plagioclase.
77.43	78.00	0.57	0.54	NQ	33.33	Coarse grain to Medium	Pinkish to grey to Black	Epidote, Allanite	Syenite	The core consists of a coarse- to medium-grained syenite with epidote vein, displaying a pinkish-grey colour. The rock is predominantly composed of alkali feldspar, with minor plagioclase.
78.00	80.00	2.00	1.95	NQ	92.00	Coarse grain to Medium	Pinkish to grey to	Epidote, Allanite	Syenite	The core consists of a coarse- to medium-grained syenite with epidote vein, displaying a pinkish-grey colour. The rock is

							Black			predominantly composed of alkali feldspar, with minor plagioclase.
80.00	81.00	1.00	0.97	NQ	71.00	Coarse grain to Medium	Pinkish to grey to Black	Allanite	Syenite	The core consists of a coarse- to medium-grained syenite. displaying a pinkish-grey colour. The rock is predominantly composed of alkali feldspar, with minor plagioclase.
81.00	84.00	3.00	2.95	NQ	85.66	Coarse grain to Medium	Pinkish to grey to Black	Zeosite, Epidote, Allanite	Syenite	The core consists of a coarse- to medium-grained syenite with epidote vein, displaying a pinkish-grey colour. The rock is predominantly composed of alkali feldspar, with minor plagioclase.
84.00	85.00	1.00	0.98	NQ	92.00	Coarse grain to Medium	Pinkish to grey to Black	Zeosite, Epidote, Allanite	Syenite	The core consists of a coarse- to medium-grained syenite with epidote vein, displaying a pinkish-grey colour. The rock is predominantly composed of alkali feldspar, with minor plagioclase.

23.11 Annexure XI- Sanction Order

Government of India
Ministry of Mines
National Mineral Exploration Trust

File No. 23/464/2024-NMET/131 **New Delhi, 10th June, 2024**

OFFICE MEMORANDUM

Subject: Approval of mineral exploration project through NMET fund (Preliminary Exploration (G-3) for REE and associated minerals in Borana block, Rajsamand district, Rajasthan).
Agency: M/s Geo Expore Pvt. Ltd.

On the recommendation of the Technical-cum-Cost Committee (TCC) in its 63rd meeting, Executive Committee (EC) of NMET in its 35th EC meeting held on 16th May, 2024 approved the mineral exploration projects of M/s Geo Expore Pvt. Ltd. Ltd through NMET fund as per following details:

S. No	Project/Block Name	Agency	Duration (Months)	Approved Cost (₹ Including GST)
1	Preliminary Exploration (G-3) for REE and associated minerals in Borana block, Rajsamand district, Rajasthan	M/s Geo Expore Pvt. Ltd.	12 (up to 09.06.2025)	**1,46,98,108/-**
Total (Rupees One crore forty six lakh ninety eight thousand one hundred and eight only)				**1,46,98,108/-**

2. M/s Geo Expore Pvt. Ltd. shall submit progress on monthly basis to NMET Secretariat. The TCC, NMET shall review the progress of project and provide update to the Executive Committee enclosed in **Annexure,** as summarized below: -

•	**Field Mobilization**	:	1st month (up to 09.07.2024).
•	**Exploration**	:	2nd to 11th month (up to 09.05.2025).
	(incl. Pitting, Trenching, Drilling and sampling)	:	
•	**Laboratory Studies**	:	4th month to 11th month (up to 09.05.2025)
•	**Report Writing with Peer Review and submission to NMET**	:	11th month to 12th (up to 09.06.2025)

3. M/s Geo Expore Pvt. Ltd. shall complete the project as per the above terms.

4. Further, as per clause 3.2(viii) of the Office Memorandum no. 6/3/2015-NMET/380 dated 12th December 2023 regarding Mode of engagement of Notified Private Exploration Agencies and funding by NMET for exploration of Critical and Strategic Minerals, NPEA may avail mobilization advance (up to 30% of the approved project cost) upon submission of Bank Guarantee (BG, including e-bank guarantee) of equal value of advance to NMET.

Yours faithfully,

(Geetika Sharma)
Deputy Secretary & HoD, NMET

Copy for information and further necessary action

1. M/s Geo Expore Pvt. Ltd., MP,2nd A Main,2nd Cross Chandra Layout, Vijaynagar Bengaluru Karnataka 560040.
2. Dr. S. Ravi, Dy. Director General and Chairman, TCC-NMET, Geological Survey of India, SU: Karnataka & Goa, Bangalore-560078.
3. Executive Committee (EC) Meeting file (F.No.6/2/2015-NMET)
4. Grant-in aid Sanction order file.

Annexure 9A

Cost Estimation For Preliminary exploration (G3 stage) for REE and associated minerals in Borana block, Dist: Rajsamand, Rajasthan
Total Area 1.14 Sq.Km, Mapping 1:2000 Scale, No.of Boreholes : 6 ,Time line: 12 months, Review: After 6 months

Sl.No	Item of work	Unit	NMET SoC-Item -Sl No.	NMET Rates (2020)	Qty	Amount INR	Remarks
A	GEOLOGICAL WORK						
i	Geologist Party days H Q	Days	1.3	9000	30	270000	
ii	Geologist Party days - Field (DM Scale-1:2000, Topographic Survey	Days	1.3	11000	120	1320000	
iii	Labourers (Rs 504/day/labour)	Days	5.7	504	240	120960	Amount will be reimburse as per the notified rates by the Central Labour Commissioner (Rs. 504/- per day) or respective State Govt. whichever is higher
iv	Sampler Party days (1party)	Days	1.5.2	5100	55	280500	
v	Labour for Sampling	Days	5.7	504	220	110880	Amount will be reimburse as per the notified rates by the Central Labour Commissioner (Rs. 504/- per day) or respective State Govt. whichever is higher
	TOTAL A					2102340	
B	SURVEY						
i	Surveyor Party Days (1 party)	Days	1.6.1a	8300	30	249000	
ii	Labourers (Rs 504/day/labour) for Survey Party (4 Nos)	Days	5.7	504	120	60480	Amount will be reimburse as per the notified rates by the Central Labour Commissioner (Rs. 504/- per day) or respective State Govt. whichever is higher
iii	DGPs Survey- Fixation of BHS.Determination of Coordinates & Reduced Levels + 1 Base Station	Per point	1.6.3	19200	0	0	
	TOTAL C					309480	
C	PITTING & TRENCHING (120 cu m)						

8/4/2024.

08/04/2024

i	Pitting(1m x 1mx 1 m) - 5nos	Per Cu.M	2.1.2	3800	100	380000	
	TOTAL D					**380000**	
D	**DRILLING**						
	Drilling (150 m for 1 BH and 250m in 5 BHs)	mts	2.2.1.4a	11500	400	4600000	
	Drillcore preservation charges- "One complete borehole plus mineralised cores of all the BHs of the Block, all cost included "150m for one borehole, 50m mineralised zone for remaining 5 Bhs, "	per mts	5.3	1590	400	636000	
	Approach Road making for Rugged-Hilly terrain	per km	2.2.10b	32200	3	96600	
	Land Compensation	per borehole	5.6	20000	6	120000	
	Construction of concrete Pillar (12" x12"x30")	per borehole	2.2.7a	2000	6	12000	
	Accommodation	per month	2.2.9	50,000	3	150000	
	Drilling Camp setting cost	per project	2.2.9a	250000	1	250000	
	Drilling Camp Winding cost	per project	22.9b	250000	1	250000	
	Transportation of drill rig and truck associated with it (To & pro)	km	2.2.8	36	3400	122400	
	TOTAL E					**6237000**	
E	**LABORATORY STUDIES**						
i	**a.Chemical analyses**	Nos					
	Analyses of Geochemical -BRS, Trench/Pit Samples REE Analysis 14 elements -ICPMS	Per sample	4.1.13	5380	200	1076000	
ii	**Primary + Check Sample (other than drill core)**						
	(a)Check Samples- 10% External	Per sample	4.1.13	5380	20	107600	
iii	**Drill Core Samples**						
	Analyses of Geochemical REE Analysis 14 elements	Per samples	4.1.13	5380	200	1076000	
iv	**Primary + Check Sample (Drill core)**						
	(a)Check Samples- 10% External	per sample	4.1.13	5380	20	107600	

8/4/2024.

08/04/2024

v	**b.Petrography studies**						
	(a) Preparation of thin sections	Per sample	4.3.1	2353	10	23530	
	(b)Complete petrographic /ore microscopic study/Mineragraphic studies	Per sample	4.3.4	4232	10	42320	
	(c)Preparation of Polished Sections	Per sample	4.3.2	1549	10	15490	
	c) EPMA Studies	Per hour	4.4.1	8540	10	85400	
	d)Whole Rock Analysis	Per samples	4.1.15a	4200	10	42000	
	TOTAL F					**2676940**	
F	**GEOTECHNICAL STUDIES**						
i	Specific Gravity Determination	Per Sample	4.8.1	1605	5	8346	
	TOTAL G					**8346**	
	TOTAL A+B+C+D+E+F+G					**11613106**	
G	**PREPARATION OF EXPLORATION PROPOSAL (5+1 Softcopy)**	Per Project	5.1		1	**232262**	EA has to submit the Hard Copies and the soft copy of the final proposal along with Maps and Plan as suggested by the TCC- NMET in its meeting while clearing the proposal.
H	**PEER REVIEW**	As per EC committee				**30000**	
	TOTAL A to I	Per Project				**11875368**	
I	**GEOLOGICAL REPORT PREPARATION (@3%)**	Per Project	5.2 ii		1	**680656**	
	TOTAL A to J					**12456023**	
	GST 18%					**2242084**	
Total with GST 18%						**14698108**	
				Rs. In lacs		**146.98**	
Note:							
1	**Strict adherence to the Ministry of Finance's and GFR guidelines is mandatory. Every transaction must adhere to GFR rule 21.**						
2	**In case of delay/non- performance, the appropriate action will be taken by competent authority against delinquent agency as per prevailing govt. of India rules/guidelines on procurement.**						
3	**If any part of the project is outsourced, the amount will be reimbursed as per the Paragraph 3 of NMET SoC and Item no. 6 of NMET SoC. In case of execusion of the project by NEA on its own, a Certifiate regarding non outsourcing of any component/project is required.**						
4	**Necessary efforts should be made to minimize any adverse impact on the environment during exploration activities.**						

8/4/2024

08/04/2024

Government of India
Ministry of Mines
National Mineral Exploration Trust

F.No.23/464/2024-NMET/ 881 **New Delhi, 21st February, 2025**

REVISED OFFICE MEMORANDUM

Subject: Additional cost of the project "Preliminary Exploration (G-3) for REE and associated minerals in Borana block, Bhilwara District, Rajasthan" .

Agency: M/s GeoExpore Pvt. Ltd.

On the recommendation of Technical-cum-Cost Committee (TCC) of NMET the Executive Committee (EC) in its 35th meeting held on 16th may, 2024 had approved the mineral exploration project namely **"Preliminary Exploration (G-3) for REE and associated minerals in Borana block, Bhilwara District, Rajasthan"** with timeline of 12 months and at an approved cost of **₹1,46,98,108/-** (including GST) to be executed by M/s GeoExpore Pvt. Ltd.

2. On the request of M/s GeoExpore Pvt. Ltd. and recommendation of TCC, the Executive Committee (EC) of NMET in its 39th meeting held on 24th January, 2025, has accorded approval of additional cost of **19,31,669/- (₹ Nineteen lakh thirty one thousand six hundred sixty nine only)**

3. The total approved cost of the project is revised as under:-

S. No.	Project / Block Name	Commodity	Stage	Duration (Months)	Revised Cost (including GST).
1	Preliminary Exploration (G-3) for REE and associated minerals in Borana Block, Bhilwara District, Rajasthan	REE and associated minerals	G3	12 month (up to 09.05.2025)	₹1,66,29,777/-

(₹ One crore sixty six lakh twenty nine thousand seven hundred seventy seven only)

4. The uploading of final Geological Report (GR) on NGDR portal is sole responsibility of the exploration agency. The final payment will be made only after receiving the confirmation of the same. The screenshot/acknowledgement of successful uploading of GR is to be submitted to NMET with the final bill.

5. The other conditions of the earlier issued OM No. 23/464/2024-NMET/131 dt. 10.06.2024 remain same.

Yours faithfully,

(Geetika Sharma)
Deputy Secretary & HoD, NMET

Copy for information and further necessary action:-

1. The Director, Directorate of Geology and Mining, Uttar Pradesh Khanij Bhawan 27/8 Raja Ram Mohan Rai Marg, Hazratganj, Lucknow Uttar Pradesh-226001.
2. I.F. Division, Ministry of Mines, Shastri Bhawan, New Delhi.
3. Executive Committee (EC) Meeting file (F.No.6/2/2015-NMET)
4. The Chairman, TCCs of NMET.
5. Grant-in aid Sanction order file.

PRELIMINARY EXPLORATION (G-3) FOR REE AND ASSOCIATED MINERALS IN BORANA BLOCK, BHILWARA DISTRICT, RAJASTHAN

23.12 Annexure XII- Officials Involved in the Exploration Project

Sr. No.	Name	Designation	Signature
1	Ms. Mansi Kesarwani	Assistant Manager- Geoscience Strategy	
2	Dr. Abrar Ahmed	Senior Geologist	
3	Mr. Mohammad Muslemeen	Senior Geologist	
4	Mr. Manoj Kumar	Senior Geologist	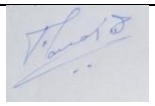
7	Dr. R. Chandrasekaran	Project Coordinator	
9	Mr. Sandeep Hamilton	Project Coordinator	
6	Mr. Channamalikarjun B. Patil	Project Director	
8	Dr. Yerriswamy Pateel	Project Director	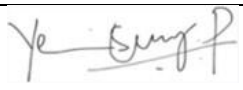

PRELIMINARY EXPLORATION (G-3) FOR REE AND ASSOCIATED MINERALS IN BORANA BLOCK, BHILWARA DISTRICT, RAJASTHAN

23.13 Annexure XIII- Project Reviewed At Various Stages

Preliminary Exploration (G-3) for REE and Associated Minerals in Borana Block, Bhilwara District, Rajasthan SO F.No.23/464/2024-NMEDT/131 dated 10th June 2024

1. Revised SO F.No.23/464/2024-NMEDT/881 dated 21st February 2025

2. The 03rd TCC II the project has been reviewed.

3. The 4th TCC II has been reviewed again and recommended revised estimated cost of ₹166.30 Lakh.

4. The 16th TCC II the project has been reviewed and rrecommended extentiondate till 08.02.2026

5. During the 21st TCC II II meetingther timeline extension for 3 months up to 7th May 2026 was requested by the agency.

6. During 24th TCC 2 meeting held on 2nd March 2026. The committee recommended the proposal for approval of PSC for “Timeline extension of 3 months up to 7th May 2026 for GR submission”. The committee advised completion of the remaining work followed by peer review & submission of the final geological report.

7. During 28th TCC 2 meeting held on 7 th and 8 th May 2026, the Committee recommended the proposal for approval of PSC for “timeline extension of 2 months up to 6 th July, 2026 for Peer Review and submission of final GR.

8. During 31st TCC 2 meeting held on 16th and 17th June, 2026, the committee recommended the proposal for approval of PSC for Timeline extension up to 31st July 2026 for submission of final Geological Report.

PRELIMINARY EXPLORATION (G-3) FOR REE AND ASSOCIATED MINERALS IN BORANA BLOCK, BHILWARA DISTRICT, RAJASTHAN

23.14 Annexure XIV- Field Inspection Photographs

GSI Visit on 18.07.2025: Mr. Rajesh Kumar Sahoo, Senior Geologist from the Geological Survey of India (GSI) Jaipur, visited the Borana project.

CHAPTER 24 - ANY OTHER INFORMATION

24.1 References

1. Bhattacharya, A.K., and Kapoor, A.K., (1988): Report on the study of high-grade sequences and associated rocks of the Sandmata Complex in parts of Udaipur district, Rajasthan.
2. Bhattacharya, A.K., and Guha, D.B., (1989): Report on the study of high-grade sequences and associated rocks of the Sandmata Complex in parts of Udaipur district, Rajasthan
3. Bhowmik, S.K., Bernhardt, H.-J., Dasgupta, S., (2010): Grenvillian age high-pressure upper amphibolite–granulite metamorphism in the Aravalli–Delhi mobile belt, northwestern India: new evidence from monazite chemical age and its implication. Precambrian Research 178, 168–184.
4. Buick, I.S., Allen, C., Pandit, M., Rubatto, D., Hermann, J., (2006): The Proterozoic magmatic and metamorphic history of the Banded Gneiss Complex, central Rajasthan, India: LA-ICP-MS U–Pb zircon constraints. Precambrian Research 151, 119–142.
5. Chishti, A., and Mahadevappa, P., (2005): Geochemical Mapping in Toposheet No. 45K/3, districts Bhilwara & Rajsamand, Rajasthan.
6. Gopalan, K., Macdougall, J.D., Roy, A.B., Murli, A.V., (1990): Sm–Nd evidence for 3.3 Ga old rocks in Rajasthan, northwestern India. Precambrian Research 48, 287–297.
7. Gupta, B.C., 1934. The geology of central Mewar. Memoirs of the Geological Survey of India 65, 107–168.
8. Hacket, C. A., (1881): The geology of the Aravalli region, central and eastern. Rec. G.S.I. Vol. XIV, pt. A
9. Heron, A.M., (1953): The geology of central Rajputana. Memoirs of the Geological Survey of India vol. 79, 389 pp.
10. Johri, R., and Roy, J., (2014-15): Compilation, Interpretation and Evaluation of Geochemical data of degreesheet 45K covering parts of Ajmer, Bhilwara, Chittorgarh, Pali and Rajsamand districts, Rajasthan.
11. Kulrani, A.V., Siriboyana, B.B., Goyal, K., (2014). Regional gravity and magnetic mapping in parts of degree sheet 45 K falling in Bhilwara, Rajsamand, Chittorgarh and Udaipur district, Rajasthan.
12. Kumar, S., et., al., (2016): Final Report on Geochemical Mapping in Toposheet Nos. 45K/3, 4 & 7 districts Bhilwara & Rajsamand, Rajasthan.

13. Misra, K.S., (1992): Search for metasedimentary enclaves in the banded gneissic complex of Udaipur -Chittorgarh area, Rajasthan.
14. Mohnaty, M., and Guha, D.B., (1990): High grade sequences and the associated rocks of the Sandmata Complex, Rec. Geol. Surv. Ind., v.123 (7), pp.1-2.
15. Mrutyunjay Das, and Jawed Ahmad, (2019): Reconnaissance survey for REE mineralization in and around Borana area, Rajsamand district, Rajasthan (UNFC STAGE: G4)
16. Neogi, S., and Raza, A., (2017): Final report on Specialized Thematic Mapping of the Anjana granitoid in Madaria-Raipur-Karera area northeast of Amet, Rajsamand district, Rajasthan. 393.
17. Patel, S.N., (1990): Report on Regional Geochemical Mapping of the Mangalwar complex and Berach Granite Belt in parts of Bhilwara and Chittaurgarh districts, Rajasthan. Up. GSI. Rep.
18. Roy, A.B., Kroner, A., (1996): Single zircon evaporation ages constraining the growth of the Archean Aravalli Craton, northwestern Indian shield. Geological Magazine 133, 333–342.
19. Roy, A.B., Kroner, A., Bhattacharya, P.K., Rathore, S., (2005): Metamorphic evolution and zircon geochronology of Early Proterozoic granulites in the Aravalli Mountains of northwestern India. Geol. Mag. 142, 287–302.
20. Sharma, V.K., (1992): Search for metasedimentary enclaves and associated mineralisation, using remote sensing techniques in parts of Bhilwara, Ajmer and Tonk districts, Rajasthan.
21. Shekhawat, L.S., Garkhal, R.S., (1990): Geochemical Mapping in parts of Bhilwara, Chittaurgarh and Udaipur districts, Rajasthan. Up. GSI. Rep.
22. Sinha-Roy, S., Guha, D.B., and Bhattacharaya, A.K., (1992): Polymetamorphic granulite facies peletic gneisses of the Precambrian Sandmata Complex, Rajasthan, India. Ind. Minerals. V.46, pp.1-12.
23. Verma, R.P., (1996): Study of regional structural patterns of the delhi fold belt between south of bhim and sambhar using remote sensing techniques. Wiedenbeck, M., Goswami, J.N., (1994): An ion-probe single zircon 207Pb/206Pb age from the Mewar Gneiss at Jhamarkotra, Rajasthan. Geochimica et Cosmochimica Acta 58, 2135–2141.

24.2 Locality Index

Sr. no.	Name of Locality	Latitute	Longitude	Toposheet no.
1	Amet	25°18'309.00"	73°55'46.2"	45K/03
2	Anjana	25°31'35.24"	73°57'39.81"	
3	Bhanja	25°24'43.30"	74°05'56.90"	
4	Bhatewar	25°26'28.17"	74°05'44.16"	
5	Bocana	25°25'27.8"	14°07'09.6"	
6	Bocana Ka Khera	25°26'2.6"	74°07'59.4"	
7	Chattol	25°23'17.80"	74°03'44.7"	
8	Deogarh	25°31'42.7"	73°54'78.82"	
9	Dhikani	25°24'23.00"	74°07'40.1"	
10	Gujjaron Ka Khera	25°25'53.80"	74°07'37.60"	
11	Jalarnali	25°23'18.20"	74°03'2.88"	
12	Jiti	25°24'39.96"	74°07'5.07"	
13	Kemuniya	25°23'16.0"	74°09'37.26"	
14	Kola Ka Khera	25°25'48.93"	74°03'25.38"	
15	Koli Khera	25°22'56.92"	74°03'02.23"	
16	Kosithal	25°18'46.78"	74°10'59.68"	
17	Kumahariya Khera	25°25'26.61"	74°09'24.94"	
18	Ladki	25°24'23.90"	74°05'44.4"	
19	Madariya	25°31'13.73"	74°00'36.19"	
20	Mandal	25°25'20.67"	74°05'39.44"	
21	Palra	25°21'88"	74°07'45.98"	
22	Panri	25°24'52"	74°00'29.00"	
23	PithaKaKhera	25°22'32.80"	74°06'3.3"	
24	Raipur	25°24'05.50	74°09'46.87"	
25	Rama	2°23'26.23"	74°05'48.94"	
26	RawatonKaKhera	25°26'35.88	74°05'07.6"	
27	Sephtiya	25°25'10.63"	74°03'10.76"	
28	Umri	25°27'21.49"	73°02'49.91"	

24.3 Reviewer's comments

Comments by Dr. Alok Porwal, Professor, Department of CSRE, IIT Bombay

Sr. No.	Reviewer's Comment	Action Taken / Compliance
1	**OVERVIEW**: The work has established that the block contains an REE-anomalous lithological association, especially in syenite/alkali syenite and migmatite gneiss. The data presented justify continued G-2 investigation, but they do not yet justify a strong conclusion regarding economic REE potential. Elevated bulk REE values are demonstrated, however whether REEs occur in sufficiently abundant recoverable REE minerals, remains to be seen. The mineralogical work is largely descriptive. Allanite and monazite are reported, but their modal abundance, grain size distribution, liberation characteristics, spatial continuity and quantitative contribution to bulk REE grade are not established.	Modal abundance, grainsize distribution, liberation characteristics, spatial continuity and quantitative contribution to bulk REE grade are not included in the NQT, therefore these studies were not included in the report.
1.1	**Geology and REE profile of the project area**	
a	The presently described system is best characterised as a low- to moderate-grade LREE-enriched syenite–migmatite system, not as a moderate to high grade REE orebody.	Corrected
b	The report should clearly distinguish among: 1. REE geochemical anomaly, 2. REE mineralization, 3. recoverable REE mineralization, and 4. economically viable REE resource. At present, the project has demonstrated the first and partly the second. It has not yet demonstrated the third or fourth.	The project has demonstrated the first and partly the second only. Three and fourth needs further in-depth studies which were not included in the NQT
2	**Comments on individual work components**	
2.1	**Geological mapping**: The mapping does not yet establish the geometry of mineralised bodies at a level	The syenite body boundaries,

	required for 50 m × 50 m drilling. The report needs clearer maps showing syenite body boundaries, contact relationships, internal lithological variation, alteration zones and grade distribution. It should also distinguish between massive syenite, syenitic bands/lenses in gneiss, feldspathized gneiss and pegmatitic material.	contact relationships were corrected in the maps so as to facilitate 50m X 50m drilling in future work.
2.2	**Petrography**: The identification of allanite and monazite is important, but the petrography is not sufficiently quantitative. The report does not answer the most important exploration question: how much allanite and monazite are present? Photomicrographs show the presence of allanite or monazite grains, however, they do not establish that these minerals occur in sufficient abundance to account for the bulk REE values or to support economic recovery. For an REE project, petrography must go beyond identification. It should quantify: • modal abundance of allanite, monazite, zircon, titanite and apatite; • grain size and shape; • whether the REE minerals are liberated or locked inside feldspar, quartz, amphibole or epidote; • whether allanite is primary, metamorphic, hydrothermal or altered; • whether monazite is widespread or rare; • whether high-grade samples contain visibly more REE minerals than low-grade samples; • whether the REE minerals occur continuously or sporadically	The petrography work has been outsourced to GSI, as per the reviewer's suggestions these details were discussed with GSI and details were updated accordingly.
2.5	**EPMA**: Only a small number of selected samples were analyzed. The reported outcome confirms the presence of minerals such as monazite, zircon, chalcopyrite, pyrite, and magnetite. However, the EPMA work is not used for a robust REE deportment model. The report states or implies that allanite and monazite explain the REE enrichment, but this is not demonstrated quantitatively. The critical question is not "Is allanite present?" but "Is allanite sufficiently abundant, continuous and recoverable?"	As per NQT only 5 samples were analysed, therefore robust REE Deportment Model could not be established. Allanite has been identified in petrographical studies only but not in EPMA.
2.6	**Geochemistry:** A more exploration-focused use of major oxides would be to examine correlations between REE and CaO, P_2O_5, TiO_2, Fe_2O_3, Na_2O, K_2O and Al_2O_3.	Corrected

2.6a	**Trace element geochemistry**: The report should present correlation plots such as: TREE vs P_2O_5, Th, U, Zr, Y, Nb, CaO, TiO_2, Fe_2O_3, modal allanite/monazite (if available).	Corrected
2.6b	**REE geochemistry**: The resource grades of about 0.137–0.144% total REE are geochemically meaningful but not exactly high-grade. They may be viable only if the material is bulk mineable, low-cost, near surface, laterally continuous and beneficiable into a concentrate. None of these conditions has yet been demonstrated. Equating "above 1000 ppm TREE" with ore can be problematic. A 1000 ppm cut-off is an exploration screening threshold, not an economic cut-off unless supported by mining, metallurgical and economic assumptions.	Beneficiation studies were beyond the scope of NQT. Basing exploration threshold REE resources were calculated for 1000 ppm and 1200ppm cutoff grade.
2.11	**Resource estimate:** The resource estimate reports: * 29.49 Mt at 1370 ppm total REE using a 1000 ppm cut-off. * 26.71 Mt at 1440 ppm total REE using a 1200 ppm cut-off. This is an inferred resource based on a limited number of boreholes. The tonnage is notable, but the average grade is low to moderate. The term "moderate to high-grade" may not be justified.	The term "moderate to high-grade" has been replaced with "low to moderate".
3	**Critical issue: allanite is reported, but how much?** Mineral deportment needs to be followed up and studied. For example, automated mineralogy by MLA/QEMSCAN/TIMA; SEM-EDS mapping of REE phases; EPMA traverses across allanite, monazite, epidote, titanite and apatite; modal estimates of REE-bearing minerals; grain-size distribution; liberation study after crushing and grinding; mineral-specific REE budget and Th-U distribution by mineral phase.	Mineralogy by MLA/QEMSCAN/TIMA; SEM-EDS mapping of REE phases and Economic viability studies were beyond the scope of our NQT.

	Economic viability requires several additional conditions such as : sufficient grade in oxide-equivalent terms, not just elemental ppm, favourable distribution of valuable REEs, especially Nd, Pr, Dy, Tb and Y, recoverable mineral hosts, low penalty elements, sufficient tonnage at mineable thickness, continuity of mineralization, beneficiation into a marketable concentrate, metallurgical recovery at reasonable cost, environmental acceptability and positive economics after mining, processing, separation and refining.	
4	**In nutshell** The report submitted GeoExpOre Pvt. Ltd documents high quality G-3 level work carried out on the project. It demonstrates that the Borana Block contains a low- to moderate-grade, LREE-dominant REE-anomalous system hosted mainly by syenite/alkali syenite and migmatite gneiss.	Thank you, corrected to “low to moderate grade”
4 a	Close spaced drilling may eventually be justified, but only after the following are completed: : (a) quantitative REE mineral deportment; (b) modal abundance of allanite, monazite, zircon, titanite and apatite; (c) liberation and beneficiation testing; (d) Th-U evaluation; (e) detailed lithology-grade modelling; and finally (f) selective 50 m × 50 m drilling in the best syenite hosted zones where trenching and drilling overlap.	Agreed

CHAPTER 25 - CERTIFICATE FROM THE QUALIFIED PERSON WITH NAME, DATE AND SIGNATURE

This is to certify that geological report has been prepared in respect of Preliminary Exploration (G-3) for REE and Associated Minerals in Borana Block, Bhilwara District, Rajasthan. The report was prepared by GeoExpOre Private Limited on behalf of the National Mineral Exploration and Development Trust (NMEDT). The report adheres to the Minerals (Evidence of Mineral Contents) Rules, 2015, as specified under the Mineral Auction Rules, 2015 and amended up to 2021.

NAME: Mr. Sandeep Hamilton
DESIGNATION: Project Coordinator
DATE: 31/07/2026